AGARD-CP-516

AGARD-CP-516

AGARD

ADVISORY GROUP FOR AEROSPACE RESEARCH & DEVELOPMENT
7 RUE ANCELLE 92200 NEUILLY SUR SEINE FRANCE

AGARD CONFERENCE PROCEEDINGS 516

High Altitude and High Acceleration Protection for Military Aircrew

(Les Equipements de Protection pour le Vol Haute Altitude et Grande Accélération à Bord des Avions Militaires)

Papers presented at the Aerospace Medical Panel Symposium held in Pensacola, Florida, United States 29th–30th April 1991.

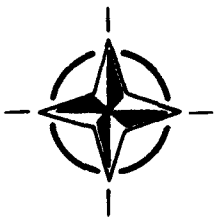

NORTH ATLANTIC TREATY ORGANIZATION

Published October 1991

Distribution and Availability on Back Cover

AGARD
ADVISORY GROUP FOR AEROSPACE RESEARCH & DEVELOPMENT
7 RUE ANCELLE 92200 NEUILLY SUR SEINE FRANCE

AGARD CONFERENCE PROCEEDINGS 516

High Altitude and High Acceleration Protection for Military Aircrew

(Les Equipements de Protection pour le Vol Haute Altitude et Grande Accélération à Bord des Avions Militaires)

Papers presented at the Aerospace Medical Panel Symposium held in Pensacola, Florida, United States, 29th—30th April 1991.

North Atlantic Treaty Organization
Organisation du Traité de l'Atlantique Nord

The Mission of AGARD

According to its Charter, the mission of AGARD is to bring together the leading personalities of the NATO nations in the fields of science and technology relating to aerospace for the following purposes:

- Recommending effective ways for the member nations to use their research and development capabilities for the common benefit of the NATO community;
- Providing scientific and technical advice and assistance to the Military Committee in the field of aerospace research and development (with particular regard to its military application);
- Continuously stimulating advances in the aerospace sciences relevant to strengthening the common defence posture;
- Improving the co-operation among member nations in aerospace research and development;
- Exchange of scientific and technical information;
- Providing assistance to member nations for the purpose of increasing their scientific and technical potential;
- Rendering scientific and technical assistance, as requested, to other NATO bodies and to member nations in connection with research and development problems in the aerospace field.

The highest authority within AGARD is the National Delegates Board consisting of officially appointed senior representatives from each member nation. The mission of AGARD is carried out through the Panels which are composed of experts appointed by the National Delegates, the Consultant and Exchange Programme and the Aerospace Applications Studies Programme. The results of AGARD work are reported to the member nations and the NATO Authorities through the AGARD series of publications of which this is one.

Participation in AGARD activities is by invitation only and is normally limited to citizens of the NATO nations.

Published October 1991

ISBN 92-835-0638-3

Printed by Specialised Printing Services Limited
40 Chigwell Lane, Loughton, Essex IG10 3TZ

Preface

Several NATO nations are developing highly-agile fighter aircraft that are capable of operating at altitudes well above 50,000 feet (15 km) and at sustained accelerations much greater than +6Gz. These include the United States with its F-22 Advanced Tactical Fighter, Germany, Italy, Spain and the United Kingdom with the European Fighter Aircraft, and France with the Rafale. Protection against both high sustained acceleration and loss of cabin pressurization at high altitude in these aircraft requires the judicious use of pressure breathing in combination with counterpressure to the limbs, trunk and abdomen. There is also the requirement for protection against other harmful environmental stressors; and there are the problems associated with effectively integrating the various protective assemblies so as to impose the minimum encumbrance and discomfort on the wearer. The purpose of this Symposium was to consider the physiological and technical requirements for protection of aircrew in the environment of high altitude and high acceleration, and against exposure to NBC threats and cold water immersion; and survey recent developments in aircrew life support equipment for counteracting the harmful effects of these stressors.

A number of topics were addressed, including:

- the problems of decompression sickness and ebullism at high altitude;
- the effects of high acceleration in relation to G-induced loss of consciousness (GLOC), positive pressure breathing (PBG), the anti-G straining manoeuvre (AGSM), and neck injury protection;
- mathematical models of the effects of high acceleration on the heart and circulatory system;
- physiological requirements and equipment for very high altitude protection; and
- integrative protective equipment to high altitude, high acceleration, NBC threats and cold water immersion.

Préface

Un certain nombre de pays membres de l'OTAN travaille sur le développement d'avions de combat à grande manoeuvrabilité capables d'effectuer des missions à des altitudes supérieures à 55 000 pieds (15 km) et à des accélérations continues bien supérieures à 6Gz.

Parmi les pays en question on distingue les Etats-Unis avec son avion de combat tactique avancé F-22 (ATF), l'Allemagne, l'Italie, l'Espagne et le Royaume-Uni avec l'avion de combat européen (EFA) et la France avec le Rafale. Pour ces avions, la protection contre les grandes accélérations continues et la dépressurisation cabine à haute altitude ne peut être assurée que par l'emploi judicieux de la respiration sous pression, associée à l'application de la contrepression aux membres, au tronc et à l'abdomen.

Il est également nécessaire de protéger les équipages contre d'autres éléments stressants et nuisibles dans leur milieu environnant, sans compter les problèmes associés à l'intégration effective des différents ensembles de protection de façon à imposer le minimum de gêne et d'embarras à l'utilisateur. Le symposium a eu pour objet d'examiner les besoins techniques et physiologiques en ce qui concerne la protection des équipages dans un environnement haute altitude, grandes accélérations, contre la menace NBC, l'immersion dans les eaux froides et également, de faire le point des derniers progrès enregistrés dans le domaine des équipements de survie conçus pour contrer les effets indésirables de ces éléments stressants.

Parmi les sujets examinés lors du symposium on distingue:

- les problèmes du mal de décompression et de l'ébullisme à haute altitude;
- l'incidence des grandes accélérations sur la perte de connaissance liée aux accélérations (G-LOC), la respiration en surpression (PBG), la manoeuvre anti-G (AGSM) et la protection du cou;
- les modèles mathématiques des effets des grandes accélérations sur le coeur et sur l'appareil circulatoire;
- les normes physiologiques et les équipements de protection à très haute altitude;
- les équipements intégrés de protection contre la haute altitude, les grandes accélérations, la menace NBC et l'immersion dans les eaux froides.

Aerospace Medical Panel

Chairman: Prof. G. Santucci
Sous-Directeur de Recherche de
L'E.A.S.S.A.A. et du C.E.R.M.A.
Base d'Essais en Vol
91228 Brétigny sur Orge Cedex
France

Deputy Chairman: Prof. Dr Med. L. Vogt
Institut für Flugmedizin – DLR
Postfach 90 60 58 – Linder Hohe
D-5000 Köln 90
Germany

TECHNICAL PROGRAMME COMMITTEE

Chairman: Dr J.P. Landolt
DCIEM
1133 Sheppard Avenue West
P O Box 2000
North York, Ontario M3M 3B9
Canada

Members

AVM J. Ernsting
RAF Institute of Aviation
Medicine
Farnborough, Hants GU14 6SZ
United Kingdom

Colonel P.I. Burgers
IDDKLu/HOOFD Luchtv.
Postbus 153
3769 Soesterberg
The Netherlands

Dr R. Burton
Chief Scientist USAF School
of Aerospace Medicine
Brooks AFB, TX 78235
United States

Dr J.M. Clère
CEV/LAMAS
B P 2
91228 Brétigny/Orge
France

HOST NATION COORDINATOR

Capt J.A. Brady
MSC, USN
Commanding Officer
Naval Aeromedical Research Laboratory
Naval Air Station
Pensacola, FL 32508-5700
United States

PANEL EXECUTIVE

Major W.D. Lyle, CAF

Mail from Europe:
AGARD–OTAN
Attn: AMP Executive
7, rue Ancelle
92200 Neuilly sur Seine
France

Mail from US and Canada:
AGARD–NATO
Attn: AMP Executive
APO AE 09777

Tel: 33(1) 47 38 57 60
Telex: 610176 (France)
Telefax: 33(1) 47 38 57 99

Contents

TECHNICAL EVALUATION REPORT

by

Jack P. Landolt, Ph.D.
Defence and Civil Institute of Environmental Medicine
North York, Ontario, Canada M3M 3B9

1. INTRODUCTION

The Aerospace Medical Panel held a Symposium on "High Altitude and High Acceleration Protection for Military Aircrew" at the Conference Support Center, Naval Air Station, Pensacola, Florida, USA, 29 - 30 April 1991. Twenty-eight papers and an invited Keynote Address were given by authors from six NATO countries. There were 162 registrants at the Symposium.

2. THEME

At its 68th Business Meeting, the Aerospace Medical Panel accepted proposals on high altitude protection from the Special Clinical and Physiological Problems Committee, and high acceleration (G or +Gz) protection from the Biodynamics Committee for a single Symposium that combined both topics. Its theme was a consideration of the physiological and technical requirements for protection of aircrew operating aircraft:

a. above 50,000 feet (15 km) against the effects of loss of cabin pressurization; and

b. at high sustained acceleration (greater than +6 Gz, greater than 15 s).

3. PURPOSE AND SCOPE

The USA with its F-22 Advanced Tactical Fighter, the four nations developing the European Fighter Aircraft (GE, IT, SP and UK) and France with its Rafale have need for life support systems which must be effective, but, at the same time, will impose the minimum encumbrance and discomfort on aircrew. The purpose of the Symposium was to review what the different countries are doing in regard to protective assemblies, and describe methods of performance enhancement and integration of these assemblies with other protective subsystems in the specific environment of high altitude, high acceleration and other harmful stressors.

The scope of the Symposium was broad covering:

a. the requirements for ameliorating decompression sickness and ebullism at high altitude;

b. the incidence of accidents resulting from G-induced loss of consciousness (GLOC);

c. the concomitant effects of positive pressure breathing (PBG) and gas counterpressure on the lungs and cardiovascular system during sustained high acceleration;

d. subjective reports on COMBAT EDGE, the US Air Force's new positive pressure breathing system;

e. mechanisms underlying GLOC to slow and rapid G onset rates;

f. a head support system for preventing neck injury to high acceleration;

g. mathematical models that simulate the cardiovascular system to high acceleration;

h. the physiological requirements for high altitude protection; and

i. the integration of protective equipment to high altitude, high acceleration, NBC threats and cold water immersion.

4. SYMPOSIUM PROGRAM

The Symposium consisted of a Keynote Address on the operational requirements for high altitude and high acceleration in NATO by LCol K.M. Waage, Royal Norwegian Air Force, SHAPE Headquarters, BE and five scientific sessions which were chaired as follows:

a. *Session I* — *Decompression Sickness and Ebullism*
Chairmen: Dr J.P. Landolt, CA and
Col P.I.Burgers, NE;

b. Session II — Effects of High Acceleration
Chairmen: (i) Dr R.R. Burton, US and
Dr J.M. Clère, FR,
(ii) Dr R.R. Burton, US and
Col P.I. Burgers, NE;

c. Session III — Modelling of Effects of Acceleration
Chairmen: Dr J.M. Clère, FR and
Dr R.R. Burton, US;

d. Session IV — High Altitude Protection
Chairmen: Dr J.M. Clère, FR and
Dr J.P. Landolt, CA; and

e. *Session V* — *Equipment for High Altitude and G Protection*
Chairmen: Col P.I. Burgers, NE and
Dr R.R. Burton, US

The Session Chairmen and AVM J. Ernsting, RAF IAM, UK formed the Technical Programme Organizing Committee.

5. TECHNICAL EVALUATION

In his Keynote Address, LCol Waage spoke of NATO's continuing commitment to the defence of territory of its member nations. Moreover, air power with its capability for manoeuvrability, speed and flexibility will maintain a vital role in any future NATO operations. Concomitant with the needs for such air assets is the continuing and evolving requirements for protection against high altitude, high acceleration and other harmful stressors.

5.1 High Altitude - Decompression Sickness and Ebullism

Attempts at defining the physiological requirements for protection against altitude decompression sickness and ebullism on loss of cabin pressurization at high altitudes were addressed in Session I. As Pilmanis and Stegmann (papers #1 and 3) have pointed out, much is known about decompression sickness for altitudes below 40,000 feet (12 km) regarding the dynamics of formation and growth of bubble nuclei in human tissues. Additionally, much effort has gone into understanding the pathophysiology of decompression sickness; currently, there are attempts to assess its contribution to long-term damage of the central nervous system. However, there is a paucity of good data on the physiological hazards of decompression sickness for altitudes greater than 45,000 feet (13.7 km). To address this concern, a model is being developed at the USAF Armstrong Laboratory that is extrapolated from lower-altitude data bases which will be used, it is hoped, to assess the clinical severity of decompression sickness experienced by aircrew operating at these higher altitudes. Moreover, Pilmanis and Stegmann suggested that data base inconsistencies could be improved by devising a better classification system for describing the symptoms of decompression sickness. The model will be used to test the efficacy of pre-breathing 100% oxygen to reduce the incidence of altitude decompression sickness (paper #4).

The mechanism by which decompression sickness is produced in rabbits decompressed to altitude was studied by Ward and his colleagues (paper #2). Rabbits that normally experience decompression sickness can be made immune if their blood complement enzyme system is inactivated. Interestingly, the decomplementation procedure does not inhibit bubble nucleation formation during decompression. This implies that complement activates one or more unknown biochemical components of the circulatory system which contribute to the onset of decompression sickness. That suggests that a pharmacological approach may help in the amelioration and/or prevention of decompression sickness insults.

Regarding the problem of ebullism, Pilmanis and Stegmann (paper #1) are concerned with the fact that integrated partial pressure suits, which will be used at these high altitudes, offer no protection to the exposed head and upper extremities. Case reports in the literature describe swelling and pain in exposed limbs, and surface eye freezing. They feel that a better understanding of the pathophysiology of ebullism, its potential for increased risk of decompression sickness, improved protective measures and special medical procedures will help with survival.

5.2 Effects of High Acceleration

Session II addressed aeromedical concerns regarding aircrew exposed to sustained accelerations considerably greater than +6 Gz. Lyons and his colleagues (paper #5) cited 18 USAF accidents involving 14 fatalities between 1982 to 1990 that resulted from GLOC during single-seat sorties. Interestingly, the average accident rate per million flying hours decreased from 4.0 during 1982 - 1984 to 1.3 for the period 1985 - 1990. It may be significant that the accident rate dropped during the period in which the number of hours flown in single seat aircraft increased by 30%. The fall in accident rate may also be due to a better awareness of GLOC and the institution of G-training programmes on the human centrifuge. Inexperience in flying; G level (+4 to +9 Gz), duration and rate of onset; and (possibly because of the stress of apprehension) high systolic blood pressure were cited as potential factors contributing to GLOC.

Glaister (paper #6) reviewed the effects of positive pressure breathing on the lungs during sustained high +Gz (PBG). Positive pressure breathing (PPB) has been used for many years for emergency protection against altitude hypoxia following the accidental loss of cabin pressurization. By controlling the hypertensive side effects of positive pressure breathing through the effective application of counterpressure to the chest, abdomen and lower limbs, +Gz protection is also afforded. Glaister described how the regional variations in lung ventilation/perfusion ratio resulting from sustained +Gz contribute to hypoxemia; and he reemphasised the fact that the combination of wearing a G suit, breathing pure oxygen and pulling G results in acceleration atelectasis (i.e., lung collapse).

Safety concerns to PBG were addressed by several other speakers as well. Buick and his colleagues at DCIEM (paper #7) demonstrated that the intrathoracic pressure produced by combining PBG with a maximal anti-G straining manoeuvre (AGSM) does not exceed the pressure produced by invoking a maximal AGSM by itself. This was explained as being due to the limited chest counterpressure, and to the maximal pressure characteristics of the expiratory muscles. Preliminary work by Burns, Fanton and Desmond, (paper #10) using the swine as a representative model, showed that increases in intraventricular pressures from pressure breathing are well balanced by intrathoracic pressures that are supported by the application of gas counterpressures, with the result that pressures across the heart wall remain within normal limits. Reducing the potential increase of work by the heart, through counterpressure techniques during PBG, has important implications if long-term deleterious effects to pressure breathing are to be minimized or avoided.

Subjective reports by McCloskey and her colleagues (paper #11) from check-out tests on COMBAT EDGE, the US Air Force's new PBG system, were also informative. Subjects estimated that they obtained an increase in G-level tolerance of +2 Gz with COMBAT EDGE. However, subjects reported distracting pain in the arms approximately 49% of the time, the tendency to hyperventilate, and a disturbing oro-nasal mask leakage during pressurization in 30% of cases when using COMBAT EDGE. Interestingly, arm pain does not appear to be a factor in high performance aircraft sorties in the F-15 or when the arms are raised to heart level in the centrifuge. Most subjects reported significant improvements in breathing as the number of centrifuge runs increased, and a reduction in the requirements for straining at the higher +Gz levels. In fact, subjects reported that AGSMs were not needed at all; the tensing of leg muscles was quite sufficient to counter the effects of high acceleration. The work of Krock and Cornwall (paper #8) suggested that there is a preferential use of leg muscles in performing the AGSM, and this fact should be considered during high acceleration

protection training.

Forgetting the basic AGSM when using COMBAT EDGE is a distinct possibility. Although pressure breathing has the same effect in improving +Gz-level tolerance, it is not meant to replace the properly-executed AGSM. To do otherwise might imperil the aviator should equipment malfunction occur. Moreover, COMBAT EDGE alone will not completely protect the pilot during high acceleration onsets greater than 1 Gz per second. In a related paper, Clère and Burns (paper # 13) reported that French equipment employing counterpressure techniques for producing PBG increased +Gz-duration tolerance in subjects in the human centrifuge, but did not significantly improve +Gz-level tolerance to very rapid acceleration onset rates.

Two papers in the session discussed ways of improving +Gz protection. Prior from the RAF Institute of Aviation Medicine (paper #14) demonstrated that good Gz enhancement may be achieved by combining PBG with anti-G trousers that provide compression to 90% of the lower body. However, arm pain of vascular origin occurred and became progressively worse with increasing +Gz levels and mask pressures. Prior argued that a compromise must be made between +Gz protection and discomfort if the system is to find acceptance by aircrew. The USAF Armstrong Laboratory has developed ATAGS, an anti-G suit that provides extensive bladder coverage to the buttocks, knees, ankles and feet. Meeker (paper #15) described studies showing that current pressurization schedules can be reduced from present standards without affecting the Gz tolerance and endurance afforded by ATAGS

At an AGARD Aerospace Medical Panel Symposium in 1989 (AGARD Conference Proceedings No 471), it was mentioned that 50% or more of pilots have reported neck injury while flying high performance aircraft. At this Symposium, Marshall (paper #16) discussed a project, the Military Aircrew Head Support System, which British Aerospace has initiated to reduce neck fatigue and injuries, and assist the pilot in making head movements during high acceleration manoeuvres. The concept employs a servo system that stabilizes the pilot's head and upper body by adjusting the tension in a set of cables attached to the helmet that is under the control of a microprocessor according to the prevailing G forces measured by means of accelerometers. The system has been tested to 6 G in the human centrifuge and subjective responses have been favourable. However, the question of pilot acceptance still needs to be addressed.

Two other papers were given in Session II. Van Lieshout and his colleagues (paper #9) noted that the Valsalva manoeuvre has no predictive value for screening aircrew for +Gz tolerance. Quandieu and his colleagues (paper #12) differentiated between GLOC to slow G onset rates, which can be explained on the basis of cerebral hypoxia, and GLOC to rapid G onset rates, which is basically biomechanical in nature and can be modelled as such. During rapid G onset, the sudden change in flow rate causes a venous collapse in circulation which prevents the blood from leaving the brain giving rise to loss of consciousness through "intracranial hypertension".

5.3 Modelling of Effects of Acceleration

Session III dealt with mathematical models of the effects of high acceleration on the heart and circulatory system. Such models are required to assess the potential for cardiac tissue damage resulting from high acceleration loading and external pressure augmentation, and to better understand the mechanisms underlying GLOC. They also have important implications for developing Gz protective equipment and techniques. Preliminary results from the cardiovascular model developed by Jaron, Moore and Vieyres (paper #17) have demonstrated the additive nature of different modes of acceleration protection; e.g., the anti-G suit, AGSMs, and PBG. The authors intend to use their model to optimize the use of PBG with other protective means. Moore and his colleagues (paper #20) developed a finite element model from reconstructed three-dimensional Magnetic Resonance or Echocardiographic images that will be used to determine the stress/strain relationship of the human left ventricle myocardium during sustained +Gz accelerations. Such a model has utility in predicting gross heart fibre changes for high accelerations where human experimentation is not possible. Gaffie and his colleagues described work underway at ONERA and CERMA (paper #19) of a model of the circulatory system that takes into account concomitant heart action, external pressures and blood flow forces to study GLOC. Results show that GLOC is related to reduced blood flow. Collins and Mateeva (paper #18) argued that a relatively-simple model of the coronary circulation provides quite a comprehensive framework for investigating effective countermeasures against high sustained acceleration.

5.4 High Altitude Protection

The three papers in Session IV discussed protection to hypoxia resulting from rapid decompression at high altitudes considerably greater than 40,000 feet (12 km). Macmillan (paper #21) described the physiological and operational requirements for using partial pressure assemblies in combination with breathing gases produced by means of molecular sieve concentrators which deliver at most 95% oxygen. In establishing the protective requirements for short-term exposure (1 to 2 minutes) to 60,000 - 65,000 feet (18 - 20 km), Macmillan emphasized that compromises must be made between providing adequate pilot protection and maintaining an acceptable level of physiological stress. In that regard, Gradwell (paper #23) demonstrated that it was possible to appropriately configure partial pressure assemblies to reduce bulk and thermal load, improve donning and doffing, and limit subjective discomfort without compromising physiological protection for the pilot.

Marotte, Vieillefond and their colleagues (paper #22) described partial pressure equipment that France has developed and tested successfully to a maximum altitude of 65,000 feet (20 km), for a maximum duration above 40,000 feet (12 km) of 2 to 3 minutes and an aircraft pressurization schedule of 35 kPa.

5.5 Equipment for High Altitude and G Protection

The major focus of papers in Session V was on the development and integration of high altitude, high

acceleration and other aircrew protective equipment. Marotte, Beaussant and their colleagues (paper #24) described new technologies in molecular sieve oxygen concentrators and electronics which France is employing in integrating protective systems within the same ensemble against high sustained acceleration, high altitude, cold water immersion and NBC contaminants. Similarly, Ernsting and Macmillan (paper #28) discussed the physiological, technical and safety aspects required for designing an integrated protective system for the RAF against high sustained acceleration short duration exposure to high altitude and NBC contaminants. Ernsting and Macmillan placed great emphasis on the difficulty imposed by "integrating" partial pressure assemblies with NBC protection. The system envisaged does not provide NBC protection following descent into water: water occludes current NBC filters. Again, as in other papers, both sets of authors placed great emphasis on the operational constraints and compromises that must be met for providing and integrating protective equipment that imposes minimum physiological encumbrances and discomfort on aircrew while enabling acceptable levels of performance to be met.

Hay and Aplin (paper #26) described an experimental partial pressure assembly that the RAE is developing to improve aircrew protection against high sustained +Gz and high altitude. The system employed anti-G trousers designed to give an anthropometric close fit, full coverage of the abdomen and legs to provide rapid inflation in response to high acceleration onset rates. By utilizing these anti-G trousers in conjunction with a PBG schedule in which chest garment counterpressure is applied directly from the breathing gas regulator, the physiological requirements for protection can be realized. In a related paper, Farrell and his colleagues (paper #25) described a computer model of a multi-bladder system which can simulate conceptual physiological protection concepts and systems such as that proposed by Hay and Aplin.

Lovett (paper #27) discussed the successful work that Normalair Garrett Limited has conducted in combining the anti-G valve, breathing gas regulator and other components into a seat-mounted combined valve -- the so-called BRAG valve. Moreover, new developments in aircrew garmentry in the United Kingdom and the United States such as those that were discussed in this Symposium have negated the need for electronically-controlling this valve; a mechanically-controlled valve is quite sufficient, responding quickly enough for providing aircrew protection. Future work by Normalair-Garrett will focus on integrating both altitude and acceleration protection into a single small unit.

6. CONCLUSIONS AND RECOMMENDATIONS

This Symposium has drawn attention to the many different physiological and engineering factors that must be considered if adequate protection is to be realized in aircrew operating in the harsh environment of high altitude, high acceleration and other stressors. As indicated, much progress has been made in improving protective life support equipment and in our understanding of GLOC. However, many of the papers given in this Symposium on other topics were preliminary or incomplete studies, and, accordingly, more research is required if aircrew are to operate effectively and safely in these environments. Probably no research area is as important as that pertaining to the short-term and long-term effects of PBG and high acceleration, singly and in combination, on the cardiovascular and respiratory systems. The problem of arm pain when instituting high acceleration protective measures also requires further study. As well, if aircrew are to operate to altitudes to 70,000 feet (21 km), then there are the continuing research challenges of decompression sickness, hypoxia, ebullism and thermal load that must be addressed. On the supply side, there is a requirement for further improvements in the efficiency of on-board oxygen generation systems. Other thrusts that promote joint development and the standardization of aircrew protective equipment should also be considered by the NATO aeromedical community.

7. ACKNOWLEDGEMENTS

I thank Capt (N) C.J. Brooks and Dr F. Buick for comments, and Mrs N. Wisteard and Ms June Parris for typing.

DCIEM Report No. 91-41.

KEYNOTE ADDRESS - HIGH ALTITUDE AND HIGH G - AN OPERATIONAL PERSPECTIVE

by

Lt. Col. Knut M. Waage, RNOAF
Supreme Headquarters Allied Powers Europe
Operations Division
Air Section, Combat Requirements Branch
B-7010 SHAPE, Belgium

Mr. Chairman, Ladies and Gentlemen,

Thank you for your introduction. Let me start by saying that I am very happy and honored to be here today to address such a distinguished group of people. The work you are doing in the field of high altitude and high acceleration protection for military aircrew is of the utmost importance for those of us who are involved in this business on a day to day basis. It is quite obvious that good results in these areas mean a safer environment, leading to better effectiveness which again ensures a high degree of mission success. And that is what it is all about - to get the weapons on the right target at the right time.

To set the scene for the conference, I will look into some of the thoughts being discussed in SHAPE at the present time that concerns the future structure of NATO with special emphasis on the air side. I will shortly touch upon some of the tendencies we see in the aircraft of the future and finally touch upon some of the problems experienced by pilots operating the aircraft of today.

With all the dramatic political changes that have happened in the world the last couple of years and with the signing of the CFE treaty in Paris in November last year, it became quite clear that NATO needed to reassess its strategy and its future structure. This is a work that has not been completed but is an ongoing process. NATO's future strategy, emerging from the London Declaration, will be a mix of continuity and change. The Alliance will remain committed to defend all territory of member nations and nuclear forces will continue to play an important role in the strategy. Crisis management, arms control and mutual security are examples of the new emerging principles. The future military strategy will be largely influenced by smaller standing forces with lower states of readiness and a greater dependence on force generation. It will require increased conventional flexibility and mobility and will rely more on multinational forces. A continued presence in Europe of significant forces from the North American democracies is indispensable.

Where NATO efforts previously have been focused on ensuring adequate resources to defend against potential aggression by a numerically superior Warsaw Pact, the changed security environment permits NATO to prepare for stability in Europe through the protection of peace. Arms control has become the linchpin in securing peace. The political and military volatility of Europe have decreased with the evolution of a matrix of treaties and agreements on INF, CFE, START and CSCE, the withdrawal of chemical weapons and anticipated SNF negotiations. However, much more remains to be accomplished. Future force structures must fully comply with all treaties and agreements and must be transparent to aid in verification.

The overall aim of the arms control process is to achieve stability among the nations involved to a degree where the use of force for the implementation of political aims and objectives is not a feasible option. Every nation should maintain a sufficient military capability, in concert with its allies, to defend against any form of aggression. Therefore, the military aim of the arms control process is to arrive at a balance of forces at the lowest level practicable. In addition, confidence building measures must complement the balance of forces to enhance transparency. Defence sufficiency is difficult to determine. Such factors as geography, population, wealth and industrial capabilities, trade lines, vulnerabilities, quantity, quality and type of weapon systems, as well as the size of armed forces have to be taken into account, balancing the capabilities between nations or groups of nations. A satisfactory formula to include all these factors does not exist. However, one is striving to develop a methodology that reflects the interdependency of the various factors. In absence of any better methods, a comparison of numbers of armed forces and of specific weapons systems has been taken as a suitable measure. This is a quantitative comparison, but a measure of the quality of assets has to play a greater role in determining the future balance.

As far as geography is concerned, restricting numbers of air assets to specific regions does not take into account the ability of aircraft to redeply quickly into other areas. Therefore the balance of air power must be achieved by looking at the whole of the signatories area of interest and responsibility. The basic question seems to be which quantity of forces may be considered sufficient for the Soviet Union, not only looking towards the rest of Europe, but also considering its Asiatic area. With regard to air power the SU must be viewed as a whole with differentiations being made for long range or rapidly deployable assets as compared to relatively static air power assets. Therefore, sufficiency for defence can not be determined by looking at the east - west relationship alone. For the SU, the quantity and quality of forces will, to a great extent, depend on the situation in east and south-east Asia as well as on its southern flank. For European nations the balance of forces and the political relations with respect to the Near East and some African nations will be determining factors as well as the relationship to the SU. Worldwide commitments for some NATO nations have also to be taken into consideration.

The quality and quantity of air power necessary for a defender can by the very nature of air power also be used to enhance aggression. But - since air power by itself has no invasion capability, and since it reduces the odds for the defender particularly in the beginning of a conflict, it should be considered as a factor which enhances overall stability as long as decisive disparities between potential opponents can be avoided through arms control agreements.

The change in east - west relations from confrontation to cooperation, the anticipated reduction and disengagement of forces in the relevant geographical area, as well as the military capabilities in other areas, mean that a large scale invasion into the Alliance area is less likely to occur and will not be possible without longer preparation times. However, growing instability around the borders of the Alliance could lead to crisis and spillover conflicts. In this context, the role of air power as the most flexible of the military instruments for defence will increase in the future. The verification of arms control arrangements is enhanced by reconnaissance and surveillance provided by air assets, including those positioned in space. Effective reconnaissance and surveillance will also monitor force disposition, displacement and possible buildup against any nation of the Alliance, thus providing for the necessary political and military warning time. The ability to increase quickly the state of readiness of Alliance air power, is a strong deterrent to a potential aggressor. Air power's inherent flexibility in changing the state of readiness, becomes an effective tool in crisis management escalation and de-escalation.

Nevertheless, a determined aggressor may be able to concentrate forces before the defender is able to react effectively, with land or sea power. Air power must therefore be used to counter any concentration with air to ground assets and to protect the buildup of own forces with air defence assets. Air power has become the instrument whereby smaller in-place land forces, at reduced readiness, can be permitted an adequate buildup.

As now, it is conceivable that a future aggressor will commence an attack with an offensive counter air campaign to prevent sortie generation of Alliance air assets. At the same time or in subsequent operations, the aggressor will use his air power to prevent Alliance ground forces from joining the battle while maintaining a favorable air situation.

The tasks for our air forces remain basically the same as they are today. The overall number of targets and areas of operation may be reduced, but because of the inability of surface forces to react immediately to concentrations of an aggressor, our own air forces will be needed to fulfill many of the Key Mission Components at the same time in several theaters of war. This will, as before, create a high demand and the availability of air power from the very beginning of a conflict. Offensive air operations in conjunction with Defensive Counter Air will continue to play a vital role for the success of defence. The absence of air forces would greatly enhance the chance of an enemy's aggression to succeed, especially with the reduced number of ground forces available. And the absence of air power would inhibit our ability as defenders to enforce a change in an aggressor's posture.

To sum up this portion of my introduction, I think we can state that the inherent capabilities of air power such as flexibility, mobility, speed and the abilitiy to concentrate force and firepower make it very well suited for rapid adaption to the requirements of the future security environment. Air power must be seen as a synergy of weapons systems (aircraft, SAMs etc), air bases (with necessary infrastructure and logistic support) and a command and control capability for nuclear and conventional force postures. Only the balanced provision of all three elements can constitute an effective deterrent and, if necessary, fighting force. Concerning the future force levels, it seems to be clear that even if the CFE treaty has set a ceiling on the number of combat aircraft NATO may possess in the ATTU, political and economic constraints suggest that forces will be well short of those limits, making the need for flexibility and mobility to concentrate necessary forces in a potential conflict area all the more important.

Now then, after having established the fact that aircraft will remain a very important part of the military future, let us take a quick look at what we can expect to find in the field of future developments. There is a lot of activity going on these days with controversy attached to many of the projects. On the "other side" of the fence we have seen the introduction of some very capable aircraft lately, like the Mig-31 Foxhound, the follow on to Foxbat; the Mig-29 Fulcrum and the Su-27 Flanker, all of which have narrowed the technology gap between the East and the West. They are formidable aircraft with formidable performance as shown by numerous demonstrations at different airshows the last few years. And after the unification of Germany we have been able to carry out hands on testing with the Mig-29. In a simulated air combat engagement against a F-16 at the German Luftwaffe's test center at Manching, the Fulcrum engaged and destroyed the F-16 at a distance of 37 NM, which is outstanding, and which shows the capabilities of the weapon platform. Throughout the 1990's, updated versions with improved engines and improved performance can be expected, as well as the emergence of the next generation fighter in the beginning of the next century. More capable bombers are also being introduced, which means that we will be facing a reduced air force in size, but with much improved capabilities.

And what about ourselves? The discussions about the future are strong and heated. Which way to go, what do we need, how much do we really need and how much are we willing to spend on the air force of the future? They are all very important questions, and I

feel that a lot of the lessons learned from the recent war in the Middle East certainly will add arguments to the discussion. Tendencies: Stealth has been a big issue for some time and the principle of stealth was proven in the Gulf war. But one of the problems associated with stealth so far has been price. The future of the B-2 is uncertain and the A-12 has been cancelled (at least for the time being). On the fighter side there are several projects running. The two contenders to become the US Air Force's ATF are the Northrop/McDonnell Douglas YF-23 and the Lockheed/Boeing/General Dynamics YF-22. Either, or maybe both, may prove to be ideal as the USAF's primary interceptor of the future. Both aircraft are stealthy and can cruise at supersonic speeds without the use of afterburners, thus gaining great range. Advanced use of the nozzles give improved maneuverability. These capabilities combined with advanced BVR and short range air-to-air weapons will allow the aircraft to penetrate deep into enemy territory with a high degree of survivability, again a point that was emphasised during the Gulf war. A decision on which ATF to acquire was actually made on the 23rd of April in favour of the YF-22. On the European side of the Atlantic we hear most about aircraft like the EFA, the Rafale and the JAS Gripen. The European Fighter Aircraft which is a coproduction between Britain, Germany, Italy and Spain will eventually replace aircraft like the Tornado, the Phantoms and the UK Jaguars. The Rafale will update the French Air Force while the Gripen will do the same for the Swedish Air Force. In addition we also see that updates to aircraft like the F-14, F-15, F-16 and F-18 are being proposed, updates that will improve the overall capabilities of all these aircraft.

But what about Unmanned Air Vehicles, or UAVs as we call them? They have been in existence for quite some time but had not been put to extensive use until recently. The breakthrough for the long range cruise missile came during the Gulf war where a substantial number of weapons were used against high value targets within the Iraqi air defence systems and command and control sites. It seems logical that other high value targets will be included in the list of possible targets for these weapons in the future, possibly reducing the need for the manned aircraft to penetrate deep into enemy territory to attack their targets. Other applications for the UAVs are in surveillance, reconnaissance and target acquisition and also as jammers and as hard kill systems used in Suppression of Enemy Air Defenses (SEAD). From this we can expect these UAVs to be valuable additional assets in a future air power structure. But within what we can call the overseeable future, it is quite obvious that the main instrument in any air force will be the manned aircraft.

When the coalition of forces in the Middle East managed to establish absolute air supremacy at an early stage of the war, the attackers could fly their missions at middle to high altitudes, allowing them to stay out of range of any anti air artillery or small arms fire that could pose a threat to their operations. This may not, and will most probably not, be the case in any other future conflict. With the very strong SAM and AAA envisaged used by the enemy, the need to fly low and at high penetrating speeds will still exist in the future. So there will not necessarily be any big changes to the way we physically do our business when looking 20-25 years down-stream. Our war fighting system - i.e. the manned aircraft - still depend on the man in the cockpit as a decision-maker and controller. This man is better trained and more knowledgeable than ever before, but the fact remains he is just a man with his well known limitations. His tolerance for vibration, heat, hypoxia and G-forces has not improved. His visual perception and information-processing capacity are unchanged. His decision-making ability remains susceptible to fatigue, illusions and the stress of combat. To try to solve these problems you have tried to, and are still working at, improving the personal equipment necessary to enhance the pilot's capabilities in the aircraft. But this also encumbers the pilot considerably. For myself, the situation has been that I have grown up in an environment in Norway where we have to fly with an emersion suit the whole year. And that piece of kit in combination with long underwear, a G-suit, a sweater and a flight suit is certainly good to have the moment you have to leave the aircraft for any operational reason, but at the same time fatigues you when you are in the midst of a long mission with high-G maneuvering and a high work load. Add to this a chemical protective equipment - which is something I have not tried myself, but several air forces have developed systems that are reaching maturity, and add also a possible body armor, a helmet mounted sighting system or a night vision apparatus, and it all adds up to something that exacts a physiological toll on the pilot and at a certain point may compromise his performance capacity. The tendency to attach more and more devices to the head is a particular concern with respect to head mobility and neck fatigue.

As for the neck problem, this is a well documented phenomenon, especially in conjunction with the high performance aircraft of today where a 9 G pull is something that is part of almost every mission. It is something that every pilot needs to get used to by preparing himself both mentally and physiologically through training and mental awareness. Even with today's lightweight helmets there is a definite problem present if you as a pilot are caught off guard. And it seems obvious that if we keep adding bulky equipment for different purposes to the helmet, which was originally constructed to give the pilot added protection, we migh create a new problem while trying t solve other problems. But there is obviously the tendency that modern technology when properly packaged, will come up with compact solutions that are acceptable both for the weapons system and for the pilot.

Another obvious problem area associated with high G is the G-induced loss of consciousness, or better known as G-loc. Systems for the prevention of this to happen in high performance fighter aircraft have received increasing attention in the past few years. There are many ideas as you are all very aware of, but no consensus on how a G-loc system should be implemented has been reached. What is interesting to notice is that according to information I have, there has not been made any reference to include a G-loc system in the specification for the ATF. But when that is said, it seems that the YF-23 includes an assisted positive pressure breathing system that should increase the pilot's ability to tolerate G-forces. And until the magic solution appears we just have to keep the awareness of the problem alive and have the pilots practice and use the different techniques and systems that are known and available today. One thing we have started using in the Norwegian Air Force is a simple warming up process before going out to do air combat to enable you to establish your tolerance level of the day and to accustom your body to the strain of high G before having to react to the first surprise attack of the day, invariably the one where you find you'll employ the most Gs. On the development side of the house I am sure that you all are familiar with the system called Combat Edge, which is an "Enhanced Design G-Ensemble". This system is a simplified version of a fully developed Tactical Life Support System, and should to the extent possible use components already incorporated in the F-15 and F-16 aircraft and in the personal kit of the pilot. What needed to be changed or improved were a new G-valve and a new oxygen regulator in the aircraft. For the pilot's equipment a modification to the helmet was needed, a new oxygen mask, a new positive pressure vest and a new connector piece. Tests have shown the equipment to be very effective, and at a price of less than 10.000 $ per copy, it seems to be a small price to pay for the added protection it gives. But there is still quite a way to go before we have a system that is ideal. Additional features that will need to be incorporated are:

- improved G-protection by an improved anti-G suit of the full body type
- better protection against hypoxia in case of decompression (there will still be a need to fly high to reach highflying bombers, surveillance a/c etc, and for own transit)
- better protection against NBC
- an "onboard oxygen generating system" - already in use in some systems
- a system to keep the pilot nice and cool (liquid cooled vest like the one the Canadians are using)
- the use of all the above in combination with an exposure suit that will remain water-tight

These are the capabilities we as pilots want to have in our aircraft to improve the performance of the weapons system we have been trained to operate, and put together so it does not hamper us in our job performance.

But along with this we also see that our more complex and sophisticated weapons systems require their operators to do more in less time. In more complex scenarios where a pilot is preparing his attack, has to get his weapons ready, is on the lookout for enemy aircraft, has to respond to warnings received on his RWR or MAW and, at the same time, has to fly his aircraft to stay clear of the ground and to obtain the right position to deliver the weapons, situations can develop where a suitable description for the cockpit workload is "too high". So what do we do? We design cockpits which have the ultimate goal to reduce the workload. But is this work done in conjunction with all the other work that goes into trying to improve the situation for the pilot and improve on mission effectiveness? Is the integration good enough between the different agencies working all these complex problems? As a pilot I certainly hope that that is the case. Because with that as a starting point I feel certain that we can avoid what has happened before when one agency has come up with a solution to their particular problem, without taking into account the problem of other agencies trying to solve different problems, but with the same ultimate goal in mind - to make the working conditions for the pilot as good and as safe as possible.

Ladies and gentlemen. I hope that I have made it quite clear to you that the manned aircraft will remain a very important part of the future armed forces, that it will be necessary to continue to fly both at low and high altitude and that high Gs will continue to be the lot of fighter pilots also in the future, in order to perform the required mission in the years ahead. Undoubtedly, the excellent work you have been doing until now and that, obviously, you intend to carry on, will be of the utmost importance to the guy in the cockpit and to the successful completion of his mission. I know you will have some very good working days here in Pensacola and look forward to attend the presentations to be made. Good luck on your work! Thank you for your attention.

Decompression Sickness and Ebullism at High Altitudes

Andrew A. Pilmanis, PhD and Barbara J. Stegmann, MD
Armstrong Laboratory, Brooks AFB ,Texas 78235
and KRUG Life Sciences, San Antonio Texas 78279

SUMMARY

The use of high altitude air space for military activities exposes flight crews to the hazards of near vacuum ambient pressures. Both the US Advanced Tactical Fighter and the National Aerospace Plane will travel at heights where unprotected exposure to the environment leads to severe physiological consequences, including decompression sickness (DCS) and ebullism. Information about DCS occurring at or above altitudes of 40,000 feet is minimal. Theoretically, bubble growth will be rapid and latency of symptoms short. The ultimate DCS consequences of such high exposures, even very short ones, may be influenced by the pre and post events of a rapid decompression (RD), including prebreathing, and post-exposure medical intervention.

Ebullism, or the vaporization of body fluids, poses additional physiological risks to flight above 63,000 feet. Medical treatment protocols for ebullism in the event of accidental manned exposures to extreme altitudes do not exist. As research, training, and operational flights of new aircraft increase, the potential for exposure increases. The establishment of new protective measures and treatment protocols becomes essential.

1. Introduction

The new generation of aircraft such as the US Advanced Tactical Fighter (ATF), the European Fighter Aircraft (EFA), and various National Aerospace Plane (NASP) derivatives are expected to routinely fly above 40,000 feet. In addition to potential high altitude human exposure in new aircraft, research and training altitude chamber activities involving rapid decompressions are expected to increase. Although their mission is less glamorous in mission, such chamber activity will be vital for the development of safe operational capabilities.

In any high altitude operation, the inherent risk of rapid decompression must be considered. Potential physiological hazards associated with emergency rapid decompressions include hypoxia, ebullism, DCS, cerebral arterial gas embolism (CAGE), extreme thermal exposure, and trapped gas problems. Conventional protection against these hazards include cabin pressurization, full pressure suits, and potentially, partial pressure suits. Measures to deal with the failure of these systems must be defined. Currently, full pressure suits are used in high altitude reconnaissance aircraft such as the TR-1. They are also employed in space for extravehicular activity (EVA). These suits may not be practical in the new fighter aircraft because of restricted mobility, poor comfort, and logistical problems. For these aircraft, partial pressure ensembles that provide both G-protection and hypoxia protection are expected to be implemented. These garments only provide partial protection against the severe physiological consequences of DCS and ebullism. Human experiments at very high altitudes have demonstrated that conscious survival for very short "get-me-down" scenarios is possible wearing partial pressure protection with positive pressure breathing. However, the physiological risks of positive pressure breathing at very high intrapulmonary pressures are being re-evaluated. In addition, the onset and severity of DCS, and the catastrophic effects of ebullism at these very high altitudes also need elucidation.

This paper is limited to a discussion of the conditions of DCS and ebullism associated with exposure to altitudes above FL 400. The general purpose of the paper is to discuss the current understanding of these two conditions, and to explore critical areas of physiological research necessary for expanded flight operations to higher altitudes. The specific objectives include: 1) to review some recent DCS research results and apply them to an example scenario of a future aircraft, and 2) to develop a hypothesis for an expanded window of survival after ebullism.

2. Decompression Sickness Above Fl 400

DCS is a potentially serious condition, especially in single seat tactical aircraft. In the USAF, DCS occurs most frequently in unpressurized aircraft or in aircraft whose pressurization systems allow the crew to be exposed to cabin altitudes above 20,000 feet for long periods. A report published in 1988 describes a fatal accident in which a pilot was exposed to an unpressurized flight to 28,000 feet for 30 minutes (29). In 1989, another report described a co-pilot's loss of consciousness from DCS in a unpressurized commercial aircraft. The exposure was at 29,000 feet for approximately 15 minutes with no prebreathing (51). A recent study at the Armstrong Laboratory showed that 1 hour prebreathing followed by 4 hour exposures to 29,500 feet resulted in 73% bends and 80% intravascular bubbles (35). USAF high altitude reconnaissance aircrews are routinely exposed to altitudes of 28,000 to 29,000 feet for periods of approximately 9 hours. Meader (27) described 36 cases (958 flights) of DCS in U-2 pilots and, more recently, Sherman reviewed the current DCS incidence in high altitude reconnaissance operations (40). He described 18 cases reported between 1976 and 1990 resulting in an incidence of 0.06%. This is a very small incidence when compared to the research results cited above. However, it is generally accepted that there is a reporting reluctance in the operational setting due to career considerations (33).

Unlike the TR-1/U-2, the new high altitude fighter aircraft will presumably not have preflight denitrogenation procedures for protection against DCS. Yet it is likely that there will be a 5 psi differential pressurization schedule above 23,000 feet aircraft altitude. Thus, cabin altitudes may reach levels known to have significant DCS risk when exposure times exceed one hour. Furthermore, if an accidental RD occurs during such a flight, DCS risk may become paramount.

There are very few studies on DCS above 40,000 feet. In 1945, Sweeney reported that "about 20% of the subjects decompressed to altitudes above 40,000 feet suffered bends during the ensuing five minutes at altitude (43)." Annis and Webb (45) noted a DCS incident in one of their subjects within 5 minutes of being exposed to 80,000 feet simulated altitude, even though he had prebreathed for 3 hours. These subjects were wearing an elastic suit with positive pressure breathing capability. On the other hand, much data exists for DCS below 40,000 feet, and an altitude decompression model is currently being developed at the Armstrong Laboratory (36). Based on DCS databases from the lower altitudes, this model will be applied to flight scenarios above 40,000 feet. Such a model incorporated into appropriate hardware will provide both real time and predictive DCS risk assessment capability. Research to verify model generated data is planned. This research will also address the severity of clinical manifestation, onset times, and decompression effects in "get-me-down" scenarios. When this computer becomes available, immediate DCS risk prediction will greatly assist the development of future life support systems. Since computerized DCS predictive capability is not immediately available, this discussion will attempt to assess DCS risk for flight above FL 400 by combining results of several recent research projects with research results dating back to the 1940's and 1950's.

2.1 DCS and Bubbles

It is well known that DCS severity increases and onset times decrease with altitude (14). Furthermore, rapid decompression to altitudes above 40,000 feet carries higher risk than slow ascents or ascents to lower altitudes. However, few data are available on DCS in humans at high altitudes. *In vitro* bubble growth experiments have shown that, at relatively low altitudes, i.e. less than 25,000 feet, bubbles grow at a gradually decreasing rate and reach relatively small diameters as dictated by Boyle's Law (Fig 1). At high altitudes, i.e. over 30,000 feet, the bubbles maintain a period of rapid growth before tapering off, and attain proportionately larger diameters (30). Asymptomatic intravenous bubbles have been detected as low as 10,250 feet (10), while at higher altitudes, venous gas emboli (VGE) and symptoms frequently occur in close succession (48). In a recent paper, Olson and Krutz (31) related the bubble growth curve in Figure 1 to the latent period of DCS symptoms and concluded that the rate of bubble growth and the resulting bubble size is the critical factor in the latency and development of DCS

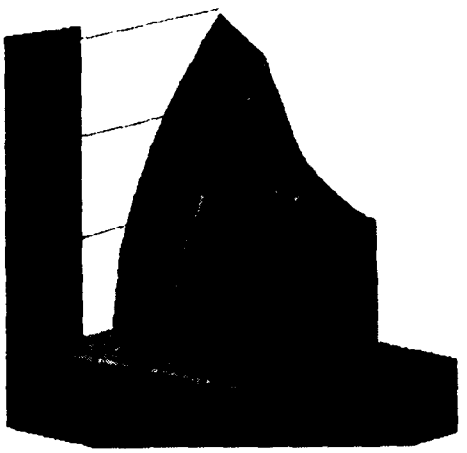

Figure No. 1. Three-dimensional graph of bubble size as a function of altitude and time (from Olson and Krutz (30)).

The onset of symptoms is probably dictated not only by the size of the bubbles, but also by the number and location of these bubbles. Bubble formation is not well understood. The concept of bubble nuclei has gained acceptance in recent years. However, the definition of bubble nuclei is controversial and has ranged from "tiny" bubbles to "potential" for bubble formation (44). As decompression progresses, there are more bubbles and they are larger at all levels of the spectrum represented in Figure 2. Although it can be generalized that symptoms are at their worst at the upper right of the spectrum, in some tissues problems can certainly occur with fewer and smaller bubbles. Conversely, the advent of *in-vivo* bubble detection methods has confirmed that the appearance of nonpain-producing bubbles, or "silent bubbles" can indeed occur well before the clinical manifestations of DCS (37).

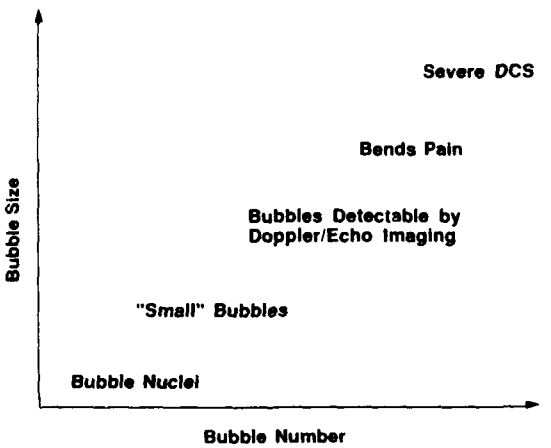

Figure 2. Relationship of bubbles to DCS

During the last decade, DCS research efforts have often used noninvasive precordial Doppler bubble detection techniques (32). DCS studies at the Armstrong Laboratory currently use a

combination of Echocardiogram and Doppler for simultaneous visual and aural monitoring of precordial venous gas emboli (2). All subjects are monitored with the Echo/Doppler to document the onset and degree of bubble formation. For example, Echo/Doppler can give an indication of how effective the prebreathe period was by indicating how quickly bubbles develop. Bubbles are recorded with the Echo by viewing a four chamber window of the heart. The Doppler is aimed at the right heart, and sound recordings are made as the bubbles enter the right sided circulation. Bubbles are graded from 1 to 4 depending on the aural and visual assessment of the number passing through the right heart. Grade 1 bubbles are defined as occasional bubbles. Grade 4 bubbles are so numerous that they are heard continuously and obscure the heart sounds.

Although the use of precordial Echo/Doppler recording has great research value, its clinical use is very limited. It is difficult to correlate the occurrence of decompression sickness symptoms and the appearance of intravascular bubbles. Indeed, subjects frequently have grade 4 bubbles without complaining of pain and some have pain without any precordial bubbles. This is understandable because intravascular bubbles may not correlate with extravascular bubbles and it is believed that the extravascular bubbles produce most symptoms. Thus, the Echo/Doppler data should not be used as an endpoint in place of clinical decompression sickness symptoms (47).

2.2 DCS *Incidence and Onset*

Results from almost 10 years of DCS research at the Armstrong Laboratory are compiled in a database described in Webb et al. (46). The incidence of both bubbles and DCS symptoms for altitudes up to 30,000 feet are shown in Table 1. As was mentioned, bubbles first appear at 10,250 feet, while bends is first seen at 15,000 feet. Again, it is evident that as altitude increases, DCS incidence increases.

It has generally been assumed that there is a short "grace" period (5 to 10 min) before DCS onset at any altitude above 30,000 feet due to the "inertia" of symptom onset. However, since essentially no hard DCS data for altitudes above 40,000 feet exist, the real onset times at these low pressures are unknown. For lower altitudes, if latency of DCS is plotted against altitude, there appears to be a linear relationship. Figure 3 shows the latency of DCS with no prebreathing, and Figure 4 shows the latency with one hour of prebreathing. The data for these plots were obtained from the above mentioned database (46), and a number of papers from the 1940's and 1950's (6, 8, 12, 16, 28, 42,). The results were screened to only include experiments that used mild exercise and defined the onset of DCS as the point at which mild (Grade 2) symptoms were noted. There are no plots above 38,000 feet because usable data could not be found. When these linear bands of

ALTITUDE	PREBREATHE	EXPOSURE DATA			INCIDENCE/MEAN LATENCY	
					DCS	VGE (Any grade)
(feet)	TIME (min)	% O_2	h/exp	#exp/#subj	(%/min)	(%/min)
30,000	60	100	8	38/30	87/ 86	82/ 65
27,500	60	100	8	83/33	80/142	67/ 96
25,000	60	100	8	28/27	79/144	89/ 90
22,500	60	100	8	46/19	54/188	59/127
16,500	0	50	6	94/32	0/---	53/107
16,000	0	50	6	25/25	0/---	48/113
15,000	0	50	6	20/20	5/261	25/118
14,500	0	50	6	10/10	0/---	30/178
13,000	0	50	6	23/22	9/173	35/ 86
11,500	0	50	6	6/ 6	0/---	17/112
10,250	0	50	6	9/ 9	0/---	22/242
9,000	0	50	6	2/ 2	0/---	0/---

Table 1. Incidence and latency data for male subjects exposed to various altitudes (from the Armstrong Laboratory DCS Database (46)).

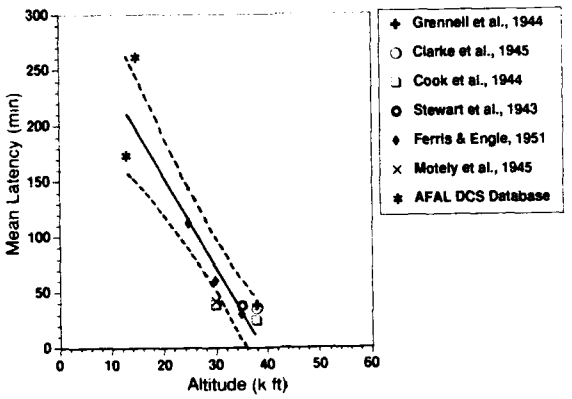

Figure 3. Mean DCS latency vs. exposure altitude (k represents 1,000 feet) with no denitrogenation. (Linear regression line with upper and lower bounds of 95% confidence interval has been superimposed over the data points.)

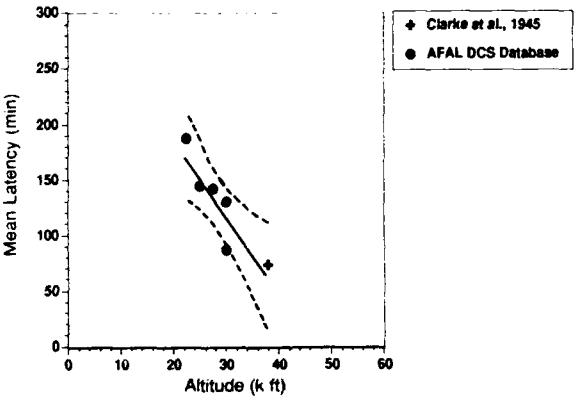

Figure 4. Mean DCS latency vs. exposure altitude (k represents 1,000 feet) with one hour of denitrogenation. (Linear regression line with upper and lower bounds of 95% confidence interval has been superimposed over the data points.)

latency are extended above 40,000 feet, it can be concluded that the time to onset of symptoms becomes "very short", probably shorter than was previously believed. Therefore, if the linearity in Figures 3 and 4 holds, there may be a significant DCS hazard in high altitude "get-me-down" scenarios even with very short exposure times. Studies using Echo/Doppler Imaging Systems are planned at the Armstrong Laboratory on chamber flights above 40,000 feet in an attempt to verify this theory.

2.3 Inflight Denitrogenation

It was recognized in the 1940's that denitrogenation at altitude, if as effective as at ground level, would have operational advantages. Aircrews could take off sooner and "prebreathe" enroute. It was found that for exposures between 35,000 and 40,000 feet, prebreathing at altitudes up to 20,000 feet decreased the DCS incidence rate significantly from exposures with no prebreathing (13, 15, 18, 26). The effectiveness was found to be equal to or slightly less than with prebreathing at ground level. Prebreathing above 20,000 feet was much less effective, if at all.

A recently completed study at the Armstrong Laboratory has confirmed this concept of "inflight" denitrogenation (35). This study followed flight profiles similar to those used in USAF high altitude reconnaissance operations. Each subject had a one-hour or two-hour prebreathe period at varying altitudes ranging from ground level to 16,000 feet, followed by a 4 hour exposure to 29,500 feet. It showed that there was no significant difference in either bubble or bends incidence between ground level prebreathing and prebreathing at 8,000, 12,000, or 16,000 feet of altitude. In fact, there appears to be a trend toward a reduction in DCS when prebreathing is done at 16,000 feet. The study also confirmed the value of longer prebreathe times at ground level. For example, the mean

DCS incidence with one hour of prebreathe was 75%, while with two hours it was 44%. The mean DCS latency was 130 min and 184 min respectively. These data indicate that operational situations which require high cabin altitudes and unexpected takeoffs, and that have 100% oxygen capability, will have similar or improved DCS risk by denitrogenating enroute as long as the cabin altitude is maintained below 16,000 feet.

2.4 Example Scenario

The application of this information can be illustrated by an example scenario of a hypothetical future fighter aircraft not using inflight denitrogenation equipment. Assumptions include the use of a current USAF oxygen system and regulator and the standard 5 psi differential cockpit pressurization schedule. There is no ground level prebreathing capability due to response time. During most of the climb to altitude the pilot is breathing 50% O_2. When the aircraft levels off at 60,000 feet, the cabin is at approximately 24,000 feet and the breathing gas is now 80% O_2. This altitude is maintained for 1 hour. Bubbles are now growing, but are "small". The closest corresponding exposure in the Armstrong Laboratory DCS database is a 25,000 feet exposure with 1 hour prebreathing. Table 1 shows a DCS incidence of 79% (8 hour exposure) with a mean onset time of 144 minutes. The detectable bubble incidence is 89% with a mean onset time of 90 minutes. Because there is no prebreathing and the breathing gas is less than 100% O2 during flight, these incidences and onset times will be substantially worse. If this exposure was one hour or less and the aircraft returned to ground level or lower altitudes without any complications, the pilot would have a minimal DCS risk. However, suppose there is an RD to 60,000 feet. Because the stay at 24,000 feet has precipitated the growth of "small" bubbles. Boyle's Law and the rapid growth phase take effect and the result is "lots of big bubbles." The time of exposure at 60,000 feet becomes extremely critical. Assuming consciousness is maintained with positive pressure breathing, and the pilot responds rapidly with a return to lower altitude and then lands, DCS risk is probably minimal. But, if the pilot must stay at a relatively high altitude, such as 40,000 feet, for a period of time before descending, whatever "grace" period might have existed for onset of DCS at 60,000 feet is now gone. The quantity and size of bubbles have grown rapidly, and the potential for severe and debilitating DCS is very high. The risk may be so high that this pilot may not survive.

Severe DCS risk could be greatly reduced by breathing 100% O_2 from takeoff to landing. If the pilot can maintain a cabin altitude of 16,000 feet (approximately 33,000 feet aircraft altitude) or less for the first hour of his mission, DCS risk is greatly reduced. The potential problem of O_2 and acceleration atelectasis that originally led to the use of low O_2 levels in breathing systems at lower altitudes may be tolerable for this situation. Since this pilot will have positive pressure breathing, it is likely that the acceleration atelectasis problems will be greatly reduced, and the impact of breathing 100% O_2 will be minimal. Thus, inflight denitrogenation with 100% O_2 must be considered as an option for reducing DCS risk for future high altitude fighter aircraft.

3. Ebullism

If the aircraft in the above scenario was flying at altitudes higher than 63,000 feet and had an RD, an additional physiological hazard known as ebullism would occur in the unprotected or partially protected individual. Ebullism is the spontaneous boiling and degassing of body fluids and tissues as well as evaporative cooling and loss of body water, heat, and other materials (4). Conditions necessary for ebullism are present when the body is exposed to pressures below about 47 mmHg (63,000 feet or 0.91 psi) for a human with a core temperature of 37 °C. This altitude is referred to as the Armstrong Line (49). However, due to variations of pressures and temperatures in the body, it is perhaps better to think of this limit as a band of altitude rather than a line. Ebullism in exposed human tissue may begin as low as 55,000 feet (39). Table 2 relates vapor pressure with altitude and temperature.

TEMPERATURE		VAPOR PRESSURE	EQUIVALENT ALTITUDE
Deg C	Deg F	mmHg	Feet
100	212	760.0	Sea Level
90	194	525.8	10,000
80	176	355.1	19,500
70	158	233.7	29,000
60	140	149.4	39,000
50	122	92.5	49,000
40	104	55.3	59,000
37	**98.6**	**47.0**	**63,000**
30	86	31.8	71,000
20	68	17.5	84,000
10	50	9.2	97,000

Table 2. Altitudes at which the ambient pressure is equivalent to the vapor pressure of water for different temperatures (39).

3.1 Physiological Consequences of Ebullism

When the vapor pressure of a tissue is reached, liquid changes to its gaseous state and gas cavities are formed in the tissue. Due to slight pressure and temperature differences among various tissues, the extent of these gas pockets will vary. Likewise, when recompression occurs, the gas pockets will spontaneously collapse into the fluid phase.

The pathophysiology of ebullism in animals was extensively studied in the 1950's and 1960's (5, 7, 11, 17, 23, 38). The animals in these studies were exposed to altitudes above 70,000 feet without protective equipment. Table 3 lists many of the effects of such exposures, some of which will be prevented by the addition of positive pressure breathing.

Severe tissue hypoxia immediately on decompression
Body volume doubles in 5-10 secs
Vomiting/defecation/urination in 5-10 secs
Unconsciousness/collapse in 9-12 seconds
Loss of voluntary control in 10 secs
Freezing of secretions (e.g. urine, salvia) by evaporation
Body temperature lowered by evaporation
Rapid increase in venous pressure
Circulatory arrest in seconds
Tonic and clonic seizures in 10-30 seconds
Apnea and spastic rigidity within 30 seconds
Total flaccid paralysis around 30 seconds

Table 3. Some observed effects of ebullism in animals.

In the cardiovascular system, the sequence of events is as follows. Ebullism bubbles form first in the low pressure areas of the vascular tree when ambient pressure decreases. Bubble formation increases the pressure in the venous and pulmonary system, reverses the normal cardiovascular pressure gradient and circulation ceases (22, 50). These changes normally resolve upon recompression. Water vapor bubbles move back into solution, pressures fall, and circulatory integrity is re-established to some degree as long as asystole has not occurred. However, microvasculature damage does not resolve and thus hinders recovery of peripheral and cerebral tissues. Still, survival is possible. Animals survive after exposure to hard vacuum from 90 to 210 seconds (5, 17, 23, 38). The significant factors influencing immediate survival are re-establishment of circulatory integrity and the degree of pulmonary and cerebral damage.

The degree of damage to the lungs is critical to survival. Autopsies of animals exposed to vacuum universally show massive pulmonary damage which can range from petechiae to severe atelectasis to frank hemorrhage (11). Unless pulmonary exchange can be re-established, survival is not possible. If pulmonary exchange is possible, cerebral resuscitation may be successful depending on the exposure time.

Of specific concern are the eyes (39). Unprotected exposure of the head may result in drying and freezing of corneal surfaces and lacrimal fluid. Cooke (9) noted ocular cloudiness in dogs after recompression from low pressure environments. He believed this was due to water being forced into the inner corneal surface after extreme evaporation of the outer corneal surface. He also noted retinal blanching and venous congestion that appeared to be more marked with air breathing. These changes resolved within 7 to 10 minutes, with a questionable visual field deficit noted afterwards. Whether these changes are of long term significance is not known. While boiling of the intraocular fluid is unlikely until higher elevations and longer exposures are encountered, surface eye freezing may impair vision. However, during short exposures to extreme altitudes, major tissue damage is unlikely. Little is known about this aspect of ebullism, and research is indicated.

Finally, decompression sickness (DCS) must be added to these concerns. DCS and ebullism may be additive. Nitrogen bubbles almost certainly exist in the tissues as ascent passes the Armstrong Line and may be predisposing to ebullism. Studies by Bancroft showed a better survival with a denitrogenation period prior to exposure, indicating that DCS may play an important role in survival of ebullism (3, 5).

3.2 Human Exposures

Humans have been exposed accidentally to hard vacuum. There is one published case report in the literature of a prolonged unprotected exposure (24). In addition, several anecdotal reports of human exposures to vacuum exist. In these cases, people survived with limited or, in one case, no protection. During such unprotected exposures, the subjects lost consciousness rapidly and had varying degrees of injury, ranging from no significant symptoms to massive cerebral and pulmonary injury requiring intensive medical intervention. In the cases of partial protection (19), subjects described swelling and pain in exposed limbs. Whether these changes were severe enough to prevent a pilot from manipulating flight controls, or controlling the aircraft, is unknown. In one videotaped case (25), a subject was testing a space suit, lost suit pressure, and was instantaneously exposed to an altitude of 120,000 feet . He remembers the saliva boiling on his tongue prior to passing out, and then recalls the chamber monitor calling 14,000 feet as the chamber was being recompressed. He suffered no complications from this incident and was not hospitalized afterwards . The one published case history involved an individual who was exposed to approximately 74,000 for 3 to 5 minutes in an industrial accident (24). He was aggressively treated with hyperbaric oxygen and full ICU support. Neurological

tests one year after the incident were above baseline levels. The authors did report the need to intubate the patient to avoid respiratory compromise due to frank pulmonary bleeding.

Vapothorax adds another complication to this multifaceted picture. Vapothorax occurs when the terminal pressures in the respiratory tree are lower than the vapor pressure of the body. A positive intrapleural pressure results with subsequent collapse of the lungs (7, 22). Increases in intrapleural pressures cause pleural tears and may lead to CAGE by allowing large amounts of air to enter directly into the pulmonary tree. Upon recompression the lungs again expand, but the pulmonary damage interferes with oxygen exchange and may lead to hypoxia.

Cerebral anoxia/hypoxia results from a combination of the above. Since cerebral tissues tolerate low O_2 tensions poorly, cerebral oxygen supplies must be re-established to avoid long term neurologic sequelae. In addition, cerebral tissue itself can undergo mechanical disruption by bubble formation Despite these potential problems, most animal research reports show good recovery of neurologic function after as much as 2.5-3.5 minutes of exposure (23, 38) The industrial accident patient had decerebrate posturing and coma after his exposure; however, all neurologic measurements were returned to baseline levels within one year.

3.3 Protective Measures

Human exposure to very low pressure can occur in one of three environments: 1) space, 2) high altitude aviation, and 3) altitude chamber operations. Any manned operations above 63,000 feet carries an inherent risk of ebullism. Obviously, this life-threatening hazard exists in all space operations. In particular, EVA operations provide the greatest potential for this hazard. It has been estimated that the assembly of Space Station Freedom will require approximately 1600 crew member hours of EVA time (21). That number will probably decrease with the resizing of the Station, but it will still be high compared to past experience. In addition, the annual maintenance of the Station will require many additional exposures. Furthermore, with every year there are more and more man-made objects in orbit, increasing the risk of collision. In addition to collision with micro meteoroids and space debris, accidental suit punctures and tears may occur during the assembly and maintenance of the Station. For space activity beyond Station new protective measures and medical treatment protocols for ebullism will be even more important since emergency return to earth will not be possible.

Future fighter aircraft will routinely fly at or above 63,000 feet. At present, crew protection against ebullism consists of cabin pressurization and full coverage pressure suits. For example, in the U-2/TR-1 reconnaissance aircraft, a full pressure suit is normally worn deflated. If there is an accidental loss of pressure, the suit automatically inflates. Full coverage suits, however, severely limit mobility. In an effort to protect the pilot from both high altitude exposure and high acceleration, yet retain mobility, integrated partial pressure/G-suits are now being tested. The disadvantage of these suits is that no protection is provided to the head or upper extremities, resulting in the potential for severe injury in the event of rapid decompression.

Recent efforts to develop a limited coverage partial pressure assembly for high altitude protection have centered around the use of a high pressure oronasal mask, torso vest, and anti-G suit arrangement similar to that evolved by the RAF in the early 1950's. Several such systems have been developed and are now being considered for short term protection at altitudes of 70,000 feet and above. A few laboratory studies have been conducted using limited coverage garments at altitudes between 65,000 feet and 80,000 feet. Notably, in the late 1970's, the Canadians successfully conducted studies to 80,000 feet in their laboratories using a limited coverage partial pressure system (20). Since most human exposures to altitudes above 63,000 feet have entailed the use of pressure suits with nearly full coverage of the head and extremities, much of our current understanding of ebullism involves speculation based on findings from earlier animal studies and the few human studies with eyes and/or extremities unpressurized or unprotected.

Although these systems have been designed to provide short term protection against several physiological hazards following decompression to high altitude, hypoxia is generally considered the most immediate concern due to the reduction in the partial pressure of oxygen in the gas delivered to the lung. Vaporization of tissue fluids in the exposed areas of the body at the more extreme altitudes has had little attention.

It was noted above that as ebullism progresses, body size can double, depending on the species. Webb and Annis (1,45) tested the concept of containing the body with elastic garments combined with positive pressure breathing and thoracic bladder counterpressure. Although several problems were evident, they were able to successfully demonstrate the concept in man to altitudes of 80,000 feet. Research on this approach to protect against ebullism has not been pursued since the late 1960's.

3.5 Medical Treatment of Ebullism

There is no medical treatment protocol for ebullism, probably because it is generally accepted that exposure to a vacuum is not survivable. That opinion is based, at least in part, on the results of the 1960's animal research. In addition, operational constraints dictated a fatalistic view. Survival was simply not considered possible. That view changed in 1982 when the industrial accident case history (24) was published describing the successful use of hyperbaric oxygen therapy. The ultimate objective of any medical treatment for ebullism is rapidly to reverse CNS anoxia requiring the following: 1) establishment of effective gas exchange in the lung, 2) restoration of circulation and reoxygenation of tissues, 3) resolution of gas bubbles, and 4) reversal of cerebral edema (41).

The immediate objective is to re-establish pulmonary exchange. No research data are available. However, the use of PEEP and High Frequency Ventilation have been suggested for combating the massive atelectasis. Unless the lung is viable, death will result from cerebral anoxia. The other 3 objectives would appear to be best met by the use of hyperbaric oxygen therapy (HBO). The rationale for use of HBO for decompression accidents includes 1) bubble size reduction, 2) hyperbaric oxygenation of hypoxic tissues, 3) bubble resolution, and 4) reduction of neurological edema (34).

Exposure to near vacuum can lead to the development of at least three other conditions known to respond to HBO therapy: DCS, hypoxia, and CAGE. HBO increases oxygen tensions in the body and may help in the post-anoxic conditions, especially if the vascular tree has been disrupted. While bubbles occurring from exposure to low ambient pressures will resolve when pressures are returned to normal, the secondary effects do not resolve immediately. Logically, HBO should be included in any ebullism treatment protocol. The efficacy of HBO on animals exposed to ebullism is currently being investigated at the Armstrong Laboratory.

4. Conclusions

As altitude increases the incidence of DCS increases. Cabin altitudes in future high altitude aircraft may reach levels known to have significant DCS risk. If an RD occurs, DCS risk may become critical. The rate of bubble growth and the resulting bubble size determine the latency and development of DCS symptoms. When plots of DCS from below 40,000 feet are extended to higher altitudes, DCS onset time appears to go to zero and risk of DCS rapidly increases between 40,000 and 50,000 feet. Recent data indicate that there is no significant difference in either bubble or bends incidence between ground level prebreathing and prebreathing at altitudes up to 16,000 feet. The occurrence of DCS symptoms actually decreased with increasing prebreathe altitude. The study also confirmed the value of longer prebreathe times at ground level. The risk of DCS would be greatly reduced if future high altitude aircraft utilized a 100% oxygen system for aircrews from takeoff to landing.

Human exposure to very low pressure environments can occur in space, high altitude aviation, and hypobaric chamber operations. Exposure of unprotected or partially protected humans to altitudes above 63,000 feet results in tissue fluid vaporization, increase in body size, rapid loss of consciousness, cardiac "vapor lock", and, if not recompressed, death. This condition is called ebullism. Special emphasis should be placed on effects of ebullism on the eye and the potential for increased risk of decompression sickness.

Two documented cases of humans accidentally exposed to near vacuum indicate that survival is possible. One was aggressively treated with hyperbaric oxygen and made a complete recovery. The second patient had minimal injuries from the exposure and did not require treatment. The objective of any medical treatment for ebullism is rapidly to reverse CNS anoxia. Survival can undoubtedly be improved with a better understanding of the pathophysiology of ebullism, improved protective measures, and the development of specific medical protocols.

5. Acknowledgements

The authors gratefully acknowledge Captain Terrell E Scoggins USAF, and James T Webb PhD for their assistance in manuscript preparation, and Joseph R Fischer M.S. for statistical support.

6. References

1. Annis JF, Webb P. Development of a space activity suit. NASA Contractor Report CR-1892. Washington D.C. 1971;138pp.

2. Baas CL, Olson RM, Dixon GA. Audio and visual ultrasonic monitoring of altitude decompression. 1988 (Abstract) 26th SAFE Symposium, Las Vegas.

3. Bancroft RW. Comments and review of decompression hazards in manned orbiting systems. Orbital International Laboratory and Space Sciences Conference, Cloudcraft, New Mexico ;223-229.

4. Bancroft RW, Cooke JP, Cain SM. Comparison of anoxia with and without ebullism. J. Applied Physiol., 1968;25:230-237.

5. Bancroft RW, Dunn JE. Experimental animal decompression to a near vacuum environment. Aerospace Med., 1965;36:720-725.

6. Clarke RW, Humm FD, Nims LF. The efficacy of preflight denitrogenation in the prevention of decompression sickness. Comm. Aviat. Med. Report #472. 1945;12pp.

7. Cole CR, Chamberlain DM, Burch BH, Kemph JP, Hitchcock FA. Pathological effects of explosive decompression to 30 mmHg, J. of Applied Physiol., 1953;6:96-104.

8. Cook SF, Williams OL, Lyons WR, Lawrence JH. A comparison of altitude and exercise with respect to decompression sickness. US NRC CAM Report No. 245, 26 Jan. 1944.

9. Cooke JP. Intraocular pressure and retinal responses of dogs at 45,000 and 80,000 feet. Aerospace Med., 1970;41:283-289.

10. Dixon GA, Adams JD, Harvey WT. Decompression sickness and intravenous bubble formation using a 7.8 psia simulated pressure-suit environment. Aviat. Space Environ. Med., 1986;57:223-228.

11. Edelmann A, Whitehorn WV, Lein A, Hitchcock FA. Pathological lesions produced by explosive decompression. WADC-TR-51-191.

12. Ferris EB, Engel GL. The clinical nature of high altitude decompression sickness. In: Fulton, JF (Ed.) Decompression Sickness. WB Saunders, Philadelphia. 1951; Chap. 2.

13. Fraser AM. The effect of stepwise ascent on the incidence of decompression sickness. C-2436 Assoc. Comm. on Avia. Med. Res., NRC Canada. 1943.

14. Fryer DI. Subatmospheric decompression sickness in man, North Atlantic Treaty Organization. NATO AGARDograph #125, 1969.

15. Gray JS. The effect of denitrogenation at various altitudes on aeroembolism in cadets. U.S Army Air Force School of Aviat. Med. Report: Project #216. 1944.

16. Grenell R, Humm FD, Nims LF, Somberg HM. The reliability of the decompression subcommittee's 90 minute preselection test. US NRC, CAM Report No. 355, 5 Sept. 1944;4pp.

17. Hall WM, Cory EL. Anoxia in explosive decompression injury. Amer. J. of Physiol., 1950;160:361-365.

18. Henry FM. Aviators "bends" pain as influenced by altitude and in-flight denitrogenation. WADC Technical Report #53-227, 1953.

19. Henry JP, Greeley, PO, Meehan, JP, Drury, DR. A case of sudden swelling of the hands occurring at 58,000 ft simulated altitude. Aeromedical Labs. Univ. of So. Calif., Los Angeles, CA. OSRD Contract: OEM CMR-288, Report #393, 1 Dec. 1944.

20. Holness DE, Porlier JAG, Ackles KN, Wright GR. Respiratory gas exchange during positive pressure breathing and rapid decompression to simulated altitudes of 18.3 and 24.4 km. Aviat. Space Environ. Med., 1980;51:454-458.

21. Horrigan DJ. Shuttle and space station eva. In: Pilmanis AA (ed.), The proceedings of the 1990 hypobaric decompression sickness workshop. USAF Armstrong Laboratory Special Report., 1991 (in preparation).

22. Kemph JP, Hitchcock FA. Cardiovascular effects of high intrapulmonic pressure at ground level and at a simulated altitude of 72,000 ft (30 mmHg), WADC-TR-53-191, Wright Air Development Center *Dayton, OH 1953.*

23. Koestler AG, Reynolds HH. Rapid decompression of chimpanzees to a near vacuum. J. Applied Physiol., 1968;25:153-158.

24. Kolesari GL, Kindwall EP. Survival following accidental decompression to an altitude greater than 74,000 feet, (22,555 m). Aviat. Space Environ. Med., Dec., 1982;53(12):1211-1214.

25. LeBlanc JC. Personal communication. 1990.

26. Marbarger JP, Kadetz W, Paltarokas J, Variakojis D, Hansen J, Dickinson J. Gaseous nitrogen elimination at ground level and simulated altitude and the occurrence of decompression sickness. USAFSAM Report #55-73. 1956.

27. Meader WL. Decompression sickness in high altitude flight. Aerospace Med., 1967;38:301-3.

28. Motely H, Chinn HI, Odell FA. Studies on bends. Aviat. Med., 1945; 16:210-34.

29. Neubauer JC, Dixon JP, Herndon CM. Fatal pulmonary decompression sickness: a case report. Aviat Space Environ. Med., 1988;59:1181-4.

30. Olson RM, Krutz RW Jr. Significance of delayed symptom onset and bubble growth in altitude decompression sickness. Aviat. Space Environ. Med., 1991,62:296-9.

31. Olson RM, Krutz RW Jr. Latent period of symptoms in decompression sickness. (Abstract) Aviat. Space Environ. Med., 1991;61:A8(#45).

32. Olson RM, Krutz RW Jr, Dixon GA, Smead KW. An evaluation of precordial ultrasonic monitoring to avoid bends at altitude. Aviat. Space Environ. Med., 1988;59:635-9.

33. Pilmanis AA (ed.). The proceedings of the 1990 hypobaric decompression sickness workshop. USAF Armstrong Laboratory Special Report. 1991 (in preparation).

34. Pilmanis AA. Hyperbaric oxygen therapy for decompression accidents - potential applications to space station operations. Proceedings of the 16th ICES Conference, San Diego, CA. 1986.

35. Pilmanis AA, Olson RM. The effect of inflight denitrogenation on altitude decompression sickness. (Abstract) Aviat. Space Environ. Med., 1991;61:A8(#46).

36. Pilmanis AA, Scoggins TE, Melkonian A. *Altitude decompression computer development.* In Pilmanis, AA (ed.), The proceedings of the 1990 hypobaric decompression sickness workshop. USAF Armstrong Laboratory Special Report. 1991 (in preparation).

37. Powell MR. Silent bubbles: the asymptomatic gas phase. In: Pilmanis AA (ed.), The proceedings of the 1990 hypobaric decompression sickness workshop. USAF Armstrong Laboratory Special Report. 1991 (in preparation).

38. Rumbaugh D. Learning ability of the squirrel monkey after exposure to a near vacuum. Aviat. Med. 1965;36(1):8-12.

39. Sears WJ. Vaporization of tissue fluids at extreme altitudes - a review. (Abstract) SAFE Symposium, San Antonio, TX. 1989.

40. Sherman RE. High altitude reconnaissance decompression sickness: Strategic Air Command *experience.* In: Pilmanis AA (ed.), The proceedings of the 1990 hypobaric decompression sickness workshop. USAF Armstrong Laboratory Special Report. 1991 (in preparation).

41. Stegmann BJ. Considerations for the survival of ebullism. M.S. Thesis, Wright State Univ. 1989.

42. Stewart CB, Warwick CH, Thompson JW, Bateman GL, Milne DJ, Gray DE. A study on decompression sickness: observations on 6,566 men during 16,293 exposures to a simulated altitude of 35,000 ft Assoc. Comm. Aviat. Med. Rpt. [illegible]-2683, 1943;64pp.

43. Sweeney HM. Explosive decompression. Air Surg. Bull. 1944;1(10):1-4.

44. Vann RD, Gerth WA. Physiology of decompression sickness. In: Pilmanis AA (ed.), The proceedings of the 1990 hypobaric decompression sickness workshop. USAF Armstrong Laboratory Special Report. 1991 (in preparation).

45. Webb P. The space activity suit: an elastic leotard for extravehicular activity. Aerospace Med. 1968;39:376-383.

46. Webb JT, Krutz RW Jr, Dixon GA. An annotated bibliography of hypobaric decompression research conducted at the Crew Technology Division, USAF School of Aerospace Medicine, Brooks AFB, Texas from 1983 to 1988. USAFSAM Technical Paper 88-10R. 1990;22pp.

47. Webb JT, Olson RM, Pilmanis AA. Bubbles are not acceptable endpoints in hypobaric decompression sickness research. (in preparation).

48. Webb, JT, Pilmanis, AA. Resolution of high bubble grades at altitude. (Abstract) Aviat. Space Environ. Med., *1991;61:A37(#219).*

49. Wilson, CL. Production of gas in human tissues at low pressures. AF-SAM-61-105, 1961. USAF SAM, Brooks AFB, TX.

50. Whitehorn WV, Lein A, Hitchcock FA, The effect of explosive decompression on the occurrence of intravascular bubbles, WADC-TR-53-191, Wright Air Development Center, Dayton OH, 1953.

51. Wolf CW, Petzel DH, Seidl G, Burghuber OC. A case of decompression sickness in a commercial pilot. Aviat. Space Environ. Med., 1989;59:990-3.

BUBBLE NUCLEATION THRESHOLD IN DECOMPLEMENTED PLASMA

C. A. Ward
D. Yee
D. McCullough
W. D. Fraser*

Department of Mechanical Engineering,
Institute of Biomedical Engineering
University of Toronto
5 King's College Road
Toronto, Canada M5S 1A4
*Defence and Civil Institute of Environmental Medicine
1133 Sheppard Avenue West
North York, Canada M3M 3B9

SUMMARY

Previous work has indicated that rabbits that are more susceptible to decompression sickness (DCS) are also more sensitive to complement activation by air bubbles, and further that rabbits can be protected from DCS if they are pharmacologically decomplemented before they are subjected to the pressure profile. We have investigated a possible means by which decomplementing a rabbit could protect it from DCS. Since DCS is thought to be produced by bubbles that are formed in the tissues of an animal because of its tissues becoming oversaturated with dissolved gas as the animal undergoes a pressure profile, we have investigated the possibility that decomplementing an animal protects it from DCS by making it more difficult to form bubbles in one of the tissues of primary concern, blood plasma. This investigation was performed with three test liquids: 1) water, 2) native rabbit plasma, and 3) decomplemented rabbit plasma. We find that the threshold for bubble nucleation in water is greater than that in either plasma or decomplemented plasma, but we do not find any difference between the nucleation threshold of the two types of plasma. Thus the indications are that the protection from DCS that results from decomplementing a rabbit does not appear to develop because of a change in the nucleation threshold of the decomplemented plasma.

1. INTRODUCTION

Previous work [1] has indicated that rabbits that have native complement systems that are insensitive to activation are less susceptible to decompression sickness. The method that was used to establish this observation was to collect a blood sample from each of 12 rabbits, then separate the plasma from each blood sample and store the plasma sample for later determination of the sensitivity of the rabbit to complement activation at the time the blood sample was taken. After the blood sample had been collected, each rabbit was placed in a an apparatus that served as both a pressure chamber and a treadmill. This allowed the rabbit to be subjected to a pressure profile that was severe enough to produce DCS in some rabbits. After completing the pressure profile, the rabbit was returned to its cage and allowed to rest for at least three days before another blood sample was taken to determine its sensitivity to complement activation at that time. The results showed that those rabbits that were susceptible to DCS were also more sensitive to complement activation.

It was also found that a rabbit that was susceptible to DCS could be made immune to DCS on the same pressure profile by pharmacologically decomplementing it [1]. To see that decomplementing a rabbit *in-vivo* changed its susceptibility to DCS, a second group of rabbits was examined. First, each rabbit of this group was subjected to two consecutive pressure profiles that were at least five days apart. The rabbits that were found to be susceptible to DCS on both of these pressure profiles were taken to be susceptible to DCS. After at least seven day of recovery from these last of these pressure profiles, each were given an injection on the next three days of an agent that is known to reduce strongly the complement components C5a and C3a *in-vivo*. Before each injection of the decomplementing agent, blood samples were taken from each rabbit, the plasma separated and stored for later examination. Approximately 24 hours after the last injection, a blood sample was taken and each rabbit was subjected to the same pressure profile for the third time. None of the decomplemented rabbits showed any symptoms of DCS on this occasion.

The rabbits were then allowed to recover for three days. This period is sufficient for the

complement system of the rabbits to return to its normal sensitivity. A sample of plasma was then collected from each rabbit and the rabbit was subjected to the pressure profile for a fourth time. On this occasion, each rabbit again showed symptoms of DCS!

After again allowing the rabbit to recover for more than three days, a blood sample was taken, plasma was collected and an aggregation test was used to examine the complement activation sensitivity. The measured complement activation sensitivities obtained from the plasma samples when the rabbits experienced DCS were about twice that obtained from the plasma samples when the rabbits were decomplemented and did not show any symptoms of DCS.

The results clearly indicate that decomplementing the rabbits protects them from decompression sickness on certain pressure profiles. Our objective in this study was to investigate possible explanations for these observations. One possibility is that the decomplementing process changes one or more physical properties of a rabbit's plasma, such as its gas solubility and/or its surface tension, and as a result, it is more difficult to form bubbles within the circulatory system of the rabbit and thereby the rabbit becomes less susceptible to DCS. A second possibility is that the cause of DCS is the complement fragments that are produced when the complement system is activated by the air bubbles. These fragments are known to initiate a number of other effects on cell membranes and to produce cellular aggregation [2, 3]. If these complement fragments are the source of DCS, then decomplementing a rabbit before it is subjected to a pressure profile would prevent DCS. As a hypothesis, we suppose that the first of these alternatives is valid, and we test this hypothesis by comparing the nucleation characteristics of native plasma with that of decomplemented plasma.

2. EXPERIMENTAL PROCEDURES

2.1 Experimental Animals

The animals used in this study were New Zealand white rabbits that weighed 2 to 2.5 *kg*. Each was held in the animal care facility for approximately one week before they entered the study. During this period they were dewormed, vaccinated against and maintained on medicated food (50 *mg/kg* Robendine Hydrochloride and 22 *mls* Amprol per 10 litres water).

2.1.1 Control Rabbits

After each of the six rabbits in this group had been maintained in the animal care facility for a period of one week, they were ready to enter the study. A blood sample was then collected from each of these rabbits. Thus when their blood sample was collected, their complement system was fully intact.

2.1.2 Decomplemented Rabbits

Each of the four rabbits in this group entered the study after they had been in the animal care facility for at least one week. On each of three successive days each rabbit received an injection of 1.5 mls cobra venom factor *Naja n naja* (CVF_n, Dimension Labs, Toronto). On the following day, blood was collected in preparation for measuring the nucleation threshold.

2.1.3. Plasma Collection

Blood samples were collected from each of the rabbits so that their plasma could be later tested using the PMN leukocyte aggregation test. The blood samples were collected from each rabbit by placing it in a restraining cage so as to minimize the trauma. The rabbit's margin ear artery was cleaned with alcohol, a 21 gauge butterfly needle was then carefully placed within the artery, a syringe containing Heparin was then attached to the needle and blood was slowly and carefully withdrawn (10 IU Heparin/*ml* blood). Once the blood had been collected the syringe was capped and placed in an ice bath until it was ready to be centrifuged, while making sure that no air bubbles were introduced during the handling process.

The blood was centrifuged for 10 minutes at 1033 *g*. Afterwards it was transferred from the syringe into a 10 *ml* polypropylene tube and capped. The clear plasma was then carefully removed using a polypropylene Pasteur pipette, placed in another 10 *ml* polypropylene tube, capped and stored in a -80°C freezer for later examination.

2.2 Water Preparation

The water was prepared by deionizing and filtering distilled water using a (Gelman Sciences WATER-I™) water purifier to

produce a resistivity at least 18 Megohm. The surface tension of this water was measured to be 71.22 ± 0.18 *mJ/m* at 24.1 ± 0.1 °C.

2.3 Nucleation Threshold in Plasma, Decomplemented Plasma and Water

The nucleation characteristics of the plasma, decomplemented plasma and water were determined by measuring the nucleation temperature at different levels of gas supersaturation. A schematic of the experimental apparatus is shown in Fig. 1. Each liquid sample (control plasma, decomplemented plasma or water) was saturated with nitrogen at a particular pressure, ± 0.7 *kPa* sensitivity, and at constant temperature, ± 0.1°C sensitivity, in a saturation chamber. The liquid sample was saturated by stirring with a teflon coated magnetic stirring bar until the system reached steady state. After a liquid sample had been saturated, the stirring was halted and a liquid droplet was injected at the lower end of the column of host liquid. The droplets of the test liquids were created using a glass capillary connected to a fine metering valve and were of approximately 1 *mm* diameter. The host liquid was Benzyl Benzoate which is denser than any of the test liquids and is also immiscible with them. Thus once a droplet had been injected, it would rise in the column of host liquid.

The container for the host liquid was double walled. The host liquid filled both of these glass cylinders and was heated with a teflon covered nichrome heating wire wrapped around the outside of the inner wall at the section where the nucleation occurred. The temperature of the host liquid was adjusted by means of the nichrome wire connected to a Powerstat™. As the droplet rose it would experience an increasing temperature. The temperature of the host liquid was adjusted so that each drop would obtain a sufficiently large temperature to cause a bubble to nucleate within the rising droplet. The position at which the droplets nucleated was noted visually and the temperature at this section was measured using five thermocouples. Each thermocouple had a sensitivity of ± 0.1°C. After locating the point where the nucleation occurred, the nucleation temperature was measured by interpolation.

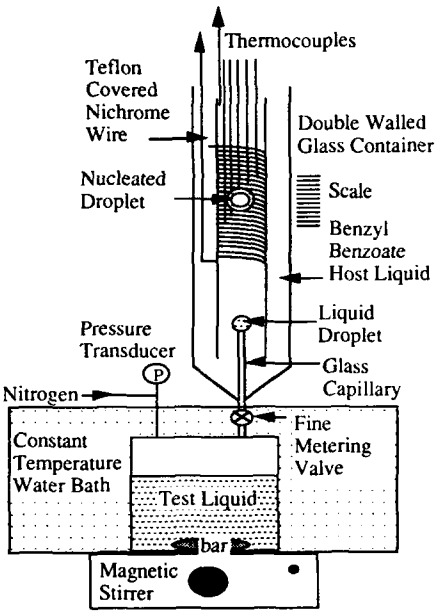

Fig. 1. Schematic of the apparatus to measure the nucleation temperature of decomplemented and control plasma and water.

3. Results and Conclusion

The measured temperature at which nucleation occurred in water and in native and decomplemented plasma has been plotted against the nitrogen gas saturation pressure. The results are shown in Fig. 2. At a particular saturation pressure, water was observed to have a higher nucleation temperature than that of native or decomplemented plasma. Thus, this experimental technique was able to distinguish between the nucleation threshold of water and of plasma.

At a particular saturation pressure, we also observed that the decomplemented plasma nucleated at apparently lower temperatures than that of the samples of control plasma. However the difference was not significant. Thus this experimental technique is not able to identify any significant difference between the nucleation threshold of native and decomplemented rabbit plasma.

If this conclusion is confirmed by other techniques, the indication would be that the reason decomplementation protects rabbit from DCS is not because of any change in the bubble nucleation characteristics of the decomplemented plasma as compared to that of native plasma. Thus the possibility that the complement fragments produced during the activation of the complement system by bubbles should be investigated at a possible explanation for the reason that decomplementation reduces the susceptibility of rabbits to DCS.

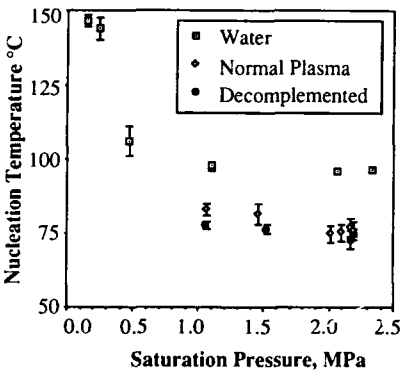

Fig. 2. Nucleation temperature of control and decomplemented plasma and water at different nitrogen saturation pressures.

4. REFERENCES

[1] C. A.Ward, D. McCullough, D. Yee, D. Stanga and W. D. Fraser, "Complement activation involvement in decompression sickness of rabbits", Undersea Biomed. 1990, **17**: 51-66.

[2] D. Bitter-Suermann, The Anaphylatoxins in: *The Complement System*, eds. K. Rother, G. O. Till, Springer Verlag, Berlin, (1987) p. 367.

[3] C. A. Ward, D. McCullough and W. D. Fraser, "Relation between complement activation and susceptibility to decompression sickness", J. Appl. Physiol. 1987, **62**: 1160-1166.

ACKNOWLEDGEMENT

This work was supported by the Defence and Civil Institute of Environmental Medicine, North York, Ontario.

1990 Hypobaric Decompression Sickness Workshop: Summary and Conclusions

Andrew A. Pilmanis Ph.D
High Altitude Protection Function
USAF Armstrong Laboratory/VNBD
Brooks AFB, Texas 78235

SUMMARY

Decompression sickness resulting from exposure to the hypobaric environment was reviewed and discussed at a three-day workshop hosted by the US Air Force Armstrong Laboratory in October 1990. This milestone meeting updated the current understanding of this condition. Gaps in this understanding were identified based on input from both research and operational participants. The results of this workshop are summarized in this paper

1. INTRODUCTION

Decompression sickness (DCS) is the clinical condition resulting from evolved inert gas bubbles in tissues caused by a reduction of environmental pressure. Originally described in 1670 by Robert Boyle, this disease can occur under both hyper- and hypobaric conditions such as diving, caisson work, aviation and space operations. Altitude DCS has been studied for over 50 years. During the last two decades, major advances in understanding decompression sickness have been made. The pathophysiology of DCS is still elusive, but has been clarified. Non-invasive bubble detection has provided a semi-objective means of studying DCS in humans. The physics and physiology of gas bubble formation and growth have been extensively studied. There is now more concern over long-term CNS damage. Modeling of DCS prediction and prevention has been extensively expanded with the advancements in computing capabilities.

An accurate accounting of operational DCS incidence in the USAF does not exist. The total reported number of DCS cases appears to be approximately 100 to 120 cases per year. The vast majority of these cases occur with altitude chamber training flights. However, there is a reluctance to report DCS because of career considerations. Large numbers of highly trained personnel are routinely exposed to altitudes that, in controlled chamber studies, produce high levels of bubbles and bends. Yet reports of DCS from the field are minimal to non-existent. Nevertheless, it is recognized that DCS continues to be an operational limitation in both aviation and space activities. It is expected that the crews of the next generation of military aircraft will be exposed to even higher altitudes than those of today.

In order to document the current understanding of altitude decompression sickness and ascertain the operational significance of this disease, a workshop was held at the USAF Armstrong Laboratory (AL) (formerly USAF School of Aerospace Medicine), Brooks AFB, Texas, on 16 to 18 October 1990. The meeting was sponsored by: (1) USAF AL, (2) NASA Johnson Space Center, and (3) AF Office of Scientific Research , and was attended by over 50 participants representing the Department of Defense (DOD), NASA, and university researchers. The objectives of the workshop included:

1. reviewing the current understanding of the pathophysiology of DCS,
2. evaluating existing and proposed options for DCS prediction,
3. defining the problems of decompression in space,
4. documenting the current incidence of DCS in aviation,
5. discussing the "acceptable risk" of altitude DCS, and
6. listing areas of needed DCS research.

The proceedings of this workshop are in preparation and are expected to be available in 1991 from the Armstrong Laboratory

2. PATHOPHYSIOLOGY OF DCS

The workshop was opened with a historical perspective of altitude decompression sickness. It was emphasized that although early researchers did excellent work with inadequate equipment, their results should not be ignored. There are specific differences between hypobaric and hyperbaric DCS, but the disease is basically the same in both environments and altitude DCS should be viewed as part of an overall condition resulting from changes in the atmospheric pressure continuum. DCS involves many pathophysiological processes occurring both in parallel and in series, and it follows dose-response characteristics rather than all-or-none thresholds.

The current conceptions on bubble physics and dynamics were reviewed. The concept of bubble nuclei is still unclear, but was defined as "a collection of gas molecules that remain together even without supersaturation." Viscous adhesion in the normal motion of joints can result in sufficient cavitation to cause a "vacuum phenomena", which, in turn, may contribute to DCS bubble precipitation. The DCS bubbles should be viewed as dynamic, rather than static. New bubbles are growing while old bubbles are shrinking. A video tape of in vivo bubbles in human subjects at altitude as recorded by the latest Echo Imaging technique was shown to the meeting. Clear bubble imaging in the right heart is now possible

The cardiopulmonary effects of bubbles are currently the focus of research because of the potentially severe consequences of such emboli. Most of the documented altitude DCS deaths are considered the result of severe cardiopulmonary bubbles. Pulmonary vascular resistance and right-sided pressures increase with an increasing load of gas bubbles, which can lead to circulatory collapse and death and can also theoretically cause right-to-left shunting of bubbles resulting in cerebral arterial gas embolism. However, some recent human altitude DCS research in the US Navy did not find evidence of right-to-left shunting in subjects with patent foramen ovale. The concern over the presence of patent foramen ovale in flyers and astronauts may have been exaggerated. More work is needed.

The 19 recorded altitude DCS deaths were reviewed. Except for one, all of these deaths occurred prior to the initiation of routine oxygen prebreathing and hyperbaric therapy. The one exception is a case history published in 1988, and was fatal despite hyperbaric therapy.

Of great concern in the diving field is the recent accumulation of data on chronic CNS pathology linked to diving. Diffuse spinal cord degeneration, often asymptomatic, has been well documented. Damage to the eyes and the brain has also been documented. Comparable studies in the altitude field have not been done. The treatment of altitude DCS with standard hyperbaric oxygen treatment tables is well established and highly successful. The origin of the extensive USAF Hyperbaric Medicine Program was historically linked to the need for altitude DCS therapy capability. The USAF has treated over 650 cases of altitude DCS with hyperbaric oxygen since 1977.

3. PREDICTION AND PREVENTION OF ALTITUDE DCS

Decompression modeling was reviewed. The overall objective of decompression tables or computers in the diving field is to prevent or reduce DCS injury. Today, the majority of divers wear decompression computers for real-time decompression guidance. Classic Haldanian diffusion/perfusion techniques used for diving tables are inadequate for altitude decompression risk assessment

For 50 years, guidelines for safe altitude exposures have been developed by costly time-consuming studies, each specific to a unique exposure scenario. The application of such studies to new operational requirements is very difficult, often requiring new studies or "best guess approximations". Therefore, the development of an altitude decompression computer is long overdue and is currently underway in the USAF. The primary problem facing such a development is the lack of a "standard" altitude decompression algorithm. The model being developed will include Haldanian theory, bubble dynamics, and the application of maximum likelihood statistics. This model will then be incorporated into appropriate hardware and will provide both real-time and predictive DCS risk assessment capability. Models must evolve empirically. Thus, both operational and research DCS databases are required for this development. It was repeatedly pointed out that the operational DCS incidence numbers may be grossly inaccurate due to aircrew and chamber operator reporting problems.

Denitrogenation or prebreathing is standard practice in both aviation and space operations for DCS risk reduction. Prebreathing has been most effective in the reduction of the serious DCS symptoms, less so with bends pain. Prebreathe times vary among operational situations and need more standardization. Hard data on the effect of interrupted prebreathe and on denitrogenation/renitrogenatior processes with repetitive prebreathe/altitude exposure cycles are lacking. Denitrogenation is enhanced by increased temperature, immersion, negative pressure breathing and supine posture. For example, immersion in 37°C water can accelerate denitrogenation by almost 50%. The inverse of these conditions tends to slow denitrogenation.

4. DECOMPRESSION IN SPACE

The second day of the Workshop began with a discussion of the problems of decompression in space. The history and current practice of NASA's extravehicular activity (EVA) decompression procedures were reviewed. The current Shuttle procedure uses a combination of oxygen prebreathing and 10.2 PSIA stage decompression based on an "R-value" (ratio of tissue PN2 over ambient pressure) of 1.65 and the 360 minute half-time tissue compartment. For these conditions, ground-based NASA and USAF research predict an incidence of 23% mild DCS symptoms, and 5-10% DCS symptoms severe enough to result in a mission abort. However, to date no reported DCS has occurred in the Shuttle program.

This apparent discrepancy may have two possible explanations. From the astronaut perspective, admitting to DCS symptoms is "not exactly a career-enhancing move". Second, weightlessness may improve denitrogenation and reduce DCS. Due to the very large number of projected EVA missions required to construct and maintain of Space Station Freedom, there is a NASA recommendation to change the "R-value" to 1.40 resulting in a more conservative decompression schedule. There is also support in the European Space Agency (ESA) for the 1.40 value. The ESA has proposed a 7.3 psia EVA suit.

Because of the potentially severe consequences of DCS in space, hyperbaric treatment capability has been designed into the Space Station. The design calls for a 2.8 ATA hyperbaric chamber. This facility would not be limited to DCS; it could also be used to treat air embolism and ebullism.

5. THE INCIDENCE OF ALTITUDE DCS

In the next session, a series of papers were presented documenting the DCS incidence and DCS reporting problems in the operational environment. Reports were presented on USAF operations including high altitude reconnaissance, high altitude parachuting, flight training in unpressurized aircraft, altitude chamber training operations, and Vietnam War high altitude operations. US Army flight and chamber operations, US Navy flight and chamber operations, RAF experience, and US civilian experience were also covered. The largest number of reported DCS cases occur in DOD altitude chamber training (approximately 120/year). The incidence, however, is small (1-3 cases/1000 exposures). In contrast, the Europeans reported essentially no DCS problems in their chamber training.

In USAF aircraft operations, 18 DCS cases were officially reported in 1989, more than double the number in previous years. Two possible explanations were postulated. A 1989 change in USAF Regulations permitting a waiver process for Type II DCS was thought to have encouraged more reporting. The 1988 published account of an altitude DCS fatality may also have contributed. However, it was emphasized repeatedly that the official reports represent a subset of the unknown true incidence. Despite the regulation change, there is a strong reluctance on the part of both chamber and flight personnel in the USAF to report DCS. There are multiple reasons for this reluctance, but the primary cause is career protection.

Perhaps the single most important conclusion of the workshop was that aviators must be allowed to report DCS with impunity. It was emphasized that DCS should be viewed as an occupational illness in the same way we view other physiological responses to environmental stress, such as hypoxia. Why should an aviator who responds to decompression in the expected manner be penalized? If the treatment is successful, why ground a healthy aviator?

6. THE CLINICAL MANIFESTATIONS OF DCS

The results of a recent workshop in England on the classification of DCS manifestations were reported and discussed. The current Type I/Type II classification is inconsistently defined and arbitrarily applied resulting in treatment variations and making multicenter trials and database comparison almost impossible. The workshop recommended a new classification scheme based on specific description of the disease. For example, a case might be described as "acute relapsing neurological decompression illness," or "acute spontaneously resolving cutaneous decompression illness." The proceedings of the workshop will be available in 1991 from the Undersea and Hyperbaric Medical Society.

It was also emphasized that thorough neurological exams are crucial to DCS diagnosis, classification and treatment. Concern was expressed that proper patient examination is too often ignored with cases of altitude DCS. Some of the problems with the inaccuracy of DCS databases can be traced to improper and inadequate patient examination. Since hyperbaric treatment procedures are defined by the specific diagnosis, doing a complete but expeditious baseline examination is mandatory. Since DCS is a very dynamic disease, following examinations during the course of therapy are also required. Specifics of DCS patient examination were reviewed

7. ACCEPTABLE RISK

A panel discussion followed on "acceptable risk" of altitude DCS. It was pointed out that a definition of acceptable risk varies with the mission and ultimately must be decided by the operational people responsible for that mission. It is the responsibility of the investigators to equip these field managers with the best available research information to enable them to make informed and rational decisions. In turn, the investigators must have access to accurate and complete feedback from the field in order to frame the research in proper perspective.

8. CONCLUSIONS

The 1990 Hypobaric Decompression Sickness Workshop provided a forum for a thorough review and in-depth discussion of the evolved gas problems associated with manned exposure to hypobaric environments. Altitude DCS is a potentially hazardous condition that is treated by oxygen prebreathing and hyperbaric therapy. DCS is a potential hazard in the space program, and will continue to affect EVA operations in future efforts. An altitude decompression model and an altitude decompression computer need to be developed to permit real-time and predictive DCS risk assessment. The reported incidence of altitude DCS is likely inaccurate due to potential career consequences associated with the reporting of DCS. Efforts toward reporting with impunity were recommended. The current classification of DCS manifestations was considered arbitrary and inaccurate. A new method of classification was recommended. The need for improvements in the examination of DCS patients was stressed. What level of DCS risk is acceptable varies and is defined by mission requirements. Such decision-making should be based on information provided by controlled laboratory research.

9. REFERENCES

1. Pilmanis, A.A. (Ed.), THE PROCEEDINGS OF THE 1990 HYPOBARIC DECOMPRESSION SICKNESS WORKSHOP. USAF Armstrong Laboratory Special Report. 1991 (in preparation).

Prebreathing as a Means to Decrease the Incidence of Decompression Sickness at Altitude

Barbara J. Stegmann, MD and Andrew A. Pilmanis, PhD

KRUG Life Sciences, San Antonio Texas 78279
and Armstrong Laboratory, Brooks AFB ,Texas 78235

SUMMARY

Prebreathing with 100% oxygen for protection against serious decompression sickness (DCS) is standard practice in the United States Air Force (USAF). Before prebreathing became routine, there were 18 reported deaths directly related to altitude DCS. Since prebreathing has been instituted, only one death has been reported. However, DCS cases still occur and are primarily associated with *training in altitude chambers.* At *the Armstrong Laboratory (AL), Brooks Air Force Base, Texas,* research on the use of prebreathing to enhance denitrogenation is directed at optimizing schedules for current operational requirements in both aviation and space. Concurrently, development of a decompression/denitrogenation computer is also underway. This analytical model is based on both *laboratory and operational databases, and will have both real-time and predictive capability.* However, the accuracy of these databases is in question. DCS reporting problems, inconsistencies in medical diagnoses, arbitrary classification of symptoms, historical variations in symptom definition, and the subjectiveness of intravascular bubble detection techniques must be taken into *account before reasonable reliability can be applied to this model*

1. INTRODUCTION

In the 1940's, investigators realized that aviators were being afflicted with an illness that was similar in many ways to a disease in divers known as dysbarism. If these two processes were truly related, then the pathology-producing event in both would be the formation of nitrogen bubbles in tissues. Once it was recognized that nitrogen bubbles were responsible for the disease, investigators began looking for a way to decrease nitrogen bubble formation at altitude. Unlike the diver, aviators can breathe oxygen both prior to and during the altitude exposure. This assists in the wash-out of nitrogen from body tissues. Behnke (2), postulated that if the aviator breathed pure oxygen, then the nitrogen stores in the body would decrease, and nitrogen bubble formation would correspondingly go down. In fact, if pure oxygen was breathed for a long enough time period, the nitrogen stores in the body would be completely depleted, and the risk of decompression sickness (DCS) would be eliminated (8). By the 1960's, prebreathing prior to high altitude flights became a standard practice, and the occurrence of severe altitude DCS symptoms diminished significantly.

However, the protection afforded by a prebreathe period is inconsistent (18). Prebreathing is known to decrease the occurrence of severe DCS symptoms, but may not significantly influence the appearance of mild DCS symptoms. Tissue denitrogenation is multi-dimensional and does not follow simple linear dynamics and this may account for some of the inconsistencies. The optimal time of prebreathe for different scenarios has not been established since the perfusion rates of various tissue beds vary from moment to moment. Work that had been done in the diving field may not correlate with altitude work because of differences in gas and bubble dynamics at altitude. These difficulties prompted the initiation of new studies on prebreathing. The goal of this paper is to outline the process of denitrogenation, review the old literature, and present new work being done to aid in the prediction of decompression sickness in the aviator.

1.1 Nitrogen Washout

Prebreathing is based on the nitrogen washout theory introduced by Behnke (2). When 100% oxygen is breathed continuously, a partial pressure gradient develops between the bloodstream and the lungs. Breathing nitrogen-free oxygen maximizes this gradient by drastically lowering the nitrogen content of the lungs, thus causing nitrogen to diffuse out of bloodstream. As the nitrogen content of the blood decreases, a second gradient is established, this time between the blood and the tissues. As the nitrogen-poor blood passes through a tissue with a high nitrogen content, nitrogen leaves the nitrogen-rich tissues and enters the bloodstream. The rate of elimination varies depending on the perfusion rate for each tissue type (7). By using this technique to decrease the

amount of nitrogen in the body prior to altitude exposure, Behnke (2) believed the risk of altitude induced nitrogen bubbles would be substantially reduced and the aviator would be protected against decompression sickness. Lundin (13) demonstrated that nitrogen elimination could be quantified by measuring the end-tidal air with a nitrogen meter during oxygen breathing. Various individuals have predicted nitrogen desaturation curves from these measurements (1, 2, 10, 13). These curves show that 95% +/- 2% of the total body stores of nitrogen are eliminated in the first four hours of prebreathe, and that by six hours 98% +/- 2% of total body stores are removed. Behnke (2) had predicted five hours prebreathe with 100% oxygen would completely desaturate tissues and give perfect protection against DCS.

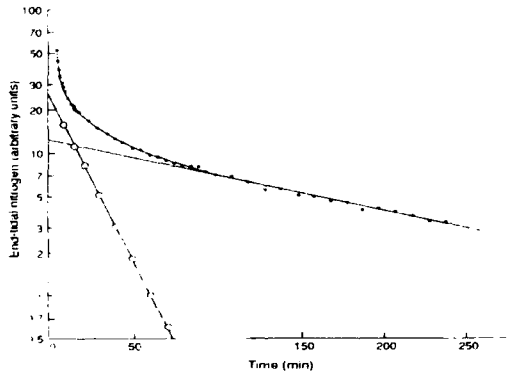

Figure 1. Tissue nitrogen washout over time while breathing 100% oxygen (13). Open circles represent fast tissue desaturation, solid line represents slow tissue desaturation, and closed circles represent total body washout times.

1.2 The Effect of Prebreathing on DCS

Studies in the 1940's and 1950's substantiated the prebreathing theory. Since the introduction of prebreathing as standard procedure in the USAF in the 1960's, only one death from DCS has been documented (14). Prior to that time, 17 DCS deaths were reported (4). There is general agreement that oxygen prebreathing significantly reduces the incidence of DCS as well as delaying the onset of severe DCS symptoms. However, the onset and occurrence of mild symptoms may not be altered to the same degree by oxygen prebreathing. Gray (9) exposed subjects to 38,000 feet for two hours after a 45 minute prebreathe with 100% oxygen. He found an 88% reduction in the incidence of severe bends, and a reduction of 100% in the incidence of chokes. No significant decreases in mild symptoms after prebreathing were found. This study defined a severe symptom as intolerable pain at altitude. Mild symptoms were any pains that were tolerable at altitude. However, during this time period, most investigators did not feel mild pain was of significance, and its onset was often not reported. Additionally, there were varying definitions of "significant" symptoms. Because of these opinions, the results of some of the old prebreathing experiments are difficult to interpret.

Symptomatic subjects often remained at altitude in these studies. For example, in a study by Fryer (6), 90% of the subjects remained at 35,000 feet for one hour. Fifty five percent were at this altitude for four hours. Almost all of these subjects had symptoms that would today terminate the exposure. When subjects remained at altitude with mild to moderate pain, the natural progression of the disease was seen. In some, pain resolved while at altitude. In other subjects, pain did not increase to a point requiring descent. However, at the end of two hours, greater than 20% of runs were aborted due to severe symptoms. Clark et al. (3) collected data from 500 flights to 38,000 feet. Again, flights were not terminated unless the subject experienced severe pain. Onset of symptoms was delayed as prebreathe times increased. These investigators graded DCS pain as follows:

Grade 1+ (mild) - signs and symptoms are noted, and there is a definite degree of discomfort.
Grade 2+ (severe) - definite discomfort which had progressed sufficiently to cause interference with performance of normal activities or duties. At this point, subjects were usually removed from the chamber.

Grade 2+ (chokes) - characterized by a cough on deep inspiration. Flights were terminated when this symptom was present.

Despite the prebreathing, protection was not universal and there was a great deal of intrasubject variability. These data are summarized in Table 1.

Bateman (1) developed the concept of threshold decompression altitudes by calculating tissue half times for both slow and rapid nitrogen elimination phases (Table 2). He predicted the nitrogen load remaining in both slow and fast tissues after oxygen prebreathe. He then used this to determine the maximum exposure altitude where DCS protection could be expected based on both tissues nitrogen loads. For example, this method predicted that a 2 hour prebreathe of 100% oxygen would provide complete protection up to an altitude of 36,419 feet. Only after exceeding this level would the nitrogen differential between the body and the ambient environment be high enough to cause bubble formation.

Onset of Symptoms

Hours O_2	Altitude (feet)	Grade 1 (min)	Grade 2 (min)
0	38,000	33	40
1	38,000	71	76
2	38,000	100	100

Table 1. Protection against decompression sickness. Data from Clark et al. (3).

Time Spent Breathing O_2 at Sea Level (hours)	Fraction of Initial Nitrogen Remaining (mmHg)	pN_2 (mmHg)	Equivalent Total Pressure for Person Breathing Air (mmHg)	Threshold Decompression Pressure (mmHg)	Threshold Decompression Altitude (feet)
0	1.000	573	760	266	26,263
0.5	0.908	520	697	240	28,630
1.0	0.820	470	635	208	31,765
2.0	0.672	385	528	167	36,419
2.5	0.608	348	482	150	38,800

Table 2. Threshold decompression altitudes for bubble formation in slowly desaturating tissue following breathing of pure oxygen (1).

In more recent studies, Waligora et al. (19) found prebreathing eliminated both severe and mild symptoms during a 4.3 psia (30,000 feet) exposure simulating extravehicular activity in a space suit. They determined that an 8 hour prebreathe would completely eliminate DCS symptoms as well as venous bubbles (as measured by precordial Doppler). This work is summarized in Table 3.

Hours of O_2 Prebreathe	# Subjects	%DCS Symptoms	%Venous Bubbles
3.5	23	30	65
4.0	28	21	46
6.0	38	10	29
8.0	8	0	0

Table 3. Results of exposure to a decompression to 4.3 psia (30,000 feet) simulating extravehicular activity (19).

2. CURRENT PREBREATHE REQUIREMENTS

Prebreathing is a standard USAF procedure prior to all high altitude exposures. Prebreathe schedules have been developed by the USAF for various operational settings. Use of these guidelines has reduced, but not eliminated DCS. Table 4 lists the AL prebreathe requirements for research subjects and inside observers in altitude simulators (12). Prebreathing is required for any chamber flight exceeding 18,000 feet for more that 15 minutes. Prebreathe times are extended as the altitude and time of exposure increase. For example, a flight to 35,000 feet for 20 minutes requires a prebreathe time of 30 minutes, while a flight to 19,000 feet for 20 minutes requires a 15 minute prebreathe. The AL maintains a DCS database built from all in-house decompression work (20). Modifications to existing prebreathe procedures stem from this database.

3. DECOMPRESSION/DENITROGENATION MODEL

For 50 years guidelines for safer altitude exposures have been developed by costly time-consuming studies, many specific to unique exposure scenarios. The results of such studies are difficult to apply to new operational requirements. Thus, as new requirements arise, more specialized studies are undertaken. This accumulated wealth of data provides an opportunity for the development of an organized method of predicting DCS risk. The AL is presently developing such a model (17). The work combines sophisticated decompression algorithms with the vast collection of databases available from 50 years of experience, and will result in a state-of-the-art computerized model. This standardized decompression/denitrogenation computer will provide both real-time and predictive DCS risk assessment capability for the USAF

Maximum Altitude	Maximum Exposure Time	Prebreathe Time Required
45,001-50,000 ft	≤ 3 minutes	45 minutes
	≤ 5 minutes	60 minutes
40,001-45,000 ft	≤ 5 minutes	30 minutes
	≤ 15 minutes	60 minutes
35,001-40,000 ft	≤ 10 minutes	30 minutes
	≤ 20 minutes	60 minutes
	≤ 45 minutes	90 minutes
25,001-35,000 ft	≤ 15 minutes	30 minutes
	≤ 30 minutes	60 minutes
	≤ 60 minutes	90 minutes
	> 60 minutes	90+(T-60) min (up to 3 hour max)
18,001-25,000 ft	≤ 15 minutes	0 minutes
	≤ 30 minutes	15 minutes
	≤ 60 minutes	30 minutes
	> 60 minutes	1:1 to 3 hour max
ground level-18,000 ft	no limit	none

Table 4. Armstrong Laboratory prebreathe requirements.

Improved operational safety and effectiveness is an obvious outcome with this computer, as well as a reduction in DCS research costs. Operational safety will be enhanced by rapidly defining the DCS risk for any altitude exposure in an organized and standard manner. Figure 3 depicts a conceptual cockpit computer showing the DCS risk display and input controls for the primary risk variables. A weighing system for individual risk factors will be incorporated into the model, and will include the aviators age, percent body fat, and prebreathe time.

After assessing the risk factors, the model will provide individualized real-time analysis of the decompression sickness risk during the flight and will permit immediate deviations in the flight plan to increase safety. During high altitude mission planning, this model can be used as a predictive aid in the selection of flight options. If risk is too high, protective measures can be added in advance to decrease the risk to a mission acceptable level.

This computer could be used when defining protective limitations during the development of new aircraft systems such as the ATF and NASP. Answers to field inquiries about altitude DCS risk will not need costly research protocols, and DCS research costs will be reduced. Currently, altitude chamber exposures contribute the largest portion of USAF DCS cases (15). The computer could be used to individually assess DCS risk for all occupants and allow protective measures to be used, thus increasing chamber safety.

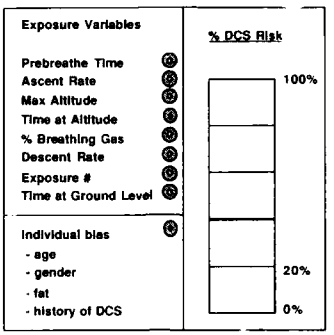

Figure 2. Conceptual Altitude Decompression Computer

4. INCONSISTENCIES IN DCS DATA

During the early stages of model development, a major deterrent to the successful completion of the described decompression computer concept surfaced. This problem is the accuracy of the various databases that are to be used in the model design. There are several aspects to this problem. Significant inconsistencies exist between databases. For instance, investigators frequently used different endpoints in their work, but did not adequately define these endpoints. As described earlier, mild to moderate symptoms were of little interest to early investigators, and therefore, were frequently ignored. Attitudes about the significance of mild symptoms have since changed, and now mild symptoms are considered the endpoint in many studies.

However, in the operational arena, mild symptoms are probably ignored as well. Concerns about career and mission impact may lead to under-reporting of symptoms, especially if "grounding" is a consequence of reporting DCS (15). This attitude is reinforced when decompression sickness symptoms resolve on descent and the aviator does not have pain at ground level. Without some type of immunity in the reporting of DCS symptoms, the true frequency of symptoms will remain obscure and field reporting will continue to be much lower than laboratory reporting and biased towards severe cases. In a recent study at the AL (16), it was found that the lowest percent of decompression sickness observed during four hour exposures at 29,500 feet with either one or two hours of prebreathe time was still 44%, which is significantly higher than the number of cases reported by field units. This is in spite of the fact that the flight protocol was identical to that used in the field. This will make interpretation of the effectiveness of the model in the real conditions difficult.

Another pitfall in the evaluation of decompression sickness is the Type I and Type II classification. This classification system tells the investigator little about the severity of the disease. Decompression sickness exhibits a continuum of symptoms (Figure 3). Any symptoms can be the initial presentation. The disease can then remain constant or progress in either direction on the scale. In addition, the course of decompression sickness is extremely variable (11,15). Symptoms can resolve on descent, remain constant, or resolve and recur. A simple Type I or Type II classification gives no indication of this dynamic situation. Finally, various organizations have different criteria for the Type I and Type II classifications. Some agencies consider hip pain as a Type I symptom, while others consider this to be a Type II symptom. Therefore, for both the investigator and the clinician, the Type I and Type II classification provides inadequate information about the disease.

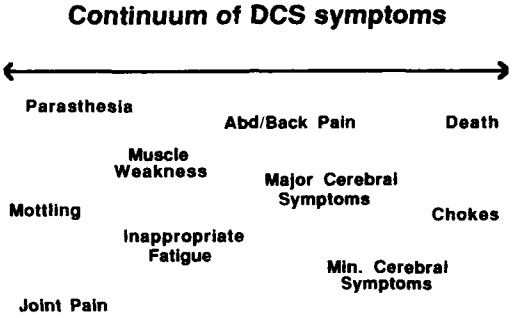

Figure 3. The DCS Continuum of Symptoms

Recently, a new classification scheme has been proposed (5). This approach uses a specific description of the illness instead of broad classification. Under the present system, knee pain is listed as Type I DCS. The new scheme describes knee pain as acute, static, limb-pain, decompression illness. Visual field changes that resolve on descent and then recur would formerly have been called Type II decompression sickness. Now, however, it will be described as acute, relapsing, neurologic decompression illness. Some of the guesswork required between investigators would be eliminated with this new system. From this description alone, the investigator nas an idea about the presentation of the symptoms and the course of the disease. If such a system were universally adopted, there would be vast improvements in database recording. This, in turn, would provide more reliable data for the development of the decompression sickness risk assessment model.

5. CONCLUSIONS

In summary, prebreathing is the main protective measure used against altitude decompression sickness. Current prebreathe schedules are based on work dating back to the 1940's and 1950's. However, while prebreathe schedules do prevent significant decompression sickness occurrences, optimum schedules for specific mission scenarios need to be identified. With the development of a more useful reporting system, databases will provide the necessary information for the development of a decompression sickness risk assessment model. This model can then be used to predict the prebreathe time needed to protect high altitude aviators in specific and new situations and to help reduce further the occurrence of all decompression sickness events.

6. ACKNOWLEDGEMENT

The authors gratefully acknowledge Captain Terrell E. Scoggins, USAF, for his assistance in manuscript preparation.

7. REFERENCES

1. Bateman JB. Preoxygenation and nitrogen elimination: part I - review of data on value of *preoxygenation in prevention of decompression sickness*. In: Fulton JF (ed.), Decompression Sickness. Philadelphia: W.B. Saunders. 1951: 242-77.

2. Behnke AR. The application of measurements of nitrogen elimination to the problem of decompressing divers. U.S. Naval Medical Bulletin. 1937; 35: 219-40.

3. Clarke RW, Humm FD, Nims LF. The efficacy of preflight denitrogenation in the prevention of decompression sickness. Comm. Aviat. Med. Report #472, 1945: 12pp.

4. Dixon JP. Death from altitude-induced decompression sickness: major pathophysiological factors. In: Pilmanis AA (ed.), The proceedings of the 1990 hypobaric decompression sickness workshop. USAF Armstrong Laboratory Special Report. 1991 (in preparation).

5. Francis TJR. Classification of decompression sickness manifestations. In: Pilmanis AA (ed.), The proceedings of the 1990 hypobaric decompression sickness workshop. USAF Armstrong Laboratory Special Report. 1991 (in preparation).

6. Fryer DI. Subatmospheric decompression sickness in man, North Atlantic Treaty Organization. NATO AGARDograph #125. 1969.

7. Fryer DI, Roxburgh HL. Decompression sickness. In: Gilles, JA (ed.), Textbook of aviation physiology. New York: Pergamon Press, 1965: 122-51.

8. Gibson WC, Manning GW. The effect of the pre-breathing of oxygen upon the incidence of decompression sickness. National Defence Institute of National Medicine, D.S. 3-7 (C.I.U. Problem No. 12): Toronto, 1942: 8pp.

9. Gray JS. The prevention of aeroembolism by denitrogenation procedures. U.S. NRC Comm. Aviat. Med. Report #123. 1942: 7pp.

10. Groom A, Morin R, Farhi LE. Determination of dissolved nitrogen in blood and investigation of nitrogen washout from the body. J. Appl. Physiol., 1967; 23: 706-12.

11. Heimbach RD, Sheffield PJ. Decompression sickness and pulmonary overpressure accidents. In: DeHart RL (ed.), Fundamentals of aerospace medicine. Philadelphia: Lea and Febiger, 1985: 132-161.

12. Hill R. Generic protocol - altitude chamber experimentation using human subject volunteers. USAF Human Use Protocol #SGO R88-004). Jan., 1988.

13. Lundin G. Nitrogen elimination during oxygen breathing. Acta Physiol. Scand. 1953; 30: 130-43.

14. Neubauer JC, Dixon JP, Herndon CM. Fatal pulmonary decompression sickness: a case report. Aviat. Space Environ. Med., 1988; 59: 1181-4.

15. Pilmanis AA (ed.), The proceedings of the 1990 hypobaric decompression sickness workshop. USAF Armstrong Laboratory Special Report. 1991 (in preparation).

16. Pilmanis AA, Olson RM. The effect of inflight denitrogenation on altitude decompression sickness. (Abstract) Aviat. Space Environ. Med., 1991; 61:A8(#46).

17. Pilmanis AA, Scoggins TE, Melkonian AD. Altitude decompression computer development. In: Pilmanis AA (ed.), The proceedings of the 1990 hypobaric decompression sickness workshop. USAF Armstrong Laboratory Special Report. 1991 (in preparation).

18. Stegmann BJ. Prebreathing-theory and history. In: Pilmanis AA (ed.), The proceedings of the 1990 hypobaric decompression sickness workshop. USAF Armstrong Laboratory Special Report. 1991 (in preparation).

19. Waligora JM, Horrigan DJ, Conkin J. The effect of extended O_2 prebreathing on altitude decompression sickness and venous gas bubbles. Aviat. Space Environ Med., 1987; 58(9, Suppl.): A110-2.

20. Webb JT, Krutz RW, Dixon GA. An annotated bibliography of hypobaric decompression research conducted at the Crew Technology Division, USAF School of Aerospace Medicine, Brooks AFB, Texas from 1983 to 1988. USAFSAM Technical Paper 88-10R. 1990; 22pp.

G-INDUCED LOSS OF CONSCIOUSNESS ACCIDENTS: USAF EXPERIENCE 1982-1990

by
Terence J. Lyons,
Richard Harding,
James Freeman,
and
Carolyn Oakley

Armstrong Laboratory
Brooks AFB, Texas 78235-5301
and
U.S. Air Force Inspection and Safety Center
Norton AFB, CA 92409-7001

SUMMARY

Discussion of acceleration protection measures should be based on analysis of relevant accident data including determination of high risk aircraft, G profiles, and pilot. Eighteen accidents attributed to G-induced loss of consciousness (GLOC) occurred in the USAF during the 9-year period 1982-1990 resulting in 14 fatalities. All 18 occurred during single crewmember sorties for an average rate of 2.1 per million single-seat flying hours. The rate for 1982-1984 of 4.0, decreased significantly for 1985-1990 to 1.3. Accident records were reviewed for cofactor data and compared to normal data for USAF pilots for age, height, weight, systolic blood pressure, diastolic blood pressure, heart rate, total flying time, and aircraft-specific flying hours. Only for systolic blood pressure (higher) and aircraft-specific flying hours (shorter) were the mishap pilots significantly different from other USAF pilots. No evidence was found in this review to support the role of weight training vs aerobic training, missed meals, or heat in the causation of GLOC accidents. Thus the mishap pilots appeared to be a representative cross-section of USAF pilots with respect to personal variables. More significant factors appeared to be G duration, G magnitude, use of G-trousers, and experience in assigned aircraft.

INTRODUCTION

Previous studies of centrifuge subjects have demonstrated positive correlations between maximum G-level attained without the use of an anti-G straining maneuver (AGSM) and the following variables: age (1,2), weight (2,3), systolic blood pressure (1,4,5), and total flying experience (2). A negative correlation has been demonstrated between height and G tolerance (1,3,4,5). Aerobic training has not been shown to enhance G-level tolerance (6). Diurnal rhythm has been demonstrated to have a small but measurable effect on G-level tolerance (7), (peak tolerance in the early morning). Weight training has been demonstrated to increase G tolerance times in subjects performing an AGSM (8). Except for Hull who studied pilots and navigators, all of these studies used non-pilot subjects.

Recently Webb et al. (9), in a study of 1,434 USAF fighter pilots, again demonstrated statistically significant, but very low, correlations between relaxed G-level attained on the centrifuge and the following variables: age (r=+.17), height (-.18), weight (+.08) systolic blood pressure (+.10), and diastolic blood pressure (+.06). Only height, however, was significantly correlated with G-level tolerance in pilots performing an AGSM on rapid onset runs (negative correlation). None of these variables was associated with GLOC on the centrifuge. Another study of the same variables also in pilots performing an AGSM on rapid onset runs, demonstrated only a positive correlation between weight and G-level tolerance and a negative correlation between resting heart rate and G-level tolerance (10).

Other studies have addressed in-flight incidents of GLOC which did not result in aircraft accidents (GLOC physiologic mishaps). One such study of USAF student pilots determined the incidence (1.7 episodes per month in USAF training) and predisposing acrobatic maneuvers of GLOC physiologic mishaps (split-s maneuver resulted in 30% of GLOC physiologic mishaps and spin/dive recovery, 23%)(11). A study of US Navy pilots determined the incidence of GLOC physiologic mishaps in various aircraft and found no significant association between these mishaps and age, height, or weight (12).

Following recognition of GLOC as a significant cause of USAF accidents in the early 1980's (1,13), continuous and intensive high G centrifuge training for fast jet pilots was instituted in January 1985 (1,15). In 1988, the USAF started to prioritize pilots for centrifuge training on the basis of presumed risk factors of low resting heart rate (<60), low sitting systolic blood pressure (<110), height > 72 inches with slender body build, and total flying time <500 hours (personal communication HQ PAC/SGPA). In addition, pilots were

aggresively educated about the GLOC problem by means of briefings, videotapes, and safety articles (14,15).

Boards of inquiry into USAF aircraft accidents have attributed 18 mishaps to GLOC during the period 1982-1990. At least 27 scientific articles have been published on various aspects of GLOC in Aviation, Space, and Environmental Medicine alone during these years. Previous studies, however, do not provide accident details, calculate incidence rates, or describe any relationships to possible cofactors such as anthropometric features, flying experience, and lifestyle, in actual GLOC acidents.

MATERIALS AND METHODS

The first accidents coded for GLOC in either the Safety or the Life Sciences Databases of the USAF Inspection and Safety Center occurred in 1982. These databases were reviewed for accidents attributed to GLOC occurring during the 9-year period 1982-1990. The accidents were characterized with respect to date of occurrence, type and duration of sortie, and peak level and duration of +Gz immediately preceding GLOC. Data were extracted from the accident investigation reports on the following cofactors: age, height, weight, systolic blood pressure, diastolic blood pressure, resting heart rate, total flying hours, aircraft-specific flying hours, exercise habits, and eating habits. For accidents occurring after 1988, preaccident vital signs data were recorded on the mishap reports. For mishaps before 1988, these data were obtained from physical examination forms in the pilot's medical records. Data were complete except for information on exercise habits (incomplete for 3 pilots) and eating habits (incomplete for 2 pilots).

To ascertain a rate for GLOC accidents, the appropriate denominator was determined to be single seat flying hours. The total of all hours logged in the F-16, F-15 (except F-15E), A-10, A-7, F-5, F-106, and OA-37 was provided by Headquarters USAF, Training and Warrior Management Division, Directorate of Operations. To this total was added 75,000 per year for solo T-37 hours (estimate provided by Headquarters Air Training Command). Because all flying hour data are recorded by fiscal year (1 October - 30 September), fiscal rather than calendar year is used in TABLE I and in all rate calculations. Normal data on the magnitude and duration of +Gz exposure in typical F-16 sorties were obtained from a study of 34 flights (40.52 hours) over a variety of mission scenarios (HEBCO, INC, January 27,1987, Contract F34600-85-C-0174, Task EA86-06, OC-ALC/MMOA, Tinker AFB, OK).

Normal data for personal and biologic variables were obtained from a variety of sources. Age, total flying time, and aircraft specific flying times were obtained from Military Personnel Center records maintained by the USAF Human Resources Laboratory. Data as of 31 December 1984 were used for all pilots who had flown an F-16, F-15 (except F-15E), A-10, A-7, F-5, F-106, or OA-37 within the previous 6 months. Normal data for age, height, weight, systolic blood pressure, and diastolic blood pressure were obtained by using data on the 1,216 USAF fast jet pilots trained on the USAFSAM centrifuge between January 1985 and May 1988 for whom complete medical data were available. Heart rate data were not routinely obtained on centrifuge trainees, but were obtained on a random sample of 37 pilots under age 27.5 years-old who had electrocardiograms on file at USAFSAM. To determine the representativeness of this sample of USAFSAM centrifuge trainees, data for age, height, weight, and blood pressure were obtained from other sources and compared to these trainees. The mean age of single seat pilots in the Military Personnel Center database as of December 1984 was 32.6 years compared with 31 for USAFSAM trainees. Height (179 cm) and weight (79.8 kg) data obtained on 350 USAF pilots in 1990 by the Armstrong Aeromedical Research Laboratory (USAF) is almost identical to that of USAFSAM centrifuge trainees (TABLE I). A mean resting systolic blood pressure measurement of 118, obtained on 291 Air Training Command Pilots in 1978-1981 (Technical Report, Analysis and Evaluation of Trial "Heart" Program and Plan for Air Force Wide Implementation, vol I, Industrial Engineering Dept., Purdue University, 15 January 1982), is slightly higher than that of USAFSAM centrifuge trainees (116 mmHg).

Normal data for eating and exercise habits of pilots are limited. An estimate of the frequency of missed meals among USAF tactical pilots was obtained by a survey of 96 F-16 pilots, 31 T-38 pilots, 46 T-37 pilots, and 48 T-37 students in 1989 (personal communication Dr. Robert Rechtenwald). An estimate of the exercise habits of USAF tactical pilots was obtained by a survey of 107 F-16 pilots performed in 1990 (16).

RESULTS

Eighteen Class A accidents cited GLOC as a contributing cause during the 9 year period 1982 to 1990 (TABLE I). A variety of aircraft types was involved, but all mishap aircraft were being flown by a single crewmember. The number of GLOC accidents annually declined from a mean of 3.3 in 1982-84 to 1.3 in 1985-90; at the same time the number of hours flown in single seat aircraft increased by 30%. The overall rate of GLOC accidents decreased from 4.0 per million flying hours in 1982-84 to 1.3 in 1985-

90 ($p < .05$).

Fourteen of these accidents resulted in fatal injuries: 9 pilots were evidently unconscious until ground impact, 2 made an unsuccessful aircraft recovery attempt just before impact, and 3 were killed during attempted escape (2 were due to failure of ejection systems and 1 drowned after water entry). One pilot survived with injuries when uncommanded ejection followed ground impact. Three pilots successfully ejected in-flight: one sustained major injuries, one had minor injuries, and one was uninjured.

Heat was noted to be a factor in 4/18 (22%) accident reports. Most of the accidents occurred in either the summer or the winter ($p<.05$, TABLE II). All the accidents occurred between 0900 and 1530 local time, with half occurring between 1100 and 1300.

For 16 pilots the mishap sortie was their first sortie of the day and for two it was their second. Twelve of the aircraft (61%) were involved in air combat simulation, four (22%) in simulated air-to-ground attack, and two (11%) in acrobatics when the accident took place (Fig. 1). For the air combat sorties, Fig. 2 also shows the distribution of accidents by the number of engagements flown before the mishap occurred. There appeared to be a bimodal distribution of accidents by time into the sortie with a few accidents occurring very early in the sortie but most occurring late. Two of the accidents occurred before the beginning of the engagement: one during a G warm-up maneuver, and one during a collision avoidance maneuver. The largest number of accidents occurred during the third engagement.

The magnitude of the +Gz exposure immediately before GLOC is shown in Fig. 2. The maximum +Gz acceleration during the period immediately preceding the mishap varied from 4 to 9 G. In four accidents, the pilot was not wearing G-trousers: the F-106 pilot opted not to wear G trousers and the T-37/OA-37s are not equipped for G-trousers. In three further cases the pilots were thought to have had problems with their G-trousers: one was a suspected hose disconnect, one was poorly fitted and one was found with comfort zippers unzipped. Three of the five accidents occurring at <6 Gz (and both of the accidents occurring at <5 Gz) involved pilots not wearing G-trousers. All 14 accidents involving pilots wearing G-trousers occurred at > +5Gz. Five out of 14 (36%) of these accidents occurred at $\geq$ +8Gz (TABLE III) even though only 4% of the peaks above +5Gz reached this level of G exposure ($p < .05$). Four of the seven F-16 accidents (57%) occurred at $\geq$ 8 Gz and all occurred at $\geq$ 6 Gz.

The duration of G exposure above +5Gz immediately preceding the accident for pilots wearing G-trousers is shown in TABLE IV. Insufficient data on +Gz exposure were available in the accident records to estimate the duration of +Gz exposure for the G warm-up maneuver and the collision avoidance maneuver, so this TABLE is based on data from only 12 accidents. As far as can be determined unconsciousness most commonly occurred after 5 to 9 seconds of G exposure. Only 2/12 (17%) of GLOC accidents and 1/7 (14%) of the F-16 GLOC accidents resulted from +Gz exposure of less than 5 seconds duration above +5Gz even though 87% of F-16 peaks above +5Gz lasted less than 5 seconds ($p<.05$).

TABLE V compares the age, height, weight, systolic blood pressure, and diastolic blood pressure of the 18 GLOC pilots with normal data from 1,216 fighter pilots trained on the USAFSAM centrifuge between January 1985 and May 1988. Heart rate data for the 18 GLOC pilots are compared to a subsample of 37 USAFSAM trainees for whom heart rate was determined. Only for systolic blood pressure do the accident pilots differ significantly from normal (higher).

TABLE VI compares the age, total flying hours, and aircraft-specific hours of the 18 mishap pilots with 3,491 USAF pilots with recent fighter experience. The aircraft-specific hours of the accident pilots are significantly less than that of the normal pilots.

TABLE VII compares the exercise habits and eating habits of the 18 GLOC pilots with survey samples of USAF pilots. Preaccident exercise habits of the 15 pilots for who exercise habits were reported varied considerably: two were regular weight lifters only, two were regular runners only, one was an occasional runner, three did both regularly, one did both occasionally, two had recently reduced both weight and aerobic training, one had recently reduced aerobic training, and five were neither regular runners nor weight lifters. Missed meals were noted to be a factor in 7/18 accident reports. A consistent definition of missed meals, however, was not used throughout these accident and no comparison with normal data was made. For the 16 pilots for whom diet on the day of the accident could be determined, only 4 (25%) had no solid food for breakfast on the day of the mishap. This is less than the estimated 44% of F-16 pilots, 29.6% of T-38 pilots, 31.9% of T-37 instructors, or 38.1% of T-37 students who ordinarily miss breakfast (personal communication, Dr. Robert Rechtenwald).

TABLE VIII applies the USAF criteria for prioritizing centrifuge training (see INTRODUCTION) to the 16 non-student GLOC pilots and to normal pilots. Just three GLOC pilots were taller than 72 inches, but all but one were of above average weight for their height. One

GLOC pilot had a low systolic blood pressure only, one had both low systolic and diastolic blood pressures, and two had resting heart rates< 60 bpm. Four of the pilots were inexperienced with less than 500 total flying hours. Only for total flying time was the proportion of GLOC pilots identified by the parameter greater than the proportion of normal pilots identified.

Three of the GLOC pilots had undergone centrifuge training (two before their accident and one after his accident). The mean relaxed +Gz tolerance to gradual onset (0.1 G/sec) for these subjects was 5.35 (range: 4.3-6.15) compared to a USAF mean of 5.2. The straining +Gz tolerance was 7.6 (range:6.6-8.7) compared to a mean of 8.3. One of the mishap pilots had a history of an inflight G-induced loss of consciousness episode as a student: this episode, which did not result in an accident, occurred at an exposure of less than +3 Gz.

Cockpit attention management problems, such as distraction and channelized attention, were noted in half the mishaps. In some cases, factors such as misreading an altimeter or reacting to a threat call intended for a wingman were believed to have contributed to G-induced loss of consciousness. In three cases, disorientation/vertigo resulting from the period of unconsciousness interfered with recovery attempts. Self-imposed stresses, other than missed meals, were suspected in five of the accidents (multiple stresses in two cases): fatigue in three accidents, alcohol use in two , preexisting illness in two, and self-medication in two.

DISCUSSION

GLOC is most strongly associated with the rate of onset, the magnitude, and the duration of +Gz exposure. The use of G trousers and cockpit configuration (e.g., F-16 tilt back seat) apparently influence the threshold for GLOC. There appears to be a bimodal distribution of accidents by time into the sortie with a few accidents occurring very early in the sortie but most occurring late , perhaps supporting the postulated role of fatigue in the causation of GLOC accidents. Factors such as day of the week, age, height, weight, diastolic blood pressure, heart rate, eating habits, and exercise were not appreciably different among the mishap pilots than among their peers. Thus, the mishap pilots appeared to be a representative cross-section of USAF pilots with respect to these variables. Lack of flying experience in the assigned aircraft was significantly associated with GLOC accidents.

The significant association found in this study between systolic blood pressure and GLOC accident is unexplained. The direction of the association with the accident pilots having higher systolic blood pressures than the controls is opposite to that found by previous studies (8,9,10). One possible explanation is that the association occurred by chance and, in a study making multiple comparisons, this explanation cannot be discounted. A second explanation is that some as yet unidentified factor has caused this association; for example, a personal characteristic associated with both high systolic blood pressure and GLOC accident proneness.

Normative data for age, height, weight, systolic blood pressure, diastolic blood pressure, and flying experience were based on large, representative samples of USAF fast jet pilots. However, normative data for some cofactors were limited. Data for the duration and magnitude of peaks above +5 Gz were obtained from 34 sorties in the F-16 only. Normative data for exercise habits were obtained from 107 pilots at a single air base and data for eating habits from only 267 pilots. In addition, the normative data on missed breakfast do not refer specifically to a day when high G exposure was planned; perhaps pilots tend to eat a better breakfast on a morning when a high G mission is to be flown.

Data on the 18 GLOC pilots are very accurate for age, height, weight, and flying experience. Data on G magnitude and duration are estimates made by the accident board. Systolic blood pressure, diastolic blood pressure, and heart rate were based on a single reading (sitting position) obtained at the last physical examination. Data on eating and exercise habits were often deductive as most of the GLOC pilots were fatally injured. The major limitation of this study was the small size of the affected population: a fact which in itself of importance considering the emphasis placed on GLOC as a problem in military aviation. Some cofactors such as age, height, exercise habits, and total flying time showed a non-significant association in the direction indicated by previous studies. The small sample size of this study might have resulted in failure to demonstrate the role of some possibly significant cofactors.

Nevertheless , on the basis of these cofactor findings, it is strongly recommended that efforts to screen pilots for potential G tolerance on the basis of personal and anthropometric variables be discontinued. Attention is better focused on cockpit design (e.g., slant seat), protective equipment (e.g., G-trouser, anti-G valve, etc), and the magnitude and duration of G exposure. All pilots selected for training into fast jets should continue to undergo intensive training on the human centrifuge early in their training.

Finally, a major strength of this study was probably the validity obtained by directly addressing the outcome of primary interest -- GLOC accidents in military aircraft. A larger study of centrifuge subjects or inflight GLOC physiologic mishaps would probably elucidate cofactors associated with G tolerance or GLOC. Centrifuge studies, however, *do not address the multifactorial* nature of the inflight GLOC problem. And it must be remembered that an inflight GLOC physiologic mishap is clearly a different phenomenon from a GLOC accident. According to the USAF Inspection and Safety Center, of 351 GLOC physiologic mishaps (1975-1990), 313 (89%) occurred in the T-37 (primary jet trainer not equipped with G-trousers), 13 (4%) in the F-15, and 12 (3%) in the F-16, whereas only 2 (11%) of the actual accidents have occurred in the T-37, 2 (11%) in the F-15, and 7 (39%) in the F-16.

REFERENCES

1. Maat GKM (chairman). AMP working group 14, High G Physiological protection training. AGARDograph No. 332.

2. Hull DH, Wolthuis RA, Gillingham KK, Triebwasser JH. Relaxed +Gz tolerance in healthy men: effect of age. J. Appl. Physiol. 45, 1978, 626-9.

3. Gillingham KK, Schade CM, Jackson WG, Gilstrap LC.. Aviat. Space Environ. Med. 57, 1986, 745-53.

4. Klein KE, Bruner H, Jovy D, Vogt L, Wegmann HM. Influence of stature and physical fitness on tilt-table and acceleration tolerance. Aerospace Med. 40, 1969, 293-7.

5. Leverett SD, Whinnery JE. Biodynamics: sustained acceleration. IN: Dehart, ed. Fundamentals of Aerospace Medicine. Philadelphia: Lea & Febiger, 1985, 233.

6. Whinnery JE, Parnell MJ. The effects of long term aerobic conditioning on +Gz tolerance. Aviat. Space Environ. Med. 58, 1987, 199-204.

7. Glaister DH, Hall GM. Circadian variations in tolerance to +Gz acceleration. The Physiologist. 25, 1982, suppl.:S-25-28.

8. Epperson WL, Burton RR, Bernauer EM. The *effectiveness of specific weight* training regimens on simulated aerial combat maneuvering G tolerance. Aviat. Space Environ. Med. 56, 1985, 534-9.

9. Webb JT, Oakley CJ, Meeker LJ. Unpredictability of fighter pilot G tolerance using anthropometric and physiologic variables. Aviat. Space Environ. Med. 62, 1991, 128-5.

10. Mizumoto C. Relationship between +Gz tolerance and physical characteristics during gradual and rapid onset runs. Jpn. J. Aerospace Environ. Med. 25, 1988, 37-47.

11. Whinnery JE. +Gz-induced loss of consciousness in undergraduate pilot training. Aviat. Space Environ. Med. 57, 1986, 997-9.

12. Johanson DC, Pheeny BT. A new look at the loss of consciousness experience within the U.S. Naval forces. Aviat. Space Environ. Med. 59, 1988, 6-8.

13. Burton RR, Whinnery JE. Operational G-induced loss of consciousness: something old; something new. Aviat. Space Environ. Med. 56, 1985, 812-7.

14. Burton RR. G-induced loss of consciousness: definition, history, current status. Aviat. Space Environ. Med. 59, 1988, 2-5.

15. Gillingham KK, Fosdick JP. High-G training for fighter aircrew. Aviat. Space Environ. Med. 59, 1989, 12-19.

16. Wiegman JF, Hart SD, Fischer JR, Peel G. Physical conditioning for G-tolerance in Tactical Air Command pilots. 62nd Annual Scientific Meeting of the Aerospace Medical Association, May 6-9, 1991: Abstract #188.

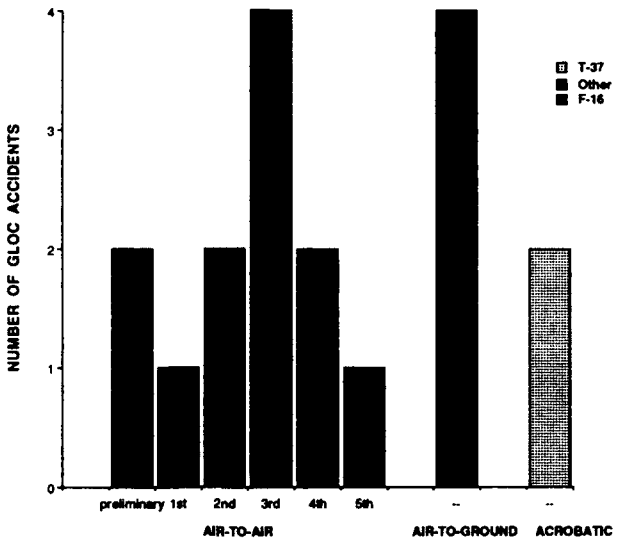

Fig. 1. Distribution of GLOC accidents by type of sortie and number of engagements for air-to-air sorties. Preliminary refers to accidents occurring before the first engagement.

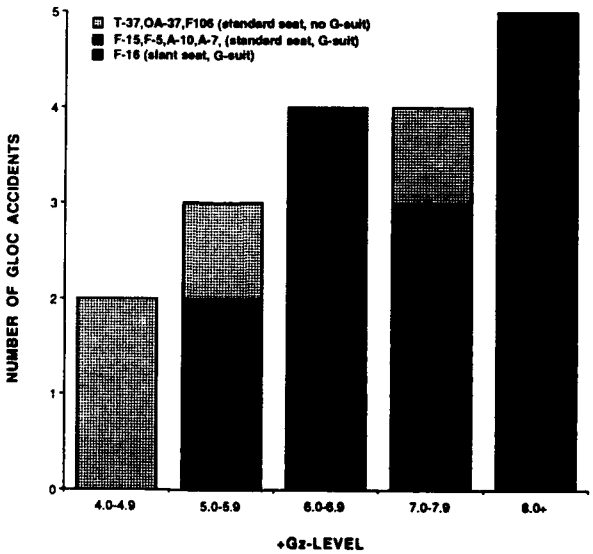

Fig. 2. Distribution of GLOC accidents by maximal +Gz level attained just prior to the accident.

TABLE I. U.S. AIR FORCE ACCIDENTS ATTRIBUTED TO G-INDUCED LOSS OF CONSCIOUSNESS: 1982-1990

YEAR	# GLOC ACCIDENTS	AIRCRAFT TYPES	TOTAL FLEET SINGLE-SEAT	RATE PER MILLION FLYING HOURS
1982	2	(F-5E, T-37B)	767,527	2.6
1983	3	(F-16A, F-16A, F106A)	846,846	3.5
1984	5	(A-10A,F-16A, A-10A, F-5E, F-16A)	887,995	5.6
PERIOD I TOTAL (1982-1984): 10			2,502,368	4.0*
1985	1	(F-16A)	944,166	1.1
1986	1	(OA-37B)	934,907	1.1
1987	0	-------	990,026	0
1988	4	(F-16A,F-16C, T-37B, A-7D)	976,395	4.1
1989	1	(F-15B)	1,137,654	0.9
1990	1	(F-15C)	1,001,561	1.0
PERIOD II TOTAL (1985-1990): 8			5,984,709	1.3*

*One sided binomial probability of this decrease in rate from PERIOD I to PERIOD II occurring by chance=.019

TABLE II. GLOC MISHAPS BY DAY OF THE WEEK AND SEASON OF THE YEAR OF OCCURRENCE.

	Winter	Spring	Summer	Autumn	Total
Monday	0	1	2	0	3
Tuesday	0	0	2	1	3
Wednesday	3	0	0	1	4
Thursday	2	0	3	0	5
Friday	1	0	1	0	2
Saturday	1	0	0	0	1
Total	7*	1*	8*	2*	18

*Chi-square rest with three degrees of freedom comparing seasonal distribution, $p<.05$

TABLE III. PEAK G LEVELS IN 14 GLOC ACCIDENTS INVOLVING PILOTS WEARING G-TROUSERS. PEAK G LEVEL IN EXCUSIONS ABOVE +5Gz FOR NORMAL F-16 OPERATIONS ARE SHOWN FOR COMPARISON.

	Column 1	Column 2	Column 3
Peak G Level	% (#) GLOC Accidents*	% (#) F-16 GLOC Accidents	% of Peaks above +5Gz in normal F-16 operations
≥5<6	14% (2)	0	58%
≥6<7	29% (4)	14% (1)	22%
≥7<8	21% (3)	29% (2)	16%
≥8	36% (5)	57% (4)	4%

Chi-square test with 3 degrees of freedom comparing Column 1 and Column 3, $p<.001$

TABLE IV. DURATION OF EXPOSURE ABOVE 5 +Gz IN 12 GLOC ACCIDENTS INVOLVING PILOTS WEARING G-TROUSERS. DURATION OF EXPOSURE ABOVE +5 Gz FOR NORMAL F-16 OPERATIONS ARE SHOWN FOR COMPARISON.

	Column 1	Column 2	Column 3
Time Above +5Gz (sec)	% GLOC Accidents*	% F-16 GLOC Accidents	% of Peaks above +5Gz in normal F-16 operations
<5	2 (17%)	1 (17%)	87%
≥5<10	7 (58%)	3 (50%)	11%
≥10	3 (25%)	2 (33%)	2%

Chi-square test with 2 degrees of freedom comparing Column 1 and Column 3, $p<.001$

* Data incomplete on duration of G exposure for 2 of the 14 mishaps

TABLE V. ANTHROPOMETRIC AND VITAL SIGNS DATA FOR THE 18 GLOC ACCIDENT PILOTS COMPARED TO 1,216 TAC PILOTS TRAINED ON THE USAFSAM CENTRIFUGE JAN 1985-MAY 1988.

	GLOC Pilots (mean)	Centrifuge Pilots (mean)	p value
Age (years)	29.7	31.0	N.S.
Height (cm)	180.2	178.8	N.S.
Weight (kg)	79.1	78.3	N.S.
Systolic BP (mmHg)	122	116	0.005
Diastolic BP (mmHg)	74	74	N.S.
Heart rate (bpm)	65	63	N.S.

* Heart rate data were not routinely collected on centrifuge subjects. This estimate was based on a sub-sample of 37 of the USAFSAM centrifuge subjects under age 27.5 years-old for whom ECGs were on file.

TABLE VI. AGE AND FLYING HOUR DATA FOR THE 16 NON-STUDENT GLOC ACCIDENT PILOTS COMPARED TO 3,491 TAC PILOTS WITH RECENT FLYING TIME IN SINGLE SEAT AIRCRAFT AS OF JAN 1985 PER MPC DATABASE.

	GLOC Pilots (mean)	TAC Pilots (mean)	p value
Age (years)	30.4	32.6	N.S.
Total Flying Time (hours)	1,554.8	1,929.9	N.S.
Aircraft Specific Flying Time	336.9	548.9	p<.05

TABLE VII. MISSED MEALS AND EXERCISE HABITS FOR THE 18 GLOC ACCIDENT PILOTS COMPARED TO AVAILABLE SURVEY DATA ON USAF TACTICAL PILOTS.

	GLOC Pilots*	Survey Data	p value
Missed Breakfast	4/16* (25%)	107/267 (40%)	N.S.
Lift Weights	8/15* (53%)	79/107 (74%)	N.S.
Run or Jog	10/15* (67%)	61/107 (57%)	N.S.

*Data incomplete on some of the 18 GLOC accident pilots.

TABLE VIII. RETROSPECTIVE ANALYSIS COMPARING THE PROPORTION OF GLOC ACCIDENT PILOTS IDENTIFIED BY TAC SCREENING PARAMETERS TO THE PROPORTION OF TAC PILOTS IDENTIFIED BY THE SAME CRITERIA.

Parameter	Proportion Meeting Criteria		Odds Ratio	p value
	16 GLOC pilots	Comparison Group		
Height>72 inches (and slender)* and Systolic BP<110	3/16 (19%)	395/1,216+ (32%)	.48	N.S.
Heart rate<60	2/16 (13%)	12/37 (32%)	.39	N.S.
Total Flying Time <500 hours	4/16 (25%)	344/3,147@ (11%)	3.0	N.S.

* Slender defined in this analysis as less than "desired weight" in USAF Table: 185 pounds for >72 inches, 190 pounds for >73 in, or 196 pounds for >74 inches.

+ USAFSAM Centrifuge subjects (see TABLE V)
@ TAC Pilots in MPC database (see TABLE VI)

PULMONARY EFFECTS OF HIGH-G AND POSITIVE PRESSURE BREATHING

Gp Capt David H Glaister

RAF Institute of Aviation Medicine,
Farnborough, Hants. GU14 6SZ, UK

INTRODUCTION

Since positive pressure breathing (PPB) can provoke syncope even at 1g, its use to support the circulation and prevent G-induced loss of consciousness (G-LOC) appears somewhat of a paradox. Furthermore, when right heart pressures are normally only a few mmHg, an alveolar pressure of 65 mmHg produced by PPB appears alarming, and concern has been expressed as to the advisability of using pressure breathing as a means for enhancing G protection (Jennings and Zanetti, 1988). This paper examines the effects of acceleration and pressure breathing on the circulation, particu-larly within the lungs, and concludes that when one considers pressure differentials across the walls of the major vessels and heart chambers, these concerns are largely unjustified.

PULMONARY PERFUSION

The influence of gravity on blood flow within the lung was clarified in studies by West and his colleagues at the Hammersmith Hospital (Dollery, Naimark and West, 1963), who used radioactive tracers to map out the vertical distribution of flow per unit lung volume. West defined three zones (to which a fourth was subsequently added) dependent upon arterial and venous pressures at each level relative to alveolar gas pressure (Fig. 1). This model was then applied to the effects of increased acceleration and validated in studies on huma[illegible]ntrifuge subjects using radioactive xenon tec[illegible]ques (Glaister, 1970).

In zone 1, the hydrostatic pressure gradient reduces pulmonary arterial pressure to below alveolar pressure, the thin walled capillaries collapse and flow becomes zero. This zone is small and restricted to the extreme apex of the lung at 1g, but rapidly expands to occupy half the total lung volume at an acceleration as little as $+3G_z$.

In zone 2, arterial pressure exceeds alveolar pressure so that the arterial ends of the pulmonary capillaries are forced open, but venous pressure is still below alveolar pressure and the venous ends of the capillaries tend to close. Flow is then controlled by the arterio-alveolar pressure difference (the so-called 'water-fall' effect). Due to the hydro-static pressure gradient down the arteries of zone 2, and its lack in the alveolar gas, flow increases with distance down the zone and its rate of increase is proportional to the level of acceleration applied.

In zone 3, venous as well as arterial pressures exceed alveolar pressure and the capillaries are fully open. However, while the arterio-venous pressure difference which determines flow stays constant down the zone, flow nevertheless increases due to passive distension (and lower resistance to flow) of the capillaries, and to the opening up of capillaries having higher critical closing pressures as hydrostatic pressures rise (capillary recruitment). Indeed, the rate of increase in flow with distance down zone 3 may be indistinguishable from that down zone 2 (Glaister, 1970).

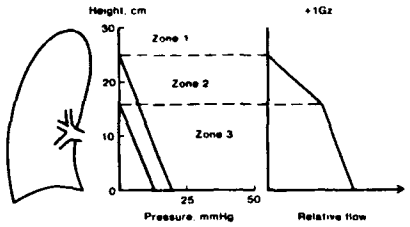

Fig. 1. West's 3-zone model for pulmonary blood flow distribution. The sloping pressure lines of the central panel refer to pulmonary venous and arterial pressures respectively. Zone 1, arterial pressure less than zero (alveolar pressure); zone 2, arterial pressure > zero > venous pressure; and zone 3, arterial pressure > venous pressure > zero.

PULMONARY VENTILATION

The idea that lung tissue would distort under its own weight to create a gradient in alveolar size was proposed by Milic-Emili (Kaneko et al, 1966) and confirmed by freezing dog lungs intact on the *IAM centrifuge (Glazier et al, 1967).* Lung mechanics predict that a gradient in alveolar size will produce a gradient in ventilation, since alveolar stiffness varies non-linearly with volume according to the lung's overall pressure-volume curve. At 5G, the lung has a weight of five times normal and this produces a gradient in transpulmonary pressure of about 1 dPa/cm, sufficient to ensure that alveoli at the lung apex are fully distended, while alveoli at the base remain at their minimal lung volume. Complete emptying of these alveoli is precluded by airway (terminal bronchioles) closure and the overall range in volume is about 5 to 1. As illustrated in figure 2, this leads to a pattern of ventilation which mirrors the slope of the pressure-volume curve for each level of inflation - from low at the apex where alveoli are relatively stiff, then increasing down the lung as alveoli become smaller and more compliant, only to fall off to zero near the base where the toe of the pressure-volume curve represents airway closure (Glaister et al, 1973).

VENTILATION/PERFUSION RATIO

The effectiveness of pulmonary gas exchange depends upon the balance between ventilation and perfusion throughout the lung, as normally expressed by the ventilation/perfusion ration, V/Q. (A value of unity indicates that a given region receives identical fractions of the total alveolar ventilation and total pulmonary perfusion). Pertinent to the present discussion is that acceleration leads to an increasing mismatch down the lung. Thus, while the lung apex is ventilated, though to a reduced extent, its perfusion is zero and its V/Q ratio becomes infinitely large, adding to the total deadspace of the respiratory system. At the lung base, in contrast, perfusion is greater than normal, but

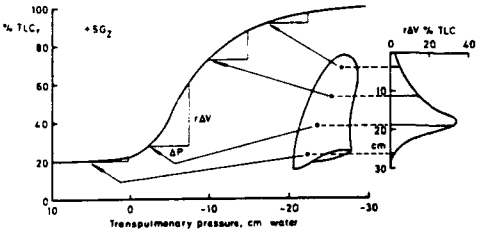

Fig. 2. The pressure-volume curve for a human lung at $+5G_z$ in which, at the same overall lung volume: alveoli at the apex are distended, stiff and poorly ventilated; alveoli in the mid-lung are compliant and well ventilated; and alveoli at the base are shrunk to their minimal volume with closed airways and zero ventilation. Alveolar volumes are expressed as percent regional total lung capacity (TLC_r) and ventilation (right hand plot) as regional volume change ($r\Delta V$) percent TLC_r.

ventilation falls to zero as airways close and the V/Q ratio also becomes zero. Once equilibrium between the venous blood and trapped alveolar gas has been achieved, a matter of seconds, further gas exchange ceases and the region constitutes a right-to-left shunt with venous admixture of arterial blood and a consequent fall in systemic arterial oxygen saturation. This may have little relevance to the subject's relaxed G tolerance which is primarily dependent upon blood *flow* to the brain, but when considering duration tolerance to a *simulated* air combat manoeuvre (SACM) in which fatigue becomes a significant endpoint, a reduction in *oxygen supply* to contracting muscles must contribute to a degradation in performance.

In practice, the situation is partly corrected by the appearance of zone 4 in the lowermost lung in which airways have closed (Fig. 3). Here, blood flow is actually less than predicted by the simple hydrostatic model, due either to a reflex vasoconstrictory response to changing alveolar gas tensions, or because airway closure allows alveolar gas pressure to rise and so to counteract the rising hydrostatic pressures. Nevertheless, centri-fuge experiments have demonstrated right-to-left shunts as great as 50% of the cardiac output in subjects exposed to accelerations of up to 7G (Glaister, 1970).

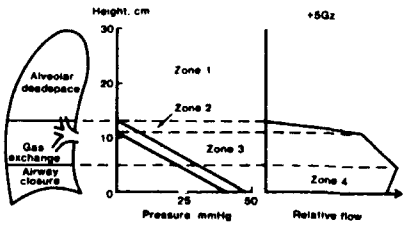

Fig. 3. As for figure 1, but calculated for an acceleration of $+5G_z$. Note the appearance of a zone 4 in which airway closure causes, or is associated with, a reduction in blood flow.

ACCELERATION ATELECTASIS

When alveolar gas is trapped by closure of terminal bronchioles, equilibrium in O_2 and CO_2 tensions between gas and venous blood will occur as described above. Normally this will leave the poorly soluble nitrogen fraction unaffected and the alveolar volume will remain virtually constant as carbon dioxide exchanges for oxygen. When 100% oxygen has been breathed, however, equilibrium is only achieved following complete absorption of the trapped gas, a process which may be completed within 30 sec or so (Glaister, 1970). This leads to the condition known as acceleration atelectasis in which the collapse persists following return to 1g due to surface tension effects, and produces symptoms of retrosternal discomfort, a tendency to cough, and difficulty in taking a deep breath (an inspiratory 'catch'). Furthermore, the right-to-left shunt will persist until resolution of the condition which, in the absence of a conscious effort to inflate the lungs, may take many hours.

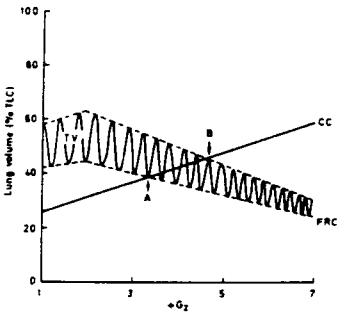

Fig. 4. The effect of $+G_z$ acceleration on tidal volume (TV), functional residual capacity (FRC) and closing capacity (CC), all expressed percent total lung capacity (TLC). Airways will start to close at end-expiration at point A, and will remain closed throughout tidal breathing from point B.

CLOSING CAPACITY

The appearance of a zone 4 is dependent upon the lung volume at which the subject is breathing - i.e., the functional residual capacity (FRC). For example, if the lung is hyperinflated, all alveoli will increase in volume and closure of airways may either be prevented, or will only occur at a higher level of acceleration. The absolute lung volume at which airway closure can first be detected (the closing capacity, CC) is increased by acceleration as indicated in figure 4. At 1g, the subject will normally be breathing at a lung volume greater than his closing capacity, but as acceleration causes his closing capacity to increase, and the inflating anti-G trousers raise his diaphragm and reduce his FRC, points are reached at which airways start to close at the end of each expiration (figure 4, arrow A), and then remain closed throughout the respiratory cycle (arrow B). From this latter point on, increasing numbers of airways will close and right-to-left shunting will develop progressively, with atelectasis if 100% oxygen had been breathed prior to closure. An increase in FRC, therefore, from whatever cause, will delay the onset and reduce the extent of closure, shunting and potential atelectasis.

POSITIVE PRESSURE BREATHING

The administration of oxygen under pressure through an aircrew mask is standard practice for protection against hypoxia in the event of loss of cabin pressurisation at altitudes above 40,000 ft. However, positive pressure breathing (PPB) has several undesirable effects on the respiratory and cardiovascular systems which limit the usable pressure and length of time for which it can be applied. The unsupported lung is fully inflated by an airway pressure of 2.7 kPa (figure 2) and will rupture if inflated to a pressure greater than 5-6 kPa, though the mechanics of the thoracic wall protect it up to 10-11 kPa and active contraction of expiratory muscles to even greater pressures. Overdistension of the lungs can be prevented, or at least contained, by training, but at a pressure of 5 kPa, the FRC is greatly increased, expiration becomes active and tiring, and tidal volume increases with a consequent increase in ventilation and fall in arterial CO_2 tension (hyperventilation).

On the cardiovascular side, an increase in intrathoracic pressure is transmitted directly to the mediastinal and pulmonary vasculature with a comparable increase in central venous, cardiac and aortic pressures (Ernsting, 1966). Blood is displaced from the thorax and cardiac output falls due to impeded venous return. Continuing arterial inflow causes peripheral venous pressures to rise with pooling and loss in circulating blood volume and, if maintained, transudation of fluid into the tissues and a further loss in blood volume.

Breathing at a positive pressure of 4 kPa for 10 min causes a decrease in the effective blood volume of 400-500 ml, but cardiac output is usually maintained at around 70% of normal. Continuation of PPB, or breathing at higher pressures, can lead to a developing *tachycardia*, loss of arteriolar tone and eventual syncope.

In order to minimise these potentially harmful physiological effects of PPB, counterpressure garments are used to support the chest, abdomen and limbs. The combination of oronasal mask, partial pressure jerkin and G-trousers allows 9-10 kPa to be tolerated, but at higher pressures head and neck discomfort occurs, and air may be forced through the lachrymal duct and eustachian tubes. At pressures greater that 13 kPa a full pressure suit must be worn, but with such a suit the sky (or ocean bed!) is the limit, hydrostatic pressure *per se* having virtually no effect on the body's physiology.

The rise in systemic arterial pressure produced by PPB also depends upon the extent of coverage of the counterpressure garments used. As illustrated in figure 5 (from Ernsting, 1966), PPB without counterpressure produces an increase equal to only 50% or so of the applied breathing pressure, while with trunk and lower limb counterpressure the increase exceeds 100%. To account for this latter phenomenon one needs to consider the role of central blood volume receptors and the baro-receptors, both intrathoracic and those in the carotid sinus. The baroreceptors are sensitive to transmural tension (stretch of the vessel wall) and the carotid sinus baroreceptor will detect the rise in systemic pressure and promote a reflex vasodilation and bradycardia. However, since pressure rises are comparable both inside and outside the aorta, the output from these receptors will remain constant and conflict with the carotid sinus signals, so permitting some overall rise in systemic pressure. Ernsting (1966) has also shown that positive pressure breathing produces a peripheral arteriolar vasoconstriction which is itself enhanced by trunk counterpressure, a possible

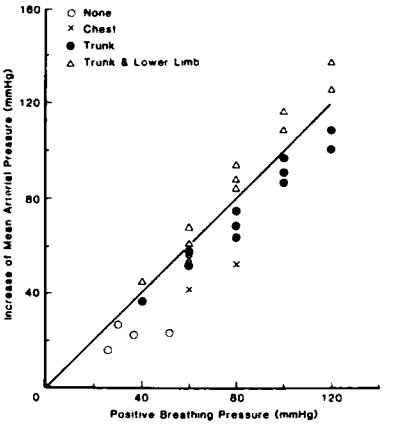

Fig. 5. The effect of breathing pressure on mean arterial pressure for voluntary human exposures to PPB using differing extents of counterpressure coverage. The line of identity is indicated (Redrawn from Ernsting, 1966).

mechanism being stimulation of low pressure receptors in the intrathoraic vasculature. It may also be noted from figure 5 that voluntary exposures to PPB at 16 kPa were made using trunk counterpressure alone, without *ill effects.*

PRESSURE BREATHING FOR G PROTECTION

As discussed above, PPB causes an increase in systemic arterial pressure, and so may be used to replace, or lessen the need for, an active straining manoeuvre to increase G tolerance. PPB was first used on the centrifuge at the IAM to assist the breathing of subjects exposed to G vectors intermediate between $+G_z$ and $+G_x$ in studies on G tolerance using reclined seats. A breathing pressure of 0.7 kPa per G balanced the increase weight of the anterior chest wall, so assisting inspiration and restoring the FRC towards its normal 1g value (Glaister and Lisher, 1976). It was noted that this level of PPB also gave a very significant increase in greyout threshold and an extension of the studies to a conventional seat confirmed a close to $+1G_z$ improvement. The increase in FRC produced by pressure breathing for G protection (PBG) was considered advantageous in that it would theoretically reduce right-to-left shunting and suscepti-bility to atelectasis (Fig 4). However, this prediction was not supported by ear oximetry on the centrifuge and aircrew preferred the use of chest counterpressure in flight trials of PBG (Harding and Cresswell, 1987), presumably due to the greater increase in systemic arterial pressure so provoked. No deliberate studies on PBG have been carried out without lower limb counter-pressure, but inadvertent loss of pressure in prototype full coverage anti-G trousers led to the expected very rapid onset of G-induced loss of consciousness (G-LOC). Pressure breathing for G protection (PBG) must, therefore, be regarded as a system which includes mandatory lower limb counterpressure with chest counterpressure as an additional option.

Figure 5 indicates a 110% transfer of pressure from airways to arteries so that, assuming a 22 mmHg per G pressure drop from heart to head level, PPB at 60 mmHg should produce a 3G improvement in tolerance, providing that trunk and lower limb counterpressure is effective. In fact, the hydrostatic fall in pressure at neck level should negate even the carotid baroreceptor's influence in preventing the 'hypertensive' effect of PPB and an even greater increase in tolerance might be expected. Full coverage anti-G trousers (FAGT) have been shown superior to the in-service cutaway garment (AGS), particularly when combined with PBG both in terms of greyout tolerance (Prior, 1990), and in maintaining eye level blood pressure (Figure 6). However, the transfer efficiency of PPB in terms of increase in eye level blood pressure per increase in breathing pressure was still only of the order of 70% (Prior, 1989), so there remains further potential for improvement.

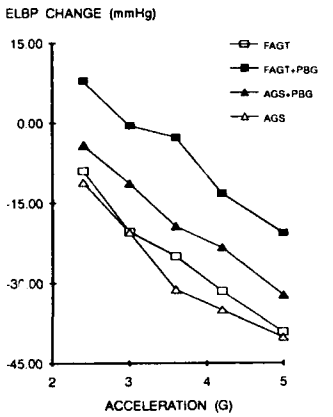

Fig. 6. The effect of $+G_z$ acceleration on eye level blood pressure (ELBP) as measured using a Finapres with hydrostatic correction (Prior, 1989). Full coverage anti-G trousers (FAGT) prevent as great a fall in pressure as a standard anti-G suit (AGS), particularly when combined with pressure breathing (PBG).

Returning to the theoretical harmful effects of PBG at, say, 65 mmHg, it is clear that, providing chest counterpressure is used to prevent overdistension of the lungs, and sufficient counterpressure is applied elsewhere to limit venous pooling and to allow venous pressures (both intra- and extra-thoracic) to rise *pari-passu* with airway pressures, then transmural pressure gradients throughout the circulation will be close to normal values. The vasculature above heart level will be protected by hydrostatic pressure falls with pressures at head level remaining below normal, and the only problem area would be the arms if allowed to lie at or below heart level, though even here normality could be regained by additional counterpresssure if required. While few studies have been carried out, Ernsting (1966) found that central venous pressures, when referenced to airway pressure, were slightly reduced by PPB, so cardiac dynamics should be virtually unaffected.

References

Dollery C. T., A. Naimark and J.B. West. (1963). Distribution of blood flow in the isolated dog lung and its relation to arterial, venous, alveolar and pleural pressures. J. Physiol. 170: 20-21P.

Ernsting, J. (1966). Some Effects of Raised Intrapulmonary Pressure in Man. AGARDograph No 106. Technivision Ltd, Maidenhead.

Glaister, D.H. (1970). The Effects of Gravity and Acceleration on the Lung. AGARDograph No 133, Technivision Services, Slough.

Glaister, D.H. and B.J. Lisher. (1976). Centrifuge assessment of a reclining seat. AGARD Conference Proceedings No 189, NATO. A4-1 to A4-8.

Glaister, D. H., R.C. Schroter, M.F. Sudlow and J. Milic-Emili. (1973). Bulk elastic properties of excised lungs and the effect of a transpulmonary pressure gradient. Respir. Physiol. 17: 347-364.

Glazier, J B, J.M.B. Hughes, J.E. Maloney and J.B. West. (1967). Vertical gradient of alveolar size in lungs of dogs frozen intact. J. appl. Physiol. 23: 694-705.

Jennings, T. and C. Zanetti. (1989). Positive pressure breathing as a G-protection device : safety concerns. SAFE Journal. 18:52-56.

Kaneko K., J. Milic-Emili, M.B. Dolovich, A. Dawson and D.V. Bates. (1966). Regional distribution of ventilation and perfusion as a function of body position. J. appl. Physiol. 21: 767-777.

Prior A.R.J. (1989). Physiological aspects of an enhanced G protection system. 11th Ann. Meeting IUPS Commission on Gravitational Physiology. Lyon, France. 25-27 Sep, 1989.

Prior A. R. J. (1990). Centrifuge assessment of the $+G_z$ acceleration protection afforded by full coverage anti-G trousers. Aviat. Space Environ. Med. 60: 504.

MAXIMUM INTRA-THORACIC PRESSURE WITH PBG AND AGSM

F. Buick PhD, J. Hartley BSc, M. Pecaric MSc

Aerospace Physiology Section
Defence and Civil Institute of Environmental Medicine
1133 Sheppard Ave. W., P.O. Box 2000
North York, Ontario, Canada
M3M 3B9

SUMMARY

Positive pressure breathing during +Gz (PBG) and anti-G straining maneuvers (AGSM) each improve +Gz tolerance by increasing blood pressure through increases in intra-thoracic pressure, but the maximal intra-thoracic pressure from their combined effect is not known. Six subjects performed: (i) maximal AGSM at +1Gz; (ii) assisted PBG (constant 60 mm Hg) at +Gz ; (iii) submaximal AGSM at +Gz (enough to maintain peripheral vision); (iv) maximal AGSM at +Gz; and (v) combined PBG and maximal AGSM at +Gz. They wore: TLSS mask/helmet ensemble, CSU-15/P G-suit, and TLSS-style jerkin. Intra-thoracic pressure was measured with a catheter tip pressure transducer in the esophagus (Pes). Gastric pressure was also measured (Pga). For both Pes and Pga, there were no significant differences among experimental conditions (i), (iv) and (v). Group mean Pes and Pga in these 3 conditions were 139 and 197 mm Hg, respectively. The similar results between maximal AGSM, and maximal AGSM and PBG are explained by: (i) limited support from the thoracic counter-pressure garment, and (ii) the characteristics of the respiratory system.

INTRODUCTION

Exposure to sustained, headward acceleration (+Gz) decreases arterial blood pressure at head level by approximately 22 mm Hg per unit +Gz increase in upright man. Near +5 Gz, compromised cerebral perfusion produces unconsciousness. +Gz tolerance can be improved by increasing blood pressure. Increases in intra-thoracic pressure act directly on the heart and great vessels producing an almost one-for-one increase in blood pressure. (Intra-thoracic pressure is loosely defined as the pressure around the heart, i.e. intra-pleural pressure.) An anti-G straining maneuver (AGSM), a vigorous expiratory effort against a closed or partially-open glottis coupled with peripheral skeletal muscle tensing, can increase intra-thoracic pressure up to 100 mm Hg. When combined with a pressurized anti-G suit, AGSM can increase +Gz-intensity tolerance up to the level of +8–9 Gz.

Performing AGSMs requires concentration and is physically demanding. By increasing intra-thoracic pressure with positive pressure breathing using a breathing regulator, the requirement for AGSM is reduced. The maximal pressure delivered by pressure breathing during +Gz (PBG) systems such as the USAF's Combat Edge, is currently set at 60 mm Hg. This pressure should increase +Gz-intensity tolerance by approximately +2.5 Gz producing a +7–8 Gz protection system. If pilots are to withstand exposure to higher +Gz levels, as may occur during aerial combat or flight emergency, PBG must be supplemented with AGSM. The degree of G-intensity protection from the combination of PBG and a maximal AGSM is not known. Several investigators have reported experimental subjects requiring moderate AGSM in order to complete PBG studies in the centrifuge (Refs 1,2,3) but the effect of maximal AGSM does not appear to have been researched. The intra-thoracic pressure is a critical issue. What is the maximal intra-thoracic pressure produced by the combination of assisted PBG (PBG with thoracic counter-pressure from a jerkin) and maximal AGSM? The study reported here addresses this question.

METHODS

Experimental Subjects

Six medically-screened volunteers participated as subjects after giving informed consent. They were experienced in riding the centrifuge with a mean +Gz tolerance of +8.3 Gz in a seat reclined 22 degrees from vertical. They received additional training in positive pressure breathing at +1G and in the centrifuge, and then in supplementing PBG with maximal AGSM.

Measurements

Mask cavity pressure (Pm) and G-suit pressure (Pg-suit) were measured with variable reluctance pressure transducers (Validyne, model DP15). Pm was obtained via a fitting fixed through the shell and facepiece of the mask. G-suit pressure was measured through a bayonet-style (Luer-Lok) fitting in the valve connector of the G-suit hose. All transducers were calibrated.

Intra-thoracic pressure was estimated by measuring pressure in the esophagus (Pes). Because abdominal pressure is important in venous return and in supporting intra-thoracic pressure, gastric pressure (Pga) was also measured. Pes and Pga were measured with miniature catheter-tip pressure transducers (Medical Measurements Inc, model 16CT). A custom brass fitting replaced the anti-suffocation valve of the mask. With the mask hanging by one bayonet from the mounted helmet, the Pes and Pga catheters were passed 40 and 65 cm respectively through two small ports in this fitting. The catheters were taped to the sleeves of this fitting to prevent sliding. A small amount of xylocaine ointment was applied to the back of the nares. With the tip dipped in a water-soluble lubricant, the Pga catheter was inserted into the nose and moved to the glottis. The subject swallowed a small amount of water as the catheter was pushed past the glottis. It was then advanced to the stomach. The procedure was repeated with the Pes catheter which ultimately rested in the lower third of the esophagus. The mask was lifted to the face, ensuring that neither catheter looped in the mask cavity. The second bayonet was then fastened. Catheter positions were checked and considered correct when, during inspiration to total lung capacity, Pes remained negative and Pga remained positive. The catheter-tip pressure transducers were pneumatically calibrated before insertion.

Cardiac function during all +Gz exposures was monitored by six-lead ECG. Centrifuge +Gz level was controlled by computer using tachometer verification. An accelerometer mounted at heart level behind the seat provided the +Gz analogue signal. All measurements were recorded on a multi-channel strip-chart recorder (Gould, model ES-1000).

Man-mounted and Pressure Equipment

The subjects wore a jerkin similar in design to the Tactical Life Support System (TLSS, Gentex Corp, PA) jerkin (Ref 4) which evolved from the Canadian Forces jerkin (Ref 5). It is a full trunk garment with a bladder over the anterior and lateral rib-cage, and in the inter-scapular space. There is no bladder over the abdomen or back. It was worn over the CSU-15/P G-suit (Irvin Industries, Ont.). The G-suit was pressurized by an anti-g valve (Alar Products, OH). The TLSS oronasal mask/helmet ensemble was used. An oxygen regulator (BF2400, ARO, NY.), designed to provide positive pressure breathing on exposure to high altitude, was used to deliver PBG and pressurize the jerkin to the same level as the mask pressure. With a needle valve on the bleed mechanism, the regulator was set to deliver a constant level of 60 mm Hg PBG. PBG to the mask was controlled using 2 one-way solenoids (Ascolectric, Ont.).

Experimental Design

The experiment consisted of the following five conditions:

1. Experimental condition no. 1 (C-1G) – maximal Valsalva/AGSM at +1 Gz;
2. Experimental condition no. 2 (C-PBG) – assisted PBG at high +Gz;
3. Experimental condition no. 3 (C-sAGSM) – submaximal AGSM at high +Gz;
4. Experimental condition no. 4 (C-mAGSM) – maximal AGSM at high +Gz;
5. Experimental condition no. 5 (C-PBG+mAGSM) – assisted PBG and maximal AGSM at high +Gz.

Experimental Procedures

The subject arrived at the laboratory with flight suit and ECG electrodes on. After the Pes and Pga catheters were inserted, the subject donned the jerkin and G-suit . The subject entered the centrifuge gondola and all the pneumatic and electrical connections were made. The briefing session reminded the subject of the well-practiced procedures. In particular, he was to produce his maximal intra-thoracic pressure, when full AGSM effort was instructed, and to maintain the normal AGSM rhythm. An LED display showing the level of intra-thoracic pressure to the subject encouraged maximal efforts.

In the first experimental condition (C-1G), three maximal straining efforts were performed separated by brief rests. Preparatory +Gz exposures were then made. The subject was exposed to a gradual +Gz onset rate centrifuge profile (0.1 G/sec) until he reached 100% peripheral light loss and/or 50% central light loss. Visual light loss was measured subjectively using a light bar similar in construction to that used by USN (Ref 6). During this centrifuge profile, PBG of 60 mm Hg was delivered at +4 Gz and maintained at that level until the visual end-point criterion was reached. The subject then released an enable switch which automatically stopped the centrifuge. For all subsequent +Gz exposures for that subject, that same peak +Gz level was used. The +Gz plateau was maintained for 20 sec.

Experimental conditions 2–5 were then presented to the subject in preassigned, semi-randomized order. The conditions requiring maximal AGSM were never consecutive. In condition C-PBG, the subject was relaxed and received 60 mm Hg PBG at +4 Gz and for the remainder of the profile. No PBG was provided in C-sAGSM. Submaximal straining was used but only as necessary to avoid reaching the visual end-point.

In C-mAGSM, moderate straining was performed as required during the +Gz onset, and then on reaching the +Gz plateau, maximal AGSM was instructed. (In C-sAGSM and C-mAGSM, the jerkin was worn but was not pressurized.) PBG was provided at +4 Gz in C-PBG+mAGSM and was supplemented with maximal AGSM on reaching the +Gz plateau. At these plateau +Gz levels, subjects could concentrate on performing maximal AGSM without fear of losing consciousness.

Data Analysis

All pressures and +Gz levels were analyzed on the strip chart record. Measurements of Pes, Pmask, Pg-suit, and +Gz were referenced to zero. Values for Pga were taken as displacement above baseline (ΔPga). The "maximal" Pes in an experimental condition was defined as the greatest pressure over a 0.5 sec period. All other Pes levels were measured as the greatest pressure over a 1 sec period. Cardiac artifacts complicate analysis of the Pes waveform, but the effects are negligible at these high Pes levels. All other variables were analyzed over the same time interval as the respective Pes measurement.

The data were statistically studied by repeated measures analysis of variance (alpha level at 0.05). Scheffe post-hoc tests followed significant F-ratio results. Variability about mean values are reported as standard error of the mean (±sem).

RESULTS

Group mean Pes at the end-expiratory lung volume position while sitting in the gondola at +1 Gz was -10 (± 2.9) mm Hg. At end tidal volume, mean Pes was -19.2 (± 3.4) mm Hg. The increase in Pes with PBG was calculated as the difference between Pes at mid-inspiration before PBG and Pes at mid-inspiration with PBG. During C-PBG when group mean Pm was 57.7 (± 0.6) mm Hg, Pes had increased by 55.0 (± 1.6) mm Hg (Figure 1) producing a mean Pes-increase ratio of 0.95 (±0.03).

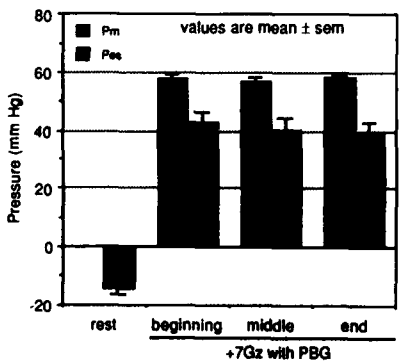

FIGURE 1. Comparison of mask pressure (Pm) and esophageal pressure (Pes) from 3 breaths during condition C-PBG at beginning, middle, and end of +7Gz plateau.

Secondary parameters were uniform for comparison of Pes between C-mAGSM and C-PBG+mAGSM. The +Gz level (mean = +7 Gz) and Pg-suit (mean = 394 mm Hg) were constant for individual subjects.

Pes for all parts of the various experimental conditions are shown in Figure 2. Pes was significantly greater when maximal straining was used (C-1G, C-mAGSM, C-PBG+mAGSM) compared to submaximal efforts (C-sAGSM) or PBG alone (C-PBG). Pes in C-sAGSM was slightly greater compared to the levels in C-PBG. Pes before AGSM started in C-PBG+mAGSM was not statistically different from Pes during C-PBG. Within each 20 sec period in all experimental conditions, the variation in Pes with different breaths/AGSMs was not statistically significant.

The bars marked "max" in C-1G, C-mAGSM, and C-PBG+mAGSM of Figure 2 show maximal Pes over 0.5 sec in their respective conditions. There was no statistical difference among these values. Their average value is 138.9 (± 1.9) mm Hg.

Figure 3 shows ΔPga corresponding to each measurement of Pes in the previous figure. Similar to Pes, ΔPga was greatest when maximal straining was performed. ΔPga was similar in C-sAGSM and C-PBG. At the time of maximal Pes, the ΔPga levels in C-1G, C-mAGSM, and C-PBG+mAGSM were not statistically different. The average ΔPga at maximal Pes was 197.2 (± 3.9) mm Hg, but there were no instructions to the subjects to increase Pga specifically during maximal straining.

DISCUSSION

PBG, both without and with the aid of thoracic counter-pressure, provides substantial increases in G-duration tolerance compared to AGSM tests (Refs 1, 3, 7). However, increases in G-intensity tolerance have not been documented. Due to increases in blood pressure from the potential extra increases in intra-thoracic pressure from PBG and straining maneuvers, improvements in +Gz-intensity tolerance might be expected. If the combination of assisted PBG and maximal AGSM had produced an additive effect on intra-thoracic pressure, maximal Pes would have reached levels approximately 60 mm Hg greater than the observed values. Instead, Pes from straining and PBG was not different from Pes produced by maximal AGSM alone at +7Gz, or by a maximal strain at +1 Gz.

It is unlikely that the difference between the perfect additive effect on maximal Pes and the findings presented here was due to methodological or experimental subject limitations. Reasons for this

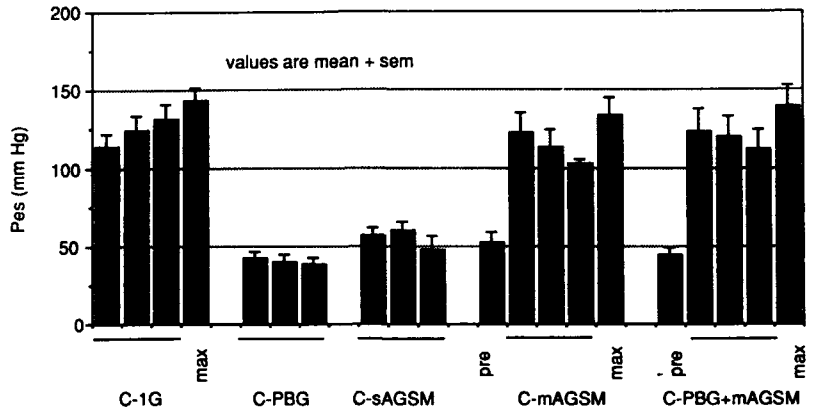

FIGURE 2. Esophageal pressure in all experimental conditions.

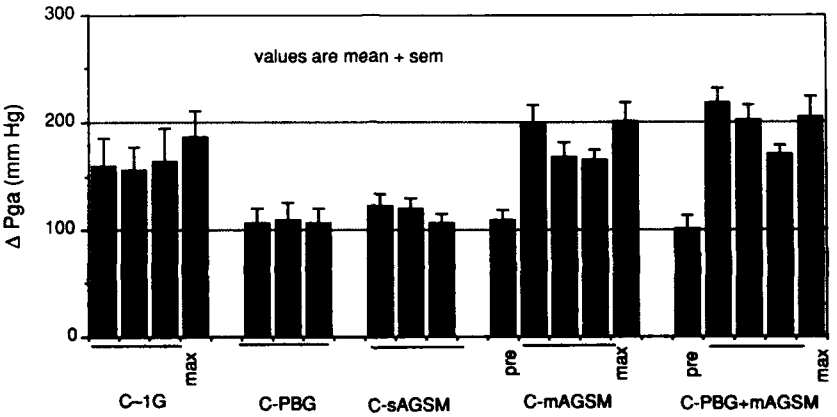

FIGURE 3. Change in gastric pressure in all experimental conditions.

Legend for Figures 2 and 3.
C-1G: maximal valsalva/AGSM at +1Gz.
C-PBG: PBG at high +Gz.
C-sAGSM: submaximal AGSM at high +Gz.
C-mAGSM: maximal AGSM at high +Gz.
C-PBG+mAGSM: PBG and maximal AGSM at high +Gz.
_____ : 3 bars underlined are pressures measured over 1 sec and represent pressures at beginning, middle, and end of high +Gz plateau.
pre: pressure measured before start of maximal AGSM.
max: greatest pressure over 0.5 sec in that experimental condition.

are as follows:

1. Methodological. (a) Pes was measured as an index of intra-thoracic pressure. Although it does not record the absolute pressure around the heart (Ref 8), changes in Pes agree well with changes in pleural pressure (Ref 9). (b) The miniature esophageal pressure transducer performs satisfactorily when compared to the standard esophageal balloon system (Ref 10).

2. Experimental subjects. (a) The maximal Pes recorded at +1Gz agrees with the observations of others (Refs 11, 12). (b) The subjects were highly motivated and performed consistently. Maximal Pes values during +Gz exposure were as high as at +1Gz.

We believe the observations are explained by: (i) inadequate support from thoracic counter-pressure during PBG, and (ii) the characteristics of the expiratory musculature.

Inadequate support from thoracic counter-pressure

We view the thorax during AGSM to behave as the piston model shown in Figure 4. Part of the thorax is represented by the rigid walls. The piston surface represents all the compliant regions of the thoracic wall. All the muscles participating in AGSM, primarily expiratory muscles, are represented by the contractile unit pulling the piston. The inspiratory muscles are ignored. (The effect of +Gz on the chest wall is also omitted. +Gz impedes normal elevation of the chest wall but PBG dampens that effect by assisting to lift the chest.) The model's recoil characteristics are represented by the spring. The spring ensures that the piston returns to the same position in the absence of muscular contraction and in the absence of a pressure differential across the piston surfaces, as in the resting condition shown in Figure 4a.

Figure 4b simulates the situation during AGSM alone. The glottis closes. Concentric contraction pulls the piston inward causing gas compression and an increase in intra-thoracic pressure of 130 mm Hg relative to outside. Boyle's Law describes the proportional relationship between volume reduction and pressure increase.

In Figure 4c, PBG delivers pressurized gas: (i) to the airway, as would occur with an oronasal

FIGURE 4. Mechanical model of some respiratory system components and interaction of anti-G straining manuevers and positive pressure breathing during +Gz.

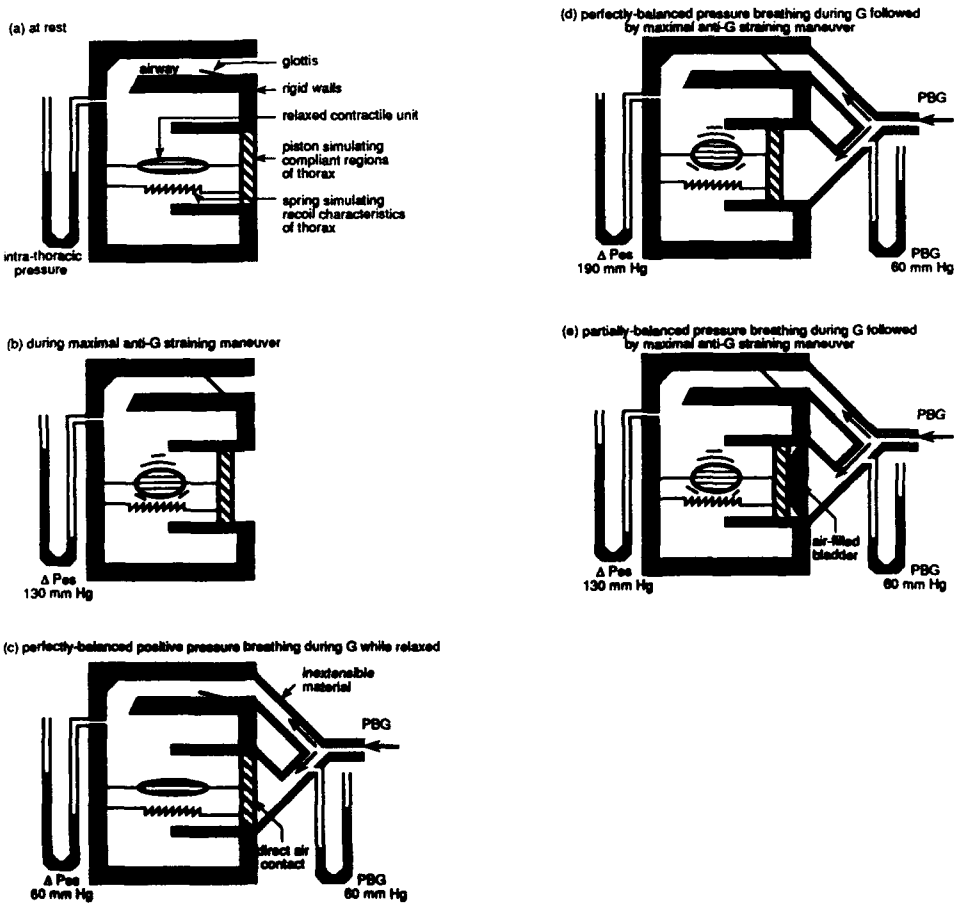

mask with a reflected seal, and (ii) directly to the compliant part(s) of the thorax, most effectively performed by a device similar to an iron lung in which equal pressure is applied to all parts of the thorax. In this figure, the intra-thoracic pressure increase is similar to the elevation in mask cavity pressure and is perfectly balanced by pressure on the piston exterior.

An AGSM is added to perfectly-balanced PBG in Figure 4d. First the muscle is relaxed and intra-thoracic pressure is increased 60 mm Hg by PBG. Then the glottis is closed and AGSM is performed. The straining muscles generate the same transmural pressure difference across the two surfaces of the piston as in Figure 4b. This increment in pressure then adds to the already-elevated intra-thoracic pressure producing 190 mm Hg.

Figure 4e represents PBG with mask and less-than-ideal jerkin. This situation differs from the previous figure by the presence of a bladder interface between the body or piston surface and external pressure. This type of counter-pressure would reproduce the counter-pressure effect of Figures 4c and 4d provided the interface is highly compliant and covers completely, and is supported by a reliable pressure source. This is not the case and the increased intra-pulmonary pressure becomes only partially-balanced at the body surface. Although the jerkin limits chest wall displacement outward, counter-pressure acting in the inward direction is not widely distributed.

There are several indications that the type of counter-pressure used was less than optimal.

1. The physiological consequences of pressure breathing are minimized when counter-pressure garments maintain the subdivisions of vital capacity near the normal levels, particularly that of the end-expiratory position (Ref 13). Only complete trunk coverage with a bladder was successful in this regard. A capstan suit and chest-only counter-pressure with a vest were only slightly better than no counter-pressure at all (Ref 13). The TLSS-style jerkin does not maintain the normal end-expiratory position during PBG. Chest wall shape studies during pressure breathing with 70 mm Hg at +1 Gz indicated that the rib-cage component of lung volume was markedly inflated. The rib-cage had a configuration similar to that at 2 litres above the end-expiratory position without pressure breathing. Only by abdominal compression through pressurization of the G-suit (at 4x Pm)was resting lung volume during pressure breathing brought close to pre-pressure breathing levels (Ref 14).

2. Although the outer shell of the TLSS-style jerkin covers the entire trunk, the bladder only covers the inter-scapular space and the anterior to mid-lateral portion of the rib-cage. (Some lower trunk support is provided by the abdominal bladder of the G-suit). This is significantly less than the all-encompassing bladder of the RAF jerkin which, from the view of respiratory and cardiovascular support, successfully balances pressure breathing at +1Gz. Figure 4e illustrates the problem with a bladder which does not provide complete coverage. Counter-pressure only occurs between surfaces in contact. Small bladders or ballooning of bladders reduce the contact area and the effectiveness of the counter-pressure. Unsupported body regions are compliant structures which waste the potential rise in intra-thoracic pressure. With the TLSS-style jerkin, two candidate regions for added support are the anterior and lateral aspects of the costal margin. Here chest wall movement is possible due to displacement of the diaphragm by changes in either intra-thoracic or intra-abdominal pressure.

3. Full trunk counter-pressure compared to chest only coverage increased the blood pressure elevation with pressure breathing (Ref 15). The closeness-of-fit of the jerkin is also important. During 70 mm Hg pressure breathing, blood pressure was 22 mm Hg greater with a tightly-fitted TLSS-style jerkin compared to a jerkin fitted more loosely (Ref 16). The tightly-fitted jerkin reduced vital capacity by 0.5 litre before pressure breathing.

It is also possible that contact between the inner jerkin liner and the thorax is not constant. To compress gas at the start of AGSM, muscle contraction reduces the size of the chest causing the chest wall to move inward away from the jerkin. Until pressure in the bladder and surface contact are restored, counter-pressure is incomplete.

Characteristics of expiratory musculature

From the preceding analysis, inadequate thoracic counter-pressure can account for the failure of combined PBG and maximal AGSM to increase intra-thoracic pressure to the level determined by the sum of their individual effects. That the maximal intra-thoracic pressure with PBG, jerkin, and maximal AGSM is not different from maximal AGSM alone suggests this counter-pressure is very ineffective. It may be so ineffective that assisted PBG more closely resembles unassisted PBG (PBG without a jerkin) than perfectly-balanced PBG. In unassisted PBG, the characteristics of the expiratory musculature can predict the ceiling of Pes when maximal AGSM is combined with PBG.

The ability of the expiratory muscles to generate intra-pulmonary pressure (a good indicator of Pes in this situation) is described by the maximal pressure-lung volume (PV) diagram (Figure 5).

Maximal Valsalva-type maneuvers were used in the development of the original PV diagram (Ref 11). These findings were confirmed using AGSM (Ref 12). The horizontal distance from the ordinate to the heavy dashed curve in the PV diagram show the maximal intra-pulmonary pressures that can be produced when the expiratory/AGSM muscles contract against a closed airway as measured at different lung volumes. The expiratory muscles produce the greatest intra-pulmonary pressure (approximately 172 mm Hg in this example) when lung volume is near full vital capacity at the start of the effort. The maximal pressure that can be generated decreases exponentially when lung volume decreases. This explains the success of maximal AGSM after a rapid inspiration to a high lung volume. The hyperinflation produced by pressure breathing may confer a similar benefit. It places the expiratory muscles at a more advantageous position to generate force.

During expiratory efforts against a closed glottis, the forced decrease in lung volume causes compression of gas. The lung volume decrease for a maneuver performed at 100% vital capacity is represented by the sloping line with a single arrow in Figure 5. This line joins the top of the ordinate, at a time just before the strain, with the maximal pressure produced during the strain at that lung volume. At maximal pressure, the maximal forces of the expiratory muscles attempting to further reduce lung volume are equally opposed by the elevated intra-pulmonary pressure. A sub-maximal effort AGSM at any lung volume would be represented by a pressure located within the boundaries defined by the maximal pressure curve, the volume reduction curve, and the ordinate.

The heavy dashed curve in Figure 5 indicates typical pressures achievable during maximal voluntary expiratory efforts. They do not indicate the overall maximal pressure that can be generated by the muscles. Intra-thoracic pressures as high as 300 mm Hg can be produced transiently during cough (Ref 17). Reflexive inhibition of muscle may limit the maximal pressure that can be generated voluntarily.

The shaded area in Figure 5 represents the pressure supplied by PBG. A breathing regulator can provide the work for the first 60 mm Hg of pressure. For intra-pulmonary pressure to exceed 60 mm Hg, the muscles first generate isometric tension equivalent to producing 60 mm Hg pressure without PBG (i.e. to the rightward limit of the shaded area of Figure 5). This amount of tension does not change lung volume. When additional tension from maximal AGSM compresses gas further, intra-thoracic pressure increases. The total pressure, however, would not exceed that defined by the maximal pressure curve. Since muscular contraction is used to reach any pressure beyond the PBG level, it follows that the sense of AGSM effort would be in parallel with the total pressure rather than the pressure change from 60 mm Hg to the final level. In other words, an AGSM effort which adds 2 +Gz of +Gz-intensity tolerance to 2 +Gz of tolerance already provided by PBG, will feel like a 4 +Gz strain and not like 2.

The effort needed requires experimental verification. It contrasts an earlier analysis which cites pilots' reports of reduced AGSM effort with PBG at +9 Gz (Ref 18). Perhaps part of the difference is due to: (i) the greater lung volume during PBG which optimizes the position for the chest wall to generate positive pressure, and/or (ii) the lifting of the chest wall by PBG which assists inspiration. The analysis would also predict that when thoracic partial pressure garments evolve from minimal coverage to more complete counter-pressure, AGSM adding 2 +Gz of protection to PBG will feel like a 2 +Gz AGSM; and, the effect of PBG and maximal AGSM on Pes will be additive.

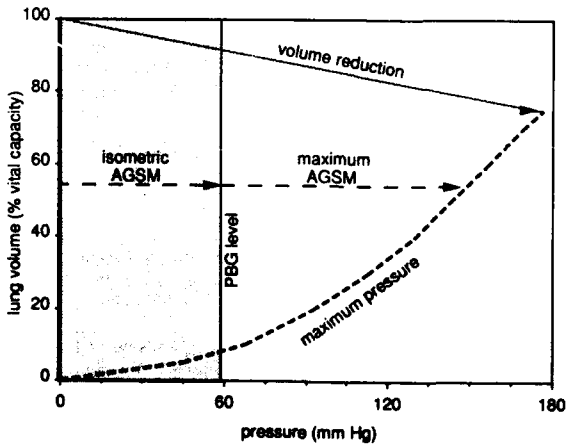

FIGURE 5. Pressure-volume diagram. Heavy dashed curve (– – –) represents maximal expiratory intra-pulmonary pressure at different lung volumes (after Rahn et al., 1946). Single arrow (—►) represents reduction in lung volume due to gas compression when maximal pressure is exerted at 100% of vital capacity. Shaded area represents intra-pulmonary pressure produced with PBG 60 mm Hg; when AGSM is added to PBG, the left dashed arrow (– –►) represents the potential intra-pulmonary pressure resulting from the submaximal isometric AGSM. The right dashed arrow(– – ►) shows the added pressure resulting from the maximal AGSM.

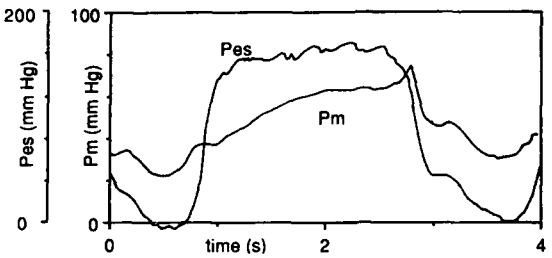

FIGURE 6. Actual record of mask cavity pressure (Pm) and esophageal pressure (Pes) during assisted PBG (approx. 60 mm Hg) and maximum AGSM at +7Gz.

Other Observations Performing AGSM with PBG.

PBG requires a reliable pressure source. The experimental records of PBG with AGSM show that Pm is greatly reduced immediately after the rapid inspiration and during the first portion of the strain compared to the normal PBG level (Figure 6). Therefore, both PBG level and counter-pressure from the jerkin were less than would be expected. A breathing regulator with insufficient capacity to meet the flow demands from inspiration and the volume demands for jerkin pressurization could explain these results.

During preliminary experiments, one subject could not increase Pes with PBG and AGSM much above his level with PBG alone, even though his maximal Pes with only AGSM was substantially greater. When his straining technique incorporated a more pronounced "hook" sound (Ref 19), Pes increased. PBG probably made closure of the glottis more difficult. Positive pressure breathing distends the upper respiratory passages (Ref 15) and the glottis may have to be moved farther to obtain complete closure. If the glottis is not completely closed during AGSM, intra-pulmonary gas compression forces air out through the mask, leading to loss of pressure.

Conclusions

1. At high +Gz, maximal intra-thoracic pressure generated by the combination of maximal AGSM and PBG with small-bladder thoracic counter-pressure garments is not greater than pressure produced by maximal AGSM alone. Therefore, the G-intensity protection obtained separately from PBG and AGSM is not additive.

2. Assisted (or balanced) PBG using thoracic garments which provide less than full trunk counter-pressure should be regarded as only partially-balanced PBG.

Implications of Findings

1. Jerkins were originally designed to limit hyperinflation of the lungs and assist expiration during positive pressure breathing for hypoxia protection. Even jerkins with smaller bladders fulfill this role. With only slight modifications, similar jerkins are being used with PBG, but the present analyses suggest that their value during PBG may have been underestimated. Greater increases in intra-thoracic pressure might be produced with larger jerkins, or with greater pressure in the jerkin compared to the mask in those jerkins with smaller bladders. Designs of thoracic counter-pressure garments should consider both hypoxia and +Gz protection roles, but expanded coverage for physiological protection must be reconciled with minimal coverage for flying comfort.

2. Breathing regulators must provide high gas flow to meet the most demanding respiratory requirements in the cockpit (Ref 20). Inspiratory flow during vigorous AGSM can reach 4.7 litres/sec BTPS (Ref 21). Design specifications must also consider frequent pressurization of high-volume thoracic counter-pressure garments during PBG and AGSM.

3. The AGSM will likely remain a vital component of any G-protection system for the upright aviator. Even with PBG, straining training in the centrifuge will be necessary.

REFERENCES

1. Shubrooks SJ. Positive-pressure breathing as a protective technique during +Gz acceleration. J. Appl. Physiol. 35 (1973): 294-298.

2. Leverett SD Jr, Burton RR, Crossley RJ, Michaelson ED, Shubrooks SJ. Physiologic responses to high sustained +Gz acceleration. Brooks AFB, TX: School of Aerospace Medicine, 1973. Report SAM-TR-73-21.

3. Burns JW, Balldin UI. Assisted positive pressure breathing for augmentation of acceleration tolerance time. Aviat. Space Environ. Med. 59 (1988): 225-233.

4. Eng KG, Gupta A, Lloyd AJP, Robinson JK. Tactical Life Support System. Brooks AFB, TX. Human Systems Division, May 1988. Report HSD-TR-87-009.

5. Michas RD, Porlier JAG, Rud RC. Development and testing of a new partial pressure jerkin. Downsview, Ontario: Defence and Civil Institute of Environmental Medicine, November 1981. DCIEM Report No. 81-R-39.

6. Hrebien L, Hendler E. Factors affecting human tolerance to sustained acceleration. Aviat. Space Environ. Med. 56 (1985): 19-26.

7. Shaffstall RM, Burton RR. Evaluation of assisted positive pressure breathing on +Gz tolerance. Aviat. Space Environ. Med. 50 (1979): 820-824.

8. Smiseth OA, Veddeng O. A comparison of changes in esophageal pressure and regional juxtacardiac pressures. J. Appl. Physiol. 69 (1990):1053-1057.

9. Cherniak RM, Farhi LE, Armstrong BW, Proctor DF. A comparison of esophageal and intra-pleural pressure in man. J. Appl. Physiol. 8 (1955): 203-211.

10. Gilbert R, Peppi D, Auchincloss JH Jr. Measurement of transdiaphragmatic pressure with a single gastric-esophageal probe. J. Appl. Physiol.: Respirat. Environ. Exercise Physiol. 47 (1979):628-630.

11. Rahn H, Otis AB, Chadwick LE, Fenn WO. The pressure-volume diagram of the thorax and lung. Am. J. Physiol. 146 (1946):161-178.

12. Cote R, Tripp L, Jennings T, Karl A, Goodyear C, Wiley R. Effect of inspiratory volume on intrathoracic pressure generated by an L-1 maneuver. Aviat. Space Environ. Med. 57 (1986):1035-1038.

13. Roxburgh HL, Ernsting J. The physiology of pressure suits. J. Aviat. Med. 28 (1957): 260-271.

14. Buick F, Roberts J. Chest wall shape during positive pressure breathing. Paper presented at 58th Annual Scientific Meeting of the Aerospace Medical Association, Las Vegas, NV, 10-14 May 1987.

15. Ernsting J. Some effects of raised intrapulmonary pressure in man. AGARDograph 106. London: McKay, 1966.

16. Buick F, Porlier G, Maloan J. Cardiovascular responses to pressure breathing with loose and tight jerkin. Aviat. Space Environ. Med. 60 (1989) : 496.

17. Sharpey-Schafer EP. The mechanism of syncope after coughing. Brit. Med. J. 2 (1953): 860-863.

18. Harding RM, Bomar JB. Positive pressure breathing for acceleration protection and its role in prevention of inflight G-induced loss of consciousness. Aviat. Space Environ. Med. 61 (1990): 845-849.

19. Whinnery JE, Murray DC. Enhancing tolerance to acceleration (+Gz) stress: the "hook" maneuver. Naval Air Development Center, PA. 1990; Report No. NADC-90088-60.

20. White JT, Morin LME. Anti-G straining maneuver incompatibility with tactical aircraft oxygen systems. Aviat. Space Environ. Med. 59 (1988): 176-177.

21. Buick F. Inspiratory breathing resistance and +Gz tolerance. Paper presented at 61st Annual Scientific Meeting of the Aerospace Medical Association, New Orleans, LA, 13-17 May 1990

APPENDIX

This report is DCIEM publication number – DCIEM No. 91-43.

ACKNOWLEDGEMENTS

We extend our appreciation to Mr. Jim Maloan and Mr. Michel Paul for technical assistance, to LCdr Fred Maggio for medical supervision, and to Mr. Dave Eaton and Dr. John Frim for valuable discussions. Special thanks to the volunteers of the A-team for another outstanding performance in the centrifuge.

The Influence of High, Sustained Acceleration Stress on Electromyographic Activity of the Trunk and Leg Muscles

Larry P. Krock, PhD
Mark W. Cornwall, PhD

Crew Systems Directorate
Armstrong Laboratory
Brooks Air Force Base, Texas 78235-5301
United States
and the
Department of Physical Therapy
Arizona State University
Flagstaff, Arizona
United States

SUMMARY

This study investigated the level and pattern of trunk and lower extremity muscle activity in aircrew performing the anti-G straining maneuver (AGSM) at high, sustained $+G_z$. Ten male, trained centrifuge riders experienced rapid onset profiles (4G/s) to $+6\ G_z$ and sustained this level on the Armstrong Laboratory's Human Centrifuge until greyout. Surface electromyography (EMG) was recorded from the erector spinae, lateral abdominal, biceps femoris, vastus lateralis, and lateral gastrocnemius muscles of the subject's dominant side. The normalized root mean square (RMS) and mean power frequency (MPF) were calculated for each muscle at 1-second intervals throughout the exposure. The RMS amplitude for the muscles of the lower extremity showed a marked decrease (-61.45%) while muscles of the trunk exhibited a slight increase (+3.45%). The MPF of the EMG signal did not demonstrate a significant change during the exposure. Motor unit recruitment decreased in the lower extremity muscles during exposure. None of the studied muscles demonstrated a shift in the MPF suggesting evidence of fatigue. The results of the present study suggest the importance of maintaining a high level of muscle activity in the legs throughout exposure to sustained high levels of acceleration stress that require use of the AGSM.

INTRODUCTION

Physiologic techniques to counter increased acceleration stress has a moderately long history. Initiated informally by World War I pilots and used by pioneering acrobatic pilots who had experienced fainting and vision decrements (5), the technique of straining was formally defined in the early 1940s (24). Shubrooks and Leverett (16) recommended minor modifications to enhance the efficacy of the procedure. During sustained high acceleration stress encountered by pilots of high performance aircraft, the anti-G straining maneuver (AGSM) is essential to successful tolerance to these stresses, especially during the onset phase of the stress. The importance of proper AGSM performance to achieve and sustain high levels of $+G_z$ stress, is underscored by the establishment of aircrew training programs by the United States Air Force and Navy.

Untrained individuals performing the AGSM, which requires near-maximal activation of several muscle groups, generally do poorly in the straining maneuver and experience rapid fatigue. Several reports have demonstrated that a generalized (whole body) resistance (strength) training program can enhance individual tolerance to acceleration stress (8, 11, 20, 22). Compliance problems arise with collective training regimens; they require a large time investment, and yield disproportionate benefits across the population. In response to these difficulties, attempts have been made to assess the influence that specific muscle group strengthening regimens have on extending acceleration tolerance. The results of these muscle-specific programs have not demonstrated promise for improving $+G_z$ tolerance (2, 17, 21). Development of an efficient resistance training regimen to offset the shortcomings of the generalized and muscle-specific training programs makes it necessary to evaluate the contribution of regional muscular groups in performing the AGSM.

The objective of this investigation was therefore to analyze the contribution of the regional muscular groups of the trunk and lower extremities and to evaluate fatigue-related changes that occur in the frequency component of the myoelectric signal in crewmembers performing the AGSM at high sustained acceleration stress.

METHODS AND MATERIALS

Subjects: Ten males from the Armstrong Laboratory, Brooks Air Force Base acceleration panel volunteered for this experiment. Their ages ranged from 21 to 32 with an average of 27.5 years. All subjects were in good health and were experienced centrifuge riders. The voluntary, fully informed consent of the subjects used in this research was obtained as required by AFR 169-3.

Centrifuge and equipment configuration: Subjects were seated in the upright (13° backangle) ACES II seat of the 6.1 meter Human Centrifuge at the Armstrong Laboratory, Brooks AFB. The foot plate was adjusted to position the heels at approximately 9 cm above the floor with the knee joint angle at approximately 120° in extension. Subjects wore individually fitted standard CSU 13 B/P G-trousers.

Experimental protocol: The volunteers were assisted and secured in the gondola following instrument calibration and application of the electrodes. The acceleration exposure consisted of a rapid onset ($+4\ G_z\ s^{-1}$) profile to a peak of $+6\ G_z$. The subjects sustained this acceleration level until experiencing light loss criteria (greyout) caused by fatigue. Each subject was evaluated with the G-trousers pressurized at the standard schedule (initiated at $+2\ G_z$; thereafter, the pressure increased at 1.5 psi for each additional $+G_z$). These procedures were repeated three times on separate days. A minimum of 1 day without G exposure was provided between trials.

Electromyography: placement and data processing: Surface electrodes (3 mm, Ag-AgCl) were positioned overlying the erector spinae (ES), abdominal lateral oblique (LO), bicep femoris (BF), vastus lateralis (VL) and the lateral gastrocnemius/soleus(GS) muscles of the subject's dominant limb. An interelectrode distance of 2.0 to 2.5 mm near the motor point of the muscle was selected; skin/electrode impedance was reduced to less than 10 kOhms. Electromyographic (EMG) signals were bandpass filtered at 3 and 500 Hz, differentially amplified, and recorded at 3.5 ips on intermediate band FM tape for later processing.

Electromyographic data for each trial were converted from analog to digital format at 1024 samples per second. One-second segments at quartile intervals were selected for each muscle to represent the individual acceleration exposures. Electromyographic signal amplitude was determined using a root mean square (RMS) algorithm (3). These data were normalized to a one-second RMS segment when the subject achieved the maximum $+G_z$ level. The mean power frequency (MPF), from the spectral analysis of the quartile segments, for each of the observed muscles, was also calculated (13).

Data Analysis: The RMS amplitude data were found to be nonnormally distributed; therefore, these data were logarithmically transformed (18). The values for RMS amplitude and MPF, for all muscles, at each quartile segment were averaged across trials for individual subjects, yielding a mean RMS and MPF value for each. These subject mean data were used to evaluate between and within muscle differences in RMS amplitude and MPF during the sustained acceleration exposure.

RESULTS

The mean normalized log RMS amplitude in the lower leg muscles steadily decreased (Fig 1) throughout the acceleration exposure ($F=8.7$, $df=4,36$, $p<0.05$). The amplitude decrease from the beginning to the end of the exposure was 61.5%. The response profiles for the three observed muscles of the leg were quite similar. Trunk muscles, however, demonstrated a more varied activation pattern throughout the exposure; the LO muscle exhibited the largest variability. The mean change in log RMS amplitude for the trunk muscles increased slightly by 3.5%. Furthermore, the amplitude of the muscle motor unit activity between the trunk and the leg muscles was different ($F=8.55$, $df=4,36$, $p<0.05$).

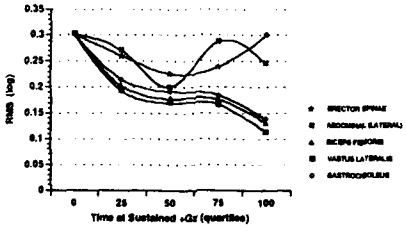

Figure 1. Group mean log RMS amplitude by muscle across the +6 Gz exposure.

Evaluation of the MPF simple main effect data indicated no substantive change (Fig. 2). The ES was the only muscle to exhibit any marked change throughout the exposure. The ES MPF shifted to a higher frequency through the middle segment of the exposure; however, the MPF returned to the frequency near that established for the earlier segment by the end of the exposure. In addition to the variable changes observed in the MPF frequency across the exposure, the ES muscle exhibited a much higher frequency of activation than the other muscles studied. Again, the leg muscles performed differently than those of the trunk.

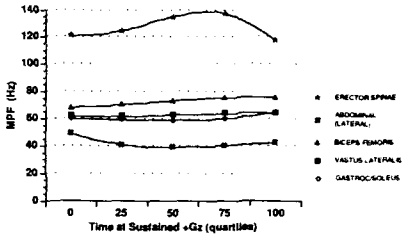

Figure 2. Group mean Mean Power Frequency by muscle across the +Gz exposure.

DISCUSSION

Tension developed by a muscle is produced and controlled by modulating the number of motor units participating in the activity—amplitude, and by varying the nerve firing frequency to the active motor units—frequency modulation (1). The present study evaluated these tension-producing characteristics for active motor units by observing surface EMG for selected muscles of the leg and trunk in subjects performing the AGSM at a high level of sustained acceleration stress. Generally, we found the leg muscles produced a consistently different response than that observed from muscles of the trunk.

Change in EMG amplitude is considered to indicate of the recruitment pattern of muscle motor units attempting to maintain a specified level of tension (4, 7). In this study, the myoelectric signal amplitude of the legs decreased throughout the $+G_z$ exposure suggesting that the subjects were able to decrease this component of generating tension in the leg muscles as the exposure to $+G_z$ continued. This recruitment pattern is different from that stated in the literature, in which a linear relationship is described between the increasing amplitude of the EMG and generated muscle tension while performing fatiguing isometric contractions (4, 7, 14). The discrepancy between the findings of the present study and those found in the literature may be attributed to the reduction in applied tension (AGSM) our subjects produced as they became more comfortable with the level of stress; i.e., they "sensed" the magnitude of the AGSM required to maintain peripheral vision. Basic EMG research generally employs a uniform resistance at a known percentage of an individual's maximum voluntary contraction capacity.

It is interesting to note that the patterns of change across the $+G_z$ exposure for the three observed leg muscles were quite similar. The BF, VL and the GS muscles participated equally in the AGSM performance. The demonstration here of the substantial contribution to the AGSM by the BF

and GS muscles is important since the LO and VL muscles were considered to be the primary agonists of the AGSM (2, 17, 21).

The surveyed muscles of the trunk demonstrated a less consistent pattern of recruitment. After an initial decline in the mean RMS amplitude, the ES and LO muscles increased their recruitment activity. This increase, approximately halfway through the $+G_z$ exposure, indicates a call for additional motor units to activation in order to maintain the necessary muscle tension as the duration of the activity progresses. These data agree with those of Balldin et al. (2), and Williams et al. (23).

The central index (the point in the spectrum where the power is equal above and below) for myoelectric firing frequencies observed in the muscles of this study were similar to those reported in the literature (10, 12, 15). The MPF viewed for the ES muscle was much higher, at approximately 120 Hz, than those for the other muscles, 40-70 Hz. This finding may indicate the activation of more fast twitch motor neurons in the ES muscle than in the other muscles studied (12, 14).

Simple main effects analysis did not indicate a substantial change in the MPF throughout the $+G_z$ exposure for the observed muscles. The MPF for the ES, however, increased through the middle phase of the exposure, and showed a trend of fatigue near the end of the trial. The other monitored muscles did not show any shift in the central index frequency indicating muscular fatigue was encountered or imminent.

The lack of evidence indicating muscular fatigue in this study is in contrast with reports describing changes in a central, biochemical index of fatigue during exposure to simulated aerial combat maneuvers (6,19). The discrepency among these findings may be due to the nature of the observed markers. Changes in venous blood lactic acid levels are systemic indicators of muscular work. The lactic acid produced must diffuse out of the muscle and into the intracellular space, then become distributed throughout the venous system before an accurate blood assay may be made (19). The MPF is a peripheral indicator of fatigue and is specific to the muscle observed. It is possible the well-defined relationship between the MPF and muscle fatigue does not apply to conditions of sustained $+G_z$ stress because of the unique type of muscle activation pattern performed during the AGSM.

The evidence of fatigue, identified by a shift of the MPF to a lower frequency, has been established for sustained contractions held at a percentage of the subject's maximum voluntary contraction. The AGSM, while viewed as a "whole body" activity consisting of predominantly maximum isometric contractions, varies with respiration and the perceived degree of intensity of the stress (remaining peripheral vision). It is possible that the shift in MPF may not be sensitive to the fatigue changes brought about by this nonuniform exercise. Likewise, the central biochemical assay may be indicating fatigue in muscles that are not primary agonists for the AGSM. Future, well-designed experiments will be required to sort out the differences in these indexes under this very complex physical activity.

Summarizing the results of the present study we found: (1) motor unit recruitment decreased in muscles of the lower extremity while muscles of the trunk remained relatively unchanged; (2) none of the muscle studies indicated fatigue; (3) the ES muscle showed some initial signs of fatigue; and (4) the posterior aspects of the thigh and the leg are active during AGSM performance. These results suggest the importance of maintaining a high level of muscle activity in the legs throughout exposure to sustained high levels of acceleration stress.

The practical implication for these data proposes that the legs should be a principal component of any strength training regimen performed to enhance acceleration endurance tolerance. Furthermore, in addition to the extensors of the leg (quadriceps), the flexors of the leg (hamstrings) and the extensors of the foot (calf) should be an integral component of these strengthening programs. While the results of this study do not indicate that the back and the abdominal muscle have a major contributory role in performing the AGSM they should not be excluded by any training regimen; they may, however, be de-emphasized in favor of leg development. Finally, in addition to maximum strength development, accomplished by high resistance, low repetition regimens, strength endurance must be enhanced. This component of strength is enhanced by decreasing the total resistance applied and increasing the number of repetitions for a specified task. This latter component of strength may well be the best method to enhance acceleration endurance tolerance.

REFERENCES

1. Adrian, E. D., & D. W. Bronk The discharge of impulses in motor nerve fibers. Part II. The frequency of discharge in reflex and voluntary contractions. J. Physiol. (Lond.). 67:199-151,1929.

2. Balldin, U. I., K. Myhre, P. A. Tesch, U. Wilhelmsen, & H. T. Anderson. Isometric abdominal muscle training and G Tolerance. Aviat. Space and Environ. Med. 56: 120-124, 1985.

3. Basmajian, J. V., H. C. Clifford, & W. D. McLeod. Computers in Electromyography. London. Butterworths, 1975.

4. Bigland, B., & O. C. J. Lippold. The relationship between force, velocity and integrated electrical activity in human muscles. J. Physiol. (Lond.), 123: 214-224, 1954.

5. Burton, R. R. G-induced loss of consciousness: Definition, history ,current status. Aviat. Space and Environ. Med. 59: 2-5, 1987.

6. Burton, R. R., J. E. Whinnery, & E. M. Forster. Anaerobic energetics of the simulated aerial combat maneuver (SACM) Aviat. Space and Environ. Med. 58: 761-767, 1987.

7. Edwards, R. G, & O. C. J.Lippold. The relation between force and integrated electrical activity in fatigued muscles. J. Physiol (Lond.) 132: 677-681, 1956.

8. Epperson, W. L., R. R. Burton, & E. M. Bernauer. The effectiveness of specific weight training on simulated aerial combat maneuvering G-tolerance. Aviat. Space Environ. Med., 56:534-539, 1985.

9. Komi P. V. & P. A. Tesch. EMG frequency spectrum, muscle structure, and fatigue during dynamic contractions in man. Eur. J. Appl. Physiol. 42:41-50, 1979.

10. Lindstrom L., R. Kadefors, & I. Petersen An electromyographic index for localized muscle fatigue. J. Appl. Physiol. Respirat. Environ. Exerc. Physiol. 43: 750-754, 1977.

11. Mizumoto, C. & M. Iwane. The effects of isotonic training on $+G_z$ tolerance. Japanese J. Aerospace Environ. Med. 25:15-29,1984.

12. Moritani, T, A. Nagata & , M. Muro. Electromyographic manifestations of muscular fatigue. Med. Sci. Sports Exercise, 14: 198-202, 1982.

13. Petrofsky, J. S. Computer analysis of the surface EMG during isometric exercise. Computers in Biology and Medicine 10: 83-95, 1980.

14. Petrofsky, J. S., R. M. Glaser, C. A. Phillips, A. R. Lind, & , C. Williams. Evaluation of the amplitude and frequency components of the surface EMG as an index of muscle fatigue. Ergonomics 25: 213-223, 1982.

15. Petrofsky, J. S., & A. R. Lind. Frequency analysis of the surface electromyogram during sustained isometric contractions. Eur. J. Appl. Physiol. 43: 173-182, 1980.

16. Shubrooks, S. J., Jr., & S. D. Leverett, Jr. Effect of the Valsalva maneuver on tolerance to $+G_z$ acceleraton stress. J. Appl. Physiol. 34:460-466, 1973.

17. Spence, D. W, M. J. Parnell, R. R. Burton. Abdominal muscle conditioning as a means of increasing tolerance to $+G_z$ stress. Washington, DC: Preprints of the Aerospace Medical Association, 1981.

18. Tabachnick, B. G., & L. S. Fidell. Using multivariate statistics. New York, Harper & Row, Publishers, 1983, p.66-83.

19. Tamir, A., R. R. Burton, & E. M Forster. Blood lactic acid levels following exposures to sustained $+G_z$. Aviat. Space and Environ. Med. 59: 54-56, 1988.

20. Tesch, P. A. Physical performance and G_z tolerance. Physiologist. 31(Suppl.):S105A-S105B, 1988.

21. Tesch P. A., & U. I. Balldin. Muscle fiber type composition and G-Tolerance. Aviat. Space and Environ Med. 55: 1000-1003, 1984.

22. Tesch, P. A., M. D. Hjort, & U. I. Balldin. Effects of strength training on G-tolerance. Aviat. Space Environ. Med. 54:691-695, 1983.

23. Williams S. A., J. E. Douglas, & G. Miller, The relationship between changes in arterial pressure, esophageal pressure and the EMG of various muscle groups during the L-1 straining maneuver at different spine-to-thigh angles: A final report.Technical Documentary Report No. AAMRL-TR-87-049, Wright Patterson AFB, Ohio, Jun., 1987, pp. 1-46.

24. Wood, E.H., & C. F. Code. The physiologic basis of voluntary (self-protective) maneuvers capable of increasing man's tolerance to positive acceleration. XVII International Physiol. Congress,1947,311-312.

The Valsalva maneuver and its limited value in predicting +Gz-tolerance.

E.J. van Lieshout (1,2), J.J. van Lieshout (2), J. Krol (3), M. Simons (3), J.M. Karemaker (4)

Dept. of Aviation Medicine (1), Royal Netherlands Air Force, Soesterberg, the Netherlands.
Dept. of Internal Medicine (2) & Dept. of Physiology (4), Academic Medical Center of the University of Amsterdam, the Netherlands.
Netherlands Aerospace Medical Centre (3), Soesterberg, the Netherlands.

address for correspondence:

E.J. van Lieshout, M.D., 1st LT RNLAF,
Academical Medical Center,
dept. of Internal Medicine, F4-257,
Meibergdreef 9,
1105 AZ Amsterdam
The Netherlands

Summary

The aim of the present study was to investigate in healthy subjects if responses to a cardiovascular reflex test, the Valsalva maneuver, might be predictive for +Gz-tolerance. The main finding is a significant correlation between blood pressure recovery during VM and peripheral light loss (relaxed, before executing the M1/L1-maneuver) ($r=0.63$, $p<0.05$). All other parameters, including baroreflex sensitivity, did not significantly correlate with +Gz-tolerance. Furthermore intact baroreflex pathways were determined in all subjects. These results indicate that the parameters derived from the cardiovascular responses to VM may only confirm baroreflex integrity. Therefore VM might be used in the diagnostic proces of fighter pilots with repeated +Gz-loss of consciousness inflight who are suspected of an orthostatic disorder. However in healthy subjects VM has limited value in predicting +Gz-tolerance.

Introduction

Cardiovascular reflexes play a major role in adaptation to downwards shift of blood induced by +Gz-stress (1). In clinical medicine the integrity of neural cardiovascular reflex control is assessed by analysing the continuous blood pressure (BP) and heart rate (HR) responses to different maneuvers, such as the Valsalva maneuver (2). In the development of screening tools to predict +Gz-tolerance in fighter pilot trainees selection the question arised if the magnitude of the cardiovascular responses upon fluid shifts and pressure changes as elicited by the Valsalva maneuver might be predictive for +Gz-tolerance.
The present study was designed to investigate the cardiovascular (i.e. BP and HR) responses to the Valsalva maneuver in healthy subjects and to correlate these findings with +Gz-tolerance in centrifuge-runs.

Methods

Subjects: 10 healthy male subjects (Mean age: 31 years (range 24-43), mean weight 77 kg (range 67-96), height 181 cm (range 168-193), mean resting systolic and diastolic auscultatory BP 127/78 mmHg (range 116-150/68-88), and mean resting HR 68 bpm (range 54-83)

Valsalva maneuver: expiratory pressure of 40 mm Hg for 15 s **without** muscle tensing.

Measurements during the Valsalva maneuver: 1: continuous non-invasive finger BP (TNO model 5 Finapres™) 2: instantaneous HR (from the electrocardiogram)

The five classical phases of the Valsalva BP response were identified with five sample points (fig. 1) and for statistical analysis were used: the initial BP rise relative to control BP (a in fig. 1), BP fall (a-b in fig. 1B) and BP recovery (c-b in fig. 1). Maximal (HR_{max}) and minimal HR (HR_{min}) (fig. 1) were determined, as well as the Valsalva ratio (HR_{max}/HR_{min}) (4).

Profiles of the centrifuge-runs: profile 1: acceleration 0.1 G/s, relaxed(R) until PLL (**PLL R**). At PLL R the subject started to strain(S) and the run was terminated when PLL (**PLL S**) re-occurred; profile 2: with anti-G-suit (**PLL Rags & PLL Sags**).

Statistical analysis: BP and HR data were correlated with +Gz-level of PLL data by means of linear regression analysis. A value of $p<0.05$ was considered significant.

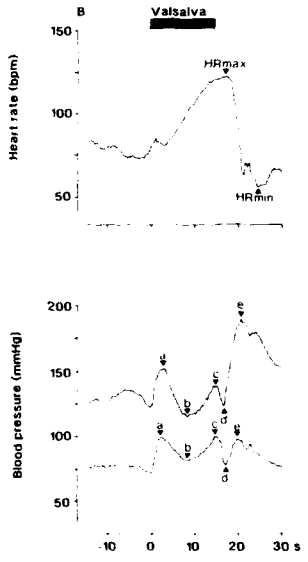

figure 1

Characteristics sample points of the **Valsalva maneuver**: a=BP rise; b=BP fall; c=last beat during strain; d=BP fall after release; e=BP overshoot. Bar marked Valsalva indicates duration of straining period.
From: (3) Ten Harkel e.a. J. Appl. Physiol. 1990; 68:147-53. Reprinted with permission.

Results

PLL R (in +Gz) was 4.2±0.9, PLL S: 7.5±1.2, PLL Rags: 5.5±1.4, and PLL Sags: 8.5±0.05.
Mean BP recovery during VM correlated significantly with PLL ($r=0.63$, $p=0.049$). Furthermore no significant correlation was found between BP and HR responses to standing (initial BP rise, fall & overshoot, maximal and minimal HR) or forced breathing (I-E difference) and PLL. Cardiovascular findings were within normal range revealing no cardiovascular autonomic dysfunction.

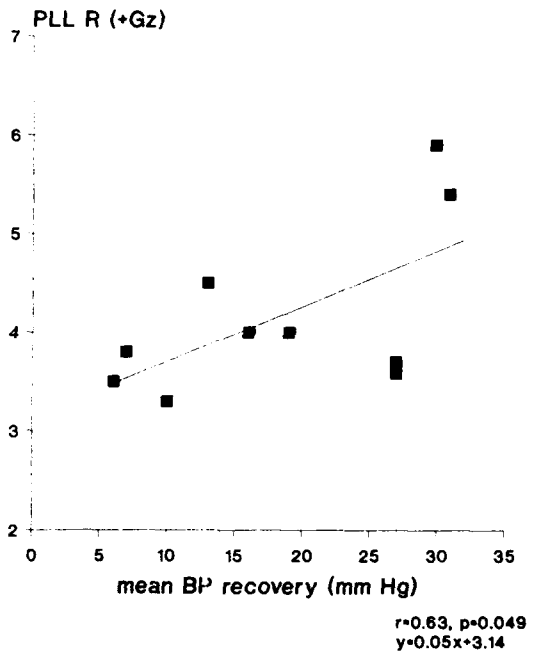

figure 2

Correlation between **mean BP recovery during the Valsalva maneuver** (c-b in fig. 1) and **PLL R** (0.1 G/s, relaxed).

Conclusions

Cardiovascular reflex tests assess integrity of the parasympathetic and sympathetic baroreflex pathways.
The cardiovascular autonomic function test used in this study, the Valsalva maneuver, has its main application as clinical tests to classify patients with orthostatic disorders. The finding of intact baroreflex pathways in the studied subjects confirms the absence of symptoms of orthostatic disorders. Therefore the Valsalva maneuver could be applicable in aviation medicine in the diagnostic proces of a pilot with repeated +Gz-loss of consciousness inflight, who is suspected of an orthostatic disorder.
However the moderate correlation found indicates that normal cardiovascular function is a condition for tolerating +Gz-stress without determining maximal +Gz-tolerance.
We conclude that responses to cardiovascular tests may only confirm baroreflex integrity. However, they have limited value in predicting +Gz-tolerance.

References

1. Bjurnstedt H, Rosenhamer G, Tydén G. Gravitational stress and autonomic cardiac blockade. Acta Physiol. Scand. 1976; 96:526-31.

2. Wieling W. Standing, orthostatic stress and autonomic function. In: R. Bannister, ed. Autonomic Failure. A textbook of clinical disorders of the autonomic nervous system. Oxford: Oxford University Press, 1988: 308-20.

3. Ten Harkel ADJ, van Lieshout JJ, van Lieshout EJ, Wieling W. Assessment of cardiovascular reflexes: influence of posture and period of preceding rest. J. Appl. Physiol. 1990; 68:147-53.

HEMODYNAMIC RESPONSES TO PRESSURE BREATHING DURING $+G_z$ (PBG) IN SWINE

JW Burns, JW Fanton, JL Desmond
Crew Technology Division
Veterinary Sciences Division
Armstrong Laboratory
Brooks AFB TX 78235-5000

Summary

Twelve chronically instrumented, unanesthetized, miniature swine were used to investigate the hemodynamic inter relationships of PBG, the AGSM, and the G-suit, during GOR and SACM $+G_z$ profiles. Maximum LVP and AP of over 300 mmHg, and LVEDP and RVEDP of over 160 mmHg and 100 mmHg, respectively, were common during the GOR and SACM exposures at 9 $+G_z$ using an ECGS. A concurrent, substantial increase in intrathoracic pressure attenuated transmural vascular pressures within the thorax. The performance of the ECGS was significantly better than the ABGS, with or without PBG. A PBG effect could not be demonstrated while using the ECGS, during either the GOR or SACM profiles.

List of Abbreviations and Acronyms

$+G_z$	acceleration in a foot-to-head vector with resultant inertial load in a head-to-foot vector
GOR	gradual onset rate of $+G_z$ (0.1 G/s)
ROR	rapid onset rate of $+G_z$ (4-6 G/s)
SACM	simulated aerial combat maneuver
PB	pressure breathing
PBG	pressure breathing during $+G_z$
AGSM	anti-G straining maneuver
ABGS	abdominal bladder G-suit
ECGS	extended coverage G-suit
LV	left ventricle; left ventricular
LVP	left ventricular pressure
dP/dt	first derivative of LVP
RV	right ventricle; right ventricular
RVP	right ventricular pressure
EDP	end-diastolic pressure
CVP	central venous pressure at the level of the right atrium
AP	aortic pressure
ELBP	eye-level blood pressure
EP	esophageal pressure
MP	mask pressure
HR	heart rate
SV	stroke volume
CO	cardiac output
RVSV	right ventricular stroke volume
RVCO	right ventricular cardiac output (RVCO=RVSV X HR)
LVSV	left ventricular stroke volume
LVCO	left ventricular cardiac output (LVCO=LVSV X HR)
TAF	Tactical Air Force
SD	standard deviation

Introduction

The imminent incorporation of COMBAT EDGE into the operational life-support inventory of the U.S. Tactical Air Force (TAF) has raised some aeromedical concerns about its safety. Some of these concerns are: barotrauma, pneumothorax, excessive transmural vascular pressures, possible cardiac valvular damage, and possible overdilation of the right ventricle following $+G_z$. Data to substantiate or refute these concerns cannot be easily or directly obtained from human subjects. Consequently this study was designed to investigate the effects of: pressure breathing during G (PBG); the anti-G suit; and the anti-G straining maneuver (AGSM), on a number of hemodynamic variables in the unanesthetized miniature swine.

Methods

Twelve female miniature swine weighing 55 ± 8 kg were chronically instrumented through a midsternal incision, using sterile technique and isoflurane/nitrous oxide anesthesia. Instrumentation included a solid state pressure transducer placed into the left ventricle (LV) through the LV free wall, between the two papillary muscles, approximately one-third the base-apex distance from the base of the heart. Another, similar transducer, was placed into the right ventricle (RV) through the RV free wall approximately 4 cm from the pulmonary valve. An electromagnetic flow transducer was placed around the ascending aorta and around the pulmonary artery, just distal to the pulmonary valve. The lead wires from the four transducers were brought to the ventral neck area and then advanced subcutaneously to the dorsum of the neck, just craniad to the shoulders. Approximately 11 cm of nylon velour had previously been glued around the ends of the wires to ensure a good skin interface for healing (6). Approximately 1 week prior to $+G_z$ exposure Teflon cannulae were placed in the right external jugular vein (.31 cm ID) and the right common carotid artery (.19 cm ID). These cannulae were used at the time of $+G_z$ exposure for: passage of a 5 or 8 French solid state catheter-tip pressure transducer into both the LV and the RV to calibrate the implanted transducers, measurement of central venous pressure (CVP) at the level of the right atrium with the catheter-tip transducer in the jugular cannula, measurement of aortic blood pressure (AP) and of eye-level blood pressure (ELBP) through the carotid cannula after removal of the catheter-tip transducer. At the time of $+G_z$ exposure each animal was fitted with a face mask for application of pressure breathing (PB) and PB during $+G_z$ (PBG), a chest counterpressure garment, and either an abdominal bladder G-suit (ABGS), or an extended coverage G-suit (ECGS). The ECGS covered the abdomen and rear legs down to the feet, completely enclosing the legs with a continuous pneumatic bladder. The chest counterpressure garment was inflated at the same pressure schedule as the mask. Pressure came on at approximately 4 G, and increased at a rate of 12 mmHg/G, to a maximum of 60 mmHg at 9 G. G-suit pressure was standard, beginning at 2 G, with a rate of approximately 1.5 psi/G, to a maximum of 10-11 psi at 9 G.

Esophageal pressure (EP), as an indicator of pleural pressure (5), was measured with a 1.5 x 6 cm balloon on a catheter containing multiple side holes within the balloon. The balloon was guided through the nose, nasopharynx,

and esophagus to heart level using fluoroscopy. The catheter was passed through a seal in the mask and connected to an external pressure transducer. The balloon was evacuated and then filled with 1-2 ml of air. ELBP was measured with a small pressure transducer sewn to the skin between the eyes after local anesthesia using bupivacaine. The transducer was connected to the carotid cannula with a saline-filled pressure line. AP was also measured with an external transducer mounted at heart level and connected to the carotid cannula with a saline-filled pressure line. Mask pressure (MP) was measured with an external transducer from a tap on the mask.

Twelve animals were exposed to a continuous 30 s pulse of 60 mmHg PB at 0 G_z, with chest counterpressure support, but without G-suit pressure. Seven animals wearing the ECGS and four wearing the ABGS were exposed to a gradual onset rate (GOR) $+G_z$ profile of 0.1 G/s to 8 G (n=1) or 9 G (n=10) with and without PBG. Five animals were exposed to a 5-9 $+G_z$ simulated aerial combat maneuver (SACM) with and without PBG while wearing the ECGS. Ten minutes were allowed for recovery between each experimental procedure.

The data were digitized at 200 Hz and formatted beat-to-beat, using left ventricular pressure (LVP) as the trigger for integration of aortic and pulmonary flow to provide stroke volume (SV). Maxima, minima, and mean of all pressure data were taken during each LVP waveform. The data were analyzed using paired and unpaired analysis of variance. The number of animals included in each test is indicated at the bottom of each table. However, because of plugged cannula and instrumentation failures there were missing data within some of the animals.

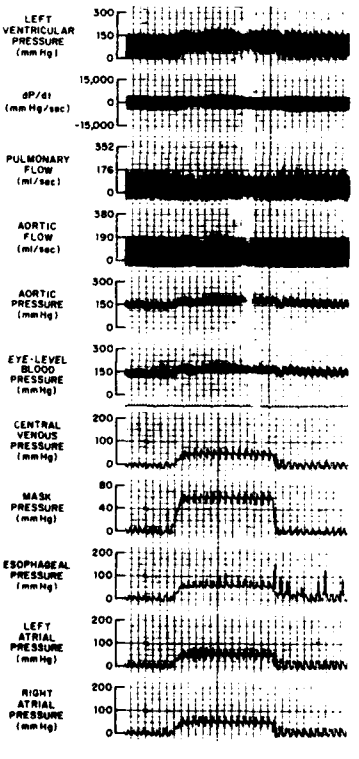

Fig 1. 60 mmHg pressure breathing at 0 $+G_z$

Table 1 Pressure Breathing at 0 Gz

		Pressure Breathing		
	Control	10 sec	20 sec	30 sec
Peak LVP (mmHg)	152±19	181±26	193±36	195±35
LVEDP (mmHg)	11±9	58±13	61±13	61±10
Peak RVP (mmHg)	45±11	89±17	95±19	93±18
RVEDP (mmHg)	1±8	48±11	50±12	49±10
AP (mmHg)				
systolic	153±13	176±23	180±25	180±22
diastolic	109±14	136±19	139±19	142±21
mean	129±13	153±20	156±20	158±21
CVP (mmHg)				
max	21±7	63±6	65±5	64±5
min	2±9	46±6	49±7	47±7
mean	11±7	54±6	57±6	56±5
EP (mmHg)				
max	12±4	67±3	71±5	71±5
min	-5±4	51±3	54±3	54±5
mean	4±3	59±2	62±2	62±3
MP (mmHg)	6±2	63±2	65±2	64±2
LVSV (ml)	28±10	19±7	20±8	18±7
LVCO (L/m)	4.0±1.1	3.1±.9	3.2±.9	3.0±.9
RVSV (ml)	24±10	17±8	17±7	17±7
RVCO (L/m)	3.7±1.1	2.9±1.0	2.9±.9	2.8±.9
HR (b/m)	149±35	171±36	172±39	175±40

Data are mean ± SD; n=12

Results

Figure 1 illustrates the response of one animal to PB at 0 G_z. Table 1 presents the mean data from the exposure of 12 animals to PB without $+G_z$ or G-suit pressure. Note that EP accurately reflects MP. During the first 10 s peak LVP lags behind the increase seen in the other pressures. Note also that LV, RV, and CV pressures increased by approximately the same amount (41-50 mmHg); whereas, AP increased by only 24-29 mmHg. Stroke volumes and cardiac outputs decreased by 20-34%, whereas heart rate (HR) increased by 15 to 17%. After the first 10 s the increase in intravascular pressures ranged from 70 to 85% of the MP increase, except for AP which increased by 46-49% of MP. During PB without $+G_z$, transmural pressure across the LV, RV, aorta, and central venous area decreased over the entire 30 s period compared to control.

Figure 2 illustrates the typical animal response to a GOR profile, with and without PBG, while wearing the ECGS. Table 2 is a comparison of the ABGS vs. the ECGS, with and without PBG, using GOR profiles to 9 $+G_z$. There was a significant difference between the two suits, both with and without PBG, as indicated in the table. Also, PBG had a significant effect on a number of variables within the ABGS data, but only right ventricular cardiac output (RVCO) was significantly different with the ECGS. Note that the changes between PBG and no PBG with the ECGS are very similar in most respects. During the GOR exposures with the ABGS, transmural pressure decreased without PBG, compared to control, and changed little with PBG. With the ECGS, transmural pressure increased with or without PBG, but to a lesser amount with PBG.

Figure 3 and Table 3 compare the PBG effect during the 5-9 $+G_z$ SACM, using the ECGS. There were no significant differences in any of the variables, comparing the change from control to the fifth 9 $+G_z$ peak, with and without PBG. Transmural pressures at the fifth 9 G exposure were in-

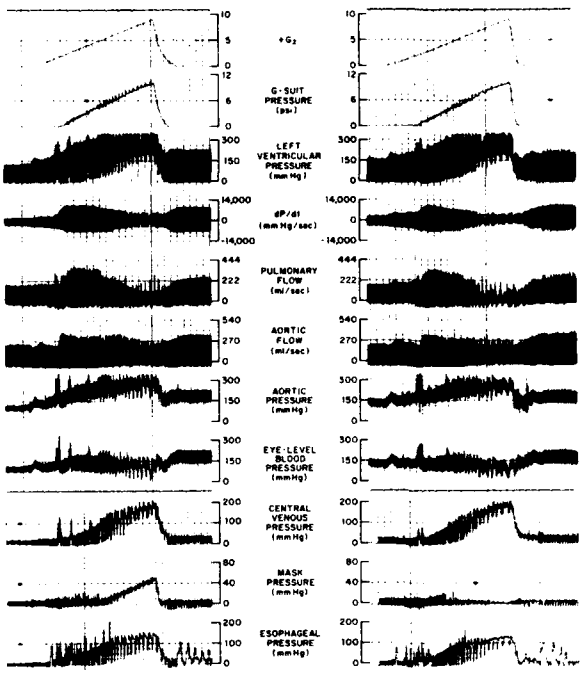

Fig 2. GOR to 9 $+G_z$ with and without PBG (see mask pressure).

creased over control, with or without PBG, except AP without PBG, which was decreased from control. In contrast to the GOR exposures with the ECGS, where PBG reduced transmural pressures compared with no PBG, transmural pressures were increased by PBG during the 5-9 SACM exposures compared to no PBG.

Discussion

One of the objectives of this study was accomplished with the demonstration of a dramatic increase in intrathoracic pressure (EP) during $+G_z$, with contributions from PBG, the AGSM and G-suit pressure. The substantial increase in intrathoracic pressure was very important in attenuating the potentially dangerous transmural vascular pressures within the thorax. There is also a concern within the aeromedical community that following high G, especially high G with PBG, RV dilation will result from a surge of venous return to the heart at the offset of $+G_z$. It is feared that repeated acute RV dilation in pilots could result in chronic dilation and possible RV pathology. There was no evidence in this study of an abnormal surge of venous return with either GOR or SACM profiles; or from a previous study using ROR exposures to 3, 5, and 7 $+G_z$/60 s (3). CVP and RVP declined in proportion to the decline in $+G_z$ and G-suit (Figs. 2 and 3).

Table 2 GOR to 9 +Gz

	ABGS						ECGS					
	Without PBG			With PBG			Without PBG			With PBG		
	Control	at 9 G	Change	Control	at 9 G	Change	Control	at 9 G	Change	Control	at 9 G	Change
Peak LVP (mmHg)	164±4	250±43	86±41[a]	168±17	222±77	47±92[b]	153±18	358±44	205±42[a]	144±16	352±19	208±22[b]
LVEDP (mmHg)	8±10	54±34	46±29[a]	9±8	77±20	68±16[b]	15±9	166±25	151±30[a]	13±9	165±28	152±29[b]
Peak RVP (mmHg)	41±9	100±28	60±25[a]	57±27	106±29	47±34[b]	48±7	179±35	131±36[a]	46±12	163±26	117±24[b]
RVEDP (mmHg)	-6±7	7±24	13±24[ac]	0±11	44±9	49±15[bc]	2±6	115±40	114±40[a]	1±9	104±21	103±17[b]
AP (mmHg)												
systolic	169±--	211±--	42±--[a]	155±8	215±--	55±--[b]	152±13	319±58	168±50[a]	145±16	305±43	159±41[b]
diastolic	117±--	140±--	23±--	112±2	162±--	51±--	106±15	199±59	93±60	103±15	209±47	107±43
mean	139±--	181±--	42±--	132±4	187±--	52±--	128±14	251±51	123±47	124±16	255±45	131±42
ELBP (mmHg)												
systolic	187±--	8±--	-179±--[a]	153±20	38±--	-129±--[b]	148±16	136±39	-13±40[a]	141±15	135±43	-6±43[b]
diastolic	113±--	-45±--	-158±--[a]	104±5	-3±--	-111±--[b]	99±14	45±46	-53±46[a]	95±16	53±34	-43±32[b]
mean	138±--	-10±--	-148±--[a]	126±11	10±--	-123±--[b]	122±13	83±44	-38±44[a]	117±16	89±38	-29±35[b]
CVP (mmHg)												
max	16±7	63±49	47±51[a]	15±9	70±33	55±41[b]	22±8	146±32	124±34[a]	21±6	145±31	124±32[b]
min	2±10	19±29	17±37[ac]	4±11	51±35	48±45[bc]	2±7	103±40	101±44[a]	1±7	106±30	106±31[b]
mean	9±8	38±35	29±41[ac]	10±10	62±34	52±44[bc]	12±7	126±32	115±34[a]	11±6	126±31	115±33[b]
EP (mmHg)												
max	11±2	99±60	89±63	10±6	70±5	60±11	15±6	103±23	88±21	12±3	113±31	101±31
min	-1±6	59±102	60±108	1±7	53±10	52±17	-2±8	59±36	61±41	-4±4	84±32	88±33
mean	5±4	82±77	77±81	6±7	62±7	56±14	6±7	84±25	78±26	5±2	99±28	95±29
MP (mmHg)	6±1	5±2	-1±3	4±2	58±7	54±8	6±1	6±4	0±4	7±1	53±4	47±4
LVSV (ml)	20±6	13±3	-7±7	23±13	9±3	-11±11	35±4	19±5	-16±6	33±3	21±7	-11±8
LVCO (L/m)	3.4±.9	1.5±.8	-1.9±1.5	3.3±1.6	1.5±.4	-1.9±1.6	4.5±1.0	1.8±.8	-2.7±1.1	4.2±.7	2.0±.7	-2.2±1.4
RVSV (ml)	20±6	29±34	9±33	20±14	13±8	-7±6	34±4	23±13	-11±16	32±4	24±9	-8±9
RVCO (L/m)	3.4±.9	1.9±.4	-1.5±.5	3.4±1.9	2.1±1.1	-1.2±.9	4.4±1.2	2.6±.9	-1.8±1.6[d]	4.1±.9	2.7±.8	-1.3±1.3[d]
HR (b/m)	175±24	128±84	-46±105	164±55	178±17	-9±32	142±34	109±50	-33±62	132±18	111±50	-21±53

Data are mean ± SD; n=4 for ABGS; n=7 for ECGS
a-d indicate significant differences between similarly labeled changes at p<.05

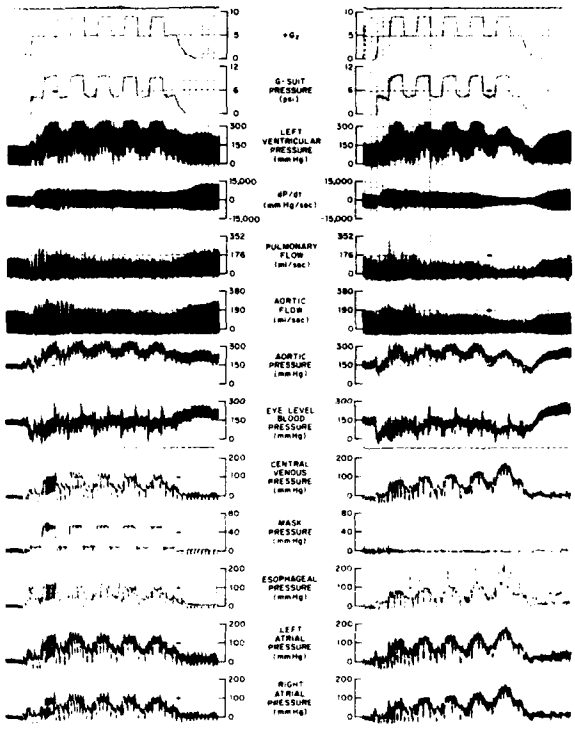

Fig 3 5-9 +G_z SACM with and without PBG (see mask pressure).

The positive differential pressure across the coronary vascular bed (AP-CVP) during both the GOR and SACM exposures suggests that coronary blood flow was not compromised.

This study was not designed to compare the two G-suits that were utilized. However, the striking hemodynamic improvement seen with the ECGS over the ABGS deserves reporting. The performance of the ECGS was exceptional, supporting peak LV and RV pressures of over 350 mmHg and 160 mmHg, respectively, and end-diastolic pressures (EDPs) of over 160 mmHg and 100 mmHg, respectively, with or without PBG during the GOR exposures. Even at these high pressures left ventricular stroke volume (LVSV) and right ventricular stroke volume (RVSV) decreased by only 25% to 45%. The increase in LVP, RVP, AP, and CVP with a concurrent decrease in HR, SV, CO and dP/dt suggest that the major effect of the ECGS is an increase in peripheral resistance. Any improvement in hemodynamics from PBG with the ECGS was masked by the dramatic increase in intravascular pressures associated with G-related pressurization of the ECGS, during both GOR and SACM profiles.

Table 3 5-9 SACM with ECGS

	Without PBG			With PBG		
	Control	5th 9 G	Change	Control	5th 9 G	Change
Peak LVP (mmHg)	153±17	310±38	162±44	152±12	316±30	164±35
LVEDP (mmHg)	14±6	180±25	169±20	12±9	170±49	158±54
Peak RVP (mmHg)	48±10	194±52	148±41	51±13	171±70	119±66
RVEDP (mmHg)	-1±13	150±40	149±27	1±11	130±65	130±57
AP (mmHg)						
systolic	158±17	243±27	88±12	156±10	275±37	119±32
diastolic	109±19	189±36	83±25	107±12	207±31	100±22
mean	131±18	214±32	85±19	131±12	238±34	107±26
ELBP (mmHg)						
systolic	156±18	86±12	-67±8	156±10	107±41	-49±43
diastolic	102±20	39±23	-61±20	100±13	51±20	-49±15
mean	125±18	58±20	-66±15	124±12	73±28	-51±24
CVP (mmHg)						
max	22±11	150±26	127±30	26±10	137±52	111±51
min	-1±9	125±23	127±23	1±10	115±50	114±49
mean	10±9	138±24	129±24	12±10	126±51	114±50
EP (mmHg)						
max	14±4	135±20	120±22	14±3	102±28	88±27
min	-3±4	117±20	120±20	-5±3	85±24	90±24
mean	6±3	126±20	121±21	5±2	94±26	89±26
HP (mmHg)	7±0	4±1	-3±1	7±1	55±5	48±5
LVSV (ml)	27±6	11±3	-14±4	31±9	12±3	-18±8
LVCO (L/m)	3.9±.9	1.4±.3	-2.1±1.0	4.4±1.4	1.7±.7	-2.7±1.3
RVSV (ml)	23±5	10±7	-13±2	25±5	14±2	-11±3
RVCO (L/m)	3.1±.1	1.3±.5	-1.8±.4	3.5±.9	1.9±.6	-1.6±.5
HR (b/m)	147±17	140±32	-8±26	144±10	141±35	-3±37

Data are mean ± SD, n=5

These data substantiate previous observations by others (1,2,4) of a significant increase in intravascular pressures with the application of PB without acceleration. The PB effect was easily observed (Fig 1 and Table 1) without +G_z. However, during +G_z the intravascular changes related to PB were more difficult to separate from the influence of the AGSM and G-suit pressure (Figs. 2 and 3 and Tables 2 and 3).

In conclusion, although this study does not address all of the concerns listed in the introduction, such as barotrauma and pneumothorax, the data demonstrate that the increases in intrathoracic vascular pressures were supported, in a large part, by a concurrent increase in esophageal pressure (reflecting pleural pressure), thus minimizing large and potentially dangerous transmural pressures. Moreover, there was no evidence of a surge in venous return to the RV following +G_z and PBG. A PBG effect could not be demonstrated while using the ECGS. The PBG effect was most likely masked by the excellent +G_z protection provided by the ECGS. Additional studies are needed to investigate lower G-suit pressures for a better definition of ECGS performance and to unmask the PBG effect.

References

1. Ackles, KN, JAG Porlier, DE Holness, GR Wright, JM Lambert and WJ McArthur. Protection against the physiological effects of positive pressure breathing. Aviat. Space Environ. Med. 49:753-8, 1978.

2. Balldin, UI and B. Wranne. Hemodynamic effects of extreme positive pressure breathing using a two-pressure flying suit. Aviat. Space Environ. Med. 51:851-5, 1980.

3. Burns, JW, MJ Parnell and RR Burton. Hemodynamics of the miniature swine during $+G_z$ stress with and without anti-G support. J. Appl. Physiol. 60:1628-37, 1986.

4. Ernsting, J. Some effects of raised intrapulmonary pressure in man. AGARDograph 106. London: McKay, 1966.

5. Fry, DL, WW Stead, RV Ebert, RI Lubin and HS Wells. The measurement of intraesophageal pressure and its relationship to intrathoracic pressure. J. Lab. Clin. Med. 40:664-73, 1952.

6. Witt, WM, JW Burns and MH Laughlin. Nylon velour for protection against percutaneous sinus tract formation in instrumented swine. SAM-TR-80-7, 1980.

SUBJECTIVE REPORTS CONCERNING ASSISTED POSITIVE PRESSURE BREATHING UNDER HIGH SUSTAINED ACCELERATION

Kathy McCloskey
Lloyd D. Tripp
Daniel W. Repperger
and
Stephen E. Popper

Armstrong Laboratory, Det 1 (AL/BBS)
Human Systems Division
Air Force Systems Command
Wright-Patterson Air Force Base,
Ohio 45433-6573
United States

SUMMARY

Assisted positive pressure breathing, as found in the COMBAT EDGE system, was shown to have distinct advantages and disadvantages concerning subjective opinion of the system under sustained acceleration. Advantages include subjects' perceptions of the system as an advancement in G-protection technology, personal projections of increased tolerance to G-forces, decrease in fatigue due to a lessening of straining maneuver effort, and an increase in breathing ease during acceleration, at least for subjects with COMBAT EDGE experience. Disadvantages include an increased incidence of arm pain, breathing difficulties for subjects new to the system, and a tendency to rely too much on the system in lieu of traditional straining maneuvers. It is recommended that a training regimen be established to address these issues before the COMBAT EDGE system is deployed operationally.

INTRODUCTION

Positive pressure breathing with an external counterpressure vest (known as assisted positive pressure breathing, or APPB) has been suggested as a means to increase G-tolerance and endurance (time-at-G) which would give an operational flight advantage to the fighter pilot. Pressures of 45 to 70 mmHg presented to the lungs via an oro-nasal mask during APPB have been shown to increase G-tolerance and endurance by increasing intrathoracic pressures, reducing the mechanical effects of G on respiration, and reducing the amount of effort needed to perform straining maneuvers [2,5,6,7]. Experience with APPB in the Royal Air Force (RAF) of the United Kingdom has shown that, when coupled with full-coverage anti-G trousers, relaxed G-tolerance was increased to +8.3Gz and fatigue was reduced to a minimum during flight [4]. Thus, APPB allows the pilot to maintain high-G flight profiles for longer periods of time, as well as perform more high-G profiles in succession.

At the present, the U. S. Air Force is preparing to man-rate an APPB apparatus for inclusion into a new G-protection system known as the Combined Advanced Technology Enhanced Design G Ensemble (COMBAT EDGE). However, with the fielding of the COMBAT EDGE, questions have arisen as to the effects of APPB on the normal flight regime of pilots. Subsequently, an experiment was conducted on the Dynamic Environment Simulator (DES) man-rated centrifuge at Wright-Patterson Air Force Base, Ohio, in an effort to obtain subjective responses to APPB while subjects were under sustained acceleration. A series of manned regulator engineering tests provided an early opportunity to obtain subjective data which may help predict the range of pilots' reactions to the COMBAT EDGE. Hopefully, the results presented here will eliminate any surprises concerning pilot opinion and degree of acceptance during operational deployment, as well as assist in identifying important training issues.

METHODS

The COMBAT EDGE System. Figure 1 depicts the pressure hose leads and a detailed breakdown of the COMBAT EDGE apparatus. The anti-G suit worn with the ensemble was the standard CSU-13B/P suit, and was worn over the bottom portion of the counterpressure vest. The pressures to the anti-G suit were controlled independently of the mask or vest pressures through an Alar high-flow G-valve. The anti-G suit pressure schedule was 77.7 mmHg (1.5 psi) per +1Gz, with pressure onset occurring at +2Gz, for a maximum pressure of 621.6 to 699.3 mmHg (12 to 13.5 psi) at +9Gz.

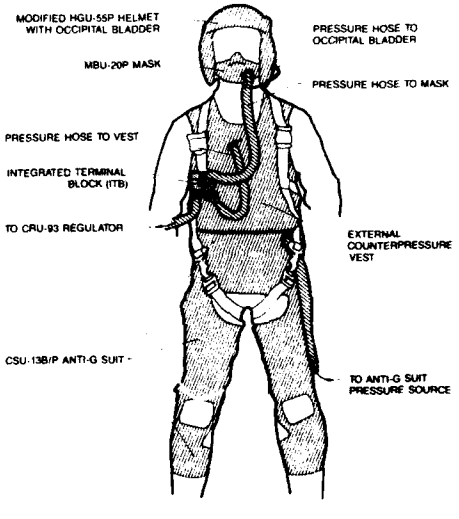

FIGURE 1
A detailed schematic of the COMBAT EDGE System

A Litton CRU-93 regulator controlled the breathing pressure to the MBU-20P mask and chest counterpressure to the vest. The main pressure hose from the CRU-93 fed into an Integrated Terminal Block (ITB) which split off to provide the same pressures to

the mask and vest. Thus, equal pressures were assured to provide approximately one-to-one external counterpressure at the chest area to those pressures being delivered to the lungs.

The helmet was a modified HGU-55P helmet with an occipital bladder which inflated simultaneously with the onset of mask pressure. A small pressure line from the main mask hose fed into the occipital bladder. This assured equal pressures at the back of the head and at the mask point-of-contact to reduce the incidence of the mask "riding away from the face."

APPB Profiles. The CRU-93 was designed to smoothly deliver pressures at a rate of 12 mmHg (0.23 psi) per +1Gz, with an onset at +4Gz. The maximum pressure delivered to the mask and vest was 60 mmHg (1.16 psi). Thus, maximum pressure occurred at +9Gz. The reason for the manned regulator engineering test and evaluation was to determine the smoothness and accuracy of this pressure profile. Overall, the regulator design performed reasonably well, although some problems precipitated a redesign effort. The results of the engineering evaluation are to be addressed in a future report.

High-G Sustained Acceleration Profiles. Subjects underwent four different acceleration profiles while seated in the cab of the DES (Figure 2) in a simulated F-16 configuration seat with a 30 degree seatback angle. The four acceleration profiles are depicted in Figure 3. The first run was +9Gz maximum with a gradual onset rate (GOR) of +0.1Gz per second and an offset rate of -0.5Gz per second. The second run was +5Gz maximum with a more rapid onset rate (ROR) of +0.5Gz per second, a plateau of fifteen seconds in length, and an offset rate of -0.5Gz per second. The third and fourth runs were identical to the +5Gz ROR, except the maximum G levels were +7Gz and +9Gz, respectively. Each subject experienced all profiles during a half hour daily session.

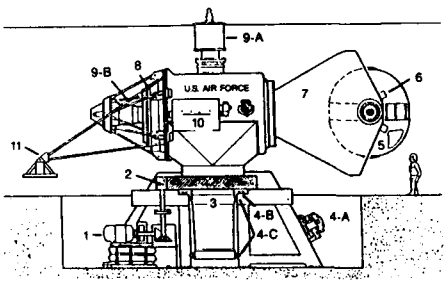

FIGURE 2
The Dynamic Environment Simulator (DES)
1) Main arm drive motor; 2) Drive pinion; 3) Main rotating travian and bull gear; 4A) Hydraulic pumps; 4B) Trust pad; 4C) Upper and lower radial pads; 5) Cab; 6) Cab drive motor; 7) Fork; 8) Fork drive motor; 9a) Main arm axis slip rings; 9B) Fork axis slip rings; 10) Motor-driven counterweight; 11) Experimental platform.

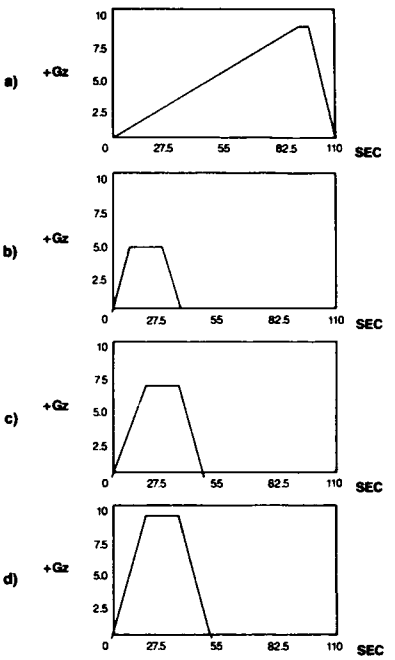

FIGURE 3
Acceleration Profiles
a) +9Gz max with +0.1 Gz/sec onset rate, -0.5 Gz/sec offset rate;
b) +5Gz max with +0.5 Gz/sec onset rate, -0.5 Gz/sec offset rate;
c) +7Gz max with +0.5 Gz/sec onset rate, -0.5 Gz/sec offset rate;
d) +9Gz max with +0.5 Gz/sec onset rate and -0.5 Gz/sec offset rate.

Experimental Design. The order in which centrifuge subjects experienced the high-G profiles was determined by the requirements of the regulator evaluation, as well as the need for consistency with centrifuge tests conducted previously at Brooks Air Force Base, Texas. Because of the limitations of these requirements, the order of exposure was not counterbalanced to eliminate learning effects for the subjective evaluation (the following results should be interpreted with this in mind). The +9Gz GOR profile was always followed by the +5Gz ROR, the +7Gz ROR, and the +9Gz ROR profiles.

Elicitation of Subjective Responses. There were four major categories of COMBAT EDGE system performance obtained through verbal protocol at the end of each of the four high-G profiles. The first was the incidence of body awareness or pain. Subjects were asked if they were aware of pain or discomfort in any body part. The second category was straining characteristics. Subjects were asked if they had used a straining maneuver, and if so, what type of maneuver was used. The third category was mask quality. Subjects were asked to relate any instances of mask leakage or changes in mask pressure smoothness. The fourth category was breathing ease. Each subject was asked to give opinions as to ease of breathing. Unfortunately, non-parametric statistical analyses of these data

were not able to be performed due to the small numbers in each cell. In addition, the experimenters recorded any incidence of extremely fast and deep breathing (hyperventilation). Data were also collected after each profile concerning reasons for terminating high-G exposure during the profile, the effectiveness of using arm wraps to reduce the incidence and severity of arm pain, and talking ability during APPB. However, the nature of these data did not allow for systematic collection and serve as anecdotal evidence only. If a subject withdrew from the study, the reasons for this were also noted.

Ratings concerning seven overall categories were obtained through a questionnaire administered at the end of all four high-G profiles. Subjects had egressed the centrifuge and were finished for the day when the questionnaire was given. The seven categories included severity of petechiae (tiny red hemorrhage spots on the body, or "G measles"), overall fatigue, ratings of the COMBAT EDGE as a means of G-protection, recommendation/rejection of the COMBAT EDGE for use in the cockpit, choosing between the COMBAT EDGE and the standard anti-G suit, difference in personal G-tolerance while wearing the COMBAT EDGE, and the maximum projected G-tolerance while wearing the COMBAT EDGE.

Subjects. Eleven male subjects, ages 26 to 39, participated in the study. All subjects had passed detailed physical examinations to qualify as members of the Acceleration Subject Panel. Other subject characteristics which could influence responses to the COMBAT EDGE system included total number of sessions, flight experience (G-exposure and familiarity with positive pressure breathing), altitude chamber experience (familiarity with positive pressure breathing), days since last centrifuge run (G-tolerance) and total experience on the DES centrifuge before the study (G-exposure and G-tolerance). These characteristics are shown in Table 1.

TABLE 1
Experience Profiles for Subjective Evaluation

Subject Code	Total Number of Sessions	Flight Experience	Alt. Chamber	Days Since Last Centrifuge Run	Total Centrifuge Experience
AA	18 at USAFSAM# 4 checkouts 5 sessions	120 hours F-111, F-4 med. observer	1.5 hours	5	94.0 hours
BB	4 sessions	80 hours T-41, T-37 ex-pilot	3.0 hours	29	3.0 hours
CC	4 sessions	none	none	23	10.5 hours
DD	3 sessions	2-3 hours flight surgeon	3.0 hours	33	12.5 hours
EE	3 sessions	114 hours T-37, T-38 ex-pilot trainee	4.0 hours	38	8.5 hours
* FF	2 sessions	150 hours ex-F-16 pilot	5.0 hours	34	5.5 hours
GG	2 sessions	none	0.5 hours	23	17.5 hours
HH	2 sessions	none	none	31	3.5 hours
** II	1 session	none	none (licensed scuba diver)	23	4.0 hours
JJ	1 session	none	0.5 hours	12	17.5 hours
KK	1 session	none	0.25 hours	38	37.0 hours

* Extreme arm pain. Subject withdrew from program after first run of the second session

** Extreme arm pain and numbness 24 to 72 hours after first session. Subject withdrew from program one day after acceleration exposure

USAFSAM is the U.S. Air Force School of Aerospace Medicine at Brooks Air Force Base, Texas

RESULTS

Verbal Protocol Results. The following results were obtained by averaging responses across subjects. A total of 26 scorable runs were determined for the +9Gz GOR profile, 27 runs for the +5Gz ROR profile, 26 runs for the +7Gz ROR profile, and 25 runs for the +9Gz ROR profile. Considering all profiles, a total of 104 scorable runs were obtained.

Incidence of pain. Table 2 shows the incidence rates of pain in various body parts. Arm pain was the most often reported, followed by no pain at all, leg pain, ear pain, buttock pain, facial pain, and rib pain. Pain occurred most often during the +9Gz ROR run, followed by the +9Gz GOR, +7Gz ROR, and +5Gz ROR profiles.

TABLE 2
Reports of Pain (percentages in parentheses)

	Acceleration Profile				
Type of Pain	+9Gz GOR [26 runs total]	+5Gz ROR [27 runs total]	+7Gz ROR [26 runs total]	+9Gz ROR [25 runs total]	Total:
None	8 (08)	17 (16.5)	9 (09)	4 (04)	38 (36.5)
Arm pain	14 (13)	5 (05)	15 (14)	17 (16.5)	51 (48.5)
Leg pain	2 (02)	2 (02)	2 (02)	2 (02)	8 (08)
Facial pain	0 (00)	0 (00)	0 (00)	1 (01)	1 (01)
Buttock pain	1 (01)	0 (00)	0 (00)	1 (01)	2 (02)
Rib pain	1 (01)	0 (00)	0 (00)	0 (00)	1 (01)
Ear pain	0 (00)	3 (03)	0 (00)	0 (00)	3 (03)
Total Incidence of Pain:	16 (17)	10 (10)	17 (16)	21 (20.5)	

Overall χ^2 = Not Significant (75% of cells had counts less than 5)

Types of straining maneuvers. Table 3 shows the most common types of straining maneuvers reported. Tensing of the legs was the most common, followed by no straining at all, tensing of the abdomen, the arms, a whole body strain, the chest, the buttocks, and the M-1 or L-1 straining maneuvers. Straining was required most often in the +9Gz ROR profile, followed by the +7Gz ROR, the +9Gz GOR, and the +5Gz ROR profiles. Two interesting types of

TABLE 3
Types of Straining Maneuvers (percentages in parentheses)

	Acceleration Profile				
Type of Straining Maneuver	+9Gz GOR [26 runs total]	+5Gz ROR [27 runs total]	+7Gz ROR [26 runs total]	+9Gz ROR [25 runs total]	Total:
None	11 (10)	17 (16)	9 (09)	1 (01)	38 (36)**
Legs	7 (07)	6 (06.5)	13 (12)	14 (13)	40 (38.5)
Abdomen	6 (06.5)	2 (02)	4 (04)	5 (05)	17 (16.5)
Arms	2 (02)	1 (01)	4 (04)	5 (05)	12 (12)
Whole body	2 (02)	1 (01)	1 (01)	4 (04)	8 (08)
Chest	0 (00)	0 (00)	1 (01)	2 (02)	3 (03)
Buttocks	0 (00)	0 (00)	1 (01)	1 (01)	2 (02)
M-1 or L-1	1 (01)	0 (00)	0 (00)	1 (01)	2 (02)
Total Incidence of Straining**:	18 (17)	10 (10)	24 (23)	32 (30)	

**Subjects reported more than one type of straining maneuver for each run

Overall χ^2 = Not Significant (99% of cells had counts less than 5)

NOTES:					Total:
Straining Forgotten:	2 (02)	1 (01)	3 (03)	1 (01)	7 (07)
"Spontaneous" visual recovery without straining:	0 (00)	0 (00)	0 (00)	2 (02)	2 (02)

subjective reports were obtained here also. There were seven instances where subjects forgot to perform any straining maneuver at all, even though it was needed. In addition, there were two instances where subjects lost vision during the +9Gz ROR profile, yet spontaneously recovered their vision at plateau with no straining required.

Mask quality. Table 4 shows the responses obtained concerning mask quality. No experience of mask problems was the most common, followed by leakage at the nose and eyes, leakage at the chin, general seal leakage, mask raised away from the face, and mask "chatter." Mask quality decrements occurred most often during the +9Gz GOR profile, followed by the +9Gz ROR, +7Gz ROR, and +5Gz ROR profiles.

TABLE 4
Reports of Mask Quality (percentages in parentheses)

	Acceleration Profile				
	+9Gz GOR (26 runs total)	+5Gz ROR (27 runs total)	+7Gz ROR (26 runs total)	+9Gz ROR (25 runs total)	
Type of Mask Quality					Total:
No leakage	13 (12.5)	25 (24)	17 (16.5)	16 (15)	71 (68)
Leakage at nose and eyes	6 (05.5)	0 (00)	3 (03)	4 (04)	13 (12.5)
Leakage at chin	2 (02)	1 (01)	4 (04)	3 (03)	10 (10)
General leakage	4 (04)	0 (00)	1 (01)	1 (01)	6 (05.5)
Mask raised away from face	1 (01)	0 (00)	1 (01)	0 (00)	2 (02)
Pressure "chatter" and unevenness	0 (00)	1 (01)	0 (00)	1 (01)	2 (02)
Total Incidence of Mask Problems:	13 (12.5)	2 (02)	9 (09)	9 (09)	

Overall X^2 = Not Significant (79% of cells had counts less than 5)

Breathing ease. Table 5 shows the subjects' ratings of breathing ease, as well as the experimenters' identification of hyperventilation occurrence. There were nine instances where subjects were breathing extremely fast and deep, and the results of these occurrences ranged from "talking the subject down" into more normal breathing rates to where subjects stopped the centrifuge by using the emergency B-stop (B-stop is defined here as the subjects' termination of the high-G profile before the prescribed end point). Subjects reported more breathing ease than breathing difficulty, however. More difficulties were reported during the +9Gz GOR profile than during the other profiles. Conversely, more reports of breathing ease were obtained during the +9Gz ROR profile than during the other profiles.

TABLE 5
Reports of Breathing Ease (percentages in parentheses)

	Acceleration Profile				
	+9Gz GOR (26 runs total)	+5Gz ROR (27 runs total)	+7Gz ROR (26 runs total)	+9Gz ROR (25 runs total)	
Breathing Type					Total:
Needed coaching ("talked down" from hyperventilation)	1 (01)	1 (01)	2 (02)	0 (00)	4 (04)**
Hyperventilation	1 (01)	2 (02)	1 (01)	1 (01)	5 (05)
Very hard	6 (05.5)	3 (03)	1 (01)	3 (03)	13 (12.5)
Hard	6 (05.5)	4 (04)	2 (02)	1 (01)	13 (12.5)
Easy	6 (05.5)	7 (07)	7 (07)	6 (05.5)	26 (25)
Very easy	4 (04)	9 (09)	9 (09)	7 (07)	29 (29)
Outstanding	1 (01)	1 (01)	1 (01)	5 (05)	8 (08)
**Some subjects respond more than once, some not at all					
Overall ease:	11 (10)	17 (16)	17 (16)	18 (17)	63 (61)
Overall difficulty:	14 (13)	10 (10)	6 (05.5)	5 (05)	35 (34)

Overall X^2 = Not Significant (85% of cells had counts less than 5)

Anecdotal data. Table 6 shows the reasons for subjects' B-stops which ended their acceleration exposures before the prescribed time. Notice the overall low percentage of occurrence (approximately 12.5 percent). Arm pain was the reason most reported, followed by breathing difficulties, straining forgotten, vertical nystagmus, and fatigue. B-stops occurred most often during the +9Gz ROR profile, followed by the +9Gz GOR and +7Gz ROR profiles. There were no B-stop occurrences during the +5Gz ROR profile.

TABLE 6
Reasons for B-stop (percentages in parentheses)

	Acceleration Profile				
	+9Gz GOR (26 runs total)	+5Gz ROR (27 runs total)	+7Gz ROR (26 runs total)	+9Gz ROR (25 runs total)	
Reason					Total:
Arm pain	3 (03)	0 (00)	0 (00)	2 (02)	5 (05)
Breathing difficulty (including hyperventilation)	2 (02)	0 (00)	0 (00)	2 (02)	4 (04)
Straining forgotten	0 (00)	0 (00)	2 (02)	0 (00)	2 (02)
Vertical nystagmus	0 (00)	0 (00)	0 (00)	1 (01)	1 (01)
Fatigue	0 (00)	0 (00)	0 (00)	1 (01)	1 (01)
Total Incidence of B-stop:	5 (05)	0 (00)	2 (02)	6 (05.5)	

Overall X^2 = Not Significant (100% of cells had counts less than 5)

Two subjects withdrew from the study. Subjects FF and II dropped out due to extreme arm pain. It was determined during the standard debriefing period that subject FF had injured his right elbow within the last two years severely enough to require corrective surgery. However, this subject reported extreme pain in both arms and general dislike for the system as the reasons for withdrawal. It should be noted that subject FF was an ex-pilot with 150 hours of flight experience in the F-16 aircraft, as well as 5 hours of altitude chamber experience. Subject II reported that he could not raise his left arm due to extreme shoulder/elbow pain and muscle numbness 24 to 72 hours after his first daily session. Consequently, subject II withdrew from the study. Subject II had no flight experience, no altitude chamber experience, and only 4 hours of centrifuge experience before participating in this COMBAT EDGE evaluation.

The high incidence of pain in the arms was most probably due to the shunting of blood into those body parts not protected by external counterpressure. As early as 1966, Ernsting stated that a full body counterpressure garment used with postive pressure breathing would eliminate pain due to blood shunting and blood pressure increases in uncovered areas [1]. Thus, arm wraps (ACE elastic bandages or surgical support hose) were used with four subjects in an attempt to alleviate arm pain. For two of those subjects, AA and BB, arm pain was eliminated using arms wraps during a total of 12 profiles of varying G levels. For subject EE, arm pain still occurred during the +9Gz GOR and +9Gz ROR profiles, but was eliminated at the +5Gz ROR profile. Subject HH reported no arm pain wearing the arm wraps until the +9Gz ROR run, where he could manipulate the degree of pain by squeezing and tensing his arms.

Another anecdotal finding concerned talking ability during A³PB. Two subjects, AA and FF, attempted to talk during the +9Gz ROR profile while at plateau. The subjects were instructed to repeatedly count from 0 to 9. Subject AA could not talk during the first two runs. During the third run at +9Gz ROR, talking could

be heard but not understood. Subject FF could not talk during his only run at +9Gz ROR.

Finally, there were two subjects who reported virtually no problems with the system (other than intermittent arm pain), and thoroughly enjoyed the extra high-G protection of the APPB capability of the COMBAT EDGE. The first subject, AA, had the most experience with the COMBAT EDGE of any of the subjects (this subject also came closest, with the exception of FF, an ex-F16 pilot, to emulating an experienced operational pilot in terms of overall high-G/positive pressure breathing experience). Conversely, subject KK had no flight experience, 0.25 hours of altitude chamber experience, and 37 hours of centrifuge exposure. Yet this subject reported that "I couldn't believe I was at 9 G."

Questionnaire Results. Nine of the eleven subjects completed the questionnaire. It should be kept in mind that the two subjects who withdrew from the study are not represented in the following results. One subject (FF) strongly recommended against the use of the COMBAT EDGE system for operational deployment. Figures 4 and 5 show the results of the questionnaire in graphic form.

Severity of petechiae. When compared to the standard anti-G suit, six of the nine subjects said that the severity of petechiae was the same or better (less severe) with the COMBAT EDGE system (Figure 4a).

Overall fatigue. When compared to the standard anti-G suit, all nine subjects said that fatigue level was the same or better (less severe) with the COMBAT EDGE system (Figure 4b).

COMBAT EDGE as a means of G-protection. All nine subjects rated the COMBAT EDGE system as either an advancement or "a great leap forward" in high-G protection (Figure 4c).

Use of the COMBAT EDGE in the cockpit. All nine subjects recommended the use of the COMBAT EDGE system in the cockpit (see Figure 4d). Four subjects suggested changes to the system before deployment, specifically, custom-fitting of the helmet and mask and implementing a training program aimed at familiarizing pilots with the system under simulated G before use in the cockpit.

Choice between COMBAT EDGE and anti-G suit. If given a choice, seven of the nine subjects would choose to be protected from high sustained G using the COMBAT EDGE system (Figure 5a).

Difference in personal G-tolerance. All nine subjects indicated that the COMBAT EDGE increased their G-tolerance. The average change in G-tolerance was an increase of +2.2Gz (Figure 5b).

Maximum G-level with the COMBAT EDGE and anti-G suit. Subjects were asked to estimate (project) their maximum G-tolerance when using either the standard anti-G suit or the COMBAT EDGE. The average G-level for the standard suit was +8.9Gz, while for the COMBAT EDGE system the average was +10.9Gz (Figure 5c).

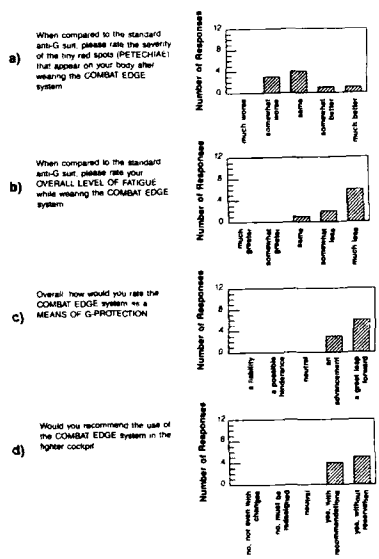

FIGURE 4
Questionnaire Results

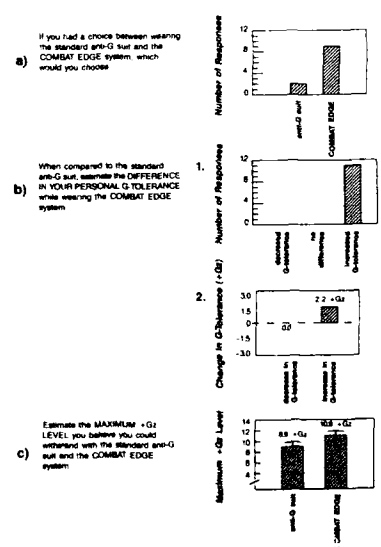

FIGURE 5
Questionnaire Results (continued)

DISCUSSION

Arm pain is expected to cause problems during operational deployment of an APPB system for G-protection, unless counteracted by some method of arm counterpressure [1]. Although there seems to be wide individual differences for incidence of arm pain, as well as tolerance to the pain, it seems likely that a small percentage of pilots will find arm pain unacceptable due to the APPB portion of the COMBAT EDGE system. In addition, breathing problems due to "backwards" breathing patterns with APPB (passive inhalation/forceful exhalation) seemed to be prevalent with people new to the system. Straining maneuvers were also fundamentally changed with APPB. Tensing of the legs, followed by no straining at all, were the most common types of straining effects reported. At first glance, this aspect of APPB seems to confer only an advantage in terms of increased G-tolerance. However, as pilots begin to rely on APPB in lieu of a traditional straining manuever, they may become complacent when letting the system "do the work for them." Under extremely rapid onset (2 to 4 +Gz/sec), as found in F-15 and F-16 aircraft [3], pilots cannot rely solely on APPB as protection against G-induced loss of consciousness.

These three points, arm pain, breathing quality, and changes in straining maneuvers, should be addressed through an APPB training program designed to alert pilots to these effects. In addition, pilots should also be alerted to the advantages which APPB may convey. Reduction in fatigue levels and increased G-tolerance are important advantages which should be stressed to facilitate operational acceptance of APPB.

CONCLUSIONS

The assisted positive pressure breathing portion of the COMBAT EDGE system conveys an added dimension of G-tolerance and endurance for humans experiencing sustained acceleration. Advantages include reduced fatigue due to lessening of anti-G straining maneuver effort and an increase in tolerance to higher levels of G-force. Disadvantages include increased arm pain and the need for training pertaining to modified breathing and straining techniques.

ACKNOWLEDGEMENTS

The authors wish to thank Maj Tom Morgan (U.S. Air Force, HSD/YAL) for allowing us the opportunity to test the COMBAT EDGE at our facility, and Squadron Leader Andy Prior (Royal Air Force, IAM, United Kingdom) for allowing us to adapt and use his concepts for the questionnaire forms.

REFERENCES

1. Ernsting, J. Some effects of raised intrapulmonary pressure in man. The Advisory Group for Aerospace Research and Development of the North Atlantic Treaty Organization (AGARD/NATO). London, England: W. J. Mackay, Ltd, 1966.

2. Chambers, R. M., Kerr, B. S., Augerson, W. S., and Morway, D. A. Effects of positive pressure breathing on performance during acceleration (NADC-MA-6219). Johnsville, Pennsylvania: U. S. Naval Air Development Center, 1962.

3. Gillingham, K. K., Plentzas, S., and Lewis, N. L. G environments of F-4, F-5, F-15, and F-16 aircraft during F-15 tactics development and evaluation (USAFSAM-TR-85-51, Restricted distribution). Brooks Air Force Base, Texas: U.S. Air Force School of Aerospace Medicine, 1985.

4. Prior, A. R. J. and Cresswell, G. J. Flight trial of an enhanced G protection system in the HAWK XX327 (IAM Report # 678). Farnborough Hampshire, United Kingdom: Royal Air Force Institute of Aviation Medicine, 1989.

5. Burns, J. W. Prevention of loss of consciousness with positive pressure breathing and supinating seat. Av. Sp. and Env. Med., 59, 1988, pp. 20-22.

6. Shaffstall, R. M., and Burton, R. R. Evaluation of assisted positive pressure breathing on +Gz tolerance. Av. Sp. and Env. Med., 50, 1979, pp. 820-824.

7. Shubrooks, S. J. Positive-pressure breathing as a protective technique during +Gz acceleration. J. of Ap. Phys., 35, 1973, pp. 294-298.

G-LOC

GZ ET HYPOXIE CÉRÉBRALE !
GZ/S ET HYPERTENSION INTRACRANIENNE ?
SYNTHESE.

*P.QUANDIEU, **D.GAFFIÉ, ***PH.LIÉBAERT, *M.BRIANE,
***J.C.SARRON, *A.GUILLAUME, *D.TRAN., *J.PH.HAYMAN.

*Centre d'Etudes et de Recherches de Médecine Aérospatiale, Division de Biomécanique
Base d'Essais en vol 91228 Brétigny sur Orge (France)
**O.N.E.R.A.,Département Energétique 29, avenue de la division Leclerc
92320 Chatillon sous Bagneux (France)
*** Direction des Recherches Etudes et Techniques Tour D.G.A.
Service des Recherches/G9, 26 Bvd Victor Paris 00457 Armées (France).

Have you ever had a loss of consciousness episode?

"I can't remember"

Réponse d'un pilote de chasse américain à une enquête anonyme sur les pertes de connaissance en vol.

I)INTRODUCTION

Lors de changement de direction, les pilotes de chasse subissent pendant le virage de leur avion, des accélérations qui les tassent sur leur siège. Elles peuvent parfois, être plus nocives et provoquer des pertes de connaissance en vol (PCEV). Depuis cinquante ans ces PCEV ou GLOC (Gz loss of consciouness), provoquées par les accélérations $+G_z$ d'installation relativement lente sont attribuées à une cause clairement orientée vers la physiopathologie: l'hypoxie cérébrale (Hy.C.). Cette explication physiopathologique est aujourd'hui admise par l'ensemble des spécialistes de médecine aéronautique.

Cette Hy.C. est consécutive à l'accroissement de la composante hydrostatique hpG_z de pression sanguine. Cette composante augmente linéairement avec l'accélération G_z (h étant la hauteur de la colonne sanguine entre le cerveau et la base du cœur). G_z étant colinéaire à l'axe longitudinal des grands vaisseaux aortocarotidiens et jugulocaves, les forces d'inertie (on parle alors de charges ou de "facteurs de charges" lorsqu'on les confond avec G) s'opposent à la progression du sang vers la tête. La pression hydrostatique augmentant, la somme des composantes pression motrice et pression hydrostatique de la pression sanguine tend vers zéro. Dès lors la distribution sanguine artérielle a tendance à s'effectuer vers les membres inférieurs. La compliance veineuse étant bien supèrieure à la compliance artèrielle, le phénomène est encore plus marqué dans le système vasculaire à basse pression.

Schématiquement le territoire cérébral devient hypovascularisé, donc hypoxique.

La mise en pression d'un vêtement anti-G (compression de l'abdomen et des membres inférieurs) s'oppose à cette redistribution sanguine vers le bas du corps. C'est donc un excellent moyen de protection contre les PCEV d'installation lente (+Gz GOR - gradual onset rate- des anglosaxons), puisqu'il augmente le "temps de conscience utile" du pilote, cette période de temps qui précède la perte de conscience.

Non seulement cette explication est d'une grande cohérence, mais elle est de plus confirmée expérimentalement. Notre laboratoire, parmi beaucoup d'autres, s'est attaché depuis des années à

Cette étude est financièrement soutenue par La Direction des Recherches Etudes et Techniques (DRET/G9).

améliorer la compréhension du phénomène tant au point de vue de la physiologie que de la biomécanique cardiovasculaire. [Borredon (1,2,3,4,), Liscia (30), Briane & Quandieu (7,37), Quandieu (38) Tran (47,48)].

L'hypoxie cérébrale ne se produit pas sans créer d'altérations des fonctions sensorielles et les troubles de la vision sont bien connus des pilotes de chasse. Ils se traduisent par la réduction de la vision périphérique (voile gris) puis de la disparition de la vision centrale (voile noir) précédant immédiatement la PCEV. L'échelle des temps est alors de la dizaine à la vingtaine de secondes en fonction de la charge.

Au début des années 80 l'amélioration de la motorisation accroit la manœuvrabilité des avions de chasse. En effectuant très vite, des virages très serrés et de longue durée, les pilotes subissent des accélérations - fait nouveau- d'installation très rapide (+Gz ROR, rapid onset rate), de très forte amplitude et de très longue durée. Le taux de variation de l'accélération est connu sous le nom de "Jolt". Il s'exprime en $G.s^{-1}$.

Au début de ces mêmes années 80 les rapports concernant les effets de ce nouveau type d'agression des pilotes de chasse font état d'une nouvelle forme clinique des PCEV, essentiellement marquée par l'absence de voile. L'individu soumis à ces accélérations d'installation très rapide ne présente plus les signes visuels d'alerte si utiles pour engager une manœuvre d'annulation du facteur de charge. Cette nouvelle symptomatologie fait des Gz-ROR "un vrai problème majeur de sécurité en aéronautique militaire" (Poirier 36).

En outre, la PCEV est parfois concomitante de la mise en accélération, c'est à dire que le temps de conscience utile est pratiquement réduit à rien. Enfin, il est fréquent que le pilote ne se souvienne de rien (amnésie lacunaire).

En résumé, la nouvelle symptomatologie des PCEV engendrées par les accélérations d'installation rapide est la suivante: immédiate (mais peut parfois être retardée), sans prodromes visuels, sans souvenir de l'accident.

L'échelle des temps quand l'accident est précoce, est alors de la seconde, voire inférieure à la seconde!

Malgré ces différences capitales - changements des caractéristiques physiques de l'agent agressif et changements de la symptomatologie de la réponse - les milieux médicaux spécialisés gardent tout son crédit à l'étiologie hypoxique selon l'assertion:

*Le facteur de charge est plus rapidement établi, donc l'hypoxie cérébrale également!

*Corollaire: puisque l'hypoxie est immédiate, il faut mettre en pression le pantalon antiG précocement, voire anticiper son action.

Une raison, au moins, s'oppose à une telle explication, elle est d'ordre physiologique: il est clair que les "temps caractéristiques" des phénomènes physiques mis en jeu dans cet accident, sont de plusieurs ordres de grandeur plus brefs que les temps de réponse des "phénomènes physiologiques" sur lesquels ils s'exercent.

En d'autres termes, nous posons l'hypothèse qu'une hypoxie cérébrale ne peut être créée en quelques centaines de millisecondes.

Une autre explication, strictement biomécanique, des PCEV d'installation rapide mérite d'être envisagée. Elle ne s'oppose pas à la théorie hypoxique mais elle la complète et s'appuie sur les réalités suivantes:

-le pilote se trouve subitement placé dans un champ de forces de forte intensité
-ces forces sont des forces de volume et non des forces de surface
-le comportement mécanique des structures nerveuses est de type visco élastique
-la masse sanguine circulant à l'intérieur de l'encéphale possède d'évidentes propriétés d'inertie.

Sur ces bases l'hypothèse est faite que les structures nerveuses cérébrales, soumises à une accélération +Gz à fort G/s, deviennent fonctionnellement inefficaces non par manque d'oxygène (Hy.C.), mais par accroissement brutal des contraintes mécaniques intracérébrales, réalisant au sens strict une hypertension intracrânienne précoce (H.I.C.).

Dès lors la mise en pression rapide du vêtement antiG, en même temps que la prise d'accélération, deviendrait potentiellement dangereuse en risquant de créer, au niveau cérébral, un "coup de bélier hydraulique" dans le système vasculaire, ce que nous allons nous attacher à analyser.

2) ANALYSE BIBLIOGRAPHIQUE

Amplitude

Les nouvelles générations d'avions d'armes développent des accélérations de forte intensité de longue durée et surtout dans un temps d'installation extrêmement court. Gilligham (18) rapporte que l'avion A10 possède un jolt de 10 G/s et Knudson (24) publie un jolt de18G/s pour le F-18.

Temps physiologiques

L'arrêt total du débit sanguin dans l'artère temporale précède le voile gris de 2 à 20 secondes (Pelligra 34), la perte de vision périphérique (voile gris) survient pour une pression artérielle oculaire systolique de 50 mm de Hg (Burton 10; Souder 45). La perte de vision centrale (voile noir), intervient

alors pour une pression systolique de 20 mm de Hg dans l'artère ophtalmique (Burton 10; Simmons 44).

La perte de conscience est en général plus tardive que la perte de la vision. L'explication communément rapportée fait intervenir un effet de siphon (au cours des accélérations) i.e. la fuite du sang veineux engendre une aspiration du sang artériel et protége le cerveau (Clère 15, Howard 21, Nickell 33). Cette explication mériterait d'être finement analysée au plan expérimental, car elle ne tient pas compte du fait fondamental selon lequel il n'y a d'effet de siphon que dans les tuyaux rigides et ouverts, ce qui n'est pas le cas pour le système artèrioveineux, essentiellement assimilable à un modèle de tuyaux collabables fermés.

Fréquence

Les PCEV sont des accidents connus depuis le début de l'aviation. L'un des premiers signe de voile décrit dans la littérature est celui survenu chez un pilote qui présenta une "perte de vision périphérique" lors de la compétition pour l'attribution de la coupe Schneider. Entre 1966 et 1971 Rayman (40) rapporte 36 cas de PCEV dans l'USAF ayant entraîné sept fois le décès des pilotes. Seuls neuf cas sont en relation directe avec les accélérations: cinq cas sont liés à des manœuvres M1 mal pratiquées, un cas est dû à une asystolie au cours de l'application de Gz négatifs, enfin trois cas sont dus à une étiologie qui devait être reconnue par la suite comme une trop faible tolérance aux accélérations. De 1970 à 1980 le même Rayman (40) dénombre dans l'USAF quarante PCEV dues aux accélérations ; trente-sept sont liés à des manœuvres M1 mal pratiquées et trois à une trop faible tolérance aux accélérations.

Burton (11) et Hood (19) rapportent qu'entre 1980 et 1986 les PCEV ont occasionné la destruction de trente appareils, au moins, de l'USAF (en général avec mort des pilotes) dont 8 F16 et 4 F15 capables d'accepter des facteurs de charges très élevés. Vingt pour cent des sujets d'une population de pilotes de F16 interrogés de façon anonyme reconnaissent avoir probablement présentés des épisodes de PCEV. Au cours de la troisième réunion des Flight Surgeon de L'OTAN (Ramstein Air Force Base 1987) il a été rapporté, que 10% environ des 1000 pilotes de chasse de l'USAFE ayant subi un test dans la centrifugeuse de Sösterberg selon un profil d'accélération simulant un combat aérien moderne, ont présenté une perte de conscience; 140 de ces pilotes par ailleurs reconnaissent avoir fait au cours d'un vol des épisodes qui pourraient être assimilés à des PC n'ayant pas laissé de trace dans la mémoire des individus.

Une enquête anonyme de l'armée de l'air française (1320 questionnaires) rapportent 98 PCEV, 9 pilotes pensent avoir fait une amnésie lacunaire associée (17).

Séquence

De nombreux auteurs étudient aujourd'hui ce phénomène. Burton (11), Hood (19), Landry (27), Leguay (28) et Whinnery (51) subdivisent la PC en deux étapes : une période d'incapacité absolue où la conscience est totalement abolie et une période d'incapacité relative qui s'accompagne de confusion et de désorientation. La première phase dure de 15 à 30 secondes selon les cas. Whinnery (52) note une bonne corrélation entre la durée de cette phase et le niveau d'accélération. Il ajoute que la P.C. est plus longue au cours des accélérations d'installation progressive que lors des accélérations d'installation brutale. Houghton (20) confirme ce fait : 23,7 secondes pour les accélérations brutales, 32 secondes pour les autres. La phase d'incapacité relative n'est pas corrélée au niveau d'accélération, elle dure en moyenne 20 à 30 secondes (Hood 19) et Whinnery (52). Le pilote ne retrouve sa pleine capacité à faire face à une situation complexe qu'au bout d'environ trois minutes.!! (Hood & Houghton).

Pertes de connaissance sans signes visuels

Le nombre des publications concernant les PCEV est très élevé et il n'est pas question d'en faire ici une analyse exhaustive. En outre, les accélérations dont il est question ci-après ne concernent que les Gz.

" Il est généralement admis que plus le temps d'installation des accélérations est long, plus les possibilités de mise en jeu des phénomènes de compensations physiologiques interviennent ". C'est ainsi que s'exprimait il y a 25 ans déjà Kydd et ses collaborateurs (22) travaillant sur des primates. "Toute étude concernant la tolérance aux accélérations devrait inclure des informations concernant la nature de l'accélération". Cette réflexion apparaît dans la discussion où Kydd relate les travaux de Rossen effectués en 1943 lequel interrompait brutalement la circulation sanguine cérébrale chez l'animal et obtenait des effets identiques à ceux engendrés par les accélérations.

Par conséquent, la relation "pression sanguine vs. accélération", fait intervenir deux fonctions: la diminution de la pression artèrielle, elle-même fonction du mode d'application des accélérations et la mise en jeu des régulations physiologiques d'autant plus intenses que la chute de pression est importante.

Edelberg (16) en 1956 avançait l'hypothèse purement théorique, que la contribution des réflexes physiologiques mis en jeu pour lutter efficacement contre les accélérations n'est maximale que s'ils ont le temps de s'opposer à l'accroissement de la composante hydrostatique de la pression artérielle. Ce temps nécessaire à l'adaptation cardiovasculaire suivant l'excitation des baro-récepteurs aortiques et carotidiens est, approximativement, de huit secondes.

Une notion s'est donc tout de suite imposée: <u>la présence ou l'absence de prodromes visuels est une fonction du temps</u>.

Pluta (35) montre (étude en centrifugeuse-USAFSAM) que la PC qui survient lors de la mise en accélération rapide peut ne pas s'accompagner des prodromes classiques de voiles gris et noirs tels qu'il est de règle dans les applications à forts facteurs de charges lentement établis. Une enquête anonyme conduite à la même époque rapporte un épisode de PC.(12% des pilotes) pour lequel la rapidité

d'installation de l'accélération arrive également en premier lieu. Cette PC sans prodromes est d'autant plus dangereuse pour le pilote que "la diminution du champ visuel périphérique est un excellent signe d'alarme" (Wood 53).

Jaron et coll.(26) fixent à 1Gz/s la limite de jolt pouvant provoquer des pertes de connaissance sans prodromes visuels. C'est cette valeur qui sera prise comme référence aux U.S.A.

Analyse de l'article de Whinnery JE,Burton RR,Boll Pa,Eddy DR(52). Characterization of the resulting incapacitation following unexpected +Gz induced loss of consciousness. Cette étude examine les PC observées en centrifugeuse selon deux types d'exposition aux Gz: installations rapides 2,5 Gz/s et 6 Gz/s, installation lente 0,1 G/s.

Cinquante cinq PC sont rapportées (âge moyen 32,7 ans ±6,2 (extrêmes 24 à 48). Moyenne des G +7,9 Gz ±1,2 (extrêmes 8-4Gz). Distribution selon les $Gz.s^{-1}$, $Gz.s^{-1}$=0,1 62%, $Gz.s^{-1}$=2 52%, $Gz.s^{-1}$=6 36%.

Deux modalités de récupération sont appréciées et définissent soit une incapacitation objective dite "incapacitation totale" (éteinte d'une alarme visuelle ou sonore), soit une incapacitation subjective (appréciée par l'observateur) dite "incapacitaton absolue".

Les résultats montrent que les temps d'incapacitation totale sont de 34,9 s (GOR), 24,8 s (ROR) et que les temps d'incapacitation absolue sont de 19,3s (GOR), de 12,2s (ROR) la différence étant extrêmement significative. Cette étude fait apparaître clairement l'existence de deux types de syndromes qui ne peuvent être rapportés aux seuls $Gz.s^{-1}$ puisque les temps d'application des accélérations sont moins longs pour les lancements rapides de la centrifugeuse. Enfin l'absence de mémorisation de la PC est rapportée en première place dans la liste des phénomènes associés.

Implicitement les auteurs rapportent les phénomènes observés à des phénomènes d'hypoxie, quelles que soient les vitesses d'accélération.

Whinnery et Jones souligneront ultérieurement, la fréquence de l'amnésie lacunaire chez la plupart des sujets qui se sont soumis volontairement à une PC. Il faut parfois les convaincre de la réalité du fait, même si quelques uns d'entre eux la suspecte.

A noter que la perte de connaissance s'accompagne parfois de mouvements cloniques cessant ensuite spontanément.

Rapidité de mise en pression du pantalon anti-G

L'effet du pantalon anti G est tout à fait clair du point de vue hémodynamique. Son efficacité n'est plus à démontrer et son étude bibliographique ne sera pas reprise ici. En augmentant les résistances vasculaires périphériques par voie externe, il améliore la perfusion cérébrale et diminue la migration sanguine dans les vaisseaux du bas du corps, (diminution du gradient de pression entre l'encéphale et la base du cœur). L'idée de son utilisation en pratique chirurgicale est déjà ancienne et son application est aujourd'hui d'usage courant. Brinquin et Coll (9) publient les résultats d'une étude conduite chez l'homme en position assise concernant l'utilisation d'un pantalon anti G pour lutter contre le choc neurochirurgical. Les résultats sont tout à fait démonstratifs. Ils sont obtenus pour des pression de 30 mmHg au niveau des membres inférieurs et de 25 mmHg au niveau abdominal. Chez le pilote -qui lui est soumis à un champ de force- les valeurs de pression atteintes dans le vêtement sont de l'ordre de 500 mmHg.

La théorie hypoxique admise même pour les forts jolts, justifie les recherches d'un gonflement accéléré du vêtement anti-G. Moore et ses collaborateurs(32) essaient (à l'instar de Van patten-30- qui tente d'améliorer la réserve d'oxygéne cérébral) de développer un vêtement à gonflement pulsé en opposition de phase avec les temps de la révolution cardiaque de telle sorte que la baisse de pression au niveau de l'encéphale soit la plus faible possible.

Beaucoup de laboratoires sont à la recherche d'un autre mode de protection contre les effets des accélérations. Mais d'une façon générale toutes les recherches spéculent sur des bases physiologiques. Krutz et Coll.(25) espèrent une amélioration des résistances vasculaires périphériques par la mise en oeuvre d'une technologie améliorée d'un vêtement pneumatique à pression uniforme. L'amélioration des lois de comportement de nouvelles valves se poursuit (Meeker et coll. 31) tandis que les inconvénients d'un déclenchement trop rapide sont surtout rapportés à un inconfort plutôt qu'à un risque augmenté de perte de connaissance (Ratajczak 39).

R.R.Burton(12) analyse les différentes méthodes de lutte contre les effets des accélérations. Il souligne qu'un certain nombre de questions n'ont pas encore trouvé de réponse en matière d'établissement d'une pression intrathoracique supérieure à 100 mmHg (50 mmHg de respiration en pression positive associée à 100 mm Hg de manœuvres antiG).

Certains auteurs et non des moindres comme E.Wood(53) n'hésitent pas à dire que les très hautes pressions appliquées pour maintenir l'efficacité de la circulation cérébrale d'un pilote assis et soumis à de forts facteurs de charges peuvent être potentiellement dangereuses. Cet auteur d'ailleurs, rappelant les travaux anciens effectués dans les laboratoires de la Californie du sud pose à nouveau la question d'une position allongée des pilotes, celle là même qui avait été envisagée pendant la deuxième guerre mondiale.

Analyse d'un article de R.R.Burton (13)sur les conditions de rapidité de mise en pression du vêtement anti G.

L'auteur analyse les résultats d'études conduites chez des sujets placés en centrifugeuse et soumis à des accélérations sous jolts croissants. Tous les sujets portent un pantalon anti-G. Le vêtement utilise une valve électronique programmable avant l'exposition aux G, quel que soit le niveau de la charge. Les résultats montrent que la tolérance sous 6G/s est de 2,3 G inférieure à la tolérance mesurée à 1G/s (en

position relâchée). Cette différence est attribuée au temps de mise en jeu des baro-récepteurs. Un délai de 3,3 secondes en moyenne du gonflement du pantalon antiG ne change pas la tolérance aux accélérations (en position relâchée) à $6G.s^{-1}$.

Les explications physiologiques données par l'auteur pour les légères différences de tolérance aux accélérations observées chez des sujets détendus sont reliées à la fonction des baro-récepteurs (le taux de 1G/s donne plus de temps au réflexe d'entrer en action). Il n'en reste pas moins d'après Burton que la vitesse de mise en accélération est un facteur important de tolérance aux Gz d'un sujet détendu. Enfin, une vitesse de gonflement extrêmement rapide n'est pas nécessairement utile et peut avoir un effet opposé sur le confort du pilote et par conséquent sur son acceptabilité.

En réalité, il n'existe pas, à notre connaissance, de faits expérimentaux qui démontrent définitivement la nécessité d'une mise en pression immédiate du vêtement anti-G.

3)RAPPELS ÉLÉMENTAIRES DE MÉCANIQUE

Forces de surface et forces de volume.

La mécanique des milieux continus distingue la mécanique des solides élastiques et la mécanique des fluides. Le cerveau est, au plan de la mécanique, un milieu continu, caractérisé par des champs m(r,t), P(r,t), v(r,t) T(r,t)...masse volumique, pression, vitesse d'ensemble, température...précisés en chaque point de position r de la masse cérébrale étudiée et à tout instant t.

Considérons le cerveau comme un système physique; le volume V du milieu (cérébral continu) intérieur à la surface corticale S fermée. On distingue deux types de forces qui peuvent être appliquées à l'encéphale: les forces de surface qui s'appliquent à S, les forces de volume (forces à distance) qui s'exercent sur la matière contenue dans V.

Les forces de volume s'exercent sur chaque élément de volume dv de sorte que la force agissant sur un élément de position r à l'instant t est telle que: $dF_V = \mathbf{f}_V(r,t)dv$. Habituellement en mécanique on s'intéresse en pratique, au seul champ de pesanteur; dans ce cas $F_V = mG$ où m est la masse volumique de l'élément de volume.

Contraintes mécaniques

En notant dF_S la force de surface qui s'exerce sur un élément d'aire dS situé autour d'un point M de S, cet élément étant caractérisé par le vecteur-surface $\vec{dS}=\vec{n}dS$ ($\vec{n}$ vecteur unitaire normal à S et dirigé vers l'extérieur) on appelle contrainte en M le vecteur $\vec{\tau}_s = \frac{d\vec{F}}{dS}$ où $\vec{\tau}_s$ définit la densité superficielle de force.

La norme de la contrainte a donc les dimensions d'une pression (Pa). Le vecteur peut être considéré comme la somme d'une contrainte **normale** à S et d'une contrainte **tangentielle** (vecteur contenu dans le plan tangent en M à S)

Si la contrainte s'exerce vers l'extérieur du cerveau elle est dite de **traction**, vers l'intérieur elle est dite de **compression**.

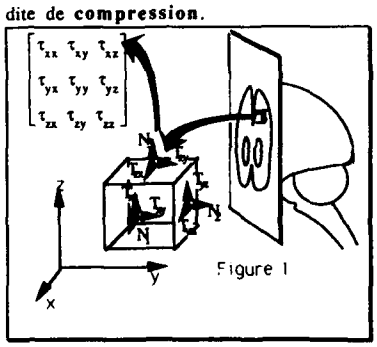

Figure 1

Figure 1: lorsqu'un petit cube élémentaire de matière cérébrale de côté dx,dy,dz est en équilibre l'ensemble des forces auxquelles il est soumis est équivalent à 0. On montre que la matrice représentative de [t] dans un repère Oxyz jouit des propriétés mathématiques qui définissent un tenseur, elle est donc appelée tenseur des contraintes dans lequel:

τ_{xx} est la contrainte de tension dans la direction de x sur la surface normale à l'axe x

τ_{xy} est la contrainte de cisaillement dans la direction de y sur la surface normale à l'axe x

τ_{xz} est la contrainte de cisaillement dans la direction de z sur la surface normale à l'axe x etc..

Quand des variations de contraintes sont engendrées dans un élément de volume élémentaire elles provoquent des variations de géométrie dans ce volume élémentaire qui correspondent à la superposition de trois déplacements: une translation, une rotation, une déformation qui est seule créatrice d'une "dilatation" et d'un "glissement" (la translation et la rotation étant des déplacements d'ensemble).

Au total pour un petit élément de volume de masse volumique invariable en équilibre dans un champ de forces on doit considérer l'état des contraintes et l'état des déformations.

Solide élastique, solide plastique

Un corps dans l'état solide se déforme sous l'action de contraintes tangentielles. Cependant sous l'action d'une contrainte tangentielle donnée il atteint nécessairement une position d'équilibre au bout d'un temps plus ou moins long (en cas contraire se serait un fluide). Si la déformation ainsi acquise disparaît entièrement le solide est dit élastique s'il retrouve sa forme initiale; dans le cas contraire il est

dit plastique.

Dans les conditions normales chez le vivant, le cerveau est donc un solide élastique. Mais il possède également des propriétés mécaniques de viscosité: son comportement sous l'effet de l'application d'une force est celui d'un solide viscoélastique dans lequel les contraintes sont liées aux déformations et aux vitesses des déformations.

Nous considérerons dans ce qui suit, que le crâne osseux est rigide devant le tissu cérébral qui sera considéré comme mou dans le cas d'application d'une charge. Le caractère "mou" est une caractéristique physique qui ne doit pas être confondue avec l'aspect "flasque" de la pièce anatomique.

Equilibre des milieux continus déformables

Nous,médecins spécialistes de médecine aéronautique avons toujours pris comme modèle mathématique appliqué au comportement mécanique des structures biologiques, le modèle de la dynamique du point matériel

$$\vec{F} = m\,\vec{\Gamma}$$

Or, les organes anatomiques peuvent difficilement être assimilés à un point matériel. Le modèle est donc insuffisant, celui de la dynamique des milieux continus déformables sans être totalement satisfaisant est déjà plus proche de nos problèmes:

$$\vec{Div}\,\bar{\bar{\sigma}} + \vec{F} - \rho\,\vec{\gamma} = 0$$

dans lequel:

$\rho\,\vec{\gamma}$ est la densité de force d'inertie par unité de volume

$\vec{F}$ est la densité de force de volume (par unité de volume)

$\vec{Div}\,\bar{\bar{\sigma}}$ rend compte du comportement du tenseur des contraintes lors de la variation de l'un des deux autres paramètres.

Une action sur la densité de force de masse par unité de volume ne peut prendre naissance que si le "temps physique" d'application du facteur de charge est suffisamment grand devant le "temps biologique".

Si le "temps physique" d'application du facteur de charge (cf infra: "temps caractéristiques" de D.Gaffié) n'est pas *suffisamment grand devant* les temps de réaction biologiques, ce sont les contraintes qui augmentent.

Enfin si γ augmente trop et trop vite, les effets mécaniques sur les structures cérébrales débordent les possibilités des régulations physiologiques.

4)PROPOSITION D'UN MODELE

Description (figure 2).

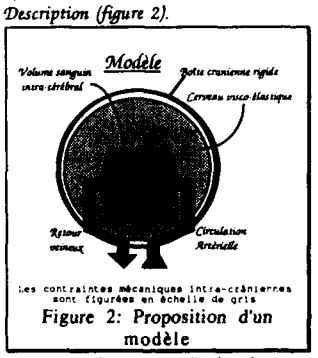

Figure 2: Proposition d'un modèle

Dans une première approche du comportement biomécanique de l'encéphale on se contentera de considérer cet organe comme une masse sphérique déformable enfermée dans une enveloppe totalement rigide (le crâne), le cerveau étant séparé de cette enveloppe par un film liquidien (le liquide céphalo rachidien). Le cerveau lui-même est composé de deux phases:

-une phase solide (le tissu nerveux)

-une phase liquide: le volume sanguin

contenu dans un système vasculaire complexe à l'intérieur de la phase solide.

Le système vasculaire est arborescent selon la description la plus classiquement élémentaire du système artériel vers le réseau capillaire puis du réseau capillaire veineux vers le système collecteur de retour. La géométrie des gros troncs vasculaires est coudée pour prendre en compte les difficultés des écoulements.

Deux paramètres sont à étudier dans ce modèle:

-les contraintes dont les variations d'amplitude sont représentées par une échelle de gris

-les déformations globales liées à la diminution de la masse sanguine sous l'effet des accélérations (redistribution vers la partie basse du corps). Les comportements mécaniques appliqués à ces différentes structures sont les suivants:

-purement rigide: crâne osseux

-fluide et faiblement visqueux : LCR

-viscoélastique pour la matière cérébrale

5)ANALOGIE

L'image d'une éponge gorgée de liquide sur laquelle s'exerce une force manuelle (bien qu'il s'agisse d'une force de surface, nous l'assimilerons à une force de volume i.e. accélération d'installation lente) permet d'éclairer notre propos:

*si la pression sur cette éponge est suffisamment lente, les contraintes mécaniques dans l'éponge ne seront jamais très élevées car le fluide ayant le temps de s'échapper, l'éponge ne présente pas de résistance et la pression manuelle reste faible, mais de longue durée (figure 3 haut).

*les termes de la proposition précédente s'inversent si la pression sur l'éponge est très rapidement réalisée, les contraintes mécaniques intraspongieuses s'élèvent très fortement avec la pression manuelle car le fluide n'ayant pas eu le temps d'être exprimé à l'extérieur oppose une résistance maximale (figure 3 bas)

Dans cet exemple d'application de la loi d'action et de réaction, la viscosité du fluide est évidemment un facteur déterminant quant à ses possibilités d'écoulement hors de l'éponge.

L'exemple que nous avons pris devient un peu moins trivial si on réalise la même expérience, l'éponge étant cette fois plongée dans un vase rempli de liquide. On sent bien intuitivement que l'expression du liquide hors de l'éponge - donc le niveau des contraintes dans l'éponge- est directement fonction de la pression dans le vase, et non seulement fonction de la vitesse d'application des forces manuelles.

Même si la pression sur l'éponge est suffisamment lente, les contraintes mécaniques dans ses parois sont d'autant plus élevées que la pression extérieure est plus grande!

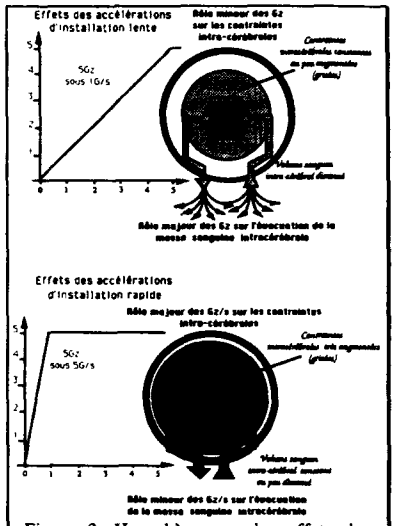

Figure 3. Hypothèses sur les effets des modalités d'application des accélérations +Gz sur les contraintes intracrâniennes.

5.1.Hypothèses

5.1.1.EFFETS DES ACCELERATIONS +GZ DE FORTE AMPLITUDE ET A FAIBLE GZ.S^{-1} . (+GZ-GOR)

La pression dans l'éponge (encéphale) est maintenant le fait d'une force de volume (accélération).

Dans le cas des accélérations +Gz de forte amplitude et à faible Gz.s^{-1} l'interprétation qui prévaut en matière de PCEV est évidemment une interprétation de type physiopathologique.

Les accélérations +Gz interviennent de façon majeure en fonction de leur amplitude et de leur durée (cas classique de la tolérance aux accélérations proposée par A.Stoll 46- fig.4). La cible est la composante hydrostatique de pression sanguine. L'effet est celui d'une redistribution de la masse sanguine vers la partie inférieure du corps. La conséquence est une hypoxie cérébrale avec apparition des voiles gris, puis noir et perte de conscience au-delà.

Les contraintes intratissulaires restent égales à elles-mêmes ou augmentent peu et ne sont de toute manière pas nocives.

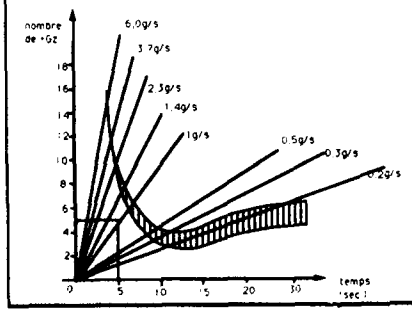

Figure 4. Courbe de tolérance humaine aux accélérations d'après Stoll (46).

Ce graphique établi en 1956 donne la tolérance aux accélérations + Gz en fonction du temps .

Au delà de la courbe en trait plein existe, quelque soit le niveau d'accélération, une perte de conscience du pilote. En deçà de la courbe en pointillé, le pilote conserve une conscience normale.

La zone hachurée constitue la zone des voiles : transition continue depuis le rétrécissement du champ visuel périphérique jusqu'au voile noir et la perte de conscience.

5.1.2. HYPOTHESES SUR LES EFFETS DES ACCELERATIONS +GZ D'AMPLITUDE VARIABLE SOUS FORT G.S^{-1} (+GZ/GOR)

Dans ce cas l'interprétation qui prévaudrait en matière de PCEV serait de type purement biomécanique. Les accélérations +Gz interviendraient de façon majeure par leur amplitude et surtout leur vitesse d'application.

La cible ne serait plus la composante hydrostatique de pression sanguine intravasculaire, mais le niveau de contraintes mécaniques intratissulaires.

Les effets d'inertie, de viscosité et probablement de géométrie du système vasculaire s'opposeraient à une expression de la masse sanguine hors de l'encéphale. Il n'y aurait pas d'apparition d'une hypoxie

Figure 5: Représentation graphique
En haut: Cas d'une prise de virage serré mais lentement établi i.e. 5Gz sous 1G/s (graphe a). Au centre: cas d'une prise de virage serré rapidement établi i.e.5 Gz sous 5G/s (graphe b).
En bas(graphe c) schéma d'une P.C par HIC avec cessation immédiate de l'accélération.

Les traits en pointillé indiquent ce que deviendrait le niveau de contraintes intra-encéphaliques si la redistribution sanguine hors du crâne ne se faisait pas.

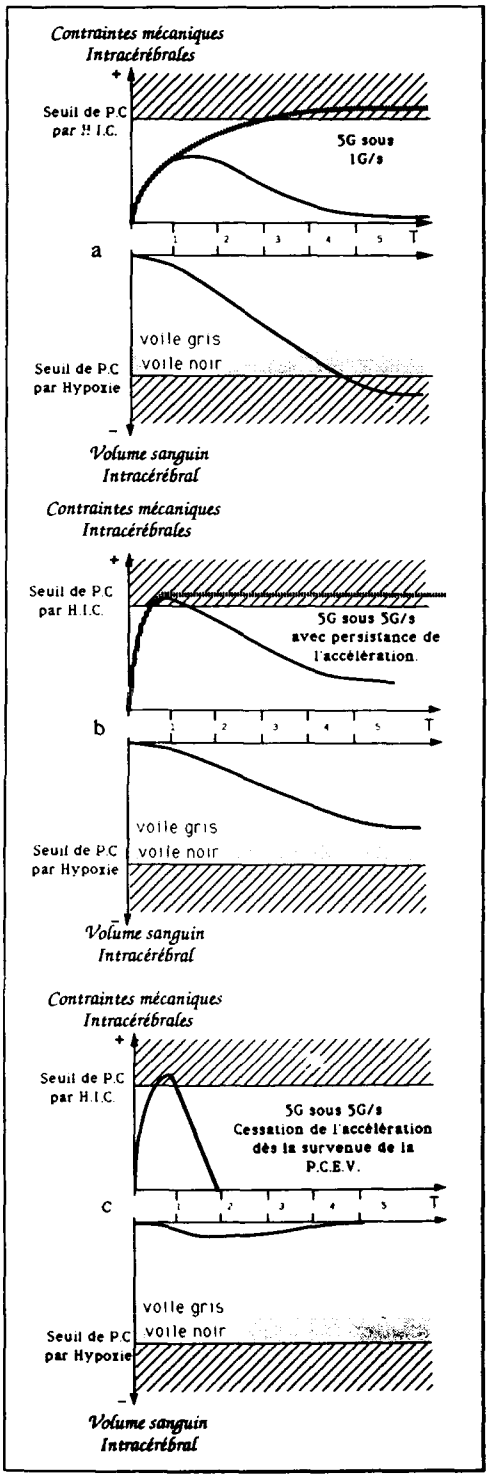

cérébrale faute de temps. La perte de conscience serait alors due à une augmentation brutale des contraintes intratissulaires cérébrales engendrées par l'application brutale des forces de volume.

Les contraintes étant homogènes à des pressions, la PCEV serait bien, au sens strict, très exactement due à une brutale hypertension intracrânienne (H.I.C.).

5.2.) Eléments de représentation graphique

Dès lors la représentation graphique de l'hypothèse d'hypertension intracrânienne est donnée figure n°5, pour laquelle l'axe des ordonnées figure en haut:

les variations positives des pressions intratissulaires et en bas les variations négatives de la masse sanguine intracérébrale pour chacun des graphes a,b,c.

5.2.1. CAS D'UNE PRISE DE VIRAGE SERRE MAIS LENTEMENT ETABLI (5Gz SOUS 1G/s, GRAPHE A).

Au début de l'application du facteur de charges, les contraintes mécaniques intracérébrales augmentent avec les forces de volume appliquées à l'encéphale (trait plein-a haut). Puis la diminution du volume sanguin intracérébral (viscoélasticité) intervenant en son temps (a bas), les contraintes mécaniques diminuent (haut) tandis que le risque s'accroît d'atteindre le seuil d'hypoxie précédé des voiles gris et noir. En quelque sorte, le cerveau "bénéficie", (en terme de diminution du niveau de contraintes mécaniques) de la diminution de la masse sanguine intratissulaire, il en "souffre" (en terme d'oxygénation).

5.2.2. DANS LE CAS D'UNE PRISE DE VIRAGE SERRE ET RAPIDEMENT ETABLI (5 Gz SOUS 5G/s graphe b).

Nous admettons pour des facilités d'explication que cette amplitude d'accélération atteint le seuil critique de tension mécanique intracrânienne. Là encore, au début de l'application du facteur de charges, les contraintes mécaniques intracérébrales augmentent avec les forces de volume appliquées à l'encéphale(b haut). Mais elles continuent d'augmenter et atteignent le seuil critique d'H.I.C. car le volume sanguin intracérébral est séquestré dans son enceinte de confinement crânienne. En quelque sorte, le cerveau "souffre", (en terme d'augmentation de contraintes mécaniques), de ce qu'il "bénéficie", (en terme d'oxygénation) de la conservation de la masse sanguine intratissulaire.

Dès lors la PCEV est immédiate et la sidération fonctionnelle des structures nerveuses, sans prodromes visuels, peut expliquer l'amnésie lacunaire.

6) ELÉMENTS DE VÉRIFICATION ANALYTIQUE (38)

Ce chapitre ne sera que très rapidement évoqué, car il est très précisément développé dans l'article de Gaffié et coll. (cf infra).

Le domaine d'étude est tel que la boîte crânienne est rigide, le tissu nerveux qui intègre un réseau de vaisseaux sanguins a un comportement viscoélastique et baigne dans le liquide céphalorachidien visqueux newtonien. La modélisation adoptée repose sur une étude découplée du comportement du matériau viscoélastique, des fluides périphériques et de l'écoulement du sang dans le système

Nomenclature

$K(z)$ Rigidité du tube	R Distance de l'axe à la paroi	F accélération centrifuge
f Loi analytique de profil de vitesse longitudinale	R_o Rayon au repos	F_z Composante axiale de l'accélération
L Longueur du tube	$S(t,z)$ Section du tube	$\alpha(z,t)$ Fonction introduite par l'intégration radiale
$P(z,t)$ Pression dynamique du sang	S_o Section du tube au repos	ρ Masse volumique du sang
$P_e(z,t)$ Pression extérieure s'exerçant sur la paroi latérale du tube	t Variable de temps	τ_p Contrainte visqueuse moyenne de cisaillement à la paroi
$P_t(z,t)$ Pression transmurale	$U(z,t)$ Vitesse moyenne	
r Variable d'espace de la direction transversale	V_z Vitesse locale longitudinale	
	z Variable d'espace de la direction longitudinale	

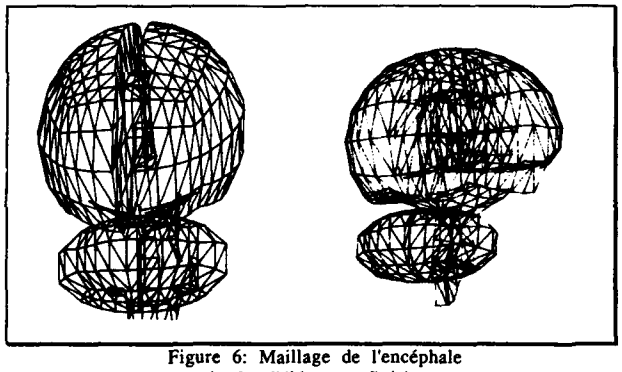

Figure 6: Maillage de l'encéphale
(code d'éléments finis)

6.1) Comportement de l'encéphale et du L.C.R.

L'étude expérimentale concernant la détermination des contraintes intracérébrales sera conduite à partir d'informations obtenues sur les déformations, c'est la raison pour laquelle un code d'éléments finis est en voie de développement au sein de la division de biomécanique du CERMA.

Le maillage nécessaire à l'utilisation de ce code est reproduit figure 6.

Toutefois les premiers résultats qui seront exposés plus loin ont été obtenus sur une structure plus simple.(cf: les niveaux de contraintes maximales dans le tissu nerveux sous une accélération de 6 Gz. §6.4).

On étudie deux cas limites:

a) cerveau viscoélastique seul pour lequel les évolutions du champ des contraintes sont obtenues numériquement par éléments finis

b: cerveau rigide dans le L.C.R. pour lequel la déformation du film visqueux est donnée par l'équation de la lubrification (42)

$$M\frac{\partial^2 h}{\partial t^2} + 3\mu\pi R^4 \frac{\partial h/\partial t}{h^3} = M\left(1 - \frac{\rho_0}{\rho}\right)\gamma$$

intégrée sur la base du cerveau supposée rigide et résolue numériquement par un schéma explicite en temps. Ces deux modèles fournissent, au cours du temps , les champs de contraintes dans la masse cérébrale et dans le L.C.R. respectivement. Ils délivrent un ordre de grandeur des perturbations qui affectent l'écoulement

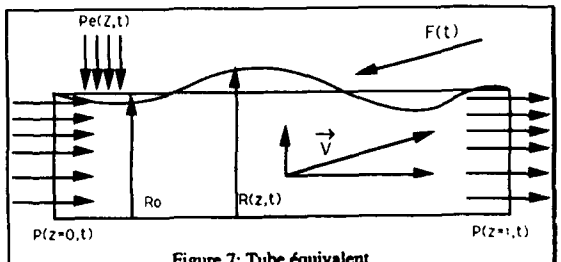

Figure 7: Tube équivalent.
Géométrie élémentaire du réseau de circulation sanguine
Cf.infra: Gaffié et coll.

sanguin décrit ci-après.

6.2) Modélisation de l'écoulement sanguin

Le choix est fait de modéliser par un tube équivalent élastique unique un ensemble de vaisseaux possédant des caractéristiques physiques voisines. Ces tubes équivalents sont ensuite reliés pour obtenir un modèle du système complet. Le tube équivalent dans lequel s'écoule un fluide visqueux incompressible est soumis à l'action simultanée du cœur, d'une distribution de pression extérieure s'exerçant sur les parois latérales et d'un champ de forces volumiques (figure 7).

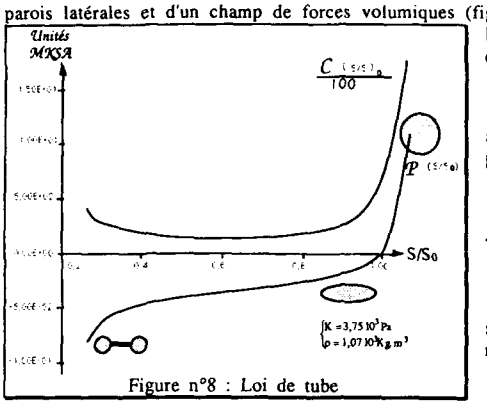

Figure n°8 : Loi de tube

Les équations locales de conservation de la masse et de la quantité de mouvement

$$\vec{Div}.\vec{V} = o \quad \text{et} \quad \rho \frac{d\vec{V}}{dt} = \vec{F} + \vec{Div}\,\bar{\bar{\sigma}}$$

ainsi que la formulation unidimensionnelle du problème

$$\begin{cases} \dfrac{\partial S}{\partial t} + \dfrac{\partial}{\partial z}(US) = 0 \\ \dfrac{\partial U}{\partial t} + (1-\alpha)\dfrac{\partial S}{\partial t}\dfrac{U}{S} + \alpha U \dfrac{\partial U}{\partial z} = \dfrac{1}{\rho}\left[-\dfrac{\partial P}{\partial z} + \dfrac{P_s}{S}\tau_p + F_z\right] \end{cases}$$

sont simplement évoquées ici (cf Infra: A detailed numerical model to study the GLOC).

6.3)La loi de tube (figure 8) est rappelée en raison de son importance

Le couplage entre le comportement mécanique du fluide et de la paroi est pris en compte par une loi d'état, la loi de tube suivante: $P-P_e=K(z)P(S/S_0)$. La forme analytique P est non linéaire par rapport à S. Ainsi la célérité de propagation des ondes dépend fortement de l'état local et instantané du tube. Si la pression transmurale est positive, le tube est dilaté, son comportement est quasi-rigide de sorte que la célérité des ondes dans la paroi devient très grande. Dans le cas contraire, le tube subit un écrasement, il devient moins rigide et la célérité est plus faible. Mais s'il est collabé avec un écoulement persistant il prend une forme d'haltères et l'on voit la célérité augmenter à nouveau (figure n°8).

En fonction du type de perturbations rencontrées, des écoulements supercritiques (U>C) sont observables qui peuvent être suivis de chocs de transition au régime subcritique (41).

6.4) Résultats

La figure n°9 donne les niveaux de contrainte maximale dans le tissu nerveux sous une accélération de +6 Gz. Dans la zone inférieure, la contrainte dépasse la pression des veines collectrices de l'encéphale prise comme référence (650 Pa). La figure n° 10 montre la variation de pression du fluide écrasé à la base du cerveau, au cours du temps à 1 et 7 G/s.

Dans ce dernier cas (hypothèse de perturbation brutale) la pression de référence est atteinte aux environs d'une seconde. L'écrasement du tube équivalent lors de l'application d'une distribution de pression extérieure sur sa paroi latérale est montré figure n°11. Cette distribution engendre des ondes pariétales qui se propagent le long du tube et font apparaître des collapsus vasculaires. Ces déformations soulignent une brusque modification du régime de l'écoulement sanguin (cf:infra: étude de Gaffié et collaborateurs).

Ainsi, Les premiers résultats de la modélisation indiquent bien qu'une accélération +Gz d'installation rapide pourrait engendrer une augmentation des contraintes mécaniques dans le tissu nerveux.

Figure n°9:
Contraintes intracérébrales

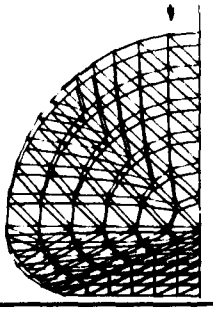

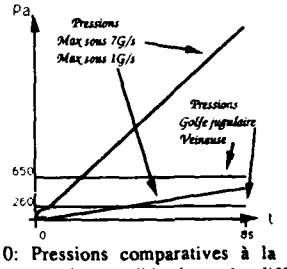

Figure10: Pressions comparatives à la base du crâne pour des accélérations de différents taux de variation

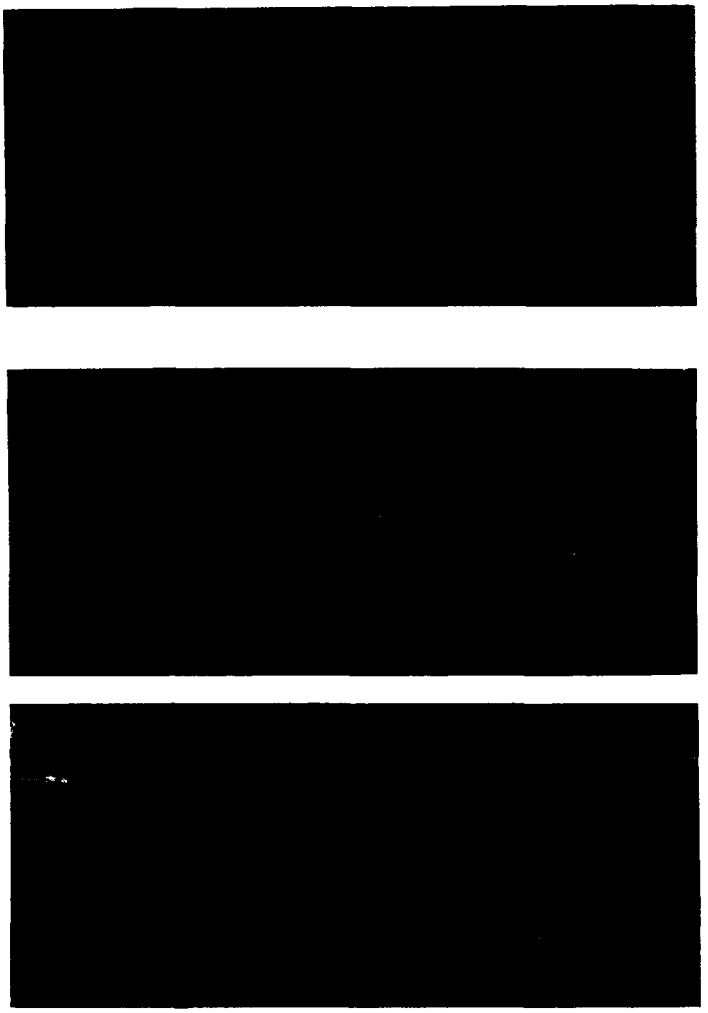

Figure n°11. Les brusques modifications du régime de l'écoulement sanguin (cf:infra: étude de Gaffié et collaborateurs)sont à l'origine de chocs aux transitions des régimes subcritique à supercritique de l'écoulement sanguin

6.5. Hypothèses sur les effets de la mise en pression du pantalon antiG.

Quels sont les effets hypothétiques de l'augmentation des résistances vasculaires périphériques de la partie inférieure du corps, relativement aux résultats qui viennent d'être obtenus?

En d'autres termes: à quel moment le vêtement antiG doit il être mis sous pression?

Les hypothèses sur les effets du vêtement antiG sont synthétisées sur la figure n°12. Il est tout à fait indispensable de noter l'existence d'un facteur d'échelle des temps qui peut être extrêmement important (soixante par exemple quand la mise en accélération passe de 0,1 $Gz.s^{-1}$ à 6 $Gz.s^{-1}$).

Comme précédemment, l'axe des ordonnées donne en haut les variations positives des contraintes intratissulaires et en bas les variations négatives de la masse sanguine intracérébrale.

Dans le cas des accélérations à faible $Gz.s^{-1}$ (graphe a en haut), l'augmentation des résistances vasculaires périphériques de l'abdomen et des membres inférieurs par pression du vêtement antiG, tend à s'opposer à la diminution de la perfusion sanguine cérébrale. Elle a donc un effet **bénéfique** sur l'oxygénation du tissu nerveux central ce qui est bien connu et utilisé depuis un demi siècle.

Selon le paramètre considéré, il permet soit de supporter un plus grand nombre de G pendant un temps donné, soit d'augmenter le temps de conscience utile pour une valeur constante d'accélération.

L'effet sur les contraintes mécaniques intracérébrales reste mineur lorsque la compression de la partie basse du corps est suffisamment retardée.

Dans le cas des accélérations à fort Gz.s^{-1} (graphe b, en bas), le champ de force volumique ayant été établi en quelques centaines de millisecondes, l'augmentation des résistances vasculaires périphériques basses tend à augmenter faiblement la perfusion sanguine cérébrale si la mise en pression du vêtement est rapide. Par contre, l'augmentation des résistances périphériques basses augmente la post charge ventriculaire. Ses effets, particulièrement l'effet **"coup de bélier hydraulique"**, se distribuent préférentiellement au territoire supracardiaque augmentant encore le risque de perte de conscience (utilisation du concept d'onde : transfert d'énergie sans transfert de matière).

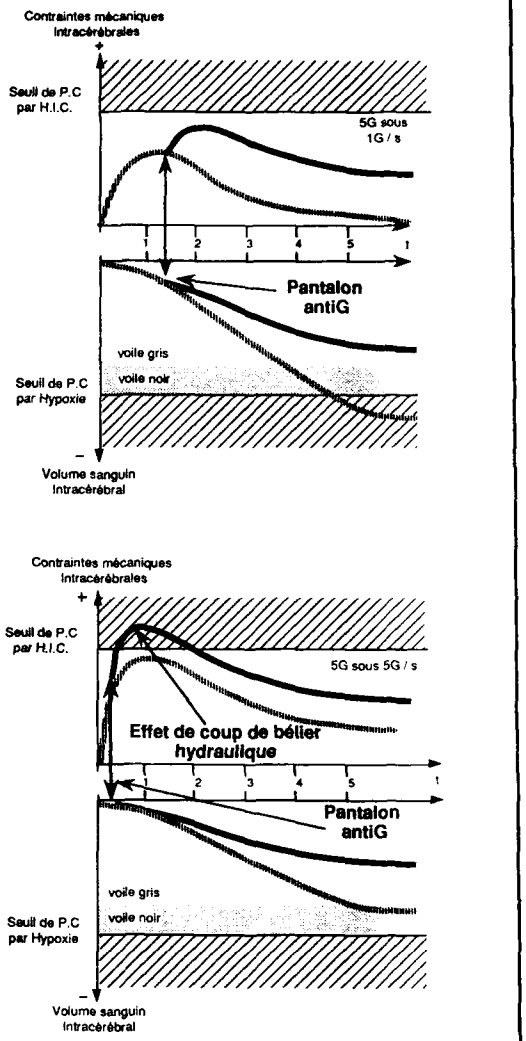

Figure 12: Hypothèses sur les effets d'une mise en pression rapide du vêtement antiG au cours d'une accélération d'installation lente (en haut) et d'installation rapide en bas.

Au travers de cette remarque se fait jour l'importance d'un troisième facteur: la valeur instantanée de la pression artérielle au moment de l'application du facteur de charges.

La pression artérielle intervient au travers de ces différentes composantes:

*la chronologie de la révolution cardiaque et l'instant d'application du facteur de charge

*la valeur maximale de la pression artérielle elle-même fonction de plusieurs paramètres dont:

-l'état physiologique du pilote (émotion, stress...)i.e. niveau du tonus sympathique, des taux de catécholamines et hormones hypertensives circulantes etc... (inotropisme myocardique): cet état basal, physiologique, de la pression artérielle, propre à chaque pilote à un moment donné (sensibilité individuelle), est certainement un des paramètres essentiels dans l'atteinte du seuil critique d'HIC.

-le volume d'éjection systolique qui peut être également fonction de la valeur instantanée du facteur de charge.

Ces différents aspects méritent d'être sérieusement examinés car ils permettront sans nul doute de répondre un jour, à cette angoissante question :

Pourquoi tous les pilotes soumis à une accélération sous fort jolt ne présentent-ils pas ,tous identiquement, une PCEV ?

Ce serait manquer de lucidité de croire que la réponse est donnée par la seule existence de cette sensibilité individuelle, que nous venons d'évoquer. Ce serait en outre admettre qu'il n'y a pas de parade envisageable. En fait ce qu'il faudra connaître c'est le niveau de pression intracrânienne auquel se situe le seuil de PC. Plus tard il faudra étudier les conditions physiologiques de fluctuations de la pression autour de ce seuil.

Dans notre hypothèse, l'agression physique impose le niveau du seuil de tension, l'état physiologique détermine l'amplitude des fluctuations autour de ce niveau. C'est évidemment sur ces fluctuations que

nous pouvons intervenir.

Les études suivantes ne prétendent pas donner la solution, mais elles nous apportent des éléments de réflexion et quelques éléments de réponse sur ce délicat problème.

7)NIVEAU DE PRESSION ARTERIELLE ET SEUIL CRITIQUE DE H.IC

7.1.Chronologie de la révolution cardiaque et instant d'application du facteur de charge

En se souvenant que seule la diastole est susceptible de présenter des variations de durée, en considérant la figure n°13 qui rappelle les durées des différentes séquences de la révolution cardiaque, prenons les deux cas d'espèce suivants:

1) le cœur d'un pilote d'avion de chasse, battant à une fréquence de 120 bpm et soumis à une accélération de +6Gz, à raison d'un taux de variation de 0,5 G/s

2) le même pilote, dont le cœur bat toujours à 120bpm subit à nouveau +6Gz, sous12Gz/s

Dans le premier cas, 12 cycles cardiaques ont le temps de se produire pendant la durée de l'accroissement de la charge avant l'application maximale des +6 Gz. Dans le second cas, le cœur n'effectue qu'un seul cycle pendant toute la phase de variation, considérée comme linéaire entre 1Gz et 6Gz!

On conçoit aisément que les effets sur le système cardiovasculaire de ces deux modalités d'application de facteurs de charges risquent d'être très différents.

Dans le premier cas, la redistribution sanguine vers le bas du corps dont nous avons déjà parlé, a le temps de s'effectuer autant dans le réservoir veineux que dans le lit artériel. Elle engendre par inefficacité du retour veineux une diminution progressive du volume de remplissage ventriculaire, donc une diminution de la précharge ventriculaire (en première approximation, la force exercée par la masse sanguine télédiastolique). Par conséquent, elle favorise l'établissement d'une faible pression artèrielle au maximum d'installation du facteur de charges qui va être contrebalancée ultérieurement par les différentes composantes physiologiques de la régulation de la pression artèrielle qui ont largement le temps d'être mises en œuvre.

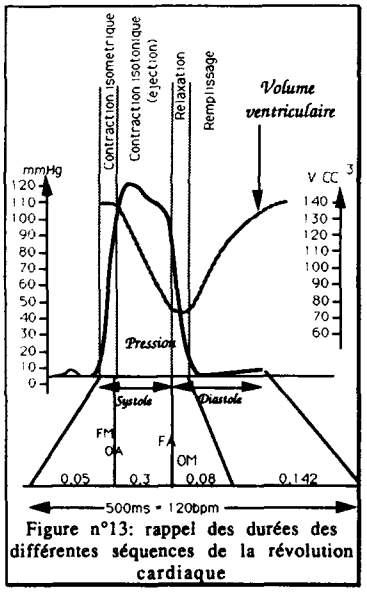

Figure n°13: rappel des durées des différentes séquences de la révolution cardiaque

Ceci est bien connu et a été rapporté comme un état de "surprise du cœur" qui précède les régulations neurohormonales (Borredon 1-3).

Lors d'une accélération à fort taux de variation, on peut supposer que la charge étant totalement établie sur une seule révolution cardiaque, la précharge ventriculaire est directement fonction de la valeur instantanée de l'accélération et s'en trouve multipliée d'autant. Le synchronisme de la première ondée systolique et de l'accélération sous fort jolt risque-t-il alors d'être déterminant pour l'atteinte du seuil critique d'HIC.?

Deux hypothèses extrêmes peuvent être envisagées.

a) Le début d'une systole coïncide avec le début de l'accélération

Les deux événements sont parfaitement synchronisés (figure n°14). Les effets de l'accélération commencent à se faire sentir au début de la relaxation. Dans l'exemple, l'accélération s'effectuant sous 12 G/s la valeur maximale du facteur de charges est atteinte au début de la systole suivante.

*Au cours de la phase systolique isovolumique la précharge est maximale puisqu'elle s'exerce sur un volume télédiastolique dont la masse plusieurs fois accélérée intervient de façon majeure sur la pression motrice (le ventricule doit pousser un volume télédiastolique 140 cc, qui oppose une force résistante supérieure à: 0,140*6=0,840 daN (la masse volumique ≈ 1)

*Au cours de la phase systolique isotonique, la post-charge est, en première approximation, également très élevée puisque l'effet normalement favorable de stockage du sang dans le système compliant veineux n'ayant pas lieu, les résistances artèrielles périphériques sont multipliées par 6, en raison de la rapidité d'application du champ de force (500 ms). C'est seulement au cours de la révolution suivante (850 ms après le début d'application du facteur de charges) que va commencer la diminution du volume télédiastolique par séquestration partielle du sang.

b) Le début d'une diastole coïncide avec le début de l'accélération (fig 15).

Les deux phénomènes sont désynchronisés et les effets sont opposés à ceux qui viennent d'être décrits.

L'accroissement du facteur de charge pendant la phase isotonique exerce, certes, un effet défavorable mais encore limité puisque la charge mécanique maximale est atteinte à la fin de la période de relaxation tandis qu'apparaissent les effets de déplacement solide des fluides intravasculaires.

Alors que l'aspect chronologique de la relation "révolution cardiaque-accélération" est aisément abordable conceptuellement, la relation "volume télédiastolique-accélération" nécessite, par contre, la mise au point d'un modèle de ventricule qui prenne également en compte le niveau de contraintes mécaniques dans le myocarde ventriculaire.

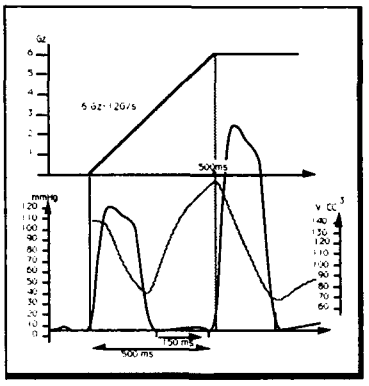

Figure 14 (à gauche): L'accélération de la masse sanguine télédiastolique maximalise les effets de la première chasse ventriculaire.

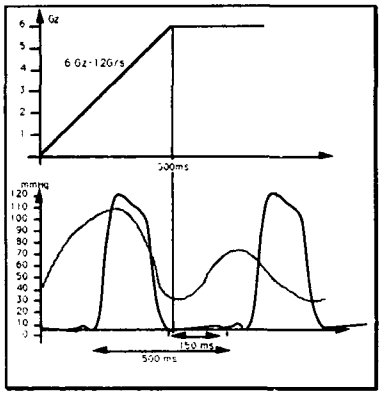

Figure 15 (à droite): Si les deux effets sont désynchronisés la précharge ventriculaire diminue.

7.2 Variation du volume télédiastolique avec le facteur de charges: modèle de ventricule (Briane et collaborateurs 5,6,7,8).

Le ventricule est modélisé par un cylindre vertical à paroi épaisse. La section inférieure du cylindre (l'apex ventriculaire) est libre alors que la section supérieure n'est soumise qu'à une déformation radiale, permettant au cylindre de garder sa forme cylindrique pendant la déformation. La paroi est constituée par un fluide incompressible dans lequel baigne des fibres élastiques (figure 16).

Ces fibres forment deux réseaux d'hélices régulières de même axe que le cylindre. Leur orientation varie de manière continue dans la paroi. Ces deux réseaux sont symétriques par rapport à un plan passant par l'axe du cylindre si bien que l'on ne prend pas en compte la torsion du volume. La déformation radiale et longitudinale est mesurée par rapport à une configuration de référence, dans laquelle n'existe aucune contrainte mécanique. L'étude suppose de grandes déformations.

La loi d'orientation des fibres $\Gamma(R)$ varie linéairement $\pi-\gamma(r)$ entre l'angle Γ_o à l'endocarde (R = Ri) et $-\Gamma_o$ à l'épicarde(R= R_e) suivant la loi: $\Gamma(R)= \Gamma_o\left(\frac{R_i+R_e-2R}{R_i-R_e}\right)$

7.2.1 ETUDE DE LA DEFORMATION DE LA PAROI

On définit le coefficient l d'allongement du cylindre par z = l Z

L'incompressibilité locale du fluide dans la paroi s'écrit: rdrdz=RdRdZ

Il vient en intégrant: $r^2= \frac{1}{\lambda}\left(R^2+\frac{v-V}{\pi L}\right)$

En comparant les pas d'une fibre hélicoïdale dans la configuration déformée et dans la configuration de référence on obtient la relation: r tg $\gamma = \lambda$ R tg Γ

Le coefficient d'allongement α des fibres est le rapport de la longueur d'un élément de fibre dans la configuration déformée par la longueur de ce même élément dans la configuration de référence. Les fibres étant hélicoïdales il vient:

$$r \operatorname{tg}\gamma = \lambda R \operatorname{tg}\Gamma \qquad \text{et} \qquad a^2= \frac{r^2+r^2(\operatorname{tg}\gamma)^2}{R^2+R^2(\operatorname{tg}\Gamma)^2}$$

On en déduit la relation: $$\alpha^2= \frac{r^2}{R^2} + (\cos\Gamma)^2 + \lambda^2(\sin\Gamma)^2 \qquad (1.1)$$

Dans la configuration déformée, les directions des fibres des deux réseaux sont données par:

$$\tau^+= \cos\gamma\, e_\theta+\sin\gamma\, e_z \text{ et } \tau^-=-\cos\gamma\, e_\theta+\sin\gamma\, e_z$$

où (e_r, e_θ, e_z) est la base cylindrique locale.

7.2.2. HYPOTHESES MECANIQUES

***la déformation est constituée d'une suite d'équilibres quasi statiques,**

***le fluide intraventriculaire est un fluide parfait incompressible,**

***le ventricule est soumis à une force d'inertie verticale et constante $\rho a e_z$ qui correspond à une accélération centripète $-a\, e_z$**

***sous l'effet de l'inertie, la surface latérale de la paroi ventriculaire est soumise à un champ de pression hydrostatique**

$$\Delta p = \rho a \Delta z \qquad (3.1)$$

***par contre la surface inférieure du cylindre est soumise à une pression externe nulle, autrement dit le ventricule ne baigne pas dans un fluide soumis à une pression hydrostatique.**

7.2.3.Description des contraintes dans la paroi myocardique

Les contraintes dans la paroi sont dues à la pression p = p(r,z) du fluide et à la tension T des fibres.

La contrainte due à la pression du fluide supposé parfait est isotrope. La contrainte due aux fibres agit dans la direction des fibres c'est à dire τ^+ et τ^-. Les contraintes internes sont représentées par une matrice Σ.

Si n est une direction de l'espace, alors le vecteur Σn représente la force à laquelle est soumise la face d'un cube élémentaire du matériau dirigé selon n. Dans le cas présent, la matrice des contraintes Σ de la paroi ventriculaire a pour composantes:

$$\Sigma_{ij} = - p\,\delta_{ij} + T\,(\tau_i^+ \tau_j^+ + \tau_i^- \tau_j^-) \qquad (3.2)$$

La tension T s'écrit (Chadwick -14)

$$T = [(1-\beta)E + \beta E^*](\alpha - 1) + \beta T_0 \qquad (3.3)$$

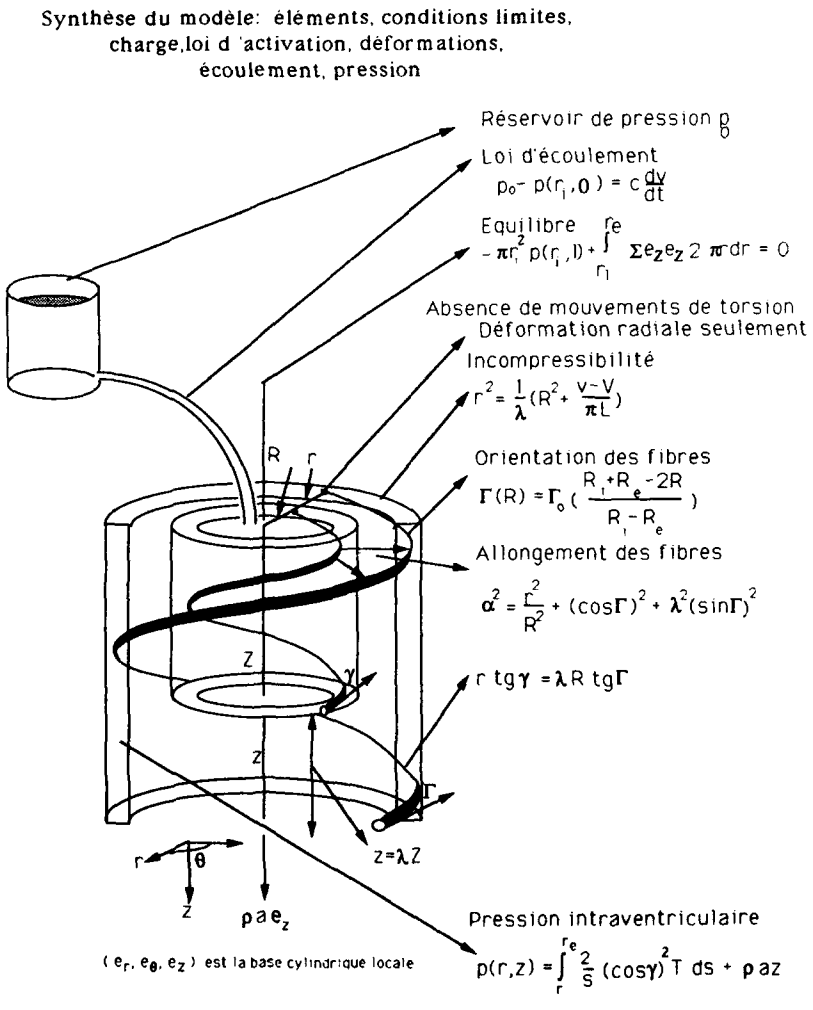

Figure n°16. Synthèse du modèle de ventricule

β est une fonction du temps comprise entre 0 et 1 qui représente l'activité des fibres cardiaques durant le cycle cardiaque. On a donc $\beta = 0$ état passif (fin de diastole), $\beta = 1$ état actif (fin de systole). Dans l'état passif, la tension T est équivalente à une force de rappel élastique proportionnelle à l'allongement relatif α-1: $T = E(\alpha - 1)$.

Par contre, dans l'état actif, la fibre ne se comporte pas comme un simple matériau élastique.

La différence de comportement est représentée par la tension "physiologique" maximale T_o déployée par la fibre.

7.2.4. EQUATIONS D'ÉQUILIBRES

L'équation d'équilibre d'un milieu continu dans le cas quasi statique s'écrit:

$$\text{div } \Sigma + f = 0$$ où f représente les forces volumiques d'inertie .

Dans le cas présent on a: $\text{div } \Sigma + \rho a e_z = 0$ où la divergence est exprimée par rapport aux coordonnées cylindriques (r,θ,z) de la configuration déformée.

On déduit de cette équation d'équilibre le système différentiel donnant le gradient de la pression en fonction de la tension T et de la coordonnée verticale z:

$$\begin{cases} \dfrac{\partial p}{\partial r} = -\dfrac{1}{r} + (\cos\gamma)^2 T \\ \dfrac{\partial p}{\partial z} = \rho a \end{cases} \qquad (3.5)$$

La pression extra ventriculaire à la côte z=0 est prise comme pression de référence .

En vertu de la loi hydrostatique (3.1) on obtient la condition limite:

$$p(r_e,z) = \rho a z$$

Avec le système (3.5) et la condition limite (3.6) l'expression de la pression intraventriculaire p(r,z) devient :

$$p(r,z) = \int_r^{r_e} \frac{2}{s} (\cos\gamma)^2 T \, ds + \rho a z$$

Une seconde équation est nécessaire pour calculer le coefficient d'élongation l qui détermine, par les équations 1.4 et 1.6 la déformation du cylindre. Cette équation est donnée par l'équilibre de la base du cylindre z=l sous l'effet des forces interne et externe de pression. La pression cavitaire à la côte z=l exerce une force constante et égale à: $-\pi r_i^2 p(r_i,l)\, e_z$

Le vecteur Σe_z représente la résultante des forces surfaciques auxquelles est soumise la base de la paroi ventriculaire.

L'équilibre de la base du cylindre se traduit par l'annulation de la somme des projections e_z de ces forces, ce qui donne l'équation:

$$-\pi r_i^2 p(r_i,l) + \int_{r_i}^{r_e} \Sigma e_z \, e_z \, 2\pi r dr = 0 \quad \text{avec} \quad \Sigma e_z \, e_z = -p(r_i,l) + 2T(\sin\gamma)^2$$

On en déduit l'équation suivante:

$$\int_{r_i}^{r_e} T\,[4(\sin\gamma)^2 - 2(\cos\gamma)^2]\, r dr = \rho a r_e^2 l$$

7.2.5. EQUATION D'ECOULEMENT

Pour achever l'étude mécanique du modèle, il reste à modéliser l'écoulement sanguin lorsque l'une des valves mitrale (phase de remplissage) ou aortique (phase d'éjection) est ouverte. On suppose que les valves mettent le ventricule en contact, au niveau de la base (z=0), avec un réservoir de pression constante p_o. Pendant la phase de remplissage, ce réservoir représente l'oreillette gauche et pendant la phase d'éjection, il représente le système artériel. La loi de Poiseuille modélise l'écoulement du sang à travers les valves: $p_o - p(r_i,0) = cQ$ (c : résistance de la valve Q : débit sanguin)

Dans le cas où la valve est cylindrique, c s'exprime par:

$$c = \frac{8\mu l_v}{\pi r_v^4}$$

(μ:viscosité sanguine, l_v:longueur de la valve, r_v:rayon de la valve). On relie le débit sanguin Q et le volume cavitaire v

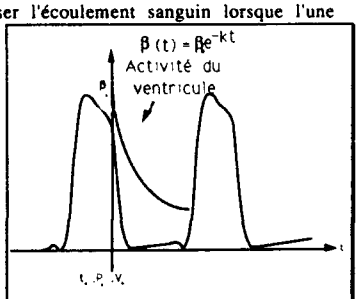

figure n°17: loi de l'activation décroissante de la fonction ventriculaire

du ventricule par la relation $Q = \frac{dv}{dt}$

On obtient alors la loi d'écoulement suivante:

$p_o - p(r_i, 0) = c \frac{dv}{dt}$

7.2.6. RESULTATS

Principes de la simulation

La phase de remplissage du ventricule gauche sous différentes accélérations a été prise comme modèle. On se donne la pression auriculaire p_o qui coïncide avec la pression $p(r_i,0)$ à l'ouverture de la mitrale prise comme origine des temps et le volume avant remplissage v_o. On en déduit de cette pression et des équations 2.7 et 2.8 l'activité initiale du ventricule $\beta = \beta_o$.

La loi d'activation $\beta(t)$ exponentiellement décroissante (figure 17) en fonction du temps est donnée en prenant la valeur β_o à l'instant initial. Connaissant la loi d'évolution $\beta(t)$, on calcule à chaque pas de temps:

*la pression intraventriculaire $p(r_i,0)$,

*le volume intraventriculaire v

*l'élongation du cylindre λ.

Les différentes simulations sont faites en prenant pour a les valeurs successives $0G_z$, $1G_z$, $3G_z$, $5G_z$

Données numériques.

Données géométriques de référence R_i = 1,5 cm, R_e = 2,4 c, V = 50cc, Γ_o=70°, c = 5 U.S.I. (résistance de la loi de Poiseuille)

Modules d'élasticité (mmHg): E=23,07; E*=171,54 ; T_o=19,23

Données initiales p_o = 11,5 mmHg, v_o = 100 cc

Les différentes simulations sont réalisées sur une durée Δt = 0,5 s.

(les données sont relatives à des données animales et correspondent à une viscosité de 5.10^{-3} Pa.s)

Résultats

Les résultats sont représentés par les séries de courbes successives suivantes:

Courbes Pression-Volume : $p(r_i,0)$ en fonction de v

Courbes Pression-temps : $p(r_i,0)$ en fonction de t

Courbes Volume-temps : v en fonction de t

Dans chaque série les courbes sont représentées en fonction des accélérations.

Calculs de { Pression intraventriculaire p(ri,0) ; Volume intra ventriculaire v ; élongation du ventricule l } sous { Gz = 0 ; Gz = 1 ; Gz = 3 ; Gz = 5 }

Graphe Pression-volume (figure n°18)

La pression intraventriculaire présente des variations intéressantes à l'ouverture de la valve mitrale. Elle diminue au début de la diastole avec la relaxation myocardique et augmente ensuite avec l'augmentation de volume. Le phénomène est d'autant plus prononcé que l'accélération dans l'axe longitudinal du ventricule est plus intense. Ainsi, pour un volume donné, la pression télédiastolique sous 5 Gz est beaucoup plus faible que sous un champ de gravité normal. Ce phénomène est d'autant plus marqué que la capacité de stockage est importante. Dans l'étude où cette capacité n'est pas limitée, il faut atteindre des volumes supérieurs à 250 cc sous 5Gz pour obtenir une valeur de pression diastolique égale à celle observée normalement chez un sujet placé dans le champ de pesanteur terrestre.

Graphe Pression-temps (figure n°19)

Les conditions de variation de pression en fonction du temps indiquent clairement la baisse de pression dans la phase diastolique initiale précoce. Ainsi il faut attendre environ 230 ms à 5GZ pour retrouver la valeur de pression ventriculaire existant au tout début de la phase de relaxation. Si un tel laps de temps correspond à une fréquence de 103 bpm, le volume associé à cette valeur de pression est tout à fait irréaliste puisqu'il atteint des valeurs extrêmes de l'ordre de 250 cc .

Si l'on se place dans le cas d'une fréquence de 120 bpm (temps diastolique de 150 ms) on constate aisément que la pression intraventriculaire sous 5Gz est très inférieure à celle qu'elle présenterait sous 1G.

Dans ce dernier cas les valeurs de pression, volume et temps sont tout à fait cohérentes avec celles observées dans la réalité.

Graphe Volume-temps (figure n°20)

Les remarques effectuées sur les graphes précédents s'appliquent évidemment au diagramme volume-temps où l'on constate que l'application d'un champ de force au début de la phase de relaxation provoque une augmentation de volume ventriculaire d'autant plus importante que l'intensité de la force est élevée. Il convient de noter que les champs de force mécaniques sont considérés établis et stables et qu'aucune notion de taux de variation des forces volumiques n'intervient.

7.2.7.DISCUSSION-PERSPECTIVES

Les résultats obtenus mettent en évidence une influence très sensible des accélérations +Gz sur la fonction diastolique du ventricule.

Schématiquement les accélérations croissantes ont les effets principaux suivants sur le modèle:

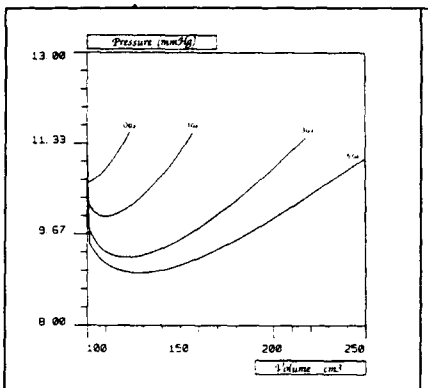

Figure 18: relation Pression volume

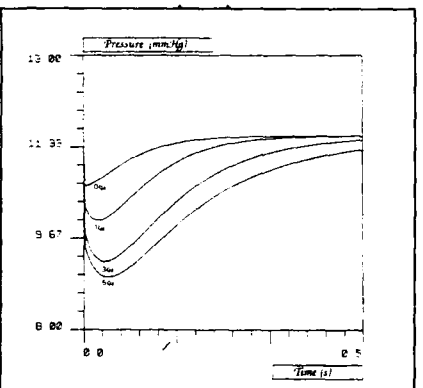

Figure 19: relation Pression temps

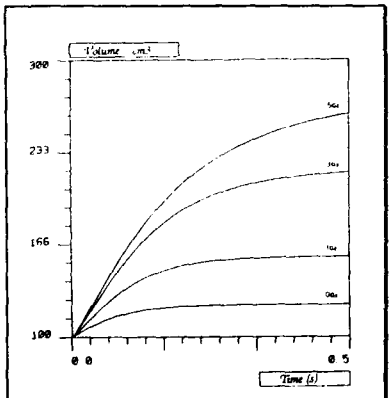

Figure 20: relation volume temps

*une baisse de pression au début de la phase de remplissage qui traduit une accentuation du phénomène d'aspiration de la chambre ventriculaire à partir de l'oreillette

*une augmentation du volume diastolique

*une accélération de la vitesse de remplissage.

Deux critiques peuvent être faites à propos de cette étude: les unes sont structurelles et portent sur le modèle, les autres sont analytiques.

Un modèle cylindrique est évidemment particulier et ne correspond pas à l'aspect tronconique d'un ventricule anatomique. Le choix de cette géométrie est du à l'acquis bibliographique qui le justifie partiellement et présente l'avantage de permettre un traitement analytique. Enfin ce modèle est évidemment démuni de péricarde.

Les autres critiques sont des conséquences des carences qui viennent d'être énoncées.

*la configuration cylindrique du modèle, repose sur l'hypothèse d'une pression hydrostatique à l'extérieur de la surface latérale du cylindre alors que sa section inférieure est en contact avec une pression nulle. Une modélisation plus réaliste consisterait à prendre une pression nulle à l'extérieur du ventricule. Une telle condition est malheureusement incompatible avec un modèle cylindrique.

*le modèle présenté ne tenant pas compte du rôle du péricarde qui empêche les étirements excessifs du myocarde permet d'atteindre des volumes de remplissage importants L'utilisation réaliste des résultats impose une limite temporelle (150ms) à l'exploitation des calculs. Cette durée est tout fait compatible avec l'application d'un facteur de charges sur un cœur en régime de 120 bpm.

*enfin, contrairement à la réalité physique, l'application de ce facteur de charges n'est pas continûment variable jusqu'à l'établissement d'un plateau. Les résultats obtenus sont donc ceux d'un processus évolutif dans le temps en présence de différents champs de force dont le taux de variation à l'origine est infini.

Ces restrictions étant faites, on constate - sur un temps de 150ms - que les accélérations +Gz

diminuent la pression intracavitaire au début de la diastole et augmentent le volume télédiastolique. En d'autres termes les accélérations +Gz sous fort jolt améliorent considérablement la fonction diastolique de pompe aspirante du cœur.

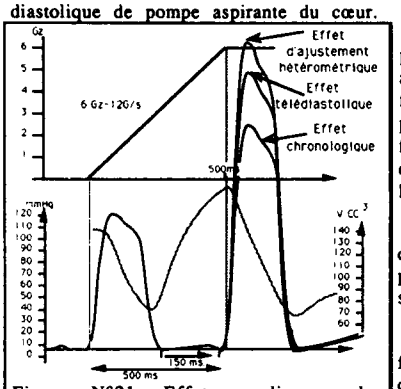

Figure N°21: Effets cardiaques des accélérations +Gz à fort taux de variation, dans le cas où les deux événements sont parfaitement synchronisés

Ainsi, en l'absence de toute régulation physiologique, les forces d'inertie dues à une accélération +Gz d'installation extrêmement rapide favorisent l'afflux de sang durant la diastole de la première révolution d'un cœur soumis à ce champ de force et augmente de façon conséquente le volume d'éjection systolique donc la pression artèrielle lors de la contraction ventriculaire suivante.

Il résulte de cette constatation que notre schéma concernant les hypothèses d'un effet chronolo- gique sur la pression systolique quand les deux événements sont synchronisés, doit être revue à la hausse.

Quatre effets interviennent (figure 21):

trois sont directement liés au taux de variation du facteur de charges.Deux de ceux-ci sont primaires, les effets chronologiques et volumiques, le troisième est secondaire i.e. l'effet loi de Starling (ajustement hétérométrique du myocarde) dû à l'augmentation du volume d'éjection systolique.

Le dernier effet, enfin est autonome, il concerne l'ajustement inotrope neurohormonal du fonctionnement cardiaque (ajustement homéométrique) et l'ajustement de la motricité vasculaire.

9 CONCLUSIONS

L'inclinaison des aéronefs au cours d'un virage lentement établi, mais néanmoins serré, fait subir au pilote une accélération colinéaire à l'axe longitudinal du corps dont l'amplitude peut atteindre, pour un avion de chasse, plusieurs fois l'accélération G de pesanteur.

L'effet centrifuge qui tasse l'individu sur son siège existe également pour les fluides. La redistribution du sang dans les vaisseaux de la partie basse du corps est responsable d'une hypoxie cérébrale, engendrant parfois une perte de connaissance *en vol, précédée de voiles gris et noir*. La compression de l'abdomen et des membres inférieurs par un vêtement antiG qui s'oppose à la redistribution sanguine vers les zones infracardiaques est donc un bon moyen de protection.

Avec les nouvelles technologies mises en œuvre pour la construction des avions d'arme qui sont capables d'accélérations +Gz d'installation rapide, une nouvelle symptomatologie des pertes de connaissance en vol est apparue: rapide, sans prodromes visuels, sans souvenir de l'accident. L'échelle des temps est alors de la seconde, voire inférieure à la seconde!

Le but du travail rapporté est de proposer une explication, strictement biomécanique, des PCEV d'installation rapide: les structures nerveuses cérébrales, soumises à une accélération +Gz à fort taux de variation, deviendraient fonctionnellement inefficaces non par manque d'oxygène, mais par accroissement brutal des contraintes mécaniques intracérébrales, réalisant au sens strict une HYPERTENSION INTRACRANIENNE PRÉCOCE (H.I.C).

Un modèle simple est proposé qui permet d'étudier trois paramètres

*la distribution de pression dans le L.C.R.

*la répartition des contraintes et des déformations dans l'encéphale

*la modification de l'écoulement sanguin pulsé dans l'enceinte crânienne osseuse de confinement.

Les calculs montrent l'influence d'une brusque modification du régime de l'écoulement qui fait apparaître des phénomènes de collapsus et des écoulements à caractère supercritique qui peuvent être suivis de chocs intravasculaires.

Ainsi, les premiers résultats de la modélisation indiquent qu'une accélération +Gz d'installation rapide pourrait engendrer une augmentation des contraintes mécaniques dans le tissu nerveux donc une hypertension intracrânienne brutale.

Le niveau de pression intracrânienne (seuil) pour lequel une perte de connaissance peut éventuellement survenir peut être discuté en fonction du niveau instantané de la pression artérielle et de paramètres physiologiques cardiovasculaires. Quatre effets sont analysés:

*les effets chronologiques de la révolution cardiaque en fonction de l'instant d'application du facteur de charge

*les effets volumiques de l'éjection systolique

*l'ajustement hétérométrique du myocarde

*l'ajustement inotrope neurohormonal du fonctionnement cardiaque (ajustement homéométrique).

Sous ces hypothèses la mise en pression rapide voire anticipée du vêtement antiG est suspectée

d'être défavorable créant un "coup de bélier hydraulique" dans le système vasculaire à destination encéphalique, augmentant ainsi les risques d'H.I.C. précoce. Bien entendu, l'utilisation - en son temps - du pantalon antiG reste une précaution indispensable, car le même pilote qui échappe à une HIC précoce n'est pas à l'abri de faire une PCEV par hypoxie cérébrale, dans les quelques secondes qui vont suivre.

Les hypothèses d'H.I.C. ne s'opposent pas à la théorie hypoxique mais elles la complètent. Ainsi, les études en cours qui concernent le "délai de mise en pression du vêtement antiG en fonction du taux de variation des accélérations " restent parfaitement justifiées, si l'on ne veut pas prendre le risque de créer des accidents chez des sujets portés artificiellement aux limites de leur tolérance qui sont dans un premier temps biomécaniques puis, dans un second, physiologiques.

Les auteurs remercient chaleureusement monsieur le Pr. P.Borredon pour les critiques amicalement constructives qu'il a bien voulu apporter à la rédaction de ce texte.

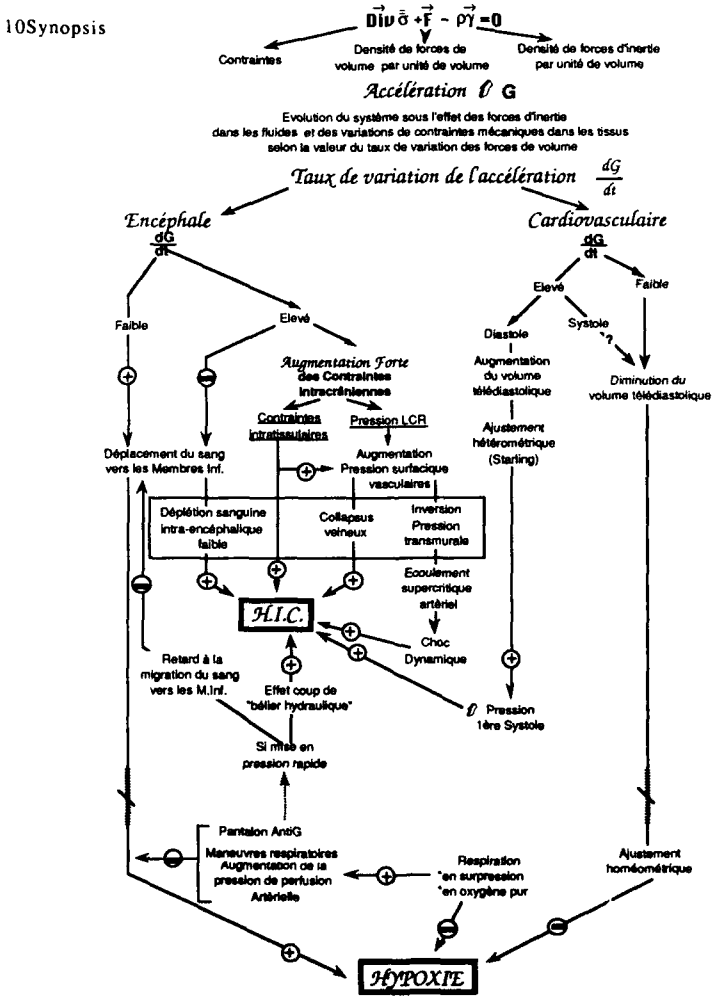

Figure 22: Synthèse des hypothèses concernant la survenue d'une PCEV par H.I.C. des pilotes de chasse soumis à des accélérations d'installation rapide et leur intégration dans la théorie hypoxique classique (les temps respectifs de survenue de l'HIC et de Hy.C. ne sont pas respectés).

BIBLIOGRAPHIE

1)Borredon P. Liscia P. Haziot A. Quandieu P.: Expositions répétées aux accélérations +GZ de haut niveau:Conséquences sur le myocarde et le système cardiovasculaire. Médecine Aéronautique et Spatiale 1982, XXI (84) 420-424.

2)Borredon P. Paillard F. Liscia P. Nogués C.: Hypertension induced by repeated exposure to high sustained +GZ stress. Aviation Space and Environmental Medicine. 1985, 56 (4) 328-332

3)Borredon P,Paillard F. Liscia P. Cailler B. Ilie H. Didier A.: Cœur droit et accélérations +Gz soutenues et de haut niveau. Med Aér.Spat.1986,XXV (98),139-144.

4)Borredon P. Paillard F. Liscia P. Bouscaillou P. Milhaud C. Nogues C.:Hypertension fonctionnelle provoquée par des expositions répétées aux accélérations +Gz soutenues et de haut niveau. Trav Scient. S.S.A., 1984, (3), 1-6.

6)Briane M., Quandieu P., Henry J., Liébaert Ph.: Modelling of changes in mechanical stress of left ventricular myocardium (diastolic phase) under +Gz acceleration. A paraître dans "The Physiologist".

7)Briane M., Quandieu P., Henry J., Liébaert Ph.:Modélisation de la fonction diastolique sous accélération à fort jolt. I Modélisation mathématique. Médecine aéronautique et spatiale:1990, XXIX (113)

8)Briane M., Quandieu P.,Henry J.:Modélisation des variations de contraintes mécaniques du myocarde ventriculaire gauche (phase diastolique) sous accélération +Gz - CERMA 90-32 (22 pages)

9)Brinquin L., Bizouarn Ph., Rousseau J.M., Diraison Y., Bonsignour J.P., Buffat J.J.: Le pantalon anti-choc pour la neuro-chirurgie en position assise. Médecine et Armées 1988,16,(5),353-355.

10)Burton RR, Leverett SD, Michaelson SD : Man at high sustained +GZ acceleration : a review. Aerospace Med 1974, 45 (10) 1115-1136.

11)Burton RR, Whinnery JE : Operational G-induced loss of consciouness. Something old, something new : Aviation Space and Environmental Medicine 1985, 56 (8) 812-817.

12)Burton R.R.: A conceptual model for predicting pilot group G tolerance for tactical fighter aircraft.Aviat.Space Environm. Med. 1986 57 ;733-44

13)Burton R.R.: Anti-G suit Inflation rate requirements Aviat. Space Environm.Med. 1988. 59, (7),601-605

14)Chadwick R.S.: "Mechanics of the Left Ventricle", Biophys. J., 39,1982, 279-288.

15)Clere J.M, Vieillefond H, Poirier JL: Interêt du siége incliné pour l'amélioration de la tolérance aux accélérations +GZ. CR n°1132 Contrat DRET n° 82/1131 Rapport 14952:/DRET/SDR/M du 20/9/1982.

16)Edelberg R.,Henry J.P.,Maciolek J.A,Salzman E.W.,Zuidema J.D.; Comparison of human tolerance to acceleration of slow and rapid onset; Aviation Medicine Decembre 1956

17)Féron X.:Pertes de connaissance dues au facteur de charges. Bulletin de sécurité des vols, Janvier 1991, 12-16, SV EMAA.

18)Gilligham KK, Makalons DL,Tays MA : G stress on A10 pilots during Jaws II exercise Actes du congrés de US Aerospace Medical Association (ASMA)1980 89-91

19)Hood LA : Lock from High G. Flying safety 1983,7 ,5-9.

20)Houghton JO, Dennis K, Bride MC, Hannah K: Performance and physiological effects of acceleration induced (+GZ) loss of consciousness: Aviation Space and Environmental Medicine 1985, 56 (10) 956-965.

21)Howard P,: Cardiac function, acceleration: In Principles and practice of human physiology (OG Edholm JS Weiner edit.Academic Press) 1981 191-240.

22)Kydd G.H, Fenichel R.L, Crosbie R.J: Relationship of carotid pressure and end point of acceleration J.Applied Physiol. 1960 15(5) 903-906

23)Kokova I: Hemodynamics parameters as related to different tolerance to head pelvis acceleration : Kosmicheskaya Biologica I Aviakosmicheskaya Meditsina 1985 19 (5) 56-60.

24)Knudson R, Mc Millan D, Doucette D, Seidel M : A comparative study of G-induced neck injury in pilots of the F/A-18, A-7 and A-4. Aviation Space and Environmental Medecine 1988 59 (8) 758-760.

25)Krutz R.W.,Krueger A.G.,Burton R.R; Comparaison entre vêtement anti-G à pression uniforme Safe Journal 1988,18,(2) 14-18

26)Jaron D, Moore T,Shankara Reddy BR, Hrebien L,Kepics F; Reflectance photoplethysmography as an adjunct to assessment of gravitational acceleration tolerance:preliminary findings.Aviat.Space Environm.Med. 1987;504-12

27)Landry RF: : G-induced loss of consciousness : AGARD Conference proceedings distribué par O.N.E.R.A. 92220 Chatillon/Bagneux CP 377 1985 B2-1,B2-3 .

28)Leguay G, Seigneuric A : Tolérance cardiovasculaire aux accélérations +GZ soutenues et de haute intensité . Revue générale. Médecine Aéronautique et spatiale 1984 XXIII (90) 137-156.

29)Liébaert Ph., Gaffié D., Quandieu P., Tran C.C.: Numerical évaluation of pressure developed in cerebrospinal fluid at the base of the skull during +Gz accelerations simulating a short hypergravitation: 1990 The Physiologist 33, (1), 145-146

30)Liscia P. Drogou C.Quandieu P. Borredon P: Accélération +Gz et catécholamines plasmatiques. A paraitre dans revue de médecine aéronautique et spatiale

31)Meeker L.J.,Krueger A.G., Love P.E. Evaluation technique de plusieurs valves antiG de conception nouvelle Safe Journal 1988,18,(2) 24-27

32)Moore TW, Fowley JF, Shankara RBR, Kepics F,J arron D : An experimental microcomputer controlled system for synchronized pulsating antigravity suit; Aviation Space and Environmental Medicine 1987, 58, (7),10-14.

33)Nickell WT, Bhagat PK, Krebeiv L, Cohen MM, :Use of ultrasonic measurement to monitor blood shift from the head during exposure to +GZ acceleration. Actes du congrés de US Aerospace medical association (ASMA). Houston 1983, 180-182.

34)Pelligra R, Sandler H, Rositano MD, Skretinland K, Mancini R : Advance technique for monitoring human tolerance to +GZ acceleration. Revue de Medecine Aéonautique et Spatiale 1973 46 301-304.

35)Pluta J.C. LOC Survey Flying Safety January 1984 25-26

36)Poirier JL, Clere JM, Vieillefond H, : L'inclinaison du siége pilote: intérêt et limites.:Médecine aéronautique et Spatiale 1986 25 (100) 318-323.

37)Quandieu P., Briane M., Henry J., Liébaert Ph.: Modélisation de la fonction diastolique sous accélération à fort jolt. II Exploitation biomécanique. Médecine aéronautique et spatiale:1990, XXIX (113)

38)Quandieu P.,Gaffié D., Liébaert Ph: Interprétation biomécanique des pertes de connaissance en vol des pilotes de chasse sous l'effet de l'application d'une accélération +Gz d'installation rapide(fort jolt). C.R. Acad. Sci.Paris 312,(II) 185-190, 1991.

39)Ratajczak M.:valves anti-G:les inconvénients d'un déclenchement trop rapide Safe Journal 1988,18,(2) 19-23

40)Rayman RB,: Sudden incapacitation in flight (january 1966 to november 1971).: Aerospace Medicine 1973 , 44, (8), 953-955.

41)Rayman RB, Mc Naughton GB: Sudden incapacitation in flight : USAF experience 1970-1980 : Aviation Space and Environmental Medicine 1980 54 (2) 161-164.

42)Roseau M.: Vibration des systèmes mécaniques. Méthodes analytiques et applications 1984 (Masson édit)

43)Shapiro A.H : Physiologic and medical aspects of flow in collapsible tubes 1977 Proc.6th Canad Cong. Appl. Mech.Vancouver 883-906

44)Simons DG, Johnson RL, : Heart rate pattern observed in medical monitoring : Aerospace Medicine.1965 36 (6) 504-513.

45)Souder ME, Bachert RF, Henry CL, Slonim A : Time series analysis ECG/ cardiovascular changes as a result of prolonged acceleration in baboon. Congrés de US Aerospace medical association (ASMA) Bal Harbour 1982.

46)Stoll A.M.: Human tolerance to positive G as determined by physiological end point. Journal of Aviation Medicine 1956 ,8 , (4), 356-367.

47)Tran C.C.,Bonnin P,Paillard F,Quandieu P.Borredon P. :Biodynamique cardiovasculaire et rythmologie cardiaque sous accélérations + Gz de longue durée. SSA 1987

48)Tran C.C.:Utilisation de la vélocimétrie doppler pulsé pour l'étude des effets des accélérations sur la biodynamique cardiovasculaire:mémoire pour l'obtention du D.E.A. de physiologie et de physiopathologie des appareils respiratoire et circulatoire 1988,Paris 65pages.

49)Tricot F.: Modélisation de structures anatomiques par utilisation de méthodes aux éléments finis. Mémoire de stage de fin d'études (Ecole Polytechnique Chaire de mécanique option biomécanique) 126 pages.

50)Van Patten R.E. Un autre mode de protection contre les accélérations de haut niveau Safe Journal 1988,18,(2) 8-10

51)Whinnery JE, Shafstall RM : Incapacitation time for +GZ induced loss of consciouness : Aviation Space and Environmental Medicine 1979 50 (1) 83-85

52)Whinnery JE, Burton RR ,Boll P, Eddy DR : Characterisation of the resulting incapacitation following unexpected +Gz induced loss of consciousness. Aviation Space and Environmental Medecine 1987 58 (7) 631-636.

53) Wood EH: Development of antiG suits and their limitations. Aviat.Space Environm. Med. 1987;58:699-709

G-LOC.

Gz AND BRAIN HYPOXIA !

Gz/s AND INTRACRANIAL HYPERTENSION ?

A SYNTHESIS

*P.QUANDIEU, **D.GAFFIÉ, ***PH.LIÉBAERT,
*M.BRIANE, ***J.C.SARRON, *A.GUILLAUME, *D.TRAN., *J.PH.HAYMANN.

*Centre d'Etudes et de Recherches de Médecine Aérospatiale, Division de Biomécanique
Base d'Essais en vol 91228 Brétigny sur Orge (France)
**O.N.E.R.A.,Département Energétique 29, avenue de la division Leclerc
92320 Chatillon sous Bagneux (France)
***Direction des Recherches Etudes et Techniques Tour D.G.A.
Service des Recherches/G9, 26 Bvd Victor Paris 00457 Armées (France).

Have you ever had a loss of consciousness episode?
"I can't remember"

Answer of a US fighter pilot to an anonymous survey on inflight LOC
(Flying safety Jan. 1984)

I- INTRODUCTION[1]

When fighter aircrafts change directions, their pilots are subject to accelerations which crush them into their chairs. Sometimes these accelerations can be high enough to induce loss of consciousness. For fifty years, G-LOC induced by gradual onset rate + Gz acceleration (GOR + Gz) have been ascribed to a clearly pathophysiological cause: brain hypoxia, and this explanation is now accepted by all specialists of aviation medicine.

This brain hypoxia results from increased hrGz hydrostatic component of blood pressure. This component increases linearly with the Gz acceleration (h being the height of the blood column between the brain and the base of the heart). Since Gz is colinear with the long axis of large aorto-carotid and jugulocave vessels, forces of inertia (described as "load" when referring to G) oppose the migration of blood toward the head. With an increasing hydrostatic pressure, the sum of motor pressure and hydrostatic pressure components of blood pressure tend toward zero. Arterial blood tends to shift toward lower limbs, and as venous compliance is much higher than arterial compliance, this phenomenon is even more patent in low pressure blood circulation.

Schematically, with reduced blood flow, the brain becomes hypoxic.

Inflation of an anti-G suit (compression of abdomen and lower limbs) counters this blood shift toward the lower limbs. It is therefore a highly efficient protection against GOR + Gz induced LOC since it increases the "useful time of consciousness" of pilots, i.e. the period of time before LOC.

Not only is this explanation highly coherent, but it also has received experimental confirmation. As in many other laboratories, our department has tried, for years, to have a better understanding of this phenomenon, both from the standoint of physiology, and cardiovascular biomechanics (Borredon (1,2,3,4) Liscia (29), Briane & Quandieu (6,36), Tran (46,47)).

Brain hypoxia cannot occur without disturbing sensory functions. Visual disorders are very familiar to fighter pilots, with reduced peripheral vision (grey-out) and loss of central vision (black-out), immediately preceding LOC within a few tenths or twentieths of a second, depending on the load.

In the early 80s, improved motor technology increased the maneuverability of fighter aircraft. Long steep turns generated high sustained rapid onset rate + Gz acceleration (ROR + Gz), which was new. The rate of change in acceleration is expressed in $G.s^{-1}$.

At this same period, reports on the effects of this new type of aggression on fighter pilots mention a new clinical form of inflight LOC, essentially characterized by the absence of a grey-or black-out. The pilot exposed to these ROR accelerations no longer experienced the warning visual symptoms which he could use as signal to initiate a maneuver cancelling the load. This new symptomatology turned ROR + Gz into "a real major problem for military flying safety" (POIRIER , 35).Sometimes, LOC can also occur during acceleration, i.e. the time of useful consciousness is practically reduced to zero. Often, the pilot does not remember anything (lacunar amnesia).

In brief, the new symptomatology of inflight LOC caused by ROR accelerations is immediate (sometimes delayed), with no visual warning, and no recollection of the accident.

When the accident occurs in the early phase of acceleration, the time scale is as small as a second, sometimes even less!

In spite of these major differences-changes in physical characteristics of the aggressing agent, the response symptomatology-specialized medical communities continue to give credit to the hypoxic etiology:

- "since the load factor develops more rapidly, so does hypoxia!
- "corollary : since hypoxia is immediate, the anti-G suit must be inflated early, even prior to ROR + Gz acceleration.

However, one physiological reason at least defies this reasoning: it is clear that times characteristic of physical phenomena implied in this accident are shorter, by several orders of magnitude, than the response times of physiological phenomena they induce. In other words, brain hypoxia cannot be elicited within a few hundredths of a millisecond.

Another strictly biomechanical explanation of sudden inflight LOC deserves attention. It does not contradict the theory of hypoxia but complements it, based on practical facts:

- "the pilot is suddenly placed into a high intensity force field.

[1]This work was supported by DRET G9

*these forces are volume (mass) forces, and not surface forces.
*the mechanical behavior of nerve structures is viscoelastic.
*the blood mass circulating inside the brain possesses obvious properties of inertia.

Brain nerve structures thus hypothetized to be exposed to a high onset + Gz stress become functionally inefficient, not because of the lack of oxygen (brain hypoxia), but because of a sudden increase in intracerebral mechanical stresses, creating, stricto sensu, early intracranial hypertension. In this biomechanical approach, the concept of energy becomes paramount.

Rapid inflation of the anti-G suit, even concomitant with the onset of acceleration, could then become potentially hazardous, with the risk of generating a "hydraulic ram effect" in the brain vascular system. This is the subject of our analysis.

II- LITERATURE REVIEW

Amplitude

New generations of fighter aircraft are developing high sustained accelerations within extremely short periods of time. Gillingham (17) reported that the A-10 aircraft can develop 10G/s and Knudson (23) 18 G/s for the F-18.

Physiological times

Total interruption of blood flow in the temporal artery precedes grey-out by 2-20 seconds (Pelligra (33)); loss of peripheral vision (grey-out) occurs for an arterial systolic eye pressure of 50 mm Hg (Burton (9), Souder (44)). Loss of central vision (black-out) occurs for a systolic pressure of 20 mm Hg in the ophthalmic artery (Burton (9), Simons (43)).

Loss of consciousness occurs generally later than loss of vision. The commonly reported explanation incriminates a "siphon" effect (during accelerations), i.e. the escape of venous blood sucks arterial blood and protects the brain (Clere (14), Howard (20), Nickell (32)). This explanation should be analyzed in detail, using experimental procedures, as it does not take into account the fundamental fact that there is no siphon effect except in rigid open pipes, which does not apply to the arterial venous system, basically similar to a model of collapsible closed tines.

Frequency

Inflight LOCs are accidents known since the early days of aviation. One of the first manifestations of a veil described in the literature was "loss of peripheral vision" during a contest for the Schneider cup. Between 1966 and 1971, 36 cases of inflight LOC were reported by Rayman (39) for the USAF, causing seven deaths. Only nine cases were directly associated with accelerations: five were due to incorrect M1 maneuvers, one to asystole during negative Gz, and three to an etiology later identified as poor tolerance to accelerations. From 1970 to 1980, Rayman (40) reported forty cases of acceleration-induced inflight LOC in the USAF. Thirty-seven were caused by incorrect M1 maneuvers, and three by poor tolerance to acceleration.

Burton (10) and Hood (18) reported that, between 1980 and 1986, inflight LOC caused the destruction of at least 30 USAF aircraft (generally with loss of human life) among which eight F-16 and four F-15 capable of exposure to very high loads. During anonymous interviews, twenty per cent of a population of F-16 pilots acknowledged that they probably experienced LOC episodes. During the third meeting of NATO's Flight Surgeons (Ramstein AFB, 1987), it was reported that approximately 10% of the 1,000 USAF fighter pilots exposed to the centrifuge test in Sôstesberg, according to an acceleration profile simulating modern air combat, experienced LOC. 140 of these pilots also admitted that they had experienced inflight episodes which could be identified as LOC and left no trace in their memory.

An anonymous survey (1,320 questionnaires) run by the French Air Force in 1991 (Féron 16) reported 98 cases of inflight LOC. Nine pilots believed they had an episode of associated lacunar amnesia.

Sequence

The LOC phenomenon is now investigated by many authors. Burton (10), Hood (18), Landry (26), Leguay (27) and Whinnery (50) are dividing LOC into two phases : a period of total incapacitation where consciousness is totally extinct, and a period of relative incapacitation, associated with confusion and disorientation. The first phase lasts 15-30 seconds. Whinnery (51) established a good correlation between the duration of this phase and the level of acceleration. He added that LOC is longer during GOR + Gz than during ROR + Gz . This observation was confirmed by Houghton (19): 23.7 seconds for ROR, 32 seconds for GOR. The phase of relative incapacitation is not correlated with the level of acceleration ; it lasts 20-30 seconds (Hood (18) and Whinnery (51)). The pilot recovers his full ability to handle a complex situation after approximately no less than three minutes! (Hood & Houghton).

LOC with no visual prodromes

The number of publications on LOC is too high for an exhaustive review in this paper. In addition, accelerations studied here are only Gz. "If the rise time to maximum G is long enough, physiological compensation tends to oppose the fall of pressure". Those were the words of Kydd et al. (21) 25 years ago as they worked on primates. "A statement regarding G tolerance should include information about the nature of the acceleration", can be read in the discussion where Kydd reports Rossen's investigations in 1943, where sudden interruption of brain blood flow, in animals, caused effects similar to those of accelerations.

The relationship "blood pressure vs acceleration" thus involves two functions: decreased arterial pressure itself a function of the mode of application of accelerations, and the action of physiological regulations which are all the more efficient as the pressure drop is significant.

In 1956, Edelberg (15) hypothetized the theory that the contribution of physiological reflexes acting to efficiently counteract accelerations is only maximum if these reflexes have time to resist the increasing hydrostatic component of arterial pressure. This time necessary for cardiovascular adaptation, according to the excitation of aortic and carotid baro-receptors, is approxatimately eight seconds.

A new concept early developed: the presence or absence of visual prodromes is a function of time.

In the USAFSAM centrifuge Pluta (34) showed that LOC caused by ROR acceleration may not be preceded by grey-out or black-out which do not fail to appear during gradual application of heavy loads. An anonymous survey run at the same time revealed LOC episodes for 12 % of pilots exposed to ROR acceleration. This LOC without prodromes is all the more dangerous for the pilot as "the preceding visual loss quite certainly serves as a very valuable premonitory warning." (Wood (52)).

Jaron et al (25) set at 1 $Gz.s^{-1}$ the onset limit which can induce loss of consciousness without visual prodromes.

Whinnery et al. examined centrifuge induced G-LOC during two types of + Gz exposure : 1) rapid onset runs (ROR), 2.5$G.s^{-1}$ and 6.0$G.s^{-1}$, and 2) gradual onset runs (GOR), 0.1$G.s^{-1}$. Fifty-five cases of LOC were reported. The mean age for the group was 32.7 ($\pm$6.2 S.D.) years, ranging from 24 to 48 years. The mean + Gz level of centrifuge exposure was +7.9 ($\pm$1.2) Gz (maximum + 9 Gz; minimum + 4 Gz). The percentage of subjects having a LOC episode for 0.1$G.s^{-1}$ was 62 %, for 2.5 $G.s^{-1}$, 52 %, and for 6 $G.s^{-1}$, 36 %. Two modes of recovery were compared, either from an objective incapacitation called "total incapacitation" (turning off visual or auditory alarm), or from subjective incapacitation (appreciated by the investigator) called "absolute incapacitation". Results showed that total incapacitation times were 34.9 s (GOR), 24.8s (ROR), and that absolute incapacitation times were 19.3s (GOR), and 12.2s (ROR), the difference being highly significant. This investigation clearly showed two types of syndromes which cannot be solely ascribed to $Gz.s^{-1}$ since the acceleration times were shorter for ROR. Unawareness of the LOC episode is the first item on the list of + Gz-induced LOC symptoms. The authors implicitely compared these phenomena with hypoxic syndromes for all acceleration rates.

Whinnery and Jones subsequently emphasized the frequency of lacunar memory in most volunteers exposed to LOC. They sometimes had to be convinced that LOC did occur even if some actually suspected it did.

LOC may sometimes be associated with flail movements which stop spontaneously.

Inflation rate of the anti-G suit

The anti-G suit has unquestionable hemodynamic effects. Its efficiency has been extensively documented and will not be reviewed here. It increases peripheral vascular resistance by external pressure, thus improving cerebral irrigation and reducing blood shifting in lower limb vessels (decreased pressure gradient between brain and apex). The idea of using it in surgical practise is not new and it is currently common practise. Brinquin et al (8) published results of an investigation run on sitting subjects to evaluate the effect of the anti-G suit against neurosurgical shock. Results were highly conclusive. Pressures of 30 mmHg were applied to lower limbs and 25 mmHg to the abdomen. For aircrew exposed to a force field, anti-G suit pressures are approximately 500 mmHg.

The theory of hypoxia, even for high G-onset rates, justifies research to develop a quick inflation system for the anti-G suit. Alike Van Patten (49) attempting to improve brain oxygen stores, Moore et al. (31) attempted to develop a pulsating anti-G suit, the pressure perturbation being out of phase with the cardiac cycle to create the lowest possible pressure drop in the brain.

Many laboratories are working to develop another system of protection against the effects of acceleration. But, generally, all research relies on physiological principles. Krutz et al. (24) hope to improve peripheral vascular resistance by an improved uniform-pressure pneumatic suit. Progress in behavior laws of new valves continues (Meeker et al. (30)) while problems associated with premature inflation are mostly described in terms of discomfort rather than of increased potential for LOC (Ratajczak, (38)).

R.R. Burton (11) analyzed the various methods used to counter the effects of accelerations, and emphasized that a number of questions remain unanswered, such as how to establish a thoracic pressure higher than 100 mmHg (50 mmHg pressure breathing associated with 100 mmHg anti-G maneuvers).

Some authors, and not the least, as E. Wood (52), clearly say that very high pressures applied to maintain efficient brain circulation in a pilot sitting under exposure to high loads can be potentially hazardous. Quoting older investigations by southern California laboratories, Wood *brings forth again the question of the positions, extensively studied during World War II.*

Burton (12) analyzed results of investigations run on subjects exposed to increasing G-onset rates in a centrifuge. All subjects wore an anti-G suit, equipped with an electronic valve programmed before G exposure, for all loads. Results show that tolerance to $6G.s^{-1}$ is 2.3G lower than tolerance to $1G.s^{-1}$ (relaxed position). This difference is ascribed to the time necessary for baroreceptor action. A 3.3 second delay in inflation does not affect tolerance to $6G.s^{-1}$ in the relaxed position. The physiological explanations given by the author for the small differences in tolerance observed in relaxed subjects address the function of baroreceptors (the 1G/s onset rate gives the reflex more time to act). However, Burton considers the G-onset rate as an important factor for Gz tolerance of a relaxed subject. An extremely rapid inflation rate may not necessarily be useful, and may adversely affect the pilot's comfort and therefore the system's acceptability.

The truth is that, to our knowledge, no experimental tests have given a final demonstration of the need for immediate anti-G suit inflation.

III) A REVIEW OF SIMPLE MECHANICS.

Surface and volume forces.

The mechanics of continuous media is divided into the mechanics of elastic solids and fluid mechanics.

Mechanically, the brain is a continuous medium characterized by fields m(r,t), P(r,t), v(r,t), T(r,t)... density, pressure, velocity, temperature... determined at each point of position r of the investigated brain mass and at any moment t.

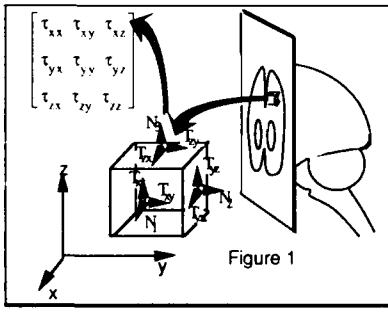

Figure 1. When a small cube of brain matter with sides dx, dy, dz is in equilibrium, the sum of all forces acting upon it equals zero. The matrix representative of (t) in a system of reference Oxyz is shown to have the mathematical properties defining a tensor. It is therefore called stress tensor, where
t_{xx} is the tension stress in direction x on the surface normal to axis x,
t_{xy} is the shearing stress in direction y on the surface normal to the x axis,
t_{xz} is the shearing stress in direction z on the surface normal to axis x, etc. .

If the brain is considered as a physical system, volume V of the continuous brain substance is contained inside the closed cortical surface S. Two types of forces can be applied: surface forces acting upon S, and volume forces (at a distance) acting upon the matter contained in V. Volume forces act upon each volume element dv so that the force acting upon a position r at time t is expressed as

$$dF_v = f_v(r,t)\, dv$$

In mechanics, what is usually taken into consideration is the field of gravity. In this case

$$\vec{F}_v = m\vec{G}$$

where m is the mass of the volume element.

Mechanical constraints

Defining as $d\vec{F}_S$ the surface force acting upon a surface element dS located around a point M of S, this element being characterized by surface-vector

$$\vec{dS} = \vec{n}\, dS$$

($\vec{n}$ unit vector perpendicular to S and directed toward the outside), vector

$$\vec{\tau}_S = \frac{d\vec{F}}{dS}$$

where $\vec{\tau}_S$ defines the surface force density is called stress in M.

Therefore, the mechanical stress is counted in pressure unit (Pa). The vector may be considered as the sum of a stress normal to S and of a tangent stress (vector contained in plane tangent to S in M).

If the stress exerts a pulling action toward the periphery of the brain it is a traction, if the pull exerts itself toward the inside of the brain it is a compression.

Changes in stress inside an elementary volume induce changes in its geometry. These changes correspond to the superimposition of three motions: a translation, a rotation, and a deformation which itself causes a "dilatation" and a "shift".

In brief, for a small volume element of invariable density, in equilibrium in a force field, stresses and deformations must be taken into consideration.

Elastic solid, plastic deformation

In a solid state, a body is deformed under the effect of tangent stresses. However, under the action of a given tangent stress, it necessarily reaches a position of equilibrium after a certain amount of time (if not, it is a fluid). If the deformation then completely disappears, the solid is said to be elastic. It recovers its initial configuration. If it does not, it is said to be plastically deformed.

Under normal conditions, in living creatures, the brain is an elastic solid. But it also possesses mechanical properties of viscosity: its behavior under the effect of a force is that of a viscoelastic solid, where stresses are associated with deformations and deformation rates.

In the following paragraphs, we shall consider that the skull is rigid and the brain tissue soft under load exposure. "Soft" is a physical property not to be confused with the flaccid aspect of the brain.

Equilibrium of deformable continuous media

Aeromedical specialists have always used the model of dynamics of a single particle

$$\vec{F} = m\vec{G}$$

as mathematical model applied to the mechanical behavior of biological structures.

However, since anatomic organs can hardly be compared with a material point, the model is inadequate and should be replaced by the model of dynamics of deformable continuous media which is certainly not perfect, but a better representation of our problem:

$$\vec{\mathrm{Div}}\,\bar{\sigma} + \vec{F} = \rho\vec{\gamma}$$

where

$\rho\vec{\gamma}$ is the density of inertial force per unit volume,

$\vec{F}$ is the density of volume force per unit volume,

$\vec{\mathrm{Div}}\,\bar{\sigma}$ represents the behavior of stress tensor when one of the other two parameters is modified .

The pilot's problem submitted to a ROR+Gz acceleration is a conflict between the "physical time" of application of the load ("characteristic times" of D. Gaffié) and the "biological time".

IV) PROPOSED MODEL

Description (Fig. 2)

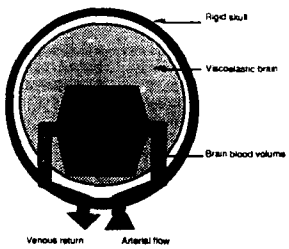

Figure 2: Proposed model.
Brain mechanical stresses are shown as grey shaded areas

In a first approach of the biomechanical behavior of the brain we will just consider this organ as a deformable spheric mass confined in a totally rigid enveloppe (the skull), and separated from this envelope by a fluid film, the cerebro-spinal fluid. The brain itself contains two phases:- a solid phase (nerve tissue).

- a fluid phase (blood) contained in a complex vascular system inside the solid phase.The vascular system is tree-shaped according to the most classically elementary description of the arterial system, branching from arteries to capillaires, then from venous capillaries to the return system. The geometry of the large vascular trunks is curved to ease flow obstacles.

Two parameters will be studied :

- stresses : their variations are represented by shades of grey.
- overall deformations resulting from a reduced blood mass under the effect of acceleration (blood pooling in lower limbs).

The mechanical behaviors applied to these different structures are :

*strictly rigid : skull.
*fluid, slightly viscous : CSF.
*viscoelastic : brain.

V) ANALOGY

The image of a sponge soaked with liquid, and exposed to a manual force can be used to illustrate our hypothesis. Although it is a surface force, we can compare it to a volume force, i.e. a GOR acceleration.

* if pressure is exerted on this sponge slowly enough, mechanical stresses inside the sponge will never be very high. The liquid has time to escape, the sponge does not resist, and manual pressure remains light but prolonged (figure 3, top).

The terms of the above proposal are inverted if pressure is rapidly exerted on the sponge. Mechanical stresses increase very sharply inside the sponge as the liquid has not had time to escape and offers maximum resistance (figure 3, bottom).

In this example of the law of action and reaction, fluid viscosity is, naturally, a determining factor with respect to fluid flow out of the sponge.

The example we chose becomes a little less trivial if the same experiment is run with the sponge immersed in a bowl filled with liquid. Intuitively, we suspect that liquid flow out of the sponge - therefore stresses within the sponge- directly depends on the pressure in the bowl and not only on the application rate of manual surface forces .

Even if the pressure is acting on the sponge sufficiently slowly, mechanical stresses inside its walls are increased if the outer pressure augments !

5.1 Hypotheses

5.1.1: EFFECTS OF GOR + GZ ACCELERATION

Pressure is maintained inside the sponge (brain) by a volume force (acceleration).

For GOR+Gz acceleration the interpretation applying to inflight LOC is naturally a pathophysiological interpretation. +Gz accelerations act through their high amplitude and duration (classical case of tolerance to acceleration proposed by A. Stoll (45), fig. 4).

The target is the hydrostatic component of blood pressure. The effect is that of blood pooling in the lower limbs, causing brain hypoxia with grey-out, black-out and loss of consciousness. Tissue stresses remain equal or slightly increase but never become noxious.

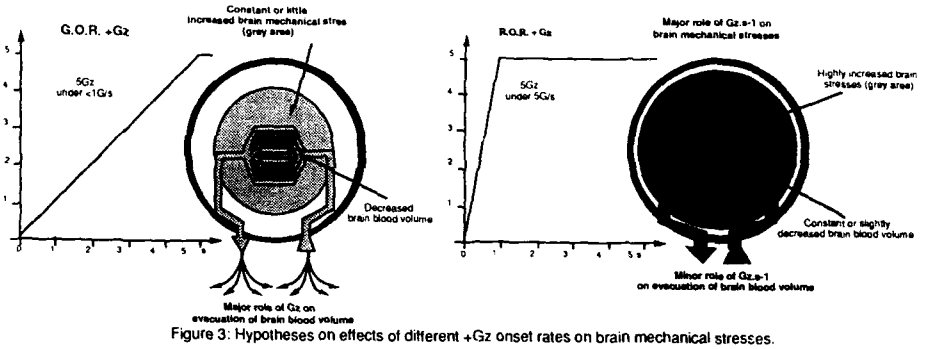

Figure 3: Hypotheses on effects of different +Gz onset rates on brain mechanical stresses.

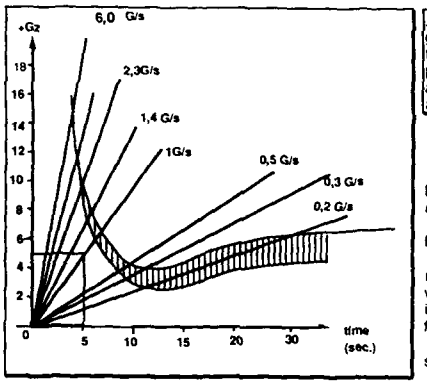

Figure 4 : Human tolerance to accelerations according to Stoll (45). This graph, drawn in 1956 shows tolerance to + Gz acceleration vs time. Beyond the upper line, any acceleration induces LOC. Under the lower curve the pilot remains normally conscious. The slashed area is the grey-and black-out area : continuous transition from narrowing peripheral visual field to black out and, ultimately, loss of consciousness.

5.1.2- HYPOTHESES ON EFFECTS OF ROR + GZ ACCELERATION

In this case, the interpretation of inflight LOC would be strictly biomechanical. The number of + Gz would play a significant role but the onset rate an even greater one.

The target would no longer be the hydrostatic component of vascular blood pressure, but rather mechanical stresses within tissues.

Inertia, viscosity, and probably geometry of the vascular system would resist the blood mass, expelling to escape from the brain. Brain hypoxia would not have time to develop, and LOC would be caused by a sudden increase in brain tissue stresses resulting from the abrupt impact of volume forces.

As stresses are similar to pressures, inflight LOC could be, stricto sensu, the result of sudden intracranial hypertension.

5.2- Graphic representation

The brain hypertension hypothesis is graphically represented in Figure 5 with positive tissue pressure changes on the upper ordinate, and negative brain blood mass changes on the lower ordinate, for the three graphs .

5.2.1 CASE OF A SLOW STEEP TURN AT 5 GZ, <1 G.S^{-1} (Figure 5, left)

When the load was first applied, intracranial mechanical stresses increased concomitantly with volume forces applied to the brain (solid line, top). As brain blood volume decreases (bottom), mechanical stresses also decrease (top) while the risk of reaching the hypoxic threshold preceded by grey- and black-out augments. The brain somehow "benefits" (in terms of reduced mechanical stresses) from the smaller tissue blood mass but also "suffers" from less oxygen.

5.2.2 CASE OF A RAPID STEEP TURN AT 5 GZ, 5 G.S^{-1} (Figure 5, right)

To make things easier to explain, we can decide that this acceleration reaches the critical threshold of brain mechanical tension. When the load is first applied, mechanical stresses in the brain increase concomitantly with volume forces applied to the brain (top). But they continue increasing and reach the intracranial hypertension threshold as blood volume is confined inside the skull. The brain "suffers" (through increased mechanical stresses) while "benefiting" from the oxygen of the retained tissue blood mass. Inflight LOC is immediate and sideration of nerve structures, without visual prodromes, can explain lacunar amnesia

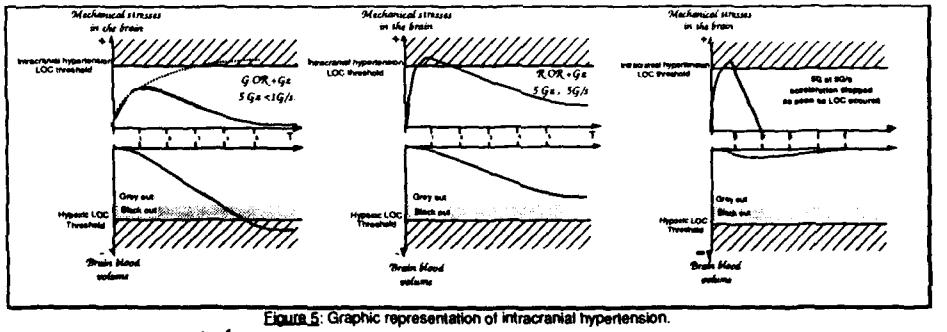

Figure 5: Graphic representation of intracranial hypertension.
left: slow steep turn at 5 Gz, 1 G.s^{-1}. Dotted lines show the course of brain stresses if blood was not drawn out of the brain. Middle: rapid steep turn 5Gz, 5G/s. Right diagram of LOC by intracranial hypertension with immediate release of acceleration.

VI) ANALYTICAL TEST APPROACH (37)

The analytical test approach will not be discussed in detail as it has been extensively developed by Gaffié et al.

Baseline assumptions are that the skull is rigid, nerve tissue connected to the blood vessel network has a viscoelastic behavior and is immersed in the Newtonian viscous CSF. The selected model is based on a decoupled study of the behavior of the viscoelastic material, of peripheral fluids, and of blood flow through the system.

Nomenclature

K(z) Vessel stiffness	r Space variable of tranverse direction.	V_z longitudinal local velocity.
f analytic law of longitudinal velocity.	R distance from the centerline to the wall.	z space variable of longitudinal directionF
ı Vessel length	R_0 Radius at rest	centrifuge acceleration
P(z,t)Blood dynamic pressure	S(t,z) Vessel cross area	F_z axial component of acceleration
P_e(z,t) External pressure acting on the vessel wall.	S_0 Resting vessel cross area	α(z,t)function induced by radial integration
P_t(z,t) Transmural pressure	t time variable	r blood volumic mass
	U(z,t)mean velocity	τ_p Mean viscous shear stress of wall

6.1- Behavior of brain and CSF

The experimental investigation of brain stresses will use information on deformations. CERMA's Biomechanics Department is now developing a code of finite elements. The mesh necessary to use this code is described in Figure 6. The first results which are reported later were obtained on a simpler structure (ref. maximum stresses in nerve tissue under + 6 Gz acceleration ; § 6.4).

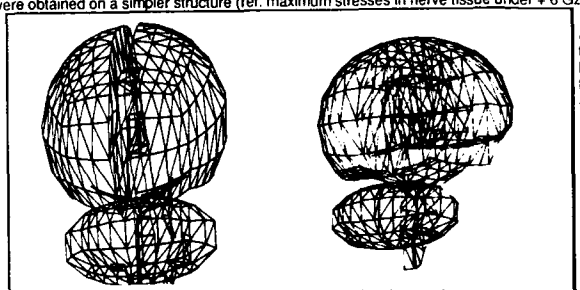

Figure 6 : Brain mesh (code of finite elements)

Two extreme cases were investigated :

a) viscoelastic brain alone, the changes in stress fields being digitally represented by finite elements.

b) rigid brain in CSF, the deformation of the viscous film being described by the lubrification equation (41) :

$$M\frac{\partial^2 h}{\partial t^2} + 3\mu\pi R^4 \frac{\partial v/\partial t}{h^3} = M\left(1 - \frac{\rho_0}{\rho}\right)\gamma$$

integrated on the skull base assumed to be rigid and digittaly represented by a two-phase diagram.

These two models provide, in the course of time, stress fields inside the brain and CSF. They also provide an order of magnitude of perturbations affecting blood flow.

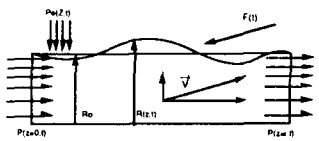

Figure n°7: Elementary geometry of elastic equivalent vessel.cf. Gaffié et al., below

6.2- Modeling blood flow

A decision was made to use a single elastic vessel to represent a group of blood vessels having similar physical characteristics. The different tubes were then connected to form a complete model of the vascular system. The tube in which an incompressible viscous fluid is flowing is simultaneously subject to the action of the heart, of a distribution of external pressure on the walls and cf a field of density (figure 7).

Local equations for mass and motion conservation

$$\vec{Div}.\vec{V} = 0 \quad \text{and} \quad \rho\frac{d\vec{V}}{dt} = \vec{F} + \vec{Div}\,\bar{\bar{\sigma}}$$

and the uni-dimensional problem formulation

$$\frac{\partial S}{\partial t} + \frac{\partial}{\partial z}(US) = 0 \quad ; \quad \frac{\partial U}{\partial t} + (1-\alpha)\frac{\partial S}{\partial t}\frac{U}{S} + \alpha U\frac{\partial U}{\partial z} = \frac{1}{\rho}\left[\frac{\partial P}{\partial z} + \frac{P_s}{S}\tau_p + F_z\right]$$

are simply quoted here (see below: A detailed digital model to study G-LOC).

6.3- Review of the vessel behavior law (Fig. 8)

Coupling between the mechanical behavior of the fluid and the wall is represented by a law of state, vessel behavior $P-P_e=K(z)P(S/S_0)$. The non analytic P form is non linear with respect to S. Wave propagation is therefore highly conditioned by the local, instantaneous condition of the tube. If transmural pressure is positive, the tube dilates and has a quasi rigid behavior so that waves travel at very high velocity in the wall. Under negative transmural pressure the wall tends to collapse, become less rigid and wave velocity is diminished. But if the flow persists, the collapsed vessel takes the shape of a dumbbell and flow velocity increases (Fig. 8).

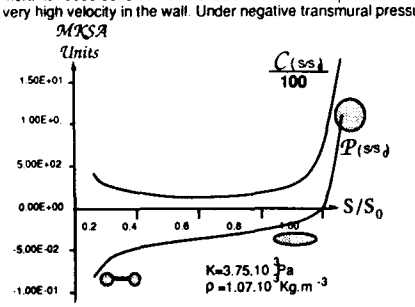

Figure 8 : Arterial vessel behavior law (vessel configuration vs. pressure) Supercritical (U>C) flows may be observed for certain types of perturbations, sometimes followed by shocks during transition to sub-critical flow conditions (41).

6.4- Results

Fig. 9 shows maximum stresses in nerve tissue under + 6 Gz. In the lower half, stress exceeds pressure of brain collector veins taken as reference (650 Pa).

Fig. 10 shows the pressure change in the fluid pressed at the base of the skull during runs at 1 and 7 G/s. In this case (hypothesis of sudden perturbation), the reference pressure is reached in approximately one second.

The crushing effect acting on the tube during the application of external pressure distributed on its wall is shown in Fig. 11. This pressure distribution causes parietal waves which propagate along the tube, inducing vascular collapsus. These deformations are the expression of a sudden change in blood flow rate (ref. below: experiment of Gaffié et al.).The first results of this modeling approach do show that ROR,+Gz acceleration can augment mechanical stresses in nerve tissue.

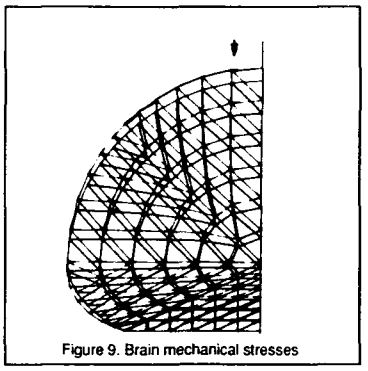

Figure 9. Brain mechanical stresses

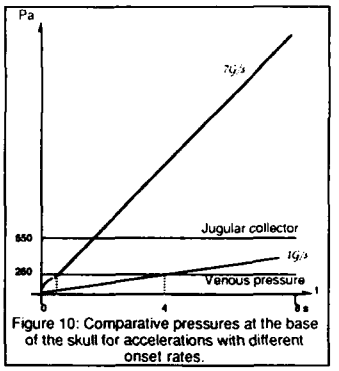

Figure 10: Comparative pressures at the base of the skull for accelerations with different onset rates.

6.5- Hypotheses on the effects of anti-G suit inflation

What are the hypothetical effects of increased peripheral vascular resistances in the lower part of the body compared to results obtained above?

In other words : when should the anti-G suit be inflated ?

Hypotheses on the effects of the anti-G suit are graphically presented in Fig. 12.

The time scale factor must be taken into consideration as it could be extremely high (sixty, for example, when the G-onset rate rises from 0.1 $Gz.s^{-1}$ to $Gz.s^{-1}$).

As in previous figures, the axis of ordinates shows, increases in tissue stresses (top), and decreases in brain blood mass (bottom). At low $Gz.s^{-1}$ (left), the increased abdomen and lower limb peripheral vascular resistances under inflation of the anti-G suit tend to counter the decrease in brain blood flow. They have a beneficial effect on central nervous system tissues, which has been known and used for over fifty years.

Depending on the considered parameter, this beneficial effect either enhances tolerance to a higher number of G for a given period of time, or prolongs useful consciousness under exposure to constant acceleration. The effect on brain mechanical stresses remains minor when compression of the lower part of the body is sufficiently delayed.

Under high $Gz.s^{-1}$ acceleration (right) the field of volume force is established within a few hundred milliseconds, and the increased low peripheral vascular resistances tend to cause a slight increase in brain blood flow if anti-G suit inflation is rapid. On the opposite, increased low peripheral resistances augment ventricular post-load, causing a hydraulic ram effect mostly affecting the supracardiac area with an enhanced risk of loss of consciousness.

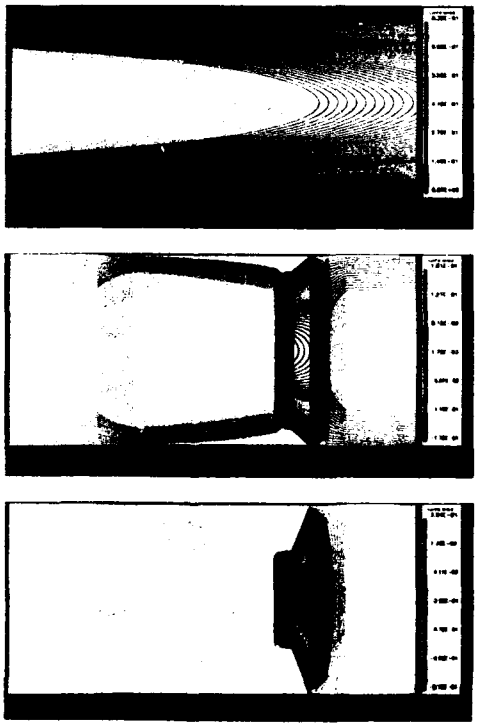

Figure 11 Sudden blood flow rate changes (ref. below: experiment of Gaffié et al.) create shocks during transition from sub-critical to supercritical blood flow rates.

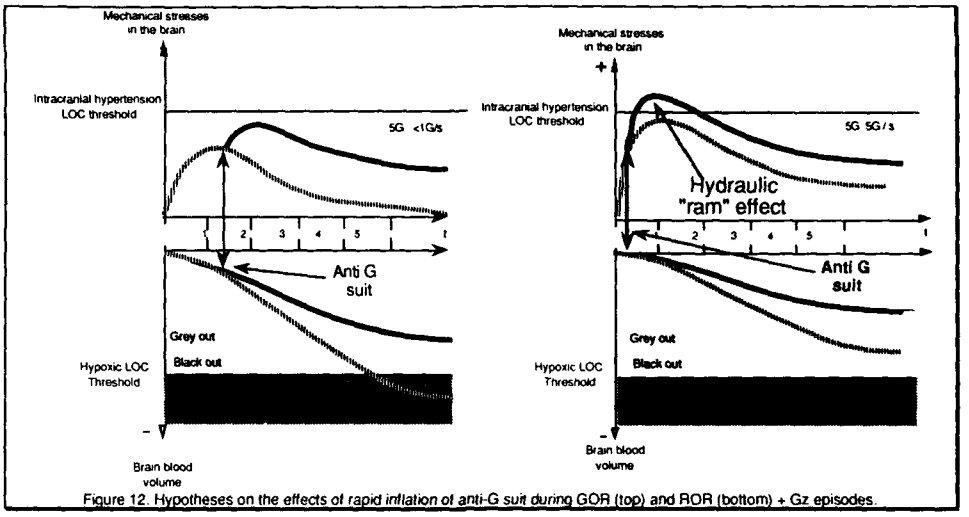

Figure 12. Hypotheses on the effects of rapid inflation of anti-G suit during GOR (top) and ROR (bottom) + Gz episodes.

his comment evidences the significance of a third factor: the instantaneous arterial pressure at the instant when loads are applied.

Arterial pressure is expressed through its different components:

*the chronological sequence of cardiac cycle and the instant when loads are applied.

*the maximum arterial pressure, itself depending on several factors :

-the pilot's physiological condition (emotion, stress, etc...), i.e. sympathic tone, circulating catecholamine and hypertensive hormones, etc. (myocardic inotropism): this basal, physiological state of arterial pressure, specific to each aircrew at a given instant (individual sensitivity) certainly is one of the major parameters determining the critical LOC threshold.

-the sytolic stroke volume which can also depend on the instant load value.

These various aspects deserve to be seriously examined as they may someday provide an answer to this puzzling question: **Why don't all fighter pilots subject to ROR acceleration similarly exhibit the same inflight LOC ?**

VII) ARTERIAL PRESSURE AND CRITICAL INTRACRANIAL HYPERTENSION THRESHOLD.

7.1- Chronology of cardiac cycle and moment of load application .

Remembering that only diastole may show some time fluctuations, and considering Figure 13 which is a review of the various sequences of cardiac revolution, two cases will be considered :

1- The heart of a fighter pilot beating at 120 bpm and exposed to + 6 Gz at 0.5 $G.s^{-1}$.

2- The heart of the same pilot still beating at 120 bpm is exposed to another + 6 Gz acceleration at 12 $G.s^{-1}$.

In the first case, twelve cardiac cycles can take place while the load increases up to + 6 Gz maximum. In the second case, the heart has only time for a single revolution during the entire phase from 1 Gz to 6 Gz, considered as linear.

It is easy to imagine that these two load application schedules can induce very different cardiovascular responses !

In the first case (6Gz, 0.5 $G.s^{-1}$) blood has time to pool both in the venous and in the arterial vessels of the lower limbs, gradually reducing ventricular filling, and ventricular preload (the force exerted by the end-diastolic blood volume, as first approximation) This will result in a low arterial pressure when loads reach their maximum, later counterbalanced by various physiological components of arterial pressure regulation which have all the time necessary to come into action.

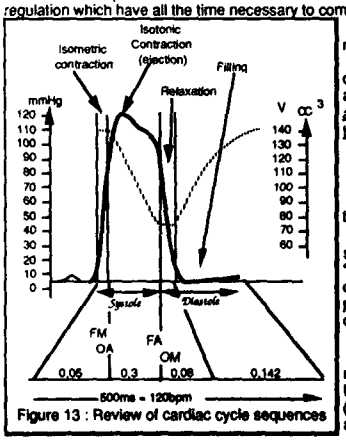

Figure 13 : Review of cardiac cycle sequences

This is a well known fact, described as the "surprise effect" on the heart preceding neuro hormonal regulations (Borredon , 1-3).

During high onset acceleration, the load can be assumed to develop over only one cardiac cycle. Ventricular preload is directly determined by the instantaneous acceleration and is multiplied by as much. Synchronisation of the first systolic wave and high onset acceleration may then be the determining factor for the critical threshold of intracranial hypertension.

Two extreme situations may be hypothesized :

a) the beginning of a systole coincides with the beginning of acceleration.

Systole and acceleration are perfectly synchronized (Fig. 14). They appear at the beginning of relaxation.

In this example, at 12 $G.s^{-1}$, maximum load is reached at the beginning of the following systole.

* During the isovolumic systolic phase, preload is maximum since it acts on an end-diastolic volume whose mass, accelerated several times, drastically acts on motor pressure (the ventricle must push an end-diastolic volume of 140 cc, resisting with a force of 0.140 *6=0.840 daN (density =1)

* During the isotonic systolic phase, post-load is, at first sight, very high since the normally positive effect of blood pooling in the venous compliant system did not occur. Peripheral arterial resistances were increased sixfold under the rapidly applied force field (500 ms). Not until the following cardiac revolution (850 ms after the beginning of load application) will end-diastolic volume start to diminish, by partial blood confinement.

b) The beginning of a diastole coincides with the beginning of acceleration (Fig. 15)

The two events are not synchronized and their effects are inverse of those just described above.
The increased load during the isotonic phase has an adverse effect, still limited since the maximum mechanical load is reached at the end of the relaxation period, when effects of "solid displacement" appear in intravascular fluids.

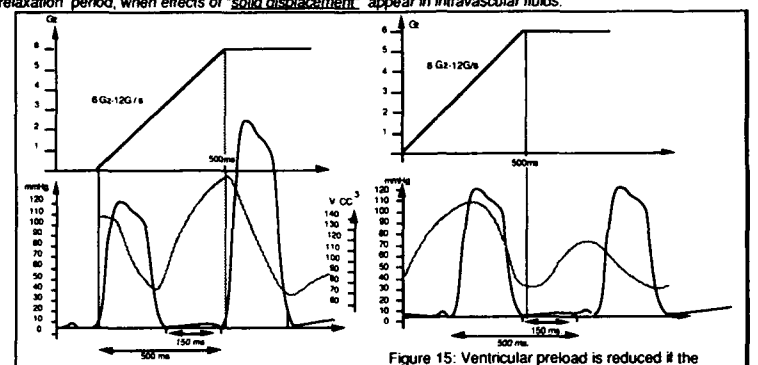

Figure 14: The acceleration of end-diastolic blood mass brings to a maximum the effects of the first ventricular ejection.

Figure 15: Ventricular preload is reduced if the beginning of diastole coincides with the beginning of acceleration.

The chronological aspect of the relation cardiac revolution-acceleration can easily be comprehended in its concept whereas the relation end-diastolic volume-acceleration requires the development of a ventricle model which also takes into account the magnitude of mechanical stresses in the ventricular myocardium.

7.2- Changes in end-diastolic volume under load: model of ventricle (Briane et al. (5-7))

The ventricle was represented by a thick walled vertical cylinder. The lower portion of the cylinder, modeling the apex, was free whereas the upper portion was exposed to radial deformation. The cylinder kept its cylindrical shape during deformation. The wall was made of an incompressible fluid in which elastic fibers were bathing (Fig. 16).
These fibers formed two networks of regular helices having the same centerline as the cylinder. Their orientation continuously changed inside the wall. These two networks were symmetrical with respect to a plane passing though the cylinder centerline and volume torsion was not taken into account. The radial and longitudinal deformations were measured with respect to a reference configuration with no mechanical strain. In this investigation great deformations were assumed to take place.

The law of fiber direction $\Gamma(R)$ varied linearly

$$\pi - \gamma(r)$$

between angle Γ_o at the endocardium (R=Ri) and $-\Gamma_o$ at the epicardium (R=Re) according to the law

$$\Gamma(R) = \Gamma_o\left(\frac{R_i+R_e-2R}{R_i-R_e}\right)$$

7.2.1 WALL DEFORMATION

The cylinder elongation coefficient was defined using $z = \lambda Z$. Local fluid incompressibility was expressed as: rdrdz=RdRdZ
By integration, we obtained

$$r^2 = \frac{1}{\lambda}\left(R^2+\frac{v-V}{\pi L}\right)$$

When the pitch of an helicoidal fiber was compared in the deformed configuration and in the reference configuration, we obtained the relation

$$r \operatorname{tg} \gamma = \lambda R \operatorname{tg} \Gamma$$

The fiber elongation coefficient α is the ratio of the length of a fiber component in the deformed configation to the length of this same component in the reference configuration. Since fibers were helicoidal, we obtained

$$r \operatorname{tg} \gamma = \lambda R \operatorname{tg} \Gamma \qquad \text{and} \quad a^2 = \frac{r^2+r^2(\operatorname{tg}\gamma)^2}{R^2+R^2(\operatorname{tg}\Gamma)^2}$$

We can also write

$$\alpha^2 = \frac{r^2}{R^2} + (\cos\Gamma)^2 + \lambda^2(\sin\Gamma)^2 \qquad (1)$$

In the deformed configuration fiber directions of both networks were given by

$$\tau^+ = \cos\gamma\, e_\theta + \sin\gamma\, e_z \quad \text{and} \quad \tau^- = -\cos\gamma\, e_\theta + \sin\gamma\, e_z$$

where (e_r, e_θ, e_z) were the base vectors in cylindrical coordinates.

7.2.2 MECHANICAL HYPOTHESES

*the deformation consists in a sequence of quasi static equilibria.
*the intraventricular fluid is an incompressible perfect fluid.
*the ventricle is submitted to a constant vertical inertial force $\rho a e_z$ which corresponds to a centripetal acceleration $-a\, e_z$
*under the effect of inertia, the lateral surface of the ventricle wall is subjected to a field of hydrostatic pressure

$$\Delta p = \rho a \Delta z \qquad (2)$$

*but the inner surface of the cylinder is subjected to a null external pressure ; in other words, the ventricle does not bathe in a fluid subject to hydrostatic pressure.

7.2.3 DESCRIPTION OF STRESSES IN THE MYOCARDIAL WALL

*Stresses in the myocardial wall are caused by fluid pressure p=p(r,z) and tension T of fibers.

*Stress caused by the fluid pressure supposed to be perfect is isotropic. Stress caused by fibers acts in the direction of fibers, i.e. τ^+ and τ^-

*Inner stresses are represented by a matrix Σ. If n is a direction in space, vector Σn represents the force applying to the side of an elementary cube of the body oriented in direction n. In the present case, the stress matrix Σ of the ventricle wall is given by :

$$\Sigma_{ij} = - p\,\delta_{ij} + T\,(\tau_i^+\,\tau_j^+ + \tau_i^-\,\tau_j^-) \qquad (3)$$

Tension T is expressed as (Chadwick, (13))

$$T = [(1-\beta)E + \beta E^*](\alpha - 1) + \beta T_0 \qquad (4)$$

where β is a time function between O and 1, representing the activity of cardiac fibers during the cardiac cycle.

We obtain

β= O passive state (end of diastole)

β= 1 active state (end of systole).

In the passive state, tension T equals a force of elastic recovery proportional to the relative elongation

α-1 : $T = E\,(\alpha - 1)$.

However, in the active state, the fiber does not behave as simple elastic material. The difference in behavior is represented by the maximum "physiological" tension T_0 applied by the fiber.

7.2.4 EQUATION OF DEFORMABLE CONTINUOUS MEDIA EQUILIBRIUM

The equation of deformable continuous media equilibrium in a quasi static state is

$$\mathrm{div}\ \Sigma + f = 0$$

where f represents the inertia force per unit volume.

In the present case we obtain

$$\mathrm{div}\ \Sigma + \rho a e_z = 0$$

where divergence is expressed with respect to cylindrical coordinates (r, θ, z) of the deformed configuration.

Using this equilibrium equation we obtained the differential system giving the pressure gradient as a function of tension T and vertical coordinate z

$$\begin{cases} \dfrac{\partial p}{\partial r} = -\dfrac{1}{r} + (\cos\gamma)^2 T \\ \dfrac{\partial p}{\partial z} = \rho a \end{cases} \qquad (5)$$

The reference pressure was the extra-ventricular pressure at z=O.

According to the hydrostatic law (2) we obtained the boundary condition

$$p(r_e, z) = \rho a z \qquad (6)$$

Using the system (5) and the boundary condition (6) we obtained the intra-ventricular pressure p (r,z)

$$p(r,z) = \int_r^{r_e} \frac{2}{s}(\cos\gamma)^2 T\,ds + \rho a z$$

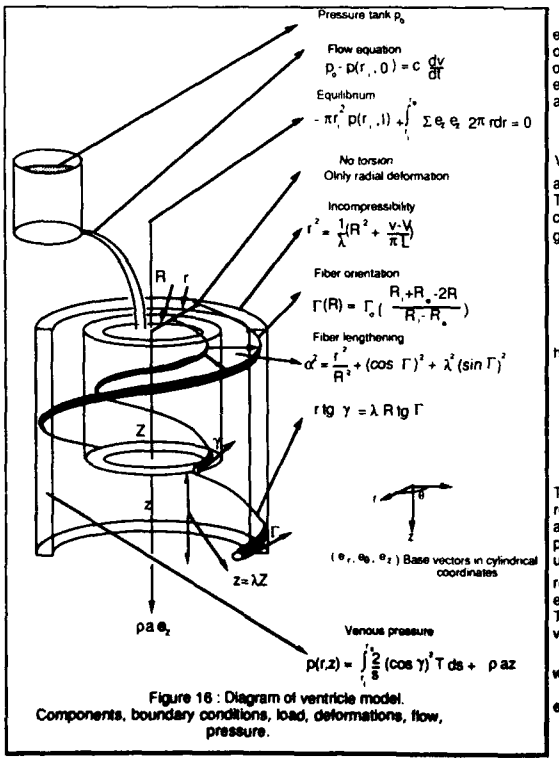

Figure 16 : Diagram of ventricle model. Components, boundary conditions, load, deformations, flow, pressure.

A second equation was necessary to calculate the elongation coefficient l which determines the deformation of the cylinder. This equation was given by the equilibrium of the cylinder base z=1 under the effect of internal and external pressure forces. The cavity pressure at z=1 applies a constant force

$$-\pi r_i^2\, p(r_i, l)\, e_z$$

Vector Σe_z represents the resultant of surface forces acting on the base of the ventricle wall.

The equilibrium of the cylinder base corresponds to the cancelling of the sum of projections e_z of these forces, giving

$$-\pi r_i^2\, p(r_i, l) + \int_{r_i}^{r_e} \Sigma e_z\, e_z\, 2\pi r\, dr = 0$$

with $\Sigma e_z\, e_z = -p(r_i, l) + 2T(\sin\gamma)^2$

hence

$$\int_{r_i}^{r_e} T\,[4(\sin\gamma)^2 - 2(\cos\gamma)^2]\,dr = \rho a r_e^2 l$$

7.2.5 FLOW EQUATION

To complete the mechanical study of this model, we had to represent blood flow when one of the mitral valves (filling) or aortic valves (emptying) is open. Valves are assumed to put the ventricle base (z=o) in contact with a reservoir under constant pressure p_o. During the filling phase, this reservoir represents the left atrium, and during the emptying phase it represents the arterial system.

The Poiseuille equation describes blood flow through the valves

$$p_o - p(r_i, 0) = cQ$$

where c is the valve resistance and Q the cardiac output.

If the valve is cylindrical, resistance c can be expressed as

$$c = \frac{8\mu l_v}{\pi r_v^4}$$

where μ is blood viscosity, l_v is the length and r_v the radius of the valve.

The cardiac output Q and the ventricle cavity volume V are related as $Q = \frac{dv}{dt}$

We obtain the following flow equation

$$p_o - p(r_i, 0) = c\frac{dv}{dt}$$

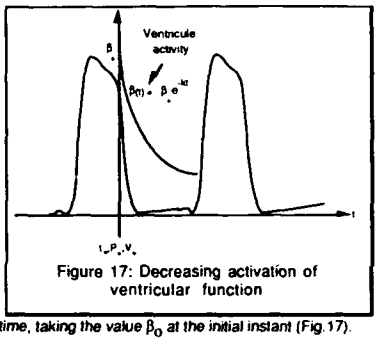

Figure 17: Decreasing activation of ventricular function

7.2.6 RESULTS

Simulation principles

The left ventricle filling phase, used as model, was studied under various acceleration profiles. Given an atrial pressure P_o coinciding with pressure $p(ri,O)$ at the opening of the mitral valve taken as time origin, and a pre-filling volume V_o, we derived from this pressure the initial ventricle activity $\beta=\beta_o$.

We applied the activation principe $\beta(t)$ exponentially decreasing as a function of time, taking the value β_o at the initial instant (Fig.17).

Knowing the effect the time law $\beta(t)$ we calculated at each time increment

*the intraventricular pressure p (r_i,o), *the intraventricular volume V, *the cylinder stretched length λ .

Different simulations were run with increasing accelerations OGz, 1 Gz, 3 Gz and 5 Gz

Data

Geometrical reference data. R_i = 1.5 cm,R_e = 2.4 c, V = 50cc, G_o=70°, c = 5 U.S.I. (Poiseuille law resistance).

Elasticity modulus (mmHg) E= 23.07; E'= 171.54; T_O = 19.23

Initial data P_o= 11.5 mmHg, V_o = 100 cc

The different simulations were run for Δt= O.5s (Data correspond to a viscosity of 5.10^{-3} Pa.s).

Results

Pressure-volume curves: $p(r_i, 0)$ as a function of v . Pressure-time curves: $p(r_i, 0)$ as a function of t. Volume-time curves: v as a function of t. In each series curves are represented as a function of accelerations.

Calculation of { intraventricular pressure p (r_i, O); intraventricular volume v; ventricle elongation l } under { Gz = 0; Gz = 1; Gz = 3; Gz = 5 } Results are plotted in several curves

Pressure-volume curve (Fig. 18)

The intraventricular pressure shows interesting fluctuations at the opening of the mitral valve. It decreases at the beginning of diastole with myocardial relaxation and rises when volume increases. This phenomenon is enhanced as acceleration in the longitunal axis of the ventricle increases. For a given volume, end-diastolic pressure under 5 Gz is much lower than under a field of normal gravity, and even more so if the ventricle has a high storage capacity. In this study where storage capacity is not limited, volumes greater than 250 cc have to be reached under 5Gz to obtain a diastolic pressure equal to that normally observed in a subject placed in the field of earth gravity.

Pressure-time curve (Fig. 19)

The pressure-time curve clearly shows reduced pressure in the early diastolic phase. Not before 230 ms at 5 Gz can the ventricular pressure recover the value it had at the very beginning of the relaxation phase. If this lapse of time corresponds to a heart rate of 103 bpm, the volume associated with this pressure is entirely unrealistic since it reaches extreme values of 250 cc.

Considering a heart rate of 120 bpm (diastolic time 150 ms), intra ventricular pressure under 5 Gz is much lower than what it would be at 1 G. Here, pressure, volume, and time are thoroughly consistent with what is observed in reality.

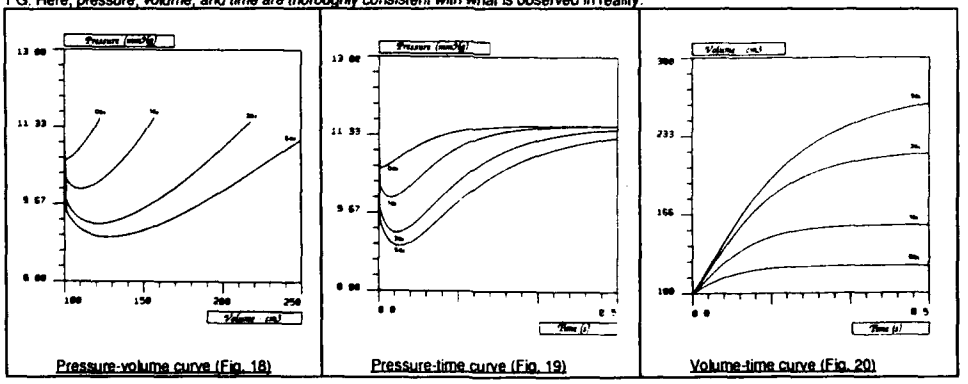

Pressure-volume curve (Fig. 18) | Pressure-time curve (Fig. 19) | Volume-time curve (Fig. 20)

Volume-time curve (Fig. 20)

Comments on pressure-volume and pressure-time curves also apply to the volume-time curve where the application of a force field at the beginning of the relaxation phase induces an increase in ventricular volume, proportional with the magnitude of this force. Mechanical force fields are considered as established and steady, and no concept of rate of change in volume forces is applied.

7.2.7 DISCUSSION - PROSPECTS

Results show a very clear influence of + Gz accelerations on the diastolic ventricular function. Schematically, the most significant effects of increasing accelerations on the model are :

* reduced pressure at the beginning of the filling phase expressing increased suction of atrial blood by the ventricle.
* increased diastolic volume
* higher filling rate.

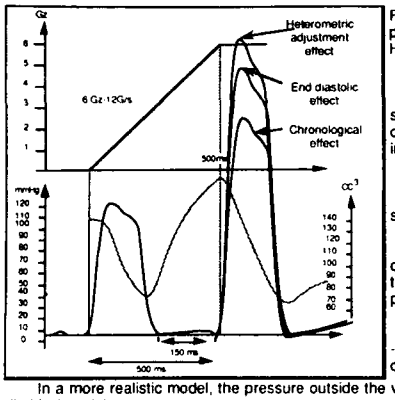

Figure 21: Cardiac effects of ROR + Gz acceleration when both events are perfectly synchronized
Hypothesis on the sum of the three effects
1)chronological
2)volume
3) heterometric
superimposing on the basal effect of myocardial homeometric adjustment capable of raising the instantaneous intracranial pressure and explaining inter-and intra-individual G-LOC differences.

Two critical comments can be made on these results : one relative to the structure of the model, the other relative to result analysis.

A cylindrical model is naturally different in aspect from a real ventricle. The choice of this particular geometry is partially justified by the literature and offers the advantage of an analytic processing. This model evidently does not include a pericardium.

Analytical criticism often pertains to these imperfections.
- the cylindrical configuration relies on the hypothesis of a hydrostatic pressure outside the cylinder wall while its lower portion is in contact with a null pressure.

In a more realistic model, the pressure outside the ventricle would be null, but such a condition is incompatible with the design of a cylindrical model.

- the model does not take into account the role of the pericardium which prevents excess stretching of the myocardium. Large filling volumes can thus be obtained. The realistic use of results imposes a time limit (150 ms) for calculations. This limit is thoroughly compatible with the application of a load to a heart beating at 120 bpm.-finally, contrary to experimental protocols, the application of this load does not continuously vary until a plateau is reached. Results are those of a process which changes in time in the presence of various force fields whose fluctuation rate at the origin is infinite.Under these conditions, the effects of + Gz accelerations over 150 ms are a decrease in intracavity pressure at the beginning of diastole and an increase in end - diastolic suction pumping of the heart.

As a result, if no physiological regulation takes place, inertial forces due to ROR + Gz acceleration (infinite onset rate in this study) enhance the inflow of blood during the diastole of the first cycle of a heart subject to this force field, and significantly increase the systolic stroke volume, hence arterial pressure during the following ventricular contraction.

Our hypotheses on a chronological effect of synchronized events on systolic pressure should be revised and upgraded. Four factors influence the situation (Fig. 21). Three are directly related to the load rate of change, two being primary,i.e. chronological and volume effects. the third being secondary, i.e. the Starling law effect (heterometric myocardial adjustment) under increased systolic stroke volume. The fourth effect is autonomous. It concerns the neurohormonal inotropic adjustment of cardiac function (homeometric adjustment), and the adjustment of vascular motricity.

Finally the synthetic diagram, summing all the hypotheses, can be establish. Figure 22 is the diagram of hypothesis relative to inflight LOC intracranial hypertension in fighter aircrew exposed to ROR acceleration, and integration into the classical theory of hypoxia under GOR acceleration (respective time courses of intracranial hypertension and brain hypoxia are not accurately represented).

VIII) CONCLUSIONS

The tilt of aircrraft during a slow steep turn subjects the pilot to an acceleration which is colinear to the longitudinal axis of the body and can reach several times the acceleration of earth gravity.

The centrifuge effect which crushes the pilot in his seat also acts on fluids. Blood is shifted toward the lower limbs, causing cerebral hypoxia, sometimes associated with inflight loss of consciousnes, preceded by grey-out and black-out. The compression of the abdomen and lower limbs by an anti-G suit which resists blood pooling in areas below the heart therefore provides good protection.

With the use of new technologies to build fighter aircraft capable of generating ROR + Gz, a new symptomatology of inflight LOC developed : rapid, without visual prodromes, without recollection of the accident. The time scale is of the order of a second, probally even less !

The purpose of this study is to propose a strictly biomechanic explanation of sudden inflight LOC, i.e. brain nerve structures subject to ROR + Gz become functionally inefficient, not because of a shortage of oxygen, but because a sudden rise in brain mechanical stresses causes, stricto sensu, sudden intracranial hypertension.

A simple model is proposed to analyze three parameters :
* pressure distribution in CSF.
* distribution of stresses and deformations throughout the brain.
* changes in blood flow pulsed into the skull.

Calculations show the influence of a sudden change in flow rate causing collapses and supercritical flows sometimes followed by intravascular shocks.

The first results of this modeling study indicate that ROR + Gz acceleration could augment mechanical stresses inside nerve tissues, and therefore result in sudden intracranial hypertension hypertension.

The threshold intracranial pressure at which LOC could occur can be discussed with respect to the instantaneous arterial pressure and heart parameters. Four effects were analyzed :

* chronological effects of the cardiac cycle vs load application time.
* volume effects of systolic stroke.
* heterometric adjustment of myocardium.
* neurohormonal inotropic adjustment of cardiac function (homeometric adjustment).

Under these hypotheses, rapid pressurization, sometimes anticipated, of the anti-G suit is suspected of being noxious, creating a "hydraulic ram effect" in the brain-bound vascular system, thus increasing the risk of early intracranial hypertension.

The use of the anti-G suit naturally remains an indispensable protection as a pilot who escapes early intracranial hypertension may well suffer inflight LOC by cerebral hypoxia a few seconds later.

Hypotheses on cerebral hypertension do not contredict the theory of hypoxia, they complement it. Current studies on delayed anti-G suit inflation respective of acceleration onset rates are perfectly legitimate if we want to avoid the risk of causing accidents in subjects artificially carried to resistance limits which are first biomechanical, then physiological.

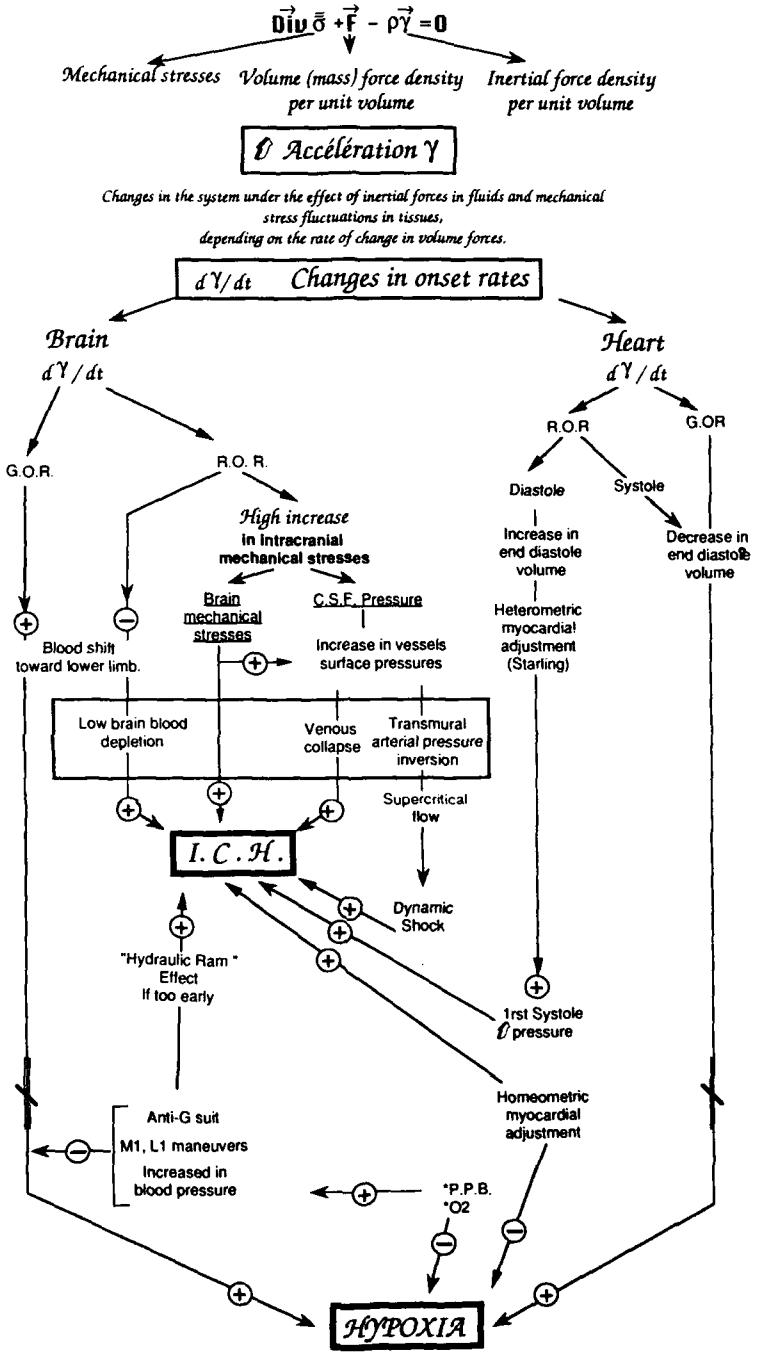
Div σ̄ + F - ργ = 0
Mechanical stresses
Volume (mass) force density per unit volume
Inertial force density per unit volume
∅ Accélération γ
Changes in the system under the effect of inertial forces in fluids and mechanical stress fluctuations in tissues, depending on the rate of change in volume forces.
dγ/dt Changes in onset rates
Brain
dγ/dt
Heart
dγ/dt
G.O.R.
R.O. R.
R.O.R
G.OR
Diastole
Systole
High increase in intracranial mechanical stresses
Increase in end diastole volume
Decrease in end diastole volume
Brain mechanical stresses
C.S.F. Pressure
Heterometric myocardial adjustment (Starling)
Blood shift toward lower limb.
Increase in vessels surface pressures
Low brain blood depletion
Venous collapse
Transmural arterial pressure inversion
Supercritical flow
I. C. H.
Dynamic Shock
"Hydraulic Ram" Effect If too early
1rst Systole ∅ pressure
Homeometric myocardial adjustment
Anti-G suit
M1, L1 maneuvers
Increased in blood pressure
*P.P.B.
*O2
HYPOXIA

Acknowledgements.
The authors express their gratitude to Professor Paul Borredon for his positive and constructive comments, to *Danielle Freund* for the English translation of this text, and to Catherine Dal Bosco for the typescript.

REFERENCES

1)Borredon P. Liscia P. Haziot A. Quandieu P.: Expositions répétées aux accélérations +GZ de haut niveau:Conséquences sur le myocarde et le système *cardiovasculaire. Médecine Aéronautique et Spatiale 1982, XXI (84) 420-424.*

2)Borredon P. Paillard F. Liscia P. Nogués C.: Hypertension induced by repeated exposure to high sustained +GZ stress. Aviation Space and Environmental Medicine. 1985, 56 (4) 328-332

3)Borredon P,Paillard F. Liscia P. Cailler B. Ille H. Didier A.: Cœur droit et accélérations +Gz soutenues et de haut niveau. Med Aér.Spat.1986, XXV, (98),139-144.

4)Borredon P. Paillard F. Liscia P. Bouscaillou P. Milhaud C. Nogues C.:Hypertension fonctionnelle provoquée par des expositions répétées aux accélérations +Gz soutenues et de haut niveau. Trav Scient. S.S.A., 1984, (3), 1-6.

5)Briane M., Quandieu P., Henry J., Liébaert Ph.: *Modeling of changes in mechanical* stress of left ventricular myocardium (diastolic phase) under +Gz acceleration. A paraître dans "The Physiologist".

6)Briane M., Quandieu P., Henry J., Liébaert Ph.:Modélisation de la *fonction diastolique* sous accélération à fort jolt. I Modélisation mathématique. Médecine aéronautique et spatiale:1990, XXIX (113)

7)Briane M., Quandieu P.,Henry J.:Modélisation des variations de *contraintes mécaniques* du myocarde ventriculaire gauche (phase diastolique) sous accélération +Gz - CERMA Report 90-32 (22 pages)

8)Brinquin L., Bizouarn Ph., Rousseau J.M., Diraison Y., Bonsignour J.P., Buffat J.J.: *Le pantalon anti-choc* pour la neuro-chirurgie en position assise. Médecine et Armées 1988,16,(5),353-355.

9)Burton RR, Leverett SD, Michaelson SD : Man at high sustained +GZ acceleration : a review. *Aerospace Med* 1974, 45 (10) 1115-1136.

10)*Burton RR, Whinnery JE* : Operational G-induced loss of consciousness. Something old, something new : Aviation Space and Environmental Medicine 1985, 56 (8) 812-817.

11)Burton R.R.: A *conceptual model* for predicting pilot group G tolerance for tactical fighter aircraft.Aviat.Space Environm. Med. 1986 57 ;733-44

12)Burton R.R.: Anti-G suit Inflation rate requirements Aviat. Space Environm.Med. 1988. 59, (7),601-605

13)Chadwick R.S.: "Mechanics of the Left Ventricle", Biophys. J., 39,1982, 279-288.

14)Clere J.M, Vieillefond H, Poirier JL: *Interêt du siège incliné* pour l'amélioration de la tolérance aux accélérations +GZ. CR n°1132 Contrat DRET n° 82/1131 Rapport 14952/DRET/SDR/M du 20/9/1982.

15)Edelberg R.,Henry J.P.,Maciolek J.A,Salzman E.W.,*Zuidema* G.D.; Comparison of human tolerance to accelerations of slow and rapid onset; Aviation Medicine 1956 27, (6) 482-489

16)Féron X.: Pertes de *connaissance dues au facteur de charges. Bulletin* de sécurité des vols Janvier 1991, 12-16, SV EMAA.

17)Gilligham KK, Makalons DL,Tays MA : G stress on A10 pilots during Jaws II exercise Actes du congrés de US Aerospace Medical Association (ASMA)1980 89-91

18)Hood LA : L.O.C.from High G. Flying safety 1983,7 ,5-9.

19)*Houghton* JO, Dennis K, Bride MC, Hannah K: Performance and physiological effects of acceleration induced (+GZ) loss of consciousness: Aviation Space and Environmental Medicine 1985, 56 (10) 956-965.

20)Howard P,: Cardiac function, acceleration: In Principles and practice of human physiology (OG Edholm JS Weiner edit.Academic Press) 1981 191-240

21)Kydd G.H, Fenichel R.L, Crosbie R.J: Relationship of carotid pressure and end point of *acceleration* J.Applied Physiol. 1960 15(5) 903-906

22)*Kokova I: Hemodynamics* parameters as related to different tolerance to head pelvis acceleration : Kosmicheskaya Biologia I Aviakosmicheskaya Meditsina 1985 19 (5) 56-60.

23)Knudson R, Mc Millan D, Doucette D, Seidel M : A comparative study of G-induced neck injury in pilots of the F/A-18, A-7 and A-4. Aviation Space and Environmental Medicine *1988* 59 (8) 758-760.

24)Krutz R.W.Jr,Krueger A.G.,*Burton* R.R; A comparison of uniform pressure anti-G suits. Safe Journal 1988,18,(2) 14-18

25)Jaron D, Moore T,Shankara Reddy BR, Hrebien L,Kepics F; Reflectance photoplethysmography as an adjunct to assessment of gravitational acceleration tolerance:preliminary findings.Aviat.Space Environm.Med. 1987;504-12

26)*Landry RF*: : G-induced loss of consciousness : AGARD Conference Proceedings N° 377 distribué par O.N.E.R.A. 92220 Chatillon/Bagneux CP 1985 B2.1-B2.3 .

27)Leguay G, Seigneuric A : Tolérance cardiovasculaire aux accélérations +GZ soutenues et de haute intensité . Revue générale. Médecine Aéronautique et spatiale 1984 XXIII (90) 137-156.

28)Liébaert Ph., Gaffié D., Quandieu P., Tran C.C.: Numerical evaluation of pressure developed in cerebrospinal fluid at the base of the skull during +Gz accelerations simulating a short hypergravitation: 1990 The Physiologist 33, (1), 145-146

29)Liscia P. Drogou C.Quandieu P. Borredon P: Accélération +Gz et catécholamines plasmatiques. A paraître dans Médecine Aéronautique et Spatiale

30)Meeker L.J.,*Krueger* A.G., *Love* P.E. *An engineering* test and evaluation of several new anti-G valves. Safe Journal 1988,18,(2) 24-27

31)Moore TW, Fowley JF, Shankara RBR, Kepics F,J arron D : An experimental microcomputer *controlled system* for synchronized pulsating antigravity suit; Aviation Space and Environmental Medicine 1987, 58, (7),10-14.

32)Nickell WT, Bhagat PK, Krebelv L, Cohen MM, :Use of ultrasonic dimension measurement to monitor blood *shift from* the head during exposure to +Gz .Preprints of 1983 Annual Scientific Meeting, Aerospace Medical Association 1983, Houston, 180-181.

33)Pelligra R, Sandler H, Rositano MD, Skretinland K, Mancini R : Advance technique for monitoring human tolerance to +GZ acceleration. Revue de Medecine Aéonautique et Spatiale 1973 46 301-304.

34)Pluta J.C. LOC survey . Flying Safety, January 1984 25-26

35)Poirier JL, Clere JM, Vieillefond H, : L'inclinaison du siége pilote: intérêt et limites.:Médecine Aéronautique et Spatiale 1986 25 (100) 318-323.

36)Quandieu P., Briane M., Henry J., Liébaert Ph.: Modélisation de la fonction diastolique sous accélération à fort jolt. II Exploitation biomécanique. Médecine Aéronautique et Spatiale:1990, XXIX (113)

37)Quandieu P.,Gaffié D., Liébaert Ph: Interprétation biomécanique des pertes de connaissance en vol des pilotes de chasse sous l'effet de l'application d'une accélération +Gz d'installation rapide(fort jolt). C.R. Acad. Sci.Paris 312,(II) 185-190, 1991.

38)Ratajczak M.: AntiG valves: when is fast, too fast. Safe Journal 1988,18,(2) 19-23

39)Rayman RB,: Sudden incapacitation in flight (January 1966 to November 1971).: Aerospace Medicine 1973 , 44, (8), 953-955

40)Rayman RB, Mc Naughton GB: Sudden incapacitation in flight : USAF experience 1970-1980 : Aviation Space and Environmental Medicine 1980 54 (2) 161-164.

41)Roseau M.: Vibration des systèmes mécaniques. Méthodes analytiques et applications 1984 (Masson édit)

42)Shapiro A.H :,Physiologic and medical aspects of flow in collapsible tubes 1977 Proc.6th Canad Cong. Appl. Mech.Vancouver 883-906

43)Simons DG, Johnson RL, : Heart rate pattern observed in medical monitoring : Aerospace Medicine.1965 36 (6) 504-513.

44)Souder ME, Bachert RF, Henry CL, Slonim A : Time series analysis of ECG/ cardiovascular changes as a result of prolonged acceleration in baboons. *Preprints of 1982 Annual scientific Meeting. Aerospace Medical Association 1982, Bal Harbour.*

45)Stoll A.M.: Human tolerance to positive G as determined by the physiological end points. Journal of Aviation Medicine 1956 ,27, (4), 356-367.

46)Tran C.C.,Bonnin P,Paillard F,Quandieu P,Borredon P. Biodynamique cardiovasculaire et rythmologie cardiaque sous accélérations + Gz de longue durée. Travaux Scientifiques des chercheurs du Service de Santé des Armées. S.S.A. 1988 (9) 185-186

47)Tran C.C.:Utilisation de la vélocimétrie doppler pulsé pour l'étude des effets des accélérations sur la biodynamique cardiovasculaire:mémoire pour l'obtention du D.E.A. de physiologie et de physiopathologie des appareils respiratoire et circulatoire 1988,Paris V, 65pages.

48)Tricot F.: Modélisation de structures anatomiques par utilisation de méthodes aux éléments finis. Mémoire de stage de fin d'études (Ecole Polytechnique Chaire de mécanique option biomécanique) 1990. 126 pages.

49)Van Patten R.E. An alternative approach to high G protection. Safe Journal 1988,18,(2) 8-10

50)Whinnery JE, Shafstall RM : Incapacitation time for +GZ induced loss of consciousness : Aviation Space and Environmental Medicine 1979 50 (1) 83-85

51)Whinnery JE, Burton RR ,Boll P, Eddy DR : Characterization of the resulting incapacitation following unexpected G-induced loss of consciousness. Aviation Space and Environmental Medicine 1987 58 (7) 631-636.

52) Wood EH: Development of anti-G suits and their limitations. Aviat.Space Environm. Med. 1987;58:699-706

RESPIRATION EN PRESSION POSITIVE:

EFFETS SUR LA TOLERANCE HUMAINE AUX ACCELERATIONS $+G_z$.

ASSISTED POSITIVE PRESSURE BREATHING:

EFFECTS ON $+G_z$ HUMAN TOLERANCE IN CENTRIFUGE.

J.M. Clère, J.W. Burns*

Laboratoire de Médecine Aérospatiale,
Centre d'Essais en Vol,
F-91228 Brétigny sur Orge Cedex, France.

* Acceleration effect Laboratory
Crew Technology Division
USAF Det.4 AL/CFTF Brooks AFB. TX 78235-5301, USA.

RESUME: Le but de cette expérimentation est d'évaluer, sur la centrifugeuse de la Crew Technology Division, le gain de tolérance aux accélérations $+G_z$ apporté par la respiration en pression positive. Les six volontaires masculins participant à cette étude étaient équipés d'un casque avec une poche occipitale, d'un masque, d'une veste et d'un pantalon anti-G connectés à un système de régulation d'air à haut débit. Le siège éjectable était incliné à 30° (inclinaison Rafale). Chaque sujet a effectué avec et sans surpression respiratoire les deux séries de profils d'accélérations suivantes: la première série comportait deux lancements à 9 $+G_z$ avec plateau de 10 s (mises en accélération à 1 et 4 $G.s^{-1}$), la seconde simulant le combat aérien (succession de plateaux de 10 s à 5 et 9 $+G_z$ avec des mises en accélération de 4 $G.s^{-1}$). Les sujets effectuaient des manoeuvres de protection anti-G. Le contrôle physiologique est effectué par un électrocardiogramme et un test de champ visuel. RESULTATS: La respiration en pression positive n'améliore pas la tolérance lors de mises en accélération rapides et n'a pas d'action sur la fréquence cardiaque. En revanche, elle augmente le temps de tolérance aux accélérations (167.9 $\pm$ 38.4 s avec surpression 88.4 $\pm$ 23.1 s sans surpression, $p < 0.001$). Ces résultats sont similaires à ceux de la bibliographie et montrent l'intérêt de cette méthode.

ABSTRACT. The goal of this paper is to present an experiment on the effect of APPB as a method of increasing G-time tolerance and improving very rapid onset rate (VROR) tolerance using French APPB equipment. Six male volunteers were used on the USAF School of Aerospace Medicine centrifuge. The French equipment used was a helmet with an occipital bladder for automatic mask tightening, mask, jerkin and G-suit, breathing regulator and high flow G-valve. A standard USAF ejection seat was used, positioned at 30° (F-16 configuration). Acceleration profiles were 9 $+G_z$ for 10 sec at 1 $G.s^{-1}$ or 4 $G.s^{-1}$ and a 5-9 $+G_z$ SACM profile at 4 $G.s^{-1}$, with and without APPB. The anti-G straining maneuver (AGSM) was used as necessary to maintain adequate vision. APPB was a maximum of 9 kPa (68 mmHg) at 9 $+G_z$. Heart rate was calculated and heart rhythm anomalies were detected by an EKG. APPB had no significant effect on VROR tolerance or heart rate. APPB statistically increased G-time tolerance (167.9 $\pm$ 38.4 s with APPB and 88.4 $\pm$ 23.1 s without APPB ($p < 0.001$). These results are consistent with those obtained in previous studies.

1. INTRODUCTION.

La respiration en pression positive sous facteur de charge a été suggérée comme moyen de protection anti-G il y a une trentaine d'années. Plusieurs auteurs ont démontré que cette méthode améliorait la tolérance aux accélérations par réduction de la fatigue et de l'inconfort. Elle serait équivalente à la manoeuvre M1 (Shubrooks, 1973). Associée à la manoeuvre M1, elle augmente la tolérance à des niveaux d'accélération supérieurs aux niveaux atteints par les avions à hautes performances tels que les F 16, F 14, F 15 et M 2000 (Clère et coll., 1988). Le temps de tolérance mesuré lors d'un profil

1. INTRODUCTION.

The Assisted Positive Pressure Breathing (APPB) during acceleration was first suggested as an adjunct to acceleration protection some 30 years ago. Since then several authors have reported APPB to be effective in raising G_z threshold and reducing fatigue and discomfort. Shubrooks (1973) has reported APPB to be approximatively equivalent to the M1 manoeuvre in increasing $+G_z$ tolerance. Clère et al. (1988) have demonstrated that APPB used with a good anti-G straining manoeuvre increased the G level tolerance to more than the maximum G performance of F 16, F 14, F 15 and M 2000. Burns and Balldin (1988) have demonstrated that mean acceleration tolerance time during a Simulated Aerial Combat Manoeuvre (SACM) was significantly increased by 108 % at

d'accélération simulant le combat aérien est augmenté de 108 % pour une valeur de pression de 6.7 kPa (50 mmHg) et de 88 % pour une valeur de pression de 9.3 kPa (70 mmHg) par rapport à une situation sans respiration en pression positive (Burns et Balldin, 1988).

Le but de notre expérimentation, effectuée dans le cadre d'une coopération entre le Laboratoire de Médecine Aérospatiale et l'Acceleration Effect Laboratory, Crew Technology Division, est d'évaluer le gain de tolérance apporté par la respiration en pression positive lors de mises en accélération rapides. D'autre part, nous avons voulu vérifier son effet positif sur le temps de tolérance à des accélérations simulant le combat aérien.

2. METHODES.

2.1. MATERIEL.

2.1.1. Equipement.

Chaque sujet est équipé d'une veste (VHA 90), d'un masque (IN MP 90) et d'un casque (0S 500), prototypes fabriqués par des équipementiers français, et d'un pantalon anti-G (ARZ 820) (photographie n°1).

Un ensemble régulateur-valve anti-G de laboratoire fournit la pression à l'intérieur de l'équipement (fig.n°1).

La loi de surpression respiratoire est de 4.5 kPa.G^{-1} (33,7 mmHg.G^{-1}) pour des niveaux d'accélération compris entre 4 et 6 +G_z. Un bouton poussoir permet de déconnecter la surpression respiratoire. Une surpression de base de 0.5 kPa (4 mmHg) est automatiquement établie quelque soit le niveau d'accélération.

La pression dans le pantalon anti-G est de 7 kPa.G^{-1} (1 psi.G^{-1}) à partir de 2,2 +G_z. La pression maximum fournie est de 50 kPa (7,25 psi). Une pression de base de 1 kPa (0,14 psi) est établie entre 1 et 2.2 +G_z.

2.1.2. Moyens d'essais.

L'expérimentation est menée dans la centrifugeuse humaine de la Crew Technology Division. Le siège est incliné de 30°. Les sujets sont surveillés grâce à un circuit de télévision. Chacun d'eux est capable d'arrêter à tout moment la centrifugeuse avec le «système de veille automatique de contrôle du maintien d'appui». Il en est de même pour le responsable de l'expérimentation qui est en contact avec tous les intervenants.

PPB_{50} (6.7 kPa) and by 88 % at PPB_{70} (9.3 kPa) compared to tolerance time without PPB.

The goal of this paper is to present a joint experiment between the Crew Technology Division of the US Air Force School of Aerospace Medicine and the Biodynamic Division of the Aeropace Medical Laboratory concerning the effect of APPB on the G onset tolerance and concerning the time tolerance during a SACM profile.

2 METHODS

2.1 MATERIAL.

2.1.1. Equipement

The equipment includes a personnal equipment and a regulator anti-G valve ensemble (picture n°1).

Subjects wore equipment with an anti-G suit (ARZ 820), a jacket (VHA 90), a mask (IN MP 90) and a helmet (OS 500) which were produced as prototypes by French manufacturers.

The APPB was produced by a laboratory regulator anti-G valve ensemble (fig. n°1).

Figure N° 1

ANTI-G SUIT INFLATION AND BREATHING PRESSURES SCHEDULES

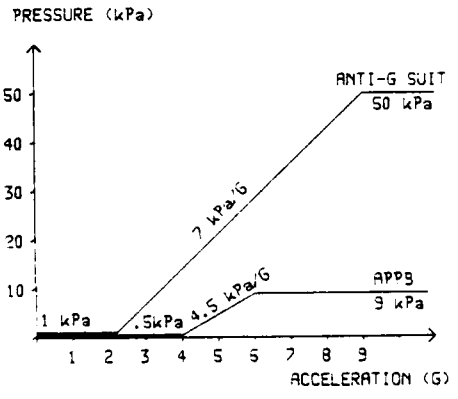

Photographie n° 1

Equipement de surpression respiratoire avec la veste VHA 90 et le pantalon anti-G ARZ 820.

2.2. MESURES.

Plusieurs paramètres sont mesurés et enregistrés sur des enregistreurs magnétique et papier. La plupart sont numérisés sur un ordinateur PDP 11/34.

Le fonctionnement de l'équipement est vérifié grâce à la mesure en continu des pressions dans le pantalon anti-G et la veste.

The schedule of inhaling pressure was 33.7 mmHg.G^{-1} (4.5 kPa.G^{-1}) between 4 and 6 G_z. A switch permitted disconnecting APPB before the runs. A ready pressure of 4 mmHg.G^{-1} (0.5 kPa) was set.

The anti-G valve pressure schedule was 1 psi.G^{-1} (7 kPa.G^{-1}) in the anti-G suit from 2.2 G_z. The maximum pressure provided is 7.25 psi (50 kPa). A ready pressure of 0.14 psi (1 kPa) was set at 1 G.

2.1.2. Experimental set.

The experiment was carried on the 6.1 m radius USAFSAM centrifuge. The seat was reclined of 30 degrees. Subjects were visually observed via closed-circuit color television. Each subject was able to stop the centrifuge with a «dead man» switch at any time, as was the central observer, who maintained voice contact with each member of the team.

2.2 MEASUREMENT.

Several parameters were measured, recorded on a strip chart and on a magnetic tape recorder. Most of them were digitized on a PDP 11/34 computer

An electrocardiogram (EKG) was recorded before, during and after the different runs. It permitted to detect EKG anomalies but also to calculate the heart rate.

The visual field is evaluated subjectively with the standard light bar used in Brooks. On this bar is mounted a central red light for fixation and testing of central vision and two green lights 0.355 meter on either side of the central light for testing of peripheral vision (visual angle set by both green lights is 48 degrees). The G_z tolerance criterion of peripheral light loss (PL) is set for all runs since this end point has been found to occur at a highly consistent G level and decreases the risks of blackout and unconsciousness.

2.3 SUBJECTS.

Six male volunteers of Brooks centrifuge panel participated at this experiment. They were required to pass a Class II flying physical examination.

They were ranging in age from 23-28 yrs (x = 25 yrs),

ranging in height from 1.67-1.97 m (x = 1.82 m) and

ranging in weight from 60-97 kg (x = 81.00 kg).

L'électrocardiogramme est enregistré avant, pendant, et après les différents lancements dans le but de détecter les anomalies mais aussi de calculer la fréquence cardiaque.

Le champ visuel est évalué subjectivement grâce à la rampe standard utilisée à Brooks. Une lumière rouge centrale permet de fixer le regard et d'évaluer la vision centrale; deux lumières vertes placées à 0,355 m de part et d'autre de la lumière rouge permettent de tester la vision periphérique. L'angle visuel entre les deux lampes vertes est de 48°. La limite de tolérance est déterminée par la perte de vision périphérique, c'est à dire la perte des deux lampes vertes. Cette méthode évite le risque de voile noir et de perte de connaissance.

2.3. SUJETS.

Six volontaires masculins du groupe des sujets d'expérimentation de Brooks ont participé à cette étude, après avoir subi avec succès les examens médicaux d'aptitude aéronautique classe II.

Leur âge variait entre 23 et 28 ans (m = 25 ans), leur taille entre 1,67 et 1,97 m (m = 1,82 m) et leur poids entre 60 et 97 kg (m = 81 kg).

2.4. PROTOCOLE.

L'expérimentation comporte deux séries de lancements de la centrifugeuse durant lesquels les sujets portent l'équipement complet et effectuent des manoeuvres anti-G.:

La première série consiste en 4 lancements dont les profils sont les suivants:

- 9 +G_z à 1 $G.s^{-1}$ sans surpression respiratoire.

- 9 +G_z à 1 $G.s^{-1}$ avec surpression respiratoire.

- 9 +G_z à 4 $G.s^{-1}$ sans surpression respiratoire.

- 9 +G_z à 4 $G.s^{-1}$ avec surpression respiratoire.

Pour chaque lancement, l'accélération de 9 +G_z est maintenue pendant un plateau de 10 s.

La deuxième série de lancements simule les accélérations produites lors du combat aérien. Il consiste en une répétition de plateaux de 10 s. à 5 et 9 +G_z avec une vitesse de mise en accélération de 4 $G.s^{-1}$. Il est effectué avec et sans surpression respiratoire.

Les critères d'arrêt sont la perte de la vision périphérique (secondairement celle de la vision centrale) la fatigue musculaire, les difficultés respiratoires, les anomalies électrocardiographiques ou une fréquence cardiaque supé-

2.4 PROTOCOL.

Two different sets of runs were performed during this experiment.

a) Subjects have to run a +9 G_z 10 s. plateau with different G-onset rates (1 $G.s^{-1}$ and 4 $G.^{-1}$) to check the efficiency of APPB on G_z tolerance.

We have the following profiles:

9 G_z at 1 $G.s^{-1}$ without APPB,

9 G_z at 1 $G.s^{-1}$ with APPB,

9 G_z at 4 $G.s^{-1}$ without APPB,

9 G_z at 4 $G.s^{-1}$ with APPB.

b) Subjects also ran the centrifuge with SACM profiles to recheck the effect of APPB on the G-time tolerance and to also check the efficiency of French equipment during these profiles. The SACM profile was a repetition of 5 and 9 G 10 s. plateau with a G onset rate of 4 $G.s^{-1}$. The G-tolerance is determined by the PLL and CLL. The subjects have to run the centrifuge until exhausted. The run could be stopped for other reasons like fatigue, difficulty in breathing, EKG anomalies, heart rate more than 200 $beats.min^{-1}$. Two rest days were observed during the two SACM profiles.

All subjects have to perform an anti-G straining manoeuvre with and without APPB. The equipement was worn in every case. The combination of the 6 runs was randomised for statistical purposes.

2.5 STATISTICAL ANALYSIS.

An analysis of variance was used to test for APPB effects, G onset rate effects, subject effects and interaction.

3 RESULTS.

Physical measurements have permitted to see proper functioning of the regulator anti-G valve ensemble. The pressure in the jacket is set with one second delay after the beginning of the G plateau.

3.1 EFFECT OF APPB WITH 1 AND 4 $G.S^{-1}$ ONSET RATES AT 9 G_z.

3.1.1 Visual field.

The central visual field is most of the time not influenced by the different experimental situations since most

rieure à 200 battements.min^{-1}. Les deux lancements (avec et sans surpression) sont séparés par une période de deux jours de repos.

L'ordre des six lancements est randomisé.

2.5. ANALYSE STATISTIQUE.

Les effets de la surpression, de la vitesse de mise en accélération, l'effet sujet et les interactions ont été testés par analyse de variance.

3. RESULTATS.

Les mesures de pression dans la veste et le pantalon anti-G mettent en évidence le bon fonctionnement de l'ensemble de l'équipement. La pression dans le veste est établie avec une seconde de retard par rapport au début du plateau d'accélération.

3.1. EFFET DE LA SURPRESSION RESPIRATOIRE A 9 +G_z LORS DE MISES EN ACCELERATION A 1 ET 4 G.S^{-1}.

3.1.1. Champ visuel.

La vision centrale, conservée dans la plupart des cas, n'est pas influencée par les différentes situations expérimentales.

La vision périphérique est diminuée systématiquement au cours de chacun des lancements (fig.n°2).

Sans surpression respiratoire, la réduction moyenne du champ visuel est de 28 % pour les profils à 1 G.s^{-1} et de 32 % pour les profils à 4 G.s^{-1}.

Avec surpression respiratoire, elle est de 15 % pour les profils à 1 G.s^{-1} et de 10 % pour les profils à 4 G.s^{-1}

La réduction moyennée du champ visuel est moins importante avec surpression que sans surpression mais l'analyse statistique ne met pas en évidence de différence significative.

3.1.2. Fréquence cardiaque.

Sans la surpression respiratoire, la fréquence cardiaque moyenne est de 165 c.min^{-1} à 1 G.s^{-1} et de 163 c.min^{-1} à 4 G.s^{-1} (fig. n°3).

Avec la surpression respiratoire, la fréquence

of the time, the subjects did not lose it.

The peripheral visual field is decreased during the different situations (fig.n°2). This decrease is less important when APPB is set. It is of 15 percent for the 1 G.s^{-1} onset and 10 per cent for the 4 G.s^{-1} onset when APPB is set. The subjects are less protected against G when APPB is not set. In this case, the values of PLL are 28 percent at 1 G.s^{-1} onset and 32 percent at 4 G.s^{-1}. These values are only a tendency but are not sustained by statistics since there is no statistical difference between the presence or absence of APPB. In this study, there exists no statistical difference of PLL between the G onset rates.

Figure n° 2

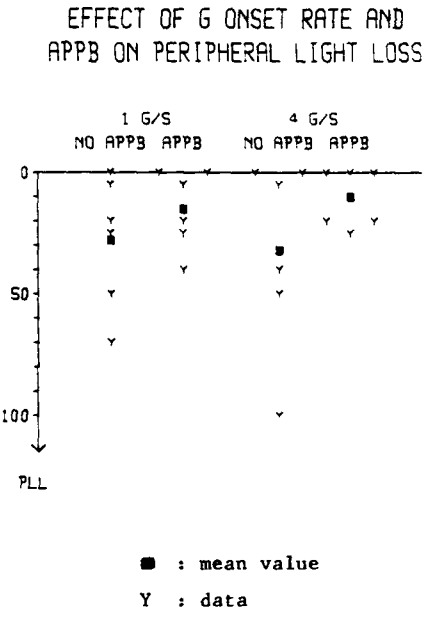

3.1.2 Heart rate.

Maximum heart rate does not seem influenced either by onset or by APPB. Differences are minimal, and there is only a tendancy for a higher heart rate with APPB (fig. n°3).

cardiaque est de 167 c.min^{-1} à 1 G.s^{-1} et de 166 c.min^{-1} à 4 G.s^{-1}.

L'analyse de variance montre que la fréquence cardiaque n'est pas influencée par la vitesse de mise en accélération ni par la surpression respiratoire.

3.2. EFFET DE LA SURPRESSION RESPIRATOIRE DURANT LES PROFILS DE COMBAT AERIENS.

3.2.1. Temps de tolérance aux accélérations.

Le temps de tolérance moyen est augmenté de 89 % par la surpression respiratoire. Avec la surpression respiratoire, le temps de tolérance est de 167.85 $\pm$ 38.40 s. Sans surpression, le temps de tolérance est de 88.42 $\pm$ 23.08 s. Cette différence est statistiquement significative ($F = 32.35$, $p > 0.001$).

3.2.2. Champ visuel.

A la fin du profil d'accélération, la perte de champ visuel périphérique est de 28.57 % avec la surpression et de 61.42 % sans surpression. Cette différence n'est pas statistiquement significative.

Pour résumer l'ensemble de ces données, la surpression respiratoire augmente de façon statistiquement significative le temps de tolérance aux accélérations appliquées selon un profil de combat aérien. Cette technique tend seulement à augmenter la tolérance lors des mises en accélérations rapides.

Enfin, notons que des fuites entre le bord du masque et le visage sont apparues pour un certain nombre de sujets, provoquant un inconfort oculaire. Des douleurs dans les bras accompagnées de pétéchies ont aussi été notées.

4. DISCUSSION.

L'absence d'effet de la surpression respiratoire sur la tolérance à des mises en accélération rapides et le bénéfice apporté par cette technique sur le temps de tolérance au profil d'accélération simulant le combat aérien amènent certains commentaires.

Ernsting (1966) avait démontré que la surpression respiratoire augmentait la pression artérielle systémique du fait de l'accroissement de la pression intrathoracique. Pour cette raison, nous nous attendions à ce qu'elle améliore la tolérance lors des mises en accélération à 1 et 4 G.s^{-1}. L'absence d'effet observé peut avoir plusieurs causes.

L'efficacité de la manoeuvre anti-G serait plus grande que celle de la surpression respiratoire et masquerait

Without APPB, heart rate is 165 B.min^{-1}. at 1 G.s^{-1} and 163 B.min^{-1} at 4 G.s^{-1}.

With APPB, the heart is somewhat higher: 167 B.min^{-1} at 1 G.s^{-1} and 166 B.min^{-1} at 4 G.s^{-1}. There exists no statistical difference between these values.

Figure n° 3

EFFECT OF G ONSET RATE AND APPB ON HEART RATE

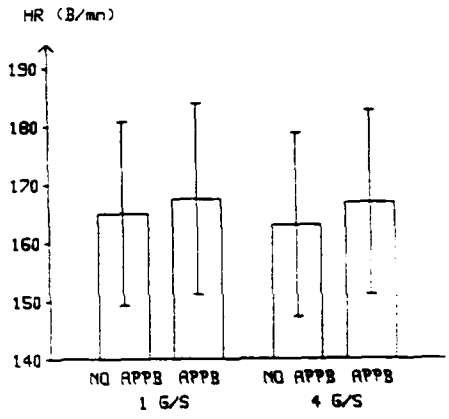

3.2 EFFECT OF APPB DURING SACM PROFILES.

3.2.1 G-tolerance time.

The G-tolerance is increased by APPB. With this G-countermeasure, G-tolerance time is 167.85 $\pm$ 38.40 s. Without APPB, G-tolerance time is 88.42 $\pm$ 23.08 s. The improvement is of 89 %. The difference is statisticaly proven ($F = 32.35$, $p > 0.001$).

3.2.2 Visual field.

PLL at the end of SACM profile is further decreased when the subject is not protected by APPB. without APPB, PLL is 61.42 % and with APPB, PLL is 28.57 %.

l'effet de celle-ci. En effet, de nombreux auteurs ont démontré que cette manoeuvre est très efficace et peut augmenter la tolérance aux accélérations de 4 G; en extrapolant, ceci correspond à une augmentation de la pression artérielle de 22 mmHg x 4 soit de 88 mmHg (11.7 kPa). Ceci est à rapprocher de mesures de pression intrathoracique lors d'une manoeuvre anti-G effectuées au Laboratoire de Médecine Aérospatiale qui ont montré que cette pression pouvait être augmentée de 12 kPa (90 mmHg) à 8 $+G_z$. Il s'agit donc d'une valeur supérieure à celle que délivre le dispositif de surpression respiratoire (9 kPa ou 68 mmHg). De plus, la manoeuvre anti-G est réalisée par le sujet juste avant la mise en accélération et le met en condition pour ce stress. Ceci est un argument en faveur de la prédominance de la manoeuvre sur la surpression respiratoire d'autant plus que celle ci est établie avec une seconde de retard.

Enfin, l'effet bénéfique escompté de la surpression respiratoire peut avoir été masqué du fait du faible nombre de sujets.

En revanche, nous avons pu montrer l'efficacité de la surpression respiratoire lors de profils de combat aérien. Une surpression de 9 kPa (68 mmHg) améliore de 89 % le temps de tolérance moyen observé sans surpression. Ce résultat est très comparable aux résultats de Burns et Balldin (1988) qui ont mis en évidence une amélioration du temps de tolérance de 108 % avec une surpression de 6.7 kPa (50 mmHg) et de 88 % avec une surpression de 9.3 kPa (70 mmHg). D'après ces auteurs, il y aurait un lien entre tolérance aux accélérations et fatigue musculaire. Cette fatigue, provoquée par les manoeuvres anti-G, serait diminuée par la surpression respiratoire d'où l'effet bénéfique sur le temps de tolérance. Par cet effet sur la fatigue, la respiration en pression positive favoriserait indirectement la tolérance à des mises en accélération très rapides et répétées. En conséquence, elle permettrait au pilote d'effectuer pendant un temps prolongé des manoeuvres anti-G efficace et le protègerait donc contre le risque de perte de connaissance (Harding and Bomar, 1990). Ceci expliquerait que, lors de lancements de brève durée où la fatigue n'a pas eu le temps de s'installer, l'effet bénéfique de la surpression n'apparaisse pas.

L'intérêt de la surpression respiratoire étant établi, l'optimisation de la loi doit prendre en compte des facteurs dits secondaires. Nous avons vu que le masque fuyait. Dans l'étude de Burns et Balldin (1988), la surpression semble plus efficace à 6.7 kPa (50mmHg) qu'à 9.3 kPa (70 mmHg). En revanche, une autre étude (Clère et coll. 1988) a mis en évidence une tolérance supérieure avec le niveau de surpression le plus élevé à savoir 9 kPa (68 kPa); mais le risque de fuite est alors potentiellement plus important. Ceci amènerait une certaine réticence des pilotes à adopter ce système dans les nouveaux avions. Pour cette raison, il pourrait être suggéré que la valeur de surpression maximale soit inférieure à 9 kPa (68 mmHg); le choix d'une valeur de 6.7 kPa semble être un bon compromis.

To summarize this data, APPB statistically increases the SACM G-tolerance time and tends to improve the G-tolerance, but statistically there is no difference.

At the end of this experiment, a part of the subjects noted that some leaks appeared between the lips of the mask and the skin of the face, causing eye discomfort. Some pains were observed in the arms with some petechia.

4 DISCUSSION.

The lack of effect of APPB on the VHOR tolerance and the benefit of APPB on G-tolerance time must be discussed.

Ernsting (1966) has demonstrated that PPB raises systemic arterial blood pressure. Indeed, the raise in intrathoracic pressure involves a raise in arterial pressure. For this reason, we expected a better G_z tolerance of subjects during ROR and VHOR profiles. Several resons would explain the lack of effect of APPB on the ROR and VHOR tolerance:

The effectivness of M1 manoeuvre is greater than the APPB and hides the effect of APPB. Several authors have demonstrated that this manoeuvre is very efficient and could increase the G level tolerance above 2 or 3 G and even 4 G, which is an increase of arterial pressure of 22 mmHg * 4 = 88 mmHg (11.7 kPa). Several measures done in the Aerospace Medical Laboratory (Clère et al., 1988) have shown that the intrathoracic pressure could be increased by 90 mmHg (12 kPa), greater than APPB which is at 68 mmHg (9 kPa). This level of pressure could hide the effect of APPB.

Lastly, the low number of subjects could explain these results. The profit of APPB for VHOR improvement is too low and statistically cannot be demonstrated.

The efficiency of APPB for G-tolerance time observed in this experiment must be compared with the work done by Burns and Balldin (1988). They demonstrated an improvement of G tolerance time of 108 % with PPB at 50 mmHg (6.7 kPa) and 88 % with PPB at 70 mmHg (9,3 kPa). It is extraordinary to observe similar results with our experiment which is 89 % for APPB at 9 kPa. This second observation confirms the advantages of APPB as a system to improve G tolerance time by reducing fatigue as it is explained in the work by Burns and Balldin (1988). APPB is indirectly useful for increasing VHOR tolerance. It protects pilots against G-Loss of Consiousness (Harding and Bomar, 1990). In effect, the most important protection against VHOR is induced by the M1 manoeuvre. This manoeuvre itself induces fatigue. If APPB reduces this fatigue, APPB protects against VHOR stress.

We must now discuss the schedule to be chosen for APPB. APPB at 70 mmHg (9.3 kPa) is perhaps to high for protecting pilots against G stress. In the experiment of Burns and Balldin (1988), the efficiency of APPB at 50 mmHg (6.7 kPa) seems better than at 70 mmHg (9.3 kPa). In the work of Clère et al. (1988), they observed the best G tolerance with the highest

5. CONCLUSION.

Dans le cadre de cette expérimentation, la surpression respiratoire à 9 kPa (68 mmHg) ne s'est pas avérée efficace dans la protection des pilotes lors de mises en accélération rapides et peu soutenues. En revanche, conformément aux données de la bibliographie, elle réduit la fatigue et accroît le temps de tolérance lors de profils simulant le combat aérien. Une surpression respiratoire de 6.7 kPa (50 mmHg) pourrait être un bon compromis entre efficacité et confort.

level of APPB. On the other hand, there is a potential risk of leaks with the highest level of APPB. The discomfort induced by these leaks could cause pilots to object to APPB in new aircraft. For this reason, it could be suggested that a schedule lower than 68 mmHg (9 kPa) be preserved.

5 CONCLUSION.

This experiment has not proven the direct effect of APPB 68 mmHg (9 kPa) for counteracting VHOR stress. On the other hand, APPB reduces fatigue and increases G tolerance time for SACM profile. This improvement is statistically true and already observed during the experiment of Burns and Balldin. However, APPB at 50 mmHg (6.7 kPa) could be a good compromise between efficiency and comfort.

6. REFERENCES.

J.W. Burns, U.I. Balldin. Assisted positive pressure breathing for augmentation of acceleration tolerance time. Aviat. Space Environ. Med., 1988; 59:225-33.

J.M. Clère, D. Lejeune, D. Tran-Cong-Chi, H. Marotte, J.L. Poirier. Effect of different schedules of assisted positive pressure breathing on G-level tolerance. SAFE proceedings, 1988:76-8.

J. Ernsting. Some effects of raised intrapulmonary pressure in man. AGARDograph, 1966, 106.

Harding R.M., Bomar J.B. Positive pressure breathing for acceleration protection and its role in prevention of inflight G-induced loss of consciousness. Aviat. Space Environ. Med. 1990, 61: 845-9.

Shubrooks S.J.,Jr. Positive pressure breathing as a protective technique during $+G_z$ acceleration. J. Appl. Physiol. 1973, 34: 460-466.

7. REMERCIEMENTS / ACKNOWLEDGEMENT.

Les auteurs souhaitent remercier le colonel Tedor et Monsieur Fournol qui ont organisé cette expérimentation et désirent également remercier les personnels de la division de la Crew technology et tout particulièrement Monsieur Wayne Isdhal qui a consacré toute son énergie pour faire en sorte que cette expérimentation se déroule de façon parfaite. Enfin, ils désirent remercier les sujets d'expérimentation qui nous ont consacré une partie de leur temps malgré leurs activités professionnelles.

The authors wish to thank Colonel Tedor and Mister Fournol which have managed this experiement. They also wish to thank the acceleration team of the Crew Technology division and particulary Mister Wayne Isdhal who has made important efforts in running this 10 day experiment. Lastly, they wish to thank the subjects which have run the centrifuge during a short period despite their professional activities.

THE OPTIMISATION OF A POSITIVE PRESSURE BREATHING SYSTEM FOR ENHANCED G PROTECTION

Sqn. Ldr. A.R.J. Prior
RAF Institute of Aviation Medicine
Farnborough, Hampshire. GU14 6SZ. UK.

SUMMARY

An electronic, computer controlled, system has been developed that allows full control of mask pressure and anti-G trouser inflation pressure in a pressure breathing anti-G system (PBG) installed on the RAF IAM human centrifuge. The apparatus has been used to investigate the effect of different mask and trouser inflation pressures upon G protection in four subjects exposed to +Gz acceleration in the range 3 to 7 G whilst wearing full coverage anti-G trousers and a chest counterpressure waistcoat. Eye level arterial blood pressure was used as an objective measurement of G protection whilst subjective assessment of peripheral vision, anti-G trouser inflation pressure, mask pressure and arm discomfort was measured using a ten centimetre line technique. The results show that eye level arterial blood pressure is better maintained as both mask and trouser inflation pressure are increased, however, peripheral vision was degraded to only 34% of normal under any of the experimental circumstances. Subjectively, the preferred schedule of inflation for the anti-G trousers was 1.3 psi/G with a cut-in of about 2Gz; for the PBG mask pressure it was 14 mmHg/G with a 3Gz cut-in point. Arm pain under G occurred in all subjects and its intensity may, from theoretical calculations, be linearly related to forearm venous pressure.

INTRODUCTION

In order to realise the hypertensive benefits of positive pressure breathing in its role of +Gz protection (PBG), it is essential to ensure that cardiac output is maintained despite the tendency towards peripheral venous pooling which is a consequence of raised intrathoracic pressure and +Gz acceleration. Counterpressure to the lower body is mandatory in order to provide support of the circulation and to avoid a catastrophic fall of heart level arterial blood pressure leading to loss of consciousness. If counterpressure is provided by a standard, five bladder, anti-G garment, PBG improves relaxed G tolerance by 0.4 - 0.8 G depending upon the mask pressure used (Glaister and Lisher, 1976; Prior, 1986). However, counterpressure provided by a full coverage anti-G garment, that covers 93% of the lower body from the level of the umbilicus to the feet, results in PBG improving relaxed G tolerance by 1.8 G (Prior, 1988). Under high G, inflation of an anti-G garment results in a headward translocation of blood, the displaced volume is greater with a full coverage garment than following inflation of a standard anti-G suit (Prior, 1989; Krutz et al, 1990). The effectiveness of PBG in enhancing G tolerance is thus dependant upon the efficiency of the lower body counterpressure garment in providing the necessary circulatory support under conditions of high +Gz acceleration and raised intrathoracic pressure.

Generally, the higher the inflation pressure within an anti-G suit the better the G protection (Wood and Lambert, 1945), although, in practice, aircrew discomfort limits the maximum pressure which may be tolerated. Raising the PBG mask pressure, for any given level of +Gz acceleration, also tends to increase G protection (Domaszuk, 1983; Burns and Balldin, 1988; Clere et al, 1988) but is limited by discomfort and the ability to seal the pressure within an oro-nasal mask.

PBG enhancement of G tolerance is, therefore, dependant upon the mask pressure, the anti-G trouser pressure and the lower body coverage of the trousers. As mask pressure increases, at any given +Gz acceleration, it would seem reasonable that the anti-G trouser pressure should also increase to counter the increased tendency to venous pooling. However, given that full coverage lower body counterpressure is more efficient in supporting the circulation during pressure breathing than the standard coverage garments, then it is possible that inflation pressures for the former garment may be reduced to levels less than the in-service pressurisation schedules, without any decrement in G protection.

The study reported here investigated the relationship between PBG mask pressure, anti-G trouser inflation pressure and +Gz acceleration when wearing full coverage anti-G trousers. G protection was assessed by the measurement of eye-level arterial blood pressure and by recording subjective opinion of protective worth and comfort.

ACCELERATION									
3.0G		4.0G		5.0G		6.0G		7.0G	
AGT.P (psi)	MASK.P (mmHg)	AGT.P (psi)	MASK.P (mmHg)	AGT.P (psi)	MASK.P (mmHg)	AGT.P (psi)	MASK.P (mmHg)	AGT.P (psi)	MASK.P (mmHg)
0.0	0	1.5	0	3.0	0	4.5	10	6.0	20
1.0	0	2.5	0	4.0	0	5.5	10	7.0	20
2.0	0	3.5	0	5.0	0	6.5	10	8.0	20
3.0	0	4.5	0	6.0	0	7.5	10	9.0	20
1.0	10	1.5	10	3.0	10	4.5	20	6.0	30
2.0	10	2.5	10	4.0	10	5.5	20	7.0	30
3.0	10	3.5	10	5.0	10	6.5	20	8.0	30
1.0	20	4.5	10	6.0	10	7.5	20	9.0	30
2.0	20	1.5	20	3.0	20	4.5	30	6.0	40
3.0	20	2.5	20	4.0	20	5.5	30	7.0	40
		3.5	20	5.0	20	6.5	30	8.0	40
		4.5	20	6.0	20	7.5	30	9.0	40
		1.5	30	3.0	30	4.5	40	6.0	50
		2.5	30	4.0	30	5.5	40	7.0	50
		3.5	30	5.0	30	6.5	40	8.0	50
		4.5	30	6.0	30	7.5	40	9.0	50
				3.0	40	4.5	50	6.0	60
				4.0	40	5.5	50	7.0	60
				5.0	40	6.5	50	8.0	60
				6.0	40	7.5	50	9.0	60

Table 1. Combinations of anti-G trouser inflation pressure (AGT.P) and PBG mask pressure (MASK.P) used at each +Gz acceleration.

METHODS

Four, highly experienced, centrifuge subjects each performed 106 runs in 16 sessions, at +Gz accelerations in the range 3.0 - 7.0 G, over a period of five days. During each run the PBG pressure schedule and anti-G trouser inflation schedule were set so that, at peak G, the mask pressure and trouser pressure achieved values according to Table 1. Thus, at each level of acceleration all combinations of mask and anti-G trouser pressure, within the given ranges, were tested. Those combinations that called for an increased mask pressure but no anti-G trouser inflation were not tested.

All subjects were dressed in flying coverall, Mk 14; full coverage anti-G trousers (FAGT); chest counter-pressure waistcoat (CCP); life preserver; flying boots; aircrew helmet, type 10 and oxygen mask, type P/Q.

Each centrifuge run was performed at 1 G/s onset and offset rates with 15 seconds duration at peak G. Subjects were strapped into a modified type II, Martin Baker, ejection seat with a 19°seat back angle and instructed to relax throughout the runs. If, according to the subjects' own judgement, the particular combination of mask pressure and trouser pressure seemed to be inadequate, then they were instructed to strain in order to avoid blackout, then report their actions. The subject's left arm was supported on an arm rest at heart level; the right hand held a centrally positioned aircraft control stick such that the hand was approximately 35 cm vertically below heart level. The right arm position was representative of the European Fighter Aircraft (EFA) cockpit configuration.

Control of PBG and anti-G trouser inflation

PBG mask pressure was supplied by a modified Mk 21 oxygen regulator. The aneroid unit, normally used to provide positive pressure breathing for altitude protection was removed and replaced by a solenoid which produces a force linearly proportional to the current flowing through its actuating coil. In order to minimise hysteresis, the solenoid was driven by a pulse width modulated (PWM) signal, via a power field effect transistor. This signal was generated and controlled by computer digital output lines.

Anti-G trouser inflation pressure was controlled by the anti-G valve portion of a combined breathing regulator / anti-G valve (BRAG valve, Normalair Garrett Ltd., Yeovil, UK.). The valve comprises an electronically controlled torque motor acting upon a pneumatic valve. It was configured to provide an outlet pressure proportional to an analogue voltage presented to the input of its electronic control unit (ECU). This controlling analogue voltage was generated by computer, via digital to analogue conversion and a suitable scaling amplifier, so that anti-G trouser inflation pressure was under software control. Figure 1 shows the general arrangement of the system. After analogue to digital conversion (ADC), the +Gz acceleration signal was suitably processed according to the desired PBG/ anti-G trouser pressure schedule to provide an input voltage for the BRAG valve. The BRAG valve outlet pressure was measured by a pressure transducer, the signal from which was used to generate the appropriate PWM signal for the generation of pressure breathing. In this way, no increased mask pressure could be produced without coincident inflation of the anti-G trousers; conversely a failure of the anti-G trousers would result in the immediate cessation of pressure breathing.

Measurements

Eye level arterial blood pressure was measured continuously using a Finapres digital artery pressure

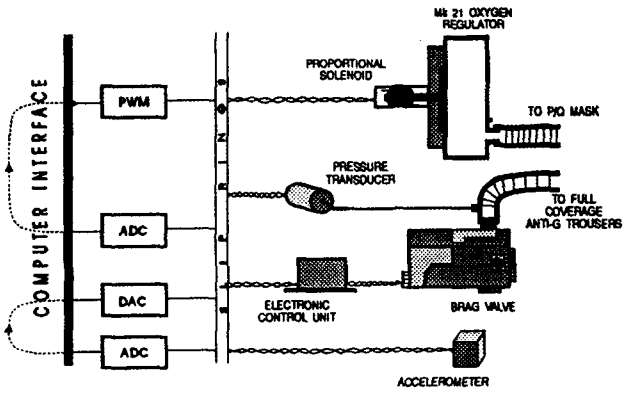

Figure 1. Schematic diagram of the apparatus used to control PBG and anti-G trouser inflation pressure.

monitor. The Finapres finger cuff was placed on the first finger of the left hand. The left hand and forearm were supported at heart level by resting the elbow on a padded support and hooking the thumb over a fixed supporting rod. In this way the fleshy part of the forearm was suspended and not prone to compression under G as would happen if a straightforward armrest had been used. A pressure transducer was mounted at the same level as the Finapres cuff and connected to a tube filled with water to the level of the eye. The upper end of the tube was fixed to the subjects P/Q oxygen mask in the mid-line so that any head movements on the subjects part would still result in the top of the water column being at eye level. The Finapresmonitor and pressure transducer outputs were subtracted from one another by an operational subtractor amplifier to give a signal representing eye level arterial blood pressure. This method also ensured that hydrostatic pressure changes, due to the -Gx acceleration component occurring during centrifuge acceleration onset and acting on the forearm positioned in the Gx axis, were cancelled in the subtraction of signals. The RS232, digital output of the Finapres monitor was also used. The information contained within the serial output was stripped to leave mean, beat-to-beat, arterial blood pressure; after digital to analogue conversion (DAC) this signal, together with the eye level arterial blood pressure waveform, was displayed on a Gould ES1000, electrostatic chart recorder (figure 2). The digital, mean arterial blood pressure data, together with a time index, was also stored on hard disc for subsequent calculation of eye level arterial blood pressure loss under G.

Subjective assessment of peripheral visual loss, mask pressure, anti-G trouser inflation pressure and right arm discomfort was made by the subject indicating his evaluation on 10 cm lines (Table 2). This was performed after the completion of each centrifuge run made with a particular combination of mask pressure, anti-G trouser pressure and +Gz acceleration. Mask cavity pressure and anti-G trouser pressure were recorded throughout the experimental period. Mean mask cavity pressure and mean anti-G trouser pressure at peak G were estimated from a chart recorder trace by eye and checked to ensure that the demanded pressures were achieved.

Centrifuge runs

At the start of each centrifuge session, the subject completed one run at 3.0 Gz, regarded as a 'warm-up' run, and one run at 4.0 Gz with an anti-G trouser pressure of 3.5 psi and mask pressure of 20 mmHg at peak G. The latter run served the purpose of checking the function of the PBG control equipment and also of checking the subjects' response to a standard centrifuge run using mask and trouser pressure schedules that were the same on each occasion. Any discrepant response, compared to runs performed on other occasions, could be detected readily. There followed a series of runs, which made up a session, selected at random from those shown in Table 1.

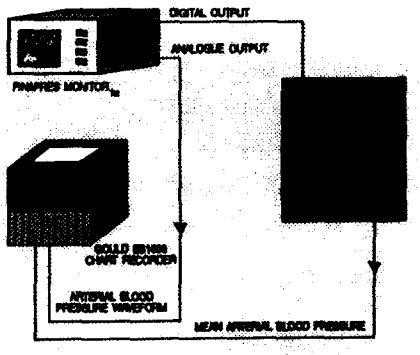

Figure 2. Using both the analogue and digital outputs of the Finapres monitor, both the arterial pressure waveform and mean, beat-to-beat, arterial blood pressure were recorded.

ASSESSMENT	EXTREMES OF THE 10 cm LINE	
G PROTECTION	BLACKED-OUT THROUGHOUT RUN	CLEAR VISION THROUGHOUT RUN
TROUSER PRESSURE	TOO LOW	TOO HIGH
MASK PRESSURE	TOO LOW	TOO HIGH
ARM DISCOMFORT	INTOLERABLE	PERFECTLY COMFORTABLE

Table 2. Terms used for subjective assessments.

RESULTS

Eye level arterial blood pressure

The arterial blood pressure at eye level was estimated both directly, by use of the Finapres monitor, and indirectly by recording the subjective assessment of loss of peripheral vision. The change in eye level arterial blood pressure under G follows a characteristic pattern of an initial fall followed, after approximately 5 seconds, by recovery to a plateau generally somewhat less than control values. In two subjects, at accelerations of 3 Gz and 4 Gz, whilst the anti-G trouser and mask pressures were at their highest settings, arterial blood pressure at eye level was observed to be in excess of resting, 1 Gz, values. In order to evaluate the protective worth of a given combination of full coverage anti-G trouser inflation pressure and PBG mask pressure, at each +Gz acceleration in the range 3 - 7 Gz, it was necessary to reduce the blood pressure data to a single value. Various parameters pertaining to the arterial blood pressure changes under G were considered, for example, the minimum blood pressure reached throughout the centrifuge run or the average fall in blood pressure over the 15 second run period, but were rejected as being insufficiently representative of the observed pressure changes. The method adopted is illustrated in figure 3. Firstly, the arterial blood pressure waveform was reduced to mean pressure. It was then assumed that if "perfect" G protection was provided there would be no change in eye level arterial blood pressure under increased +Gz acceleration. Anything less than perfect would result in a loss of blood pressure under G, the extent of which is represented by the area contained within the trace of the observed mean eye level arterial blood pressure, and the line of "perfect protection". Therefore, the unit of arterial blood pressure loss, by this definition, is that of pressure x time, or (mmHg.s).

In figure 4, the average eye level arterial blood pressure loss, as defined above, for the four subjects at each G level, is plotted for each anti-G trouser inflation

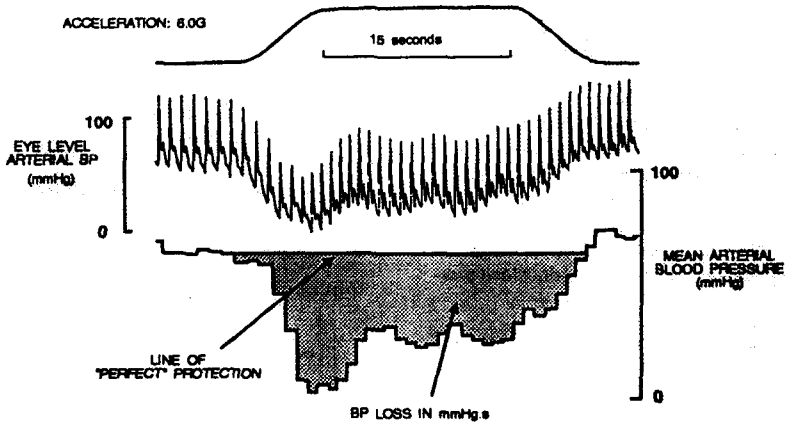

Figure 3. *Objective measurement of G protection. See text for explanation.*

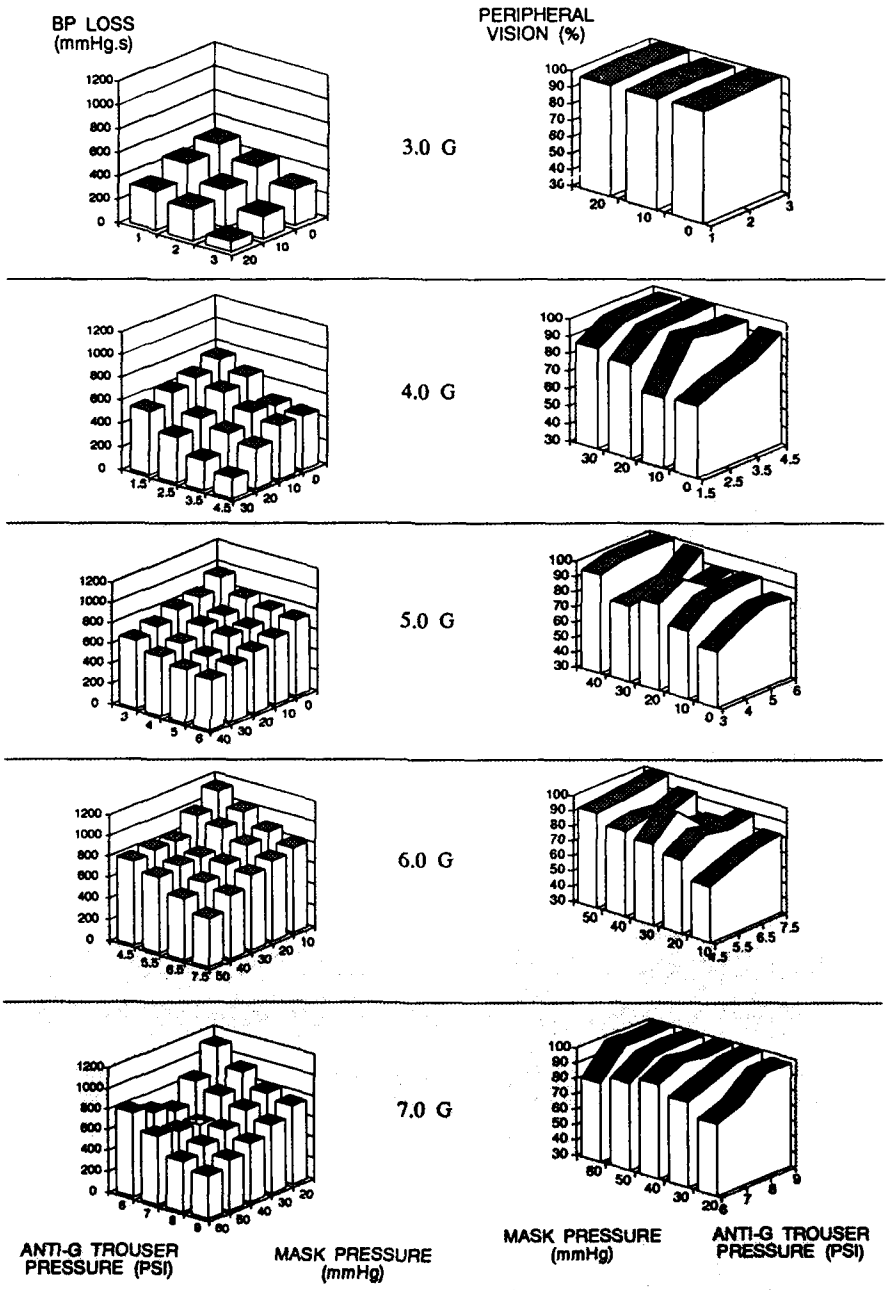

Figure 4. Eye level arterial blood pressure loss and subjective assessment of peripheral vision at each +Gz acceleration for each combination of anti-G trouser inflation pressure and PBG mask pressure.

pressure and mask pressure combination. The corresponding charts for the subjective assessment of peripheral vision under G are shown alongside. Generally, the higher the anti-G trouser inflation pressure and PBG mask pressure the smaller the loss in eye level arterial blood pressure. At 7.0 Gz, however, with low anti-G trouser inflation pressures of 6 and 7 psi, as the mask pressure increases from 20 to 40 mmHg, there is a fall in blood pressure loss but, as the mask pressure rises to 50 and 60 mmHg, this trend is reversed and the blood pressure loss increases again.

At all accelerations the loss in peripheral vision was small, no more than 34% under any condition. The average relaxed, unprotected, G tolerance, for a 70% loss of peripheral vision, for the four subjects, was 3.6 G (SD 0.16). At each acceleration, there is a general trend toward a better preservation of vision at the higher mask and trouser pressures.

Anti-G trouser inflation pressure

All subjects reported that they could readily assess anti-G trouser inflation pressure for any particular +Gz acceleration. They found no difficulty in reporting accurately the level of pressure above or below what they considered to be the ideal for the circumstances. All subjects were experienced in the use of standard anti-G trousers and were familiar with an inflation schedule of 1.25n - 1 psi, where n = the prevailing +Gz acceleration.

At each +Gz acceleration, there is no significant difference between the subjective appraisal of anti-G trouser inflation pressure at different PBG mask pressures. The mean subjective rating for each trouser inflation pressure at each +Gz acceleration is shown in figure 5 (a). Positive rating values indicate that the subject found the pressure too high, negative values indicate too low a pressure and zero rating represents the ideal.

PBG mask pressure

As with the anti-G trouser inflation pressure, subjects were able to make accurate assessments of the level of mask pressure, although it was slightly more difficult and less clear cut than in the case of trouser inflation pressure. All subjects commented that the anti-G trouser inflation pressure seemed to influence how they rated the level of mask pressure. In general, a higher mask pressure, for a particular +Gz acceleration, felt more comfortable if the trouser pressure was also tending towards the higher values. Those conditions that had a high trouser inflation pressure and a low mask pressure, or vice versa, generally felt uncomfortable and unbalanced. There are, however, no significant differences in the ratings of mask pressure for different anti-G trouser inflation pressures at each level of +Gz acceleration. The meaned, subjective assessments for each PBG mask pressure at each +Gz acceleration are given in figure 5(b).

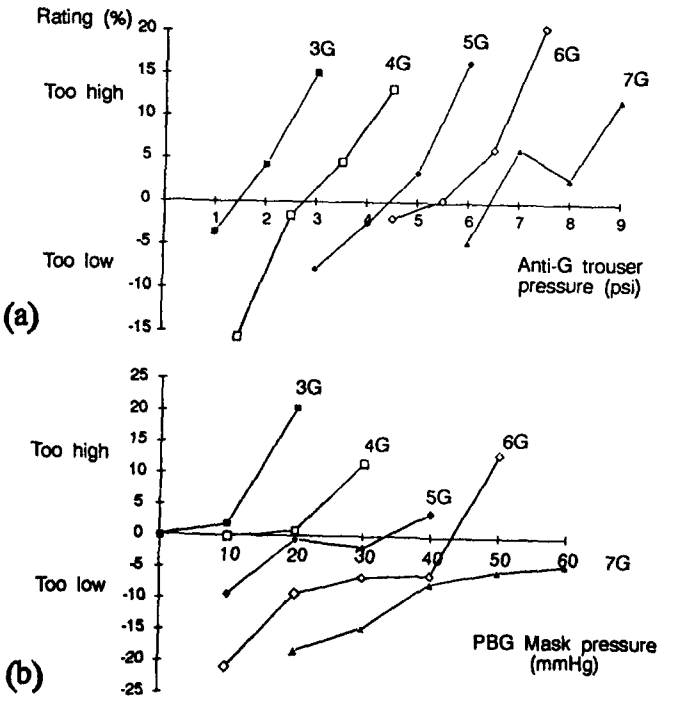

Figure 5. Mean subjective ratings for (a) the anti-G trouser inflation pressure and (b) the PBG mask pressure for each level of +Gz acceleration.

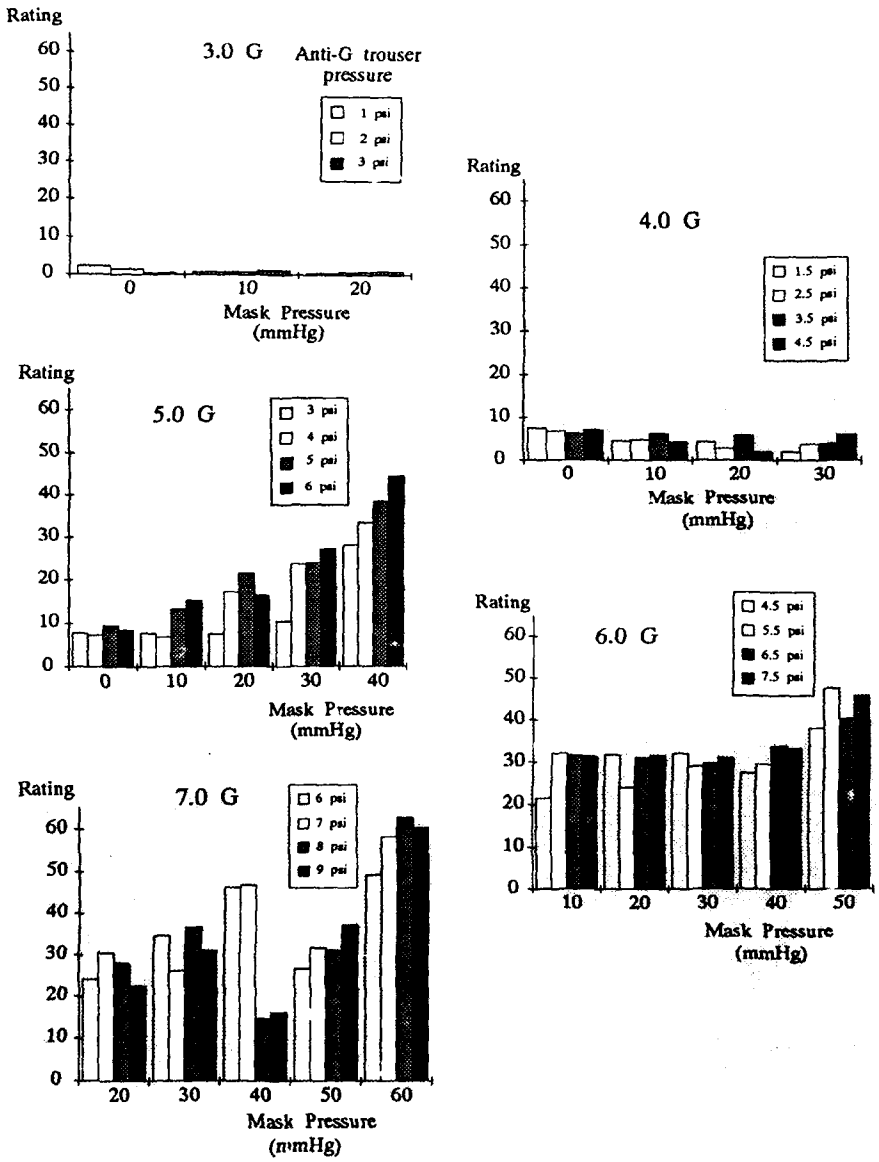

Figure 6. Subjective ratings of arm pain for each +Gz acceleration level, mask pressure and anti-G trouser inflation pressure.

Arm pain

Arm pain occurred in all subjects to a greater or lesser extent. It was described as a deep, somewhat nauseating ache, mainly in the forearm but sometimes localised around the elbow. One subject compared the pain to that which occurs when the inner aspect of the upper arm is compressed firmly. The subjective ratings of arm pain for each +Gz acceleration, mask pressure and anti-G trouser inflation pressure combination are shown in figure 6. By analysis of variance (Statgraphics, v4.0, Statistical Graphics Corp.) the results show that arm pain is made significantly worse ($P<0.05$) by increasing +Gz acceleration; it is unaffected by the anti-G trouser inflation pressure at a given level of +Gz acceleration, and the highest PBG mask pressures at 5G, 6G and 7G are associated with worsening arm pain.

Preferred pressure schedules

Lines of best fit were drawn through each of the curves of subjective ratings for mask and trouser inflation pressure at each +Gz acceleration, as shown in figure 5(a+b). The values of either anti-G trouser inflation pressure, or PBG mask pressure, which gives a zero rating (subjectively assessed ideal pressure) for each level of +Gz acceleration, are shown in figure 7 together with lines of best fit and the equations that describe them.

DISCUSSION

The anti-G system used in the experiment reported here, consisting of full coverage anti-G trousers and positive pressure breathing with chest counterpressure, is a highly effective means of enhancing G tolerance. The greatest loss in peripheral vision, under any acceleration in the range 3 - 7Gz and using any combination of mask and anti-G trouser inflation pressure, was 34% of the peripheral visual field whilst sitting, relaxed, in an "upright" seat. Objective measurement of the loss of eye level arterial blood pressure, however, (figure 4) shows that the loss falls progressively, at all accelerations investigated, as both mask pressure and anti-G trouser inflation pressure are increased. An exception is seen at 7Gz; with an anti-G trouser inflation pressure of 6 psi, as mask pressure increases from 20 mmHg to 40 mmHg, eye level arterial blood pressure loss is reduced but increases once more as the mask pressure rises to 60 mmHg. A raised intrathoracic pressure, consequent upon pressure breathing, and in conjunction with increased +Gz acceleration, causes a marked tendency to inhibit the return of venous blood from dependant areas. Ernsting (1966) estimated the immediate loss of effective blood volume, at 1Gz, whilst pressure breathing at 20 mmHg, to be approximately 150 ml, rising to 250 ml at 60 mmHg mask pressure. Counterpressure to the lower body will tend to reduce, or reverse, venous pooling depending upon the pressure within the counterpressure garment and the efficiency of pressure transmission to the underlying tissues. Maintenance of cardiac filling, and therefore arterial blood pressure, is thus a balance between raised intrathoracic pressure tending to reduce the effective circulating blood volume and the efficacy of lower body counterpressure in increasing effective blood volume. The result of these effects provides an explanation for the observed changes in eye level arterial blood pressure loss seen at 7Gz when anti-G trouser inflation pressure is only 6 psi. As the trouser pressure increases through 7 psi to 8 psi, the degree of lower body counterpressure once again becomes adequate and supports the circulation in the face of high intrathoracic pressure and high +Gz acceleration.

The results shown in figure 4 indicate that eye level arterial blood pressure is better maintained with high mask and trouser pressures, but the high pressures do not necessarily result in better peripheral vision. Lambert and Wood (1946) found that, providing retinal arterial perfusion pressure is adequate, with a systolic pressure of about 50 mmHg, then vision is not impaired

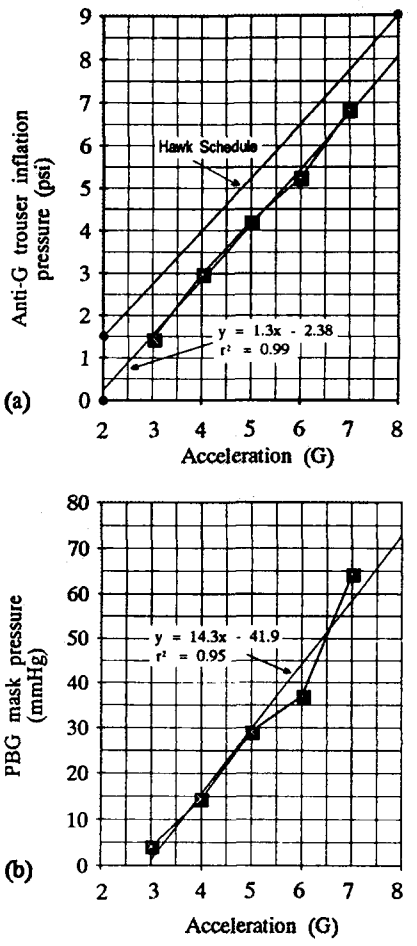

Figure 7. Preferred pressure schedules for (a) anti-G trouser inflation and (b) PBG mask pressure derived from the results of subjective assessment.

so that, providing systolic pressure does not fall below this value, arterial blood pressure may change without any degradation of vision. The pilot in air combat is concerned only with having unimpaired vision, not on the level of his arterial blood pressure, therefore, effects other than raising blood pressure must be taken into consideration if optimal conditions are to be found.

The subjective assessment of mask and anti-G trouser inflation pressure take into account the overall degree of protection afforded by the combination of pressures, the level of comfort and the general 'feel' of the system. Figure 5(a) shows that the rating of anti-G trouser inflation pressure changes quite abruptly from a pressure that feels inadequate to one that is perceived as too high. On the whole, the majority of the pressures that were used were regarded as excessive. The range of

different pressures that were used originated from consideration of the pressure schedule used in RAF Hawk aircraft. Pressures were chosen above and below this schedule. It appears that the use of full coverage trousers, with PBG, requires that the schedule of pressurisation be less than that used with standard, in-service anti-G trousers. The preferred anti-G trouser inflation pressure for each acceleration, derived from applying lines of best fit to the curves of figure 5(a), are shown in figure 7(a); the Hawk anti-G valve outlet pressure schedule is also shown for comparison.

The results of subjective assessment of PBG mask pressure (figure 5(b)), show that mask pressure can change substantially with little change being perceived by the subject. This is particularly pronounced at 7G, where mask pressure rises from 20 mmHg to 60 mmHg with only little change in the rating. The rating remains negative, indicating that the mask pressure is regarded as too low, for all mask pressures. This apparent indifference to mask pressure level is in keeping with the results of several other studies of PBG, performed both on the centrifuge and in the air, where widely different mask pressures, for a particular +Gz acceleration, have been employed and all have been found to be acceptable from a subjective point of view (Glaister and Lisher, 1976; Bagshaw, 1984; Harding and Cresswell, 1987; George and Jollett, 1987; Prior and Cresswell, 1989). Figure 7(b) indicates that, under these experimental conditions, PBG is probably unnecessary, from a protective point of view, until at least 4Gz is reached because the full coverage anti-G trousers provide a relaxed G tolerance

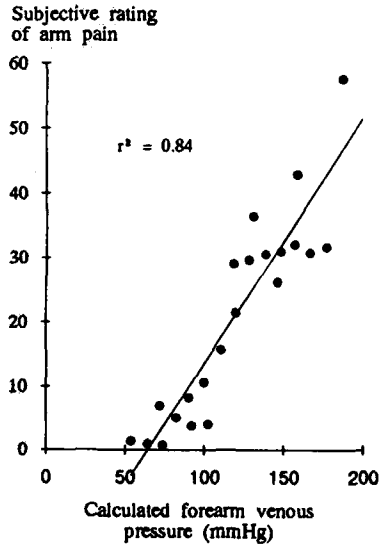

Figure 8. A subjective assessment of the severity of arm pain correlates with the calculated pressure within the forearm veins.

of about 6.0 G, using a Hawk anti-G valve to inflate the trousers (Prior, 1988). However, at 4.5 to 5.0 G the results suggest that some 25 to 30 mmHg mask pressure is required. An abrupt delivery of this pressure, as an acceleration threshold is exceeded, should be avoided for it is has been shown to be particularly distracting to aircrew and has the effect of interrupting speech in mid flow (Bagshaw, 1984). Therefore, a ramp onset of mask pressure is necessary and could reasonably be an extrapolation of the PBG pressure schedule to the baseline. In figure 7(b), a line of best fit, linear regression, is shown which indicates that PBG cut-in should occur at approximately 3G and have a subsequent slope of 14 mmHg/G. Subjects were not exposed to accelerations of 8 and 9 Gz so no data are available to indicate preferred mask pressures at these G levels but if extrapolated, the regression line of figure 7(b) would suggest that 86.8 mmHg pressure should be present in the mask at 9 Gz. This level of mask pressure is likely to be impractical on account of the difficulties in achieving an adequate mask seal on the face, especially with a system of automatic mask tensioning. On these grounds, an upper limit of 70 mmHg mask pressure is realistic but it may be necessary to substantially lower mask pressure in order to minimise the severity of arm pain.

Arm pain is a feature of pulling high G both in the air and in the centrifuge. With the arms positioned below the heart, at the level of the 'stick' and throttle controls, the pain is most pronounced at accelerations of 6 Gz and above. Raising the arms to the level of the heart markedly reduces the pain. In the Hawk aircraft, it is not uncommon for the rear seat occupant, frequently the flying instructor, to alleviate his discomfort by resting his hands on the instrument panel coaming, whilst the student is performing high G turns, to a 7G maximum in the Hawk (personal communication, RAF Brawdy, 1990). The addition of PBG to the anti-G system appears to both worsen the arm pain and to promote its occurrence at lower +Gz accelerations. Although not reflected in the subjective assessment statistical analysis, it did seem that once arm pain had occurred during a centrifuge run, subsequent exposure to conditions that were hitherto pain free, then caused pain. That the pain is of vascular origin is implied by the observation that the inflation of a arterial occlusion cuff around the upper arm reduces or abolishes the pain (Wood, 1944). If the forearm is approximately 25 cm below heart level then the hydrostatic pressure within the forearm vasculature is 18 mmHg/G. The addition of pressure breathing, with chest counterpressure, will tend to raise forearm venous pressure by an amount almost equal to the mask pressure (Ernsting, 1966) so that the forearm venous pressure, at any given +Gz acceleration, is equal to the sum of the hydrostatic pressure and the PBG mask pressure. Based upon this theoretical calculation, figure 8 shows that the subjective rating of arm pain can be related to forearm venous pressure by a simple linear model. The measurement of forearm venous pressure during increased +Gz acceleration whilst pressure breathing is required in order to check the validity of this model.

The performance of modern combat aircraft, and the physiological limitations of the pilot in tolerating high, sustained G of very rapid onset, has led to the investigation of improved anti-G systems. Given the potentially catastrophic nature of G-LOC in flight, it is natural to strive for the development of a system that provides the best possible G protection. However, this is not necessarily required by aircrew if operation of the system results in compromising their operational effectiveness, whether due to discomfort, impairment of mobility in the cockpit or on the ground, or prolonged time to dress in the protective clothing. Wood (1987) reports his experiences of anti-G suit development during the Second World War when highly efficient anti-G systems were rejected by aircrew, principally on the grounds of discomfort, distraction and inconvenience. At that time he concluded that discomfort caused by an anti-G system must be minimised to the lowest possible degree compatible with the protection required for the accelerations produced by air combat manoeuvring. A compromise between the G protection afforded by an anti-G system and the needs of the pilot in the role of air combat may be necessary now, as it was 50 years ago.

CONCLUSIONS

1. Within the +Gz acceleration range of 3 - 7 G, at 1 G/s onset rate using a human centrifuge, and wearing full coverage anti-G trousers and a chest counterpressure waistcoat, the G protection afforded by a PBG system increases as both mask pressure and anti-G trouser inflation pressure increase. However, at 7 Gz, with only 6 psi trouser inflation pressure, raising the mask pressure from 40 mmHg to 60 mmHg results in a reduction in the level of G protection.

2. Subjective assessment of anti-G trouser inflation pressure and PBG mask pressure shows a preferred schedule of 1.3 psi/G with a cut-in at about 2 G for the former and 14 mmHg/G starting at 3 G for the latter.

3. With the right hand on a control 'stick' in a position representative of that in the European Fighter Aircraft, arm pain was experienced by all subjects. The severity of the pain increased with increasing G levels and mask pressure. Theoretical calculations show that the pain might be linearly related to forearm venous pressure.

4. A compromise between the G protection afforded by an anti-G system and the degree of discomfort that it causes will be necessary for aircrew acceptance of the system.

REFERENCES

Bagshaw, M. A flight trial of positive pressure breathing during acceleration using RAF Hawk aircraft at a tactical weapons unit. RAF IAM Report No 637, 1984.

Burns, J.W. and Balldin, U.I. Assisted positive pressure breathing for augmentation of acceleration tolerance time. Aviat. Space Environ. Med. 59: 225-233, 1988.

Clere, J.M., Lejeune, D., Tran-cong-chi, D., Marotte, H. and Poirier, J.L. Effect of different schedules of assisted positive pressure breathing on G-level tolerance. In: Proceedings of SAFE Symposium, Las Vegas, NV, 1988.

Domaszuk, J. The application of positive pressure breathing for improving +Gz acceleration tolerance. Aviat. Space Environ. Med. 48: 91-96, 1983.

George, E.J. and Jollett, L.D. Limited evaluation of three prototype positive pressure breathing anti-G systems in the F16. Edwards AFB, Ca. AFFTC Technical Report 87-07, May 1987.

Glaister, D.H. and Lisher, B.J. Pressure breathing as a means of enhancing tolerance to sustained positive acceleration. ASCC WP61. Report of 17th meeting, Vol 2, pp 138-144, 1976.

Harding, R.M. and Cresswell, G.J. Royal Air Force flight trials of positive pressure breathing. In: High G and high G protection - aeromedical and operational aspects. Proceedings of the Royal Aeronautical Society symposium, 1987.

Krutz, R.W., Burton, R.R. and Forster, E.M. Physiologic correlates of protection afforded by anti-G suits. Aviat. Space Environ. Med. 61: 106-111, 1990.

Lambert, E.H. and Wood, E.H. Direct determination of man's blood pressure on the human centrifuge during positive acceleration. Fed. Proc. 5: 59, 1946.

Prior, A.R.J. Centrifuge assessment of the +Gz acceleration protection afforded by full coverage anti-G trousers. RAF IAM Aircrew Equipment Report No. 572. 1988.

Prior, A.R.J., Bass, J.A. and Tervit, J. Positive pressure breathing and chest counterpressure for enhanced +Gz tolerance using NGL anti-G module and regulator, 1654E000. RAF IAM Aircrew Equipment Report No. 537. 1986.

Prior, A.R.J. Physiological aspects of an enhanced G protection system. Eleventh Annual Meeting IUPS Commission on Gravitational Physiology, Lyon, France. p37, 1989.

Prior, A.R.J. and Cresswell, G.J. Flight trial of an enhanced G protection System in Hawk XX327. RAF IAM Report No 678, 1989.

Wood, E.H. and Lambert, E.H. Some factors which influence the protection afforded by pneumatic anti-G suits. J. Aviat. Med. 23: 218-228, 1952.

Wood, E.H. Development of anti-G suits and their limitations. Aviat. Space Environ. Med. 58: 699-706, 1987.

Wood, E.H., Lambert, E.H., Code, C.F. and Baldes, E.J. Factors involved in the protection afforded by pneumatic anti-blackout suits. Committee on Aviation Medicine, Office of Scientific Research and Development, Report No 351, 1944.

Effects on G_z Endurance / Tolerance of Reduced Pressure Schedules Using the Advanced Technology Anti-G Suit (ATAGS)

L.J. Meeker
Armstrong Laboratory
Crew Technology Division

Brooks AFB, Texas, USA 78235-5000

SUMMARY

The Armstrong Laboratory has recently developed an advanced lower body full coverage anti-G suit designated the Advanced Technology Anti-G Suit (ATAGS). Previous centrifuge studies using standard pressurization schedules, flight tests, and theoretical considerations suggest that the ATAGS might provide equivalent G protection using reduced pressures. This study was conducted to determine the G protection afforded by ATAGS using a lower pressure schedule.

Six test subjects were exposed to three separate G profiles on the Armstrong Laboratory Centrifuge, Brooks AFB, TX during each of three test sessions. The profiles were: a gradual onset with the subject relaxed, a rapid onset to 9 G for 10 seconds with the subject performing an anti-G straining maneuver (AGSM) and a rapid onset 5 to 9 G Simulated Aerial Combat Maneuver (SACM) with 10 sec at each level, repeated to exhaustion. A different anti-G suit pressurization schedule was used at each test session. Pressurization schedules began at 2 G but increased at different rates which resulted in maximum pressures of 10, 8, and 6 psig that occurred at 9 G (Fig 1).

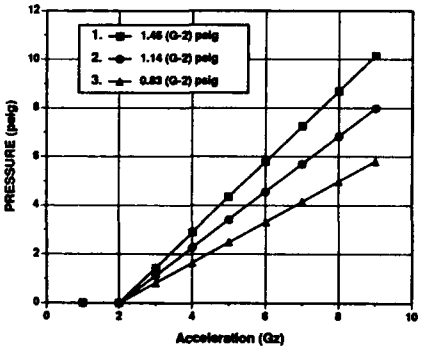

Figure 1. ATAGS inflation schedules used in this study. Schedule 1. is similar to the standard inflation schedule used in current USAF aircraft.

Data were analyzed by making statistical comparisons of performance between different pressure profiles, both for tolerance and endurance. Results suggest that the ATAGS pressurization schedule can be reduced from the present standard of 10 psig to 8 psig at 9 G without reducing G protection, but that a pressure schedule resulting in 6 psig at 9 G is insufficient.

INTRODUCTION

The anti-G suits used operationally in most countries today do not differ significantly from those used during the latter days of WWII. The majority of these anti-G suits have five pneumatic bladders which cover a portion of each calf, each thigh and one bladder which covers a portion of the abdomen. These bladders are inflated by an anti-G valve; a pressurization schedule starts at between 1.5 and 2 G and increases at a rate of between 1.25 and 1.5 psig/G. The idea that G tolerance might be improved by a more uniform pressurization of the lower body, is certainly not a new concept. In a paper published in 1953, Sieker et al. described the G protection provided by two different approaches to an extended coverage anti-G suit and compared it with the G protection provided by the standard G suit of that time. It was reported that these suits increased G tolerance by 0.7 to 0.9 G above the standard suit (7). A number of different concepts and designs have been tried but for one reason or another have been abandoned before the suit was transitioned to the operational community. One such approach was the capstan anti-G suit which used a standard abdominal bladder but each leg was covered by a layer of fabric connected to an "expandable tube" or capstan extending down each side by a series of interdigitized tapes. Since the ratio of the leg diameter to the capstan diameter was 5 to 1, these tubes required up to 50 psig to apply the same interface pressure around the leg as the standard suit (3,8). Although this design indicated a definite improvement in G tolerance (6) the difficulty of fitting and the complexity of design as well as the necessity of having an anti-G valve which could provide two different pressure schedules (one for the capstan and one for the abdominal bladder) made this suit rather impractical. Interestingly, R. W. Thompson showed that the actual interface pressure applied to the skin by the capstan anti-G suit was actually less than the pressure applied by the bladders of the standard anti-G suit (Unpublished). This fact reinforced the idea that lower pressures in a full coverage anti-G suit might provide equivalent G protection. Another approach at our laboratory was the Lower Body Full Coverage anti-G suit. This was essentially a large single bladder which covered the entire lower portion of the body. Despite G tolerance enhancement this design was extremely uncomfortable and because of the large volume was slow to respond to G changes(2,8).

Recently the need for increased G protection has caused renewed interest in several laboratories in perfecting a uniform pressure or extended coverage anti-G suit. At the Royal Air Force Institute of Aviation Medicine (RAF/IAM) in Great Britain, work is continuing on their extended coverage suit, the Full Coverage Anti-G trousers (FAGT) (5). The Royal Swedish Air Force has been conducting tests with their Extended Cover Anti-G Trousers (ECGT) at the Armstrong Laboratory Centrifuge, Brooks AFB, TX. Early data from these centrifuge tests and flight tests of the ECGT in Sweden have indicated that equal G protection might be afforded by an extended coverage anti-G suit at lower than the current standard pressure schedule.

The ATAGS system provides bladder coverage of nearly all of the lower body including the feet. The area behind the buttocks is not covered by bladders and a separate interconnected abdominal bladder is used (Fig 2,3). The ATAGS has provided dramatic improvements in G protection, both in centrifuge testing (3) and in flight evaluation (9). All of the previous ATAGS testing has been done, however, using the standard anti-G valve inflation schedule (approximately 1.5 psig per G starting at 2 G to a maximum pressure of about 10.5 psig). Because a lower pressurization schedule might provide increased pilot comfort or reduce fatigue, we conducted the following study to test the effectiveness of the ATAGS with decreased inflation schedules.

Figure 2. The ATAGS with the left boot removed to display the full bladder coverage of the foot.

METHOD

All tests were performed on the Armstrong Laboratory Centrifuge at Brooks AFB. Tests were conducted with an ACES II ejection seat mounted in the F16 position with a 30 deg back angle. A NATO standard light bar was used to asses test subject visual light loss. Blood pressure was measured during runs with an Ohmeda Finapres[1]. This measurement was compensated for eye-level pressure using a method developed by McKenzie at the RAF/IAM (personal communication). This method consists of attaching one end of a water filled tube at the subject's eye-level. The other end of the tube is connected to a pressure transducer mounted as near as possible to the Finapres cuff. The pressure measured from this water column is then subtracted from the Finapres reading to correct the measurement to eye-level. A Finapres Model 2350 was used during early tests but was substituted with a Model 2300 during later runs. A digital electronic anti-G valve built by Carleton Technologies Inc[2] was used for all tests. Pressure vs G schedules were varied in this valve by substituting appropriate PROM chips supplied by Carleton. The anti-G valve is equipped with a "ready pressure" feature which applies a pressure of 0.2 psig to the suit at 1 G filling the "dead volume" of the suit. As soon as the valve is actuated by G, pressurization of the anti-G suit is immediate. All runs were accomplished with the ready pressure activated to minimize the effects of variations in fitting the suit for different subjects. All subjects wore the ATAGS, with long underwear and standard flight boots during the test runs. No flight helmet or breathing mask was worn during these tests. Six male test subjects were recruited from the Armstrong Laboratory Acceleration Panel to participate in this study. The voluntary, fully informed consent of the subjects used in this research was obtained as required by AFR 169-3. Subjects had varying degrees of experience as centrifuge riders and some had worn the ATAGS on previous studies. Each subject was exposed to three test sessions. Each test session consisted of three separate G profiles; the subject was allowed a rest period (1 to 5 min) between each profile.

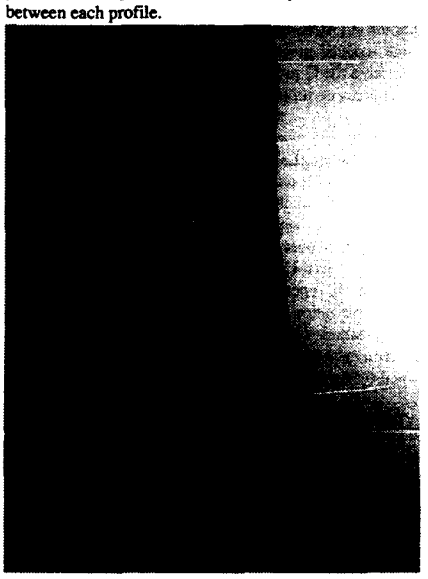

Figure 3. The ATAGS bladders with covering removed.

Any profile was terminated by the subject upon reaching either 100% peripheral or 50% central light loss using a NATO standard light bar. The first profile was a gradual onset (0.1 G / sec) to light loss with the subject relaxed. The second profile was a rapid onset (6 G / sec) to 9 G with 10 sec at the 9 G level with the subject performing an AGSM. The third profile was a high onset 5 G to 9 G Simulated Air Combat Maneuver (SACM) with 10 sec at each level; the subject performed an AGSM until reaching light loss limits or exhaustion, whichever came first. Each test subject was randomly assigned a different anti-G suit pressure schedule for each test session and did not know which schedule he was riding at that particular session. Three schedules were used. Each schedule began to pressurize the anti-G suit at 2 G and increased at rates of; (1.45), (1.14), and (0.83) psig/G, which resulted in pressures of, 10, 8, and 6 psig respectively at 9 G (Fig. 1).

At the conclusion of each session subjects were asked for comments regarding the ATAGS performance, (i.e. comfort and support of the suit as compared to previous

1. Ohmeda
1315 West Century Drive
Louisville, OH 80027 9560 USA

2. Carleton Technologies Inc
10 Cobham Drive
Orchard Park, NY 14127 4195 USA

sessions). Data taken and recorded during the study were: G level, ATAGS pressure, blood pressure, water column pressure, blood pressure corrected to eye-level (blood pressure - water column pressure), EKG, and heart rate. To compare the effects of the three pressure schedules on G endurance total run time was recorded for each SACM profile. To compare pressure schedule effects on G tolerance, G level at light loss and eye-level mean arterial blood pressure [diastolic + 1/3 (systolic - diastolic)] were determined for each gradual onset profile. Since all subjects completed the second profile (rapid onset to 9 G for 10 sec.) and since the Finapres was unreliable on this run, no data were analyzed from Profile 2. In each case, subject's performance at the presently operational pressure schedule (1.45 psig/G) was statistically compared against their performance at each of the reduced pressure schedules with either a student's one-tailed paired t-test or a one-tailed Wilcoxan Signed Rank Test. The choice of tests was based on the outcome of a previous test for normalcy. The significance criterion was alpha = 0.05. One-sided tests were chosen because the primary goal was to determine whether a reduced pressure schedule was detrimental to G tolerance or G endurance.

RESULTS

Total SACM run time is shown in Table 1 for each subject and for each pressure schedule. The last 2 columns show the changes under the 1.14 and 0.83 psig/G schedules compared to the standard 1.45 psig/G schedule. A negative number indicates a decrease in endurance time. Under 1.14 psig/G, 2 subjects showed substantial decreases in endurance time, 2 showed increases, and 2 had essentially no change (i.e., less than 10 sec). At 0.83 psig/G, 2 subjects decreased, 1 increased, and 3 had less than 10 second changes. In no case was the average change statistically significant.

Subject	Schedule 1 (1.45 psig/G)	Schedule 2 (1.14 psig/G)	Schedule 3 (0.83 psig/G)	Change vs 1.45 psig/G: Schedule 2	Change vs 1.45 psig/G: Schedule 3
1	233	189	121	-44	-112
2	122	119	113	-3	-9
3	164	150	142	-14	-22
4	180	187	188	-3	-1
5	145	231	238	+86	+93
6	187	198	183	+21	-4
Average	170	177	161	+7	-9

Table 1. SACM endurance time in seconds for each subject at each ATAGS inflation schedule. Differences between inflation schedule 1 and schedules 2 and 3 are also displayed.

Table 2 displays the gradual onset G tolerance for each subject under each pressure schedule. The last 2 columns show the changes in G tolerance at the lower pressure schedules compared to the standard schedule. Three subjects showed substantial decreases in G tolerance under the 1.14 psig/G schedule, but 2 had increases exceeding .5 G, and 1 showed no change. The average change was not statistically significant. At the 0.83 psig/G schedule, 4 subjects had decreases ranging from .8 to 1.6 G, and 2 subjects had slight increases (.2 G). The average change was significant ($p = .032$, one tailed), indicating that G tolerance was negatively affected by reducing the pressure schedule to 0.83 psig/G.

Subject	Schedule 1 (1.45 psig/G)	Schedule 2 (1.14 psig/G)	Schedule 3 (0.83 psig/G)	Change vs 1.45 psig/G: Schedule 2	Change vs 1.45 psig/G: Schedule 3
1	7.5	6.8	6.2	-0.7	-1.3
2	5.6	6.2	5.8	+0.6	+0.2
3	7.8	7.8	7.0	0	-0.8
4	7.9	6.3	6.3	-1.6	-1.6
5	6.2	6.9	6.4	+0.7	+0.2
6	8.6	7.3	7.4	-1.3	-1.2
Average	7.3	6.9	6.5	-0.4	-0.8*

*Change is significant (P=.032)

Table 2. The highest G_z attained by each subject on the gradual onset run is shown for each inflation schedule. Differences between schedule 1 and schedules 2 and 3 are also displayed.

Eye-level mean arterial blood pressure from the gradual onset profiles was plotted against G level for each pressure schedule in Figure 4. These lines represent the averages of the 6 subjects. The figure suggests that, under the 0.83 psig/G schedule, blood pressure drops more rapidly, and to a larger extent, than under the 1.14 and 1.45 psig/G schedules. However, upon inspection of individual data, inconsistent patterns were found. The apparent trend shown in the figure was caused chiefly by one subject who had a large drop in pressure at 0.83 psig/G compared to his other runs. Table 3 shows each subject's blood pressure at 5.5 G into the run, for each pressure schedule. The 5.5 G point was chosen because this was the highest point where data existed for each subject. In agreement with the figure, there is no difference between the 1.45 and 1.14 psig schedules, with 2 subjects showing decreases, 3 showing increases, and 1 showing very little change. The results for 0.83 psig/G, however, do not agree with the pattern suggested by the figure. Three subjects show some decrease in blood pressure, one shows essentially no change, and 2 actually show increases. Note the very large decrease by subject 4, thus, magnifying the average change (and the trend in the figure). Neither of the average changes in Table 3 was statistically significant.

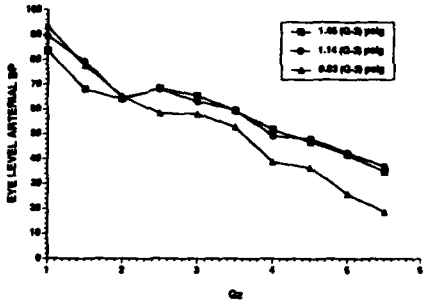

Figure 4. Average mean arterial blood pressure at eye level vs G_z level for each of the ATAGS inflation schedules tested.

Subject	Schedule 1 (1.45 psig/G)	Schedule 2 (1.14 psig/G)	Schedule 3 (0.83 psig/G)	Change vs 1.45 psig/G: Schedule 2	Change vs 1.45 psig/G: Schedule 3
1	30	50	32	+20	+2
2	35	50	35	+15	0
3	34	34	56	0	22
4	69	47	-54	-22	-123
5	36	36	53	-19	+13
6	1	21	-9	+20	-10
Average	35	37	19	+2	-16

Table 3. The eye-level mean arterial blood pressure for each subject on the gradual onset run at 5.5 G_z is shown for each inflation schedule. Differences between schedule 1 and schedules 2 and 3 are also displayed.

DISCUSSION

The performance of subject 5, as shown on Table 1, is an interesting case. Notice that the longest SACM time (238 sec) was attained by this subject at the lowest pressure. His performance with the schedule 2 pressure was almost identical (231 sec), but at the highest pressure he sustained the SACM for only 145 sec. While this performance was in line with the endurance times attained by most of the other subjects at this pressure, it was substantially lower than his other exposures. When questioned about his performance on this exposure the subject said that the abdominal bladder seemed too tight at the 9 G level and was somewhat painful. He further stated that this discomfort adversely effected his timing and AGSM and contributed greatly to his early fatigue on this ride. Interestingly, if the data from this subject is dropped from the calculations the difference in average SACM time from Schedule 3 to Schedule 1 is statistically significant ($p = .031$).

Interestingly a recent study (not yet published) done by the Royal Swedish Force at Armstrong Laboratory (using reduced pressure schedules in their extended coverage anti-G suit demonstrated similar results. Statistical analysis of the data from a number of different aspects did provide significant results in some cases which showed that the lowest inflation schedule studied (0.83 psig/G) did have a negative effect on G protection with the ATAGS. The prediction that this inflation schedule would provide a lower pressure boundary and that the optimum schedule for the ATAGS would be found between this schedule and the standard 1.45 psig/G was demonstrated to be true. Results of the analysis of mean arterial blood pressure as taken from Finapres data must be viewed with some caution. McKenzie has shown that while relative blood pressures taken with the Finapres may be valid, the variance of Finapres data with direct arterial pressure measurements is significant (4). It is interesting to note, however, that the blood pressure data shown in Figure 2 closely follow predictable trends indicated by the flattening of the curve in the 2 to 4 G area indicating the effects of the anti-G suit and baroreceptor responses. This finding, at least to some extent, validates mean arterial blood pressure recorded at eye level for the gradual onset runs. Review of the comments made by the test subjects at the conclusion of each session indicates a definite preference for the lower pressures which they felt were more comfortable. The strongest preference was for the 1.14 psig/G schedule as some felt that there was not sufficient support from the lowest pressure schedule.

CONCLUSIONS

Research in the effects of extended coverage anti-G suits will be continued. There are valid reasons to believe that a reduction in inflation schedules is desirable from the standpoint of comfort or potentially advantageous in the design of future high technology Breathing Regulator / anti-G Valve systems.

From the data collected in this study, we have shown that reducing the pressure schedule from 1.45 to 1.14 psig/G in the ATAGS has no statistical effect on G tolerance or endurance. It is important to caution, however, that these results are based on a rather small sample, and attempts will be made to corroborate these findings in future studies. This study has also shown that reducing the schedule to 0.83 psig/G has a definite negative effect on both SACM endurance and relaxed G tolerance.

The findings of this study indicate that the pressure schedule for the ATAGS may be reduced to at least 1.14 psig/G but that a schedule as low as 0.83 psig/G has a negative effect on G protection.

REFERENCES

1. Burton, R. R., M. J. Parkhurst, and S. D. Leverett. $+G_z$ protection afforded by standard and preacceleration inflations of the bladder and capstan type G-suits. Aerospace Med 44:488-494, 1973.

2. Krutz, R. W. and R. R. Burton. The effect of uniform lower body pressurization on $+G_z$ tolerance and protection. In: Preprints of the 1974 Annual Scientific Meeting, Alexandria, VA, Aerospace Med Assoc, 62-63, 1974.

3. Krutz, R. W., R. R. Burton, and E. M. Forster. Physiologic correlates of protection afforded by anti-G suits. Aviat Space Environ Med 61:106-111, 1990.

4. McKenzie, I. Non-invasive blood pressure measurement under G. SAFE Journal 21(1):26-30, 1991.

5. Prior, A. R. J. and G. J. Cresswell. Flight trial of an enhanced G protection system in Hawk XX327. RAF IAM Report No. 678, December 1989.

6. Shaffstall, R. M. and R. R. Burton. Evaluation of a uniform pressure anti-G suit concept. AsMA preprints, 96-97, 1980.

7. Sieker, H. O., E. E. Martin, O. H. Gauer, and J. P. Henry. A comparative study of two experimental pneumatic anti-G suits and the standard USAF G-4A Anti-G suit. Wright Air Development Center, WADC-TR-52-317, 1953.

8. Thompson, R. W., L. J. Meeker, G. L. Wilson, A. G. Krueger and P. E. Love. Engineering test and evaluation during high G, Vol III: Anti-G suits. SAM-TR-78-12, June 1978.

9. USAFTIPS-TR-88A-A. Limited qualitative evaluation of the advanced technology anti-G suit (ATAGS), Edwards Test Pilot School, Edwards AFB CA 93523-5000.

THE MILITARY AIRCREW HEAD SUPPORT SYSTEM (MAHSS)

A.A. Marshall
British Aerospace
Richmond Road
Kingston Upon Thames
Surrey KT2 5QS
U.K.

ABSTRACT

The Military Aircrew Head Support System (MAHSS) is designed to give the pilot extra support to his head and torso by means of cables under the control of a micro-processor. This calculates the expected tension on the cables under the prevailing G forces. It then compares these values with the actual strain on the cables. Any differences in tension to those calculated should be as a result of the pilot trying to move, and the cables will be adjusted to assist him. The MAHSS should offer benefits in terms of less fatigue and injury and the ability of the pilot to move his head while manoeuvring without the danger of getting stuck in a slumped position during high G. It could also be useful during the ejection sequence, by reeling in the cables and thus stabilising the pilot's body and spine in the line of the ejection force. A simplified system has been tested to 6 G in a centrifuge with manual control of the cable lengths. The development of the system is described, including biomechanical modelling and an investigation into its acceptability to pilots, and other human factors issues.

1. INTRODUCTION

The capacity of modern fighter aircraft to pull high levels of G can lead to a number of problems for the crew. These problems range from lack of head mobility while sustaining G, through discomfort and fatigue, to G-Induced Loss of Consciousness (G-LOC). The introduction of helmet mounted systems such as Night Vision Goggles (NVGs) and Helmet Mounted Sights (HMSs) could increase the problems of mobility, and increase the likelihood of strain and injury. This is particularly a problem if the Centre of Gravity (C of G) of the head and helmet assemblies is further forward than that of the natural C of G.

It seems likely that no single solution will be found for these problems, short of fully automated or remotely piloted aircraft. It had previously been believed that the use of longer range weapons would reduce the need to pull high G. However, evidence is emerging which suggests that these only serve to distance the aircraft in air-to-air combat without altering the need to perform high G manoeuvres. HMSs could allow aircraft to release weapons at high off boresight angles reducing the need to turn tightly. However, if an aircraft is capable of high G it is likely that tactics and circumstances will at sometime demand that the pilot utilise this capability

The need for some kind of head support system has been recognised by a number of authors, including Farley (1985). He postulated that such a system could be used to exploit more fully the high G capabilities of combat aircraft, and also act as an aid during ejection. Such a system would need to allow the pilot to move his head unrestricted during normal operations and support or aid head movements under high G. Deakin (1987) proposed a design for the Military Aircrew Head Support System (MAHSS), and this has been developed to a prototype standard (Allright, 1989)

This paper gives an outline of the MAHSS concept and design. It reports on the testing and development to date, and presents the results of an investigation into some of the human factors aspects of the system.

2. DESCRIPTION

The pilot wears a helmet to which a 'horseshoe' and slider arrangement is attached (see Figure 1). The horseshoe runs around the back of the helmet, approximately from ear to ear and is attached by pivots which allow it to move up and down in relation to the helmet. The slider is positioned on the horseshoe and is free to move along its length. Attached to the slider is a cable which runs through a series of pulleys to a drum mounted in the seat. The drum is powered by an electric stepper motor mounted off the seat. The pilot is free to move his head left and right with the slider running along the horseshoe, and up and down with the horseshoe pivoting. The horseshoe could be extended by spring loaded extensions to allow the slider to move beyond 90°, without permanently imposing upon the pilot's field of view. A second cable from a powered drum is attached to the back of the pilot's harness, to provide torso support.

The system will utilise various inputs to determine its correct operation. Accelerometers will be mounted in the aircraft to measure G in the z axis. The lengths of cable paid out will be measured via optical shaft encoders on the motors. The tension on these cables will be measured with strain gauges. A microprocessor determines the expected tension on the cable. This will vary according to the mass of the pilot's head and headgear, the head position and current G values. This will be compared to the measured value.

If the measured value is less than that expected then the pilot is assumed to be trying to raise his head (move it back) if more then he is trying to move it forward. Dead space values are needed for a band around the calculated value. The microprocessor will demand that the motor winds in or out or holds depending on the relative values of the accelerometers, cable tension and position of the head (determined by the amount of cable paid out). The system acts in effect as a servo mechanism for the pilot's neck when he is trying to raise or support his head, while still allowing rotation of the head and paying out cable to allow for forward movement.

In the event of ejection being initiated, it is proposed that the cables would be wound in to hold the head and torso against the seat head box and back. A limiting speed of about 8 meters/sec for the head to be reeled in during ejection has been suggested by the RAF Institute of Aviation Medicine (IAM). A suggested alternative position for ejection could be with the torso fully forward resting on the thighs. If the position of the head will not allow a fully upright position to be obtained, it may be preferable to accommodate this leaning forward position by allowing the cables to reel out. After ejection the cables would be severed to prevent the pilot from remaining attached to the seat.

The MAHSS is covered by British, European, Japanese and USA patents. The MAHSS differs from previous designs in that it is an active system, not based on inertia reels or passive supports.

3. DEVELOPMENT

The design raises a number of fundamental questions which can be summarised as 'Can the system be made to work safely and reliably and be acceptable to the users?'. A secondary question is whether the benefits will outweight the disadvantages, eg costs.

The development and assessment of the system comprises four main topic areas. These are centrifuge and aircraft trials, biomechanical modelling, and a survey of pilot opinion. So far some centrifuge trials have been completed with partial systems. The biomechanical modelling and the pilot survey have also been undertaken. The results of the modelling will feed into a prototype which will be ready for further centrifuge trials later this year.

3.1 Centrifuge Trials

The horseshoe and slider were tested with a fixed length of cable at up to 6 G by two subjects. This showed that the cable could support the head while still allowing it to move, although this caused high noise levels to be transmitted to the helmet from the slider.

The horseshoe and slider were re-designed and a partial prototype was built. This was tested on the centrifuge at the RAF IAM. It was incomplete in that it had no accelerometer inputs or computer programme to control the motor function. Instead this was under the control of the subject via a hand lever. Forward movement caused the wire to be paid out and backward movement made the motor reel in. The subjects had to keep the tension on the wire to prevent it from slipping off the drum. Care had also to be taken when winding in as there was no safety mechanism to prevent the helmet and head being pulled hard into the headbox. This system did not include a torso cable.

Two subjects tested the prototype at 4 G and one subject tested it at 6 G, while wearing an anti-G suit. The subjects were able to use the motor to assist head movements forward and back, and rotated their heads while in the forward position. Head mobility did not seem to be adversely affected by the system. The lack of a torso cable may have contributed to subjects reporting the uncomfortable situation of the head supporting the body while in forward positions. McKenzie (1990) describes this trial more fully.

The centrifuge trial indicated that while the concept was viable, several aspects still needed a large amount of development. These included:

1. Developing a computer programme to actively control the motor(s).
2. Assessing the acceptability and applicability of the MAHSS.
3. Making a robust system for more centrifuge work.
4. Developing an aircraft prototype

3.2 Biomechanical Modelling

An active control programme to control the MAHSS is required. There are two main methods by which such a programme could work. The first would be based on calculating the expected tension for each set of measured G forces and amount of cable paid out, depending on pilot head and helmet mass. The second method is to use look up tables of derived tensions for different conditions. These values could be derived either from models or empirically. However, if dynamic conditions are to be catered for a very large data base might be required. Gathering experimentally derived values would be difficult, costly and time consuming. This is not justified for a prototype, but it may become a viable option for a production system.

Both methods might require different data to be input for different pilots, helmets and helmet mounted equipments. This could be via a pilot 'head trim' control that could be set up early in the flight and would be valid for all conditions.

Alternatively there could be sufficient dead area to cope for the largest mass of head and helmet. In this case increasing or decreasing tension on the cable has no effect until a break out force is exceeded.

Biodynamic modelling of the head under G is being carried out to develop algorithms to calculate expected tensions for solution one. Various models of how the human body behaves under G are available, ranging from simple to very complex. A model outlined by Vulcan and King (1970) was selected as a standard with which to compare more simple versions. The model, including FORTRAN programme listings is described more fully in Vulcan's PhD dissertation (1969) which examines human biodynamic responses to high G forces, such as those found in ejection. He compared his model to measurements made on cadavers which were propelled up a disused lift shaft at the Wayne State University at varying accelerations. His programme has been copied as accurately as possible. What appear to be five small programming errors were discovered, but they have negligible effect on the output solutions. The outputs from this programme therefore match those that Vulcan obtained. Three other programmes have also been written. The first is very similar to the original and is based on a four degree of freedom model which calculates dynamic forces (or expected tensions on the support wires). The second is based on the same set of equations but only deals with steady state conditions, and the third is simpler still and is based on a joint model of the body without considering any damping or stiffening.

All four models have been compared to some of the measurements made on the cadavers at Wayne State University. The selected measurements were the forces and moments around the third lumber vertebra (L3), and the tension at a shoulder strap, which was measured for one run. The models show differing degrees of fit for different conditions. The more simple models did not necessarily show less fidelity than the Vulcan model.

There was sufficient agreement between the models and the experimental evidence to suggest that one of them could form a suitable basis for the MAHSS control laws. The rate of onset and the peak levels of G that the MAHSS has to deal with will be well within those examined. It therefore seems possible that a fairly simple model may be adequate to predict the expected tensions in the MAHSS wires. The advantage of a simple model is that it is easier to run the system at a faster rate to calculate the expected tensions and compare them to the measured tensions and adjust as necessary. Twenty Hz is the aim for the prototype. However all of the models are available for testing during the next centrifuge trials.

3.3 Survey

Assessment of the prototypes has been an important part of the development process. As these progressed and confidence in the viability of the concept grew, it was felt that a parallel study was required in order to elicit aircrew opinion on the factors which might affect its successful introduction into service. Structured interviews were conducted with five BAe test pilots. The eight topic headings given below were taken from these interviews. In addition other discussions with service aircrew have been quoted where applicable.

3.3.1 The Requirement

It has been suggested that the need for the pilot and other aircrew to move their heads under high G may not be enough to warrant the development of a system similar to the MAHSS. In another study (on the introduction of NVGs) interviews were conducted with Tornado ADV aircrew from RAF Coningsby. They tested NVGs under a variety of conditions including during Air Combat Manoeuvres (ACM). The weight and positioning of the NVGs mean that an increased strain on the neck was imposed. The crews reported that they preposition their heads before making medium G manoeuvres (4 to 5 G) and avoided putting on high G whenever possible, although up to 7 G had been reported. The development and implementation of such coping strategies could impose unnecessary limits to operational effectiveness.

The opinions of the BAe pilots are that there is a great need for head movements under G. This is especially so when flying terrain masking or ACM. The reduced Field of View (FOV) of NVGs, and the fact that the pilot has to point his head rather than his eyes to see, means he will have to move his head more to acquire targets and maintain situational awareness.

3.3.2 Application

The test pilots thought that the system would be suitable for aircraft capable of high sustained G manoeuvres. The system was considered for the ADV Tornado Weapon System Upgrade but it was found that the attack profiles of a BVR interceptor, such as ADV, did not warrant its inclusion. However, it is recognised that in two seater aircraft the Weapon System Operator or navigator may benefit more from the MAHSS, as he may be less prepared for the onset of G than the pilot who is controlling the aircraft.

3.3.3 Systems Requirements

The most important requirement identified was that the system should not limit the pilot's FOV. The proposed spring loaded extensions to the horseshoe were criticised for this, even though they may not be a permanent restriction. The removal of this design feature should not restrict head movements.

The pilot needs to be able to turn his head to approximately 150° behind and to be able to see 180° behind.

The system should also not hinder or restrict pilot head movement under normal conditions. As the vast majority or flying is done close to 1 G, any encumbrance is likely to cause the users to reject the system.

The horseshoe and headbox interface was not felt to be a problem as the pilots only position their heads against the headbox for ejection.

3.3.4 Ejection

As described above, there are two positions that are being considered for ejection. The first is the standard upright position, for when the pilot is sat upright or if the system has enough time to pull him upright. The second position is with the torso resting on the thighs, and is proposed for when there is not enough time for the pilot to become upright.

The reeling in on of the cables during the ejection sequence was treated with some suspicion. There was some debate about this restrained posture for ejection and more investigation is required in this area. Equally the possibility of the system releasing the tension on the wires to allow the torso to rest on the thighs was greeted with some alarm. However, if the MAHSS was in place then it should be more likely that the pilot could eject in the approved upright position.

It was not felt that because the MAHSS holds the head against the head box it would enable ejection while wearing current NVG's. The effects of air stream upon them were too great and unpredictable. However, the extra mass and any induced moment of an integrated and streamlined helmet system might be ameliorated on ejection by the cable tension.

3.3.5 Ingress/Egress

The capability of rapid ingress and egress is required for combat aircraft. The opinion of all the test pilots was that anything which requires longer strapping in procedures is undesirable. They also stated that it should be possible for the pilot to connect to the tension wires himself. The ability for the pilot to disconnect himself was considered essential.

3.3.6 Other Problems

It was noted that applying tension to the wires connected to the harness and the helmet is not quite the same as supporting the man directly. If it is possible for him to slip within the helmet or harness then the system could be rendered less effective.

The use of a close fitting helmet such as the 'Alpha' is an important feature of the design. The force is transmitted to the brow of the helmet, rather than to the chin strap which had been one fear.

One pilot commented that the design did not go far enough and he would like to see assistance for head side to side movements under combined y and z accelerations. It may be that by reducing the muscle tension needed against +Gz that lateral movements become easier if there is a high Gy, but this will need to be investigated further.

3.3.7 Spin Offs

Head slump due to G-LOC could be fairly readily detected by the MAHSS and could be linked to an aircraft recovery system, should such systems be introduced in the future.

Linking the system with a helmet mounted sight could have benefits for both systems in that each could cross reference the other to get more accurate head position data.

3.3.8 Testing and Confidence

A programme of centrifuge, flight and ejector seat trials is required for the system. The results of these will feed back into the design and the computer modelling and control laws.

Initially the flight trials of the MAHSS may have to be without a functional ejector seat. This is because the prototype is unlikely to be compatible with ejector seat operation. Aircraft which are capable of subjecting the system to the required G conditions are usually fitted with ejector seats. The pilots commented that they would be very reluctant to fly most aircraft without a functional ejector seat. A number of factors were identified which make the pilots more willing to consider flying without an operational ejector seat. These are that the plane should be twin engined, should have good glide characteristics, in case of engine failure, and will need to be twin seater as a safety pilot will probably be required. All these criteria may not need to be met, and to date the Hawk 100 has been identified as a good candiate. Other aircraft under consideration are the Tucano and PC 9.

It was felt by BAe test pilots that confidence in the system could be built up fairly quickly in an aircraft system, if it worked correctly. Failure could be catastrophic if, for example, the cable were to fail or reel out, under high G. Pilots felt that direct use or contact with pilots who had used the system would be needed to establish confidence in the concept amongst a wider audience.

4. CONCLUSIONS

The testing on the centrifuge has shown that the system could be viable, although there is a lot more work required before an aircraft standard prototype can be produced.

The biomechanical and programming work on the control laws for the MAHSS indicates that a sophisticated model may not be needed for the prediction of cable tensions. This needs to be ratified with more centrifuge studies.

The survey has shown that there is potential for a head support system and this is likely to increase as more agile aircraft are brought into service, such as EFA. The mass of head mounted systems is going to be critical and strengthens the demand for a MAHSS. Pilot and other opinions have tended to be reserved but are generally favourable towards such a system.

No obstacle has so far ruled out the possibility of the MAHSS being employed in mordern fighter aircraft. The way ahead after completing the development of the control laws and other work on the centrifuge, is to put a prototype into an aircraft. This will allow testing under more realistic manoeuvres and dynamic conditions.

Figure 1 - Helmet Attachment

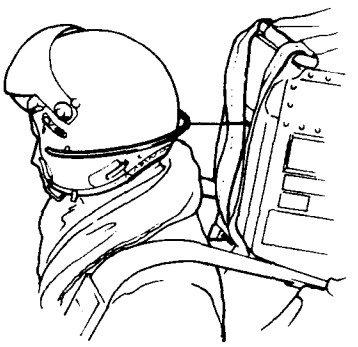

References

Allright, S J 'Military Aircrew Head Support System Development of a Prototype' Kingston Polytechnic, School of Mechanical Aeronautical and Production Engineering, B Eng Degree Project Report, 1989.

Deakin, R S 'Military Aircrew Head Support System' Kingston Polytechnic, School of Mechanical Aeronautical and Production Engineering, B Eng Degree Project Report, 1987.

Farley, J F 'Fast Jet Aircrew Safety' Flight International pp25-29, 31 Aug 1985.

McKenzie I 'Investigation of a Prototype Military Aircrew Head Support System' IAM Report No 687, Feb 1990.

Vulcan A P and King A I 'Forces and moments sustained by the Lower Vertebral Column of a seated Human during Seat-to-Head Acceleration' pp84-100 in 'Dynamic Response of Biomechanical Systems' Conference proceedings of the American Society of Mechanical Engineers, 1970.

Vulcan A P 'Response of the Lower Vertebral Column to Caudocephalad Acceleration' Ph.D. Dissertation, Wayne State University, Detroit, Michigan, 1969.

A Cardiovascular Model of G-Stress Effects: Preliminary Studies With Positive Pressure Breathing

Dov Jaron, Ph.D.
Thomas W. Moore, Ph.D.
and Pierre Vieyres, Ph.D.

Biomedical Engineering and Science Institute
Drexel University, 32nd and Chestnut Streets,
Philadelphia, PA 19104 USA

To study possible means of ameliorating the effects of gravitational acceleration on the cardiovascular system, a non-linear digital computer model has been developed. It combines a variable compliance model of the left ventricle, multi-element models of the aorta and the systemic and venous systems, and lumped models of peripheral vascular beds. The model of the left ventricle is based on work by Suga and Sagawa [1]. The vascular elements are obtained from the solution of the Navier-Stokes equations, combined with a set of simplifying assumptions [2]. This closed-loop system includes heart rate control and venous tone control, and the effects of acceleration forces. The model also can simulate the effect of several modes of G protection, including the anti-G suit, straining maneuvers, positive pressure breathing (PPB), and seat back angle. A block diagram of the simulation is depicted in Fig. 1. In the study reported here, this model was used to gain an understanding of the effects of positive pressure breathing on G tolerance and to compare these effects to other protection methods.

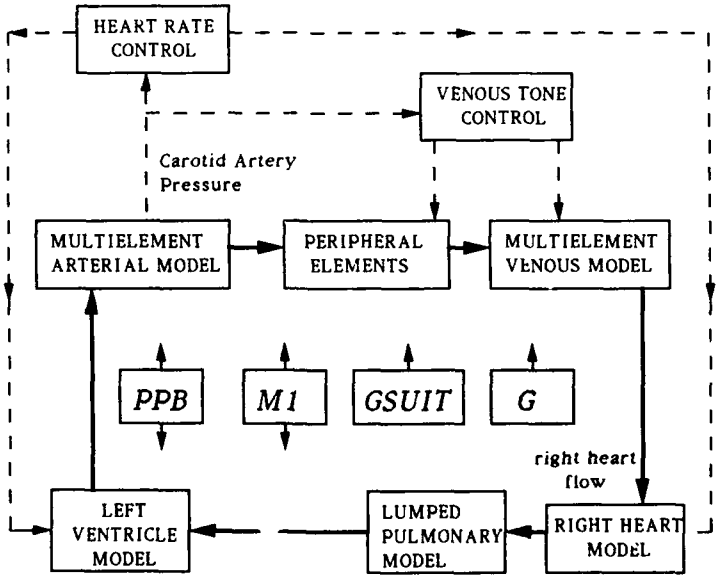

Fig.1: Block diagram of the cardiovascular model

Pressure from the G-suit, straining maneuvers, and/or PPB was coupled to the vasculature through the compliance elements of the appropriate vascular bed. Suit pressure was applied to the abdominal and leg elements; the M1 pressure was applied to the thoracic, abdominal and leg elements; and the PPB pressure was applied to the upper elements of the model representing the thoracic segments and the lower cerebral vessels. PPB pressure was applied in proportion to the +Gz level beginning at 1.2G. The amplitude of the G suit pressure followed the standard military specification: P_{suit}=1.5 (Gz-1) psi, with the pressure applied beginning at 1.5G [3]. The M1 maneuver included inspiration for 1 second and forced expiration for 3 seconds.

The effects of G stress and protection techniques were evaluated using calculated pressure and flow in the ophthalmic artery where the first symptoms indicative of G induced circulatory problems occur. It was assumed that systolic ophthalmic artery pressure above 50 mmHg maintains full vision; that peripheral light loss (PLL) begins when peak ophthalmic artery pressure falls below 50 mmHg; and that central light loss (CLL) occurs when peak pressure drops below 20 mmHg. To permit comparison of the various protection techniques, we used simulated G profiles consisting of rapid onset (1G/sec), followed by a 15 second plateau for sustained level; or alternate levels of 4 and 7 G, each for 7 second duration, for simulated aerial combat maneuver (SACM). Thus far, we have incorporated only the mechanical effects of PPB in the cardiovascular model. The rhythmic effects of respiration have not yet been included.

Sample results are presented in Figs. 2, 3 and 4, and the accompanying Table 1. Fig. 2 shows the effects on ophthalmic artery pressure of the anti-G suit alone (Panel 2b) and the effects of the anti-G suit combined with PPB adjusted to a maximum of 30 mmHg (Panel 2c). The results were obtained for a rapid onset, 15 second sustained acceleration level. The G profile is shown in Panel 2a. The pressure level at which PLL and CLL values are assumed to occur are indicated by the two horizontal lines at 50 and 20 mmHg respectively. Note that the rapid acceleration onset is followed by a decrease of the systolic pressure of the ophthalmic artery.

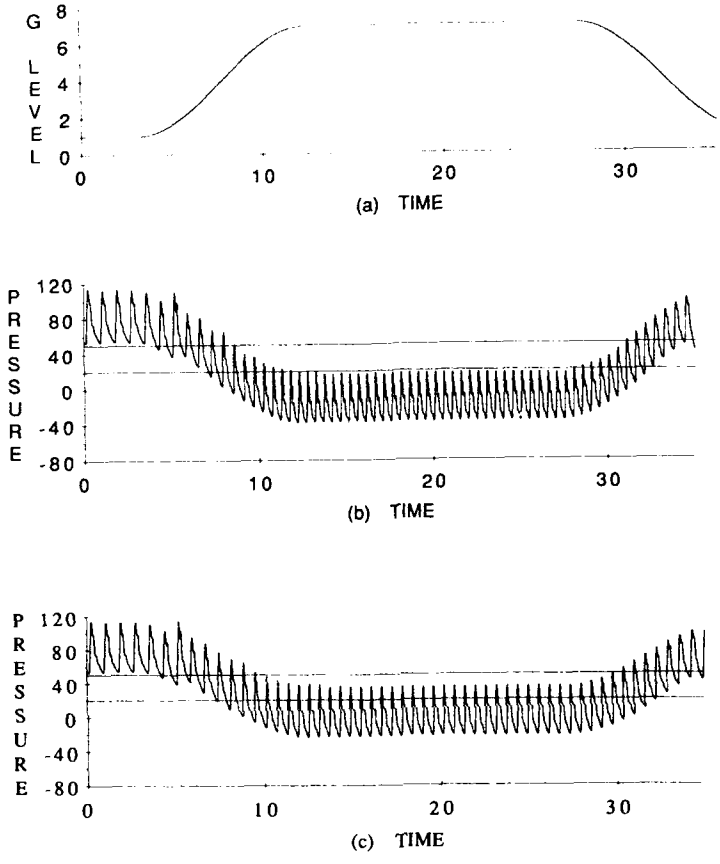

Fig. 2: Ophthalmic artery pressure for a sustained plateau (7G)
(pressure in mmHg, time in sec)
a- G Profile
b- Anti-G suit alone
c- Anti-G suit combined with PPB at 30 mmHg max.

In Panel 2b, the peak pressure fell below the critical value for CLL approximately 7 sec after the start of the acceleration stress; the anti-G suit was able to maintain a peak arterial pressure of only slightly below 20 mmHg for the remainder of the run. The ophthalmic pressure recovered its initial value when the acceleration stress was removed. When the anti-G suit was combined with PPB having a maximum value of 30 mmHg (Panel 2c), the peak pressure fell below the PLL value 8.5 sec after the start of the onset, and was maintained substantially above the CLL value for the remainder of the run. This demonstrates the benefit of positive pressure breathing, yielding (for 30 mmHg positive pressure) an additional protection of approximately 1G over the anti-G suit alone. This assumes that each additional 22 mmHg provides a 1G increment in protection.

The effects of combining different levels of PPB with an anti-G suit during SACM are demonstrated in Fig. 3 in which rapid onset is followed by 4/7G SACM. In Panel 3b, for PPB of 30 mmHg maximum level, the ophthalmic artery pressure falls below the PLL value during the 7G plateau but remains above the CLL value of 20 mmHg. The same level of protection was observed as in the sustained 7G run. A more effective protection was achieved in these runs when the PPB pressure was set to reach 60 mmHg at 7G (Panel 3c).

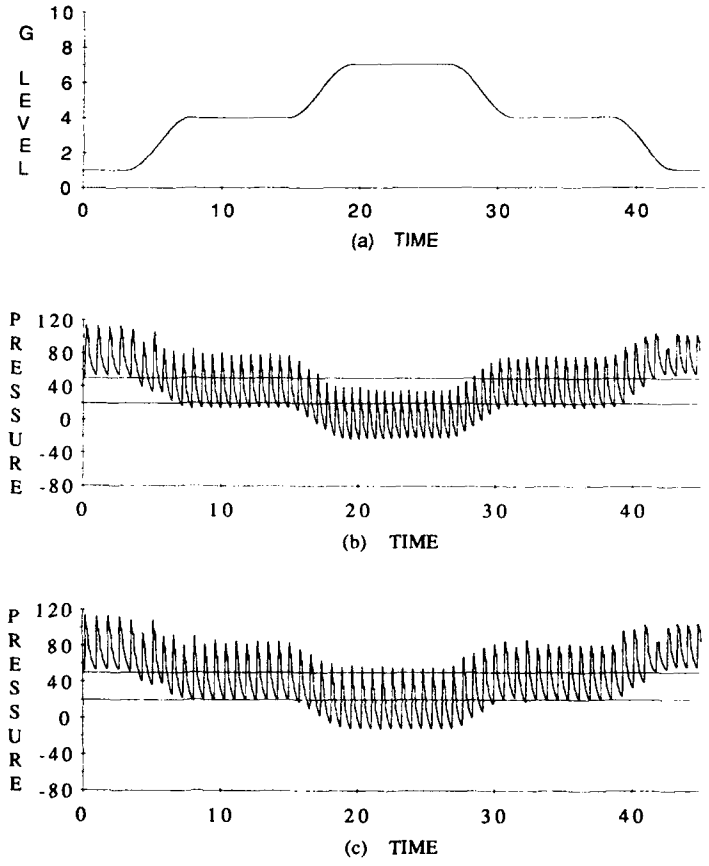

Fig. 3: Ophthalmic artery pressure for a simulated SACM maneuver (4/7G)
(pressure in mmHg, time in sec)
a- G Profile
b- Anti-G suit combined with PPB at 30 mmHg max.
c- Anti-G suit combined with PPB at 60 mmHg max.

For the SACM run, the model predicts that for an unprotected subject, during the 4G plateau, the ophthalmic artery pressure recovers to increasingly higher value for each repeated low level plateau (Panel 4b). When the Anti-G suit, the M1 maneuver (at 25 mmHg), and PPB (at 25 mmHg) were all combined during the SACM run (Panel 4c), the ophthalmic artery pressure was maintained around the PLL value, suggesting the additive effects of these techniques on gravitational acceleration tolerance. For this run, the M1 maneuver was applied only above the 4G plateau level, as the combination of anti-G suit and PPB of 25 mmHg provided a sufficient protection up to this acceleration level.

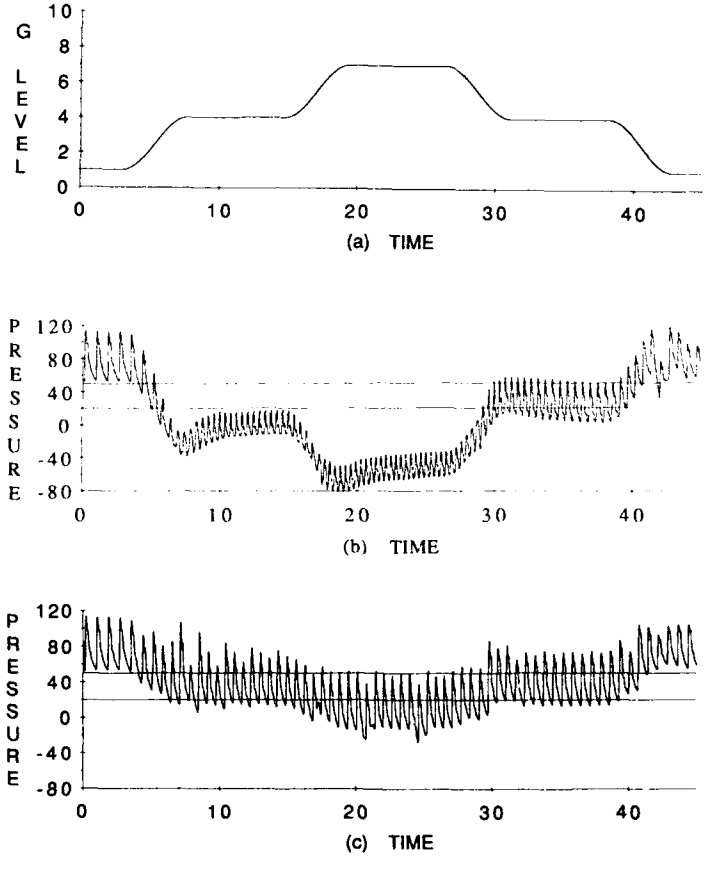

Fig. 4: Ophthalmic artery pressure for a simulated SACM maneuver (4/7G) (pressure in mmHg, time in sec)
a- G Profile
b- Unprotected
c- Anti-G suit combined with PPB at 25 mmHg max, and M-1 at 25 mmHg max.

Table 1: Protection Technique and G tolerance

Protection Technique / G Level	No	Suit	Suit+M1(30)	Suit+PPB(30)	Suit+M1(30)+PPB(30)
4	PLL: 2.2 sec CLL: 3.0 sec	No PLL No CLL	No PLL No CLL	No PLL No CLL	No PLL No CLL
7	PLL: 3.5 sec CLL: 4.1 sec	PLL:5.1 sec CCL:7.0 sec	PLL: 8.5 sec No CLL	PLL: 8.5 sec No CLL	No PLL No CLL
4/7 Alternate	PLL: 2.2 sec CLL: 3.0 sec	PLL:13.5 sec 2nd Plateau CLL: 15 sec	PLL:15 sec 2nd Plateau No CLL	PLL:15 sec 2nd Plateau No CLL	No PLL No CLL

PLL : Peripheral Light Loss-
Ophthalmic artery pressure falls and remains below 50 mmHg during the run.

CLL : Central Light Loss-
Ophthalmic artery pressure falls and remains below 50 mmHg during the run.

Table 1 summarizes the simulated results of three different protection techniques at different G levels. Note the increased delay in the occurrence of PLL and CLL when the protective effects of the anti-G suit was supplemented by 3 other combinations of protection techniques. For an unprotected subject at 7G, PLL occurred 3.5 sec after the start of the rapid onset run. The delay was increased to 8.5 sec when the anti-G suit was combined either with M1 maneuver or with positive pressure breathing. Both the M1 straining maneuver and PPB of 30 mmHg maximum level gave the same protection delay at two different G levels, suggesting that similar protection level is provided by these two techniques. Also note that no center light loss was observed when the anti-G suit was combined with M1 or with PBB. When all protection techniques were combined, peak ophthalmic artery pressure remained above the PLL value throughout the run.

We are now refining our model to include pulmonary mechanics, ventilation, perfusion and gas exchange, all of which are affected by positive pressure breathing. We anticipate that the added elements will improve the understanding of the effects of positive pressure breathing on G tolerance and will provide the means for optimizing its effects.

REFERENCES

[1] H. Suga and K. Sagawa, "Instantaneous pressure-volume relationships and their ratio in the excised, supported canine left ventricle", Circ. Res., vol. 35, pp.117-126, 1974.

[2] D. Jaron, T. W. Moore and Jing Bai, "Cardiovascular Responses to acceleration Stress: A computer simulation", Proceeding of the IEEE, vol. 76, no. 6, pp.700-707, June 1988.

[3] U.S. Military Specifications: "Valve, automatic, pressure regulating, anti-G suit". MIL-V-9370D(ASG), October 18, 1967.

ASSESSMENT OF PHYSIOLOGICAL REQUIREMENTS FOR PROTECTION OF THE HUMAN CARDIOVASCULAR SYSTEM AGAINST HIGH SUSTAINED GRAVITATIONAL STRESSES.

Richard Collins and Emilia Mateeva
Biodynamics International
5170 Bishop St., Halifax (Canada B3J 1C9)

SUMMARY

Satisfactory performance of combat pilots exposed to rapid onset of high sustained gravitational stress ($+G_z$) is compromised by caudalward fluid shifts which provoke "compensatory" responses from the central nervous system. Such neural, metabolic and humoral responses can lead to dramatic alterations in the heart rate, stroke volume, cardiac output, myocardial contractility and vascular tonus, with the clear danger of loss of vision, loss of consciousness and myocardial fibrillation and ischemia.

A simple but complete model of the coronary circulation is proposed as a framework for organizing a systematic research program for the passive and active control of this circulation under conditions of extreme g-stress. Within such a framework, preliminary conclusions can be drawn concerning the investigation of effective countermeasures designed to enhance pilot tolerance in air-combat maneuvers.

LIST OF SYMBOLS

A	cross-sectional area of vessel lumen
F	wall skin-friction coefficient
$\mathcal{F}$	Faraday constant (coul./mol. charge)
G_z	caudalward gravitational force
K^z	factor in *pressure-area law*
P^p	transmural pressure
R	universal gas constant
S_i, S_o	concentrations of S inside and outside of the cell, resp.
T	absolute temperature
V	cross-section averaged velocity
V_m	potential difference across cell membrane
Z	valence of S
x	distance along vascular tree
t	time
α, α_i	compliance and related parameters
ϕ	gravitational force potential
μ	blood viscosity
ρ	blood density

1. INTRODUCTION

The general physiological aspects of *human response* to gravitational loading have been summarized in a review article by Collins et al (1987). Two categories of cardiac pathology resulting from human exposure to $+G_z$ (caudalward) gravitational stress may be delineated: a) subendocardial hemorrhage, and b) stress cardiomyopathy (myocardial cellular damage and necrosis and myofibrillar degeneration). Human exposure to the latter could potentially be of greater functional significance. Both general categories will be considered in this paper, as well as proposed means of mitigating their effects on aircraft pilots of high performance fighters.

Human exposure to high levels of $+G_z$ acceleration (3 - 15 G) results in direct mechanical effects (caudalward shifting and distortion of the heart and blood volumes), autonomic nervous system (ANS) activity (attempting to compensate for these shifts) and alterations of the aortic pressure.

The heart rate may increase rapidly up to 180 - 200 bpm upon activation of the arterial baroreceptor reflex which transmits signals to the pacemaker via the carotid sinus nerve. Other reflexogenic areas may further modify the response. For example, activation of vagal cardiopulmonary mechanoreceptors *can reduce baroreceptor response* (Greenleaf et al 1977). Both subendocardial hemorrhage and increase in heart rate appear to be related to involvement of the sympathetic nervous system (lessened by β -adrenergic blockade). As blood volumes shift caudalward under $+G_z$ loading, from the head and thorax to the legs, human regulatory responses show many similarities with changes during standing (orthostatic fluid shifts). An increase in plasma ADH (anti-diuretic hormone) levels is likely due to this shift in blood volume and decreased activation of the cardiopulmonary receptors. The amount of pulmonary plasma volume lost is clearly a function of both the magnitude and the duration of the gravitational force fields.

On the other hand, the coronary vessels are not likely to be distorted or obstructed mechanically during the $+G_z$ acceleration (Erikson et al 1976).

In what follows, a simple preliminary mathematical model, based directly on the true physics of fluid flow in distensible vessels, is proposed to predict the time-varying coronary blood flow under conditions of external gravitational stress. As indicated above, a definitive model must take account of both the passive and active control of the coronary circulation. As this active component implicates the sympathetic nervous system, it is of interest to examine the possibilities of protecting the coronary circulation against gravitational stress using both mechanical forces (via anti-G suits) and hyperactive nervous controls (via external neuroelectric stimulation of the appropriate nerve cells).

Operation of both modes of protection may be considered simultaneously and will involve state-of-the-art and yet to be developed knowledge of both aspects through the application of an intelligent and inventive combination of theory and experiment. The purpose of this paper is to challenge the reader to consider such new perspectives.

2. A MODEL FOR THE CORONARY CIRCULATION

The coronary circulation supplies the heart muscle and myocardial cells with oxygen and nutrients. Coronary blood flow closely parallels myocardial oxygen demand as heart work increases or decreases. Coronary vasodilation during myocardial hypoxia may result from the direct effect of interstitial oxygen tension on vascular smooth muscle or may involve an intermediate link such as adenosine.

2.1 Coronary Circulation under $+G_z$ Stress:

Blood flow in the coronary circulation may tend to decrease under prolonged and sufficiently high $+G_z$ stress (Laughlin 1986). If that blood flow is no longer sufficient to satisfy the demands of the myocardium for oxygen, then only a few compensatory mechanisms can be marshalled to preserve the viability of the myocardial cells. These mechanisms may include:

(i) recruitment and dilation of the coronary vessels, and

(ii) consumption of glycogen stores and of blood oxygen dissolved in the interstitial fluid of the coronary vasculature,

(iii) modulation or cessation of active myocardial contraction. These mechanisms are capable of a combined augmentation of coronary blood flow five to sixfold. The aortic pressure observed at heart level actually increases with increasing gravitational force, confirming the function of peripheral vascular compensatory mechanisms. Such an increase in aortic pressure levels would raise the proximal coronary blood pressure and also tend to modulate the otherwise larger fall in the coronary blood flow during this type of g-stress. On the other hand, both cardiac output and stroke volume fall progressively with increasing gravitational force (Blomquist et al 1979). Table I, adapted from Blomquist et al (1979), summarizes the hemodynamic effects of $+G_z$ and $+G_x$ acceleration.

TABLE I *Hemodynamic Effects of Acceleration*

Acceleration	Cardiac Output	Heart Rate	Stroke Volume	Mean Arterial Pressure
G_z				
+2	+7	+14	−24	+9
+3	−18	+35	−37	+21
+4	−22	+56	−49	+27
G_x				
+2	−12	−2	−10	+11
+3.5	+9	+17	−7	+18
+5	+27	+40	−8	+25

Effects of head-to foot (+G_z) and transverse gravitational force (+G_x) acceleration in 6 relaxed human volunteers. Values are % change from control [Data from Lindberg et al (207, 208)]

Several factors (Fig. 1a) may explain why coronary blood flow may fall to inadequately low levels during $+G_z$ stress:

a) activation of the arterial (carotid sinus) baroreceptor reflex leads to increased heart rate (tachycardia), thus reducing the diastolic interval for coronary blood flow,

b) increased myocardial contractility, in response to augmented myocardial metabolic rate associated with tachycardia, leads to higher intramyocardial pressures (IMP) causing extravascular compression of the coronary blood vessels.

c) activation of the sympathetic nervous system, in mediated response to increased heart rate, may initially result in coronary vasoconstriction through an increase in circulating levels of norepinephrine and epinephrine (see Fig. 1b).

Adequate coronary blood flow during gravitational stress can only be assured through the functioning of the *compensatory mechanisms* described earlier as a means of maintaining sufficient coronary blood flow reserve capacity.

However, should the gravitational stress exceed the human tolerance level, compensatory mechanisms will fail and *decompensation* will occur. The characteristics of decompensation are progressively falling or zero cardiac output and aortic pressure, bradycardia and asystole (incomplete systole). Myocardial hypoxia and ischemia may ensue. Such a condition may be accompanied, or preceded by loss of vision (LOV) and/or loss of consciousness (LOC) in pilots of high performance military aircraft undergoing high $+G_z$ combat maneuvers (Collins et al 1987).

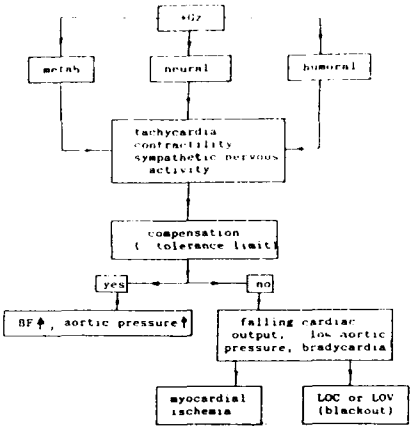

Figure 1a): Influence of $+G_z$ on the Coronary Circulation

2.2 Formulation of the Model (Passive)

The characteristics of this passive control model have been described extensively by Zhou et al (1989). Accordingly, only the principal features will be outlined here.

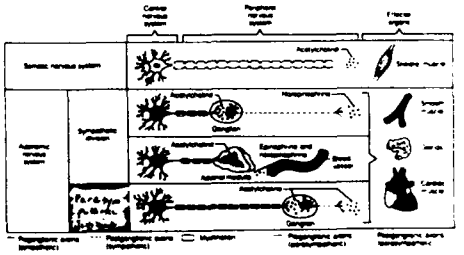

Figure 1b): Autonomic nervous system Sympathetic/Parasympathetic Divisions and Actions (Marieb)

2.2.1 Anatomy and properties of the coronary circulation

The complete human coronary circulation is modelled as a distensible branching network of piecewise rectilinear vessels distributed within the myocardial wall of the heart. Vascular volumes have been discretized into three layers within the depth of the myocardium in the epicardial/midwall/endocardial ratios of 0.83/1/1.19 respectively. The network (Fig. 2) extends from the main coronary artery, through the progressively narrowing and bifurcating medium and small arteries

and arterioles, and into the capillary bed. Most models of the coronary circulation stop here. Our model goes on to include the venous vasculature, extending from the venules, small and medium veins, into the large cardiac veins and coronary sinus, which empty primarily into the right atrium.

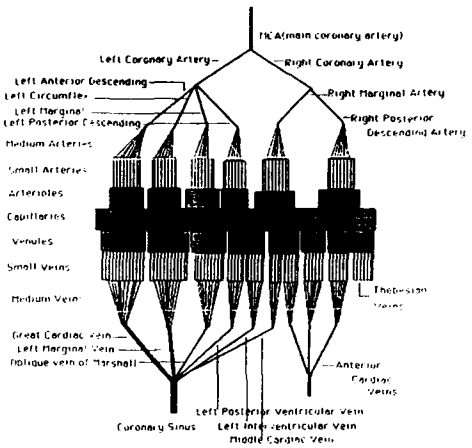

Figure 2: Schematic representation of the coronary vasculature

The dimensions of the some 55 successive generations of branching coronary vessels considered here have been documented only for the larger arteries and veins. To fill in the intermediate gap, a principle of local self-similarity for the branching of biological networks as proposed by Petukhov (1988) has been applied. Notwithstanding the global nonlinear geometric character of the branching vascular network, good accuracy and relative simplicity are afforded through use of a linear principle of local self-similarity relating the relative vessel diameters d of successive k and k + 1 th generations in the form

$$d_{k+1} = \frac{a_1 d_k + a_2}{a_3 d_k + 1} \qquad (1)$$

The three free parameters a_1, a_2 and a_3 and the relative vessel diameters d_k may be determined from measured data at three pairs of branching vessels distributed for example at proximal, medial and distal positions within the network.

2.2.2 Boundary conditions imposed at the proximal and distal ends of the complete coronary circulation

The imposed pressure boundary conditions reflect the close proximity of: a) the main coronary artery to the aortic root at the inlet to the coronary circulation, and b) the fact that the coronary sinus and Thebesian and anterior cardiac veins empty into the right atrial cavity situated distally at the outlet of the coronary circulation. Similarly, the time variation of the intramyocardial pressure, which acts externally to the coronary blood vessels, is taken to be synchronous with the left ventricular cavity pressure at the endocardium, falling off to zero (relative) pressure at the epicardium (Heineman et al 1985 and Beyar et al 1984, 1987).

2.2.3 Governing equations

The fluid and wall motions are coupled through functional relations between transmural pressure and cross-sectional area of the deformable vessels. The unsteady quasi-one-dimensional form of the fluid continuity, momentum and the wall equations are given respectively as:

Governing Equations

$$\frac{\partial A}{\partial t} + \frac{\partial}{\partial x}(AV) = 0 \qquad (2)$$

$$\frac{\partial V}{\partial t} + \frac{\partial}{\partial x}\left(\frac{V^2}{2} + \frac{P}{\rho}\right) = -F + G_z \qquad (3)$$

$$P = P(A) \quad \text{... transmural pressure} \qquad (4)$$

with

$$F = \frac{8\pi}{A}\frac{\mu}{\rho}V, \quad G_z = \frac{d\phi}{dx}$$

Wall Relations

For $p \geq 0$, $A/A_0 \geq 1$

$$p = \frac{1}{\alpha}\left(A - A_0\right) \quad \text{... } \alpha = \text{compliance.} \qquad (5)$$

For $p \leq 0$, $0.8 < A/A_0 < 1$

$$p = K_p\left[\alpha_0 + \alpha_1\left(\frac{A}{A_0}\right) + \alpha_2\left(\frac{A}{A_0}\right)^2\right] \qquad (6)$$

with $\alpha_0 = 20.9625$, $\alpha_1 = -55.9$,

$\alpha_2 = 34.9375$

For $p \leq 0$, $A/A_0 < 0.8$

$$p = -K_p\left(\frac{A}{A_0}\right)^{\frac{3}{2}} \quad \text{... similarity law} \qquad (7)$$

The laminar friction factor F has been based for simplicity on a fully developed Poiseuille flow, while G_z denotes a conservative force field, expressible as the gradient of a scalar potential ϕ. For negative values of the transmural pressure, corresponding to periods for which IMP exceeds the intraluminal pressures, provision has been made for partial collapse of the affected vasculature.

2.2.4 Numerical solution and results

A hybrid method of characteristics combined with a two-step Lax-Wendroff finite-difference scheme has been used to integrate the system of governing fluid/wall coupled equations with their boundary conditions in the x-t plane. The partial differential equations are reformulated in conservative form for this purpose. The yet unknown initial conditions may be estimated at the outset; these will converge readily to reproducible values after only a few computed cardiac cycles of periodic flow. Our computational results for the

passive control of the coronary circulation confirm that the flows developed in this vasculature are highly sensitive to:

a) *vascular architecture;* vessel diameters, lengths and branching angles, which govern corresponding pressure drops across the bifurcations, and

b) *vessel compliance or modulus of elasticity* which varies spatially over the vascular tree by several-fold under passive conditions, and even more so under active control of the vascular tonus. Negative transmural pressures result in an extremely high level of vessel compliance. Under the extravascular compression (IMP) during systolic contraction, coronary arterial blood flow can fall nearly to zero in some vessels, inducing retrograde flows (see Hoffman et al (1990).

In Figs. 3, 4 and 5 below are presented illustrative graphs (Zhou 1991) of the passive variations of coronary blood pressure through the vascular tree extending from the coronary artery to the venous drainage network.

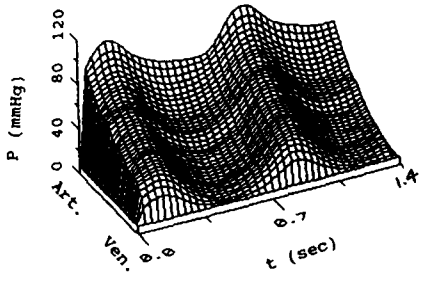

Figure 3: Computed coronary epicardial blood pressure P(x,t)

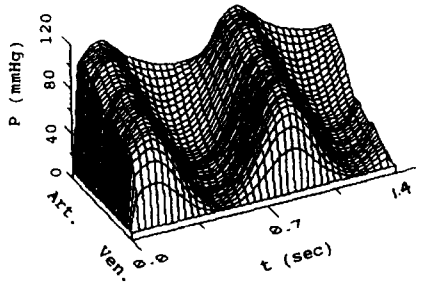

Figure 4: Computed coronary midcardial blood pressure P(x,t)

As a direct result of the nonuniform distribution of both vascular density and intramyocardial pressure (IMP) within the ventricular wall, the pressure wave forms appear to steepen markedly as one descends in depth from the epicardium towards the endocardium. Indeed, systolic levels are raised and diastolic pressures fall as one proceeds in this direction.

As expected, the computed variations in coronary blood pressure tend to mirror similar variations in the extravascular IMP, the latter attaining its maximum level at the endocardium, and falling off to near zero at the epicardial level during ventricular contractions. As a result, the systolic pressure levels progressively increase with depth through the myocardial wall.

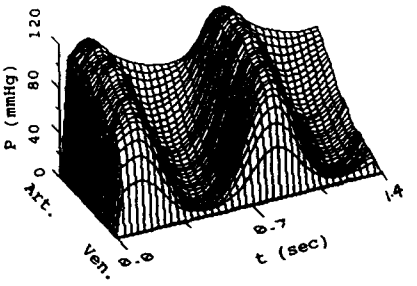

Figure 5: Computed coronary endocardial blood pressure P(x,t)

From our earlier research on pulsatile flows in collapsible vessels (Collins 1986) with longitudinal tethering, it would appear that the restoring forces on externally collapsed vessel augment with increases in longitudinal tension. It can be hypothesized that the coronary arterial vessels, particularly those in the endocardium, may be subjected to considerable mechanical distortion and longitudinal tension under the action of the ventricular contraction and enhanced IMP. This leads to substantially increased restoring forces by causing the coronary arteries to rebound, "springing open" abruptly as the IMP is released upon diastole; whereas, the compressed veins, with their higher compliance, cannot respond (re-open) as quickly. During that short time interval, the suddenly lowered arterial pressure created by virtue of the almost explosive re-opening of the coronary arteries may generate a suction, drawing blood from the veins into the arterial system. In the process, the diastolic pressures fall more rapidly than the systolic pressures as one proceeds from the arteries to the veins. In the endocardium, they fall even below the levels observed in the epicardium, with concomitant rupture of small vessels (arteries and/or veins) and possible endocardial hemorrhaging. It is logical to assume that this phenomenon should be exacerbated under $+G_z$ stress, which is accompanied by increased heart rate and ventricular contractions which raise the IMP even further. It will be seen later that this can have important consequences for myocardial ischemia and endocardial hemorrhage under high levels of sustained gravitational stress.

This effect is of sufficient interest in itself to justify undertaking in the future a more detailed investigation of the properties and response of compressed coronary vessels of differing elasticity and longitudinal stress under the influence of a strong and rapidly changing external (IMP) force field.

A typical computed midwall distribution of coronary blood flow during a cardiac cycle is depicted in Fig. 6 on the next page.

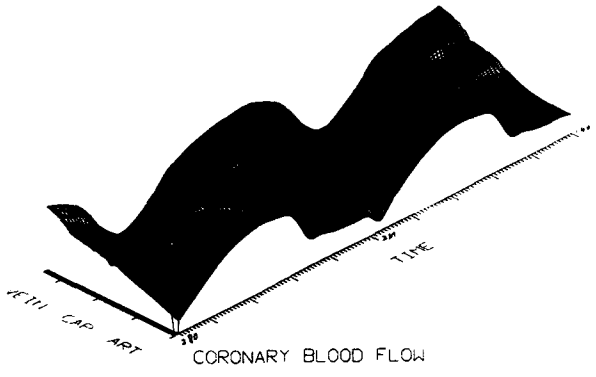

Figure 6: Computed midwall distribution of coronary blood flow during cardiac cycle

One notes during diastole the rapid drop in arterial blood flow near the capillaries. In systole, however, coronary blood flow becomes more uniformly distributed throughout the arteries and veins. This occurs because arterial flow is diminished during systole as arterial blood is squeezed out into the veins, where flow rates attain their maximal values. These rôles reverse during diastole, during which the release of IMP allows the arteries to open very rapidly, drawing back blood from the veins which tend to empty during this phase.

These blood flow distributions have been re-plotted in Figs. 7 and 8 as a function of depth through the myocardial wall, and viewed respectively from the endo- and epicardial sides of the myocardium. During systole, flow rates drop to minimal values in the endocardium under the action of IMP; whereas, epicardial flow attains maximal values. During diastole, upon release of the IMP, the compressed endocardial vessels spring back open, creating low pressures which draw blood back from the larger vessels of the epicardial layer, as the latter vessels lose blood volume.

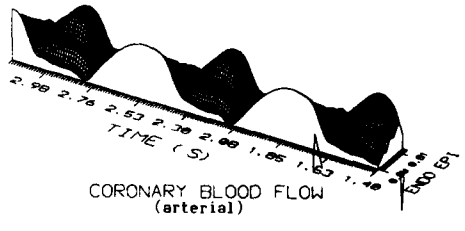

Figure 7: Computed distribution of arterial coronary blood flow within myocardial wall layers during cardiac cycle as viewed from the endocardial side

The sharply differing flow profiles between the endocardial and epicardial regions of the coronary circulation are brought out clearly in Fig. 9 which represents a superposition (shifted vertically for clarity) of computed coronary blood flow as a function of time at four wall depths ranging from the endocardium (a), via two near midwall layers (b) and (c), to the epicardium (d).

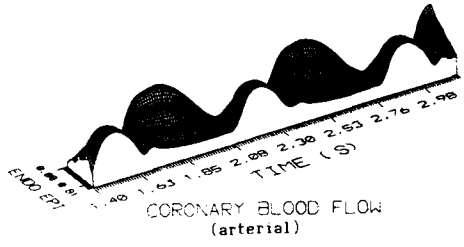

Figure 8: Computed distribution of arterial coronary blood flow within myocardial wall layers during cardiac cycle as viewed from the endocardial side

One notes larger flow amplitudes at the endocardium (a), diminishing towards the epicardium (d), indicating that at the endocardium, flow rates are higher in diastole and lower in systole than their corresponding values at the epicardium. As discussed earlier, this effect is due to both a richer (denser) vascularization and a higher systolic IMP in the endocardium, causing larger extravascular compression and hence more greatly reduced endocardial blood flow in systole. This results in faster vascular re-opening in order to draw in venous blood during diastole.

However, this property of the endocardial coronary vessels to shut down blood flow so markedly during systole renders the region highly vulnerable to ischemia during $+G_z$ loading, and is a likely factor in the occurrence of myocardial ischemia and hemorrhaging in the subendocardium in miniature swine and in humans exposed to gravitational stress.

One may note in Figs. 9c) and 9d), which correspond to the epicardial regions, the formation of notches, reminiscent of the "dicrotic notch" in aortic flow profiles. These would normally indicate the presence

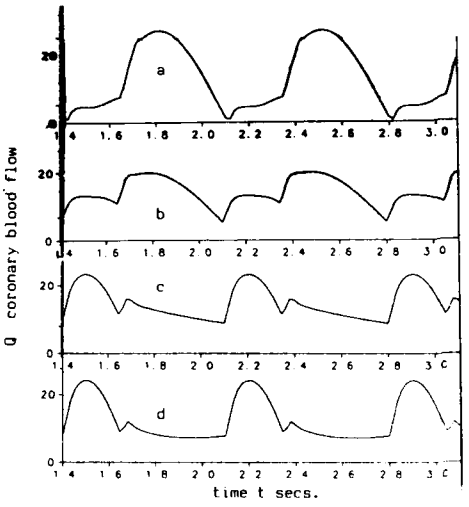

Figure 9: Computed profiles of coronary blood flow at 4 wall depths ranging from (a) endocardium through to (d) epicardium, during a cardiac cycle

of wave reflections in the epicardial layer, which are damped out in the deeper layers toward the endocardium (note the absence of "notches" in Figs. 9a and 9b), by the increased extravascular compression IMP prevailing there.

Finally, it is of interest to examine the time-phased relationship between *total* arterial and venous flows (Zhou 1991) as depicted in Figs. 10 and 11 respectively.

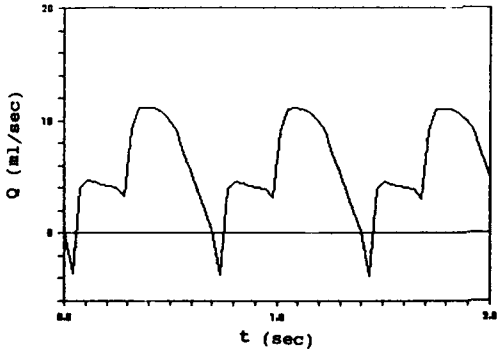

Figure 10: Total computed arterial flow

These flows represent the integration over the arterial and venous networks, respectively, of all the blood flow in the individual or grouped vessel segments. The net computed arterial flow is observed to be negative or retrograde during systole (Fig. 10) as arterial blood is forced backward (Zhou et al 1989) into the large epicardial veins (Fig. 11) under the action of the extravascular compression IMP. This corresponds to the "toothpaste tube" squeezing analogy of Hoffman et al (1990). It results in a global back-and-forth flow between arteries and veins during the cardiac cycle, with venous flow rates attaining maximal values during systole and minimal values during diastole.

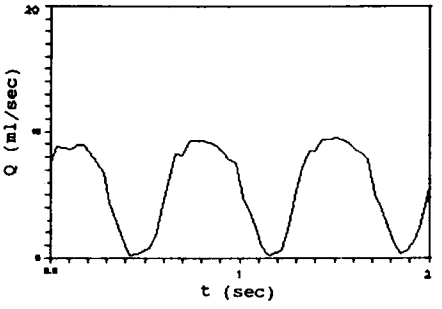

Figure 11: Total computed venous flow

One notes the good qualitative agreement between these computational predictions and the published measurements of Gregg et al (1956) in our Figure 12, at least as far as the general waveforms and sychronization of arterial maxima with venous minima and vice versa are concerned. However, this computational model can serve as a valuable framework for planning and implementing more detailed controlled experimental programs directed toward exploring fully the quantitative character and dynamic response of the coronary vasculature to time-varying external force fields derived both from IMP and $+G_z$ stresses under both passive and active control.

In the next section, some aspects of the very important active control of the coronary hemodynamics will be discussed briefly.

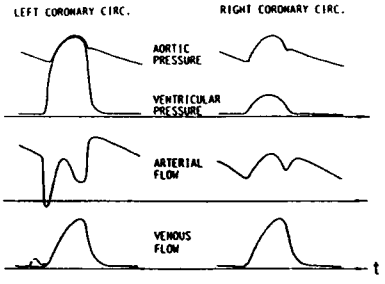

Figure 12: Measured coronary blood flow (from Gregg & Sabiston 1956)

2.3 Formulation of the Model (Active Control)

The model proposed in §2.2 for coronary hemodynamics under *passive* control is based upon the fundamental laws of fluid dynamics (continuum and momentum equations 2 and 3) for the blood flow, coupled with the vascular wall equations 4 (involving wall elasticity and eventually viscoelasticity). It

provides the basic foundation for a more generalized *actively* controlled model, accounting for the additional metabolic, nervous and hormonal controls which are invoked during exercise or exposure to varying gravitational stresses. These can modify drastically the flow field response predicted by the *passive* model of §2.2.

As described briefly in foregoing §1 and 2, high sustained levels of $+G_z$ stress tend to trigger autonomic nervous system activity (to compensate for caudalward shifts in blood volumes), provoking abrupt and substantial changes in heart rate and output, vasomotor activity and myocardial contractility. In the process, the aortic pressure and metabolic (O_2-related) rates may change significantly.

Notwithstanding these important physiological complexities, it is in principle very straightforward to generalize the passive model to incorporate these active controls.

Referring back to the governing equations (2) to (4) and the associated boundary conditions on the proximal and distal pressures, one has only to modify the following:

a) the *vascular compliances* in Eqs. 5 - 7 (to reflect alterations in ANS-induced vascular tone),

b) the *pressure boundary conditions* at the main coronary artery (to reflect changes in aortic pressure) and at the right atrial cavity (to reflect alterations in cardiac output dynamics),

c) the *intramyocardial pressure (IMP)* (to reflect changes in myocardial contractility *induced by heart rate-related* alterations in metabolic rate).

Although it has been stated that it is very straightforward to incorporate modifications of these three categories into the system of mathematical equations and computational algorithms, it is quite another matter to *formulate* the required modified expressions a) to c) above. It is here that a careful and innovative analysis must be made of the gravitational stress related data available to date. Where necessary, additional controlled experimental programs must be planned and implemented to provide expressions for the modified active relationships which may still be lacking.

Although such an experimental program represents the present state-of-the-art in the field of actively controlled circulatory physiology in general, a crude preliminary illustration is outlined below, constituting a simple first step approximation to an idealized response of the coronary circulation to an exercise simulation drawn from Zhou (1991).

In this illustrative simulation, only the main coronary arterial pressure boundary condition was altered. In lieu of modifying the vascular compliances, the cross-sections of the coronary vasculature were altered directly by imposing a simplistic ad hoc functional multiplier intended to simulate the observed relationship between elevated blood pressure elicited by increased metabolic demands and neural factors and the substantial induced dilatory effect on the coronary vasculature.

The measured response of canine coronary blood flow to treadmill exercise is depicted in Fig. 13, as reported by Khouri et al (1965).

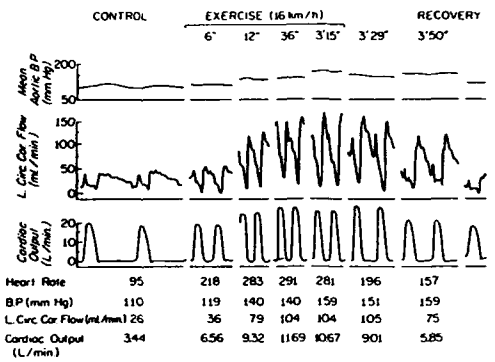

Figure 13: Experimental record of treadmill exercise on coronary flow in a dog (from Khouri et al 1965).

Using our simplified model as a basis, the heart rate was increased from 82 bpm at rest to 164 bpm during exercise, while the resting level aortic pressure of 120/80 mmHg was raised 40% during exercise, as was the IMP. The computed variations in coronary arterial pressure and flow rate are set out in Figs. 14 and 15 respectively.

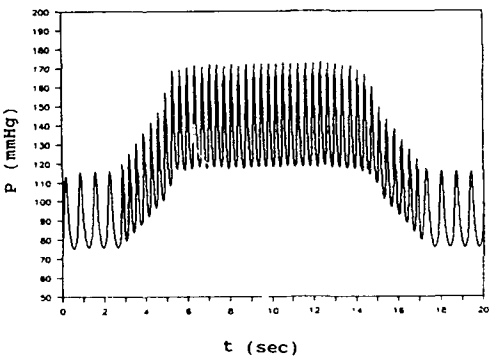

Figure 14: Computed coronary arterial pressure during exercise

The mean flow rate is seen to double simultaneously with rising coronary arterial pressures, remaining relatively stable from 6 to 14 seconds until recovery. Improved results will be forthcoming from the model upon incorporation into it of more realistic relationships for alterations in vascular tone (or compliance), from which concomitant variations in vessel lumen may be computed, instead of imposed as in the case reported here. Nonetheless, this illustration serves to give a preview of the power of the generalized model to account for extremely complex physiological responses to exercise and gravitational stress.

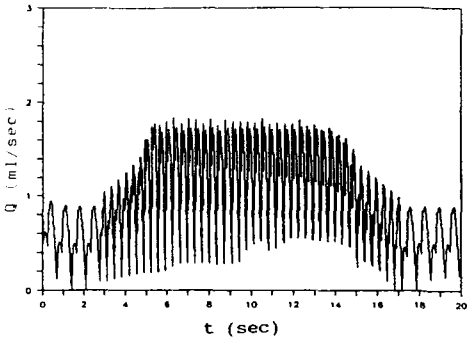

Figure 15: Computed coronary arterial flow rate during exercise (Zhou 1991)

3. PROTECTIVE COUNTERMEASURES AGAINST EXPOSURE TO GRAVITATIONAL STRESSES

The current generation of highly maneuverable fighter aircraft of the type F-14, F-15, F-16 and F-18 have propulsive power so great as to exclude the pilot from substantial portions of their operational envelopes. During aerial combat maneuvers, aircraft rates of onset of acceleration can attain 10 to 15 G in under one second, and can be sustained at these G-levels for 45 seconds or more. These flight conditions are traumatic for the pilot and aircrew, evoking simultaneous loss of vision (LOV) and loss of consciousness (LOC). Similar levels of gravitational stress can be expected during certain phases of manned space flight to Mars (National Academy of Sciences Report 1968, ed. Peterson).

Presently, pilots of combat aircraft wear an anti-G suit and engage in fatiguing continuous coordinated straining maneuvers (respiratory M-1, etc., and skeletal muscular) in an imperfect attempt to maintain vision and normal cardiac function in the face of severe $+G_z$ acceleration.

In this section will be considered briefly the anti-G suit and electrocutaneous stimulation of the autonomic nervous system ANS as potentially effective countermeasures of protection against sustained gravitational stress.

3.1 Anti-G Suits and their Limitations

An excellent review of the subject, extending back to the early work in Germany, England and the U.S. in the 1930's on the development of anti-G protective suits has been published by Wood in 1987. The clear and unequivocal conclusion developed there is that inherent limitations in the very concept of an anti-G suit render it inadequate, even in combination with currently practiced straining maneuvers, and that one should rather consider re-positioning the pilot into a more horizontal (preferably prone) position in the cockpit. The basic ideas behind this conclusion are important and merit to be summarized below.

The principle physiological objective in designing an anti-G suit is to provide the level of arterial hypertension at heart level necessary to support an arterial pressure at head level sufficient to maintain pilot vision and consciousness throughout aerial combat. In the 1930's, the prevailing concept was that caudalward gravitational stress exacerbated pooling of blood, particularly in the lower member distensible venous system, and consequently, one should design anti-G suits to prevent the presumed decrease in venous return to the heart. However, subsequent centrifuge studies (Wood et al 1946) indicate that *arterial pressure*, rather than venous return, is the major determinant of G tolerance in the sitting position. This is likely due to the intervention of the autonomic nervous system (ANS) as described in §1 and §2 above, which had not been fully appreciated in the 1930's.

Much higher levels of G protection were afforded by arterial occlusion suits than by those purpor edly designed to promote venous return. In fact, in 1942, an automated rapid inflation valve air bladder version was developed by D. M. Clark at the Mayo Centrifuge Laboratory (see Wood 1987). This suit, incorporating a very rapid high pressure inflation of the bladder system from the ankles upward toward the abdomen, provided an average protection of 2.1 G, which could be increased to 2.9 G with the addition of 2 arterial occlusive arm cuffs. However, the discomfort associated with the operation of this and slightly modified occlusive systems precluded pilot acceptance. Since World War II, only a less effective (but more comfortable) non-progressive single bladder system, incorporated into a variety of snugly-fitting garments, has found wide favor with pilots to this day. This system affords however a protection of only 1.9 G.

With the advent of the present generation of powerful modern combat aircraft, even a well-trained fighter pilot proficient in respiratory M-1 etc. maneuvers cannot always generate, while wearing an anti-G suit as well, sufficient levels of arterial pressure at the aortic valve level to prevent black-out.

That level of arterial pressure required to overcome the hydrostatic pressure gradient between the heart and brain at + 10 G_z is of the order of some 300 mmHg. Below that level, a sudden exposure to + 10 G_z results in equally sudden cessation of cerebral blood flow, and about 6 sec. later, to loss of vision and loss of consciousness in rapid succession.

More modern very high G suit protection (eg. Moore et al 1987), which may possibly extend beyond the physiologically limited levels that can presently be generated by a pilot, present a potential danger of cardiocirculatory and respiratory injury associated with the elevated cardiovascular preload and afterload needed to generate such protective levels of arterial pressure above 8 to 9 G_z exposures.

Faced with such physiological limits in the tactical operation of present-day fighter aircraft, Wood (1997) concluded that it will be necessary to reduce the heart-to-brain arterial pressure difference by re-positioning the pilot into a reclining or preferably prone position (with counterweighted head support). In the supine position at high G

levels, the heart is exposed to $+G_x$ acceleration, leading to a dramatic dorsalward displacement with concomitant severe overdistension of the ventral region of the lung (Wood 1986).

If the associated substantial re-design of the cockpit required to accommodate a prone disposed pilot is not presently practical, it may be of interest to consider a controlled intervention on the autonomic nervous system of the pilot as an alternate means of providing enhanced compensation for caudalward shifts in blood volume during exposure to high levels of $+G_z$ acceleration. This radical approach is considered briefly in the following section.

3.2 Electrocutaneous Stimulation of the Autonomic Nervous System

The effects of $+G_z$ stress on coronary blood flow were outlined in §2.1, with particular reference to the arterial baroreceptor reflex and the autonomic nervous system (ANS) as depicted in Fig. 1a and 1b. It is useful at this point to view the control system regulating the cardiovascular circulation within the broader framework depicted in Fig. 16 below:

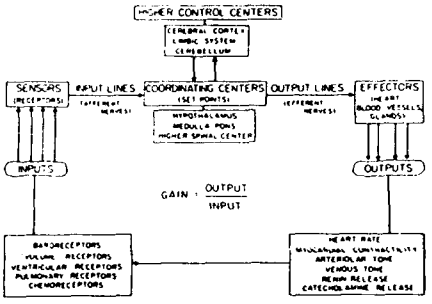

Figure 16: Overall cardiovascular control system.

Fig. 16 depicts the major cardiovascular control systems available to humans. Of particular importance are the receptors that sense the variables to be regulated. These sensors report their status to a coordinating area in the central nervous system (CNS) which must then compare the input information with a previously determined set point, which is itself alterable by higher control centers for the variable involved. Finally, the coordinating centers issue their orders to effectors which must respond accordingly to produce the desired changes.

The *baroreceptor reflex* is the best known mechanism for arterial pressure control. A rise in pressure stretches the baroreceptors (Fig. 17) and causes them to transmit signals to the CNS while efferent signals are sent back through the ANS to reduce the arterial pressure back to normal levels. The baroreceptors possess spray-like nerve endings lying within the walls of the arteries (carotid, aorta). The greatest sensitivity or maximum gain occurs over normal ranges of blood pressure. The receptors do not respond to pressures below 50 - 60 mmHg and are maximally activated at a pressure of about 200 mmHg. In the case of increased arterial pressure, the baroreceptor signals entering the brain stem inhibit the vasoconstrictor center of the medulla and excite the vagal center (Fig.16). The net effects are: a) arteriolar vasodilation, b) decreased heart rate and c) venous system dilation. Excitation of the baroreceptors by pressure in the arteries reflexly causes the arterial pressure to decrease. Similarly, low pressure has an opposite effect which reflexly causes the pressure to rise back toward its normal level.

Baroreceptor control is cited as a principal reason for the tachycardia and bradycardia which is clearly activated during exposure to g-stress. As mentioned above, the baroreceptors respond to the decrease in blood pressure initially observed during acceleration stress by increasing the heart rate. Pilot straining techniques, such as the M-1 respiratory maneuver, then raise the intrathoracic pressure, to which the baroreceptor responds by lowering heart rate. The carotid sinus nerve, when sectioned, removes the tachycardia response as well as the compensatory rise in arterial pressure during gravitational acceleration.

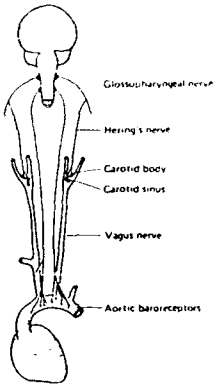

Figure 17: The baroreceptor system

The clear goal in increasing human tolerance to $+G_z$ acceleration resides in preventing substantial falls in the arterial pressure of the cardiovascular system. In view of the physiological limitations discussed earlier in §3.1 in maintaining a 300 mmHg heart-to-head pressure differential in pilots at $+10\ G_z$, rising to 450 mmHg at $+15G_z$, by purely mechanical external compression (anti-G suits), it is suggested here that one may wish to examine the possibility of "intelligent" countermeasures based on a novel stimulation or inhibition of the reflex neurotransmission in the ANS by the generation of a distributed electric field using arrays of skin-mounted non intrusive electrodes.

Such a proposition may be fraught with undesired adverse responses, and in any event requires a precise knowledge of the firing of the nerve fibres and the interaction of nerve cells with electric currents.

A very clear and concise review of the physiological basis for such interactions has been set out by Reilly (1988). The main features of electrical excitation models will be discussed briefly below.

The main functional sensory neuron

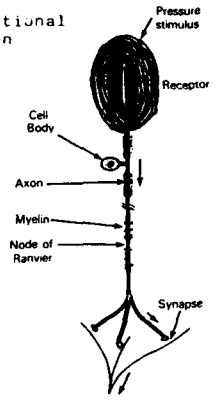

Figure 18: Sensory neuron components

Information is transmitted in the direction indicated by the arrows. Neural signals are propagated across the synapses (gaps) via chemical neurotransmitters and elsewhere by membrane depolarization (see Fig. 20). The neurons are covered with a fatty layer of insulation called myelin, and have unmyelinated (exposed) nodes of Ranvier. The conducting portion of the neuron is a long hollow structure known as the axon. The combination of axon plus myelin wrapping is referred to as a nerve fibre. Nerve impulses, called action potentials (AP) propagate from one of a variety of specialized receptors, such as the baroreceptors described above, and proceed to a synapse in the spinal column. Communication across the synapses is assisted by chemical substances known as neurotransmitters.

The cell bodies (see Fig. 18) are bounded by very thin membranes, about 8-nm thick. Electrochemical forces across the membrane help regulate chemical exchanges between the cell contents (plasm) and the outer interstitial fluid. These two fluids contain different ions of differing concentrations which set up electrochemical force gradients across the cell membrane. The semi-permeable membrane, basically a dielectric insulator, permits a controlled ionic interchange in a selective manner (Fig. 19). An active metabolic pump drives particular ions into and out of the cell. The transmembrane potential difference is about -90 mv; the inside is negative with respect to the outside.

The work required to move a mole of ionic species S across the membrane depends on the total electrochemical potential difference, which is the sum of the concentration and electrical potentials W_c and W_e respectively.

Since the concentration potential W_c is proportional to the difference of the logarithm of the concentration (S)

$$W_c = RT(\ln(S)_i - \ln(S)_o) = RT \ln \frac{(S)_i}{(S)_o} \qquad (8)$$

and the electrical potential W_e is simply

$$W_e = Z \mathcal{F} V_m \qquad (9)$$

proportional to the potential difference V_m across the membrane, then an equilibrium will exist when the total electrochemical potential across the membrane (W_t) = 0.

That point of transmembrane equilibrium

$$W_t = 0 = RT \ln \frac{(S)_i}{(S)_o} + Z \mathcal{F} V_m \qquad (10)$$

defines the transmembrane potential

$$V_m = \frac{RT}{\mathcal{F} Z} \ln \frac{(S)_o}{(S)_i} \qquad (11)$$

which is known as the *Nernst potential*.

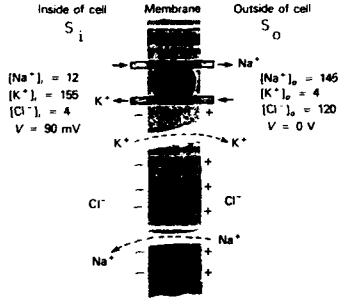

Figure 19: Schematic of a cell membrane

In the Fig. 19 above it is seen from the magnitudes and the signs of the potentials shown that a strong electrochemical force tends to drive Na^+ into the cell, while a relatively weaker force tends to drive K^+ out of the cell. A state of equilibrium would eventually be reached were it not for the action of the sodium pump, an active system fuelled by the metabolism of the cell, which works in the opposite direction, tending to maintain the disequilibrium. The conductivity of this excitable cell is closely related to membrane field; disturbances from the equilibrium state can alter dramatically the electrical properties of the membrane, and thereby, the functional responses of nerve fibre transmission.

The resulting change in membrane voltage V_m will also affect adjacent portions of the membrane, and, in a nerve, will propagate as a nerve impulse. The response of the excited membrane is known as an *action potential*. The membrane voltage change, the membrane conductance and the various and total ionic currents can be calculated as functions of time during the propagation of an action potential (Reilly 1988) for both the Hodgkin-Huxley membrane (unmyelinated nerve cells) and Frankenhaeuser-Huxley membrane (generalized to myelinated nerve cells).

The propagation of nerve impulses through the generation of action potentials can be described briefly by referring to Fig. 20. The voltage disturbance caused by a stimulating electrode will tend to decrease the

membrane potential *(depolarization)* near the cathode and increase the potential *(hyperpolarization)* elsewhere along the axon.

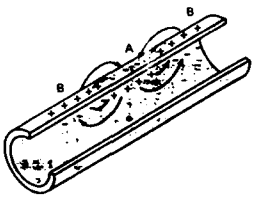

Figure 20: Propagation of depolarization wave front along an axon

As an example, consider (Fig. 20) that a point A on the axon is depolarized, causing ions to move between adjacent points on the axon. *In this way, the depolarization* wave front spreads in both directions, away from the site of stimulation by an external electrode.

After the membrane has recovered its resting potential, it cannot be re-excited until a *recovery period* has passed, known as the *refractory state* of the membrane. This recovery is progressive as the membrane becomes partially refractory during the recovery period.

As a refreshing alternative to anti-G suits and straining maneuvers to modulate the response of the cardiovascular system to g-stress, one may consider the enormous variety of electrical stimuli of the sensory neurons. Vastly different stimulation thresholds can result from alterations in the stimulus wave-form or electrode configuration (Reilly 1988). These relationships relating excitation currents imposed by external arrays of electrodes with the properties and response of the excited tissues may be computed using relatively straightforward models, of which a wide variety exists in the published literature. Although a number of these nonlinear models require a knowledge of the current wave-form and density which crosses the membrane, the myelinated fibre model of McNeal (1976) does not.

The model described by Reilly (1988) is an extension of the McNeal model, with modifications to include nonlinearities associated with the Frankenhaeuser-Huxley myelinated nerve membrane at each of several adjacent nodes. Additional extensions include a test for excitation based on AP propagation, the ability to model arbitrary stimulus wave-forms, the representation of stimulation at the neuron terminus, and the representation of stimulation by uniform electric fields.

Application of this spatially extended nonlinear nodal (SENN) model by Reilly (1988) to electrocutaneous sensory stimulation has resulted in a general determination of the spatial distribution requirements for *neural excitation*.

Fig. 21 illustrates two bipolar electrode arrangements for stimulating a nerve fibre. The electric field in the medium is the primary force governing stimulation, even though current density is perhaps a more frequently cited parameter.

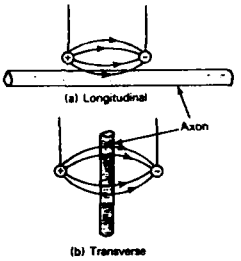

Figure 21: Electrode stimulation of a nerve fibre

The stimulation thresholds can be controlled through tailoring of the excitation pulse. A biphasic pulse may have a higher excitation threshold than a monophasic pulse by reversing a developing AP that was excited by the initial phase. Accordingly, it may be of interest to combine particular patterns of say rectangular monophasic constant-current stimuli, symmetric biphasic rectangular and sinusoidal stimuli to achieve the desired thresholds with respect to the level of g-stress exposure and its duration.

Thresholds are most elevated when the pulse is short and the current reversal immediately follows the initial pulse. Below 40 Hz, thresholds rise for sinusoidal stimulation. At low frequencies, the slow rate of change prevents the membrane from building up a depolarization voltage because of membrane leakage. In contrast, no upturn in threshold appears at low frequencies with square-wave biphasic stimuli whose rate of change is not frequency-dependent.

According to Reilly (1988), repetitive stimuli can be more potent than a single stimulus, as an integration of the multiple pulses occurs, either through a reduction in the threshold or through enhancement of the response due to multiple generation of AP's. These integrations take place at the membrane level and at higher levels within the CNS, respectively. The threshold for a 3-pulse stimulus can fall about *20% below that for a single pulse.*

However, it should be emphasized once again that external interference with the normal firing response of the autonomic nervous system under exposure to gravitational stress may have both favorable and adverse effects on the compensatory mechanisms required to maintain arterial pressure and thus enhance human tolerance to high sustained gravity.

Both the favorable and adverse implications on the ANS must be weighed very carefully in formulating effective countermeasures through direct electrocutaneous stimulation of the nervous system. This will, in itself, require a significant program of controlled research. It is suggested here that a successful *direct* control of the ANS compensatory responses to G-stress could result in a significant improvement over present methods focussed entirely on

the mechanical control of fluid volume shifts via anti-G suits and respiratory and muscular straining maneuvers, both of which appear to be reaching their physiological limits within the framework of the present generation of highly powerful aircraft and launching systems.

4. CONCLUSIONS

The field of human cardiovascular response to gravitational stress has important implications for both aviation physiology and space travel. In both applications, the technological means of propulsion and guidance appear to be far ahead of man's ability to adjust to them. Accordingly, Man can be viewed as the "weak link in the chain", and far more research must be devoted to the study of human adaptation to varying gravitational force fields.

As the physiological mechanisms which Man puts into play in an involuntary, but not always successful, effort to "compensate" for these new environmental conditions invariably involve the nervous system and its complex interaction with the cardiovascular circulation, it is evident that an important by-product of such research will be an improved understanding of cardiovascular physiology on Earth. Such clinical topics as chronic hypertension are one of many potential beneficiaries of such future research programs.

In the present work, we have proposed a comprehensive model of relative simplicity as a framework for the formulation of effective countermeasures designed to enhance G-tolerance of combat pilots operating the present generation of high performance fighter aircraft.

5. REFERENCES

1. Beyar R., S. Sideman: A computer study of the left ventricular performance based on fiber structure, sarcomere dynamics, and transmural electrical propagation velocity. Circ. Res. 55, 358-375 (1984).
2. Beyar, S. Sideman: Time-dependent coronary blood flow distribution in left ventricular wall. Am. J. Physiol. 252, (Heart Circ. Physiol. 21), H417-H433 (1987).
3. Blomquist G.G., H.L. Stone: Cardiovascular adjustments to gravitational stress. In Handbook of Physiology, §2: The Cardiovascular System, chapt. 28, pp. 1049-1063 (1979).
4. Collins R.: Pulsatile flow in a collapsible tube subjected to longitudinal tension. In Comput. Methods & Experimental Measurements, vol. I, §3: Fluid Dynamics, pp. 221-240, Springer Verlag, Berlin (1986).
5. Collins R., E.M. Collins: Cardiovascular response under accelerative loading. In Physiological Fluid Dynamics II Proc. 2nd Intl. Conf. Physiol. Fluid Dynamics, ed. L.S. Srinath & M. Singh, Tata McGraw-Hill, pp. 229-236 (1987).
6. Erikson H.H., Sandler H., H.L. Stone: Cardiovascular function during sustained +G stress. Aviat Space Environ. Med. 47, 750-758 (1976).
7. Greenleaf J.E., Brock P.J., Haines R.F., Rositano S.A., Montgomery L.D., L.C. Keil: Effect of hypovolemia, infusion, and oral rehydration on plasma electrolytes, ADH, renin activity and $+G_z$ tolerance. Aviat. Space Environ. Med. 48, 693-700 (1977).
8. Gregg D.E., D.C. Sabiston: Current research and problems of the coronary circulation. Circ. 13, 916-927 (1956).
9. Heineman F.W., J. Grayson: Transmural distribution of intramyocardial pressure measured by micropipette technique. Am. J. Physiol. 249 (Heart Circ. Physiol. 18) H1216-H1223 (1985).
10. Hoffman J.I.E., J.A.E. Spaan: Pressure-flow relation in coronary circulation. Physiol. Rev. 70, 331-390 (1990).
11. Khouri E.M., Gregg D.E., C.R. Rayford: Effect of exercise on cardiac output, left coronary flow and myocardial metabolism in the unanesthetized dog. Circ. Res. 17, 427-437 (1965).
12. Laughlin M.H.: The effects of $+G_z$ on the Coronary Circulation: A review. Aviat. Space Environ. Med.p. 5 (1986).
13. Marieb E.N.: Human Anatomy and Physiology. Benjamin/Cummings Publ., Redwood City, CA, p. 449 (1989).
14. Moore T.W., Foley J., Reddy B.R.S., Kepics F., D. Jaron: An Experimental Microcomputer-Controlled System for Synchronized Pulsating Anti-Gravity Suit. Aviat. Space Environ. Med. 58, 710-714 (1987).
15. McNeal D.R.: Analysis of a Model for Excitation of Myelinated Nerve. IEEE Trans. Biomed. Eng. BME-23, 329-337 (1976).
16. Peterson L.H. (ed.): Physiology in the Space Environment. Vol. I: Circulation. Report of a study conducted by the Space Science Board of the Nat. Acad. Sci., Nat. Res. Council 1966-1967, Publ. N°1485 A, NAS, Washington D.C., p. 144 (1968).
17. Reilly J.P.: Electrical models for neural excitation studies. Johns Hopkins APL Tech. Digest 9,1:44-59 (1988).
18. Wood E.H.: Contributions to aeromedical research to flight and biomedical science. Cause and prevention of G-LOC. Aviat. Space Environ. Med. 57 (Suppl.) A 13-23 (1986).
19. Wood E.H.: Development of Anti-G Suits and their Limitations. Aviat. Space Environ. Med. 58, 699-706 (1987).
20. Wood E.H., G.A. Hallenbeck: Voluntary (self-protective) maneuvers which can be used to increase man's tolerance to positive acceleration. Fed. Proc. 5, 118 (1946).
21. Zhou S.H.: A mathematical model of the human coronary circulation. PhD dissertation, Halifax, Canada (1991).
22. Zhou S.H., Mateeva E., R. Collins: A mathematical model for response of the coronary circulation to high sustained force fields. In Advances in Fluid Dynamics, ed. W.F. Ballhaus & M.Y. Hussaini, Springer-Verlag, 284-304 (1989a).
23. Zhou S.H., Mateeva E., R. Collins: A Computational Model for Blood Flow in the Heart Under External Force Fields. In Proc. 4th Intl. Conf. Comput. Methods Experimental Measurements, Springer-Verlag, 22 p. (1989b).

BIOMECANIQUE CIRCULATOIRE. EFFETS DES ACCELERATIONS.

(*) D. GAFFIE,(**) P. QUANDIEU, (***) Ph. LIEBAERT,
(****) D. COHEN-ZARDY, (****) T. DAUMAS, (**) A. GUILLAUME

(*) ONERA, Direction de l'Energétique,
29, Avenue de la Division Leclerc, BP. 72
92320 Chatillon-Cedex (FRANCE)
(**) Centre d'Etudes et de Recherches de Médecine Aérospatiale,
Division Biomécanique, Base d'essais en vol, 91228 Brétigny sur Orge (France)
(***)Direction des Recherches Etudes et Techniques Tour D.G.A.
Service des Recherches/G9, 26 Bvd Victor Paris 00457 Armées (France)
(****) Ecole Polytechnique, Route de Saclay,
91128, Palaiseau (France)

Sommaire

Un modèle physique général traitant du comportement de l'écoulement de sang dans les vaisseaux, est proposé dans le but de mieux comprendre les mécanismes produisant les pertes de connaissance observées chez les pilotes d'avions de chasse. Le cas est étudié en supposant l'action simultanée du coeur et des perturbations extérieures induites par le mouvement de l'avion. Ces dernières sont à la fois d'origine volumique et surfacique. Les résultats de calcul montrent que sous certaines conditions on peut observer une limitation du débit de sang dont l'origine est une modification du régime de l'écoulement. Ceci conduit à proposer une hypothèse selon laquelle dans le cas d'une application très rapide du facteur de charge, la perte de connaissance pourrait avoir une autre origine qu'une hypoxie cérébrale due à la fuite du sang vers les membres inférieurs du pilote.

Liste des symboles

C célérité des ondes pariétales.
fz composante longitudinale de la force volumique.
F force volumique imposée
M nombre sans dimension analogue au nombre de Mach.
p pression hydrodynamique du sang
Pe(z,t) pression extérieure s'exerçant sur la paroi du vaisseau.
Ps périmètre mouillé
Re nombre de Reynolds
S(z,t) section du vaisseau.
U(z,t) vitesse moyenne de l'écoulement sanguin
Vr, Vz,Vθ composantes du vecteur V
V vitesse de l'écoulement sanguin
σ tenseur des contraintes
τ tenseur des contraintes visqueuses
ε petit paramètre adimensionnel
$\alpha(z,t)$ fonction introduite par l'intégration des équations
τrz contrainte visqueuse de cisaillement
τp contrainte visqueuse moyenne de cisaillement à la paroi.

1 - Introduction

La perte de connaissance des pilotes d'avions de chasse est un phénomène connu depuis plusieurs décennies. Dans le cas d'une mise en accélération lente, son origine est hypoxique. En effet, sous l'action de la force centrifuge imposée (virages accélérés descendants), le sang s'accumule dans les territoires veineux inférieurs du fait de la grande distensibilité des veines. Ceci produit une baisse du débit sanguin cérébral.

Travail effectué sous contrat D.R.E.T.

Il apparaît alors un voile gris, puis un voile noir et éventuellement survient une perte de connaissance en vol si les mécanismes régulateurs de la pression artérielle n'interviennent pas rapidement. Le temps de conscience utile peut être prolongé grâce à l'utilisation d'un pantalon anti-G.

Dans le cas où le facteur de charge est imposé rapidement, on observe une modification sensible du syndrome de la perte de connaissance. Le voile gris n'apparaît plus. La perte de connaissance est instantanée, non reproductible et s'accompagne d'une amnésie lacunaire. La question est donc de savoir si dans le cas d'une mise en accélération rapide l'explication d'une origine hypoxique de la perte de connaissance peut être maintenue. Le modèle que nous proposons peut fournir un élément de réponse sur le plan exclusivement mécanique. Il décrit l'écoulement du sang dans un vaisseau dans le cas général où les actions du coeur et des forces extérieures sont imposées simultanément. Il montre que la nature des écoulements de sang est liée à la célérité des ondes pariétales qui se propagent à la paroi des vaisseaux et prend en compte les effets de l'évolution des contraintes dans le tissu cérébral.

2 - Formulation mathématique

2.1 Equations du problème

Les équations de conservation de la masse et de la quantité de mouvement sont écrites en considérant le sang comme un fluide visqueux et incompressible:

$$\operatorname{div} \vec{V} = 0$$

$$\rho \frac{d\vec{V}}{dt} = \vec{F} + \operatorname{div} \sigma \qquad (1)$$

F représente la force volumique, elle est une donnée du problème. σ est le tenseur des contraintes qui s'exprime en fonction de la pression hydrodynamique p et du tenseur des contraintes visqueuses τ.

$$\sigma = -p.I + \tau \qquad (2)$$

La donnée d'une loi de comportement associée à la nature du fluide permet de relier les contraintes aux déformations. Dans les applications, le sang sera considéré comme un fluide newtonien.

2.2 Hypothèses simplificatrices

Le problème élémentaire que nous traitons est représenté sur la figure suivante. Il s'agit de l'écoulement du sang dans un vaisseau déformable. Le mouvement est dû à l'action simultanée du coeur (écoulement pulsé), et d'un champ de perturbations produit par le mouvement de l'avion.

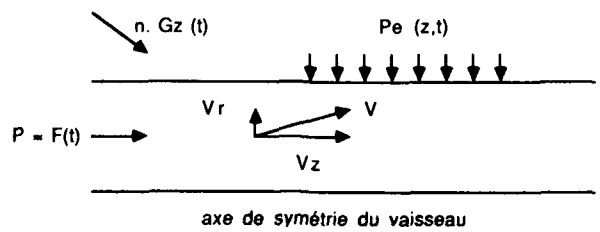

Dans le modèle considéré, ce champ de perturbations extérieures est constitué à la fois par la force volumique F qui est directement prise en compte dans les équations et par une distribution de pression extérieure que l'on répartit le long des vaisseaux . Il s'agit pour ce dernier point de prendre en compte les évolutions du champ des contraintes au sein du tissu cérébral dues à l'application du facteur de charge. Les équations locales sont naturellement écrites dans un repère de coordonnées cylindriques dans le cas le plus général. On suppose toutefois la symétrie de l'écoulement et de la déformation du tube par rapport à l'axe du conduit.

Dans le but d'évaluer l'ordre de grandeur des différents termes des équations précédentes, on introduit le paramètre ε rapport des vitesses caractéristiques dans les directions radiale et longitudinale.

Si l'axe du vaisseau peut être considéré comme la direction privilégiée de l'écoulement, on peut admettre que ε est toujours très inférieur à l'unité.

$$\varepsilon = \frac{Vo}{Uo} = \frac{Ro}{L} \ll 1 \qquad (3)$$

On suppose de plus que le nombre de Reynolds rapport des forces d'inertie aux forces de viscosité n'est pas trop grand, ceci, afin de conserver l'influence des effets de viscosité:

$$Re^{-1} = \frac{\sigma_o}{\rho . U_o^2} \quad O(1) \qquad (4)$$

Une étude de l'ordre de grandeur de ces différents termes en suivant les hypothèses (3) et (4) permettent de déduire une formulation simplifiée des équations générales (1). Nous obtenons:

$$\frac{\partial}{\partial r}(rV_r) + \frac{\partial V_\theta}{\partial \theta} + \frac{\partial}{\partial z}(rV_z) = 0$$

$$\rho\left(\frac{\partial}{\partial t}(rV_z) + \frac{\partial}{\partial r}(rV_rV_z) + \frac{\partial}{\partial \theta}(V_\theta V_z) + \frac{\partial}{\partial z}(r V_z^2)\right) =$$

$$\rho r f_z - \frac{\partial}{\partial z}(rp) + \frac{\partial}{\partial r}(r\tau_{rz}) + \frac{\partial}{\partial \theta}(r\tau_{\theta z})$$

$$\frac{\partial p}{\partial r} = \frac{\partial p}{\partial \theta} = 0 \qquad (5)$$

Ce système simplifié, montre qu'en première approximation, la pression peut être considérée comme uniforme dans chaque section. Pour les conditions aux limites, on suppose la symétrie par rapport à l'axe du vaisseau, ainsi que l'adhérence à la paroi.
En considérant le mouvement de la paroi du vaisseau, on montre aisément que cette dernière condition se traduit par la relation:

$$(V_r)_R = \frac{\partial R}{\partial t} + \left(\frac{V_\theta}{r}\right)_R + \frac{\partial R}{\partial z}(V_z)_R \qquad (6)$$

Les effets de torsion et d'étirement suivant z seront en général négligés.

2.3 Formulation unidimensionnelle

Le système précédent fait apparaître la faible dépendance de l'écoulement par rapport aux deux directions transversales. Il paraît donc naturel de rechercher une formulation unidimensionnelle des équations du problème (ref: [2], [7]). Celle-ci est obtenue par intégration des équations précédentes sur une section quelconque du vaisseau S(z,t). On définit la vitesse moyenne de l'écoulement:

$$U(z,t) = \frac{1}{S}\int_0^{2\pi} \left(\int_0^R r V_z dr\right) d\theta \qquad (7)$$

Nous obtenons finalement le système d'équations unidimensionnelles suivant:

$$\frac{\partial S}{\partial t} + \frac{\partial}{\partial z}(SU) = 0$$

$$\frac{\partial U}{\partial t} + (1-\alpha)\frac{U\partial S}{S\partial t} + \alpha U\frac{\partial U}{\partial z} + U^2\frac{\partial \alpha}{\partial z} = \qquad (8)$$

$$f_z + \frac{1}{\rho}\left(-\frac{\partial p}{\partial z} + P_s\frac{\tau_p}{S}\right)$$

U et S sont les variables principales du système. p est la pression supposée uniforme dans la section. La contrainte moyenne de cisaillement à la paroi τ_p est obtenue par la relation:

$$\tau_p = \frac{1}{P_s}\int_0^{2\pi} (r\tau_{rz})_R \, d\theta \qquad (9)$$

Le terme α qui apparaît dans l'équation de conservation de la quantité de mouvement (8) est dû à l'intégration des termes non-linéaires. Il est défini par la relation suivante:

$$\alpha(z,t) = \frac{1}{SU^2}\int\int V_z^2 dS \qquad (10)$$

2.4 Hypothèse de fermeture

Les inconnues du système unidimensionnel (8) sont la vitesse moyenne, la section du tube, la contrainte τ_p, la pression p et le paramètre α. Soit 5 inconnues pour 2 équations. On cherche donc des relations supplémentaires qui permettent l'obtention d'un système complet.
Si l'on suppose le fluide newtonien, et que l'on se place dans le cadre de l'hypothèse (3), la composante locale τ_{rz} a pour expression:

$$\tau_{rz} = \mu\frac{\partial V_z}{\partial r} \qquad (11)$$

Les relations (9), (10) et (11) font apparaître que la donnée d'une loi de profil pour la composante de vitesse V_z permet de calculer la contrainte pariétale τ_p et le paramètre α.

On introduit donc une nouvelle hypothèse dite loi des profils semblables qui suppose l'existence de profils homothétiques pour toute section du tube et à tout instant:

$$V_z(r,\theta,z,t) = U(z,t).g(\frac{r}{R}) \qquad (12)$$

On déduit de cette nouvelle hypothèse les deux relations supplémentaires suivantes:

$$\tau_p = \frac{2\pi\mu U}{P_s}(\frac{dg}{d\beta})\beta=1$$
$$\alpha = 2\int_0^1 g(\beta).\beta.d\beta \qquad (13)$$

On remarque que dans le cadre de l'hypothèse (12), α est constant. Il faut établir une dernière relation pour la pression, *celle-ci est obtenue en* exprimant la compatibilité entre le mouvement du fluide et le mouvement de la paroi du vaisseau.

2.5 Couplage fluide/paroi

Les mouvements du fluide et de la paroi n'étant pas indépendants, il est nécessaire de définir une relation supplémentaire pour l'expression du couplage *entre* les propriétés mécaniques du fluide et de la paroi. Dans le cadre d'une étude quasi-statique, en considérant la paroi du vaisseau comme un milieu isotrope et *en négligeant* les déplacements dus aux tensions axiales, l'application de la loi fondamentale de la dynamique à la paroi du tube conduit à la "loi de tube" suivante:

$$p - p_e = K(z).P\ (S/S_0) \qquad (14)$$

Le coefficient K caractérise la rigidité du tube et la loi *P* est une fonction fortement non-linéaire de la section adimensionnelle. p-p_e est la pression transmurale; différence entre la pression au sein de l'écoulement et la pression extérieure s'exerçant sur la paroi latérale du vaisseau.

Toute perturbation du système étudié va inévitablement générer des ondes de surface. Celles-ci vont se propager suivant la direction longitudinale z.

La célérité de ces ondes pariétales s'exprime en fonction de la pression transmurale par la relation suivante:

$$C^2(S/S_0) = \frac{S}{\rho}\frac{\partial}{\partial S}(p-p_e) \qquad (15)$$

Le comportement non-linéaire exprimé par la loi *P* conduit à une forte dépendance de la célérité par rapport à l'état local de déformation du vaisseau. La figure (1) représente les courbes *P* et C/100 en fonction de la section adimensionnelle. La loi de tube qui est représentée a été obtenue à l'aide d'une fonction rationnelle approchant les résultats expérimentaux de Kamm et Shapiro [1].

On peut observer que pour une pression transmurale positive, le tube est dilaté et constitue un système plus rigide. Il s'ensuit que la célérité des ondes de surface est élevée. Dans le cas contraire, où la pression transmurale est négative, le tube subit un collapsus. Il est alors moins rigide et la célérité des ondes associée à un tel état est beaucoup plus faible (ref: [9], [10], [11], [12])

On peut définir un régime d'écoulement subcritique ou supercritique selon que la vitesse moyenne U est respectivement inférieure ou supérieure à C. Par analogie avec les problèmes de dynamique des gaz, il peut être utile de définir un nombre sans dimension équivalent au nombre de Mach:

$$M = \frac{U}{C} \qquad (16)$$

Si l'on considère que la distribution de pression extérieure ne dépend que de z et de t, le couplage fluide/paroi peut être pris en compte simplement dans les équations en exprimant le gradient de pression intérieure sous la forme:

$$\frac{\partial p}{\partial z} = \frac{\partial (p - p_e)}{\partial z} + \frac{\partial p_e}{\partial z} \qquad (17)$$

Le système final que nous obtenons en introduisant dans (8), les relations (13) et (17) est le suivant:

$$\frac{\partial S}{\partial t} + \frac{\partial}{\partial z}(SU) = 0$$

$$\frac{\partial U}{\partial t} + (1-\alpha)\frac{U}{S}\frac{\partial S}{\partial t} + \alpha U \frac{\partial U}{\partial z} + \frac{1}{\rho}\frac{\partial (p - p_e)}{\partial z} = \qquad (18)$$

$$-\frac{1}{\rho}\frac{\partial p_e}{\partial z} + f_z + \frac{1}{\rho} P_s \frac{\tau_p}{S}$$

2.6 Forces extérieures et Conditions aux limites

Il apparaît clairement que la connaissance d'une distribution de pression extérieure Pe(z,t) permet le calcul de son gradient longitudinal. Ce dernier est ensuite introduit comme terme source dans l'équation du mouvement lors de la résolution numérique.

Le champ de forces volumiques induit par le mouvement de l'avion n'intervient dans la modélisation adoptée que par la seule composante axiale f_z qui est naturellement une donnée du problème.

L'action du coeur est prise en compte à l'aide de conditions aux limites. Elles sont données sous la forme de lois analytiques approchées dépendantes du temps à l'entrée et à la sortie du système. A l'entrée est considérée la pression intravasculaire carotidienne et à la sortie, il s'agit de la pression intravasculaire avant le lit capillaire. Pour la condition d'entrée l'exploitation des résultats expérimentaux issus de la bibliographie a permis d'obtenir l'approximation suivante du signal de pression:

$$p(mm\,Hg) = p_{diastole} + (p_{systole} - p_{diastole}).F(t.Hz - E(t.Hz)) \qquad (19a)$$

où Hz est la fréquence cardiaque et E la fonction partie entière. la fonction F a été obtenue de manière approchée par la méthode de Bernstein

$$\begin{aligned} F(X) = {} & -367056.2X^{20} + 3760594X^{19} - 20892181.5X^{18} + 85288929X^{17} \\ & - 266991961.5X^{16} + 625286397.6X^{15} - 1078175292X^{14} + 1363379124X^{13} \\ & - 1259926746X^{12} + 840312278X^{11} - 391387110.4X^{10} + 116992538X^{9} \\ & - 16338309X^{8} - 2096916X^{7} + 1387608X^{6} - 251940X^{5} \\ & + 21318X^{4} - 1425X^{3} + 152X^{2} - X \end{aligned} \qquad (19b)$$

3 - Résolution numérique

Une technique numérique de type volumes finis est mise en oeuvre pour la résolution du système (18). On recherche donc une écriture conservative des équations du problème, ceci, afin de pouvoir procéder ensuite à l' intégration de ces dernières sur les domaines constitués par chacune des mailles (application du théorème de la divergence). Dans le cadre du problème étudié, la non-linéarité de la loi de tube rend délicate une intégration spatiale du gradient de pression transmurale:

$$\frac{\partial(p-p_e)}{\partial z}=\frac{\partial(p-p_e)}{\partial S}\frac{\partial S}{\partial z}=\frac{\rho C^2}{S}\frac{\partial S}{\partial z} \qquad (20)$$

Cette remarque nous contraint , lors de la résolution à l'instant $(n+1)\Delta t$ pour une position quelconque du vaisseau, à l'utilisation d'une forme linéarisée de la loi de tube autour d'une valeur connue à l'instant $n\ \Delta t$:

$$P(X)-P(X^n)=\frac{dP}{dX}[X=X^n].(X-X^n) \qquad (21)$$

où X représente la section adimensionnelle S/S_0.

On en déduit une expression approchée de la célérité de propagation des ondes pariétales:

$$C^2=\frac{K}{\rho S_0}\frac{dP}{dX}[X=X^n].S=k_0.S \qquad (22)$$

L'introduction de cette expression dans le système (18) permet d'obtenir la formulation conservative des équations recherchées. Nous obtenons le système final approché suivant, écrit sous forme vectorielle:

$$\frac{\partial\vec{V}}{\partial t}+\frac{\partial\vec{F}}{\partial z}=\vec{G} \qquad (23)$$

avec:

$$\vec{V}=t(S\ ,\ S.U)$$

$$\vec{F}=t(S.U\ ,\ \alpha.S.U^2+\frac{1}{2}k_0S^2)$$

$$\vec{G}=t(0\ ,\ S.(\frac{1}{\rho}\frac{\partial p_e}{\partial z}+f_z+\frac{P_s}{\rho S}\tau_p+(\alpha-1)\frac{U}{S}\frac{\partial S}{\partial t}))$$

3.1 Construction du schéma numérique

Comme le montre la figure qui suit, l'intégration de l'équation précédente sur une cellule quelconque du maillage conduit à une nouvelle équation vectorielle qui met en jeu des quantités moyennées, sur le segment élémentaire de la maille, ainsi que les flux de ces quantités exprimés aux interfaces.

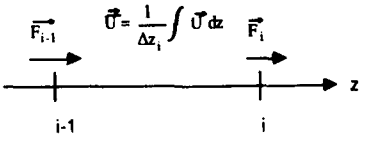

Nous obtenons pour une cellule quelconque i:

$$\Delta z_i \frac{\partial \vec{V}_i}{\partial t} + F_{i+1} - F_i = \vec{G}_i \qquad (24)$$

Le système constitué par la relation vectorielle précédente est un système ouvert qui ne peut être résolu directement. En effet, il met en jeu pour une cellule quelconque i, 4 inconnues (les deux composantes de V_i et F_{i+1}) pour uniquement deux équations. La résolution du problème impose donc d'introduire des relations supplémentaires. Ces dernières qui définissent le schéma spatial vont permettre de relier linéairement les flux aux interfaces à ceux exprimés à l'aide des quantités moyennées sur chaque cellule. On obtient donc:

$$\vec{F}_i = \sum_j \alpha_j \vec{F}_j \qquad (25)$$

A la différence des équations d'Euler, le flux F n'est pas une fonction homogène de degré 1 en V. Ceci est dû en particulier au caractère non-linéaire de la loi de tube. Toutefois, l'obtention d'une forme conservative des équations nous a contraint précédemment à la linéarisation de celle-ci dans le voisinage de la solution recherchée. On peut donc vérifier dans le cadre de cette approximation la relation suivante:

$$\vec{F} = \tilde{A}\,\vec{V} \qquad \text{avec} \qquad \tilde{A} = \begin{pmatrix} 0 & 1 \\ -\alpha.U^2 + \frac{1}{2} k_0 S & 2.\alpha.U \end{pmatrix} \qquad (26)$$

On déduit aisément d'après la relation (25) que le flux exprimé à l'interface d'une cellule de calcul à l'instant $(n+1)\Delta t$ s'écrit de la manière approchée suivante:

$$F_i^{n+1} = \sum_j \alpha_j \bar{F}_j^{n+1} = \sum_j \alpha_j \tilde{A}_j^n . \bar{U}_j^{n+1} \qquad (27)$$

Finalement, on constate que le flux à l'interface i est relié linéairement aux inconnues principales du problème V exprimées au même instant $(n+1)\Delta t$. Le schéma d'intégration dans le temps est donc de type implicite. Ce choix est justifié pour des raisons de stabilité.

3.2 Méthode de décomposition des flux

L'écriture de la relation (27), conduit à introduire des schémas d'intégration spatiale, centrés ou non, et dont la précision est liée à la fois au nombre de points choisis pour exprimer le flux F à l'interface et à la valeur des paramètres γ_j.

Bien que très largement utilisées, ces méthodes ne conduisent pas à une représentation précise des discontinuités qui peuvent être observées dans les écoulements. La technique de décomposition des flux (FLUX SPLITTING) que nous avons développée s'appuie sur les résultats issus de la méthode des caractéristiques (ref: [3], [4], [8]). Elle permet une adaptation automatique de la discrétisation en fonction des conditions locales d'écoulement rencontrées . Les travaux de Steger et Warming [13] sont à l'origine du développement de ces méthodes numériques.

Le principe de la méthode des caractéristiques est de rechercher, pour un système donné, l'existence de courbes du plan physique (z,t) et de définir, le long desquelles certaines loi d'évolution sont vérifiées (invariants de Riemann). Ces courbes sont appelées caractéristiques. Dans le cadre du système de nature hyperbolique que nous étudions, un calcul très classique permet de montrer qu'il existe deux familles de caractéristiques, notées respectivement [C+] et [C-]. La pente de ces courbes dépend de l'état local de l'écoulement. Nous avons:

$$(\frac{dz}{dt})_{C^+} = U + C \quad ; \quad (\frac{dz}{dt})_{C^-} = U - C \qquad (28)$$

où U représente la vitesse moyenne de l'écoulement et C la célérité des ondes pariétales. Ainsi, il peut être mis en évidence deux régimes d'écoulement suivant que U est inférieur ou supérieur à C. Dans le cas subcritique (U<C), la figure qui suit, montre que la solution en un point quelconque du plan physique dépend à la fois des états considérés à l'amont et à l'aval, le long des caractéristiques passant par M. En effet les deux caractéristiques C+ et C- sont respectivement de pente positive et négative. Dans le cas supercritique, les pentes des caractéristiques passant par M sont toutes deux positives, de sorte que la solution en M ne dépend que de l'amont.

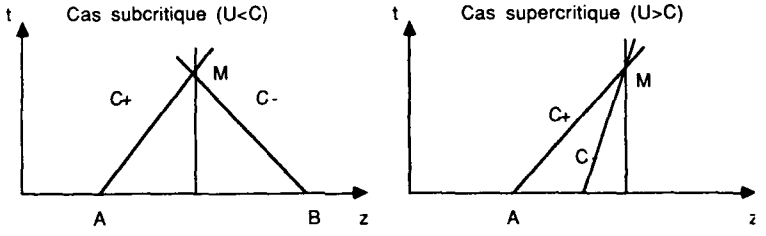

Ces considérations sur la manière de rechercher l'information en amont et en aval, ou en amont seulement, conduisent à proposer la décomposition suivante: le flux exprimé à une interface quelconque est la décomposition d'une partie F+ et d'une partie F- respectivement exprimées en utilisant les états amont et aval. Leur expression dépend de l'orientation des caractéristiques C+ et C- à l'interface considérée. Cela permet de chercher une expression du flux à l'interface sous la forme suivante:

$$F_i = \sum_m \gamma_m \cdot (\overline{F^+_{i+1+m}} + \overline{F^-_{i-1-m}}) \qquad (29)$$

Cette relation introduit une décomposition du flux F en une partie F+ et une partie F-:

$$F = F^+ + F^- \qquad (30)$$

Celle-ci est obtenue simplement, en considérant la matrice diagonale Λ associée à A:

$$\tilde{A} = P.\tilde{\Lambda}.P^{-1} \qquad (31)$$

où P et P^{-1} sont les matrices de passage de la base initiale dans la base des vecteurs propres.

La technique de décomposition des flux que nous avons adoptée, consiste à rechercher une décomposition de la matrice Λ qui respecte le caractère subcritique ou supercritique de l'écoulement. En remarquant que les valeurs propres $\lambda_{1,2}$ sont aussi les pentes des caractéristiques, on peut proposer la décomposition suivante:

$$\Lambda = \Lambda^{+} + \Lambda^{-} \qquad (32)$$

où $\Lambda+$ et $\Lambda-$ sont les matrices diagonales respectivement définies positive et négative telles que si λ est une valeur propre de Λ, alors:

$$\lambda = \frac{\lambda + |\lambda|}{2} \quad ; \quad \lambda = \frac{\lambda - |\lambda|}{2} \qquad (33)$$

De la décomposition précédente il est aisé de déduire une décomposition du flux F. Le calcul est le suivant:

$$\begin{aligned} F = \tilde{A}.V &<=> F = (P.\Lambda.P^{-1}).V \\ <=> F &= (P.\Lambda^{+}.P).V + (P.\Lambda^{-}.P).V \\ <=> F &= F^{+} + F^{-} \end{aligned} \qquad (34)$$

Par application des relation (26) et (29), nous obtenons un système algébrique associé au système aux dérivées partielles (23). Il est de la forme:

$$M.X = Y \qquad (35)$$

où M est une matrice tridiagonale ou pintadiagonale par blocs suivant la précision du schéma que l'on choisit. X est le vecteur unicolonne par blocs dont les composantes sont les inconnues V_j à l'instant $(n+1).\Delta t$. Enfin, Y est le vecteur unicolonne par blocs correspondant aux termes connus explicitement.

4 - Résultats et conclusion

4.1 Calculs préliminaires

De nombreux tests numériques ont été effectués pour tenter d'analyser précisement le comportement du système fluide/vaisseau. Nous avons signalé précédemment que le caractère non-linéaire de la loi de tube influençait considérablement l'écoulement du sang dans le vaisseau. Ceci s'explique par les brutales variations de célérité qui peuvent être obtenues même pour des variations de section du vaisseau extrêmement faibles. La figure (2) présente l'évolution de la section du vaisseau en fonction de la direction longitudinale x à différents instants et pour le cas où la loi de tube s'exprime linéairement en fonction de la section du vaisseau. Pour cette application, on choisit le repos comme état initial. A t>0, on impose instantanément au niveau du vaisseau une distribution de pression extérieure, uniforme, constante pendant toute la durée du calcul.

Deux phénomènes sont observés:

* Vers l'aval (z>0), une onde de compression se déplace dans le sens de l'écoulement sanguin. Celui-ci est lui-même accéléré. La pression transmurale varie dans le sens d'une augmentation de la pression intérieure (déplacement vers la droite sur la loi de tube).

* Vers l'amont (z<0), une onde de détente se propage dans le sens inverse de l'écoulement sanguin. A son passage la pression sanguine diminue de sorte que le vaisseau possède une pression transmurale négative et tend à s'écraser (déplacement vers la gauche sur la loi de tube).

Il convient de se souvenir que l'étude est monodimensionnelle et que par conséquent la distribution spatiale du profil des vitesses n'est pas considérée.
La célérité des ondes pariétales étant peu dépendante de la section dans le cadre de la loi de tube utilisée, on ne peut assister dans ce cas à un phénomène de focalisation des ondes pariétales.
Nous présentons sur la figure (3) un calcul analogue obtenu dans le cas de la loi de tube non-linéaire de la figure (1). On constate, dans ce cas, que les variations de la célérité de propagation sont telles que le régime supercritique peut exister. C'est le cas où l'énergie introduite par les perturbations extérieures ne peut se propager le long du vaisseau suffisamment rapidement. Il se produit alors un collapsus dynamique:
Il s'agit d'un phénomène ondulatoire (péristaltisme induit) qui se propage en avant et en arrière de la zone d'application de la distribution de pression extérieure. Dans la partie amont du vaisseau apparaît un écoulement sanguin à contre courant.

4.2 Domaine d'application du modèle

La compréhension de la perte de connaissance du pilote de chasse liée à l'application d'une accélération centripète impose d'étudier les effets de l'application simultanée d'un champ de forces volumiques aux composantes précédentes du modèle ie écoulement sanguin (conditions aux limites imposées) dans un vaisseau collabable sous l'effet d'une distribution de pression. Les conditions aux extrémités ont été précisées figure (4).

Le calcul est réalisé suivant trois phases bien distinctes:

1- La première conduit à l'obtention du régime établi d'écoulement sanguin correspondant au fonctionnement de la seule pompe cardiaque.

2 - La mise en accélération, étape dans laquelle on superpose au fonctionnement du cœur, un facteur de charge évolutif progressivement établi avec un taux d'accélération que l'on peut fixer.

3- Enfin, l'écrasement correspondant au cas complet pour lequel on rajoute à la situation précédente une distribution de pression extérieure répartie sur la paroi latérale du vaisseau. De quoi s'agit t'il?
Une image approximative, mais de bonne valeur explicative, consiste en la représentation d'un vaisseau sanguin de l'espace sous dural écrasé entre le plancher de la base du crâne et des tissus encéphaliques sus-jacents qui tendent à migrer vers le bas sous l'effet des forces volumiques. Les grandeurs prises en considération dans notre modèle sont donc les forces d'écrasement appliquées à la surface du vaisseau et traduites en terme de distribution de pression.
La réalité physique résulte en fait de l'évolution du champ de déformations (lié au champ des contraintes par la loi de comportement) sous facteur de charge. Cette évolution traduit les effets de la pression intracrânienne et des tensions d'origine purement visqueuse.
Les figures qui suivent présentent les résultats obtenus pour les trois phases de calcul:

1- La figure (5a) représente les lignes iso-vitesse à un instant donné de la phase transitoire. La fréquence cardiaque est de 120 bpm. On observe le mouvement périodique de l'écoulement et l'augmentation importante de la vitesse moyenne au passage de l'onde systolique.

2- La figure (5b) présente les lignes iso-vitesse durant la phase de mise en accélération. On observe le mouvement global (déplacement solide) de la masse sanguine jusqu'à des niveaux de vitesse très élevés (12 m/s).

3- Enfin, l'écrasement du tube est représenté sur la figure (5c). On observe la création d'un écoulement supercritique suivi d'un choc de transition du régime supercritique au régime subcritique. Le choc lui-même est défini comme une discontinuité de certaines grandeurs physiques, dans le cas d'espèce le régime des vitesses sanguines. Sa localisation se situe au niveau de l'application de la distribution continue de pression. Les

ondes de compression et de détente précédemment citées peuvent alors apparaître, avec les conséquences que l'on sait, refoulement du sang qui tend à être piégé en amont du domaine.

A ce point de notre étude, seule une analyse locale a été rapportée. Un dernier cas de calcul présenté est une analyse globale du comportement du système fluide/vaisseau du sujet, pendant toute la durée de l'application du facteur de charge sur une portion de trajectoire décrite par l'avion. Les évolutions du facteur de charge et de l'amplitude de la distribution de pression extérieure sont données sur la figure (6). On étudie l'existence d'une relation entre l'instant d'application du facteur de charge paramètré selon la phase du cycle cardiaque. Nous avons superposé sur la figure (7), les évolutions du rapport M de la vitesse moyenne du sang sur la célérité des ondes pariétales. On constate que si les conditions sont telles que le régime supercritique est atteint, il se produit un choc qui engendre une limitation du débit, puis un refoulement du sang vers l'amont.

4.3 Conclusion

L'observation d'une modification de la symptomatologie de la perte de connaissance en vol des pilotes d'avions de chasse dans le cas où le facteur de charge est imposé rapidement, nous a conduit à proposer une hypothèse différente de l'hypoxie: l'hypertention intracrânienne [QUANDIEU et all.]. Dans ce cadre, nous avons été amener à developper un modèle physique permettant la représentation de l'écoulement sanguin au niveau cérébral, sous l'influence du champ extérieur. Ce modèle s'applique à un conduit élastique dans lequel s'écoule un fluide supposé newtonien. Des équations monodimensionnelles ont été établies pour représenter le comportement de ce système. L'exploitation numérique du modèle a montré que sous certaines conditions compatibles avec les situations rencontrées en vol, il pouvait apparaître un régime d'écoulement dit supercritique, généralement instable, et immédiatement suivi d'un choc de transition. Ce dernier est à l'origine d'un phénomène de limitation du débit sanguin, voire de refoulement du sang vers l'amont. Cette analyse mécanique du problème apporte donc un élément de réponse qui, dans le cadre des forts jolts, plaide en faveur de l'hypothèse d'une hypertension intracrânienne produite par le piègeage d'une partie de la masse sanguine au niveau cérébral.

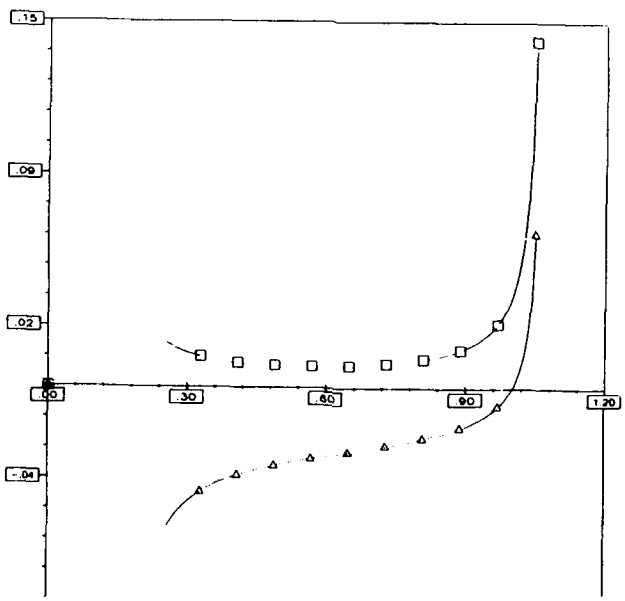

Figure 1 :

Représentation de la loi de tube (a) et de la célérité de propagation des ondes pariétales (b) en fonction de la section adimensionnelle.

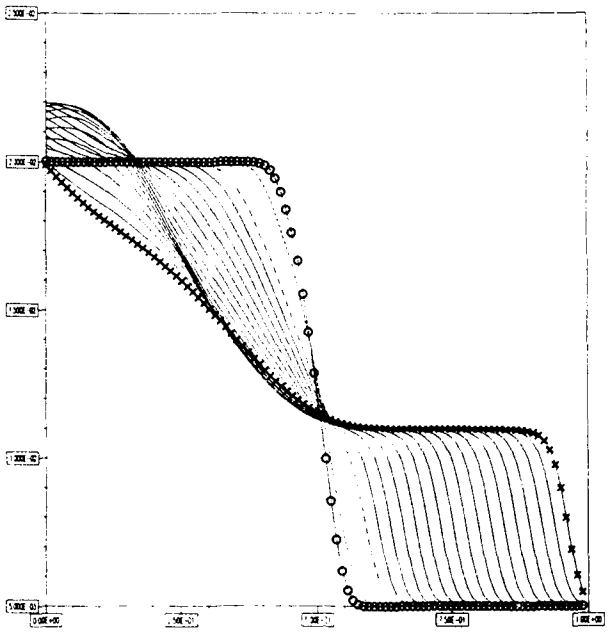

Figure 2:

Vessel section distributions along the axial direction at different instants.
Linear vessel behavior law case.

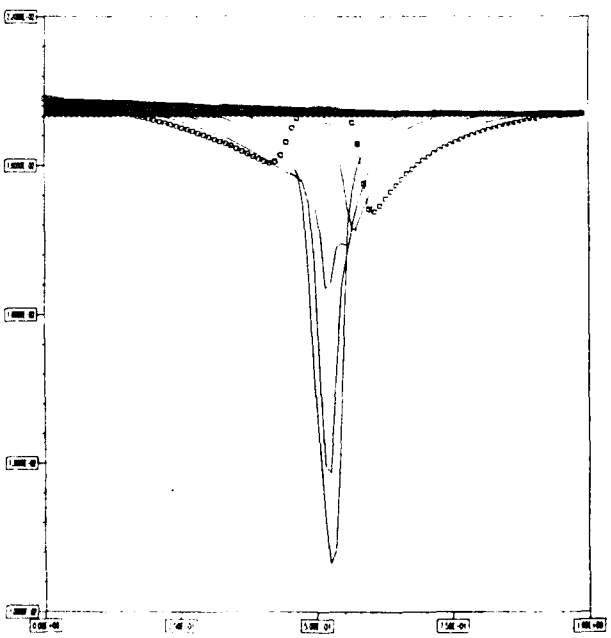

Figure 3:

Vessel section distributions along the axial direction at different instants.
Non-linear vessel behavior law case.

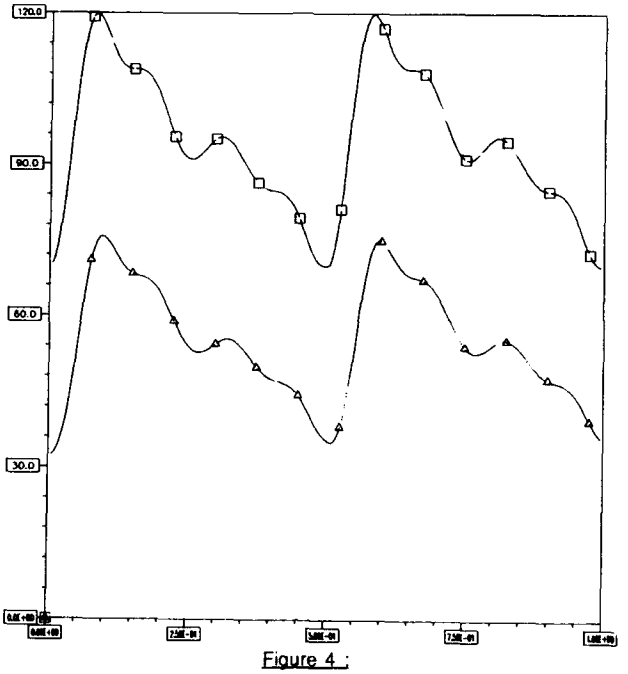

Figure 4 :

Représentation des pressions aux extrémités du vaisseau en fonction du temps.

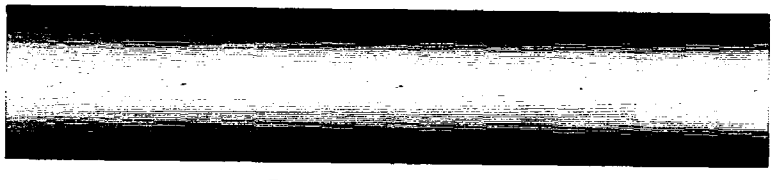

a - Etablissement du régime pulsé,

b - Action de la force volumique f_z,

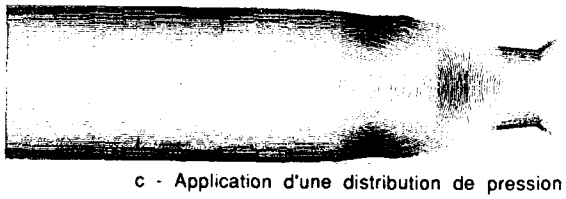

c - Application d'une distribution de pression extérieure.

Figure 5 :

Représentation des lignes iso-vitesse dans le cadre de l'application simultanée du régime pulsé (action du coeur) et du champ de perturbations extérieures (forces volumiques et surfaciques).

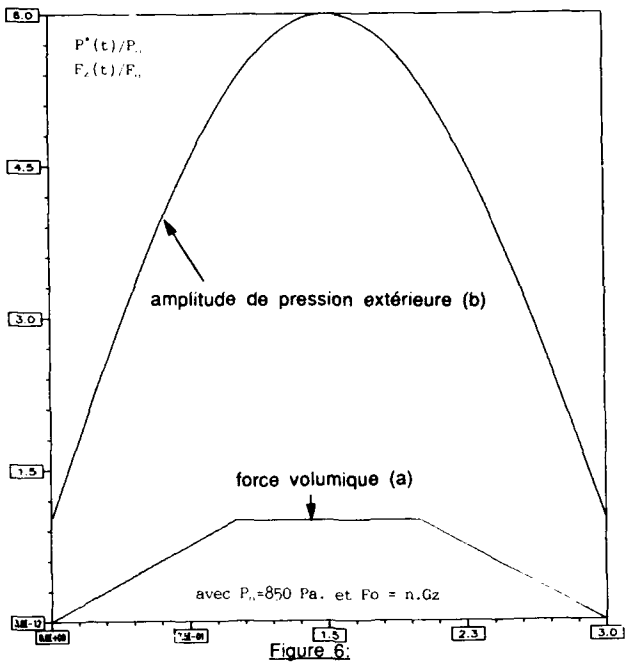

Figure 6:

Distribution imposée de la force volumique (a) et de l'amplitude de pression extérieure (b) en fonction du temps, au cours de l'évolution de l'avion sur une portion de trajectoire (virage accéléré descendant).

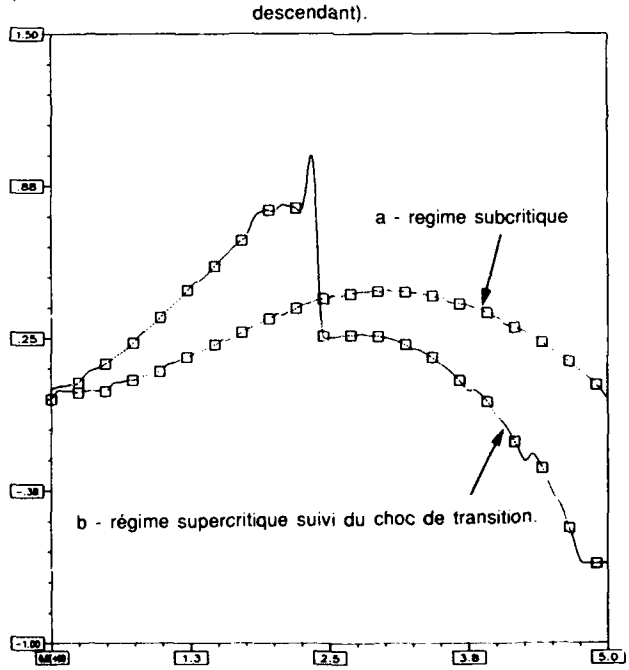

Figure 7:

Evolution du nombre sans dimension M (nombre de Mach) en fonction du temps, pour le champ de *perturbations décrit sur la figure (6).*

5 - Références

[1] KAMM, D.K., SHAPIRO, A.H., 1979.
Unsteady flow in a collapsible tube subjected to external pressure or body forces.
J. Fluid. Mech. 95, 1-78.

[2] GAFFIE D., LIEBAERT Ph., QUANDIEU P., 1990.
A mathematical modeling of the cerebrovascular system.
The Physiologist, Vol 33, n° 1 Suppl.

[3] GODOUNOV, S., 1973.
Equations de la physique mathématique.
Ed. Mir.

[4] GODOUNOV, S., ZABRODINE, A., IVANOV, M., KRAIKO, A., PROKOPOV, G., 1979.
Résolution numérique des problèmes multidimensionnels de la dynamique des gaz.
Ed. Mir.

[5] LIEBAERT Ph., GAFFIE D., QUANDIEU P., 1990.
Stresses in the brain mass and in the peripheral fluids under Gz accelerations. Study of a simple model.
The Physiologist, Vol 33, n° 1 Suppl.

[6] QUANDIEU P., TRAN C.C., LIEBAERT Ph., GAFFIE D., 1990.
Toward and univocous interprétation of cardiovascular biomechanics in hyper and microgravity.
The Physiologist, Vol 33, n° 1 Suppl.

[7] QUANDIEU P., GAFFIE D., LIEBAERT Ph., 1991.
Interprétation biomécanique des pertes de connaissance en vol des pilotes de chasse sous l'effet de l'application d'une accélération +Gz d'installation rapide.
C.R. Acad. Sci. Paris, Série II, 185-190.

[8] RICHMEYER, R.D., MORTON, K.W., 1967.
Difference methods for initial-value problems.
N.Y. Interscience publ.

[9] RUBINOW, S.I., KELLER, J.B., 1972.
Flow of viscous fluid through an elastic tube with applications to blood flow.
J. Theor. Biol., 299-313.

[10] SHAPIRO, A.H. , HAWTHORNE, W.R. 1947.
The mechanics and thermodynamics of steady one dimensional gaz flow.

[11] SHAPIRO, A.H. 1977a.
Physiologic and medical aspects of flow in collapsible tubes.
Proc. 6th Canadian Cong. Appl. Mech. Vancouver, 883-903.

[12] SHAPIRO, A.H. 1977b.
Steady flow in collapsible tubes.
J. Biomec. Engng 99, 126-147.

[13] STEGER J.L., WARMING R.I., 1981.

Flux vector splitting of the inviscid gasdynamic equations with applications to finite difference methods.
Computational Physics 40, 263-993.

CIRCULATORY BIOMECHANICS
EFFECTS OF ACCELERATIONS

(*) D. GAFFIE,(**) P. QUANDIEU, (***) Ph. LIEBAERT,
(****) D. COHEN-ZARDY, (****) T. DAUMAS, (**) A. GUILLAUME

(*) ONERA, Direction de l'Energétique,
29, Avenue de la Division Leclerc, BP. 72
92320 Chatillon-Cedex (FRANCE)
(**) Centre d'Etudes et de Recherches de Médecine Aérospatiale,
Division Biomécanique, Base d'essais en vol, 91228 Brétigny sur Orge (France)
(***)Direction des Recherches Etudes et Techniques Tour D.G.A.
Service des Recherches/G9, 26 Bvd Victor Paris 00457 Armées (France)
(****) Ecole Polytechnique, Route de Saclay,
91128, Palaiseau (France)

Abstract

A general physical model of blood flow behavior in vessels is proposed, to have a better understanding of mechanisms which cause inflight loss of consciousness (LOC) in fighter pilots. The problem is considered in the situation when heart work and external disturbances induced by aircraft motions are concomitant. Disturbances are both volume and surface changes. Calculations show that under certain conditions blood flow is limited due to a change in flow rate. It can then be hypothesized that under the effect of a sudden load, LOC could be caused by a factor other than brain hypoxia resulting from blood pooling in the pilot's lower limbs.

List of symbols.

C local speed of parietal waves.
fz axial component of the volume force.
F volume force field.
M non-dimensional number similar to Mach number.
p blood hydrodynamic pressure.
Pe(z,t) external pressure applied to the vessel wall.
Ps perimeter associated to the vessel section S.
Re Reynolds number.
S(z,t) vessel section .
U(z,t) mean blood flow velocity.
V_r, V_z,V_θ blood velocity components.
V blood velocity vector.
σ stress tensor.
τ viscous stress tensor.
ε non-dimensional parameter (<<1)
$\alpha(z,t)$ fonction issued of non-linear term integration.
τ_{rz} shear component of the viscous stress tensor.
τ_p mean wall shear stress.

I - Introduction

Inflight fighter aircrew LOC is a phenomenon known for decades. Under slow onset acceleration, it is caused by hypoxia resulting from blood pooling in highly distensible lower limb veins under the effect of the centrifuge force associated with descending fast turns. Brain blood flow diminishes, associated with grey-out, followed by black-out, and sometimes LOC if arterial pressure regulatory mechanisms do not rapidly set into action. The useful time of consciousness can be prolonged by use of anti-G suit.

This work has been supported by D.R.E.T.

If the load is applied quickly the LOC syndrome is changed. No grey-out develops, LOC is immediate, non reproducible, and associated with *lacunar amnesia*. The question is to know whether in the case of rapid onset acceleration, hypoxia can still be maintained as the cause of this new LOC. The model which is proposed here can provide a partial answer, from a strictly mechanical view. It describes blood flowing in a vessel in the general case where the actions of the heart and of external forces are concomitant. It shows that the nature of blood flow is conditioned by the velocity of parietal waves which propagate up to vessel walls and takes into account the effects of changes in brain tissue stresses.

II - Mathematical formulation

2.1- Equations

Mass and momentum conservation equations are described, considering blood as a viscous, incompressible fluid:

$$\operatorname{div} \vec{V} = 0$$

$$\rho \frac{d\vec{V}}{dt} = \vec{F} + \operatorname{div} \sigma \qquad (1)$$

Where F represents the volume force and is a datum in the problem. σ is the stress tensor, expressed as a function of the hydrodynamic pressure p and of viscous stress tensor.

$$\sigma = -p.I + \tau \qquad (2)$$

A behavior law associated with the nature of the given fluid can relate stresses to deformations. In the present application, blood will be considered as a Newtonian fluid.

2.2- Simplifying hypotheses

The elementary problem which we are processing here is presented in the figure below which illustrates blood flow through a deformable vessel. Motion is due to the concomitant action of the heart (pulsed flow), and of a field of distrubances caused by aircraft motion.

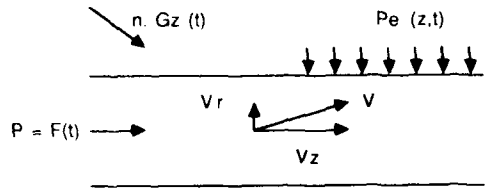

axis of symmetry of blood vessel

In this model, the external field of disturbances is composed of the volume force F, directly included in equations, and of external pressure distribution along blood vessels. Stress field changes caused by the application of the load have to be taken into account inside brain tissue (Ref: [5]). Local equations are naturally written in a system of cylindrical coordinates in the most general case. However, flow and vessel deformation are assumed to be symmetrical with respect to vessel centerline.

In order to evaluate the order of magnitude of the various terms of the above equations parameter ε is added as the ratio of characteristic velocities in the radial and longitudinal directions. If the vessel centerline can be considered as the favorite flow direction, ε can always be considered to be much smaller than 1.

$$\varepsilon = \frac{V_o}{U_o} = \frac{R_o}{L} << 1 \qquad (3)$$

We also consider the Reynolds number, ratio of inertial force to viscosity force, is not too high, in order keep into effect the influence of viscosity.

$$Re^{-1} = \frac{\sigma_o}{\rho . U_o^2} \quad O(1) \qquad (4)$$

A study of the order of magnitude of these different terms according to hypotheses (3) and (4) gives a simplified formulation of general equations (1). We obtain

$$\frac{\partial}{\partial r}(rV_r) + \frac{\partial V_\theta}{\partial \theta} + \frac{\partial}{\partial z}(rV_z) = 0$$

$$\rho \left(\frac{\partial}{\partial t}(rV_z) + \frac{\partial}{\partial r}(rV_rV_z) + \frac{\partial}{\partial \theta}(V_\theta V_z) + \frac{\partial}{\partial z}(r V_z^2)\right) =$$

$$\rho r f_z - \frac{\partial}{\partial z}(rp) + \frac{\partial}{\partial r}(r\tau_{rz}) + \frac{\partial}{\partial \theta}(r\tau_{\theta z})$$

$$\frac{\partial p}{\partial r} = \frac{\partial p}{\partial \theta} = 0 \qquad (5)$$

This simplified system shows that, as a first approximation, pressure can be considered as uniform in each vessel section. For boundary conditions, symmetry about the axis vessel with adherence to vessel walls are assumed. Considering the motion of the vessel wall, this latter condition is easily shown to be expressed by:

$$(V_r)_R = \frac{\partial R}{\partial t} + \left(\frac{V_\theta}{r}\right)_R + \frac{\partial R}{\partial z}(V_r)_R \qquad (6)$$

Torsion and stretching along the z axis are generally not taken into consideration.

2.3- <u>One-dimensional formulation</u>

The above described system shows that flow is little affected by the two transversal directions. It therefore seems natural to try and formulate the problem by a one-dimensional equation. This equation is obtained by integration of the above equations on any vessel section S(z,t) (Ref: [2], [3]). Mean flow velocity is defined as:

$$U(z,t) = \frac{1}{S}\int_0^{2\pi} \left(\int_0^R rV_z dr\right) d\theta \qquad (7)$$

And the one-dimensional equation system is given by:

$$\frac{\partial S}{\partial t} + \frac{\partial}{\partial z}(SU) = 0$$

$$\frac{\partial U}{\partial t} + (1-\alpha)\frac{U\partial S}{S\partial t} + \alpha U\frac{\partial U}{\partial z} + U^2\frac{\partial \alpha}{\partial z} = \qquad (8)$$

$$f_z + \frac{1}{\rho}\left(-\frac{\partial p}{\partial z} + P_s\frac{\tau_p}{S}\right)$$

Where U and S are the main variables of the system, p is the supposedly uniform pressure in the section. The mean shearing stress in the wall τ_p is obtained by:

$$\tau_p = \frac{1}{P_s}\int_0^{2\pi} (r\tau_{rz})_R \, d\theta \qquad (9)$$

The term α which appears in the motion conservation equation (8) results from the integration of non linear terms. It is defined by:

$$\alpha(z,t) = \frac{1}{SU^2}\int\int V_z^2 dS \qquad (10)$$

2.4- Closure hypothesis

The unknowns of the one-dimensional system (8) are the mean velocity, the vessel section, the shearing stress τ_p , pressure p and parameter α. Given 5 unknowns for 2 equations. We derive other equations, which will provide a complete system. Under the assumption that we are dealing with a Newtonian fluid, under the conditions of hypothesis (3), the local component τ_{rz} is expressed as:

$$\tau_{rz} = \mu \frac{\partial V_z}{\partial r} \qquad (11)$$

Equations (9), (10), (11) show that a law of profile for velocity componemt V_z can be used to calculate the parietal stress τ_p and parameter α.

A new hypothesis called law of similar profiles is then added, which assumes homothetic profiles for any vessel section at any instant.

$$V_z(r,\theta,z,t) = U(z,t).g(\frac{r}{R}) \qquad (12)$$

Two new equations can be derived from this new hypothesis:

$$\tau_p = \frac{2\pi\mu U}{P_s}(\frac{dg}{d\beta})\beta=1$$
$$\alpha = 2\int_0^1 g(\beta).\beta.d\beta \qquad (13)$$

In hypothesis (12) α is constant. A final equation has to be written for pressure. It is obtained writting the compatibility between fluid motion and blood vessel motion.

2.5- Fluid/wall coupling

As fluid and wall motions are not independent, another equation has to be defined to express the coupling between wall and fluid mechanical properties. In a quasi-static analysis, considering the vessel wall as an isotropic medium and neglecting displacements caused by axial tensions, the application of the fundamental law of dynamics to the vessel wall yields the vessel behavior law.

$$p - p_e = K(z).P\ (S/S_0) \qquad (14)$$

Coefficient K characterizes vessel stiffness, and law P is a highly non-linear function of the non-dimensional wall section. p-pe is the transmural pressure, i.e. the difference between in-flow pressure, and the external pressure acting on the vessel wall. Any disturbance in the studied system shall inevitably create surface waves which will propagate along the longitudinal axis z.

The velocity of these parietal waves is expressed as a function of transmural pressure:

$$C^2(S/S_0) = \frac{S}{\rho}\frac{\partial}{\partial S}(p-p_e) \qquad (15)$$

The non-linear behavior described by law P creates a strong relationship between wave velocity and local vessel deformation. Figure (1) shows curves P and C/100 vs the non-dimensional section. The vessel behavior law is derived from a rational function approaching experimental results of Kamm and Shapiro [1].

In the case of a positive transmural pressure the vessel is dilated, and forms a stiffer system. Surface wave velocity therefore increases. In the opposite case of negative transmural pressure the vessel collapses, becomes less stiff and wave velocity decreases (Ref [9], [10], [11], [12]).

A subcritical or supercritical flow rate can be defined from mean velocity U, respectively lower or higher than C. By analogy with problems of gas dynamics, it may be useful to define a non-dimensional number similar to the Mach number.

$$M = \frac{U}{C} \qquad (16)$$

If we consider that the external pressure distribution only depends on z and t, the fluid/wall coupling can be simply taken into account in equations, expressing internal pressure gradient as:

$$\frac{\partial p}{\partial z} = \frac{\partial (p-p_e)}{\partial z} + \frac{\partial p_e}{\partial z} \qquad (17)$$

The final system obtained with the incorporation of equations (13) and (17) into (8) is:

$$\frac{\partial S}{\partial t} + \frac{\partial}{\partial z}(SU) = 0$$

$$\frac{\partial U}{\partial t} + (1-\alpha)\frac{U}{S}\frac{\partial S}{\partial t} + \alpha U\frac{\partial U}{\partial z} + \frac{1}{\rho}\frac{\partial (p-p_e)}{\partial z} = \qquad (18)$$

$$-\frac{1}{\rho}\frac{\partial p_e}{\partial z} + f_z + \frac{1}{\rho}\cdot P_s\frac{\tau_p}{S}$$

2.6- External forces and boundary conditions

It clearly appears that knowledge of an external pressure distribution Pe (z,t) makes calculation of the longitudinal gradient possible. This gradient is then inserted as source term into the momentum equation for the numerical solution. The volume force field created by aircraft motion is only represented in this model by the axial component f_z, which is naturally a datum of the problem.

The action of the heart is taken into consideration using boundary conditions given as approaching analytical laws depending on the time at the input and output of the system. The input is the carotid intravascular pressure and the output is the intravascular pressure upstream of the capillary bed. Experimental results extracted from the literature yielded an approximation of the pressure signal for the input condition:

$$p(\text{mm Hg}) = p_{diastole} + (p_{systole} - p_{diastole}).F(t.Hz - E(t.Hz)) \qquad (19a)$$

Where Hz is heart rate, and E the integer part function. Function F was obtained by approximation using Bernstein's method.

$$\begin{aligned} F(X) = {} & -367056.2X^{20} + 3760594X^{19} - 20892181.5X^{18} + 85288929X^{17} \\ & - 266991961.5X^{16} + 625286397.6X^{15} - 1078175292X^{14} + 1363379124X^{13} \\ & - 1259926746X^{12} + 840312278X^{11} - 391387110.4X^{10} + 116992538X^{9} \\ & - 16338309X^{8} - 2096916X^{7} + 1387608X^{6} - 251940\,X^{5} \\ & + 21318\,X^{4} - 1425X^{3} + 152X^{2} - X \end{aligned} \qquad (19b)$$

III- Numerical solution

A finite volume numerical method was used to solve system (18). The equations have to be written in their conservative form in order to integrate them on each cell of the mesh. In this problem, the non linearity of the vessel behavior law somewhat complicates spatial integration of transmural pressure gradient.

$$\frac{\partial(p-p_e)}{\partial z} = \frac{\partial(p-p_e)}{\partial S}\frac{\partial S}{\partial z} = \frac{\rho C^2}{S}\frac{\partial S}{\partial z} \qquad (20)$$

To solve the system at instant $(n+1)\Delta t$, for any vessel position, we have to use a linearized form of the vessel behavior law around a value known at instant $n\Delta t$.

$$P(X) - P(X^n) = \frac{dP}{dX}[X = X^n].(X - X^n) \qquad (21)$$

Where X represents the non-dimensional section S/S_0.

We derive an approached expression of parietal wave propagation velocity:

$$C^2 = \frac{K}{\rho S_0}\frac{dP}{dX}[X = X^n].S = k_0.S \qquad (22)$$

Conservative formulation of the wanted equations becomes possible if this expression is included into system (18). We obtain the final appraoched system, written in vector form.

$$\frac{\partial \vec{V}}{\partial t} + \frac{\partial \vec{F}}{\partial z} = \vec{G} \qquad (23)$$

with

$$\vec{V} = t(S, S.U)$$
$$\vec{F} = t(S.U, \alpha.S.U^2 + \frac{1}{2}k_0 S^2)$$
$$\vec{G} = t(0, S.(-\frac{1}{\rho}\frac{\partial p_e}{\partial z} + f_z + \frac{P_s}{\rho S}\tau_p + (\alpha - 1)\frac{U}{S}\frac{\partial S}{\partial t}))$$

3.1- Numerical scheme

The figure below shows that integration of the above equation into any cell of the mesh generates a new vectorial equation. It involves mean quantities defined at cell centers as well as fluxes of these quantities expressed on cell interfaces.

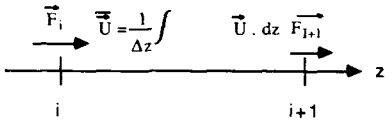

we obtain, for any cell i:

$$\Delta z_i \frac{\partial \vec{\bar{V}}_i}{\partial t} + F_{i+1} - F_i = \vec{\bar{G}}_i \qquad (24)$$

The system made of the above vector equation is an open system which cannot be directly solved. For any cell i, it actually involves 4 unknowns (the two components of V_i and F_{i+1}) for only two equations. To solve the problem, additional equations have to be used. These equations determine the spatial numerical scheme. They consist of linear relationships between interface fluxes and fluxes expressed by mean quantities for each cell. We obtain:

$$\vec{F}_i = \sum_j \gamma_j \vec{\bar{F}}_j \qquad (25)$$

Contrary to Euler equations, flux F is not a homogeneous first degree function in V, due essentially to the non-linear nature of the vessel behavior law. However, to obtain a conservative form of equation we previously linearised this law, in the vicinity of the expected solution. Then we obtain:

$$\vec{F} = \tilde{A}\vec{V} \qquad (26)$$

with $$\tilde{A} = \begin{pmatrix} 0 & 1 \\ -\alpha.U^2 + \frac{1}{2}k_0 S & 2.\alpha.U \end{pmatrix}$$

We easily deduct from equation (25) that flux expressed on the interface of a calculation cell at instant $(n+1)\Delta t$ can be written:

$$F_i^{n+1} = \sum_j \gamma_j \overline{F}_j^{n+1} = \sum_j \gamma_j \widetilde{A}_j^n \overline{U}_j^{n+1} \qquad (27)$$

Finally, we observe that flux at interface i is linearly related to the main unknowns of problem V expressed at the same instant $(n+1)\Delta t$. The diagram of integration in time is therefore implicit. This choice is justified for stability reasons.

3.2- Fluw decomposition method

Equation (27) requires the use of spatial integration schemes, centered or not, whose precision depends both on the number of points chosen to express flux F at the interface and on the value of γ_j).

Although these methods are extensively used, they do not provide an accurate representation of discontinuities which can be observed in flows. The flux splitting technique which we developed is based on results yielded by the method of characteristics (Ref [3], [4], [8], [13]). It permits automatic adaptation of discretization as a function of local flow conditions the principle of the method of characteristics is to identify curves in the physical plane (z,t) along which évolution laws, such as Riemann invariants, are verified. These curves are called characteristics. In the studied hyperbolic system, a very classical calculation can evidence two families of characteristics, respectively identified as (C^+) and (C^-). The slope of these curves depends on the local flow. In the case where $\alpha=1$, We have:

$$(\frac{dz}{dt})_{C^+} = U + C \quad ; \quad (\frac{dz}{dt})_{C^-} = U - C \qquad (28)$$

where U represents mean flow velocity, and C the velocity of parietal waves. Two flows are then identified: U lower or higher than C. In the subcritical case (U<C) the figure below shows that solution in any point of the physical plane depends on conditions upstream and downstream along characteristics passing through M. Characteristics C^+ and C^- have a positive and a negative slope, respectively. Under supercritical conditions (U > C) slopes of characteristics passing through M are both positive, and the solution in M only depends on upstream conditions.

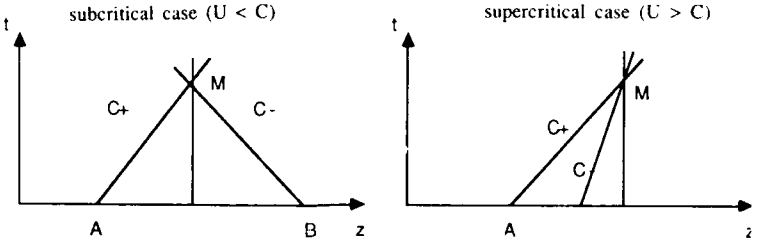

These considerations on how to look for information upstream and downstream, or upstream only, lead to the following splitting approach : flux expressed at any interface is the split of part of F^+ and part of F^-, respectively expressed with respect to upstream and downstream conditions. They depend on the orientation of characteristics C^+ and C^- at the given interface. The flux at the interface can then be written:

$$F_i = \sum_m \gamma_m (\overline{F^+_{i+1+m}} + \overline{F^-_{i-1-m}}) \qquad (29)$$

This equation induces flux splitting in F into a part F^+ and part F^-.

$$F = F^+ + F^- \qquad (30)$$

This one is easily obtained, considering diagonal matrix Λ associated with A :

$$\tilde{A} = P.\tilde{\Lambda}.P^{-1} \qquad (31)$$

where P and P^{-1} are transition matrices from the initial base into the base of eigenvectors.

The flux splitting technique was used here to identify a split of matrix Λ which takes into consideration the sub-critical or super-critical nature of flow. Observing that eigenvalues $\lambda_{1,2}$ are also the slopes of characteristics, we can propose the split:

$$\Lambda = \Lambda^+ + \Lambda^- \qquad (32)$$

where Λ^+ and Λ^- are diagonal matrices respectively defined as positive and negative, so that if λ is a eigenvalue of Λ:

$$\lambda = \frac{\lambda + |\lambda|}{2} \quad ; \quad \lambda = \frac{\lambda - |\lambda|}{2} \qquad (33)$$

A split of F flux can easily be derived from the above split:

$$\begin{aligned} F = \tilde{A}.V &<=> F = (P.\Lambda.P^{-1}).V \\ &<=> F = (P.\Lambda^+.P).V + (P.\Lambda^-.P).V \\ &<=> F = F^+ + F^- \end{aligned} \qquad (34)$$

Applying equations (26) and (29), we obtain an algebraic system, associated with the system of partial derivates (23). It is expressed as:

$$M.X = Y \qquad (35)$$

where M is a tridiagonal or pintadiagonal matrix with blocks depending on selected scheme accuracy. X is the single colum vector with blocks whose components are unknowns V_i at instant $(n + 1)\Delta t$. Finally, Y is the single colum vector corresponding to terms explicitely known.

IV- RESULTS AND CONCLUSIONS

4.1- Preliminary calculations

Numerical tests have been made to attempt to analyze with precision the behavior of the fluid/vessel system. We previously observed that the non-linear nature of the vessel behavior law significantly influences blow flow in blood vessels, due to sudden wave velocity changes, even for extremely small vessel section variations. Figure (2) shows the changes in blood vessel section as a function of longitudinal direction z at different instants, and for the case where the vessel behavior law is linearly expressed versus vessel section. Rest is selected as initial slate. At t >O, a uniform external pressure distribution is instantaneously imposed, constant over the entire calculation time.

Two phenomena were observed

. downstream ($z > O$), a compression wave travels in the same direction as blood flow, which is accelerated. Transmural pressure varies with increased internal pressure (displacement to the right on the vessel behavior law).

. upstream ($z < O$), a relaxation wave propagates in counter direction of blood flow. Blood pressure diminishes so that the vessel has a negative transmural pressure and tends to collapse (displacement the left on the vessel behavior law).

The study is one-dimensional, and therefore spatial distribution of velocity profile is not being considered.

As parietal wave velocity is little influenced by section in the vessel behavior law, a phenomenon of parietal wave focalisation cannot be observed.

Figure (3) shows a numerical calculation obtained in the case of the non-linear vessel behavior law of figure (1). Here propagation velocity changes are observed to be such that a supercritical flow can develop. This is the case where energy generated by external perturbations cannot propagate rapidly enough along the vessel. A dynamic collapse is observed . It is an ondulatory phenomenon (induced peristaltism) which propagates to the front and the rear of the area concerned by external pressure distribution . A counter blood flow develops in the upstream part of the vessel.

4.2- Model application

To understand inflight LOC in fighter pilots exposed to centripetal acceleration, we have to study the effects of the application of a volume force field to the above described components of blood flow (imposed boundary conditions) in a collapsible vessel under the effect of pressure distribution. Boundary conditions have been described (figure (4)).

The calculation is divided into three stages :

1. Blood flow rate is calculated to strictly correspond to heart pumping.

2. Acceleration, with superimposition of a load onto heart pumping. This load is graduably increased, at an acceleration rate which can be pre-determined.

3. Finally, collapsing, induced by adding external pressure distribution over the blood vessel wall. How? an approximate, but illustrative image of what happens is a blood vessel of the sub-dural area, crushed between the skull base and underlying encephalic tissues which tend to sink down under the effect of volume forces. Magnitudes taken into consideration in our model are crushing forces applying to vessel surface and expressed in terms of pressure distribution.

The physical reality results from changes in the deformation field (linked with the stress field by the behavior law) under load. These changes express the effects of intracranial pressure and strictly viscous tensions.

Figures (5) shows results obtained for the three calculation stages.

1. Figure (5-a) presents axial velocity contours at a given instant of the transient phase. Heart rate is 120 bpm. A periodic flow movement and a high increase in mean velocity of systolic ware are observed.

2. Figure (5-b) presents axial velocity contours during the acceleration onset phase. The overall blood mass displacement (solid displacement) is observed up to very high velocities (12 $m.s^{-1}$).

3. The collapsed vessel is represented in figure (5-c). A super-critical flow appears, followed by a shock marking the transition from super-critical to sub-critical flow rate. The shock is defined as discontinuity of certain physical magnitudes, here, blood flow rates. Shock location is at the external pressure discontinuity. Compression and relaxation waves appear, with the consequences we know, i.e. backflow of blood which tends to be trapped upstream.

At this point of our study, only a local analysis has been reported. A last calculation is an overall analysis of the behavior of the pilot's fluid/vessel system, over the entire application of the load on a portion of the aircraft flight path. Changes in load and external pressure distribution are depicted in figure 9. We study a possible relationship between the moment when the load is applied and the phase of the cardiac cycle. Changes in ratio M of mean blood velocity to parietal wave velocity were superimposed onto figure 10. We observe that supercritical flow conditions create a shock which in turn causes a decrease in blood flow a followed by backflow.

4.3- Conclusion

The observation of a change in the symptomatology of inflight loss of counsciousness of fighter pilots exposed to rapid onset rate load led us to suggest a hypothesis different from the thesis of hypoxia: intracranial hypertension (Quandieu and Gaffié). We developed a physical model to represent brain blood flow under the influence of external factors. This model applies to an elastic vessel in which a fluid flows which is assumed to Newtonian. One-dimensional equations were prepared to represent the behavior of this system. The numerical processing of this model showed that, under certain conditions, compatible with situations encountered inflights, supercritical flow rate could develop, generally unstable, and immediately followed by a transition shock. This mechanical analysis of the problem provides a partial response which for ROR acceleration factors the hypothesis of intracranial hypertension resulting from the trapping of part of the blood mass inside the brain.

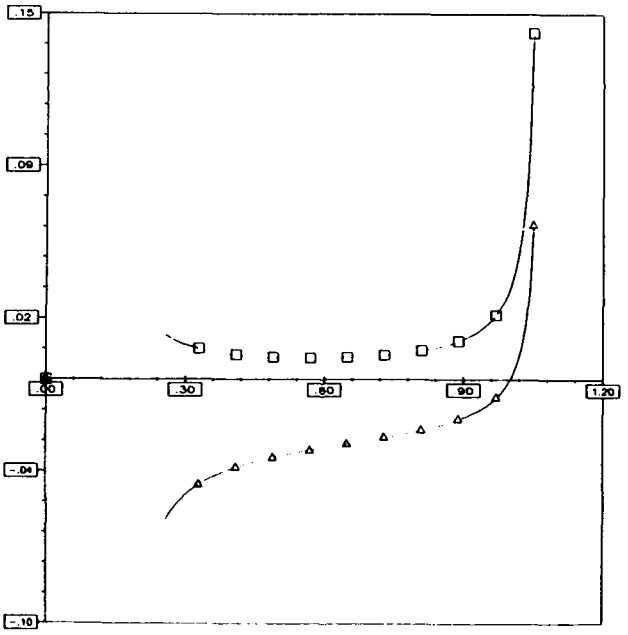

Figure 1 :

Vessel behavior law (a) and parietal wave velocity (b) versus non-dimensional section.

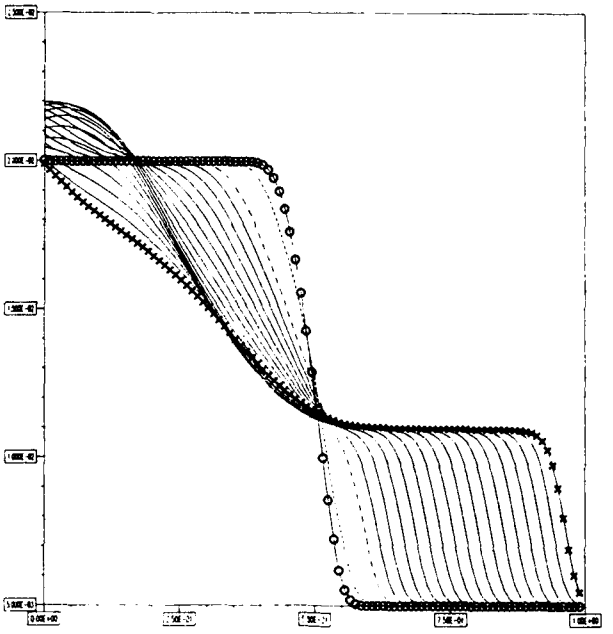

Figure 2 :

Représentation de la section en fonction de la direction longitudinale z, à des instants successifs, dans le cadre d'une loi de tube linéaire.

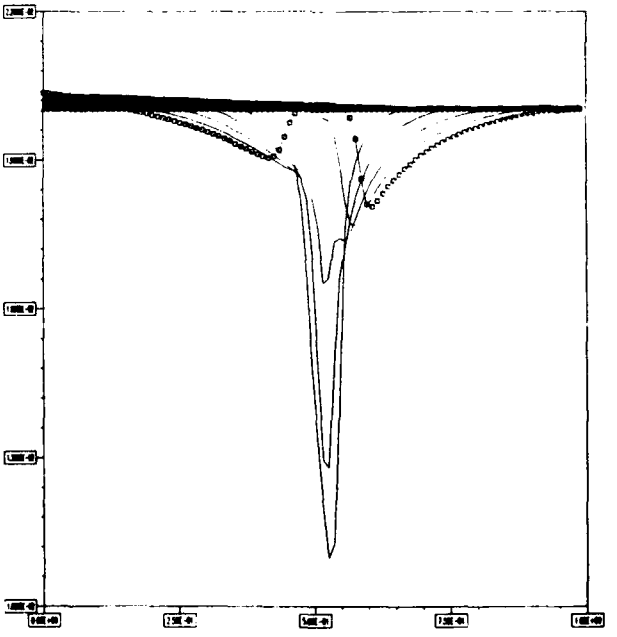

Figure 3 :

Représentation de la section en fonction de la direction longitudinale z, à des instants successifs, dans le cadre d'une loi de tube non-linéaire (c.f. figure (1)).

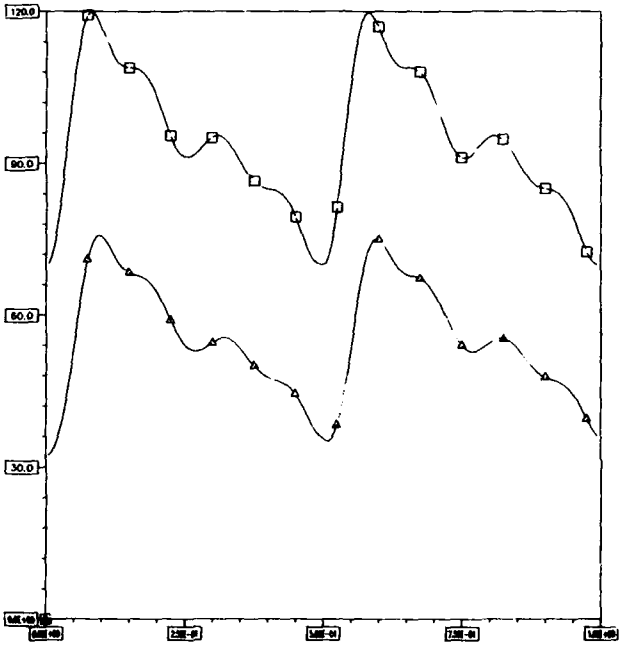

Figure 4:

Pressure time distributions at the inpout and the output of the vessel.

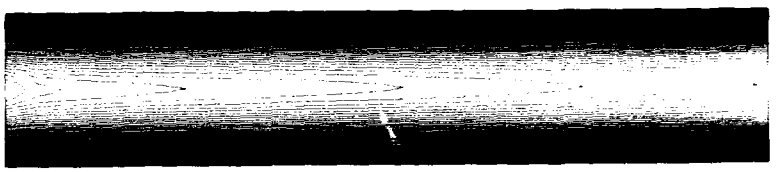

(a) - Transient phase.

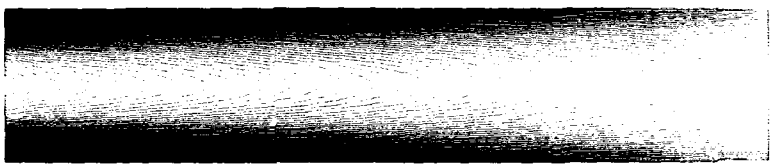

(b) - Acceleration onset phase.

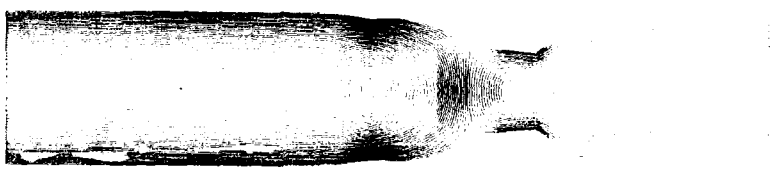

(c) - External pressure distribution.

Figure 5:

Axial velocity contours:

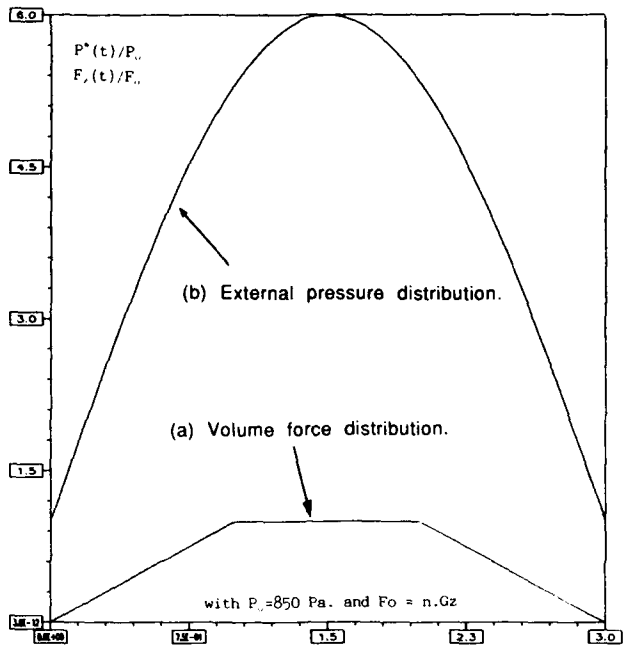

Figure 6:

External disturbance field versus the time:

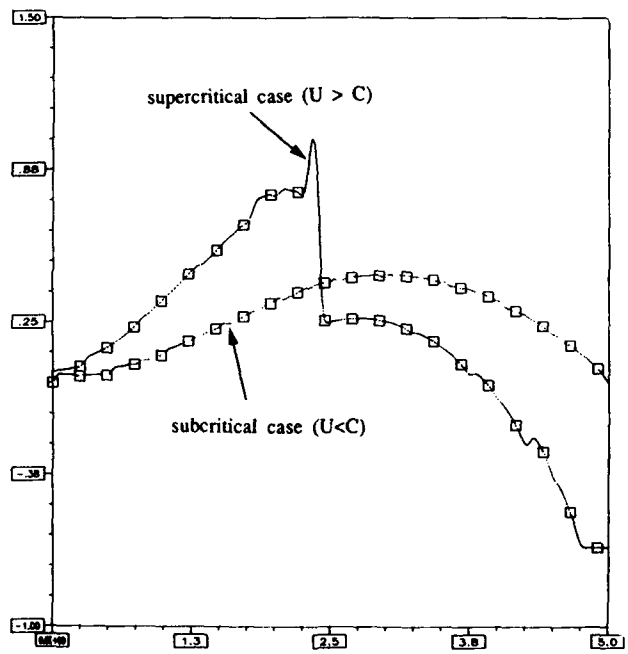

Figure 7

Distribution of the quantity M (similar to Mach number) versus time.

V - References

[1] KAMM, D.K., SHAPIRO, A.H., 1979.
Unsteady flow in a collapsible tube subjected to external pressure or body forces.
J. Fluid. Mech. 95, 1-78.

[2] GODOUNOV, S., 1973.
Equations de la physique mathématique.
Ed. Mir.

[3] GODOUNOV, S., ZABRODINE, A., IVANOV, M., KRAIKO, A., PROKOPOV, G., 1979.
Résolution numérique des problèmes multidimensionnels de la dynamique des gaz.
Ed. Mir.

[4] RICHMEYER, R.D., MORTON, K.W., 1967.
Difference methods for initial-value problems.
N.Y. Interscience publ.

[5] RUBINOW, S.I., KELLER, J.B., 1972.
Flow of viscous fluid through an elastic tube with applications to blood flow.
J. Theor. Biol., 299-313.

[6] SHAPIRO, A.H. , HAWTHORNE, W.R. 1947.
The mechanics and thermodynamics of steady one dimensional gaz flow.

[7] SHAPIRO, A.H. 1977a.
Physiologic and medical aspects of flow in collapsible tubes.
Proc. 6th Canadian Cong. Appl. Mech. Vancouver, 883-903.

[8] SHAPIRO, A.H. 1977b.
Steady flow in collapsible tubes.
J. Biomec. Engng 99, 126-147.

[9] RUBINOW, S.I., KELLER, J.B., 1972.
Flow of viscous fluid through an elastic tube with applications to blood flow.
J. Theor. Biol., 299-313.

[10] SHAPIRO, A.H. , HAWTHORNE, W.R. 1947.
The mechanics and thermodynamics of steady one dimensional gaz flow.

[11] SHAPIRO, A.H. 1977a.
Physiologic and medical aspects of flow in collapsible tubes.
Proc. 6th Canadian Cong. Appl. Mech. Vancouver, 883-903.

[12] SHAPIRO, A.H. 1977b.
Steady flow in collapsible tubes.
J. Biomec. Engng 99, 126-147.

[13] STEGER J.L., WARMING R.I., 1981.
Flux vector splitting of the inviscid gasdynamic equations with applications to finite difference methods.
Computational Physics 40, 263-993.

Finite Element Modeling of Sustained $+G_z$ Acceleration Induced Stresses in the Human Ventricle Myocardium

J. Moore and B. Tabarrok
Department of Mechanical Engineering
University of Victoria
Victoria, B.C., CA V8R 2Y2

W. Fraser
Department of National Defence and Civil
Institute for Environmental Medicine
Downsview, Ontario, CA M3M 3B9

Summary

Due to reports of endocardial hemorrhaging and myofibrillar degradation in swines undergoing high sustained $+G_z$ accelerations, questions arise as to the possibility of cardiac tissue damage in humans subjected to similar $+G_z$ forces. Non-invasive cardiological techniques used during experiments seem too insensitive to provide sufficient data to determine the presence of any localized cardiac damage. In addition, these tests involve some risk to the subject. Hence, there exists the need for a model to predict possible tissue damage under high sustained $+G_z$ accelerations. This paper presents the development of such a model for the analysis of $+G_z$ induced stresses in the human ventricle myocardium. The model is based on the finite element method where the effects of finite displacements, large strains and non-linear nearly incompressible material behaviour are accounted for. When experiments cannot be justified the computational model can provide valuable quantitative (gross distortions and predicted stresses) data on the effects of $+G_z$ induced stresses in humans. Ultimately, the goal is to provide some form of cardiac risk assessment for pilots of high performance aircraft.

1 Introduction

The development of high performance aircraft capable of providing substantial positive accelerations ($+G_z$) has created the need for a better understanding of the adverse physiological responses that can affect a pilot's judgement. This adversity ranges from the less severe temporary loss of peripheral vision to unconsciousness and, in very severe cases, permanent damage to heart tissue. For safety reasons, there is considerable interest in the cardiovascular system since it plays a vital role in the human physiological changes resulting from exposure to sustained $+G_z$ accelerations (see references [4, 9, 25]).

Under these high $+G_z$ loading conditions the heart tissue will be highly stressed and these $+G_z$ loadings have been found to be associated with abnormalities of the electrocardiogram in man [24], as well as subendocardial hemorrhage and pathological changes in the myocardial tissue of animal models [25]. Though most researchers have assumed that ischemia is the cause of the tissue damage [37], detailed pathological examination of the ventricle of the swine has indicated tearing of the heart fibres rather than damage consistent with a hypoxic or ischemic insult. It is probable that the observed damage is due to the high stresses, and subsequent strains, from a combination of i) high $+G_z$ loading acting directly on the heart fibres, ii) the elevated hydrostatic pressures in the vasculature, and iii) the stresses from normal contraction of the heart. An analysis of the heart under such conditions involves both non-linear geometric and material effects. This paper outlines the development of a computational finite element model for the determination of the stress/strain state of the human left ventricle (LV) and right ventricle (RV) myocardium during sustained $+G_z$ acceleration. The proposed mechno-myocardial study differs from previous works in that in the earlier studies only the passive diastole and active systole cyclic responses of the heart were considered in a relatively stress-free environment, for example see [6, 11, 12, 13, 14, 15, 22, 30, 31, 33, 39].

The flexibility of the finite element method for dealing with complicated shapes, and the ability to take into account material and geometrical non-linearities effects makes this technique an ideal research tool for the study of the heart. In addition, with the advent of computer-aided tomography, in particular, Mag-

netic Resonance Imaging (MRI) and data imaging, accurate reconstruction of the three- dimensional ventricular shape is possible [8, 36]. Nevertheless, there remain some limitations to the existing finite element models of the left and right ventricle myocardium that must be addressed [33]. For example, even though numerous experimental studies have been carried out on the heart, there is still considerable lack of information on the anisotropic material properties for constitutive relations of the intact myocardium.

The heart wall is composed of continuous intertwining myocardial fibers following a helical path, with varying helix angle (-50 to $+50$ degs.) through the wall thickness [38]. Theses complex fiber bundles form the left and right ventricles. In essence the heart wall behaves as a *non-linear anisotropic composite material* [32]. There exists in the literature some data on the properties of heart tissue [34, 35]. However, in recent years a number of interesting *constitutive relations for passive myocardium* have appeared. These relationships are based on a *pseudo-strain* energy function, which represents a *best fit* of the material parameters collected experimentally. Nevertheless, this approximate set of constitutive relations provide better predictive capabilities than the linear extrapolation methods (see [19, 20, 21]). Hence, it is both feasible and desirable to incorporate such a constitutive model into the finite element model.

For the above reasons, it was decided that a special purpose computer program be developed *in-house* for the non-linear analysis of the human ventricles. This approach lends itself to a much easier process of model refinement as newly available analysis techniques are developed and material/physiological data becomes available. It should also be possible to perform a comparison of numerically generated geometric responses with those measured experimentally using ultra-sound imaging techniques in a centrifuge [7].

Though the task of performing a realistic simulation of the cardiac response under sustained $+G_z$ acceleration is an enormously difficult task, progress over the past two decades in both computer/medical technology has reached a stage where a sufficiently accurate computational model of the heart can now be developed.

2 Theoretical Background

2.1 Kinematics of Deformation

In order to analyse the motion of a deformable body either a Lagrangian (material / referential) or Eulerian (current / spatial) approach may be used [26] (see Figure 1). In this study, the so called *Updated Lagrangian* approach is adopted. In this approach the reference frame, attached to each element, moves with changes in geometry. This corresponds to the special case where $r = t$ in Figure 1. Alternatively, if $r = 0$ then the *Total Lagrangian* method where all variables are referred to the initial configuration at $\tau = 0$ would have resulted. Both formulations are mathematically equivalent, however, one may possess some computational advantages over the other depending on the problem under consideration.

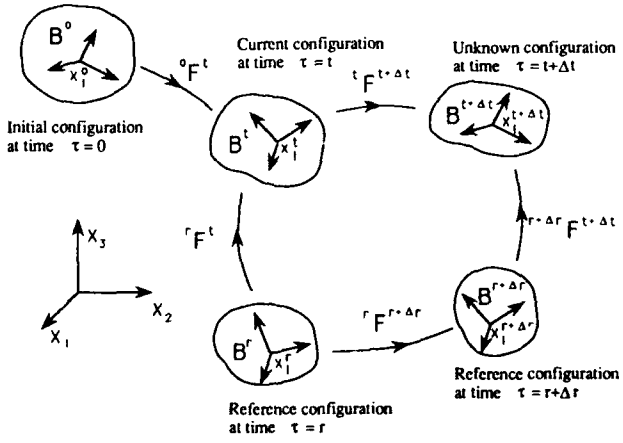

Figure 1. Incremental description of deformation (with deformation gradient: ${}^{\circ}F_{ij}^{t}=\partial x_i^t/\partial x_j^{\circ}$).

2.2 Equations of Motion

Consider the Eulerian differential field equations, or more commonly referred to as the *equations of motion*:

$$\frac{\partial \sigma_{ij}}{\partial x_j} + \rho b_i = \rho \ddot{u}_i \tag{1}$$

subject to the prescribed displacements on the boundary Γ_{g_i}:

$$u_i = g_i(\mathbf{x}, t) \tag{2}$$

and tractions on the complementary boundary $\Gamma_{g_i^*}$:

$$\tau_i = \sigma_{ij} n_j = g_i^*(\mathbf{x}, t) \tag{3}$$

With the following initial conditions:

$$u_i(\mathbf{X}, 0) = u_i^o(\mathbf{X}) \qquad \dot{u}_i(\mathbf{X}, 0) = \dot{u}_i^o(\mathbf{X}) \tag{4}$$

For the special case of a body at rest Eq.(1) is referred to as the equilibrium equations with $\dot{u}_i(\mathbf{x}, t) = 0$ for all $x \in \mathcal{B}$ and $t \in [0, \infty)$; where σ is the Cauchy (true) stress tensor, $\mathbf{x}(\mathbf{X}, t)$ is a vector of spatial coordinates, (which is a function of initial material coordinates $\mathbf{X}$ and time t), $\mathbf{b}$ is the body acceleration vector, ρ is the mass density and, $\mathbf{n}$ is a outward normal vector. Further, the indices i, j which range from 1 to 3, denote the Cartesian coordinate system relative to a fixed global frame. One can also consider the variational form of the equilibrium equations with the virtual displacements $\delta \mathbf{u}$ as:

$$\int_\Omega \left(\frac{\partial \sigma_{ij}}{\partial x_j} + \rho b_i \right) \delta u_i d\Omega = 0 \tag{5}$$

Now, applying the divergence theorem to Eq.(5) yields:

$$\int_\Omega \delta u_i \rho b_i d\Omega + \int_\Gamma \delta u_i \sigma_{ij} n_j d\Gamma - \int_\Omega \frac{\partial \delta u_i}{\partial x_j} \sigma_{ij} d\Omega = 0 \tag{6}$$

In terms of the virtual strain energy:

$$\int_\Omega \delta \cdot \rho b_i d\Omega + \int_\Gamma \delta u_i \sigma_{ij} n_j d\Gamma - \int_\Omega \delta \epsilon_{ij} \sigma_{ij} d\Omega = 0 \tag{7}$$

where $\delta \epsilon$ is the variational *strain* tensor which is conjugate to the Cauchy stress. Due to symmetry of the stress and strain tensors, $\delta \epsilon_{ij}$ can be written as:

$$\delta \epsilon_{ij} = \frac{1}{2} \left(\frac{\partial \delta u_i}{\partial x_j} + \frac{\partial \delta u_j}{\partial x_i} \right) \tag{8}$$

The finite element formulation is based on these fundamental non-linear continuum equations (equilibrium and constitutive) which are ultimately expressed in a linearized form for numerical implementation at each incremental step. A detailed description of the finite element formulation used is given in references [2, 17, 23, 28]. In this approach the non-linear system of equations are solved iteratively as a set of linear equations in each iteration. Thus a discrete load history of the responses is obtained as the load is increased in small steps.

3 Modeling and Analysis of the Human Heart

3.1 Development Stages of the Human Heart Model

The development of the human heart model can conceptually be broken down into four distinct phases. (These phases pertain only to the heart model and not to the theoretical development, implementation and verification of the FE algorithm.) In the initial phase, MRI imaging data is required for various cross-sectional planes of a healthy human heart. (see Figure 2-1). In the second phase, a 3D model of the left and right ventricles during diastole is reconstructed from a coronal, sagittal, and transverse MRI images obtained (Figure 2-2). In phase 3, an accurate 3D finite element mesh of the irregular geometry of the heart is reconstructed from the imaging data (see Figure 2-3). Finally, phase 4, which represents the vast majority of the work, involves the determination and processing of $+G_z$ acceleration induced stresses in the LV and RV from a non-linear finite element analysis (Figure 2-4). This phase should also include a comparison of the numerically generated deformation profiles with those obtained experimentally, for final validation of the FE algorithm and the heart model developed.

3.2 Geometric Modeling Considerations

An accurate description of the human heart requires the use of elements capable of conforming to the irregular geometry. For this particular problem, such elements are best developed based on a 3D continuum formulation. Further, these elements must be able to handle arbitrary large displacements and rotations while maintaining kinematically admissible displacement fields at element interfaces. Two such element types satisfying these conditions have been selected for use, making them ideal for problems involving geometric and material nonlinearities (see Figure 3). The first is a 20-node isoparametric solid stress element [2]. The second is an 8-node degenerated 3D continuum based shell element [1, 3, 18]. The 20-node solid element is ideally suited for model-

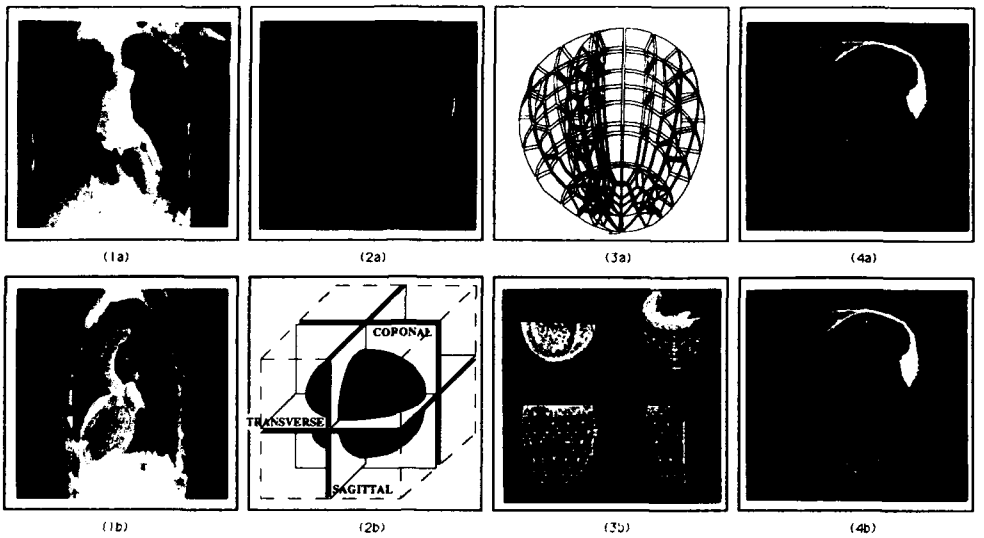

Stage 1: MRI imaging of the human heart, showing (1a) coronal and (1b) sagittal images at the end of a diastolic phase (Eiho, S. et al)

Stage 2. (1a) 3D clay model constructed from (2b) coronal, transverse and sagittal cross sectional shapes on different planes.

Stage 3: Generation of a 3D finite element mesh of the right and left ventricles; (3a) wireframe and (3b) solid representations.

Stage 4: Determination and postprocessing of +Gz stresses in the LV and RV from a FEA. (4a) without and (4b) with displacements superimposed.

Figure 3. MRI imaging, FE modeling and analysis of the human left and right ventricles.

ing of the left and right ventricles, while the 8-node shell element is used to model the pericardial sac, which is a conical fibrous membrane surrounding the heart and proximal portions of the cardiac vessel. Only by including the pericardial sac in the analysis will the correct boundary conditions be realised, and accuracy of the geometric model be assumed.

3.3 Using an Appropriate Constitutive Relation

It is vital that computational models developed use reliable data for the mechanical properties of the heart tissue. Recently, a number of three-dimensional constitutive relations for passive cardiac tissue, undergoing finite strain, have appeared in the literature by Humphrey et al. [19, 20, 21]. These relationships use uni- and bi- axial experimental stress-strain data to provide information for selecting *best fit* parameters to construct a pseudo-strain energy function, W. The feasiblility of introducing such pseudo-strain energy functions into the finite element formulation is currently being explored. However, due to the lack of a reliable constitutive relation for modeling the anisotropic material behaviour of the human heart, a non-linear isotropic relationship was adopted in this study. The constitutive relation is of the form $\Delta\sigma = [C]\Delta\epsilon$. Where the non-linear incremental stress-strain ($\Delta\sigma$-$\Delta\epsilon$) relation, using a linear Young's modulus (E)-stress relationship to construct the material matrix $[C]$ is given by: $E = a + b\sigma_m$ Pa, where $a = 4.47 \times 10^3$ and $b = 5.056$ with σ_m being the maximum myocardial principal stress [12]. Poisson's ratio (ν) is taken equal to 0.49.

3.4 Comparison with Experimental Images

Unfortunately, there is very little data available on the passive myocardial tissue properties obtained from high tri-axial stress measurements. Therefore, it becomes necessary to "project" in a rational manner, the properties in the stress-free state to those at high stress. This approach evidently builds into the finite element model a measure of uncertainty. A heuristic approach would be to compute the deformed shape of the heart, using projected material properties, and compare the results with ultra-sound images of the heart under high ($+G_z$) loading [7]. To bring about an optimum agreement between the experimentally obtained images and the response of the computational model, the assumed material prop-

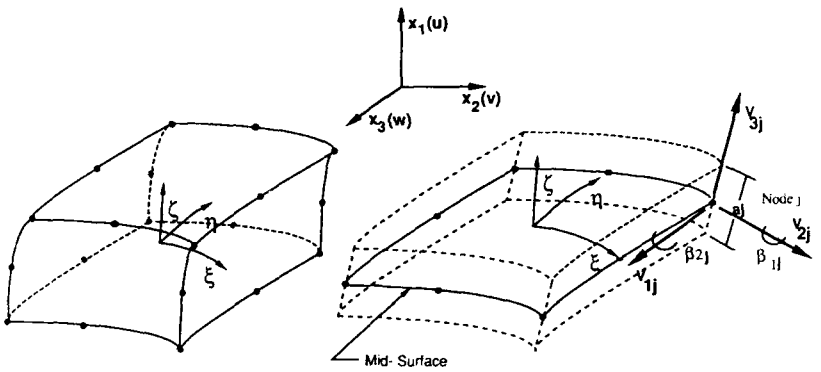

(a) 20 node isoparametric stress solid. (b) Degenerated 8-node continuum based shell.

Figure 3. Continuum based isoparametric elements used in modeling the human heart.

erties may be readjusted. By using the outlined procedure, the possibility of myocardial damage due to excessive strains, induced from the combination of high $+G_z$ loading acting directly on the heart fibres and elevated hydrostatic pressures in the vasculature, can be determined.

3.5 Computational Verification and Testing of the Heart Model

The verification of the finite element program developed was carried out in several stages. The initial stages involved using properties for isotropic engineering materials, (e.g., steel and rubber), to perform extensive tests on plates, cylindrical and spherical shell structures subject to various loadings. In the order of increasing complexity, these verification tests consisted of:

1. Linear analysis
2. Geometrical non-linear analysis
3. Material non-linear analysis
4. Material and geometrical non-linear analysis

For some of these tests analytical results are available while for others numerical results exist in the literature, (for example [3, 18]). Such information is used to verify the computer program developed.

3.6 Pre and Post Processing of Mesh and Stress Data

In order to develop a working model of the human heart it is imperative that a FE pre and post processor with 3D colour capabilities be available. Such a facility enables one to view the model as it is being built. In addition, by selecting various perspective views and colour coding elements one can easily verify the *correctness* of the FE mesh generated. Most importantly, the 3D graphics modeler enables the post processing of both stress and displacement data in a pictorial format (Figure 2-4). In addition, using colour stress contouring of stress and strain fields the analyst is able to easily locate critical regions from the the vast amount of data generated during each load increment.

Conclusions

A computational model for the analysis of $+G_z$ induced stresses in the human ventricle myocardium was presented. The model, based on the finite element method takes into account the effects of finite displacements, large strains and the non-linear nearly incompressible material of the heart. Various aspects of the heart models development and the limitations of presently available constitutive relationships were discussed. However, when experiments cannot be justified on moral grounds the computational model can provide useful quantitative (gross distortions and stresses - strains) data on the effects of $+G_z$ induced stresses in human heart.

References

[1] Ahmad, S., Irons, B.M., and Zienkiewicz, O.C., *Analysis of thick and thin shell structures by curved finite elements,* Int. J. of Num. Meth. Eng., (1970), 2:419-451.

[2] Bathe, K.J., *Finite Element Procedures in Eng. Analysis,* (1982), Prentice Hall Inc., New Jersey, 1st ed.

[3] Bathe, K.J., and Bolourchi, S., *A geometric and material non-linear plate and shell element, Comp. and Structures,* (1980), 11:23-48.

[4] Burton, R.R., and Whinnery, J.E., *Operational G-induced loss of consciousness: Something old; something new,* Aviation, Space and Environmental Medicine, (1985), 8:812-817.

[5] Chambost, G., and Turk, P. *G-induced loss of consciousness: Combat aircraft pilots head for trouble, INTERAVIA,* (1986), 5:507-508.

[6] Chen, C.J., Kwak, B.M., Rim, K., and Falsetti, M.L., *A model for an active left ventricle deformation-formulation of a non-linear quasi-steady finite-element analysis for orthotropic, three-dimensional myocardium,* Int. Conf. Finite Elements in Biomechanics, (1980), 2:639-655.

[7] Danaher, C. *Air Force Evaluates Acceleration Effects on Cockpit Design,* Aviation Space and Environmental Medicine.

[8] Eino, S., Matsumoto, N., Kuwahara, M., Matsuda, T., and Kawai, C., *3-D reconstruction and display of moving heart shapes from MRI data, IEEE Computer Society,* Computers in Cardiology 1987, (1988), pp. 349-352.

[9] Erickson, H.H., Sandler, H., and Stone, H.L., *Cardiovascular Function During Sustained $+G_z$ Stress,* Aviation, Space, and Environmental Med., (1976), 7:750-756.

[10] Fung, Y.C., *Biomechanics: Mechanical Properties of Living Tissues,* (1981), Springer-Verlag New York Inc.

[11] Ghista, D.N., and Hamid, M.S., *Finite-element stress analysis of the human left ventricle whose irregular shape is developed from single plane cineangiocardiogram,* Comp. Prog. Biomed. (1980), 7:219-231.

[12] Ghista, D.N., Roy, G., and Sahdler, H., *Cardiac assessment mechanics: I, Left ventricular mechno-myocardiography, a new approach to the direction of diseased myocardial elements and states,* Med. Biol. Eng. and Comp., (1980), 18:271-280.

[13] Gould, P., Ghista D., Brombolich, L., and Minsky, J., *In-vivo stresses in the human left ventricular wall: analysis accounting for the irregular 3-D dimensional geometry and comparison with idealized geometry analysis,* J. Biomechanics, (1972), 5:521-539.

[14] Han, G., McPherson D.D., and Chandran, K.B., *Finite Element Analysis of the Effect of Right Ventricular Ischemia on the Left Ventricular Function, ASME,* 1989 Advances in Bioengineering, (1989), BED 15:37-138, (ASME winter annual meeting, San Fransisco, Calif., Dec. 10-15, 1989).

[15] R.M., Pao, Y.C., and Ritman, E.L., *Computer Aspects of three-dimensional finite element analysis of stresses and strains in the intact heart,* Comp. and Biomed. Res., (1977), 10:271-285.

[16] Horrigmoe, G., and Bergan, P.G., *Incremental variational principles and finite element models for non-linear problems,* Comp. Meth. Appl. Mech. and Eng., (1976), 7:201-217.

[17] Hibbitt, H.D., Marcal, P.V., and Rice J.R., *A finite element formulation for problems of large strain and large displacements,* Int. J. Soild. Structures, (1970), 6:1069-1086.

[18] Hughes, T.J.R., and Cornoy, E., *Non-linear finite element shell formulation accounting for large membrane strains* Comp. Meth. in Appl. Mech. and Eng., (1983), 39:69-82.

[19] Humphery, J.D., and Yin, F.C.P., *On constitutive relations and finite deformations of passive cardiac tissue: I, A pseudo-strain energy function,* Trans. ASME, J. of Biomech. Eng., (1987), 109:298-304.

[20] Humphery, J.D., Strumpf, R.K., and Yin, F.C.P., *Determination of a constitutive relation for passive myocardium: I A new functional form,* Trans. ASME, J. of Biomech. Eng., (1990), 112:333-339.

[21] Humphery, J.D., Strumpf, R.K., and Yin, F.C.P., *Determination of a constitutive relation for passive myocardium: II Parameter estimation,* Trans. ASME, J. of Biomech. Eng., (1990), 112:340-345.

[22] Janz, R.F., Kubert B.R., Moriarty, T.F., and Grimm, A.F. *Deformation of the diastolic left ventricle - II. Nonlinear geometric effects,* J. Biomechanics, (1974), 7:509-516.

[23] Kluber, M., *Incremental Finite Element Modelling in Non-linear Solid Mechanics,* Ellis Horwood Ltd., (1989), 1st ed.

[24] Leverett, S.D., Jr., Burton, R.R., Crossley, R.J., Michaelson, E.D., and Shubrouks, S.J., Jr., *Human Physiologic Responses to*

High, Sustained $+G_z$ Acceleration, (1973). *USAFSAM* TR-73-21.

[25] Mackenzie, W.F. and Burton, R.R., *Ventricular Pathology in Swine at High Sustained $+G_z$*, (1976), AGARD Conf. Proc. No. 189, The Pathophysiology of High Sustained $+G_z$ Acceleration. ed. Clarke, N.P., Leverett, S.D., A2:1-2.

[26] Malvern L.E., *Introduction to the Mechanics of a Continuous Medium*, Prentice Hall, Inc., (1969).

[27] Meethaar, R.M., Pao, Y.C., and Retman, E.L., *Computer aspects of three-dimensional finite-elements: analysis of stresses and strains in the intact heart*, Comp. and Biomed. Res., (1977), 10:291-295.

[28] McMeeking R.M. and Rice, J.R. i *Finite-element formulations for problems of large elastic-plastic deformations*, Int. J. Solids and Structures, (1975), 11:601-615.

[29] Panada S.C., and Natarajan, R., *Finite-element method of stress analysis in the human left ventricular layered wall structure*, Med. Biol. Eng. Comp., (1977), 15:76-71.

[30] Pao, Y.C., Retman, E.L., and Wood, E.M., *Finite-element analysis of left ventricular myocardial stresses*, J. Biomechanics, (1974), 7:469-477.

[31] Pao, Y.C., Robb, R.A., and Retman, E.L., *Plain-strain finite element analysis of reconstructed diastolic left ventricular cross section*, Ann. Biomed. Eng., (1976), 4:232-249.

[32] Pao Y.C., Natarajan, G.K., Padiyar, R., and Ritman, E.L., *Derivation of myocardial fiber stiffness equation based on theory of laminated composite*, Trans. ASME, J. of Biomechanical Eng., (1980), 102:252-257.

[33] Perl, ... and Horowitz, A., *Material and structural limitations in a 3D finite element model of the left ventricle*, ed. Sideman, S., *Simulation and imaging of the cardiac system*, (1985), pp. 117-129.

[34] Pinto, J.G., and Fung, Y.C., *Mechanical properties of the heart muscle in the passive state*, J. Biomechanics, (1973), 6:597-616.

[35] Ray, G., and Ghista, D.N., *In vivo properties of normal and ischemic-infarcted myocardium*, , (1979), Proc. 7^{th} Canadian Congress of Applied Mechanics, Sherbrooke, pp. 819-820.

[36] Retman, E.L., Kursey, J.H., Robb, R.A., Gilbert, B.K., Haris, L.D., and Wood, E.H., *Three dimensional imaging of heart, lung, and circulation*, Science, (1980), 210:273-280.

[37] Stone, H.L., Sordahl, L.A., Dowell, R.T., Lindsey, J.W., and Erickson, M.M., *Coronary Flow and Myocardial Biochemical Responses to High Sustained $+G_z$ Acceleration*, (1976), AGARD Conf. Proc. No. 189, The Pathophysiology of High Sustained $+G_z$ Acceleration. ed. Clarke, N.P., Leverett, S.D., A5:1-8.

[38] Streeter, D.D. Jr., *Gross morphology and fibre geometry of the heart*, ed. Berne R.M. et al, *Handbook of Physiology - The Cardiovascular System I*, 1:61-112;

[39] Yettram, A.L., Vinson, C.A., and Gibson, D.G., *Effect of myocardial fiber architecture on the behaviour of the human left ventricle in diastole*, J. Biomed. Eng., (1983), 5:321-328.

PHYSIOLOGICAL REQUIREMENTS FOR PARTIAL PRESSURE ASSEMBLIES FOR ALTITUDE PROTECTION

by

Dr A J F Macmillan
Royal Air Force Institute of Aviation Medicine
Farnborough, Hampshire GU14 6SZ, UK

SUMMARY

Partial pressure assemblies utilising an oronasal mask, and garments providing counter pressure to the torso and lower limbs may be used to provide protection against a short term exposure (1-2 minutes) to altitudes up to 60-65,000 feet.

The performance characteristics of the delivery system used in such emergency exposures must be at least as good as that required during routine operations.

Mask cavity pressure of up to 80 mmHg may be tolerated for a short period provided adequate chest and lower limb counter pressure is provided.

When upper body counter pressure is limited to the chest, then anti-G suit pressure should be at least 3 times the breathing pressure.

Further "trade-offs" of breathing pressure and counter pressure against absolute oxygen pressure with the use of gas mixtures with less than 100% oxygen should be defined by examining the effect of these trade-offs on performance, and arterial gas tensions and cardiovascular responses.

INTRODUCTION

The next generation of high performance aircraft will be capable of sustaining operations at altitudes in excess of 50,000 feet. The principal physiological hazards associated with loss of cabin pressure at such altitudes are hypoxia, decompression sickness and cold. A full pressure suit assembly is necessary if protection against all three hazards is required over a prolonged period. However if the aircraft can descend promptly and rapidly (within 3-4 minutes) to an altitude of less than 40,000 feet, protection only against hypoxia is required. A full pressure suit assembly will provide the ideal physiological protection but it is bulky, cumbersome, impairs operational efficiency during routine flying with an intact cabin and imposes major ground procedural problems, particularly when Quick Readiness Alert or other rapid response is required.

Most Air Forces have therefore adopted positive pressure breathing (PPB) combined with partial pressure garments at altitudes in excess of 50,000 feet to provide short-term or "get-you-down" protection against hypoxia. Partial pressure garments are required to combat the undesirable physiological disturbances produced by PPB but in order to exploit the advantages of the partial pressure approach (less restriction when inflated and uninflated, greater routine comfort and lower thermal load) it is desirable that counterpressure should be applied to the minimum area of the body. Thus the design of garments represents a compromise between ideal physiological requirements and functional convenience. In addition since the protection against hypoxia using a partial pressure assembly is required for only a short period of time during emergency descent, some compromise in the level of alveolar partial pressure of oxygen which is required in the steady state is also acceptable. It is the interaction of the deleterious effects of mild

hypoxia with the undesirable consequences of positive pressure breathing which determines the admissable concession to the ideal level of oxygenation.

The practical compromises which may be applied to partial pressure assemblies for altitude protection are described in this paper.

THE OXYGEN DELIVERY SYSTEM

The performance of an optimum oxygen system even for "get-you-down" equipment should be such that it maintains an adequate partial pressure of oxygen within the alveoli whilst imposing minimal physiological stress. This physiological stress applied by an oxygen delivery system at cabin altitudes below 40,000 feet (when PPB is not required) is generally generated by the impedance of the breathing devices and limitations in the flow capacity of the demand regulator and has been well described elsewhere (Ref 1). These recommended minimum standards must be maintained when pressure breathing is delivered so that the undesirable physiological effects produced by the raised intrathoracic pressure are not augmented by cardio respiratory stresses imposed by the equipment.

Respiratory Volume Demands

In most individuals, pressure breathing causes an increase in pulmonary ventilation although the magnitude of this varies and depends to some extent upon the experience of the subject. Pressure breathing at 30 mmHg (4.0 kPa) causes, on average, an increase in the respiratory minute volume of about 50% more than the resting value. The individual responses may vary from doubling ventilation to little or no increase. Respiratory disturbances induced by pressure breathing are minimised by the application of counter pressure to the surface of the thorax and abdomen. Significant distension of the lungs is prevented and breathing remains relatively effortless even at positive pressures in excess of 100 mmHg (13.3 kPa) (Ref 2). The degree of hyperventilation induced by a given breathing pressure is also reduced and it can be concluded that an oxygen system which can adequately meet the maximum pulmonary ventilation which may be sustained in flight for longer than 30 seconds (55 L (BTPS) Ref 3) will adequately supply the volume demands required of a partial pressure assembly.

Respiratory Flow

Pressure breathing causes marked changes in respiratory flow patterns in addition to the reversal of the normal mechanism of breathing in which expiration becomes active whilst inspiration is passive. Thus the pneumotachgram inspiratory curve becomes shorter in duration and peaked with higher instantaneous flows while expiration is extended and flattened but with little or no change in peak flow. The maximum peak inspiratory flows recorded in flight using a conventional oxygen system are of the order of 160 L (BTPS)/min (Ref 3) although using a low impedance breathing system Harding (Ref 4) recorded 2.5% of breaths with peak inspiratory flows in excess of 220 L (BTPS)/min. Comparable data for in-flight pressure breathing are not available but in practice, with adequate training and experience of pressure breathing, instantaneous respiratory flows recorded in hypobaric chamber exposures are considerably lower than those recorded in flight.

The maximum flow required from an oxygen delivery system is more likely to be set by the requirement to pressurise adequately counter pressure garments whose gas supplies are derived from the same demand regulator as supplies the respiratory tract. The greater the volume of the bladders in the counter pressure garment the greater is the flow capacity required from the demand regulator. For a typical counter pressure garment covering the torso with a bladder volume of approximately 15 L (incompressible litres at a pressure of 80 mmHg) which is required to attain at least 90% of final pressure within one second of commencement of inflation a flow capacity in excess of 10 L/sec may be required. The most stringent demands on this function of the regulator will be

imposed during operation of the press-to test facility on the ground or during high G manoeuvres at low level if a PPB for enhanced acceleration protection capacity is present.

Impedance to Respiration

The physiological disturbances which might result from the imposition of a high impedance to breathing (fatigue of respiratory muscles, discomfort, alteration of pulmonary ventilation) tend to be swamped by the magnitude of the effects of PPB. However the total change of mask cavity pressure throughout the respiratory cycle (ie the difference between the minimum and maximum mask cavity pressure) should be as low as possible. Sensations of resistance to breathing or stimulation of hyperventilation may be additive to the effects of PPB particularly at lower levels of positive pressure. The maximum change of mask cavity pressure during the respiratory cycle at altitudes in excess of 40,000 feet should therefore not exceed those acceptable below 40,000 feet (Ref 1).

PREVENTION OF HYPOXIA

Minimum Oxygen Partial Pressure

The positive pressure which must be delivered in the steady state to the respiratory tract at any given altitude above 40,000 feet is determined by the degree of hypoxia or alveolar/arterial PO_2 which is acceptable in the presence of the cardiovascular stress imposed by the pressure breathing. The interaction of these two additive stresses may be modified by the extent of body cover and the inflation pressures uitilised in the counter pressure garments. 100% oxygen has in the past been used as the breathing gas and the relationship between absolute intrapulmonary pressure and performance during pressure breathing both with and without counter pressure is well established (Ref 5) for exposures not exceeding five minutes. These data were based on experiments in which the counter pressure garments were inflated to the same absolute pressure as the breathing pressure. The relationship (Table 1) demonstrates that in order to prevent significant hypoxia in these conditions it would be necessary to maintain an intrapulmonary pressure of not less than 120 mmHg absolute (Ref 5). In these circumstances, since 100% oxygen was employed as the breathing gas, the alveolar gases were principally oxygen and carbon dioxide (saturated with water vapour). If no hyperventilation is assumed then the alveolar PO_2 would be 33 mmHg. However the hyperventilation induced by the positive pressure breathing and lowered arterial PO_2 produces a higher alveolar PO_2 than would otherwise be the case. The hypocapnia which accompanies the hyperventilation influences cerebral blood flow so that the degree of cerebral hypoxia which determines the "performance" of an individual is set by the arterial PO_2, PCO_2 and cardiovascular changes induced by pressure breathing. Thus despite the higher than expected alveolar PO_2 the mean oxygen tension in the cerebral capillaries may be reduced by the reduction in blood flow caused by hypocapnia and pressure breathing itself. This latter reduction will be modified by the extent of the counter pressure applied to the body. It is this interaction of alveolar PO_2, hyperventilation (modified by counter pressure), cerebral blood flow and cardiovascular support provided by pressure garments which permit different combinations of pressure breathing levels and counter pressure to be employed to maintain acceptable levels of cerebral oxygenation in partial pressure assemblies.

TABLE 1

The Relationship Between Absolute Intrapulmonary Pressure and Performance During Pressure Breathing

Absolute Intrapulmonary Pressure mmHg	Breathing Pressure mmHg	Counter Pressure	Performance
141	0 - 141	Trunk and lower limbs	No impairment
130	0 - 70	Trunk and lower limbs	Mild impairment
120	0 - 70	Trunk only	Mild/moderate impairment
115	0 - 30	None	Moderate/ severe impairment

Area of Counter Pressure Cover and Ratio of Anti-G Suit Pressure to Chest Counter Pressure

The partial pressure assembly introduced into RAF service in the 1950s comprised a torso "jerkin" in combination with an anti-G suit. This assembly (which is still in operational use) generally derived the supply to both garments from the breathing regulator so that the bladder inflation pressure equalled breathing pressure. With a mask cavity pressure of 70 mmHg exposures to altitude of 56,000 feet were safely achieved. A differential system (higher pressure in the anti-G suit than jerkin) was however exploited in one aircraft type (Lightning) in which the anti-G valve responded both to +Gz acceleration and exposure to cabin altitudes in excess of 40,000 feet. When providing inflation of the anti-g suit for altitude protection, this "barometric-anti-G valve produced a pressure of approximately 1.5 times the breathing pressure. The advantages of improved lower limb vascular support were recognised but the magnitude of the pressure ratio between anti-G suit and torso counter pressure was rigidly controlled since the anti-G valve functioned independently and in the event of loss of suit pressure, with the maintenance of jerkin pressure, a catastrophic fall in blood pressure would occur if the ratio was much greater. Thus in systems which employ separate lower limb and chest counter pressure garments it must not be possible for the chest garment to remain inflated should failure of the supply to the lower limb garments occur.

In the investigations reported by Larsson and Stromblad (Ref 6) subjects were successfully protected at altitudes of 65,600 feet for 30 seconds following rapid decompression using a minimal chest counter pressure garment with anti-G trousers inflated to 3.2 times the breathing pressure.

Later experiments by Canadian investigators (7, 8, 9, 10) confirmed that improved protection against hypoxia could be obtained by reduced coverage chest counter pressure garments with a higher pressure in the anti-G trousers (3.2 times breathing pressure). Their findings however did suggest that the greater the bladder coverage of the torso, the better the support for the cardiovascular system even in combination with higher G- suit pressures. Thus it was found (Ref 7) that although the RAF partial pressure assembly with no differential pressures provided the highest degree of protection when assessed by the effects on heart rate, peripheral resistance, blood pressure and stroke volume the

addition of an anti-G suit pressure of 3.2 times breathing pressure significantly increased the degree of protection afforded. However, neither the Swedish nor Canadian experimental assessments (particularly the altitude exposures), followed the operational profile usually simulated in UK. Thus in UK it is generally required that when assessed in the laboratory a protective assembly should provide adequate protection at the simulated altitude for at least twice the duration expected in a realistic operational scenario followed by descent at a rate commensurate with the aircraft performance. It is also a pre-requisite that a realistic (usually worst case) gas mixture be breathed prior to the decompression since the influence of the partial pressure of oxygen in the alveolar gas prior to decompression on the impairment of consciousness following the decompression is well recognised (Ref 1).

A systematic assessment of the ability of several different counter pressure garment assemblies to protect against some of the adverse respiratory consequences of pressure breathing has been conducted (Ref 12). Pressure breathing without counter pressure increases Forced Vital Capacity (FVC) by increasing Tidal Volume (TV) and Expiratory Reserve Volume (ERV). Total lung capacity and residual volume are also increased. ERV rises to a much greater extent than FVC (because of the smaller increase in TV and a decrease in inspiratory reserve volume) resulting in an increase in the ratio of ERV/FVC. An ideal counter pressure garment assembly would prevent or minimise any increase in expiratory reserve volume and prevent a rise in the ratio of ERV/FVC during pressure breathing. This would help to protect against respiratory discomfort and fatigue, and prevent an inappropriate increase in pulmonary ventilation. The results indicate that chest counter pressure provided by a waistcoat with bladders around the chest, in combination with lower limb counter pressure provided by anti-G trousers, inflated to three times the pressure supplied to the waistcoat, offered more protection than any other counter pressure assembly tested.

Subsequent experimental exposure at altitudes up to 60,000 feet have confirmed these findings and demonstrated that adequate protection against hypoxia can be provided with this assembly.

The surface area of the lower limbs which is required to be covered by bladders to provide optimum counter pressure for altitude protection has not been so thoroughly investigated. The physiological requirements for increased coverage anti-G suits have largely been dictated by the needs for enhanced G protection. Systematic assessment of increased and full coverage anti-G suits as part of a partial pressure assembly for altitude protection with or without a higher pressure in the lower limb garments has not yet been conducted. In the UK early versions of full coverage anti-G trousers although successfully used for G protection proved to be unacceptably uncomfortable during use at simulated altitudes in excess of 50,000 feet when anti-G suit pressure was 3 times the breathing pressure in the waistcoat (Ref 14). The acceptable pressure schedule compromise for this combination has therefore still to be defined.

Maximum Acceptable Mask Cavity Pressure

In the presence of effective thoracic and abdominal counter pressure the factors which limit the level of pressure breathing which may be delivered to the respiratory tract are the undesirable effects on the head and neck. The most convenient method of delivering breathing gas to the respiratory tract is by an oronasal mask which is capable of sealing the necessary mask cavity pressures. Typical RAF oxygen masks when properly fitted and adjusted will hold pressures up to 100 mmHg without significant leakage. In practice however because support is given to only a limited area of the face well defined physiological effects limit the pressure which can be delivered.

Distension of the upper respiratory tract becomes very uncomfortable at pressures in excess of 70 mmHg and this discomfort is the main limitation to the use of an oronasal mask. Additional effects such as blephorospasm (due to gas passing up the nasalacrimal ducts) and rupture of conjuctival vessels as a

consequence of raised intrathoracic (and hence arterial) blood pressure limit the breathing pressure and duration for which an oronasal mask may be used to 70 mmHg for 3-4 minutes. However, well trained subjects can tolerate pressure breathing up to 80 mmHg for short periods (Refs 5,8) and provided an aircraft can initiate descent within 1 minute of the onset of loss of cabin pressurisation and continue descent at a rate in excess of 10,000 ft/min, mask cavity pressure of up to 80 mmHg, accompanied by adequate body counter pressure, should be acceptable. A pressure or partial pressure helmet would eliminate the pressure differentials which develop between the respiratory tract and the surface of the face and neck when an oronasal mask is employed. These helmets however are bulky, heavy, cumbersome and inappropriate for use in the next generation of high performance aircraft.

Acceptable Gas Mixtures

With the advent of Molecular Sieve Oxygen Concentrating Systems (MSOCs) for production of oxygen rich gas mixtures on board aircraft the use of a breathing gas whose composition is less than 100% oxygen has been investigated. USAF SAM (Ref 15) completed over 200 simulated decompressions to 50,000 feet without counter pressure garments in which subjects breathed gas mixtures at 30 mmHg positive pressure with oxygen concentrations which varied from 85-100%. Transient post decompression alveolar oxygen levels of less than 30 mmHg occurred and it was concluded that the maximum flight ceiling for this partial pressure regime should be reduced from 50,000 feet to 46,000 feet if oxygen concentrations below 93% were delivered. These investigations once again demonstrated the requirement for balance between alveolar PO_2 and pressure breathing levels. Extension of these investigations to examine the altitude domain in which counter pressure garments are required would complete the physiological "picture" but production of acceptable equipment to ensure that the necessary equilibration between the stresses of hypoxia and pressure breathing is maintained at all operational altitudes may be difficult.

REFERENCES

1. Ernsting, J. (1943). Operational and Physiological Requirements for Aircraft Oxygen Systems. Seventh Advanced Operational Aviation Medicine Course. AGARD Report No 697. Paper 1.

2. Ernsting, J. (1965). The Physiology of Pressure Breathing. A Textbook of Aviation Physiology. Ed. J.A. Gillies. Pergamon Press 343-373.

3. Macmillan, A.J.F., Patrick, G.A. and Root, D.E. (1976). Inspiratory Flow and Ventilation in Aerobatic Flight. Air Standardisation Co-ordinating Committee, Aerospace Medical and Life Support Systems. Working Party Report, Vol II.

4. Harding, R. (1983). In Flight Respiratory Response in High Performance Aircraft. Preprints of Annual Scientific Meeting, Aerospace Med. Assoc. 104-105.

5. Ernsting, J. (1966). Some Effects of Raised Intrapulmonary Pressure in Man. AGARDograph 106. Technivision Limited, Maidenhead, England.

6. Larsson, G.E. and Stromblad, B.C.R. (1967). Development of a Flying Suit System for the RSAF, Forsvarsmedicin 3: 17-26.

7. Ackles, K.N., Porlier, J.A.G., Holness, D.E., Wright, G.R., Lambert, J.M. and McArthur, W.J. (1978). Av. Sp. and Env. Med. 49: 753-758.

8. Holness, D.E., Porlier, J.A.G., Ackles, K.N. and Wright, G.R. (1980). Av. Sp. and Env. Med. 51: 454-458.

9. Porlier, J.A.G., Ackles, K.N., Wright, G.K. and Holness, D.E. (1978). Reduction of the Physiological Effects of Positive Pressure Breathing by Increasing G-Suit Counter Pressure. 49th Annual Mtg. Aerosp. Med. Assoc.

10. Ackles, K.N., Porlier, J.A.G., Holness, D.E., Wright, G.R. and McArthur, W.J. (1978). Comparative Physiological Changes Produced by Positive Breathing Pressure of 60 and 70 mmHg at 60,000 feet. 49th Annual Mtg. Aerosp. Med. Assoc.

11. Ernsting, J. (1978). Prevention of Hypoxia - Acceptable Compromises. Aviat. Space. and Env. Med. 49: 495-502.

12. Brown, G.W., Gradwell, D.P., Harding, R.M. and Lupa, H.T. (1991). An Evaluation of Counter Pressure Garments by Spirometric Measurements of Lung Volume. IAM Report No 669.

13. Gradwell, D.P. (1991). The Experimental Assessment of New Partial Pressure Assemblies. AGARD 71st AMD Symposium Paper 23.

14. Gradwell, D.P. (1990). Personal Communication.

15. Nesthus, T.E., Bomar, J.B. and Holden, R.D. (1988). Hypoxia Symptoms Resulting from Various Breathing Gas Mixtures at High Altitude. Proc. 26th SAFE Symp. 16-21.

L'EQUIPEMENT FRANÇAIS DE PROTECTION INTEGREE POUR EQUIPAGES D'AVIONS DE COMBAT MODERNE: PRINCIPES ET ESSAIS EN HAUTE ALTITUDE.

Col. Henri MAROTTE, M.D., Sc.D. (*)
Col. Henri VIEILLEFOND, M.D. (**)
Maj. Damien LEJEUNE, M.D. (*)
Lt-Col. Jean-Michel CLERE. M.D. (*)

(*) Laboratoire de Médecine Aérospatiale
Centre d'Essais en Vol
91228 - BRETIGNY SUR ORGE CEDEX
(France)

(**) D.C.S.S.A. - 00459 ARMEES (France)

RESUME : Un équipement personnel de vol a été fabriqué et testé en France, pour protéger les équipages d'avions de combat contre le risque de perte de pressurisation à haute altitude. Il s'agit d'un vêtement à pressurisation partielle. Plusieurs séries d'essais ont été effectuées : sur maquette fonctionnelle pour valider le principe de l'équipement, puis en décompression lente jusqu'à 60 000 ft; ces essais ont montré que la loi de surpression altimétrique était mal adaptée à ce type d'équipement. Une loi de dilution altimétrique spécifique ainsi qu'une nouvelle loi de surpression ont été imaginées. Elles ont été testées au cours d'une série d'essais en décompression rapide (2 secondes); quelques essais en décompression explosive ont enfin été réalisés. A la suite des expérimentations, l'équipement a pu être homologué pour l'altitude maximale de 65 000 ft, pour un temps limité (2 à 3 minutes avant de rejoindre l'altitude de 40 000 ft) et avec une loi de pressurisation de l'avion de 35 kPa.

SUMMARY : A personal flight equipment has been manufactured and tested in France, in order to protect combat aircraft crew against the risk of loss of pressurisation at high altitude. It is a partial pressure suit. Some series of tests were performed : on mock-up, to validate the principles of the equipment, then in slow decompression up to 60 000 ft; theses tests showed the altimetric positive pressure schedule was badly adapted for this kind of equipment. Specific schedules of altimetric dilution and positive pressure were established and tested with a series of rapid decompression experiments (in 2 seconds); some explosive decompression tests were also performed. By the results, the homologation was obtained, for the maximum altitude of 65 000 ft, maximum duration above 40 000 ft of 2-3 minutes and an aircraft pressurisation schedule of 35 kPa.

Un équipement personnel de vol a été développé en France pour protéger les équipages contre le risque de perte de pressurisation à haute altitude. Il s'agit d'un vêtement à pressurisation partielle, composé de 3 sous-ensembles : un ensemble de tête comprenant casque et masque pressurisé, un gilet respiratoire avec une vessie de contre-pression thoracique et un pantalon anti-G qui, outre sa fonction habituelle de pressurisation anti-G, assure le rôle de partie basse du vêtement à pressurisation partielle. L'ensemble est commandé par un système complexe de régulation, permettant ainsi d'assurer à la fois la protection contre l'altitude et la protection contre les accélérations +Gz de longue durée. Cet équipement est également compatible avec un vêtement d'immersion ou des équipements de protection NBC. Cet équipement a fait l'objet de plusieurs séries d'essais en haute altitude, selon différents scenarios de décompression : après quelques essais sur maquette fonctionnelle pour valider les principes de construction, une série d'essais a été pratiquée en décompression lente (en quelques minutes) puis en décompression rapide (en deux à trois secondes), suivis de quelques essais en décompression explosive. Nous présenterons donc tout d'abord cet équipement de façon succinte puis nous décrirons les essais effectués, avec les résultats obtenus, enfin les limites d'emploi de cet équipement.

Description générale de l'équipement

L'équipement stratosphérique français, décrit par ailleurs dans le détail, est constitué de 3 sous-ensembles reliés à un système complexe de régulation (figure n° 1). La partie haute se compose d'un casque avec un masque à serrage asservi à la surpression. La coque du casque est standard. Le masque est porté par un système de crémaillère. Par rapport aux masques militaires français utilisés jusque là, il s'agit d'un masque oro-nasal dont la surface d'appui sur le visage a été minimisée pour assurer une meilleure étanchéité en surpression; le masque reste étanche pour une pression de 15 kPa environ (environ 120 mm Hg). La soupape du masque est une soupape combinée, inspiratoire et expiratoire compensée, capable de laisser passer des débits gazeux très élevés, cette dernière caractéristique dans le but de minimiser les risques de surpression alvéolaire en cas de décompression explosive. L'étanchéité de la soupape, montée dans un plan parallèle à l'axe Gz, a été vérifiée jusqu'à 15 G dans chaque direction sur simulateur respiratoire.

La tenue de l'ensemble de tête à l'éjection, habituellement dévolue au masque lui-même, est reportée sur une sangle mentonnière. Une poche pressurisée est installée à l'arrière de la tête, entre le squelette de la tête et la coque du casque. Elle est montée pneumatiquement en parallèle avec le circuit respiratoire. La poche occipitale est prolongée de chaque côté par une poche auriculaire qui plaque les écouteurs sur les oreilles et qui, par un gicleur, pressurise les tympans pour limiter la différence de pression transtympanique; dans un souci d'économie de l'oxygène en cas de fonctionnement sur la source de secours, la pression de pressurisation des conduits auditifs externes était limitée pour obtenir une différence de pression transtympanique de 5 kPa.

La partie thoracique de l'équipement pressurisé est constituée d'un gilet avec poche de poitrine, sans manches. La poche de poitrine est montée en parallèle sur le circuit respiratoire. Les équipements de survie sont intégrés au gilet pressurisé. La partie basse est constituée d'un pantalon anti-G habituel, qui reçoit ainsi une double fonction, pantalon anti-G et partie basse de l'équipement pressurisé pressurisé de haute altitude.

L'ensemble de l'équipement est piloté par un système de régulation complexe, qui reçoit l'ensemble des ordres d'altitude et d'accélération, les intègre et les répartit vers les différents sous-ensembles.

L'équipement a été prévu pour pouvoir fonctionner avec un mélange d'air et d'oxygène (mélange dilué), au lieu de l'oxygène pur jusque là de règle avec tout vêtement à pressurisation partielle. La loi de dilution a été adaptée à cette fin car, en cas de décompression rapide de la cabine, le prélèvement de gaz respirables se fait pour partie dans la poche de pressurisation et pour partie à travers le régulateur d'oxygène. Le volume des poches et la répartition exacte de ces deux débits a été évaluée le plus exactement possible pour optimiser cette fonction.

Les autres fonctions de l'équipement ont été adaptées au fur et à mesure des essais et seront présentées comme résultats des différentes séries d'expériences.

Essais réalisés

Les essais ont été réalisés en quatre séries successives :

- des essais sur maquettes fonctionnelles pour tester la validité du concept, en particulier pour valider le mode de fonctionnement du dispositif de régulation incluant régulation d'oxygène et système anti-G;

- des essais en décompression lente qui avaient pour but un essai progressif de l'équipement dans ses différentes fonctions et qui ont permis entre autres de montrer l'inadaptation de la loi de surpression altimétrique initialement choisie;

- des essais en décompression rapide (en 2 à 3 secondes) qui avaient pour but de valider les principes retenus dans des conditions les plus réalistes possibles de risque hypoxique en haute altitude;

- des essais en décompression explosive, interrompus avant leur terme pour différents motifs.

Les dispositifs de mesure ont un peu varié au cours de ces quatre séries d'expériences. D'une façon générale cependant, ils ont permis de mesurer l'ensemble des modes de fonctionnement du système. Sous leur forme la plus complète, pour les deux dernières séries expérimentales, le dispositif de mesure comprenait des mesures de débits gazeux, des mesures de pressions, l'analyse gazeuse au masque, l'enregistrement du fonctionnement du régulateur d'oxygène.

Les mesures de débit gazeux ont été effectuées dans un premier temps à l'aide de trois débit-mètres : l'un à la sortie du régulateur d'oxygène, le deuxième à l'entrée au masque, le dernier sur la tuyauterie d'alimentation de la poche de pressurisation de poitrine. Les résultats ont montré que le signal obtenu par différence entre les deux premiers débit-metres recoupait à 5 p. cent près environ le signal du troisième débit-mètre. Ces mesures pouvaient donc être considérées comme redondantes et le troisième débit-mètre a pu être supprimé. Les résultats présentés sont donc les mesures effectuées à la sortie du régulateur d'oxygène et à l'entrée au masque, le débit gazeux à travers la poche de poitrine étant calculé.

Les mesures de pression ont permis de contrôler l'ensemble de l'équipement :

- pression dans le pantalon anti-G,

- pression dans la poche de poitrine,

- pression dans le masque,

- pression dans la poche occipitale,

- pression dans les poches auriculaires,

- différence de pression entre le masque et la poche de poitrine (différence de pression trans-thoracique),

- perte de charge de la soupape seule,

- contrôle de la pression d'entrée de l'oxygène au régulateur d'oxygène (entrée du circuit normal et entrée du circuit secours),

- pression ambiante (altitude)

- pression intra-oesophagienne pour les décompressions explosives

Les essais en décompression rapide et explosive ont été complétés d'une mesure de la composition gazeuse dans le masque par spectrométrie de masse, adaptée aux conditions de la haute altitude.

Enfin le signal *blinker* a été enregistré.

Les essais ont été effectués avec des sujets humains volontaires, médicalement aptes et instruits des conditions de l'essai. 8 sujets ont participé aux essais, sans cependant qu'il ait pu être possible de planifier parfaitement les essais, qui ont été effectués en fonction de la disponibilité, du volontariat et de l'aptitude physique de chacun des sujets.

Essais sur maquette fonctionnelle

Ces essais ont été réalisés suffisamment tôt dans le programme et ont permis de vérifier la validité technique des concepts de construction de l'équipement.

Essais en décompression lente

Les essais en décompression lente ont été effectués avec 6 volontaires, au cours de 16 montées en altitude simulée, 2 à 50 000 ft, 1 à 57 000 ft et 13 à 60 000 ft, à la vitesse de 30 m.s-1 (2 000 ft.min-1), avec un arrêt tous les 10 000 ft, pendant 1 min jusqu'à 30 000 ft, 45 s à 40 000 ft et 30 s à 50 000 et 60 000 ft. Les différents modes de fonctionnement du système ont été systématiquement testés (modes oxygène pur ou dilution, avec ou sans surpression permanente, pour toutes les pressions d'alimentation en oxygène, y compris en secours, c'est-à-dire dans une plage de pressions d'alimentation de 1.9 à 7.5 bars).

Ces essais ont permis de montrer deux limitations de l'équipement tel qu'il était conçu. La première limitation a été ressentie par deux des sujets, sous la forme d'une sensation très pénible de strangulation à partir de l'altitude de 50 000 ft (avec une valeur de surpression de 8.8 kPa); cette sensation de strangulation n'a pas pu être rattachée à une compression de la partie avant du cou par une pièce de l'équipement. Elle a donc été imputée à une distension de la trachée par la surpression interne aux voies respiratoires, sans contre-pression externe.

La deuxième limitation est apparue sous la forme d'une perte de conscience à l'altitude de 60 000 ft (figure n° 2). Le sujet a présenté une perte de conscience à la fin du plateau à 60 000 ft. L'historique de l'incident est le suivant : après le plateau de 30 000 ft, montée à 40 000 ft en 30 s puis arrêt à cette altitude pendant 45 s; la surpression est alors égale à 2.8 kPa; la montée puis le plateau à 50 000 ft durent respectivement 22 et 38 s; à cette altitude, la surpression est égale à 8.9 kPa; la montée et le plateau à 60 000 ft durent 16 et 37 s, altitude à laquelle la surpression est égale à 12.8 kPa. La perte de conscience survient à ce moment; elle durera 20 s environ, le temps mis pour redescendre vers 40 000 ft; nous ne disposions pas à ce moment d'enregistrements électro-cardiographiques mais nous observerons un arrêt respiratoire. L'association de la perte de conscience alors que nous contrôlions à la fois la fraction d'oxygène et la pression dans le masque permet d'éliminer la syncope hypoxique. L'arrêt respiratoire, suivi d'une reprise progressive 20 secondes après, nous a fait émettre l'hypothèse d'une syncope vagale, probablement par inhibition cardio-circulatoire due à une stimulation aberrante des baro-récepteurs sino-carotidiens (Figure 3).

Compte-tenu de la mauvaise tolérance de la surpression respiratoire dans ces conditions, du fait que les avions de combat modernes ont des taux de descente très rapides, qu'une hypoxie de degré modéré peut être supportée pendant un temps bref et que, enfin, il semble que la surpression repiratoire s'accompagne d'une certaine hyperventilation, génératrice d'une hypocapnie elle-même à l'origine d'une minoration de l'hypoxie alvolaire, la loi de surpression altimétrique a été modifiée de façon à ne pas dépasser 11.5 kPa à 60 000 ft. C'est cette hypothèse qui, en même temps que la loi de dilution altimétrique, a été validée au cours de la série suivante d'essais, en décompression rapide.

Essais en décompression rapide

Les essais en décompression rapide ont été effectués avec 4 sujets volontaires, en augmentant progressivement l'altitude et la variation de pression. Les variations de pression ont été de 5, 10, 15, 20, 25 et 30 kPa. Les essais ont été effectués

systématiquement en mode dilution et surpression permanente de 0.45 kPa. L'objectif fixé à ces essais était la validation de l'équipement dans les conditions d'emploi fixées par la France (altitude maximale : 60 000 ft, pression différentielle de la cabine pressurisée : 30 kPa); quelques essais ont été effectués à des valeurs plus élevées de l'altitude : 65 000 ft, 70 000 ft et 75 000 ft ainsi qu'à des valeurs plus élevées de la pression différentielle : 35 kPa. Ils ont été effectués à partir de l'altitude de 10 000 ft, 18 400 ft et 25 250 ft, ces deux dernières valeurs permettant d'atteindre les valeurs d'altitude de 39 000 ft et 60 000 ft respectivement à l'issue d'une décompression de 30 kPa. Pour les essais effectués avec une pression différentielle de 35 kPa, l'altitude initiale était plus faible : 16 100 ft et 22 350 ft pour arriver à 39 000 et 60 000 ft. L'essai à 75 000 ft a été effectué avec une pression différentielle de 25 kPa seulement pour des raisons techniques.

Tous les essais en décompression rapide ont été pratiqués avec une technique à deux caissons, séparés par un vanne quart de tour à ouverture rapide; les pressions étaient égalisées entre les deux caissons en 2.5 secondes environ. La commande de la vanne de décompression était à double clé : l'une à la disposition de l'opérateur technique et l'autre à la disposition du sujet lui-même. Pour éviter une surpression alvéolaire excessive, les sujets étaient entraînés à subir la décompression en fin d'expiration, en contrôlant soigneusement la position de la glotte.

La validation de la loi de dilution a été étudiée essentiellement au cours des essais à partir de 10 000 ft et de 18 400 ft (figure 4). La fraction d'oxygène dans les gaz inspirés (FI O2) était égale en moyenne à 0.70 à 10 000 ft et à 0.75 à 18 400 ft; une valeur de 0.54 a été observée au cours d'un essai. Aucun symptôme hypoxique important n'a été observé au cours des différentes décompressions, bien que deux sujets aient signalé une réduction passagère du champ visuel quelques secondes après l'arrivée à 39 000 ft (entre 5 et 15 secondes environ). Pour une pression différentielle plus importante (35 kPa), les résultats sont identiques. A partir de l'altitude de 25 250 ft, le régulateur d'oxygène délivrait de l'oxygène pratiquement pur et le problème se trouvait éliminé.

La validation de la loi de surpression altimétrique a été effectuée lorsque l'altitude atteinte dépassait 40 000 ft. A l'issue de la décompression, le plateau d'altitude était maintenu pendant 30 secondes avant la mise en descente à une vitesse comprise entre 25 000 et 40 000 ft.min-1.

Les résultats montrent l'augmentation de pression dans les différents compartiments de l'équipement, en deux phases,l'une due à l'expansion volumétrique dez gaz préalablement contenus dans les poches de l'équipement, l'autre, plus lente due à la régulation de pression par le régulateur d'oxygène. Toutes les pressions contrôlées dans l'équipement étaient à leur valeur nominale. Il ne fut observé ni symptôme hypoxique ni symptôme d'intolérance à la surpression altimétrique (figure 5). Cependant les deux tests effectués à l'altitude maximale de 70 000 ft et 75 000 ft (figure 6) ont montré que la tolérance était limitée, le sujet ayant considéré qu'il n'aurait probablement pas pu piloter un avion de façon très satisfaisante dans de telles conditions.

Essais en décompression explosive

Quelques essais ont été effectués en décompression explosive, utilisant la technique du double caisson avec membrane ruptible de 0.5 m2 entre chaque caisson. La décompression est alors obtenue en 30 millisecondes environ. Des essais ont été exécutés jusqu'à l'altitude de 30 000 ft avec une pression différentielle de 30 kPa; ils ont permis la mise au point métrologique du dispositif expérimental mais ont été interrompus à ce stade par les autorités.

Commentaires

Ces différents essais ont permis de montrer à la fois les possibilités et les limites des équipements testés. Compte-tenu des clauses techniques de construction des cabines d'avions, en particulier leurs clauses d'étanchéité, il est raisonnable de penser que toute décompression à haute altitude est nécessairement une décompression rapide ou explosive. C'est dans ce sens qu'a porté le maximum des essais de qualification de l'équipement français. Les optimisations ont également porté sur l'hypothèse d'un épisode de décompression court, ce qui explique certains des choix techniques (gilet sans manches, casque à contre-pression au lieu du casque pressurisé). La loi de surpression théorique ne pouvait donc être retenue et les choix effectués sont d'ailleurs conformes à ceux d'autres auteurs (1,3) et que nous avons motivés par ailleurs (5,6). Ne pas les respecter nous a conduits à observer une perte de conscience chez l'un des sujets (4). De même, il a été possible, sur cet équipement, de maintenir le principe de la dilution altimétrique, sans conséquence physiologique notable, résultat également en accord avec ceux d'autres auteurs (2,7,8).

En conclusions, les essais effectués avec l'équipement français de haute altitude VHA 90 associé au régulateur d'oxygène IN 439 ont permis de valider ces équipements dans les conditions suivantes :

- protection contre l'hypoxie d'altitude,

- protection en haute altitude par la surpression respiratoire compensée, jusqu'à 65 000 ft,

- limitation de la surpression pulmonaire en cas de décompression explosive,

auxquelles s'ajoutent la protection contre les accélérations +Gz et la protection contre l'immersion par l intégration du gilet de sauvetage, ainsi que la compatibilité avec des équipements de protection thermique ou chimique.

L'homologation de l'équipement a donc été proposée pour l'altitude maximale de 65 000 ft, sous réserve d'une descente à 40 000 ft en moins de 2 à 3 minutes et pour une pression différentielle de cabine maximale de 35 kPa.

BIBLIOGRAPHIE

1 - Balldin U.I., Wranne B. (1980)
Hemodynamic effects of extreme positive pressure breathing using a two-pressure flying suit.
Aviat., Sp. and Environ. Med., 51(9) : 851-5

2 - Chopp C.S., Bomar J.B., Harding R.M., Harding R.D., Holden R.D., Bauer D.H. (1990)
Rapid decompression to 50,000 ft : effect on heart rate response.
Aviat., Sp. and Environ. Med., 61(7) : 604-8

3 - Holness D.E., Porlier J.A.G., Ackles K.N., Wright G.R. (1980)
Respiratory gas exchange during positive pressure breathing and rapid decompression to simulated altitude of 18.3 and 24.2 km.
Aviat., Sp. and Environ. Med., 51(5) : 454-8

4 - Marotte H., Vieillefond H., Poirier J.L. (1985)
Syncopes non hypoxiques en altitude. A propos de deux observations en caisson hypobare.
Rev. Méd. Aéro. et Sp., 24(95) : 169-172

5 - Marotte H., Gutman G., Chrome V. (1986)
Decompression tests of the french personal flight equipment IN 439 - VHA 90.
SAFE 24th Annual Symposium Dec. 11-13 SAN-ANTONIO Conf. Proc. : 4-9

6 - Nesthus T.E., Bomar J.B., Holden R.D., O'Connor R.B. (1987)
Cognitive workload and symptoms of hypoxia.
SAFE 25th Annual Symposium Nov.16-19 LAS VEGAS (NE) Conf. Proc. : 45-47

7 - Wright C.S., O'Connor R.B., Holden R.D., Nesthus T.E. (1988)
Heart rate response after rapid decompression to 50,000 ft : the effect of 93% oxygen breathing gas.
A.S.M.A. 59th meeting May 8-12 NEW ORLEANS

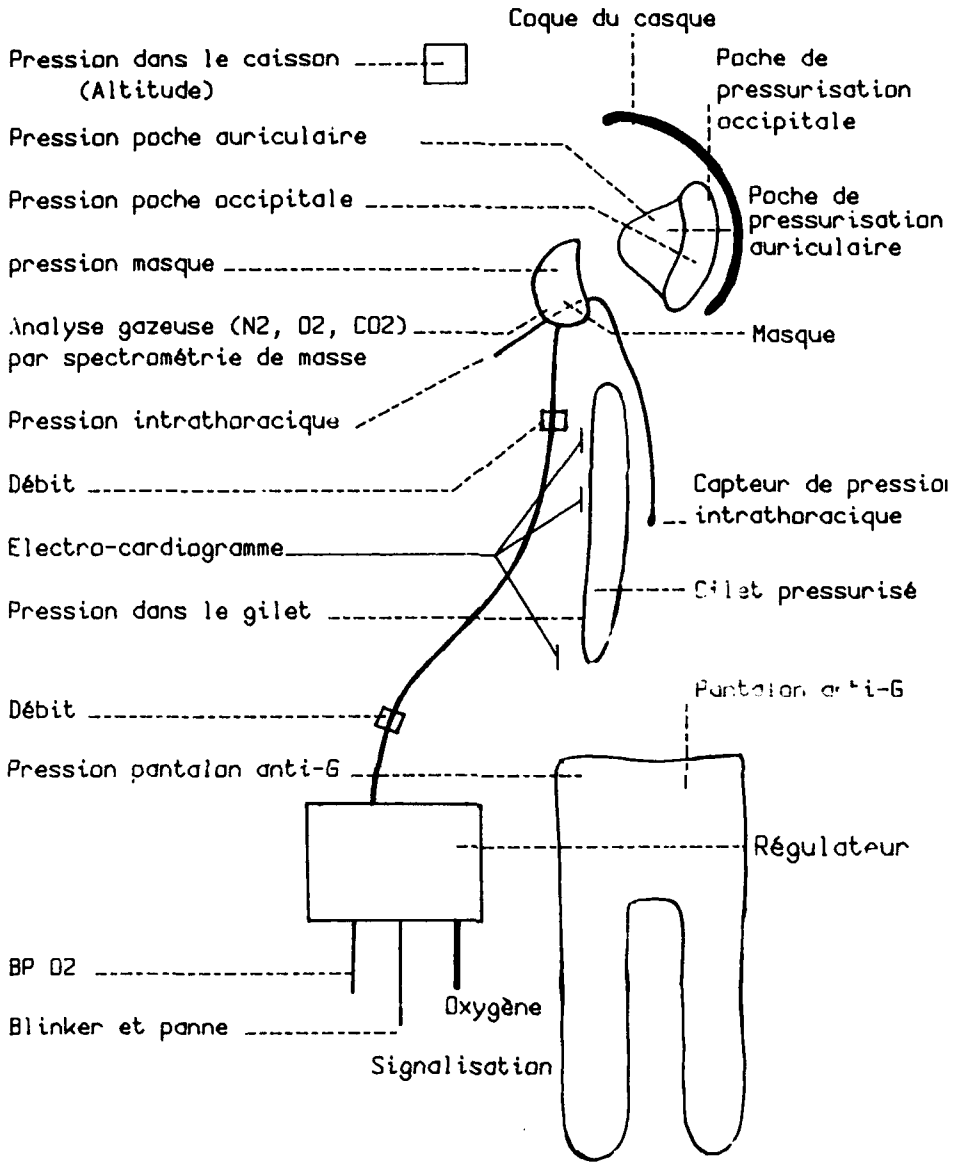

Figure 1 : Schéma de principe de l'équipement VHA 90 associé au régulateur IN 439.

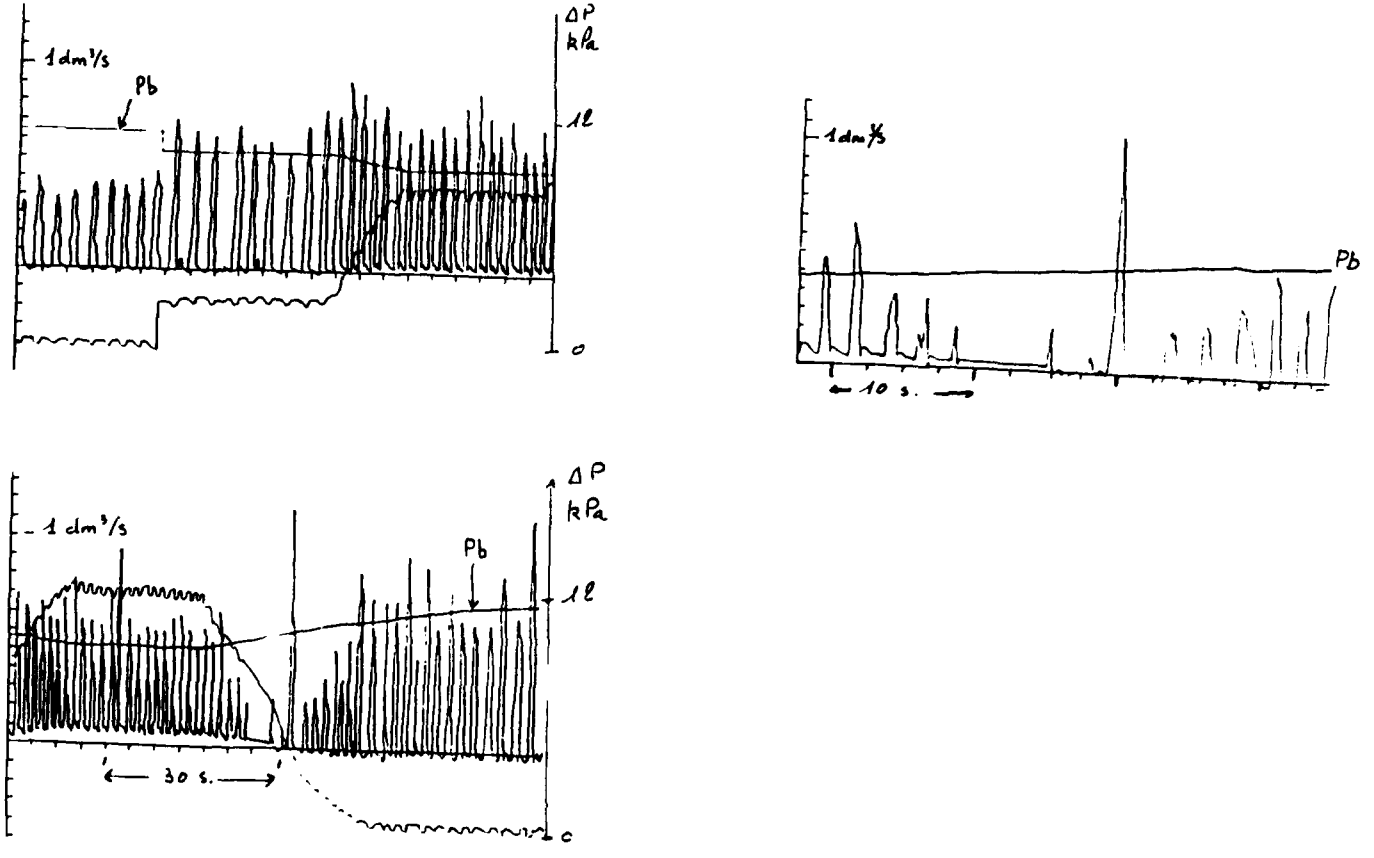

Figure 2 : Enregistrements (dV/dt, Pb, ΔP) en fonction du temps au cours d'un incident de perte de conscience à 60 000 ft.

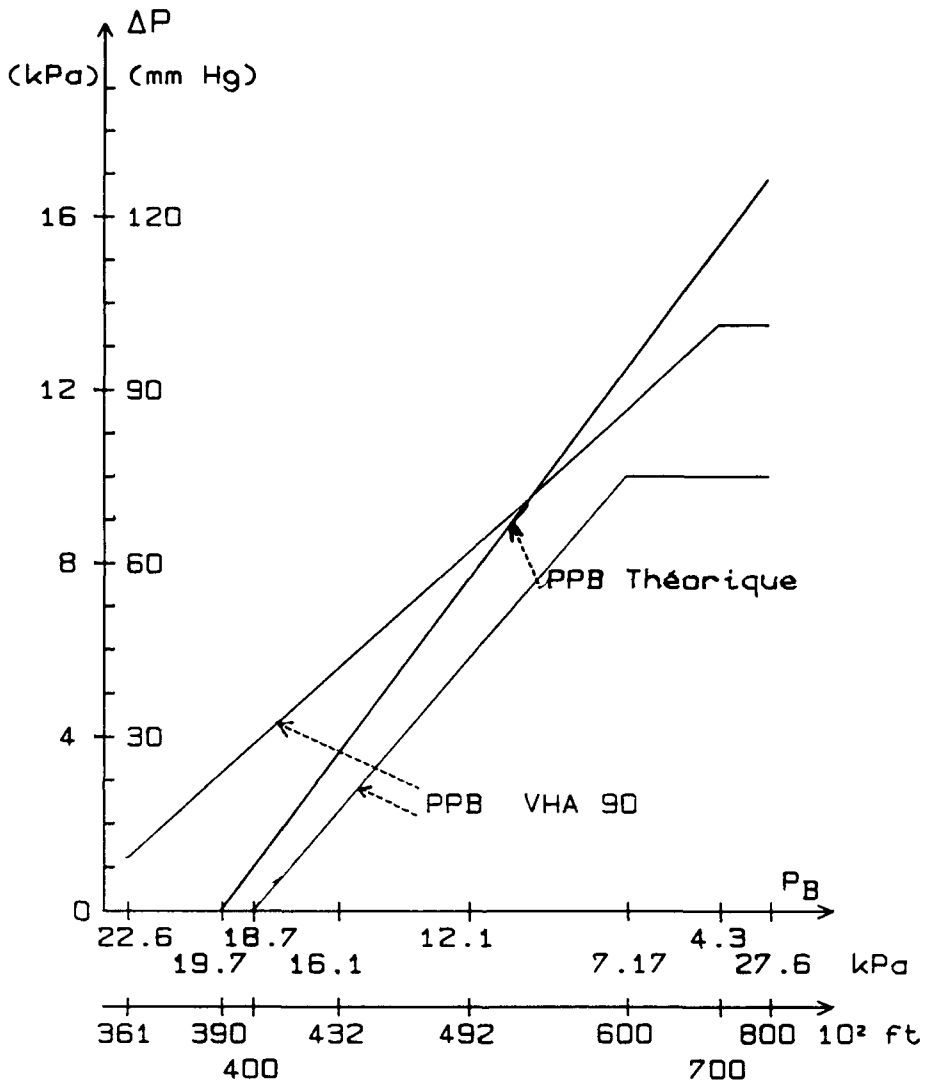

Figure 3 : Loi de surpression utilisée pour l'équipement VHA 90.

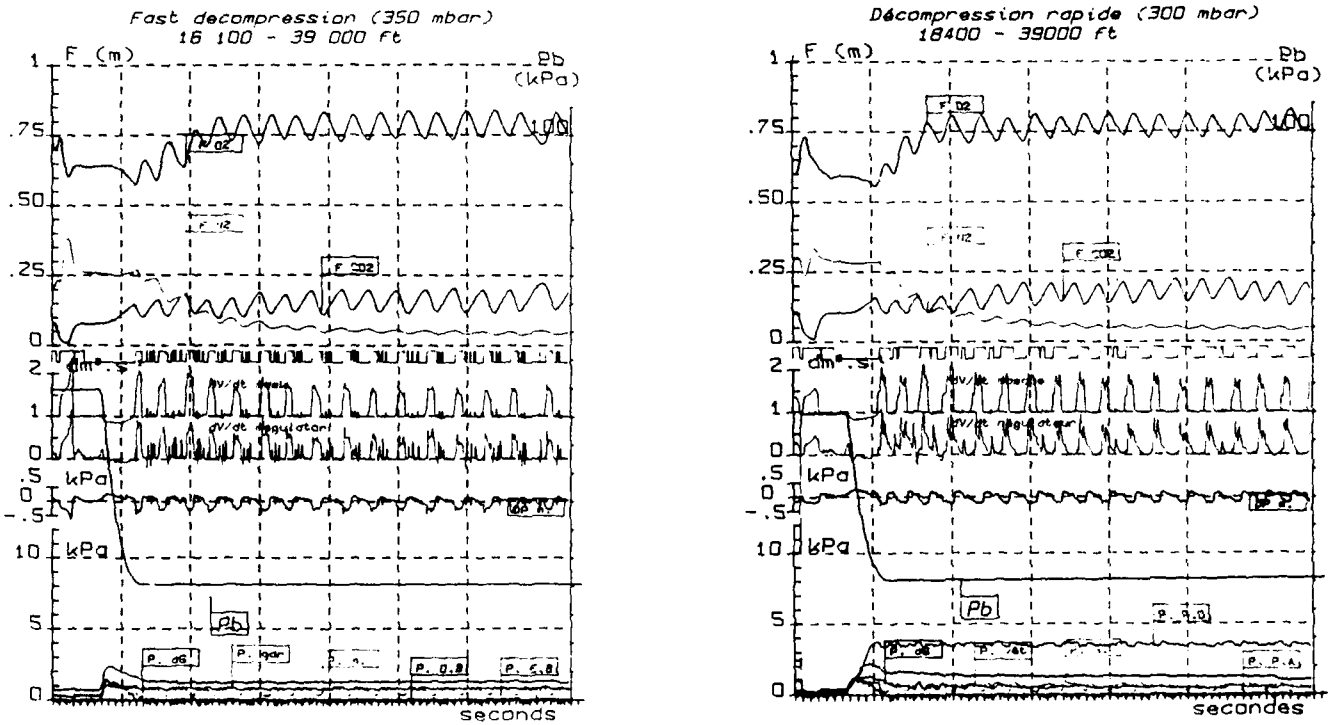

Figure 4 : Résultats d'essais de décompression rapide à 39 000 ft.
de bas en haut: pressions contrôlées dans l'équipement (anti-G, gilet, masque, poches occipitale et auriculaire), pression barométrique (Pb) perte de charge de la soupape du masque, débits gazeux (régulateur et masque, blinker, analyse gazeuse.
Le temps est exprimé en secondes sur l'axe horizontal (10 s entre deux traits verticaux pointillé).

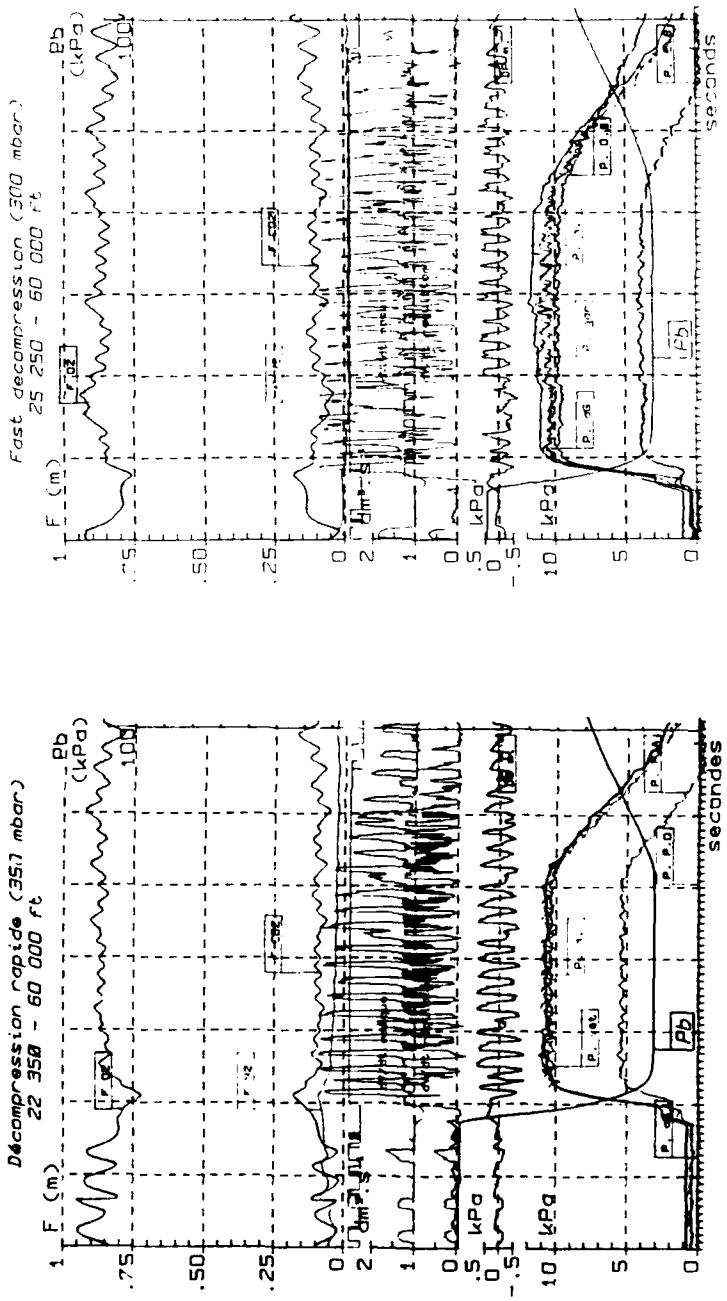

Figure 5 : Résultats d'essais de décompression rapide à 60 000 ft, même légende que figure 4

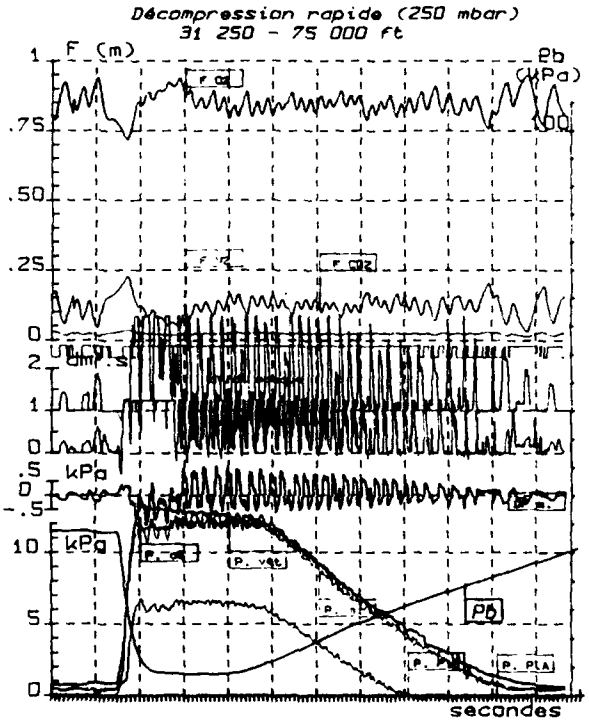

Figure 6 : Résultats d'essais de décompression rapide à 75 000 ft.
même légende que figure 4.

THE EXPERIMENTAL ASSESSMENT OF NEW PARTIAL PRESSURE ASSEMBLIES

Sqn Ldr DP Gradwell
RAF Institute of Aviation Medicine
Farnborough
Hampshire
United Kingdom

SUMMARY

A new generation of partial pressure assemblies have been assessed with particular reference to the optimization of counter-pressure relationships. A system of non-invasive assessment of the physiological consequences of using such assemblies during pressure breathing and following rapid decompression to altitudes between 45,000 and 60,000ft has been developed. The methods used are described and an outline of the results achievable with this system are discussed.

The physiological benefits of enhanced lower body counter-pressure compared with uniform levels of pressure garment inflation are described. Suggestions are made for further areas of research in this topic.

INTRODUCTION

The next generation of agile aircraft are destined to fly to altitudes of approximately 60,000ft. The Aircrew Equipment Assembly (AEA) to be worn be the pilot must provide protection in the event of a rapid decompression at such altitudes but in addition must be compatible with other requirements of the AEA such as integration with NBC protective assemblies and minimal thermal load. Therefore there has been a need to a carry out a reappraisal of high altitude emergency protective systems. In this paper the steps taken to assess the physiological performance of new forms of partial pressure assemblies intended for the protection of aircrew following loss of cockpit pressurization at altitudes in excess of 40,000ft will be outlined. The objective is to establish the physiological ideal consistent with an assembly acceptable to the user.

Co-incident with the need to re-examine high altitude protective systems has been the emergence of the requirement for pilots to use pressure breathing with G (PBG) as a mechanism of enhanced G protection and wear the associated counter-pressure assemblies. As is discussed elsewhere, PBG is an excellent technique for enhancing G protection and pressure breathing during G exposure is a more tolerable exercise than pressure breathing at simulated altitude in an hypobaric chamber at 1G.

The physiological standard adopted has been derived from the levels of protection afforded by the current high altitude partial pressure assembly in use in the Royal Air Force and elsewhere, consisting of a Mk 4 Partial Pressure Jerkin (PPJ) and conventional external anti-G trousers. The jerkin is a torso garment, extending over the saddle region to the tops of the thighs, thereby protecting the inguinal and femoral hernial orifices. Within the garment there is an extensive circumferential inflatable bladder the coverage of which encompasses essentially all those parts of the body covered by the jerkin except the saddle area. Although in itself providing adequate counter-pressure to allow short duration pressure breathing up to 50mmHg and thus conferring protection up to an altitude of 52,000ft, the jerkin is commonly combined with anti-G trousers inflated from the same source, ie breathing gas. Then the pilot may pressure breathe at up to 70mmHg above ambient and receive counter-pressure of the same magnitude over the chest, abdomen, pelvis, groin and those parts of the legs where the lobes of the anti-G trousers bladder inflates, that is essentially the muscles of the thighs and calves.

This assembly has been shown to be acceptable in physiological terms for short duration protection[1] but would present operational difficulties if adopted for use in future fighter aircraft. Therefore the opportunity has been taken to examine in detail the manner in which acceptable circulatory and respiratory support during positive pressure breathing can be provided by a smaller and lighter garment assembly which also complements the needs of enhanced G protection.

METHODS

The Partial Pressure Jerkin itself was developed from a counter-pressure waistcoat and the fundamental design was reported many years ago. In addition, Ackles and his colleagues,[2] examined at ground level the effects of pressure breathing whilst wearing a waistcoat and anti-G trouser combination and this led us to the examination of a revised UK waistcoat coupled to anti-G trousers.

In this case the inflation of the anti-G trousers was controlled in such a manner as to be a ratio of the breathing pressure. The relationships examined have been with anti-G trousers inflated to one, three and four times breathing pressure. The first ratio herefore closely reflects the situation in the jerkin assembly, where counter-pressure is equal to breathing pressure on all areas to which it is applied. In the second and third cases the counter-pressure over the abdomen and legs, applied by the anti-G trousers, is significantly greater than breathing pressure. In all cases the chest counter-pressure is equal to breathing pressure.

The device adopted to provide the control of the "ratioed" anti-G trouser pressures was designed and built at the RAF Institute of Aviation Medicine. In principle it consists of an electronic switch opening and closing solenoids to provide compressed air inflation or deflation of the anti-G trousers through a conventional G valve. Sampling the pressures in both the anti-G trousers and the mask hose and comparing them to a pre-set relationship completes the control system. Breathing gas is delivered from a modified panel mounted MK21B pressure demand regulator via a Personnel Equipment Connector (PEC). Breathing pressure rises in a linear manner from ambient plus safety pressure at 40,000ft to its maximum of 70mmHg added pressure at 60,000ft

Our studies have examined the physiological performance of the waistcoat/anti-G trouser combination at the three ratios of breathing pressure to anti-G trouser pressure as noted above. In addition we have examined the performance of the standard Mk4 PPJ/anti-G trouser system under identical conditions and using the same type of pressure demand regulator as the source of breathing gas. Performance has been examined at mask cavity pressures of 30, 45, 60 and 70mmHg above ambient on six healthy male volunteers.

The influence on spirometric measurements of lung volumes of pressure breathing with a differential counter-pressure system have been reported by Macmillan[3]. The "ratioed" waistcoat/anti-G trouser system was found to be at least as effective as the jerkin assembly in maintaining lung volumes as near normal as possible when anti-G trouser inflation pressure was three times breathing pressure.

Preliminary procedures to investigate the functional effects of various pressure breathing assemblies were conducted in a hypobaric chamber decompressed only as far as necessary to create a pressure differential across the wall equal to the desired breathing pressure. The turning of a tap in a hose from the outside of the chamber to the mask/garment assembly thereby provided pressure breathing, on air, at a negligible altitude. This "through the wall" technique has proved to be extremely useful. By this means it has been possible to train subjects in exactly the same chamber facility as used for the high altitude exposures and operate the same monitoring systems. It has yielded a large quantity of experimental data on the circulatory and respiratory effects of pressure breathing isolated from the influence of high altitude whilst familiarizing the subjects to the breathing technique and the effects of ratioed counter-pressure. It also offered the opportunity to carry out additional studies into physiological effects of pressure breathing without the hazards associated with exposure to high altitude.

Having completed preparatory training and "through the wall" exercises the subjects carried out rapid decompressions (RD) to a series of final altitudes; 45,000 ft, 50,000ft, 55,000ft and 60,000ft. In each case the base, pre-RD, altitude was chosen to reflect a 5lb.in^2 differential across the cockpit wall. The RD itself occurred over three seconds, followed by a two minute period at the final altitude. Descent from that altitude was then carried out at a recompression rate of 10,000ft/minute. At the final altitudes the subject pressure breathed at the requisite level with subsequent reduction in breathing pressure as the chamber was recompressed until by approximately 38,000ft mask cavity pressure was at ambient plus safety pressure. During descent from altitude the enhanced anti-G trouser inflation declined in parallel with breathing pressure.

The observations made and recorded have been divided into the physical and the physiological and listed in Table 1. The inflation pressure of the chest counter-pressure garment is equal to mask cavity pressure.

Table 1. Human High Altitude Rapid Decompressions,
Physical and Physiological Data Recorded

Data	Units
Ambient Pressure (Altitude)	mmHg
Mask Cavity Pressure	mmHg
Anti-G Trouser Pressure	mmHg
Electrocardiograph	-
Heart Rate	Beats.minute^{-1}
Blood Pressure	mmHg
Arterial Oxygen Saturation	%
Partial Pressures of Oxygen	mmHg
Carbon Dioxide	mmHg
Nitrogen	mmHg
Respiratory Flow	litres.minute^{-1}
Respiratory Ventilation	litres.minute^{-1}

Electrocardiograph (ECG) was displayed to the second medical officer and recorded. The beat to beat heart rate was derived from the R-R interval of the ECG. Arterial oxygen saturation was measured by indirect oximetry.

Blood pressure was monitored with the relatively novel Finapres device which provides a non-invasive continuous display of arterial blood pressure. In a comparative assessment of Finapres with intra-arterial measurement of blood pressure during pressure breathing this non-invasive monitor has

been shown to offer a high degree of accuracy.[4] Moreover, although the Finapres will operate at higher altitude than reported by the manufacturer, it was found to be more satisfactory to have the monitor on the outside of the chamber with the lead to the patient/subject interface module passing through a gas-tight seal in the chamber wall. Blood pressure is measured at the finger and the finger cuff worn by the subject is connected to the interface module by both pneumatic and electronic leads. Changes in ambient pressure and rapid decompressions do not adversely affect the measurement of blood pressure by this device but the subject is required to keep his hand at the level of the aortic valve to avoid the necessity of making a hydrostatic pressure correction to the recorded blood pressure.

Respiratory observations included the breath-by breath measurement of the partial pressures of nitrogen, oxygen and carbon dioxide, by mass spectrometry. Respiratory frequency could be observed from the traces of the mass spectrometer or from the respiratory flow. Integration of flow measurements provided an indication of ventilation.

Subject-borne instrumentation consisted of ECG chest leads and on the right hand the probe for measurement of oxygen saturation. In addition, on another finger of the same hand was worn a Finapres blood pressure cuff and the patient interface module was strapped to the back of the hand. Thus the left hand was free to rotate the pressure breathing mask toggle at the time of the rapid decompression. The subjects wore a conventional RAF flying coverall and helmet but the P/Q series mask was substantially modified to incorporate a port for the mass spectrometer probe and a pressure tapping leading to a mask cavity pressure transducer, branched to a mercury manometer used for direct observation by the medical officer in charge during the period of pressure breathing. The mask also had an additional inlet for an entirely independent supply of 100% oxygen for emergency use. Finally, over the counter-pressure waistcoat the subjects wore a conventional Life Saving Jacket.

From experience it was found preferable to take the breathing pressure sensing signal, used in anti-G trouser inflation control, from the supply hose rather than the mask cavity itself. This reduced any tendency for anti-G trouser inflation to hunt in response to breathing patterns.

The satisfactory conduct of these experiments required a team of at least eight personnel including three medical officers, in addition to a subject pool of six. One medical officer acted as a chamber safety officer, being himself decompressed to an intermediate altitude of 16,000ft in the part of the chamber adjoining the one-man capsule occupied by the subject. Throughout the procedure updates on end-tidal partial pressure of oxygen, blood pressure and heart rate were given to the medical officer in charge. This data and all other physical and physiological information measured was recorded on paper and FM tape. By prompt attention to the changing physiological state of the subject it was hoped that should an individual fail to sustain an adequate response to the challenge action could be taken immediately to prevent him suffering a collapse.

RESULTS

A full report of the results obtained in this large series of experiments is beyond the scope of a paper intended instead to detail the techniques adopted to assess the physiological responses to a specific stress. However some of the consistent patterns emerging from the data will be reviewed.

The adverse cardiovascular and respiratory consequences of positive pressure breathing are well known. The most severe effects are increasing expiratory difficulty and a falling cardiac output due to inadequate venous return in the presence of high intrathoracic pressure. This manifests itself as a rising heart rate and falling blood pressure leading to collapse. To assess the effectiveness of the support measures it is therefore appropriate to examine the increase in blood pressure induced by the pressure breathing and how that rise is influenced by the partial pressure assembly including any differential counter-pressure. The physiological optimum may be predicted to be the system that results in the greatest increase in blood pressure with the smallest increase in heart rate. The response can be examined further by taking account of any disparity between the influence on systolic and diastolic blood pressure and whether the optimal assembly at a low level of pressure breathing continues to be most favourable throughout the range of required breathing pressures.

A sample of part of a trace is given in Figure 1 and it is evident that on rapid decompression mask cavity pressure rises immediately to the required level and appropriate anti-G trouser inflation is initiated. The influence on arterial blood pressure is easily observed but we have sought to quantify that effect by calculating the change in systolic, diastolic and mean blood pressures associated with the use of the various assemblies and enhanced lower body counter-pressure. In general the greater the added pressure in the mask during pressure breathing the greater the observed elevation of arterial blood pressure.

The physiological data obtained from experiments in which subjects wore the Mk4 PPJ /anti-G trousers combination provide a standard against which the responses obtained when differential counter-pressure assemblies were worn can be measured. Although this work continues a interesting trend is appearing. This type of effect is seen in Figure 2 in which the changes in mean blood pressure and heart rate in one subject following rapid decompression to 45,000, 50,000, 55,000 and 60,000ft are shown. The associated mask cavity pressures are 30, 45, 60 and 70mmHg respectively. Data for the jerkin system and enhanced lower garment

Figure 1. A record of seven of the fourteen variables monitored during a rapid decompression from 22,500 to 60,000ft. In this experiment the subject wore standard RAF Mk4 Partial Pressure Jerkin and anti-G trousers.

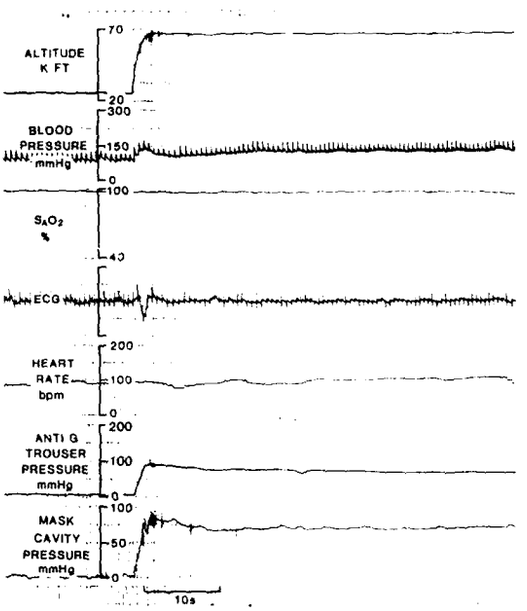

Figure 2. A record of the changes in heart rate and mean blood pressure observed in a subject during a series of rapid decompressions to 45,000, 50,000, 55,000 and 60,000ft whilst wearing uniform and enhanced lower body counter-pressure garments.

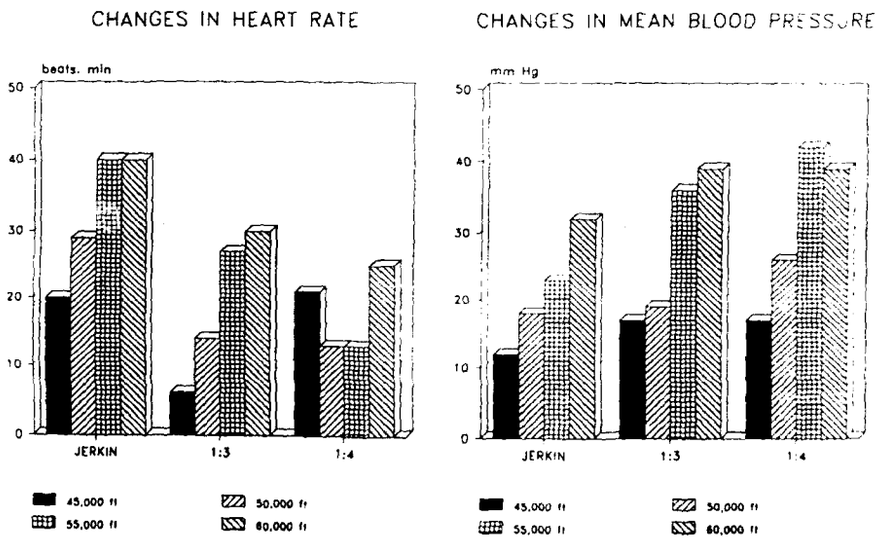

counter-pressure are presented. Blood pressure is raised consistently by pressure breathing to a level rather less than the applied pressure. However, in general, when enhanced lower body counter-pressure is used, a greater rise in BP is seen and the positive chronotropic effect is diminished.

Wearing the jerkin and anti-G trousers, ie the standard assembly, a well trained subject can generally tolerate a two minute exposure to at least 55,000ft but heart rates are raised considerably and subjective discomfort limits are being reached. Similar circulatory changes are observed when individuals use the experimental waistcoat with the anti-G trousers inflated to breathing pressure. However we have seen one case of this leading to a presyncopal state requiring an accelerated recompression. A more satisfactory response is seen with enhanced lower counter-pressure garment inflation and in several cases the use of four times breathing pressure to inflate the anti-G trousers has been observed to induce an even more physiologically advantageous response. However, this is not necessarily a significantly greater effect and may only be obtained at an unacceptable price in terms of subjective tolerability.

A consideration of the relevant inflation pressures may suggest an explanation for the effects observed. In circumstances of a one to four ratio between upper and lower counter-pressures, with a breathing pressure of 70mmHg the anti-G trouser inflation pressure is 280mmHg. Although substantially lower than trouser inflation under G, it is nonetheless a considerable load on the abdomen and legs. Indeed such an anti-G trouser inflation pressure will exceed the maximum pressure in the femoral artery at the inguinal area and therefore arterial supply to the lower limbs may be reduced or abolished in the face of such counter-pressures. There may still be benefit in terms of substantial and sustained compression of the venous compartment but it is unlikely to be significantly greater than would be achieved with an inflation of 210mmHg, i.e. as occurs with a ratio of one to three. Finally, the greater compression over the abdomen may provide a greater degree of respiratory support. However our results would suggest that the end-tidal oxygen levels are not significantly improved by use of a four to one ratio and ventilation may even by impaired since moving the diaphragm against high intra-abdominal pressure may be made considerably more difficult.

This pattern of response has been seen in both "through the wall" experiments and at simulated high altitude following rapid decompression. However hypoxia itself can have a presser effect and therefore the greatest rises in blood pressure can be expected to be associated with rapid decompressions. Heart rate is, not surprisingly, generally higher during rapid decompression experiments than "through the wall" ones but the proportionate changes can still be observed.

CONCLUSIONS

Our studies suggest that enhanced lower body counter-pressure can offer substantial benefits in respect of circulatory support during positive pressure breathing. However the subjective discomfort of high ratios has to be considered and unless a significant benefit can be offered by applying more than three times breathing pressure in the anti-G trousers it may be more appropriate to limit counter-pressure to that level. This is based on the assumption that the area of coverage provided by the anti-G trousers is that obtained with conventional garments. It remains to be seen if the adoption of increased coverage anti-G trousers for enhanced G protection may offer the possibility of reducing the ratio still further, perhaps to a mere doubling of breathing pressure.

REFERENCES

ERNSTING,J. Some Effects of Raised Intrapulmonary Pressure in Man. AGARDograph No106 Maidenhead: Technivision. 1966

2. ACKLES,K.N., PORLIER, J.A.G., HOLNESS,D.E., WRIGHT,G.R., LAMBERT,J.M. and W.J.MCARTHUR. Protection Against the Physiological Effects of Positive Pressure Breathing. Aviation, Space and Environmental Medicine, 1978, 49, 753-758.

3. MACMILLAN, A.J.F. The Physiological Requirements for Partial Pressure Assemblies for Altitude Protection. 71st AMP AGARD Symposium, 1991 Paper No 21.

4. GRADWELL, D.P. Validation of a Method of Continuous Non-invasive Monitoring of Blood Pressure During Positive Pressure Breathing in Man. J. Physiol. 1991 Suppl 1 54P.

PROTECTION PHYSIOLOGIQUE DES EQUIPAGES D'AVIONS DE COMBAT:

INTEGRATION DE FONCTIONS, PRINCIPES TECHNOLOGIQUES.

Col. Henri Marotte, M.D., Sc.D. *
Mr Raymond Beaussant, Ing. **
Mr Richard Zapata, Ing. ***
Lt-C. Jean-Michel Clère, M.D. *
Maj. Damien Lejeune, M.D. *

* Laboratoire de Médecine Aérospatiale
Centre d'Essais en Vol
91228 - Brétigny sur Orge Cédex
(France)

** INTERTECHNIQUE
BP 1
78374 - Plaisir Cédex
(France)

*** L'AIR LIQUIDE
BP 15
38360 - Sassenage Cédex
(France)

RESUME : Les avions de combat actuels sont caractérisés par le fait que leurs équipages peuvent être soumis à plusieurs types de contrainte au cours d'un même vol. De plus sont apparues de nouvelles technologies, telles que les concentrateurs d'oxygène à tamis moléculaire pour les sources d'oxygène ou les technologies électroniques pour la commande et/ou le contrôle des systèmes de régulation. Les équipements développés en France permettent de prendre en compte ces nouvelles données, allant de la génération de gaz respirable de façon illimitée par les concentrateurs d'oxygène, avec les systèmes de régulation à basse pression associés, à la protection anti-G utilisant les techniques de la surpression respiratoire; ces fonctions sont intégrées au sein d'un seul équipement avec multiplexage d'ordres au sein d'un système regroupant les fonctions respiratoires et anti-G. De nouvelles potentialités ont été développées : loi de dilution altimétrique utilisable avec un vêtement à pressurisation partielle, compatibilité de ces équipements avec ceux qui n'ont pu y être intégrés : équipements de protection contre le froid en cas d'immersion ou équipements de protection NBC.

SUMMARY : New generation combat aircraft crew can be submitted at many kinds of constraints during the same flight. New technologies also have appeared, such the molecular sieve oxygen concentrator (MSOC) or the electronic technologies for command and/or survey of the regulation systems. The equipments developed in France allow to take in account these new data, from the unlimited oxygen supply, with low pressure oxygen regulation systems, to anti-G protection thanks to the assisted positive pressure breathing (A-PPB). These functions are integrated in the same equipment with order multiplex in a system which associates respiratory and anti-G functions. New perspectives have been developed : altimetric dilution schedules, usable with a partial pressure suit, compatibility of the flight equipment with non-integrated functions : thermal (cold) protection in case of accidental immersion or NBC protection equipments.

Les avions de combat mis en service depuis 10 ans environ dans les différentes forces aériennes sont caractérisés par le fait que plusieurs contraintes physiologiques majeures sont susceptibles d'être rencontrées au cours d'un même vol. Les avions de générations précédentes en effet, du fait de leur aérodynamique, de leurs possibilités d'emport en carburant, ou encore du fait de leur système d'armes, ne pouvaient effectuer plusieurs types de mission au cours d'un même vol, même s'ils étaient réputés polyvalents. En quelque sorte leur mission était fixée dès le décollage : mission en haute altitude, mission de combat ou mission de pénétration lointaine avec survol maritime éventuel. Il était dès lors logique de ne protéger l'équipage que contre cette seule contrainte, d'où des équipements de vol qui ne répondaient qu'à une seule fonction : équipements anti-G, équipements de haute altitude ou combinaisons d'immersion. La compatibilité de ces différents équipements entre eux n'avait pas été particulièrement étudiée. Equipements stratosphériques ou équipements d'immersion étaient en général compatibles avec le pantalon anti-G mais ne l'étaient pas entre eux; il en était de même des équipements de protection chimique.

La mise en service d'avions réellement polyvalents a entraîné la nécessité de reétudier ces problèmes de polyvalence et de compatibilité (1,2,9). La France avait par ailleurs à résoudre une autre difficulté qui était que son équipement stratosphérique était très performant, de la classe 100,000 ft pendant 1 heure, ce qui veut dire aussi qu'il était jugé par ses utilisateurs trop lourd et trop encombrant; en particulier le casque était un véritable casque de scaphandre. Ensuite l'émergence de nouvelles technologies était à même de modifier certaines données : introduction des concentrateurs d'oxygène à tamis moléculaire (4,8) à autonomie quasi-illimitée mais à basse pression d'alimentation du régulateur d'oxygène, apparition de systèmes à commande

et/ou à surveillance électronique, intégrales ou partielles (6,7). Physiologiquement enfin il nous a été demandé d'une part de beaucoup mieux cerner les circonstances de mise en oeuvre des équipements, en particulier par une bien meilleure prise en compte du facteur temps, d'autre part d'inclure dans les études la nécessaire amélioration de la tolérance aux forts facteurs de charge (3,5). Les équipements étudiés en France intègrent donc plusieurs fonctions de protection au sein d'un même ensemble, système de régulation et équipement personnel de vol; ces différentes fonctions apparaissent dans le premier tableau, la France ayant développé des prototypes de systèmes de régulation dans les deux technologies disponibles, la technologie électronique et la technologie pneumatique. Ces deux systèmes ayant été développés d'après des hypothèses, des concepts physiologiques et des textes réglementaires communs, leurs performances sont très proches du point de vue de leur efficacité physiologique.

Tableau n° 1 : analyse des fonctions demandées

Fonctions réalisées :

- protection contre l'hypoxie d'altitude, de durée quasi-illimitée avec l'emploi de concentrateurs d'oxygène,
- protection contre la haute altitude (fonction de surpression altimétrique)
- protection contre la surpression alvéolaire en cas de décompression explosive
- protection classique contre les accélérations
- protection évoluée contre les accélérations +Gz soutenues de haut niveau par l'utilisation de la surpression respiratoire
- protection contre l'immersion

Fonctions compatibles :

- protection thermique en cas d'immersion (vêtement d'immersion)
- protection NBC

Les équipements étudiés en France se composent d'un système complexe de régulation et d'un ensemble d'équipements personnels de vol. Le système de régulation comprend un régulateur d'oxygène, une valve anti-G et un module de connexion entre ces deux équipements; le module de connexion agit en fait fonctionnellement par multiplexage d'ordres. Le système de régulation peut être alimenté par un concentrateur d'oxygène. L'équipement personnel de vol est décomposé en plusieurs sous-ensembles : un équipement de tête (casque et masque), un gilet pressurisé et le pantalon anti-G dont le rôle est étendu à l'ensemble des fonctions de contre-pression tégumentaire de la partie basse du corps (figure n° 1).

La fonction ventilatoire est assurée par un système à la demande basé sur un amplificateur pneumatique (figure n° 2). La France a récemment développé deux prototypes spécialement adaptés aux basses pressions d'alimentation telles que celles qui peuvent être observées en aval d'un concentrateur d'oxygène à tamis moléculaire. L'un de ces prototypes utilise la technologie pneumatique, l'autre la technologie électronique; le schéma de principe est cependant le même pour les deux équipements (figure n° 3), avec deux caractéristiques par rapport aux schémas traditionnels précédents : tout d'abord le gain de l'amplificateur est variable, asservi à la pression d'alimentation du régulateur d'oxygène, qui peut varier dans un rapport voisin de 10; ensuite l'étage de sortie du régulateur est doublé en raison des très basses valeurs de pression susceptibles d'être rencontrées dans ces mêmes conditions. Les performances d'un tel régulateur peuvent être décrites sur une courbe débit-pression (figure n° 4), qui montrent d'excellentes performances pour les valeurs nominales de pression d'alimentation du régulateur en aval d'un concentrateur d'oxygène et un écrêtement du débit de sortie du régulateur à des valeurs acceptables en cas de très basse pression d'alimentation, correspondant à une anomalie de fonctionnement de la source de gaz respirable (par exemple par défaut de pression moteur).

La loi de dilution altimétrique a été adaptée au port d'un vêtement à contre-pression tégumentaire par vessie de pressurisation. Comme il est de règle sur de tels équipements, la vessie de pressurisation thoracique est montée en parallèle sur le circuit ventilatoire. Si l'équipement fonctionne en dilution, est introduit un risque hypoxique supplémentaire en cas de décompression rapide de la cabine. En ce cas en effet, la poche de poitrine est remplie d'un mélange gazeux adapté à l'altitude de la cabine préalable à la décompression; son rinçage progressif par la ventilation du sujet apporte un retard à l'adaptation des gaz alvéolaires et impose de modifier la loi de dilution. En première analyse, il suffit d'asservir cette loi non pas à la pression-cabine mais à la pression-avion pour résoudre cette difficulté (figure n° 5). Au moment

où nous l'avons testé, l'équipement était prévu pour devoir fonctionner avec un réservoir d'oxygène liquide; il convenait donc de pouvoir économiser l'oxygène. D'autre part cette loi était en contradiction avec le STANAG 3198 puisqu'elle imposait l'oxygène pur dès 18 400 ft dans la cabine (les avions français sont pressurisés à 30 kPa). Ultérieurement enfin, elle n'était pas cohérente avec toutes les performances des concentrateurs d'oxygène. C'est une loi intermédiaire entre les deux courbes caractéristiques qui fut choisie, en même temps que le volume de la vessie du gilet respiratoire était minimisé. Les essais effectués au laboratoire en décompression rapide sur sujet humain ont montré la validité du concept d'utilisation du vêtement à pressurisation partielle avec les mélanges dilués d'air et d'oxygène choisis, pour autant que le volume de la poche de pressurisation ne dépasse pas 2 à 2.5 dm3 lorsque l'équipement est utilisé avec sa surpression normale (de 4 à 5 kPa environ). Notons pour terminer sur le problème de la dilution que la fraction d'oxygène peut être réglée soit depuis le régulateur d'oxygène soit depuis le concentrateur d'oxygène lorsque cette source de gaz respirable est utilisée. Dans ce dernier cas, le régulateur d'oxygène est dépourvu de la fonction de dilution. Connaissant les qualités du concentrateur d'oxygène comme filtre, cette caractéristique peut n'être pas dépourvue d'intérêt en cas de protection contre l'agression NBC.

La loi de surpression altimétrique a été adaptée au port d'un vêtement à pressurisation partielle. L'hypothèse est faite que la fonction de surpression altimétrique impose l'utilisation d'oxygène pur, éventuellement par l'intermédiaire d'une source de secours lorsqu'un concentrateur d'oxygène est utilisé. En effet, compte-tenu de la pressurisation des aéronefs, il est exclu de devoir utiliser la fonction de surpression altimétrique autrement qu'en cas de défaillance grave et rapide de la pressurisation. L'utilisation de la source de secours d'oxygène pur est alors licite. Nos premiers essais, réalisés avec la loi de surpression haute, correspondant au maintien strict de la pression de 19.6 kPa (147 mm Hg) dans l'alvéole pulmonaire, soit l'altitude équivalente de 39 000 ft, ont montré l'inadaptation de cette loi. En accord avec d'autres travaux, la loi de surpression a été abaissée, tenant compte d'une part de l'hypocapnie due à une constante hyperventilation au cours de la respiration en surpression, d'autre part de la brièveté de l'exposition à la haute altitude. Il est ainsi possible d'admettre une diminution de 2.5 kPa environ de la surpression par rapport à la valeur nominale à 60 000 ft. Techniquement, le pantalon anti-G est utilisé pour assurer la contre-pression tégumentaire de la partie inférieure du corps. Cette fonction est obtenue par renvoi de l'ordre de surpression altimétrique vers l'étage de sortie de la valve anti-G. Le dispositif de multiplexage des ordres pneumatiques assure la fiabilité du dispositif, en particulier pour assurer les priorités d'ordres et éviter l'envoi de la surpression anti-G vers la partie respiratoire de l'équipement.

Le risque de surpression alvéolaire en cas de décompression explosive est atténué à travers deux éléments : une soupape expiratoire spécifique pour le masque et le gilet de contre-pression thoracique. La soupape expiratoire a été dimensionnée pour permettre l'évacuation rapide des gaz au cours de la décompression. Pour la vessie du gilet respiratoire, c'est la courbe de compliance (courbe pression-volume) qui a été optimisée pour permettre l'application d'une contre-pression péri-thoracique suffisante au moment de la décompression. Les caractéristiques de cette vessie de pressurisation thoracique sont donc déterminées pour minimiser à la fois le risque hypoxique en décompression rapide et le risque de surpression alvéolaire en décompression explosive.

La protection classique contre les accélérations +Gz de longue durée est assurée de façon traditionnelle par la valve et le pantalon anti-G. Cependant, sur cet équipement, cette fonction habituelle a été fortement améliorée, en même temps qu'une fonction supplémentaire était apportée. Techniquement, le gonflage du pantalon anti-G a été accéléré par des modifications internes importantes de l'ensemble de la chaîne anti-G : augmentation des sections de passage des gaz, réduction des volumes internes de la valve anti-G, utilisation du concept de pression maximale dès le déclenchement. Ensuite le fonctionnement de la valve anti-G a été adapté à l'hypothèse du fonctionnement avec un concentrateur d'oxygène, c'est-à-dire que, seul, l'étage de commande est alimenté en gaz par le concentrateur (compatibilité vis-à-vis du système de multiplexage avec le régulateur d'oxygène), l'étage de sortie de la valve anti-G étant alimenté en gaz directement par l'air comprimé; c'est une technologie de valve anti-G dite hybride. Enfin, et peut-être surtout, la mise au point de l'équipement VHA 90 en France pour les besoins de la protection en haute altitude nous a conduits à développer un équipement qui permet de tolérer des valeurs élevées de surpression respiratoire, jusqu'à 10 kPa environ, dans des conditions de confort jusque là peu connues. Dès lors pouvait être réactivée une idée ancienne qui n'avait pu être rendue opérationnelle : l'utilisation de la surpression respiratoire pour améliorer la tolérance aux accélérations +Gz soutenues et de haut niveau. Le concept d'intégration de l'ensemble de régulation permettait de réaliser aisément cette fonction, en commandant l'étage de surpression respiratoire par un ordre en provenance de la valve anti-G : il s'agit bien d'un ordre de commande de la valve anti-G et non du renvoi de la pression anti-G elle-même dans le circuit ventilatoire. Les résultats de cette fonction ont été étudiés au sein de notre groupe par Clère, qui les présente dans une autre communication.

Une autre fonction ne présente pas de particularités physiologiques notables : **c'est la fonction anti-immersion** sous la forme du gilet de sauvetage intégré. Par contre un effort particulier et un choix spécifique ont conduit à assurer la compatibilité de cet équipement avec deux autres équipements qui ne pouvaient lui être intégrés : il s'agit de la combinaison d'immersion et d'éventuels équipements de protection NBC. Le choix a été celui de supprimer les manches de l'équipement à pressurisation partielle; à l'origine de ce choix demandé par les techniciens, nous avons fait l'hypothèse d'une

part que le réservoir vasculaire que représentent les membres supérieurs n'est pas considérable, d'autre part qu'en haute altitude les problèmes d'aéroembolisme, qui n'apparaissent pas immédiatement dès l'exposition à l'altitude, ne seront pas majeurs. Les essais réalisés, aussi bien dans les conditions de la surpression altimétrique que dans le cadre de la surpression anti-G ont démontré la validité de la première hypothèse. Les essais en altitude n'ont pas permis d'observer de cas d'aéroembolisme dans les conditions de la décompression rapide, bien que tous les essais aient été effectués sans dénitrogénation préalable, avec utilisation de mélanges gazeux air-oxygène; la deuxième hypothèse était donc considérée comme validée elle aussi.

Parmi les fonctions non encore intégrées dans les équipements personnels, figure en premier lieu la protection thermique, cette fois dans le sens de l'évacuation de chaleur hors de l'organisme du pilote, lorsque celui-ci revêt combinaison d'immersion ou équipement NBC. La protection pare-éclats n'est pas envisagée; la compatibilité de l'ensemble de tête décrit avec des dispositifs de visualisation portés par le casque n'est envisagée à l'heure actuelle que sous son aspect théorique.

En conclusion, a été développée en France depuis 10 ans environ une nouvelle génération d'équipements qui permettent d'intégrer, au sein d'un seul ensemble, diverses fonctions qui doivent permettre à un équipage d'avions de combat d'être protégé contre les différents facteurs nocifs du vol, quelles que soient les contraintes rencontrées. Ces contraintes sont aussi bien des contraintes d'environnement (altitude sous tous ses aspects, agressions thermiques de toutes formes, risques toxicologiques) que des contraintes biodynamiques, sous la forme des accélérations +Gz de haut niveau et de longue durée.

BIBLIOGRAPHIE

1- **DAMRON J., HOWARD T., MORGAN T.R., HOSKIN R.S.** (1988)
Development of an advanced high altitude flight suit.
A.S.M.A. 59th meeting May 8-12 NEW ORLEANS

2 - **ERNSTING J. (1984)**
Operational and physiological requirments for aircraft oxygen systems.
AGARD report 697 : 1.1-1.10

3 - **HARDING R.M., BOMAR J.B.** (1990)
Positive pressure breating for acceleration protection and its role in prevention of in-flight G-induced loss of consciousness.
Aviat., Sp. and Environ. Med., 61(9-1) : 845-9

4 - Ikels K.G., Bomar J.B., Miller R.L. (1987)
Performance criteria for the MSOCS.
SAFE 25th Annual Symposium Nov.16-19 LAS VEGAS (NE) Conf. Proc. : 29-34

5 - Marotte H., Vieillefond H. (1985)
La respiration en pression positive: moyen de protection contre les accélérations +Gz. Approche théorique.
Rev. Méd. Aéro. et Sp., 24(95) : 147-9

6 - Marotte H., Zapata R., Dehayes J., Clère J.M. (1988)
Study and design of an electronic oxygen regulator prototype for aircrew.
SAFE 26th Annual Symposium Dec. 6-9 LAS VEGAS (NE) Conf. Proc.: 319-320

7 - Marotte H., Clère J.M., Gutman G., Beaussant R. (1989)
Modern pneumatic technology and the challenges of physiological protection for the pilot of advanced fighter aircraft.
SAFE 27th Annual Symposium Dec.5-8 NEW ORLEANS Conf. Proc. : 29-34

8 - Miller R.L., Ikels K.G., Lamb M.J., Boscola E.J., Ferguson R.H. (1980)
Molecular sieve generator of aviator's oxygen: performance of a prototype system under simulated flight conditions.
Aviat., Sp. and Environ. Med., 51(7) : 665-673

9 - Vikan T.T., Bomar J.B., Orr T.C. (1987)
The integrated concept for aircrew life support equipment.
SAFE 25th Annual Symposium Nov.16-19 LAS VEGAS (NE) Conf. Proc.: 319-320

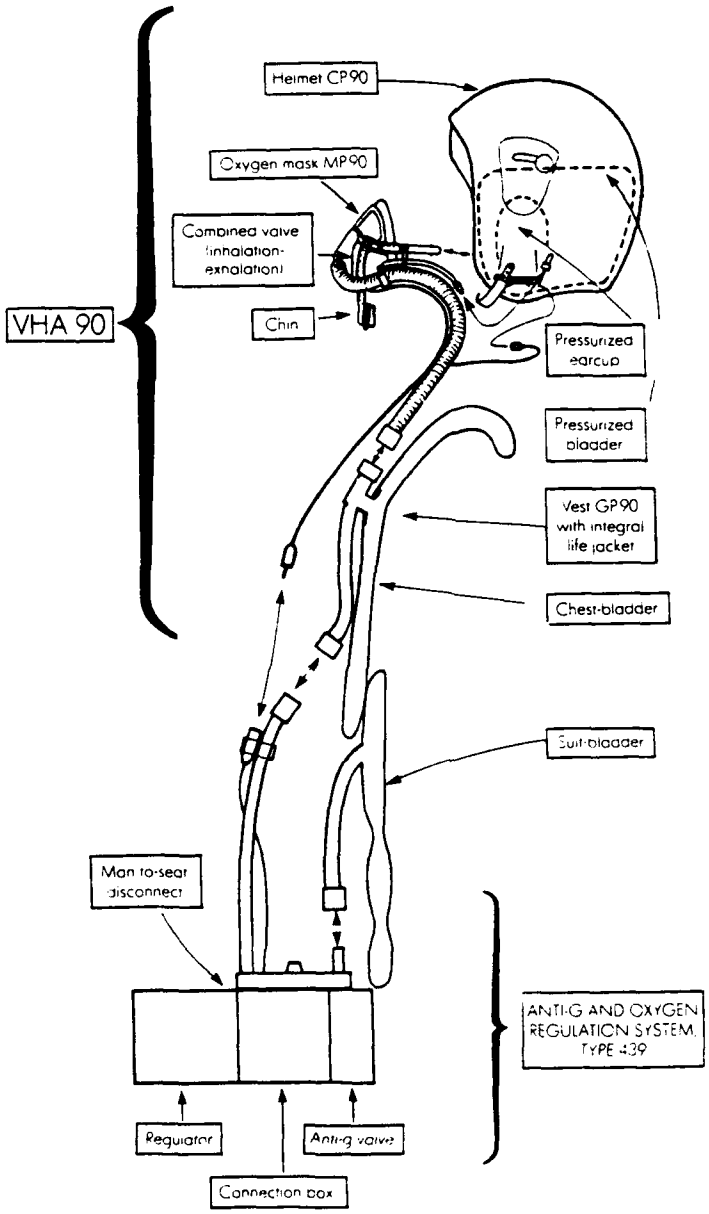

Figure 1: Schéma de principe du système de régulation et du vêtement à pressurisation partielle.

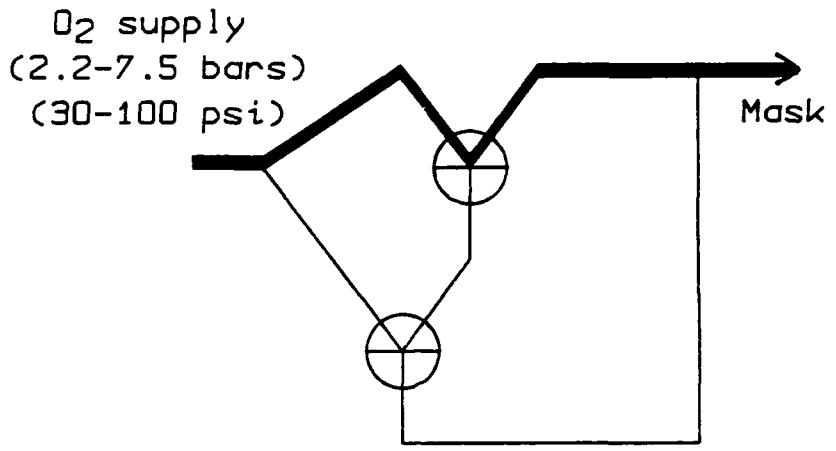

Figure 2: Schéma fonctionnel d'un régulateur d'oxygène de conception traditionnelle.

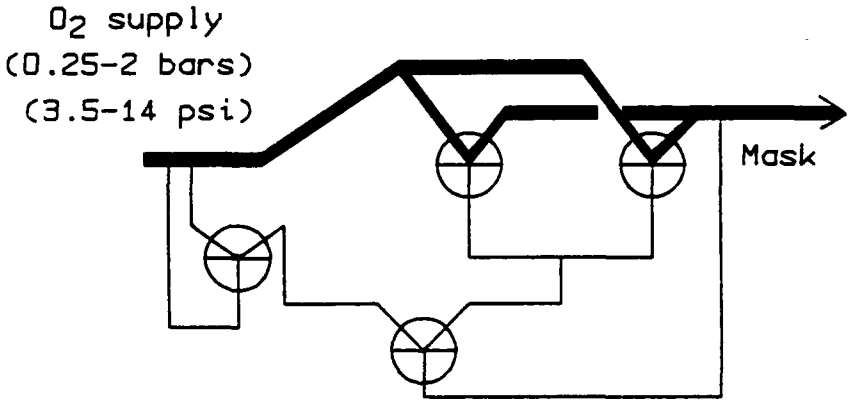

Figure 3: Schéma fonctionnel d'un régulateur d'oxygène adapté aux très basses pressions d'alimentation en oxygène (concentrateur d'oxygène).

Les schémas des figures 2 et 3 s'appliquent aussi bien en technologie pneumatique qu'en technologie électronique.

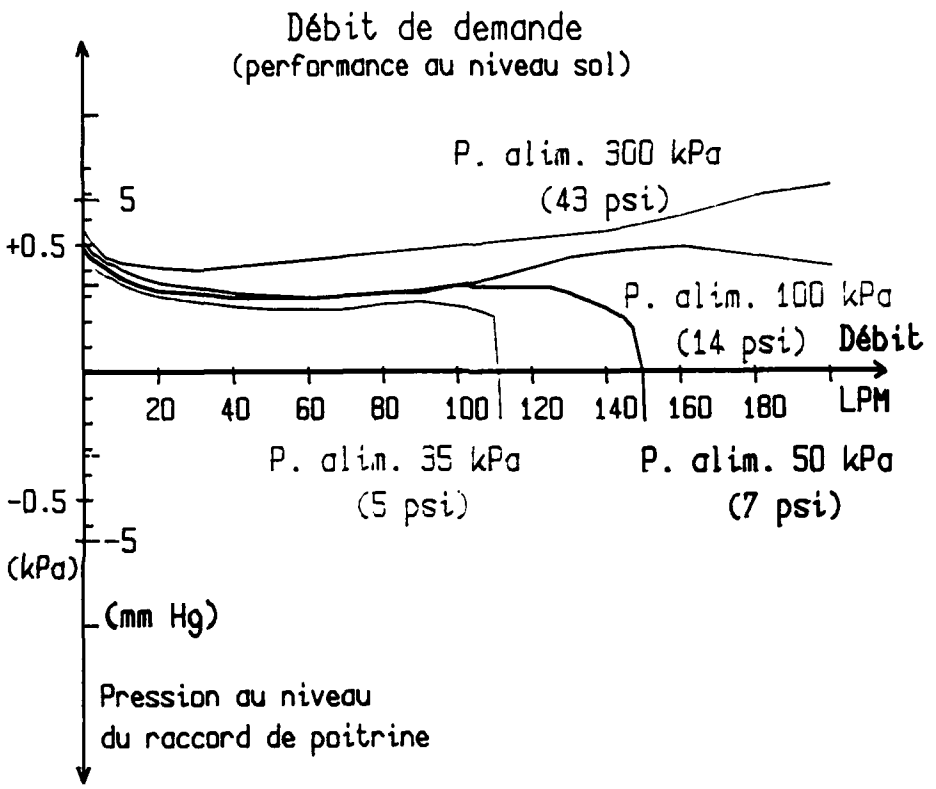

Figure 4: Courbes pression-débit au masque obtenues avec un régulateur d'oxygène adapté aux basses pressions d'alimentation.

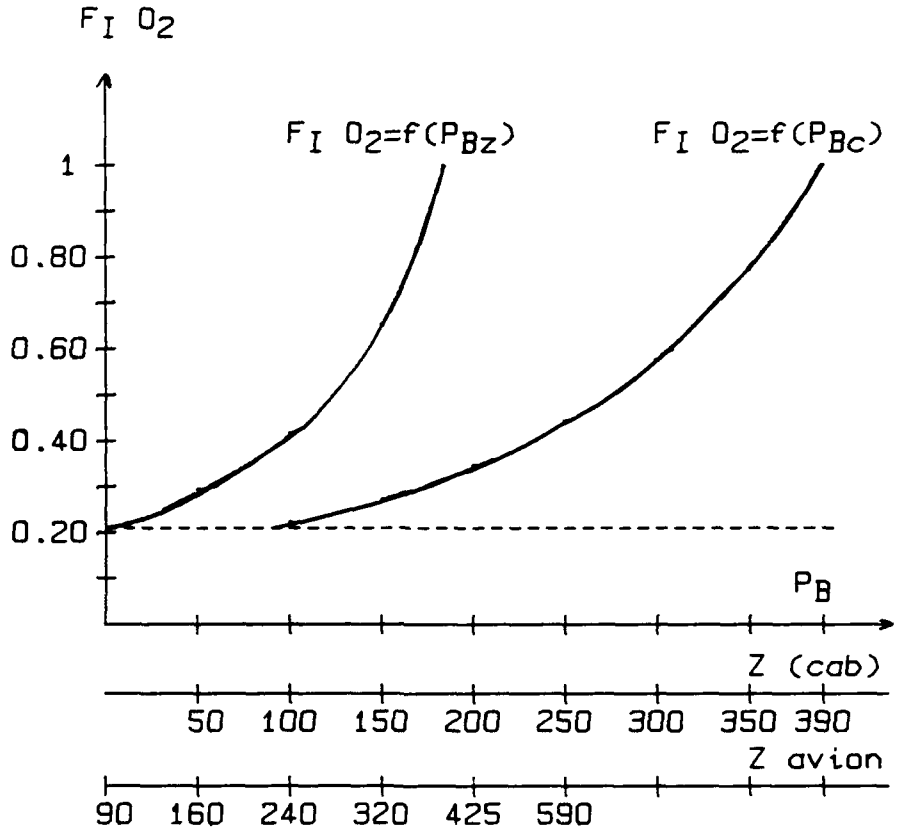

Figure 5: Loi de dilution altimétrique utilisable avec un vêtement à pressurisation partielle, comprise entre les deux courbes théoriques, établies soit en fonction de la pression cabine, soit en fonction de la pression avion.

MODEL OF AIR FLOW IN A MULTI-BLADDER PHYSIOLOGICAL PROTECTION SYSTEM

P.S.E. Farrell
D.F. James
A.A. Goldenberg
Department of Mechanical Engineering
University of Toronto
Toronto, Ontario M5S 1A4, Canada

SUMMARY

New physiological protection systems are needed in order to keep the pilot in control of the aircraft during high G and high altitude maneuvers. A model has been developed for air flow in a multi-bladder physiological protection system. Each bladder of the protection system is modelled as a flexible pressure vessel. The governing equations are derived for fluid flow from one vessel to another. The equations are simplified by five assumptions which are based on the fluid being compressible and inviscid. The result is a set of nonlinear differential equations which describe the isentropic pressure variation within the vessels. The equations are integrated numerically, and yield the thermodynamic quantities within each vessel as a function of time. Based on the differential equations, a computer simulation of the flexible pressure vessel model has been performed. The simulation allows for many possible configurations and scenarios. Five basic configurations are discussed in this paper.

LIST OF SYMBOLS

C_p	heat capacity at constant pressure
C_v	heat capacity at constant volume
e	internal energy per unit mass
h	internal enthalpy per unit mass
M	Mach number
m	mass
$\dot{m}$	mass flow rate
P	pressure
R	universal gas constant
s	entropy per unit mass
T	temperature
V	volume
u	velocity
γ	specific gas ratio
ρ	density

1. INTRODUCTION

Physiological protection from high G and high altitude environments is essential for fighter aircraft pilots. The standard G protection system consists of an anti-G suit controlled by an anti-G valve, in combination with $L1$ and $M1$ maneuvers performed by the pilot. A regulator, mask, and chest jerkin provide positive pressure breathing (*PPB*) for additional protection from high G and high altitude. However, with the increase in aircraft maneuverability, present protection systems have limited use.

New physiological protection systems have been proposed. One proposed system is a multi-bladder suit where the pressure in each bladder is controlled. The bladder coverage includes the calfs, thighs, abdomen, chest, as well as arms, forearms and hands. Other systems involve designing new regulators and G-valves. The basic mechanism of these systems is to alter the pressure within the bladders by controlling the air flow from one vessel to another. If the air flow between pressure vessels is modelled, then a generic system of pressure vessels can be generated. The objective of this research is to develop a model of the air flow in a multi-bladder physiological protection system.

With a generic mathematical model any specific system (current or proposed) can be implemented, simulated, and analysed by computer. The simulation displays the system dynamics as a function of time. With the system dynamics, bladder material and coverage, inflation priority, pressure schedules, etc., can be optimised. Thus, an iterative design procedure can be performed before the hardware is built and tested.

The governing equations for the flow are based on the general flow equations [1], simplified by five assumptions which allow the flow to be described as isentropic. The assumptions are specified in section 2 and are related to the fluid dynamics of a compressible and inviscid fluid. The system model is described as a set of first order, nonlinear, multi-variable, coupled differential equations which yield the pressure within each vessel. Included in the analysis are the mass, volume, and temperature variations due to the change in pressure within each vessel.

The mathematical model is implemented and simulated for the following basic multi-bladder configurations and scenarios:

1. Flow from a rigid pressure vessel to the atmosphere (e.g. a venting supply tank)
2. Flow from a rigid pressure vessel into a rigid pressure vessel (e.g.from a breathing regulator to a mask)
3. Flow from a rigid pressure vessel into a flexible pressure vessel (e.g. a supply tank inflating an anti-*G* suit)
4. Pressure profile of a volume driven vessel (e.g. lungs)
5. Simulation of a multi-bladder configuration (e.g. breathing regulator, mask, chest jerkin, and lungs)

2. ASSUMPTIONS

Air flow from a high pressure source into a pressure vessel is described as compressible flow of an inviscid fluid [2]. The conservation equations of mass, momentum, and energy are simplified by the following five assumptions, which reflect the nature of the flow between the vessels.

2.1. Inviscid Fluid

An inviscid fluid assumes that viscous effects are negligible in comparison to inertial effects. This is true for air and oxygen in anti-*G* suits, chest jerkins, etc..

2.2. No Body Forces

It is assumed that the body forces (e.g. gravity, electro-magnetic) acting on the fluid are negligible with respect to the change in momentum of the fluid. This is true for most gases.

2.3. Quasi-Steady Flow

Steady flow assumes that the variation of a quantity (i.e. velocity, pressure, density) with time is small in comparison to its variation in the flow direction, and thus time derivatives are neglected. Quasi-steady flow assumes that the flow is steady during a short period of time. Given initial conditions, the steady flow governing equations are solved for a short period of time. New values are found at the end of the interval, and are used as the initial conditions for the following interval, and so on.

2.4. One-dimensional

It is assumed that the fluid properties change mainly in the direction of fluid flow. Boundary layers and eddy currents are neglected.

2.5. Adiabatic

In an adiabatic process the heat entering the system from the outside is negligible. That is, the temperature change due to heat transfer from the outside is small compared to the temperature change due to pressure variation within the bladder.

2.6. Governing Equations

From these assumptions, the continuity, momentum, and energy equations are expressed as follows:

$$\frac{d(\rho u)}{dx} = 0 \qquad 2.1$$

$$\rho u \frac{du}{dx} = -\frac{dP}{dx} \qquad 2.2$$

$$\rho u \frac{de}{dx} = -P \frac{du}{dx} \qquad 2.3$$

where ρ is the density, u is the velocity, P is the pressure, and e is the internal energy of the fluid, at a point. An alternate expression for the energy equation (equation 2.3) in terms of the enthalpy h is as follows:

$$\frac{dh}{dx} = -u \frac{du}{dx} \qquad 2.4$$

where $h = e - \frac{P}{\rho}$. Substituting equation 2.2 into equation 2.4 yields a relationship between enthalpy and pressure along a streamline:

$$\frac{dh}{dx} = \frac{1}{\rho} \frac{dP}{dx} \qquad 2.5$$

In the next section, it is shown that equation 2.5 is an identical expression of the isentropic assumption which yields the isentropic relationships.

3. ISENTROPIC RELATIONSHIPS

The second postulate of thermodynamics [3] is expressed mathematically as follows:

$$ds = \frac{1}{T} de + \frac{P}{T} d\left[\frac{1}{\rho}\right] \qquad 3.1$$

where s is the entropy and T is the temperature of the fluid at a point. In terms of enthalpy:

$$ds = \frac{1}{T} dh - \frac{1}{T\rho} dP \qquad 3.2$$

The isentropic assumption states that the change in entropy is zero during the process (i.e. $ds = 0$). Therefore equation 3.2 becomes:

$$dh = \frac{1}{\rho} dP \qquad 3.3$$

Equation 3.3 is the general relationship between enthalpy and pressure, and it holds along a streamline (equation 2.5) as well as at a point as time passes. Therefore the compressible inviscid fluid flow described above is an isentropic process.

The isentropic relationships are obtained by substituting $dh = C_p dT$, where C_p is the heat capacity at constant pressure, and by integrating equation 3.3. The isentropic relationship between T and P is:

$$T = C_1 P^{\frac{\gamma - 1}{\gamma}} \qquad 3.4$$

where C_1 is a constant of integration. The ideal gas law is used to solve for the isentropic relationship between ρ and P:

$$\rho = C_2 P^{\frac{1}{\gamma}} \qquad 3.5$$

The isentropic relationships are used to find a set of differential equations for the multi-bladder system.

4. DIFFERENTIAL EQUATION

Equation 3.5 is differentiated with respect to time to yield an expression between the pressure within the bladder, the mass within the bladder, and the volume of the bladder as follows:

$$\frac{1}{\gamma P}\frac{dP}{dt} = \frac{1}{m}\frac{dm}{dt} - \frac{1}{V}\frac{dV}{dt} \qquad 4.1$$

Equation 4.1 is the differential equation which describes how the pressure changes as the vessel's mass and volume changes. Each term of the equation is discussed below.

4.1. Rate of Change of Mass

The rate of change of mass with time, $\frac{dm}{dt}$, within a control volume is equal to the sum of mass flow rates into the control volume, $\dot{m}_{in}$, minus the sum of mass flow rates out of the control volume, $\dot{m}_{out}$. That is:

$$\frac{dm}{dt} = \sum \dot{m}_{in} - \sum \dot{m}_{out} \qquad 4.2$$

$\dot{m}$ is defined as follows:

$$\dot{m} = \rho_t u_t A \qquad 4.3$$

where A is the minimum cross-sectional area of the outlet duct, and ρ_t and u_t are evaluated at the minimum cross-sectional area (or the "throat") of the duct. ρ_t and u_t are expressed in terms of ρ and P at a stagnation point within the vessel ($u = 0$), and P_t, the throat pressure. From equation 3.5, ρ_t becomes:

$$\rho_t = \rho\left[\frac{P_t}{P}\right]^{\frac{1}{\gamma}} \qquad 4.4$$

From equation 2.4 and equation 3.4, u_t is expressed as follows:

$$u_t^2 = \frac{2\gamma RT}{(\gamma - 1)}\left[1 - \left[\frac{P_t}{P}\right]^{\frac{\gamma-1}{\gamma}}\right] \qquad 4.5$$

Substituting equations 4.4 and 4.5 into equation 4.3 yields an expression for $\dot{m}$ in terms of the vessel conditions and the throat pressure:

$$\dot{m}_{out} = \frac{PA}{\sqrt{RT}}\left\{\frac{2\gamma}{\gamma-1}\left[\frac{P_t}{P}\right]^{\frac{2}{\gamma}}\left[1 - \left[\frac{P_t}{P}\right]^{\frac{\gamma-1}{\gamma}}\right]\right\}^{1/2} \qquad 4.6$$

Similarly, $\dot{m}_{in}$ is the mass flow rate from an adjacent vessel with a greater pressure, say $P_s > P$ (s refers to "supply" conditions). The expression is as follows:

$$\dot{m}_{in} = \frac{P_s A}{\sqrt{RT_s}}\left\{\frac{2\gamma}{\gamma-1}\left[\frac{P}{P_s}\right]^{\frac{2}{\gamma}}\left[1 - \left[\frac{P}{P_s}\right]^{\frac{\gamma-1}{\gamma}}\right]\right\}^{1/2} \qquad 4.7$$

A maximum flow rate is obtained when the throat Mach number is equal to one. This is called *choked flow*. The mach number is calculated by re-arranging equation 4.5, where $\mathbf{M}_t = \frac{u_t}{a_t}$, and $a_t = \sqrt{\gamma RT_t}$ is the speed of sound at the throat:

$$\mathbf{M}_t^2 = \frac{2}{\gamma - 1}\left[\left[\frac{P}{P_t}\right]^{\frac{\gamma-1}{\gamma}} - 1\right] \qquad 4.8$$

Substituting $\mathbf{M}_t = 1$, and solving for the pressure ratio yields:

$$\frac{P_t}{P} = \left[\frac{2}{\gamma + 1}\right]^{\frac{\gamma}{\gamma-1}} \qquad 4.9$$

Equation 4.9 is substituted into equation 4.6 and $\dot{m}_{\max}$ is as follows:

$$\dot{m}_{\max} = \frac{PA}{\sqrt{RT}}\gamma^{1/2}\left[\frac{2}{\gamma + 1}\right]^{\frac{\gamma+1}{2(\gamma-1)}} \qquad 4.10$$

For air and oxygen, choked flow occurs when $\frac{P_t}{P} \le 0.5283$.

4.2. Rate of Change of Volume

The rate of change of volume, $\frac{dV}{dt}$, is a function of the material properties of the pressure vessel. If the vessel is rigid, then $\frac{dV}{dt} \to 0$ and the differential equation becomes:

$$\frac{1}{\gamma P}\frac{dP}{dt} = \frac{1}{m}\frac{dm}{dt} \qquad 4.11$$

If the vessel is flexible, then $\frac{dV}{dt}$ is a function of pressure. The differential equation becomes:

$$\left[\frac{1}{\gamma P} + \frac{1}{V}\frac{dV}{dP}\right]\frac{dP}{dt} = \frac{1}{m}\frac{dm}{dt} \qquad 4.12$$

where $\frac{dV}{dP}$ depends on material properties. If the vessel volume is actively driven (e.g. a piston or a lung), $\frac{dV}{dt}$ is a known function of time.

4.3. Temperature Variation

The temperature changes within each vessel due to changes in pressure. This is seen from the isentropic relationships (equation 3.4). A detailed analysis shows that the temperature obeys the Ideal Gas Law, even when one considers the mixing of gases at different initial temperatures. Therefore, given the pressure, mass, and volume, the temperature can be calculated at a point in time and along the flow path.

5. COMPUTER SIMULATION

A differential equation has been derived which describes the pressure variation within a vessel. Given a particular multi-bladder configuration, a set of differential equations describes the system (each differential equation is of similar structure). The differential equations are nonlinear due to the isentropic relationships and the velocity varying with the square root of the temperature. The differential equations are multivariable and coupled due to the pressures which appear in the mass flow rate terms. Solutions to the differential equations must therefore be found numerically.

The objective is to implement a computer algorithm, based on the differential equations, which simulates various multi-bladder configurations and scenarios. A single vessel algorithm is generated first, then two vessels, then multiple vessels. The goal is to allow the user to obtain an overall picture of how the thermodynamic properties vary within the system.

5.1. Flow from a Rigid Pressure Vessel to the Atmosphere

The differential equation below describes the flow from a rigid vessel to the atmosphere:

$$\frac{dP}{dt} = -\frac{\gamma P}{m}\dot{m}_{out} \qquad 5.1$$

where $\dot{m}_{out}$ is given by equations 4.6 and 4.10. Note that $P_t = P_{atm}$ is constant. For a given initial pressure, temperature, volume, and cross-sectional area, the computer predicts the thermodynamic properties as a function of time. Figure 1 is the pressure within the rigid vessel as a function of time. Initially, $P = 1800$ mmHg, $P_t = 760$ mmHg, $T = 20^o$ C, and $V = 5$ liters, and $A = 1$ in^2. The plot shows P reaches P_t in 1.78 seconds.

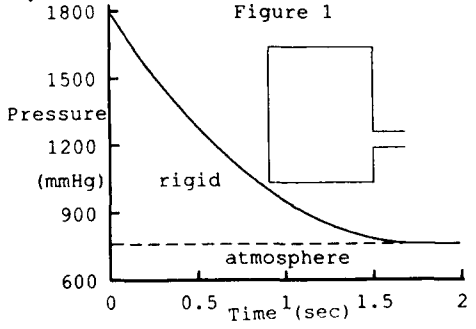

5.2. Flow From a Rigid Vessel into a Rigid Vessel

Two differential equations describe the flow from a rigid vessel into a rigid vessel. The differential equation for the higher pressure is identical to equation 5.1. The differential equation for the lower pressure, P_l, is as follows:

$$\frac{dP_l}{dt} = \frac{\gamma P_l}{m_l}\dot{m}_{in} \qquad 5.2$$

where the mass flow rate is common to both equations. Figure 2 shows four pairs of pressure versus time curves. Each pair represents identical initial configurations, except the lower pressure vessel volume is different in each case (i.e. $\frac{V}{V_l}$ is 0, ½, 1, and 2). Initially, $P = 1800$ mmHg, $P_l = 760$ mmHg, $T = T_l = 20^o$ C, $V = 5$ liters, and $A = 1$ in^2. For a given volume ratio, the system reaches its equilibrium pressure. For example, for a volume ratio of one, the equilibrium pressure is 1280 mmHg. For a volume ratio of a half, the equilibrium pressure is 1453 mmHg. The time to reach the equilibrium pressure decreases as the volume ratio increases.

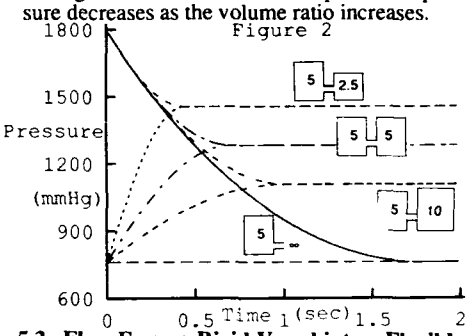

5.3. Flow From a Rigid Vessel into a Flexible Vessel

Two differential equations describe the flow from a rigid vessel into a flexible vessel. The differential equation for the rigid vessel is identical to equation 5.1. The differential equation for the flexible vessel is similar to equation 4.12, where $\frac{dV}{dP}$ was found from experimental data for a CSU 13B/P anti-G suit. The data were fitted to the following expression:

$$\frac{dV}{dP_f} = a(b - e^{-cP_f}) + gP_f \qquad 5.3$$

Figure 3 shows 3 pairs of pressure versus time curves. The lowest pair is the flow from the rigid vessel (5 liters) into a flexible vessel. The middle pair is the flow from the rigid vessel into a rigid vessel whose volume is equal to the final volume of the flexible vessel (6.1 liters). The highest pair the flow from the rigid vesse. into a rigid vessel whose volume is equal to the initial volume of the flexible vessel (2.5 liters). Initially, $P = 1800$ mmHg, $P_f = 760$ mmHg, $T = T_f = 20^o$ C, and $A = 1$ in^2. As expected, the inflation time of the flexible vessel is longer than two rigid vessels.

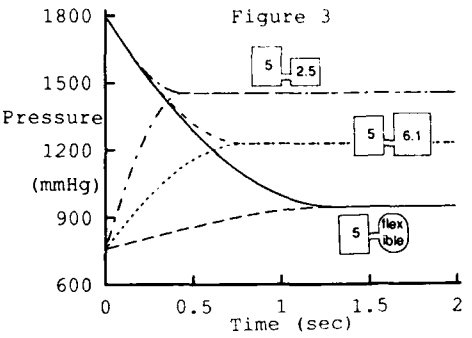

5.4. Pressure Profile of a Volume Driven Pressure Vessel

A piston open to the atmosphere has a volume which varies sinusoidally. The differential equation describing the pressure within the piston is equation 4.1, where $\frac{dV}{dt}$ is as follows:

$$\frac{dV}{dt} = \omega\left[\frac{V_{max} - V_{min}}{2}\right]\cos\omega t \qquad 5.4$$

Figure 4 shows pressure and volume versus time curves. Initially, $P = 760$ mmHg, $T = 20^{o}$ C, $V_{min} = 500$ ml, $V_{max} = 1000$ ml, $\omega = 4$ rad/sec, and $A = 1$ in^2. The pressure obtains the same frequency as the volume. In addition to the sinusoidal volume function, the algorithm includes a linear volume function (which approximates an M1 or L1 maneuver).

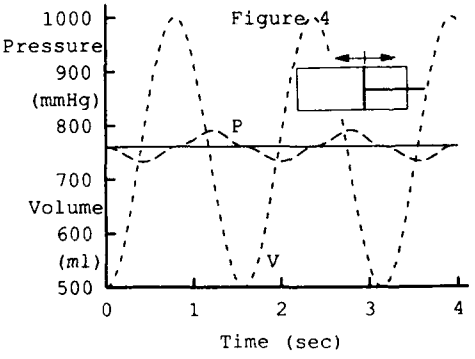

5.5. Multi-Bladder Configuration

The resultant computer algorithm allows for any number of pressure vessels connected in any configuration (parallel or series). An example of this is described below. Vessel 1 is a large, rigid vessel whose initial pressure is 1800 mmHg. All other vessels are initially at 760 mmHg. Vessel 2 is a flexible vessel. Vessel 3 is a small, rigid vessel. Vessel 4 is an active vessel with a sinusoidal input. Vessel 1 is connected to vessels 2 and 3. Vessel 3 is connected to vessel 4. The system is closed to the atmosphere. Figure 5 shows the pressure versus time curves for each vessel. The curves are reasonable, but not readily predictable.

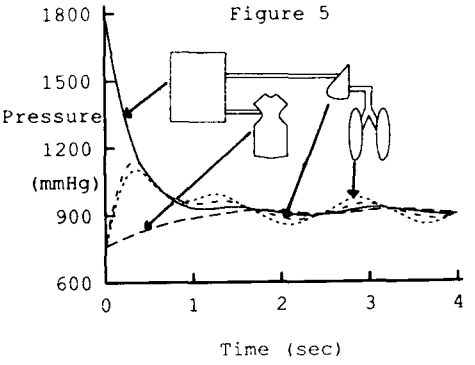

In general, this simulation is capable of determining the thermodynamic properties within each vessel connected in series and/or parallel. The vessels may be rigid or flexible, or have an actively changing volume (sinusoidal or linear). Also, various gases may be used. The possible configurations and scenarios are unlimited.

The computer algorithm generates the differential equations automatically based on the following questions:
What are the vessels' initial P, V, and T?
What is the vessel type (i.e. rigid, etc.)?
How are the vessels connected?
What is A_{min} between each vessel?
The computer then generates the appropriate differential equations for each vessel, integrates, and outputs the desired thermodynamic property for any specified vessel.

6. CONCLUSIONS

A mathematical model has been developed based on the governing equations for isentropic fluid flow. For a given multi-bladder physiological protection system, a set of differential equations are generated and integrated to yield the thermodynamic properties as functions of time. This information can be used in the design of multi-bladder physiological protection systems

Issues arising from this work include the optimisation of physiological protection systems. For instance, an anti-G suit can be modelled and simulated, and the material properties and suit dimensions can be varied and optimised over a range of supply pressures. Another issue is the development of valves and regulators controlling bladder pressures. The designer can use the model to test various valve designs and control strategies.

REFERENCES

1. White, Frank M. Fluid Mechanics, McGraw-Hill Book Company, Toronto, 1979
2. Currie, I. G. Fundamental Mechanics of Fluids, McGraw-Hill Book Company, Toronto, 1974
3. Callen, B. Herbert. Thermodynamics and an Introduction to Thermostatistics, second edition, John Wiley & Sons, Toronto, 1985

THE DESIGN AND DEVELOPMENT OF A FULL-COVER PARTIAL PRESSURE ASSEMBLY FOR PROTECTION AGAINST HIGH ALTITUDE AND G

by

A. E. Hay
Judy E. Aplin

Aircrew Integration Section (FS9)
Flight Systems Department
The Royal Aerospace Establishment, Farnborough, Hampshire, GU14 6TD, United Kingdom

SUMMARY

A partial pressure assembly comprising a chest counter pressure garment (CCPG) and full-cover anti G trousers (FAGTS) has been designed and constructed to flight standards in the Aircrew Integration Section of RAE, and is illustrated in Fig 1.

The CCPG is a simple two layer outer garment located under the life-preserver and supplied with breathing gas from the demand regulator.

The FAGTS comprise a single bladder which covers the abdomen, legs and feet retained by an outer inextensible layer of Nomex, with the ability to be donned quickly by employing zips and low friction lacing for final fit adjustment. Gas supplied from a suitably programmed G-valve inflates the garment to provide protection.

Details of the design approach and the developmental stages to date are given together with an outline of the anthropometric considerations required to provide a snug fitting assembly from a limited size roll.

INTRODUCTION

The chest counter-pressure garment (CCPG) current development began in RAE in September 1986 with a simple 'over the head' design to prove the concept and has evolved through a further three designs to it's current state of split-bladder with off-centre zip closure.

Concurrently the development of the FAGTS was commenced in April 1988, progressed rapidly through some design changes on the basis of assessments made by the RAF Institute of Aviation (IAM) using their man-carrying centrifuge, to what is essentially the current design which was first flown from RAE in the IAM Hawk aircraft in February 1989.

Developments since that time have been concerned mainly with improving comfort, mobility, sartorial elegance and with facilitating easier donning/doffing. The short time taken to produce this flight-worthy assembly is attributable to the excellent working relationship which exists between the two research organisations co-located at Farnborough whereby RAE can design and construct in its clothing laboratory, garments made to the physiological requirements and functional evaluations provided by IAM.

DESIGN CONSIDERATIONS

RAE decided from the outset that there was little benefit to be gained by trying to adapt old patterns of early pressure garments, or by modifying existing in-service garments in an attempt to extend the boundaries of the protection they provided.

New RAE designs and patterns were constructed aimed at achieving maximum bladder coverage to investigate the improvement in protection levels that this would provide, with the assumption that reduction in bladder cover would be a relatively easy matter once the functional garments had been designed. In the event, it has been found that petechial haemorrhaging occurs on areas of the skin not covered by the bladder following periods of exposure to sustained high G when garments with reduced coverage, or gaps in coverage, have been worn. These results make it seem unlikely that much reduction will be possible if the protection levels so far achieved are to be maintained.

Separate garments, CCPG and FAGTS, have been developed mainly to give ease of mobility and greater versatility of fitting than a one-piece suit would allow, but this does mean that the area of overlap in the waist/ umbilical region needs special consideration.

The question of fit of full-cover trousers is extremely important to mobility, comfort and operational effectiveness and certain critical features must be borne in mind if the best fit possible is to be achieved. For instance, the correct location of the crotch of the FAGTS is essential since it both inhibits step-up actions if it is too low, and affects the position of the articulated segment on the trouser leg which must be centred on the knee joint to be effective.

The sizing of the experimental partial pressure garments to date, has been determined mainly by the requirements to equip resident and visiting aircrew or subjects for laboratory trials, and therefore has been somewhat empirical and piecemeal.

However, as with all aircrew protective clothing, the real problem of sizing to be addressed is that of maximising the proportion of the aircrew population which can be fitted to an acceptably high standard by a limited size roll of garments

Accordingly RAE has now derived, using previously published methodology (Ref 1), a complete theoretical size roll for FAGTS which is due to be manufactured under contract in the near future. This nine size roll is based on the application of anthropometric data from the survey of 2000 RAF aircrew, (Ref 2) using waist circumference and crotch height as the control dimensions. The 3 x 3 size grid is shown in Fig 2 and is expected to accommodate 98% of the UK aircrew population.

The simple design of the CCPG renders it's sizing less of a problem and the size roll for this garment will be based on

chest circumference and cervical (or nape of neck) to waist length.

BRIEF HISTORY OF DEVELOPMENT

(a) Chest Counter Pressure Garments (CCPG)

The Type 1 was a simple garment which comprised four layers, a single bladder which surrounded the chest contained within an outer layer of non-extensible fabric and a low friction lining. The patterns for this design are shown in Fig 3. This CCPG was donned over the head like a 'pull-over', lacing adjustment was provided down each side to ensure a snug fit.

The Type 1 design was intended as a 'tool' to allow IAM to investigate schedules of positive pressure breathing with G (PBG), however the programme progressed so quickly to flight trials that this rather bulky laboratory design, albeit constructed to flight standards, attracted criticism of its fallibility for operational use rather than its demonstrable functional effectiveness (Ref 3).

Other designs, Types 2 and 3, involved variations in positioning of the bladder split, tailoring the waist, changes to the bladder shape to allow maximum freedom of arms and neck. These changes resulted in a greatly reduced dead space volume and the patterns are illustrated in Fig 4.

The Type 4 CCPG is the current design and is shown in Fig 5. It has an off-centre split with a zip closure, both shoulders are closed and adjustment is made by symmetrical side lacing adjustments. This is a two layered construction using a composite fabric of nylon-butyl-nylon on the outside and a butyl-nylon-butyl inner, which provides effective chemical hardening.

This garment has been made to locate within the life-preserver (LP) for quick donning as shown in Fig 6; combining the CCPG with the LP so as to have a single-action closure has not yet been satisfactorily resolved.

A total of 4· CCPGs has been produced in-house at RAE for development and assessment purposes.

(b) Full Cover Anti G Trousers (FAGTS)

The RAE programme for the development of FAGTS started with a two-layered design, the Type 1, which effectively meant that the bladder was the garment, but this approach was not pursued because of the difficulties in providing all the shaping necessary to provide fit and mobility, while still retaining the gas tight integrity of the trousers. However, the benefit of full-cover protection on test runs with subjects on the centrifuge was sufficiently apparent to merit an immediate follow-up design, the Type 2, which demonstrated the advantage of designing a fully tailored, easy to construct, inextensible outer layer containing a simplified bladder. The patterns for this development are shown in Fig 7. Used in conjunction with an experimental toeless wrap-around foot bladder this garment was finalised in November 1988 so as to accommodate a range of wearers.

By February 1989 the design incorporated a fourth layer, this is the current Type 3 FAGTS design Fig 8, and comprises an outer layer of flame retardant inextensible material (Nomex) which is adjustable and bearing pockets, a butyl-nylon-butyl bladder (chemically hardened) and a silk lining providing improved inter-garment slip to aid donning.

The Type 3 FAGTS have been flown extensively in the IAM Hawk from RAE by IAM/RAE pilots and by visiting European pilots, and have been provided to British Aerospace for the European Aircraft Project (EAP) integration flying assessments. A total of 41 Type 3 garments have been constructed in the RAE clothing laboratory, the latest of which have included rf welded bladders and a detachable slip-on style foot bladder which is easy to don and provides very comfortable foot protection.

(c) Laboratory and flight trials

Assessments of the CCPG and FAGTS assembly using the IAM human centrifuge has demonstrated enhanced sustained high G protection in excess of +9 G_z while at the same time allowing the trial subjects to speak.

Flight trials of this partial pressure assembly have been conducted in the IAM Hawk T Mk 1 aircraft both at RAE and off-base at a RAF Tactical Weapons Training Unit in March 1989 (Ref 4), for evaluation by experienced instructor aircrew. The findings, some of which are illustrated in Fig 9, indicate that the level of protection afforded by the installed system was rated very highly, 17 of the 19 subjects having found a dramatic improvement in their G tolerance. The ability of the aircrew to move around within the cockpit was also rated highly indicating minimum restriction imposed by full-cover garments. The comfort rating was somewhat biased by the fact that only one size of FAGT was available to the 19 aircrew who participated in the trial, and of the 19 aircrew who wore it only 9 would be deemed to have been a correct match to the garment size. If these facts are borne in mind when viewing the results of the user questionnaires in (Ref 4), the donning/doffing, comfort and mobility assessments become more meaningful.

FUTURE DEVELOPMENTS AND REQUIREMENTS

At present RAE are finalising bladder designs which will allow easier and quicker construction using rf welding techniques on polyurethane impregnated fabrics. Garment bulk and mass has been significantly reduced from the early models and the search for suitable new materials to make further reductions, continues.

The protection of the feet presents problems since almost certainly the aircrew will want to remove their external FAGTS while in the crewroom between sorties, without having to remove flying boots. The provision of a connector between the foot and leg introduces a potential problem since it must be reliable, fail safe, easy to use, small, low mass, easily integrated with the lower leg and of course be reasonably priced. To date RAE have been able to provide a connector which meets most of these requirements, however we are still seeking a lower mass and less expensive alternative.

Attempts have been made to reduce bladder coverage by using the reaction of the bladder against an inextensible outer or by removing material in areas where it was thought that little benefit would be derived from applying counter-pressure. Because of the pressure schedules employed the effects of removing material causes increased mechanical strain on the garment which results in distracting distortions of the garment for the wearer. Furthermore, areas of the wearer not covered by bladder tend to result in varying degrees of petechial haemorrhaging or haemotoma which generally receives negative comment from the subject.

In our opinion having achieved protection with a measure of latitude to accommodate the whole population it seems a retrograde step to reduce effectiveness.

With regard to the overall integration of the partial pressure assembly with the man, which meets the requirements of having a role specific aircrew equipment assembly (AEA) to protect against all threat scenarios including the NBC, some questions remain to be addressed: if the CCPG uses the breathing gas supply to pressurise it, what safeguards are needed to ensure that no BC agent can enter the breathing supply if the CCPG is to be worn as an outer layer?

Also, if the CCPG is to incorporate a compensated dump valve to cope with over inflation on rapid decompression at altitude while pulling G, then how will this valve be protected from an ingress of BC agent if the CCPG is worn on an outside garment?

The donning/doffing drills which are a major part of the ground operating procedures (GOPs) will be derived once the order of the assembly has been established and, it is expected that the RAE NBC Test Facility (Ref 5), will play an important role in the determination and finalisation of these drills.

REFERENCES

1 Aplin, Judy E., "The application of anthropometric survey data to aircrew clothing sizing". RAE Technical Report 84050 (1984).

2 Bolton, C.B., Kenward, M., Simpson, R.E., Turner, G.M., "An anthropometric survey of 2000 Royal Air Force aircrew 1970/71". RAE Technical Report 73083 (1973)

3 Harding, R.M. and Cresswell, G.J., "Royal Air Force flight trials of positive pressure breathing." In: High G and high G protection - aeromedical and operational aspects. Proceedings of the Royal Aeronautical Society Symposium, 1987.

4 Prior, A.R. and Cresswell, G.J., "Flight trial of an enhanced G protection system in Hawk XX 327". RAFIAM Report No.678, 1989.

5 Hay, A.E., "The RAE NBC Test Facility." Paper CP 457-31. In: AGARD Conference Proceedings No.457 - Aeromedical and performance aspects of air operations in a chemical environment, Madrid, May 1988.

Fig 1 Partial pressure assembly

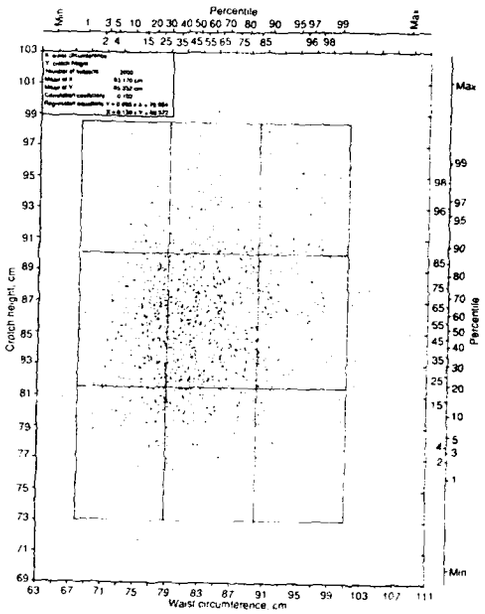

Fig 2 RAE FAGTS sizing grid

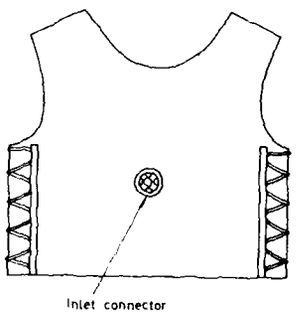

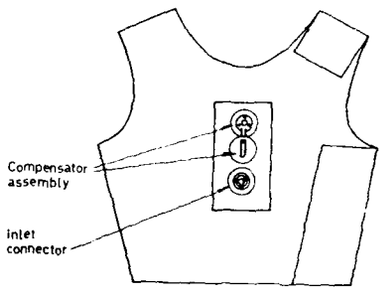

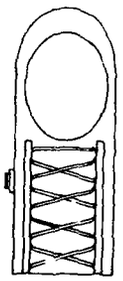

Fig 3 Type 1 CCPG patterns

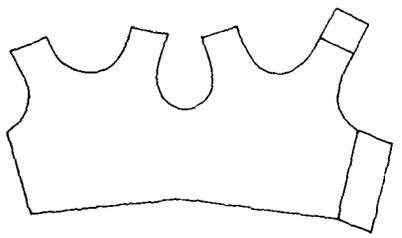

Fig 4 Type 3 CCPG patterns

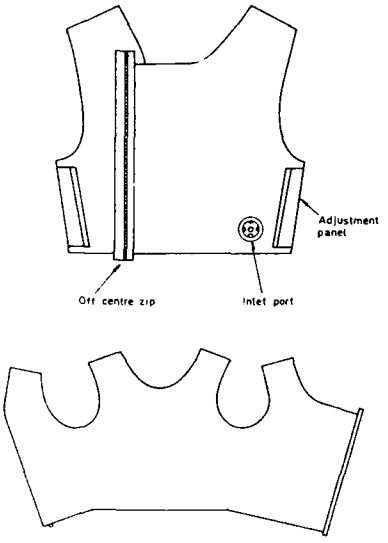

Fig 5 Type 4 CCPG patterns

Fig 6 CCPG with life preserver

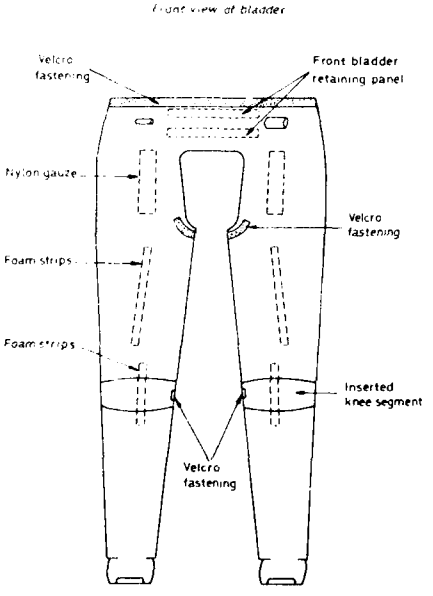

Fig 7 Type 2 FAGTS patterns

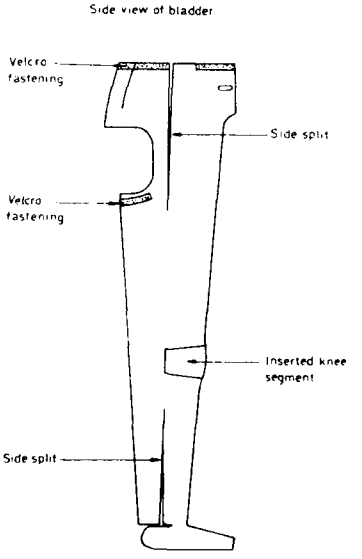

Fig 7 (continued)

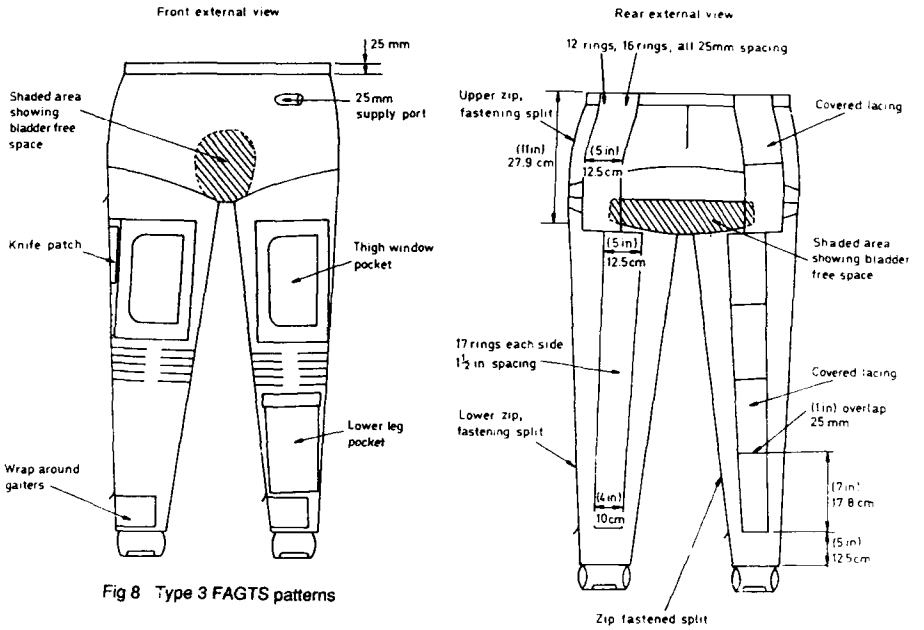

Fig 8 Type 3 FAGTS patterns

Fig 8 (continued)

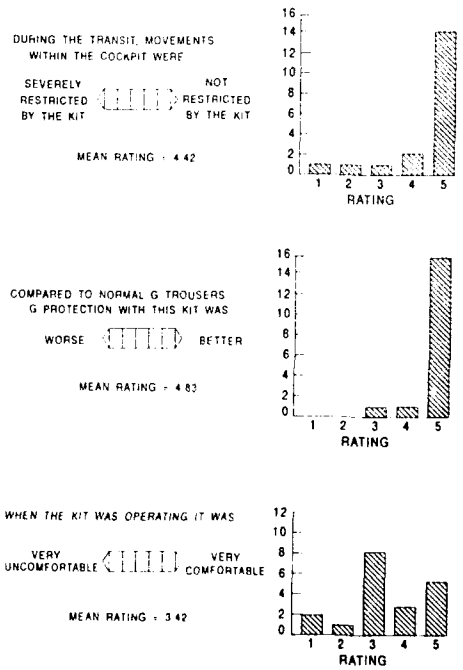

Fig 9 Flight trial ratings

ADVANCES IN THE DESIGN OF MILITARY AIRCREW BREATHING SYSTEMS WITH RESPECT TO HIGH ALTITUDE AND HIGH ACCELERATION CONDITIONS

Author : Nigel P J Lovett
Title : Project Engineer - Military Breathing Systems

Normalair-Garrett Limited
Yeovil, Somerset BA20 2YD
United Kingdom

SUMMARY

The conclusions drawn from the work undertaken by NGL indicate that for future aircraft systems the combining of an Anti-G Valve with a Breathing Regulator into one unit, provides the most compact and effective system. The advances made by the Research Establishments (both RAF IAM and USAFSAM) into the development of new aircrew garments, reduces the need for quick response, electronic controlled valves, thus suggesting that mechanically controlled systems still provide the optimum protection for aircrew under high acceleration conditions.

LIST OF ABBREVIATIONS

BRAG	Breathing Regulator and Anti-G
ECU	Electronic Control Unit
IAM	Institute of Aviation Medicine
Ins W G.	Inches of Water Gauge
mm Hg	Millimetres of mercury
NADC	Naval Air Development Center
NGL	Normalair-Garrett Limited
P.B.A	Pressure Breathing with Altitude
P.B.G	Pressure Breathing with + Gz
RAF	Royal Air Force
TLSS	Tactical Life Support System
USAF	United States Air Force

INTRODUCTION

NGL have been involved in providing military aircrew breathing systems with protection against altitude conditions since the early 1950s, this basically being the provision of a breathing regulator incorporating a pressure breathing with altitude capability (PBA).

The PBA schedules were mainly established by the Royal Air Force Institute of Aviation Medicine and they satisfied physiological requirements for altitudes of 50, 60 and 70 thousand feet.

The most common altitude requirement is that which derives from the MK17 panel mounted regulator, where a pressure of nominally 17 ins WG is provided at 50 thousand feet. This schedule was also carried forward into the miniature man mounted units and the more recent duplex seat mounted units, Type 317 and 517 respectively. Additionally other versions of the above regulators provided a pressure of nominally 37.5 ins WG at 60 thousand feet and with the aid of partial pressure suits, some units provided protection up to 70 thousand feet.

Unlike PBA, where NGL has an established history, Pressure breathing with G (PBG) is a relatively new requirement with our experience to date being two fold.

For U.S. programmes NGL provided one standard PBG schedule as identified at FIGURE 1. This initiated pressure breathing at 4g, increasing linearly at a rate of 12 mmHg g, with a plateau of 32 ins WG.

For RAF IAM programmes a number of different schedules were provided that had varying characteristics. However, the schedule currently provided for the IAM Hawk aircraft is shown at in FIGURE 2. This schedule initiates pressure breathing at 2g, increasing linearly at a rate of 11 mmHg g with a plateau of 29 ins WG.

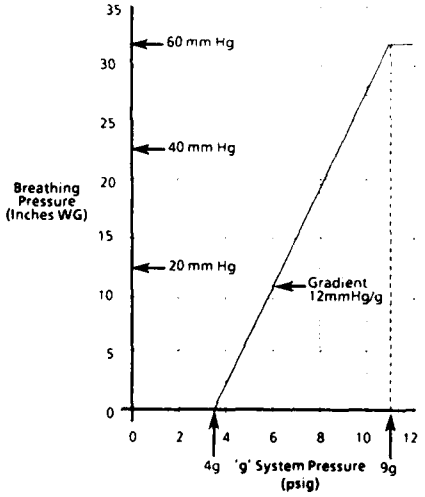

FIGURE 1 : U.S. PBG SCHEDULE

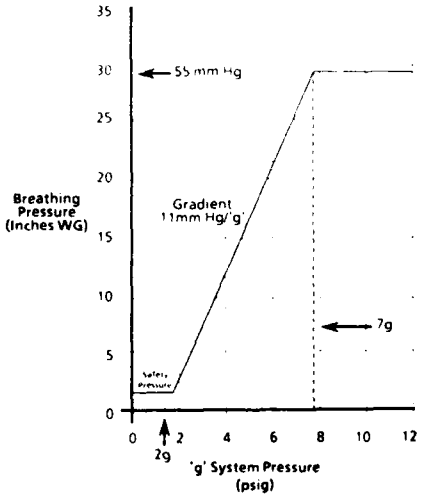

FIGURE 2 : HAWK PBG SCHEDULE

DEVELOPMENT OF PBG

The main advances in breathing regulators over recent years has been the development of PBG with NGL having approached this in two ways. Firstly adapting existing breathing regulators to provide PBG and secondly developing the concept of combining the breathing regulator and anti-g valve into a single unit, a concept more commonly referred to as BRAG Valves.

Originally, in conjunction with RAF IAM, NGL adapted the standard Hawk type 517 regulator to provide PBG in response to g using a g sensitive module. This module was adapted to the top face of the regulator and utilised the bleed flow venting from the existing Press-To-Test port. When subjected to +Gz the module reacted and instigated PBG to a predetermined schedule. Trials where conducted under the jurisdiction of RAF IAM and although successful, it was concluded that the concept of G sensitive regulators, operating independently from the aircraft anti-g system, could be physiologically unsatisfactory due to the risks of providing PBG without inflation of the aircrew anti-g suit.

For the USAF Tactical Life Support System (TLSS) programme, NGL developed the principle of only providing the aircrew with PBG when inflation of the anti-g suit had occurred. This was accomplished by providing the breathing regulator with a pneumatically activated PBG module, which connected directly to the anti-g suit supply system. This principle ensured that PBG would only be provided when pressure was supplied to the anti-g suit. Successful subjective test programmes were conducted by USAF where a further improvement in G module design was established, which was to provide the breathing regulator with a supplemental bleed flow under +Gz conditions. This supplemental bleed flow ensured the regulator control chambers were always primed to improve dynamic breathing response under rapid changes of acceleration.

A schematic diagram of a PBG breathing regulator is shown on FIGURE 3 which incorporates the improved module. When activated by the aircraft g system pressure, the valve closes to restrict regulator bleed flow, thus allowing the supplemental bleed flow to pass into the regulator control chamber. when the g system pressure decays, the valve returns to the rest position and ceases the supplemental bleed flow.

This process always ensures sufficient control pressure is supplied under acceleration conditions to ensure the regulator provides satisfactory breathing performance.

Further experimental work continued with RAF IAM to establish suitable test units for a number of centrifuge and flight test programmes. The Type 600 breathing regulator developed for the Harrier GR5 aircraft and again the Hawk Type 517 were used.
Pressure activated PBG modules, based on that provided for the TLSS programme, were developed for both regulators and subjected to a number of centrifuge test programmes and flight trials in the IAM Hawk and Hunter aircraft. The modified type 517 being now standard fit on the IAM Hawk aircraft.

More recently NGL adapted the CRU-88 P man mounted regulator, produced for the US Navy NACES programme, to provide a PBG schedule. This again employed a pressure activated module which was incorporated by deleting the existing pressure breathing aneroid. The unit was subsequently supplied to NADC for a centrifuge test programme.

Each of these aforementioned activities involving NGL, utilise separate breathing regulators pneumatically "talking to" independent anti-g valves which for low altitude requirements could be satisfactory.

For altitude conditions above 40 thousand feet however, there is a physiological requirement to provide counter pressure on the lower abdomen and limbs, when subjected to pressure breathing.

Therefore, to ensure this, an additional communication link between the anti-g valve and breathing regulator was considered together with the combination of the previously mentioned two units which in turn began the development of the BRAG Valve within NGL.

DEVELOPMENT OF THE COMBINED BREATHING REGULATOR AND ANTI-G (BRAG) VALVE

The USAF TLSS programme "really began" NGLs development programme into BRAG valves as the system provided acceleration protection up to 9G and altitude protection up to 60 thousand feet. Included in this system was a pneumatic breathing regulator and an independent electronically controlled anti-g valve. The object of the system was to pneumatically initiate PBG by linking the regulator PBG module with the supply system to the anti-g suit. For altitude protection however, both breathing regulator and anti-g valve functioned independently to provide a PBA schedule to the aircrew and chest counter pressure garment and to provide 4 times the PBA schedule to the anti-g suit for altitudes above 40 thousand feet.

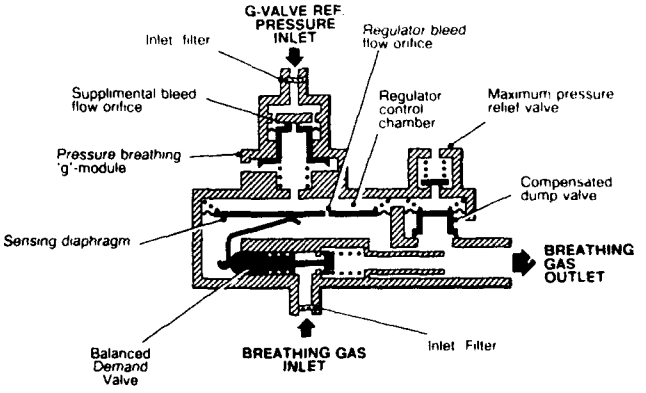

FIGURE 3 : SCHEMATIC DIAGRAM OF PBG BREATHING REGULATOR

This philosophy was further advanced by NGL when fully developing the concept of BRAG by combining the independent units into one body. NGL considered that the optimum approach would be to develop a seat mounted concept that incorporated a simple breathing regulator, an anti-g valve and a personal equipment connector (PEC) together with providing the anti-g valve with an electronic control unit (ECU), which was considered necessary to provide a rapid response system. This concept of BRAG valve enabled all the pneumatic link requirements for acceleration protection to be integrated within the one body. The altitude protection provided by the valve again relied on the breathing regulator being controlled independently to the anti-g valve, where the ECU controlled the inflation of the anti-g suit to 4 times the pressure breathing schedule above 40 thousand feet.

The PBA schedule considered for this unit is shown on FIGURE 4. PBA is initiated at nominally 39 thousand feet, and has a plateau pressure of 37.5 ins WG at nominally 53 thousand feet, which is maintained to the maximum altitude of 60 thousand feet.

The anti-g valve inflation schedule selected for the BRAG valve, with respect to acceleration protection, is shown on FIGURE 5, which follows the basic algorithm of outlet pressure = 1.5n-2.5 psig (where n = absolute 'g' level).

To fully evaluate this BRAG valve concept, NGL conducted a full performance test programme in the oxygen laboratory. This included basic performance tests in conjunction with simulated acceleration tests. Altitude tests were performed in NGLs test chamber and acceleration tests conducted on our unmanned centrifuge. To further evaluate the valve, a subjective test programme was arranged and conducted on the human centrifuge at RAF IAM.

This enabled valuable information to be assessed up to acceleration levels of +9Gz at onset rates of 1 and 2 G/sec. Under simulated conditions this BRAG valve was capable of pressurising a rigid 10 litre capacity to 9.5 psig in 0.5 seconds, equivalent to an onset rate of 18 G/second.

FUTURE DEVELOPMENTS

Since the development of NGLs BRAG valve, changes have occurred in the thinking behind aircrew protection, which have tended to move away from the need for rapid response valves.

In this case, although more accurate, the need for electronically controlled units is less apparent as mechanically controlled systems, are just as capable of fulfilling current specification requirements. As such NGL have evaluated by design and mathematical modelling the potential performance of possible mechanically controlled systems.

A weakness identified during these evaluations was the potential for the requirements of PBA and PBG to be additive. NGL has developed a principle, whereby any new system has the ability to be fully capable of ensuring that addition of breathing and anti-g pressures, will not occur, should altitude and acceleration conditions occur simultaneously and that only the higher of the two requirements will be delivered.

This requirement is being actively pursued with the U.S. Navy. A number of future applications have been addressed including the ability of a man mounted regulator to provide both pressure breathing altitude and +Gz conditions, this being based on NGLs' existing CRU-88 P regulator. Additionally NGL are addressing the possible requirement of providing a simple mechanical BRAG valve that would be capable of replacing existing cockpit mounted equipment. Both applications being based on the proven performance recorded at IAM and NADC and the benefits of extensive company input through development testing and mathematical modelling.

To further highlight NGLs future commitment to the advancement of military breathing systems, the production of an Air Dilution Panel Mounted Regulator, compatible with liquid, gaseous and OBOG systems, and having the benefits of altitude and acceleration protection, should be available within the next 12 to 18 months. This being based on a current programme to supply a trainer aircraft with a new panel mounted regulator.

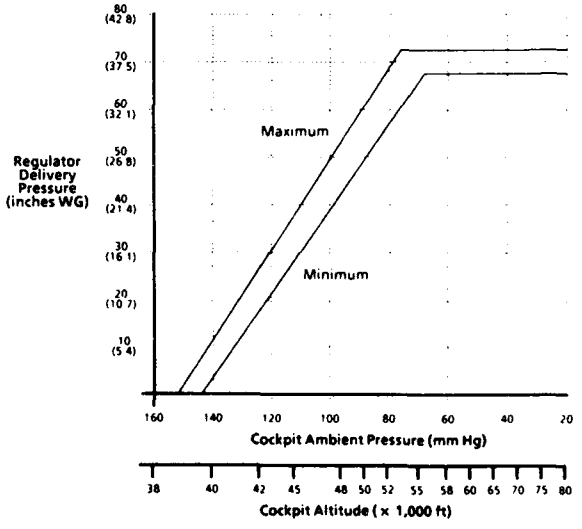

FIGURE 4 : PBA SCHEDULE

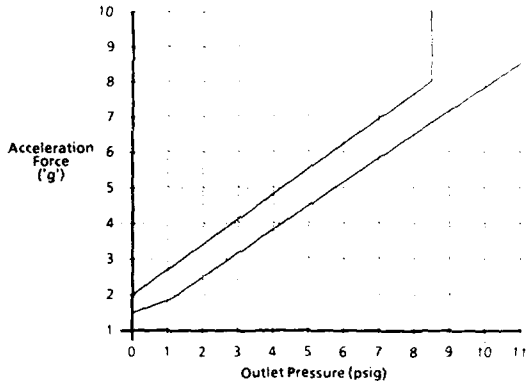

FIGURE 5 : ANTI-G VALVE INFLATION SCHEDULE

CONCLUSIONS

To conclude this short paper, NGL are aware that further work is being undertaken by a number of aeromedical research establishments worldwide and available data is obviously continually updated. Many factors will effect the design of aircrew military breathing equipment and through the close liaison NGL has maintained with a number of the research establishments we continually aim to meet new demands as they arise. Our experience to date has shown the major requirements for acceleration protection move away from Valves and response rates that operate on the principle of "the faster the better" to the improvement of aircrew garments.

These garment improvements have significantly improved aircrew protection using existing aircraft systems, thus substantiating NGL's view that mechanical control systems can still provide the optimum aircrew protection against the effects of high altitude and high acceleration conditions, but it is the integration of these systems into a small lightweight, single component which offers NGL the challenge for the future.

HIGH ALTITUDE HIGH ACCELERATION AND NBC WARFARE PROTECTIVE SYSTEM FOR ADVANCED FIGHTER AIRCRAFT - DESIGN CONSIDERATIONS

by

Dr A J F Macmillan
Royal Air Force Institute of Aviation Medicine
Farnborough, Hampshire GU14 6SZ, UK

SUMMARY

The physiological, technical and flight safety aspects of the design of an integrated system providing protection against high sustained acceleration short duration exposure to high altitude and NBC warfare agents have been discussed. The proposed system employs a molecular sieve oxygen concentrator and seat-mounted demand regulator and anti-G valve together with a source of clean filtered air and an emergency gaseous oxygen supply. The personal equipment assembly comprises counter pressure garments worn external to the NBC protective layer and a man-mounted filter. The filter assembly is used on the ground with a portable ventilator; in the air connected to the breathing gas supply; and post escape as part of a lung powered respirator system.

INTRODUCTION

Many NATO Air Forces have possessed individual NBC protective assemblies for use by aircrew for some time. UK has had chemical defence assemblies for aircrew in service for approximately 12 years. These assemblies have some limitations however since integration with in-service aircraft oxygen systems does not permit utilisation of the pressure breathing facilities of the demand regulators fitted to those aircraft. The next generation of high performance aircraft will require pressure breathing for altitude protection in emergencies and routinely during flight manoeuvres in which sustained high acceleration is experienced. It is essential therefore that the requirements for a combination of NBC protection with positive pressure breathing capabilities be recognised, the facilities required to provide this combination identified and the problems of achieving a satisfactory assembly highlighted. It must however be remembered constantly that an individual protective equipment assembly is only part of the system which is needed to provide complete protection and permit aircrew to operate in a contaminated environment. The components of the aircrew NBC protective system are; the aircrew respirator, the below neck protection, aircraft supply systems and the ground facilities of collective protection and contamination control. "Integration" therefore of partial pressure assemblies with NBC protection must by definition integrate with the other components of the protective system. It is in this area that the greatest difficulty is experienced and this paper addresses those various components and considers those design aspects of the individual protective assembly which are necessary to maintain protection against NBC agents during all phases of preparation for flight, in flight, after flight and post escape.

CHEMICAL AND BIOLOGICAL (CB) WARFARE AGENTS

The spectrum of identified CB warfare agents and potential toxins is now recognised as a continuum from classical, totally chemically produced agents through synthesised organic compounds to the true agents of biological origin. These agents, depending on their nature, the presence of additives and the mode of delivery, may be in vapour, aerosol or liquid form with the size of the drops of liquid varying over a wide range. Aircrew are at risk not only on the ground but also when they are in the aircraft if liquid contamination has been carried into the crew compartments by servicing personnel or the aircrew themselves. In addition there is evidence that some chemical warfare agents may pass unchanged

through the engines of existing aircraft and into the environmental control system, particularly when the engine power setting is low. The classical CW agents, against which effective protection is already in service, can be classified into three categories namely the vesicants, the nerve agents and other CW agents. It is the extreme toxicity of the nerve agents which in low doses affects vision by producing constriction of the pupil (miosis), and which can continue for several days, that set the standards for NATO aircrew respirators. The hazards from CW agents also include:

(i) inhalation in the respiratory tract by virtually all agents in gaseous, vapour, aerosol or liquid form;

(ii) ingestion hazard to alimentary tract;

(iii) skin hazard presented by nerve agents, primarily in liquid form, and vesicants as vapour aerosol or liquid;

(iv) hazard to the eyes by vesicants as well as nerve agents.

COMPONENTS OF THE NBC PROTECTIVE SYSTEM

Aircrew Respirator

The aircrew respirator for high performance aircraft must meet all the general requirements for such a device and should therefore envelope the head and neck in NBC proof material, provide clean breathing gas to the oronasal mask, provide clean ventilating gas to the eye compartment at positive pressure and integrate with the other items of headgear. In addition, since positive pressure breathing is to be provided, mask sealing characteristics must be better than in existing respirators, the breathing system must integrate with the counter pressure garments and ideally improved vision and head mobility should be achieved. The below neck NBC protection must also be compatible with the counter pressure garments and their gas supplies and other items of aircrew clothing such as immersion protection apparel and the lifepreserver. Consideration of the requirement to safely don and doff contaminated garments and re-use them have resulted in the most acceptable below neck protection systems utilising a "layered" principle in which an activated charcoal absorbent garment is worn beneath the outer standard aircrew clothing so that none of the functions of these outer garments is compromised. Therefore the first step in integrating these NBC protective facilities with partial pressure assemblies is to accept that the partial pressure assembly should be worn on top of the CW protective layer.

The ventilation which is necessary to maintain a slightly raised pressure in an aircrew respirator to provide the high level of protection required together with the through flow for demisting of the visor area is supplied on the ground by a portable ventilator and in the air generally by a fixed ventilator using an arrangement as indicated in Figure 1. This form of assembly which utilises a man-mounted filter and a two-compartment manifold positioned on the chest fulfills all the requirements for a NBC system for aircraft with demand oxygen regulators, thus a duplex regulator is used and oxygen from one or other of these regulators may be diverted via the changeover valve in the manifold to provide a back-up ventilating gas supply to the respirator. If however positive pressure breathing is required in this sytem then that format of backup ventilating gas would not be acceptable since gas at the raised pressure would be delivered to the hood compartment as well as the oronasal mask. Thus on exposure to high altitude ventilating gas must be provided from either an efficient blower unit or from the molecular sieve via an independent supply.

Partial Pressure Assemblies for High Performance Aircraft

The next generation of agile fighter aircraft requires positive pressure breathing both for protection against acceleration and altitude. The anti-G trousers and pressure waistcoats, which are being developed in UK to provide protection have been described by Gradwell (Ref 1), obtain their gas supplies by way of two independent valves. Higher pressures are required in the lower limb garments than in the chest counter pressure waistcoat (Ref 2). Pressure breathing is triggered during exposure to positive acceleration by a pneumatic signal from the anti-G system to the demand regulator. This arrangement ensures that should a failure of the anti-G valve occur, then pressure breathing would also cease thus avoiding the serious cardiovascular consequences of raised intrathoracic pressure in addition to pooling of blood in the lower limbs as a result of acceleration.

The evolving systems, for partial pressure assemblies required for altitude protection, generally require some multiple of the breathing pressure to be delivered to the anti-G trousers. This too is achieved by means of a pneumatic signal but in this case in the reverse sense from the demand regulator to the anti-G valve, thus at the onset of pressure breathing on exposure to altitude a signal to the anti-G valve will initiate the predetermined multiple of the breathing pressure (Ref 1).

Integration of NBC Protection with Partial Pressure Assemblies

By far the easiest concept for integrating NBC protection and partial pressure assemblies is based on the layering of aircrew protective garments as currently adopted in the UK. At present external anti-G trousers are well accepted by aircrew, since it is the last garment to be donned. Comfort and mobility on the ground, prior to donning the garment is not impaired. Similar considerations can be applied to a chest counter pressure garment and locating this garment external to the NBC protective layer is likely to be acceptable to the aircrew and would also eliminate the complex passageways which would be necessary to route gas supplies to the waistcoat through an NBC layer. In this position, however, since the chest counter pressure garment is likely to become contaminated, the gas supply to it must be isolated from the direct breathing line to the mask. This may be achieved by either;

1. Providing an independent gas supply hose from the breathing regulator, or

2. Bifurcating the hose immediately upstream of the man-mounted filter.

A jerkin isolation valve would minimise contamination during donning and doffing procedures in the contamination control area. Preliminary integration assessments suggest that the latter solution would be more acceptable but careful siting of the man-mounted filter is required.

Additional Design Considerations for Routine Flying and Emergency Egress

A key component in providing all the necessary routine and emergency facilities that are required in an integrated system is the man-mounted filter. The essential design features which must be incorporated in the man-mounted filter are shown in Figure 2. They comprise a portable ventilator connecting port so that the ground ventilator can be used during transit to and from the aircraft. A low resistance non-return valve is required in this port to prevent loss of molecular sieve product gas at low altitude. In addition however this connecting port can be used to provide inward relief in the aircraft in the event of failure of the molecular sieve followed by exhaustion of the back-up supply. Some form of barometric switch is required to ensure that the low resistance non-return valve is isolated at altitudes in excess of 8-10,000 feet. This low resistance non-return valve would also provide the route whereby air can be breathed following man-seat separation after ejection. An additional

high resistance inward relief valve might be necessary to provide a warning of failure of the oxygen supply as well as a means of breathing cabin air at altitudes in excess of 8-10,000 feet.

To ensure that positive pressure breathing may be supplied to the oronasal mask when required in flight, the manual changeover valve in the manifold must be kept in the position which separates the hood supply from the mask hose at all times. Thus back-up hood ventilation from the demand regulator is not possible, and an additional backup facility for hood ventilation gas is required in the event of failure of the primary system. This second system may be derived from product gas via a separate supply from the molecular sieve or from an enhanced performance fan unit if product gas is used as the primary system (Figure 8). The choice of which ventilating system should be considered the primary one is not yet finalised. An adequate flow of gas can be produced from a molecular sieve, but the ability of fan units to provide adequate gas flow at altitudes at which positive pressure breathing is required for protection against hypoxia is as yet unknown. Recent investigations in UK using augmented flow techniques suggest that acceptable flow from fan units may be feasible.

An additional refinement to the system described is required in the event of separation from the source of ventilating gas such as may occur following ejection or on the ground after emergency egress to ensure that post escape protection is available. This refinement permits breathing gas to be drawn across the visor compartment thus providing a degree of ventilation and preventing gross misting of the visual area. This facility will require an additional modification to the inlet of the oronasal mask within the respirator to allow inhalation (lung powered valve) (Figure 3). Routing of the inspiratory gas through the man-mounted filter is achieved by setting the changeover valve on the manifold to the "ground" position.

The various arrangements of the man-mounted filter assembly and the ground and aircraft supply systems for the different phases of a sortie are shown schematically in Figures 4, 5, 6 and 7.

The integrated NBC and partial pressure assembly discussed in this paper will provide NBC protection during all routine and emergency conditions of flight. It will not however provide protection following escape and descent into water. Immersion in water completely occludes current NBC filters and therefore some form of anti-suffocation/anti-drowning disconnect or inlet relief valve located in part of the breathing system which would be above water when worn by an aircrew member supported by an inflated lifepreserver is required. Means for producing an automatic facility of this nature are currently under investigation.

REFERENCES

1. Gradwell, D.P. (1991). The Experimental Assessment of New Partial Pressure Assemblies. AGARD 71st AMD Symposium, Paper 23.

2. Porlier, J.A.G., Ackles, K.N., Wright, G.K. and Holness, D.E. (1978). Reduction of the Physiological Effects of Positive Pressure Breathing by Increasing G-Suit Counterpressure. 49th Annual Meeting Aerospace Med. Assoc.

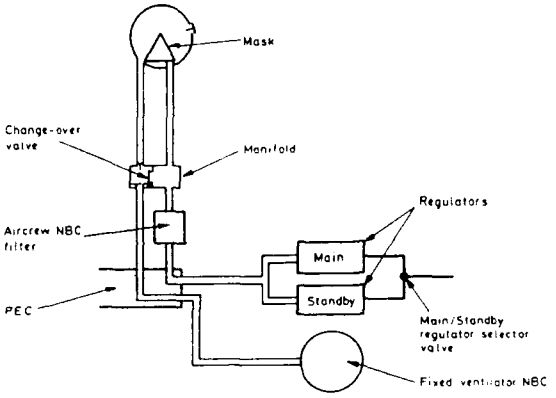

Figure 1 Supplies for Aircrew Respirator NBC No 5 Mk 3

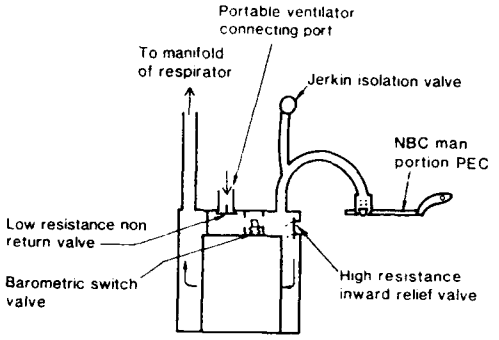

Figure 2 Features of Man Mounted Filter

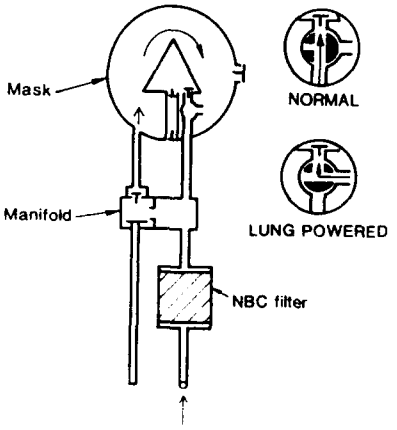

Figure 3 Schematic of "Lung Powered Facility"

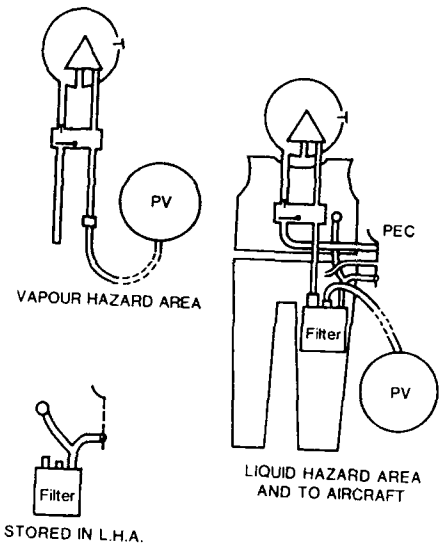

Figure 4 Assembly Used During Pre-Flight Phase

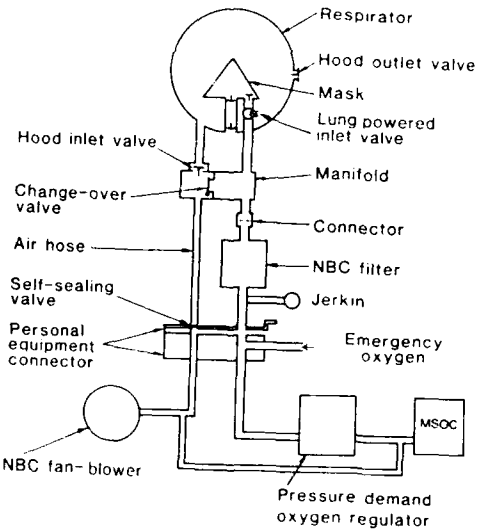

Figure 5 Schematic of Aircraft Installation

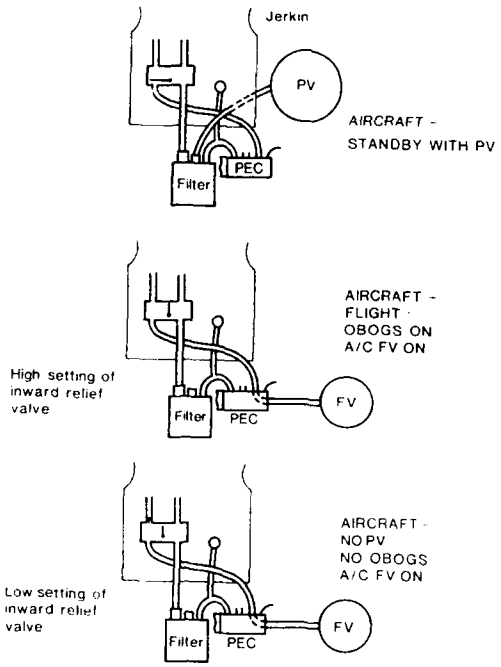

Figure 6 Assembly as Used With and Without OBOGS Functioning

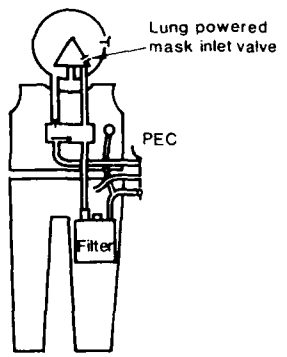

ASSEMBLY AS WORN POST ESCAPE

Figure 7

REPORT DOCUMENTATION PAGE

1. Recipient's Reference	2. Originator's Reference	3. Further Reference	4. Security Classification of Document
	AGARD-CP-516	ISBN 92-835-0638-3	UNCLASSIFIED

5. Originator Advisory Group for Aerospace Research and Development
North Atlantic Treaty Organization
7 rue Ancelle, 92200 Neuilly sur Seine, France

6. Title HIGH ALTITUDE AND HIGH ACCELERATION PROTECTION FOR MILITARY AIRCREW

7. Presented at the Aerospace Medical Panel Symposium held in Pensacola, Florida, United States, 29th–30th April 1991.

8. Author(s)/Editor(s)	9. Date
Various	October 1991
10. Author's/Editor's Address	**11. Pages**
Various	274

12. Distribution Statement This document is distributed in accordance with AGARD policies and regulations, which are outlined on the back covers of all AGARD publications.

13. Keywords/Descriptors

High altitude protection
High altitude, high acceleration protection
Integrative protective assemblies for air operations
Positive pressure breathing altitude (PPB)
Decompression sickness
Counterpressure techniques
G-Induced loss of consciousness (GLOC)
High acceleration protection (high onset, sustained)
NBC threat protection
Cold water immersion protection
Positive pressure breathing at G (PBG)
Modelling high acceleration effects
Ebullism
Anti-G straining manoeuvre (AGSM)

14. Abstract

These proceedings include the Technical Evaluation Report, the Keynote Address and the 28 papers of the Symposium sponsored by the AGARD Aerospace Medical Panel and held at the Naval Air Station in Pensacola, Florida, United States, 29th–30th April 1991.

Future NATO fighter aircraft will be highly agile and capable of operating at altitudes well above 50,000 feet (15km) and at sustained accelerations much greater than +6 Gz. Protection against the effects of these stressors involves the use of pressure breathing with counterpressure to parts of the body. Furthermore, there is also the need to protect against harmful environmental stressors such as NBC threats and cold water immersion; and for integrating different protective subassemblies so as to impose the minimum encumbrance and discomfort on aircrew. The purpose of the Symposium was to consider the different requirements for aircrew protection in such potentially hazardous environments, and survey recent developments in the requisite life support equipment.

The papers addressed a variety of topics including: (a) decompression sickness and ebullism at high altitude; (b) effects of high acceleration in terms of G-induced loss of consciousness (GLOC), positive pressure breathing (PBG), and anti-G straining manoeuvre (AGSM), and the neck injury protection; (c) modelling effects of high acceleration on the cardiovascular system; (d) very high altitude protection; and (e) integrative protective equipment to high altitude, high acceleration and other harmful stressors.

These Proceedings will be of interest to those involved in the design of protective aircrew life support equipment, and those concerned with the health and effective use of aircrew in air operations.

AGARD Conference Proceedings 516
Advisory Group for Aerospace Research and Development, NATO
HIGH ALTITUDE AND HIGH ACCELERATION PROTECTION FOR MILITARY AIRCREW
Published October 1991
274 pages

These proceedings include the Technical Evaluation Report, the Keynote Address and the 28 papers of the Symposium sponsored by the AGARD Aerospace Medical Panel and held at the Naval Air Station in Pensacola, Florida, United States, 29th—30th April 1991.

Future NATO fighter aircraft will be highly agile and capable of operating at altitudes well above 50,000 feet (15km) and at sustained accelerations much greater than +Gz. Protection against the effects of these stressors

P.T.O.

AGARD-CP-516

- High altitude protection
- High altitude, high acceleration protection
- Integrative protective assemblies for air operations
- Positive pressure breathing altitude (PPB)
- Decompression sickness
- Counterpressure techniques
- G-induced loss of consciousness (GLOC)
- High acceleration protection (high onset, sustained)
- NBC threat protection
- Cold water immersion protection
- Positive pressure breathing at G (PBG)
- Modelling high acceleration effects
- Ebullism
- Anti-G straining manoeuvre (AGSM)

AGARD Conference Proceedings 516
Advisory Group for Aerospace Research and Development, NATO
HIGH ALTITUDE AND HIGH ACCELERATION PROTECTION FOR MILITARY AIRCREW
Published October 1991
274 pages

These proceedings include the Technical Evaluation Report, the Keynote Address and the 28 papers of the Symposium sponsored by the AGARD Aerospace Medical Panel and held at the Naval Air Station in Pensacola, Florida, United States, 29th—30th April 1991.

Future NATO fighter aircraft will be highly agile and capable of operating at altitudes well above 50,000 feet (15km) and at sustained accelerations much greater than +Gz. Protection against the effects of these stressors

P.T.O.

AGARD-CP-516

- High altitude protection
- High altitude, high acceleration protection
- Integrative protective assemblies for air operations
- Positive pressure breathing altitude (PPB)
- Decompression sickness
- Counterpressure techniques
- G-induced loss of consciousness (GLOC)
- High acceleration protection (high onset, sustained)
- NBC threat protection
- Cold water immersion protection
- Positive pressure breathing at G (PBG)
- Modelling high acceleration effects
- Ebullism
- Anti-G straining manoeuvre (AGSM)

AGARD Conference Proceedings 516
Advisory Group for Aerospace Research and Development, NATO
HIGH ALTITUDE AND HIGH ACCELERATION PROTECTION FOR MILITARY AIRCREW
Published October 1991
274 pages

These proceedings include the Technical Evaluation Report, the Keynote Address and the 28 papers of the Symposium sponsored by the AGARD Aerospace Medical Panel and held at the Naval Air Station in Pensacola, Florida, United States, 29th—30th April 1991.

Future NATO fighter aircraft will be highly agile and capable of operating at altitudes well above 50,000 feet (15km) and at sustained accelerations much greater than +Gz. Protection against the effects of these stressors

P.T.O.

AGARD-CP-516

- High altitude protection
- High altitude, high acceleration protection
- Integrative protective assemblies for air operations
- Positive pressure breathing altitude (PPB)
- Decompression sickness
- Counterpressure techniques
- G-induced loss of consciousness (GLOC)
- High acceleration protection (high onset, sustained)
- NBC threat protection
- Cold water immersion protection
- Positive pressure breathing at G (PBG)
- Modelling high acceleration effects
- Ebullism
- Anti-G straining manoeuvre (AGSM)

AGARD Conference Proceedings 516
Advisory Group for Aerospace Research and Development, NATO
HIGH ALTITUDE AND HIGH ACCELERATION PROTECTION FOR MILITARY AIRCREW
Published October 1991
274 pages

These proceedings include the Technical Evaluation Report, the Keynote Address and the 28 papers of the Symposium sponsored by the AGARD Aerospace Medical Panel and held at the Naval Air Station in Pensacola, Florida, United States, 29th—30th April 1991.

Future NATO fighter aircraft will be highly agile and capable of operating at altitudes well above 50,000 feet (15km) and at sustained accelerations much greater than +Gz. Protection against the effects of these stressors

P.T.O.

AGARD-CP-516

- High altitude protection
- High altitude, high acceleration protection
- Integrative protective assemblies for air operations
- Positive pressure breathing altitude (PPB)
- Decompression sickness
- Counterpressure techniques
- G-induced loss of consciousness (GLOC)
- High acceleration protection (high onset, sustained)
- NBC threat protection
- Cold water immersion protection
- Positive pressure breathing at G (PBG)
- Modelling high acceleration effects
- Ebullism
- Anti-G straining manoeuvre (AGSM)

involves the use of pressure breathing with counterpressure to parts of the body. Furthermore, there is also the need to protect against harmful environmental stressors such as NBC threats and cold water immersion; and for integrating different protective subassemblies so as to impose the minimum encumbrance and discomfort on aircrew. The purpose of the Symposium was to consider the different requirements for aircrew protection in such potentially hazardous environments, and survey recent developments in the requisite life support equipment.

The papers addressed a variety of topics including: (a) decompression sickness and ebullism at high altitude; (b) effects of high acceleration in terms of G-induced loss of consciousness (GLOC), positive pressure breathing (PBG), and anti-G straining manoeuvre (AGSM), and the neck injury protection; (c) modelling effects of high acceleration on the cardiovascular system; (d) very high altitude protection; and (e) integrative protective equipment to high altitude, high acceleration and other harmful stressors.

These Proceedings will be of interest to those involved in the design of protective aircrew life support equipment, and those concerned with the health and effective use of aircrew in air operations.

ISBN 92-835-0638-3

involves the use of pressure breathing with counterpressure to parts of the body. Furthermore, there is also the need to protect against harmful environmental stressors such as NBC threats and cold water immersion; and for integrating different protective subassemblies so as to impose the minimum encumbrance and discomfort on aircrew. The purpose of the Symposium was to consider the different requirements for aircrew protection in such potentially hazardous environments, and survey recent developments in the requisite life support equipment.

The papers addressed a variety of topics including: (a) decompression sickness and ebullism at high altitude; (b) effects of high acceleration in terms of G-induced loss of consciousness (GLOC), positive pressure breathing (PBG), and anti-G straining manoeuvre (AGSM), and the neck injury protection; (c) modelling effects of high acceleration on the cardiovascular system; (d) very high altitude protection; and (e) integrative protective equipment to high altitude, high acceleration and other harmful stressors.

These Proceedings will be of interest to those involved in the design of protective aircrew life support equipment, and those concerned with the health and effective use of aircrew in air operations.

ISBN 92-835-0638-3

involves the use of pressure breathing with counterpressure to parts of the body. Furthermore, there is also the need to protect against harmful environmental stressors such as NBC threats and cold water immersion; and for integrating different protective subassemblies so as to impose the minimum encumbrance and discomfort on aircrew. The purpose of the Symposium was to consider the different requirements for aircrew protection in such potentially hazardous environments, and survey recent developments in the requisite life support equipment.

The papers addressed a variety of topics including: (a) decompression sickness and ebullism at high altitude; (b) effects of high acceleration in terms of G-induced loss of consciousness (GLOC), positive pressure breathing (PBG), and anti-G straining manoeuvre (AGSM), and the neck injury protection; (c) modelling effects of high acceleration on the cardiovascular system; (d) very high altitude protection; and (e) integrative protective equipment to high altitude, high acceleration and other harmful stressors.

These Proceedings will be of interest to those involved in the design of protective aircrew life support equipment, and those concerned with the health and effective use of aircrew in air operations.

ISBN 92-835-0638-3

involves the use of pressure breathing with counterpressure to parts of the body. Furthermore, there is also the need to protect against harmful environmental stressors such as NBC threats and cold water immersion; and for integrating different protective subassemblies so as to impose the minimum encumbrance and discomfort on aircrew. The purpose of the Symposium was to consider the different requirements for aircrew protection in such potentially hazardous environments, and survey recent developments in the requisite life support equipment.

The papers addressed a variety of topics including: (a) decompression sickness and ebullism at high altitude; (b) effects of high acceleration in terms of G-induced loss of consciousness (GLOC), positive pressure breathing (PBG), and anti-G straining manoeuvre (AGSM), and the neck injury protection; (c) modelling effects of high acceleration on the cardiovascular system; (d) very high altitude protection; and (e) integrative protective equipment to high altitude, high acceleration and other harmful stressors.

These Proceedings will be of interest to those involved in the design of protective aircrew life support equipment, and those concerned with the health and effective use of aircrew in air operations.

ISBN 92-835-0638-3

NATO OTAN
7 RUE ANCELLE · 92200 NEUILLY-SUR-SEINE
FRANCE
Telephone (1)47.38.57.00 · Telex 610 176
Telecopie (1)47.38.57.99

DIFFUSION DES PUBLICATIONS
AGARD NON CLASSIFIEES

L'AGARD ne détient pas de stocks de ses publications, dans un but de distribution générale à l'adresse ci-dessus. La diffusion initiale des publications de l'AGARD est effectuée auprès des pays membres de cette organisation par l'intermédiaire des Centres Nationaux de Distribution suivants. A l'exception des Etats-Unis, ces centres disposent parfois d'exemplaires additionnels; dans les cas contraire, on peut se procurer ces exemplaires sous forme de microfiches ou de microcopies auprès des Agences de Vente dont la liste suit.

CENTRES DE DIFFUSION NATIONAUX

ALLEMAGNE
Fachinformationszentrum,
Karlsruhe
D-7514 Eggenstein-Leopoldshafen 2

BELGIQUE
Coordonnateur AGARD-VSI
Etat-Major de la Force Aérienne
Quartier Reine Elisabeth
Rue d'Evere, 1140 Bruxelles

CANADA
Directeur du Service des Renseignements Scientifiques
Ministère de la Défense Nationale
Ottawa, Ontario K1A 0K2

DANEMARK
Danish Defence Research Board
Ved Idraetsparken 4
2100 Copenhagen Ø

ESPAGNE
INTA (AGARD Publications)
Pinar Rosales 34
28008 Madrid

ETATS-UNIS
National Aeronautics and Space Administration
Langley Research Center
MS 180
Hampton, Virginia 23665

FRANCE
O.N.E.R.A. (Direction)
29, Avenue de la Division Leclerc
92320, Chatillon sous Bagneux

GRECE
Hellenic Air Force
Air War College
Scientific and Technical Library
Dekelia Air Force Base
Dekelia, Athens TGA 1010

ISLANDE
Director of Aviation
c/o Flugrad
Reykjavik

ITALIE
Aeronautica Militare
Ufficio del Delegato Nazionale all'AGARD
Aeroporto Pratica di Mare
00040 Pomezia (Roma)

LUXEMBOURG
Voir Belgique

NORVEGE
Norwegian Defence Research Establishment
Attn: Biblioteket
P.O. Box 25
N-2007 Kjeller

PAYS-BAS
Netherlands Delegation to AGARD
National Aerospace Laboratory NLR
Kluyverweg 1
2629 HS Delft

PORTUGAL
Portuguese National Coordinator to AGARD
Gabinete de Estudos e Programas
CLAFA
Base de Alfragide
Alfragide
2700 Amadora

ROYAUME UNI
Defence Research Information Centre
Kentigern House
65 Brown Street
Glasgow G2 8EX

TURQUIE
Milli Savunma Başkonlığı (MSB)
ARGE Daire Başkanlığı (ARGE)
Ankara

LE CENTRE NATIONAL DE DISTRIBUTION DES ETATS-UNIS (NASA) NE DETIENT PAS DE STOCKS DES PUBLICATIONS AGARD ET LES DEMANDES D'EXEMPLAIRES DOIVENT ETRE ADRESSEES DIRECTEMENT AU SERVICE NATIONAL TECHNIQUE DE L'INFORMATION (NTIS) DONT L'ADRESSE SUIT.

AGENCES DE VENTE

National Technical Information Service
(NTIS)
5285 Port Royal Road
Springfield, Virginia 22161
Etats-Unis

ESA/Information Retrieval Service
European Space Agency
10, rue Mario Nikis
75015 Paris
France

The British Library
Document Supply Division
Boston Spa, Wetherby
West Yorkshire LS23 7BQ
Royaume Uni

Les demandes de microfiches ou de photocopies de documents AGARD (y compris les demandes faites auprès du NTIS) doivent comporter la dénomination AGARD, ainsi que le numéro de série de l'AGARD (par exemple AGARD-AG-315). Des informations analogues, telles que le titre et la date de publication sont souhaitables. Veuiller noter qu'il y a lieu de spécifier AGARD-R-nnn et AGARD-AR-nnn lors de la commande de rapports AGARD et des rapports consultatifs AGARD respectivement. Des références bibliographiques complètes ainsi que des résumés des publications AGARD figurent dans les journaux suivants:

Scientifique and Technical Aerospace Reports (STAR)
publié par la NASA Scientific and Technical
Information Division
NASA Headquarters (NTT)
Washington D.C. 20546
Etats-Unis

Government Reports Announcements and Index (GRA&I)
publié par le National Technical Information Service
Springfield
Virginia 22161
Etats-Unis

(accessible également en mode interactif dans la base de données bibliographiques en ligne du NTIS, et sur CD-ROM)

Imprimé par Specialised Printing Services Limited
40 Chigwell Lane, Loughton, Essex IG10 3TZ